



**US Army Corps
of Engineers**
Waterways Experiment
Station

Technical Report CERC-93-6
March 1994

AD-A278 368



(2)

Observations and Modelling of Winds and Waves During the Surface Wave Dynamics Experiment

Report 2

Intensive Observation Period IOP-3

25 February–9 March 1991

by *Michael J. Caruso*
Woods Hole Oceanographic Institution

Hans C. Gruber
University of Miami

Robert E. Jensen

Mark A. Donelan
Canada Centre for Inland Waters

DTIC
ELECTED
APR 19 1994
S B D

REF ID: A6425

Approved For Public Release; Distribution Is Unlimited

29/08/94-11703



94 4 18 122

REF ID: A6425

Prepared for Headquarters, U.S. Army Corps of Engineers

Under **Upgrading of Discrete Spectral Hindcasting Models**
Work Unit 32523
Office of Naval Research Contracts N00014-90-J-1464,
N00014-92-J-1546, and N00014-88-J-1028



**The contents of this report are not to be used for advertising,
publication, or promotional purposes. Citation of trade names
does not constitute an official endorsement or approval of the use
of such commercial products.**



PRINTED ON RECYCLED PAPER

Observations and Modelling of Winds and Waves During the Surface Wave Dynamics Experiment

Report 2

Intensive Observation Period IOP-3

25 February–9 March 1991

by Michael J. Caruso

Department of Physical Oceanography
Woods Hole Oceanographic Institution, Woods Hole, MA 02543

Hans C. Gruber
Rosenstiel School of Marine and Atmospheric Science
University of Miami, Miami, FL 33149-1098

Robert E. Jensen
U.S. Army Corps of Engineers
Waterways Experiment Station
3909 Halls Ferry Road, Vicksburg, MS 39180-6199

Mark A. Donelan

National Water Research Institute
Canada Centre for Inland Waters, Burlington, Ontario L7R 4A6, Canada

Report 2 of a series

Approved for public release; distribution is unlimited

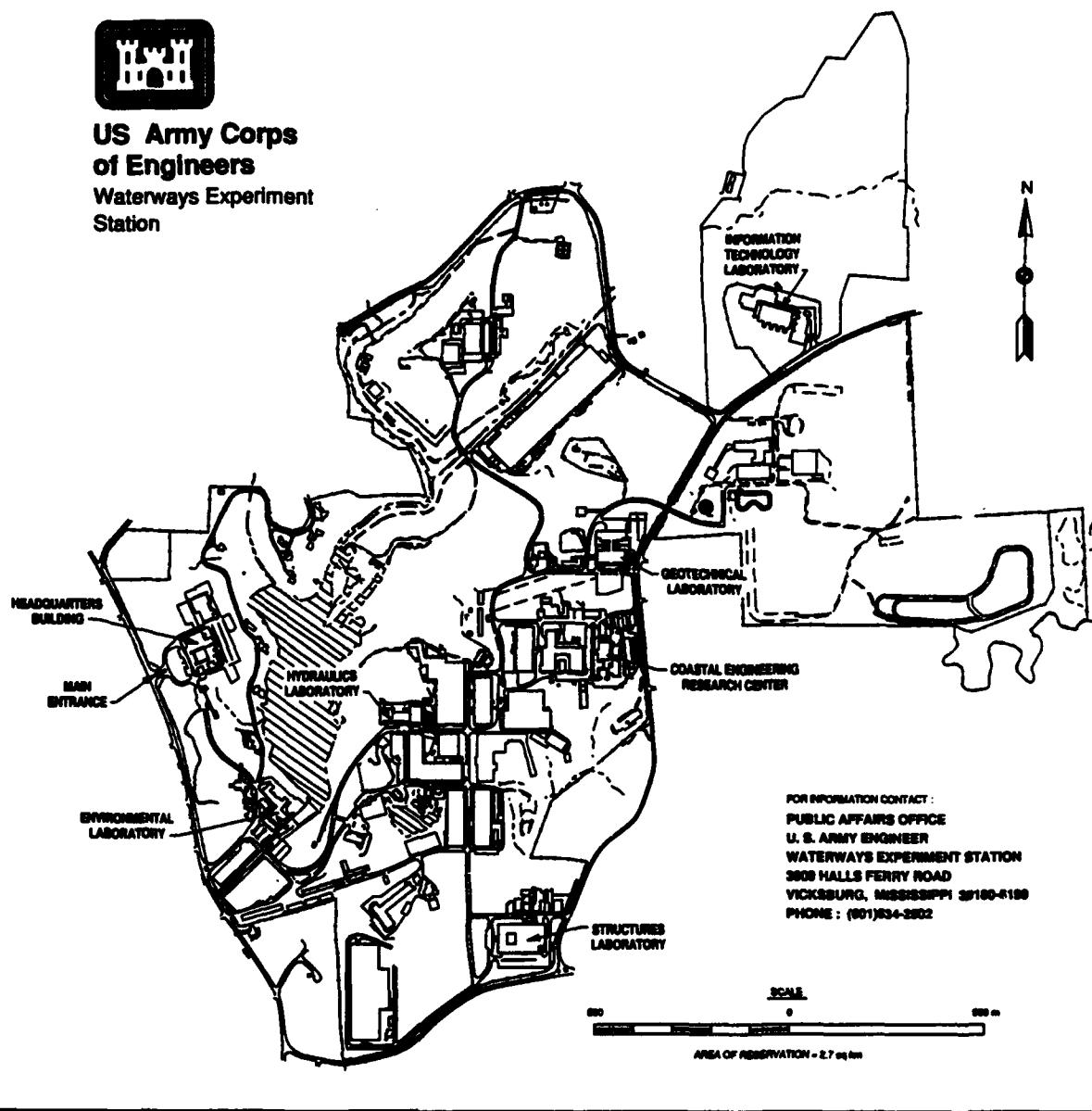
DTIC QUALITY INSPECTED 3

Prepared for U.S. Army Corps of Engineers
Washington, DC 20314-1000

Under Office of Naval Research Contracts N00014-90-J-1464,
N00014-92-J-1546, and N00014-88-J-1028
Upgrading of Discrete Spectral Hindcasting Models Work Unit 32523



**US Army Corps
of Engineers**
Waterways Experiment
Station



Waterways Experiment Station Cataloging-In-Publication Data

Observations and modelling of winds and waves during the Surface Wave Dynamics Experiment. Report 2, Intensive observation period IOP-3, 25 February-9 March 1991 / by Michael J. Caruso ... [et al.] ; prepared for U.S. Army Corps of Engineers.

167 p. : ill. ; 28 cm. — (Technical report ; CERC-93-6 rept. 2)

Includes bibliographical references.

1. Ocean waves — Atlantic Ocean. 2. Winds — Atlantic Ocean.
3. Oceanographic buoys. 4. Ocean-atmosphere interaction. I. Caruso, Michael J. II. United States. Army. Corps of Engineers. III. Coastal Engineering Research Center (U.S.) IV. U.S. Army Engineer Waterways Experiment Station. V. Series: Technical report (U.S. Army Engineer Waterways Experiment Station) ; CERC-93-6 rept 2.

TA7 W34 no.CERC-93-6 rept.2

Contents

| | |
|--|-----------|
| Preface | v |
| 1 Introduction | 1 |
| 2 Measurements | 3 |
| SWADE Buoys | 3 |
| SWATH Ship | 5 |
| Remote Sensing | 7 |
| 3 Ocean Wave Modelling and Grid Domains | 26 |
| Atlantic Basin Model | 26 |
| Western North Atlantic Model | 27 |
| SWADE Model | 27 |
| 4 Wind Fields | 28 |
| FNOC | 28 |
| ECMWF | 28 |
| NMC/GSFC | 29 |
| OW/AES | 29 |
| UKMO | 30 |
| 5 Surface Currents | 31 |
| 6 Summary | 32 |
| References | 33 |
| Appendix A: Time Series from SWADE and NDBC Buoys | A1 |
| Appendix B: Directional Wave Spectra from SWADE Buoys | B1 |
| B.1 Discus Buoy "North" | B3 |
| B.2 Discus Buoy "East" | B37 |
| B.3 Discus Buoy "Central" | B71 |
| B.4 Discus Buoy "CERC" | B105 |
| Appendix C: Custer Diagrams of Surface Current Fields | C1 |
| Appendix D: Custer Diagrams of Wind Fields and Wave Hindcasts | D1 |
| D.1 Oceanweather/Atmospheric Environment Service (OW/AES) | D3 |
| D.2 Fleet Numerical Oceanography Center (FNOC) | D17 |
| D.3 European Centre for Medium-Range Weather Forecasts (ECMWF) | D31 |
| D.4 National Meteorological Center (NMC) | D45 |
| D.5 NASA Goddard Space Flight Facility (GSFC) | D59 |

| | |
|--|-----------|
| D.6 United Kingdom Meteorological Office (UKMO) | D73 |
| Appendix E: Infrared Imagery of Sea Surface Temperature | E1 |

List of Tables

| | |
|--|----|
| 1 Buoy Positions and Logistics for SWADE IOP-3. | 3 |
| 2 Measurement Characteristics of Meteorological Variables on NDBC 3-m Discus Buoys (after Steele et al. (1992)). | 5 |
| 3 Data Availability and Sampling Modes from the SWATH Ship. | 8 |
| 4 RESSAC Radar System Characteristics. | 14 |
| 5 Positions and Times of RESSAC Directional Wave Spectra. | 16 |
| 6 Times and Positions of AXCPs (CP) and AXBTs (BT) Deployed on 5 March 1991 from the NASA NP-3A. | 22 |

List of Figures

| | |
|---|----|
| 1 Geographic location of the SWADE program and the positions of the buoys during IOP-3. | 4 |
| 2 SWATH ship <i>Frederick G. Creed</i> configured for SWADE | 6 |
| 3 Ship track of <i>Creed</i> for 25 - 27 February 1991. | 10 |
| 4 Ship track of <i>Creed</i> for 3 - 6 March 1991. | 11 |
| 5 Ship track of <i>Creed</i> for 7 - 9 March 1991. | 12 |
| 6 Directional wave spectra from SWATH ship measured at four sites. | 13 |
| 7 Wave number spectrum from RESSAC on 4 March 1991, 19:59:16 LT. | 17 |
| 8 Flight tracks for the surface radar altimeter during IOP-3. | 19 |
| 9 Directional wave number and frequency spectra from the surface radar altimeter on 5 March 1991. | 21 |
| 10 AXCP and AXBT deployments in a star-like pattern. | 23 |
| 11 Current vectors from the AXCPs and ADCP deployed on 5 March 1991. | 24 |

| | |
|---|-------------------------------------|
| Accession For | |
| NTIS GRA&I | <input checked="" type="checkbox"/> |
| DTIC TAB | <input type="checkbox"/> |
| Unannounced | <input type="checkbox"/> |
| Justification | |
| By | |
| Distribution/ | |
| Availability | |
| Dist | Avail and/or Special |
|  | |

Preface

The authors gratefully acknowledge funding support by the Small-Scale Physics Program (Code 1122SS) at the Office of Naval Research (ONR) under Grant Nos. N00014-90-J-1464, N00014-92-J-1546, and N00014-88-J-1028.

This study was authorized by Headquarters, U.S. Army Corps of Engineers (HQUSACE), under Civil Works Research Work Unit 32523, Upgrading of Discrete Spectral Hindcasting Models, Coastal Flooding Program. Messrs. John H. Lockhart, Jr., and John G. Housley were HQUSACE Technical Monitors. This report was prepared by Mr. Michael J. Caruso, Woods Hole Oceanographic Institution (WHOI), Dr. Hans C. Graber, Rosenstiel School of Marine and Atmospheric Science (RSMAS), University of Miami, Dr. Robert E. Jensen, U.S. Army Engineer Waterways Experiment Station (WES) Coastal Engineering Research Center (CERC), and Dr. Mark A. Donelan, National Water Research Institute, Canada Centre for Inland Waters (CCIW). Dr. Jensen's work was carried out under the program management of Ms. Carolyn Holmes, CERC; under the direct supervision of Mr. H. Lee Butler, Chief, Research Division; and under the general supervision of Dr. James R. Houston and Mr. Charles C. Calhoun, Jr., Director and Assistant Director, CERC, respectively.

The authors gratefully acknowledge the contributions of the following SWADE investigators: Dr. Danièle Hauser, Centre de Recherches en Physique de l'Environnement Terrestre et Planétaire (CRPE), France; Dr. Will M. Drennan, National Water Research Institute, CCIW; Dr. Lynn "Nick" K. Shay, RSMAS; Dr. Edward J. Walsh, Wallops Flight Facility/National Aeronautics and Space Administration (WFF/NASA); and Dr. Kristina B. Katsaros, Institut Français de Recherche pour l'Exploitation de la Mer (IFREMER), France.

The authors extend special thanks to the following: Models Division of the Fleet Numerical Oceanography Center, National Meteorological Center of the National Weather Service (Dr. William H. Gemmill), the Global Modeling and Simulation Branch, Goddard Space Flight Center/National Aeronautics and Space Administration (GSFC/NASA) (Dr. Dean Duffy), the European Center for Medium Range Weather Forecasts, the United Kingdom Meteorological Office, the Atmospheric Environment Service of Environment Canada, funding work conducted by Dr. Vincent J. Cardone, Oceanweather, Inc., and the National Data Buoy Center, especially Kenneth Steele. The authors are also grateful to Ram Vakkayil and Louis Chemi, RSMAS, for producing the numerous plots.

Finally, continuous support and helpful advice provided by Dr. Melbourne G. Briscoe (formerly ONR), NOAA, Dr. Alan Brandt (formerly ONR), Applied Physics Laboratory, Johns Hopkins University, and Dr. C. Linwood Vincent, CERC, were always welcomed and appreciated.

1 Introduction

The primary scientific goals of the Surface Wave Dynamics Experiment (*SWADE*) are to understand the dynamics of the evolution of the directional wind-wave spectrum and the effect of waves on fluxes of momentum, heat, and mass at the air-sea interface. During the third intensive observation period (IOP-3) opportunities existed to investigate the effect of the directional wave field on the response of various airborne sensors such as the scanning radar altimeter (SRA), the radar ocean wave spectrometer, the scatterometer, the radar altimeter and the synthetic aperture radar. A detailed discussion of the scientific and experimental objectives as well as a description of the measurement systems and sensors can be found in Weller et al. (1991). The experiment began on October 1, 1990 and lasted for a six-month period in the waters off the DelMarVa Peninsula. During three intensive observation periods (IOPs) in situ measurements from buoys were complemented by radar and remote sensing observations from aircraft and a ship.

An improved understanding of the evolution of the directional wave spectrum under a variety of spatially and temporally inhomogeneous wind fields will make it possible to determine and develop better parameterizations of the source term physics in numerical wind-wave models. Unlike previous field experiments (e.g. JONSWAP, ARSLOE) *SWADE* will provide wind data from a spatially dense array of buoys, which were deployed between Cape Hatteras and Cape Cod. The wind forcing field still remains the largest source of uncertainty in predicting the directional wave field and, hence, the sea state. An improved specification of the wind field will be suitable for examining the physics of the source functions for wind energy input, nonlinear wave-wave interactions, and dissipation by breaking. In addition the *SWADE* measuring systems included five buoys recording continuous (hourly) estimates of directional wave spectra as well as three aircraft and one ship during the third IOP.

SWADE identified several storm situations that were expected to occur during the project period. These included cold air outbreaks featuring large wind shifts; steady, off-shore blowing winds; long fetch conditions from the northeast; and cyclones developing from the south and moving northward over the *SWADE* area. Meteorological conditions during the final intensive measurement period were primarily marked by persistent south and southwesterly winds. Those conditions were interrupted by passages of two cold fronts toward the end of the IOP. Wind speeds ranged from about 5 to 15 ms^{-1} and wave heights reached up to 6 m. Of greater significance was the movement of the Gulf Stream toward the west and the emergence of a ring in the center of the *SWADE* measurement array. At that time, the directional wave field became far more complicated, with multi-modal sea states and steeper and shorter waves resulting from wave-current interactions.

In Chapter 2 a summary is presented of several remote and in-situ measurements from airborne, shipborne, and buoy-based sensors. Brief descriptions of the third-generation wave model (WAM) and the grid domains used during *SWADE* are given in Chapter 3; the six wind fields are briefly described in Chapter 4; the model currents are described in Chapter 5. Appendix A presents time series of meteorological and wave parameters,

Appendix B contains plots of directional wave spectra, Appendix C presents maps of the modelled surface current fields, Appendix D consists of maps of wind vector fields and the associated wave hindcasts, and infrared images of sea surface temperature are contained in Appendix E.

2 Measurements

SWADE Buoys

In addition to the existing operational network of buoys maintained by the National Data Buoy Center (NDBC), *SWADE* deployed two 3-m discus buoys with several modifications to their measuring capability, four MiniMet meteorological buoys, and one WAVESCAN directional wave buoy provided by SEATEX, Norway. The modified Mills-cross array was designed to provide spatial estimates of the variation in wave, wind, and flux data. At its center was the Brookhaven Spar buoy, which was replaced after it sank during the October Storm (October 26, 1990) by another 3-m discus buoy provided by NDBC and by the SWATH (Small Water Plane Area - Twin Hull) ship, *Frederick G. Creed*, from the Canadian Department of Fisheries and Oceans. The SWATH was used as a mobile research platform and with its special equipment could perform almost all tasks expected of the Spar (Donelan *et al.* 1992). The U.S. Army Engineer Waterways Experiment Station Coastal Engineering Research Center (CERC) and the Woods Hole Oceanographic Institution also contributed to *SWADE*, each providing a 3-m discus buoy. Drawings of all of the buoys can be found in Caruso *et al.* (1993). Figure 1 shows an update of the locations of the *SWADE* experimental measurement array during IOP-3. Table 1 summarizes the deployment logistics for these buoys.

Table 1
Buoy Positions and Logistics for SWADE IOP-3

| Station | WMO Code | Latitude | Longitude | Depth | Comments |
|-----------|----------|-------------|-------------|---------|---------------------|
| D-East | 44015 | 37° 29.0' N | 73° 23.9' W | 2,469 m | Reset on 1-24-91 |
| D-North | 44001 | 38° 22.1' N | 73° 38.9' W | 115 m | |
| D-Central | 44023 | 37° 32.1' N | 74° 23.5' W | 102 m | Deployed on 1-14-91 |
| Exp. Buoy | 44024 | 37° 41.1' N | 74° 42.9' W | 49 m | Deployed on 1-14-91 |
| MET-1 | 41012 | 32° 37.8' N | 73° 57.0' W | 4,572 m | Adrift on 10-3-90 |
| | 41014 | | | | Recovered 4-5-91 |
| MET-3 | 44016 | 37° 59.9' N | 72° 54.7' W | 2,617 m | Equipped with Wotan |
| | 44020 | | | | |
| CERC | 44014 | 36° 35.0' N | 74° 50.0' W | 48 m | |

Data from the buoys listed above as well as all NDBC buoys and C-MAN (Coastal-Marine Automated Network) stations along the east coast are available for the entire *SWADE* experimental period and have been archived at the National Aeronautics and Space Administration (NASA)/Wallop Data Archive Center (Oberholtzer and Donelan 1993). The NDBC portion of the buoy instrumentation transmits hourly values of wind speed and direction (two sensors), atmospheric pressure, air and water temperature, significant wave height, and average and dominant wave period. In addition, the covariance spectra for directional wave data as a function of frequency are also transmitted. The Canada Centre for Inland Waters motion sensor packages and K-Gill anemometers sampled

NDBC AND SWADE BUOY LOCATIONS

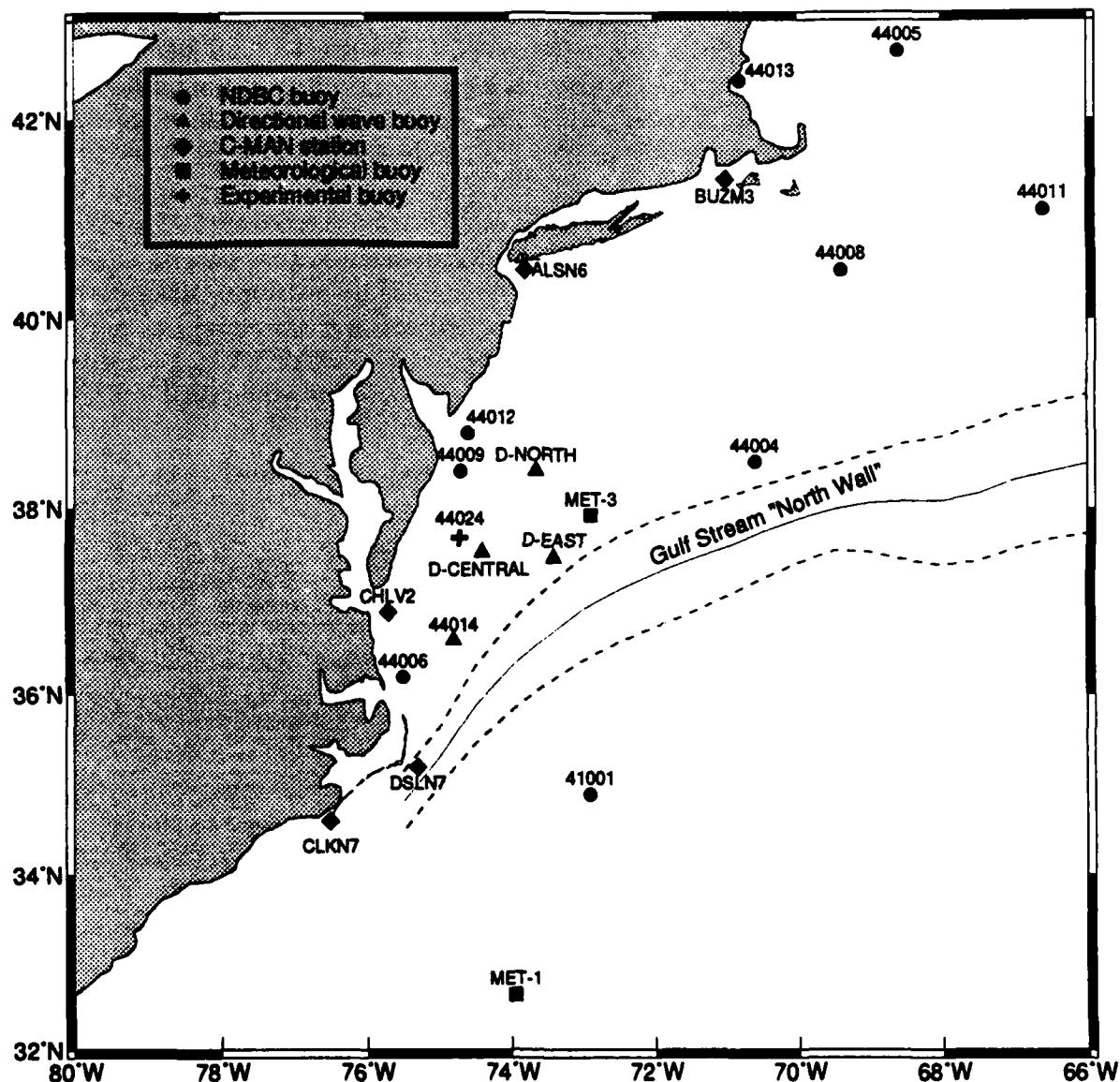


Figure 1: Geographic location of the SWADE program and the positions of the buoys during IOP-3. The mean (solid) and one standard deviation (dashed) positions of the "North Wall" of the Gulf Stream are also shown

data continuously at 1 Hz and stored the data internally on five 120-MB laser disks. A summary of the sampling interval, recording period, and system accuracy of the NDBC sensors is presented in Table 2. For details on the buoy sensors and calibration procedures, the reader is referred to Steele, Teng, and Wang (1992).

In Appendix A, time history plots of wind speed and direction, significant wave height, peak wave period, atmospheric pressure, and air and sea temperature are presented for IOP-3 from *SWADE* buoys D-East, D-North, D-Central, and CERC (44014). In addition, time series of these variables are also shown for buoys 41001, 44004, 44008, 44009, 44011, 44012, the C-MAN stations DSLN7, CHLV2 and BUZM3, and the MiniMet buoys MET-1 and MET-3.

In Appendix B, plots of the directional wave spectra and the associated one-dimensional frequency spectra are presented for buoys D-East, D-North, D-Central and CERC (44014) every 3 hr from 25 February 1991, 03:00 GMT to 9 March 1991, 00:00 GMT during IOP-3. The directional wave spectra were computed with the maximum-likelihood technique described in Drennan, Gruber, and Donelan (1993).

Table 2
Measurement Characteristics of Meteorological Variables
on NDBC 3-m Discus Buoys (after Steele et al. (1992))

| Parameter | Range | Resolution | Sample interval | Sample period | Total system accuracy |
|-------------------------|-----------------------|----------------------|-----------------|---------------|--------------------------------|
| Wind speed | 0-80 ms^{-1} | 0.1 ms^{-1} | 1 sec | 8 min | $\pm 1 \text{ ms}^{-1}$ or 10% |
| Wind direction | 0-360° | 1° | 1 sec | 8 min | $\pm 10^\circ$ |
| Wind gust* | 0-80 ms^{-1} | 0.1 ms^{-1} | 1 sec | 5 sec | $\pm 1 \text{ ms}^{-1}$ or 10% |
| Air temperature | -40 to 50 °C | 0.5 °C | 90 sec | 90 sec | $\pm 1^\circ\text{C}$ |
| Sea surface temperature | -15 to 50 °C | 0.5 °C | 1 sec | 1 sec | $\pm 1^\circ\text{C}$ |
| Barometric pressure | 900-1100 hPa (mb) | 0.1 hPa (mb) | 4 sec | 8 min | $\pm 1 \text{ hPa (mb)}$ |

* Highest 5-sec window average

SWATH Ship

The *Frederick G. Creed*, a SWATH ship operated by the Canadian Department of Fisheries and Oceans, was deployed during *SWADE* to carry out in situ high resolution meteorological and wave measurements. Only 20 m long by 10 m wide, the *Creed* was designed to cruise at speeds up to 13 ms^{-1} . Its hull is very streamlined and produces minimal flow disturbance at the water surface (Figure 2).

For the purposes of *SWADE*, a variety of special equipment was added to the *Creed*. A 9-m mast located on the foredeck held the meteorological equipment. This included K-Gill and propeller anemometers, two pairs of wet/dry bulb thermometers, Lyman- α and Rotronics hygrometers, thermocouples, and a rain gauge. Radiometers were mounted on a smaller mast behind the cabin and a barograph was inside the bridge. Additional

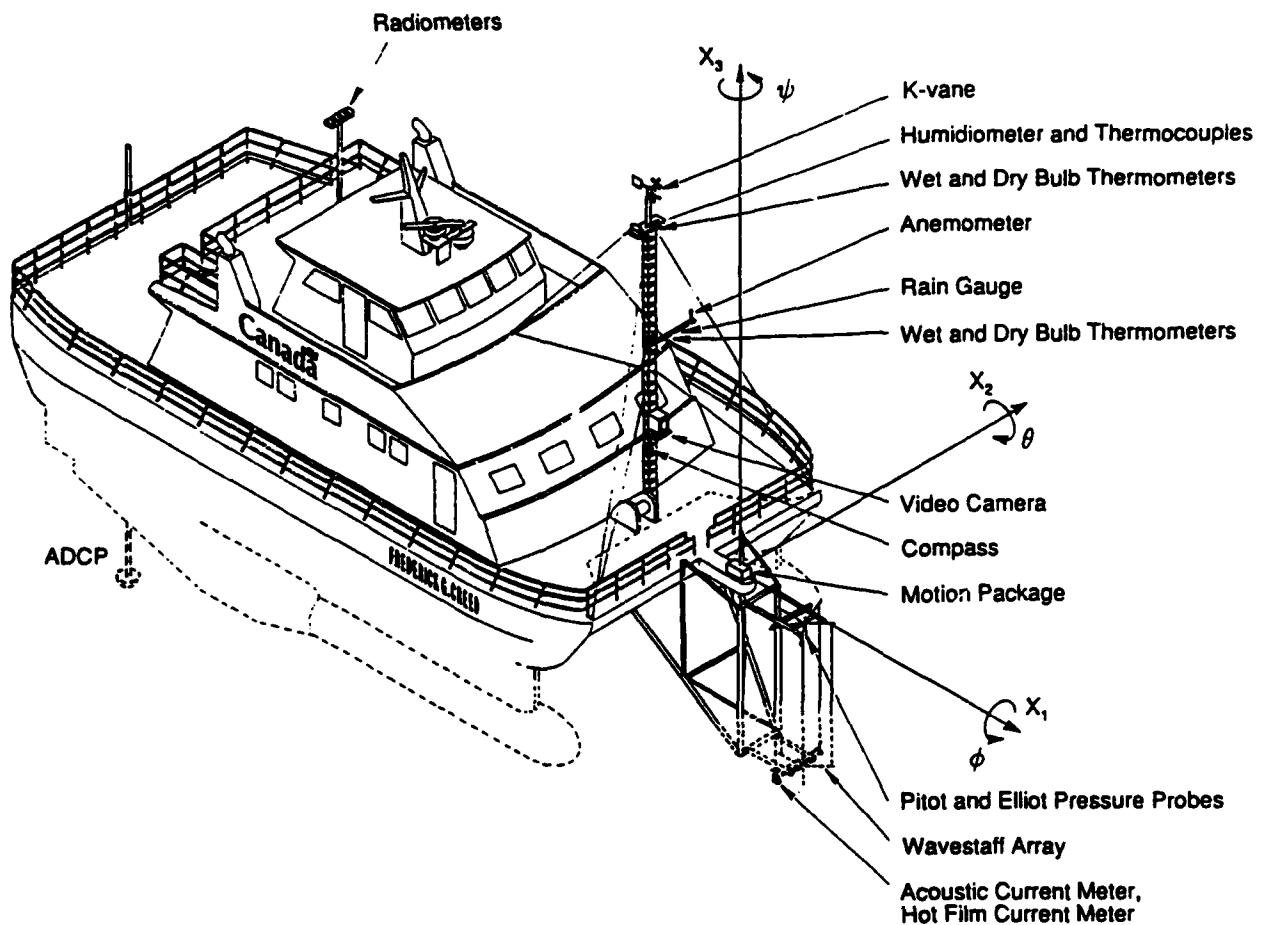


Figure 2: SWATH ship *Frederick G. Creed* configured and equipped for SWADE with special sensors to measure meteorological and wave parameters during IOP-3

meteorological measurements were made from instruments attached to 23 balloons launched from the *Creed*, and these measurements are summarized in Howard (1993).

A sprit reaching 2 m fore of the bow held an array of wave staffs and an acoustic current meter for the estimation of wave directional spectra and the kinetic energy dissipation in the near surface meters. The original array of six capacitance wave gauges and the three-axis acoustic current meter were lost on 27 February 1991. An array of three staffs was employed for the remaining duration of *SWADE*. Current profiles were made using an Acoustic Doppler Current Profiler (ADCP) mounted off the stern of the ship. The six components of ship motion (heave, pitch, roll, yaw, surge, and sway), required for the estimation of both surface fluxes and wave directional spectra were recorded with a motion sensor package and compass, both located near the bow of the ship. The ship's position was measured using a global positioning system recorder.

During IOP-3, the *Creed* carried out three cruises each lasting approximately three days. Figures 3, 4, and 5 show the ship track of these cruises by the *Creed* and the locations where data were collected. Mean meteorological data were recorded almost continuously during these periods (see Table 3). High-frequency (20 Hz) data were collected in two modes, "fast" and "slow" referring to the cruising speed of the *Creed*. In the slow mode, typically $2-3 \text{ ms}^{-1}$, the ship travelled into the wind with all sensors deployed. In the fast mode, measurements were often secondary to travel; the bow array was removed from the water and the ship followed its course, independent of the wind direction, at speeds of up to 8 ms^{-1} . The time intervals (30 min in duration) when data were collected appear in Table 3.

Two principal measurements made from the *Frederick G. Creed* were those of surface fluxes and wave directional spectra. The algorithm described in Katsaros, Donelan, and Drennan (1993) (see also Anctil et al. (1993)) was used to determine surface fluxes of momentum, heat, and water vapour via the eddy-correlation technique. Examples, along with comparisons of fluxes derived via the inertial dissipation method, are given in Katsaros, Donelan, and Drennan (1993). Estimates of wave directional spectra were determined using the algorithm of Drennan et al. (in preparation); preliminary results were presented in Donelan et al. (1992). Figure 6 shows four examples of the directional wave spectra collected from the wire wave gauge array on the SWATH ship.

Remote Sensing

RESSAC

RESSAC ("Radar pour l'Etude du Spectre des Surfaces par Analyse Circulaire") is an airborne radar, whose main characteristics are given in Table 4. During *SWADE*, RESSAC was installed on the French research aircraft "MERLIN-IV" which belongs to Météo-France (French National Weather Service). For details about the system or the processing of the data the reader is referred to Hauser et al. (1992).

Table 3
Data Availability and Sampling Modes from the SWATH Ship
(Note: x - data available; s - slow and f - fast sampling mode)

| Date | Hour of Day | | | | | | | | | | | | | | | | | | | | | | | | System | |
|--------|-------------|----|----|----|----|----|----|----|----|----|----|----|----|----|----|----|----|----|----|----|----|----|----|----|--------|---------|
| | 00 | 01 | 02 | 03 | 04 | 05 | 06 | 07 | 08 | 09 | 10 | 11 | 12 | 13 | 14 | 15 | 16 | 17 | 18 | 19 | 20 | 21 | 22 | 23 | | |
| 25 FEB | xx | xx | xx | xx | xx | xx | xx | xx | xx | xx | xx | xx | xx | xx | xx | xx | xx | xx | xx | xx | xx | xx | xx | xx | MET | |
| | | | | | | | | | | | | | | | | | | | | | | | | | ADCP | |
| | | | | | | | | | | | | | | | | | | | | | | | | | GPS | |
| | | | | | | | | | | | | | | | | | | | | | | | | | HFD | |
| | | | | | | | | | | | | | | | | | | | | | | | | | DS | |
| | | | | | | | | | | | | | | | | | | | | | | | | | Flux | |
| | | | | | | | | | | | | | | | | | | | | | | | | | CM | |
| 26 FEB | 00 | 01 | 02 | 03 | 04 | 05 | 06 | 07 | 08 | 09 | 10 | 11 | 12 | 13 | 14 | 15 | 16 | 17 | 18 | 19 | 20 | 21 | 22 | 23 | | |
| | | | | | | | | | | | | | | | | | | | | | | | | | | MET |
| | | | | | | | | | | | | | | | | | | | | | | | | | | ADCP |
| | | | | | | | | | | | | | | | | | | | | | | | | | | GPS |
| | | | | | | | | | | | | | | | | | | | | | | | | | | HFD |
| 27 FEB | 00 | 01 | 02 | 03 | 04 | 05 | 06 | 07 | 08 | 09 | 10 | 11 | 12 | 13 | 14 | 15 | 16 | 17 | 18 | 19 | 20 | 21 | 22 | 23 | | |
| | xx | x | xx | x | xx | x | xx | x | xx | x | xx | x | xx | x | xx | x | xx | x | xx | x | xx | x | xx | x | | |
| | | | | | | | | | | | | | | | | | | | | | | | | | | MET |
| | | | | | | | | | | | | | | | | | | | | | | | | | | ADCP |
| | | | | | | | | | | | | | | | | | | | | | | | | | | GPS |
| | | | | | | | | | | | | | | | | | | | | | | | | | | DS |
| | | | | | | | | | | | | | | | | | | | | | | | | | | CM |
| 03 MAR | 00 | 01 | 02 | 03 | 04 | 05 | 06 | 07 | 08 | 09 | 10 | 11 | 12 | 13 | 14 | 15 | 16 | 17 | 18 | 19 | 20 | 21 | 22 | 23 | | |
| | xx | xx | xx | xx | xx | xx | xx | xx | xx | xx | xx | xx | xx | xx | xx | xx | xx | xx | xx | xx | xx | xx | xx | xx | | |
| | | | | | | | | | | | | | | | | | | | | | | | | | | MET |
| | | | | | | | | | | | | | | | | | | | | | | | | | | ADCP |
| | | | | | | | | | | | | | | | | | | | | | | | | | | GPS |
| | | | | | | | | | | | | | | | | | | | | | | | | | | HFD |
| | | | | | | | | | | | | | | | | | | | | | | | | | | DS |
| | | | | | | | | | | | | | | | | | | | | | | | | | | Flux |
| | | | | | | | | | | | | | | | | | | | | | | | | | | CM |
| 04 MAR | 00 | 01 | 02 | 03 | 04 | 05 | 06 | 07 | 08 | 09 | 10 | 11 | 12 | 13 | 14 | 15 | 16 | 17 | 18 | 19 | 20 | 21 | 22 | 23 | | |
| | xx | xx | xx | xx | xx | xx | xx | xx | xx | xx | xx | xx | xx | xx | xx | xx | xx | xx | xx | xx | xx | xx | xx | xx | | |
| | | | | | | | | | | | | | | | | | | | | | | | | | | MET |
| | | | | | | | | | | | | | | | | | | | | | | | | | | ADCP |
| | | | | | | | | | | | | | | | | | | | | | | | | | | GPS |
| | | | | | | | | | | | | | | | | | | | | | | | | | | HFD |
| | | | | | | | | | | | | | | | | | | | | | | | | | | DS |
| | | | | | | | | | | | | | | | | | | | | | | | | | | Flux |
| | | | | | | | | | | | | | | | | | | | | | | | | | | CM |
| | | | | | | | | | | | | | | | | | | | | | | | | | | Balloon |

(continued)

Table 3 (concluded)

| Date | | Hour of Day | | | | | | | | | | | | | | | | | | | | | | | | System | | |
|--------|---|-------------|----|----|----|----|----|----|----|----|----|----|----|----|----|----|----|----|----|----|----|----|----|----|----|--------|----|----|
| 05 MAR | 00 01 02 03 04 05 06 07 08 09 10 11 12 13 14 15 16 17 18 19 20 21 22 23 | | | | | | | | | | | | | | | | | | | | | | | | | | | |
| xx | xx | xx | xx | xx | xx | xx | xx | xx | xx | xx | xx | xx | xx | xx | xx | xx | xx | xx | xx | xx | xx | xx | xx | xx | xx | xx | xx | xx |
| xx | xx | xx | x | xx | xx | xx |
| x | xx | xx | xx | xx | xx | xx | xx | xx | xx | xx | xx | xx | xx | xx | xx | xx | xx | xx | xx | xx | xx | xx | xx | xx | xx | xx | xx | xx |
| 6s | ss | ss | 1 | ff | ff | ff |
| xx | xx | xx | xx | xx | xx | xx | xx | xx | xx | xx | xx | xx | xx | xx | xx | xx | xx | xx | xx | xx | xx | xx | xx | xx | xx | xx | xx | xx |
| xx | xx | xx | x | xx | xx | xx |
| 06 MAR | 00 01 02 03 04 05 06 07 08 09 10 11 12 13 14 15 16 17 18 19 20 21 22 23 | | | | | | | | | | | | | | | | | | | | | | | | | | | |
| xx | xx | xx | xx | xx | xx | xx | xx | xx | xx | xx | xx | xx | xx | xx | xx | xx | xx | xx | xx | xx | xx | xx | xx | xx | xx | xx | xx | xx |
| xx | xx | xx | xx | xx | xx | x | xx | xx | xx |
| 6s | ss | ss | 3s | ss | s | 1 | ff | 1 | ff | 1 |
| x | x | x | x | x | x | x | x | x | x | x | x | x | x | x | x | x | x | x | x | x | x | x | x | x | x | x | x | |
| 07 MAR | 00 01 02 03 04 05 06 07 08 09 10 11 12 13 14 15 16 17 18 19 20 21 22 23 | | | | | | | | | | | | | | | | | | | | | | | | | | | |
| xx | xx | xx | xx | xx | xx | x | xx | xx | xx |
| 1 | xx | xx | xx | xx | xx | x | xx | xx | xx |
| 08 MAR | 00 01 02 03 04 05 06 07 08 09 10 11 12 13 14 15 16 17 18 19 20 21 22 23 | | | | | | | | | | | | | | | | | | | | | | | | | | | |
| xx | xx | xx | xx | xx | xx | xx | xx | xx | xx | xx | xx | xx | xx | xx | xx | xx | xx | xx | xx | xx | xx | xx | xx | xx | xx | xx | xx | xx |
| xx | xx | xx | x | xx | xx | xx |
| 6s | ss | ss | ss | ss | ss | s | ss | ss | ss |
| x | xx | xx | x | xx | xx | x | xx | xx | xx |
| 09 MAR | 00 01 02 03 04 05 06 07 08 09 10 11 12 13 14 15 16 17 18 19 20 21 22 23 | | | | | | | | | | | | | | | | | | | | | | | | | | | |
| xx | xx | xx | xx | xx | xx | x | xx | xx | xx |
| xx | x | ss | 6 | xx | x | x | xx | xx | xx |
| x | x | x | x | x | x | x | x | x | x | x | x | x | x | x | x | x | x | x | x | x | x | x | x | x | x | x | x | |

SWATH Ship Positions during IOP3, 25-27 February 91

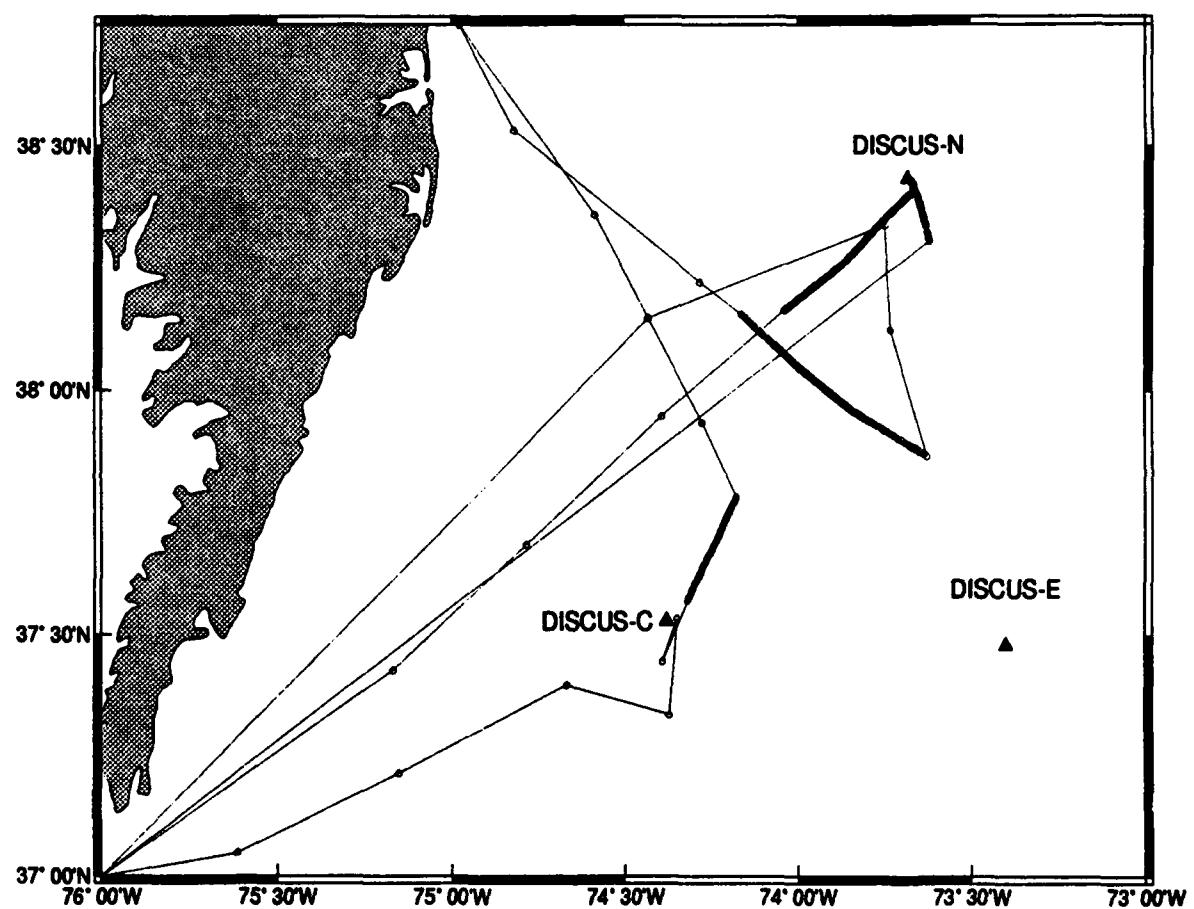


Figure 3: Ship track of *Creed* for 25 - 27 February 1991. Dots and heavy lines indicate locations where data from various sensors were collected as shown in Table 3

SWATH Ship Positions during IOP3, 3-6 March 91

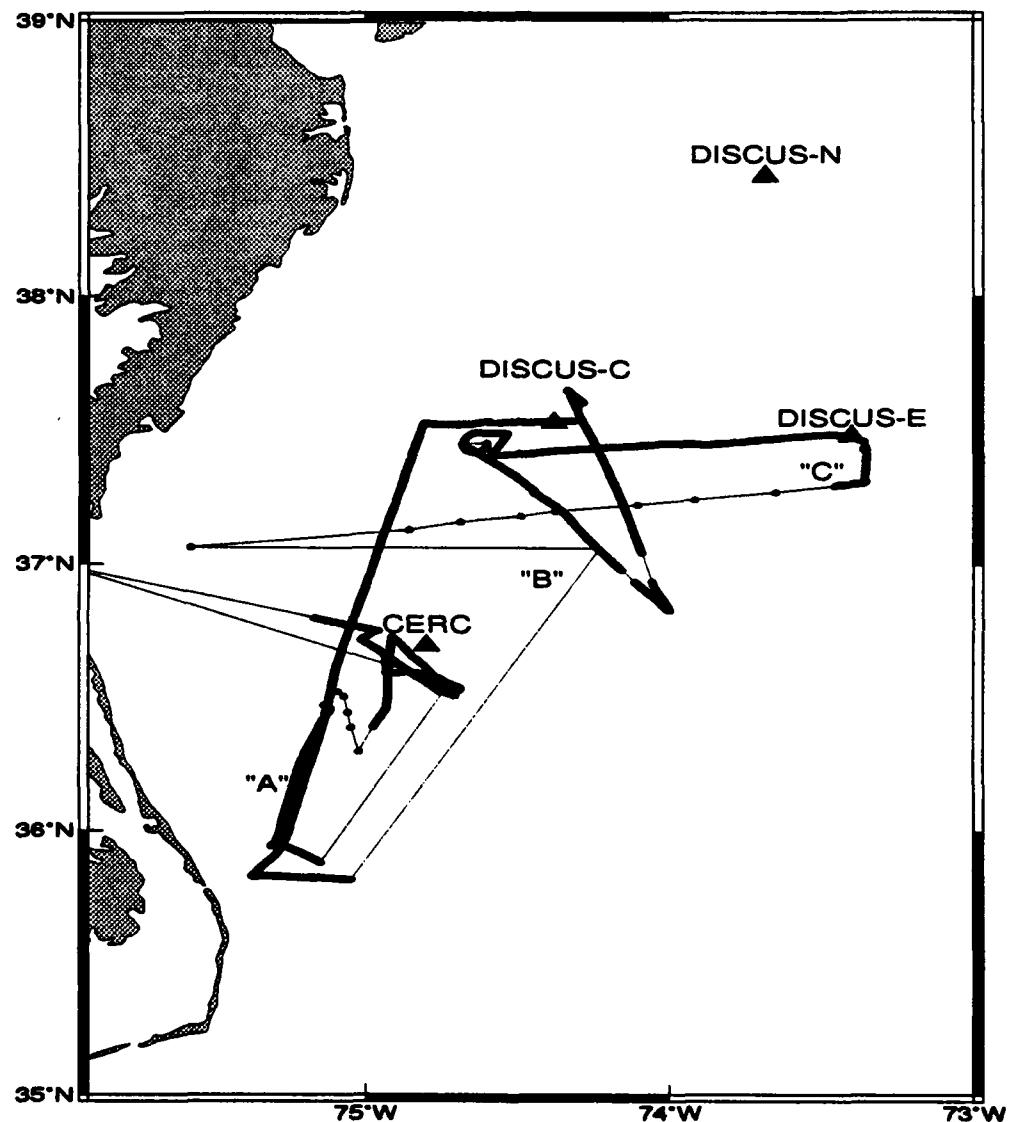


Figure 4: Ship track of *Creed* for 3 - 6 March 1991. Dots and heavy lines indicate locations where data from various sensors were collected as shown in Table 3. Note that sites "A," "B," and "C" specify the locations of sample directional wave spectra shown in Figure 6

SWATH Ship Positions during IOP3, 7-9 March 91

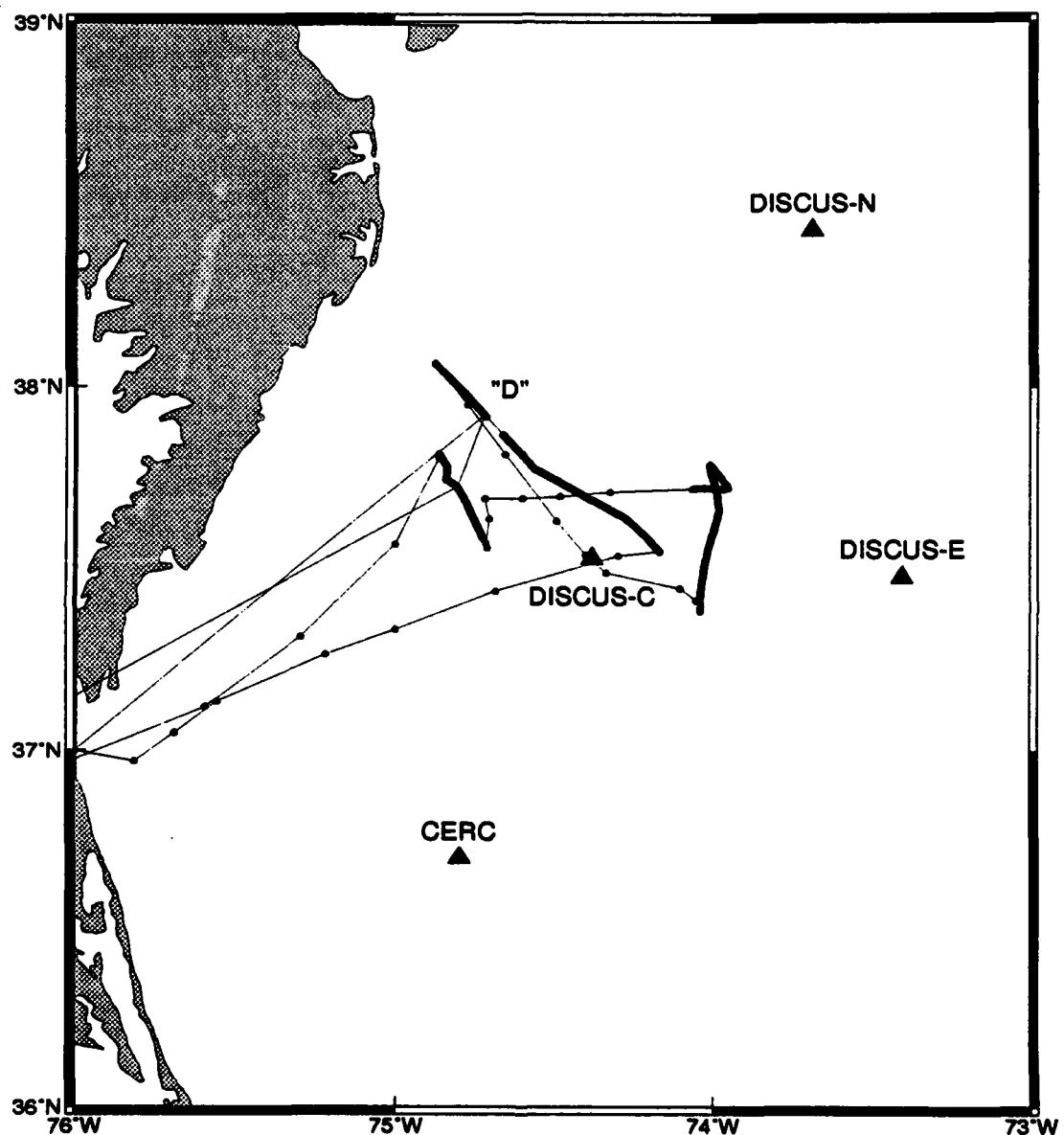


Figure 5: Ship track of *Creed* for 7 - 9 March 1991. Dots and heavy lines indicate locations where data from various sensors were collected as shown in Table 3. Note that site "D" specifies the location of sample directional wave spectrum shown in Figure 6

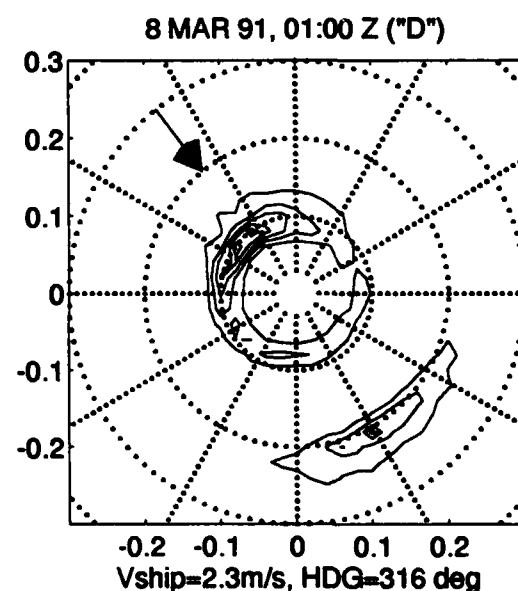
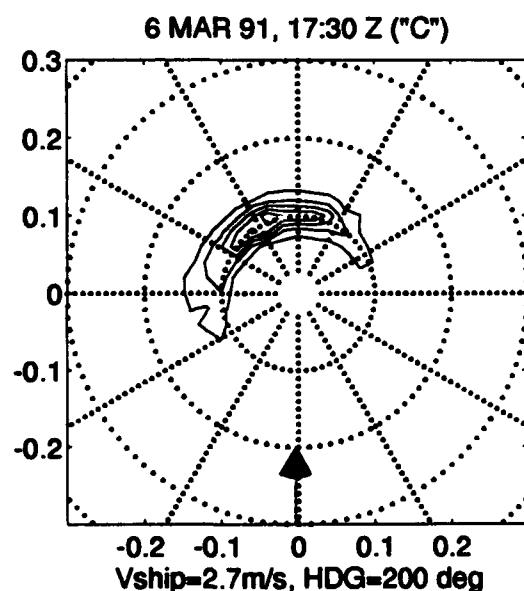
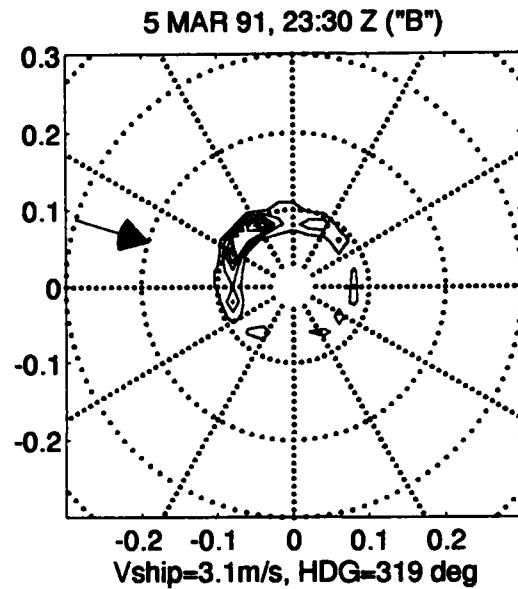
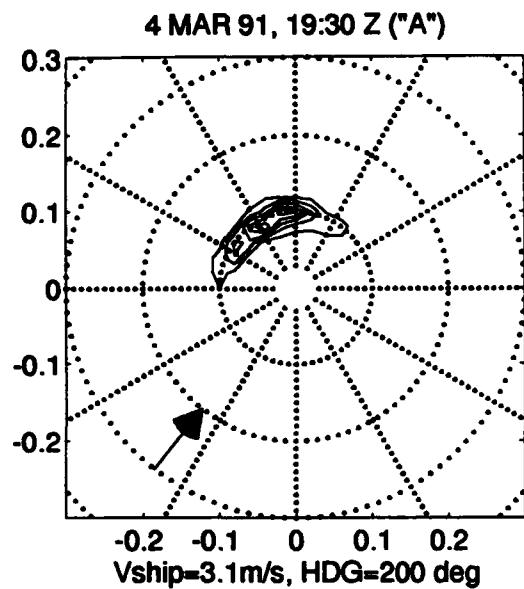


Figure 6: Directional wave spectra from SWATH ship measured at four sites. Specific locations of these spectra are marked in Figures 3 and 4

Table 4
RESSAC Radar System Characteristics

| System Component | Parameter | Value |
|-----------------------------|--|-----------------------------------|
| TRANSMITTER | | |
| | Type | FM/CW |
| | Frequency | 5.35 GHz (C-Band) |
| | Power | 32 mW or 3400 mW |
| RECEIVER | | |
| | Analysis bandwidth | 100 kHz (total range = 624 m) |
| | Resolution | 250 Hz (range resolution = 1.5 m) |
| | Dynamic range | 40 dB |
| ANTENNA | | |
| | Mean incidence angle | 14 deg |
| | Beam width in elevation | 13 deg |
| | Beam width in azimuth | 3.4 deg |
| | Polarization | HH |
| | Scanning geometry and rate | Conical at 1 rpm |
| SIGNAL MODULATION | | |
| | Upward linear frequency modulation | saw tooth |
| | Pulse duration | 5.71 ms |
| | Bandwidth | 137 MHz |
| | Pulse repetition period | 6.1 ms |
| REAL TIME PROCESSING | | |
| | FFT analyzer on 512 points | |
| | Averaging over 8, 16, or 32 samples | |
| | Recording on CCT, includes data from Inertial Navigation System of aircraft (i.e., roll, pitch, position, speed, heading, drift) | |

RESSAC measures the radar cross section of the surface at low incidence angles. High horizontal resolution is required in order to measure the modulation of the backscattered signal due to the tilt of the long waves (> 50 m in wavelength). A Fourier analysis of this modulation gives a spectrum of modulation that can be related to the slope spectrum of the waves in the look direction (Hauser *et al.* 1992). The scanning antenna allows the retrieval of the directional wave spectrum with a 180-deg ambiguity in direction.

Data processing provides directional wave spectra in terms of energy density as a function of direction and wave number of the surface waves. Generally, the directional spectra are available every 5 min, and represent an average of the data over these 5 min, which correspond roughly to 30 km along the flight track, assuming a nominal aircraft speed of 100 ms^{-1} . Each spectrum is specified by 30 wave numbers and 72 directions. Wave number bin size depends on the flight altitude. For a 6,000-m flight altitude, the spectra are

specified for 30 equally spaced wave numbers between 4.09×10^{-3} rad m $^{-1}$ and 0.1227 rad m $^{-1}$ at increments of $\Delta k = 4.09 \times 10^{-3}$ rad m $^{-1}$. The 72 directional bands cover 360 deg in azimuth at 5-deg intervals, but the ± 180 -deg ambiguity has not yet been removed. Accuracy in direction and wavelength depends on the wave number itself. For example, a 100-m wavelength is specified to within 15 deg in azimuth and 10 m in wavelength.

From the data, a parameter can also be calculated that is related to the mean square slope of the short waves (of the order of a few tens of centimeters), which in turn can be related to the local wind speed.

From the nine flights carried out between 27 February and 7 March, 1991, six flights on the following dates provided data of good quality: 27 February, 2, 4, 5, 6, and 7 March. However, the observations on 27 February consisted mainly of short waves of small amplitude, for which the radar was not sensitive enough to provide consistent wave spectra. Table 5 presents the times and positions of the directional wave spectra obtained from RESSAC for 2, 4, 5, 6, and 7 March. An example of the two-dimensional wave number spectrum obtained on 4 March 1991 by the RESSAC system is presented in Figure 7. A detailed analysis of this data set near the Gulf Stream is discussed in Hauser, Caudal, and Shay (1993) which shows that the RESSAC could also be used as a scatterometer to study small-scale variations in the wind field.

Scanning radar altimeter (SRA)

The NASA/Goddard Space Flight Center (GSFC) has a long history of measuring the directional wave spectrum using the Surface Contour Radar (SCR) (Walsh et al. 1985, 1989). SRA, which is a mode of the 36-GHz GSFC Multimode Airborne Radar Altimeter (Parsons and Walsh 1989), has replaced the SCR as the instrument of choice in the measurement of sea surface directional wave spectra. Both the SCR and SRA scan a narrow beam across the aircraft ground track, but the SRA has higher power and a wider swath. It measures the slant range to 64 points (versus 51 for the SCR) evenly spaced across the swath (at 8-m intervals for a 640-m altitude), converts them to surface elevations, and as the aircraft advances at a nominal speed of 100 ms $^{-1}$, displays the false-color coded topography on a monitor in real time. This grid of surface topography represents a snapshot of the wave field with along-track spacing of 12-13 m between points. The data over an along-track distance of 5-6 km and a cross-track swath of about 520 m are transformed into directional wave spectra by a two-dimensional Fast Fourier Transform (FFT).

The two-dimensional FFT of the wave topography produces an encounter spectrum in wave number space. This encounter spectrum must be Doppler corrected because of the finite time it takes the aircraft to acquire the data. The Doppler corrections and the transformation into the frequency domain are derived by assuming a linear dispersion relationship, and ignoring any effect of ocean current (Walsh et al. 1985). Doppler shifts in frequency (or wave number) by the ocean currents (maximum ~ 2 ms $^{-1}$) are at least of second-order in this correction compared to the speed of the aircraft (~ 100 ms $^{-1}$).

Figure 8 shows the flight tracks of the surface radar altimeter for 27 and 28 February,

Table 5
Positions and Times of RESSAC Directional Wave Spectra.

| Local Standard Time | | Mean Position | | Local Standard Time | | Mean Position | |
|---------------------|----------|---------------|--------|---------------------|----------|---------------|--------|
| Start Time | End Time | LAT | LONG | Start Time | End Time | LAT | LONG |
| 2 March 1991 | | | | | | | |
| 16:23:04 | 16:28:00 | 36.48 | -73.75 | 16:28:00 | 16:32:56 | 36.53 | -74.07 |
| 16:32:56 | 16:38:51 | 36.58 | -74.41 | 16:38:51 | 16:43:48 | 36.64 | -74.78 |
| 16:52:33 | 16:57:29 | 36.70 | -74.83 | 16:57:29 | 17:04:21 | 37.13 | -74.63 |
| 17:04:21 | 17:09:14 | 37.58 | -74.44 | | | | |
| 4 March 1991 | | | | | | | |
| 19:54:12 | 19:59:16 | 37.58 | -74.43 | 19:59:16 | 20:05:21 | 37.55 | -73.95 |
| 20:05:21 | 20:09:41 | 37.54 | -73.48 | 20:13:00 | 20:18:06 | 37.53 | -73.33 |
| 20:18:06 | 20:23:15 | 37.53 | -73.63 | 20:23:15 | 20:28:22 | 37.54 | -73.97 |
| 20:28:22 | 20:33:34 | 37.58 | -74.32 | | | | |
| 5 March 1991 | | | | | | | |
| 11:50:04 | 11:56:51 | 36.91 | -75.28 | 11:56:51 | 12:01:52 | 36.65 | -74.96 |
| 12:01:52 | 12:03:04 | 36.47 | -74.88 | 12:41:05 | 12:46:01 | 35.58 | -72.20 |
| 12:46:01 | 12:50:56 | 35.33 | -72.02 | 12:50:56 | 12:53:47 | 35.13 | -71.89 |
| 12:57:31 | 13:02:28 | 35.04 | -72.16 | 13:02:28 | 13:07:24 | 35.04 | -72.45 |
| 13:07:24 | 13:12:22 | 35.04 | -72.74 | 13:12:22 | 13:17:16 | 35.04 | -73.04 |
| 13:17:16 | 13:22:12 | 35.04 | -73.33 | 13:22:12 | 13:27:01 | 35.05 | -73.63 |
| 13:30:20 | 13:35:18 | 35.37 | -73.62 | 13:35:18 | 13:41:16 | 35.71 | -73.34 |
| 13:41:16 | 13:46:14 | 36.05 | -73.08 | 13:46:14 | 13:48:39 | 36.29 | -72.91 |
| 13:50:03 | 13:55:02 | 36.58 | -72.99 | 13:55:02 | 14:00:01 | 36.83 | -73.21 |
| 14:12:02 | 14:17:04 | 37.08 | -74.28 | 14:17:04 | 14:24:06 | 37.09 | -74.71 |
| 14:24:06 | 14:29:07 | 37.06 | -75.04 | | | | |
| 6 March 1991 | | | | | | | |
| 14:18:32 | 14:25:20 | 36.58 | -74.60 | 14:28:56 | 14:33:49 | 36.72 | -74.78 |
| 14:35:50 | 14:40:42 | 36.91 | -74.49 | 14:40:42 | 14:45:31 | 37.18 | -74.48 |
| 14:59:08 | 15:04:00 | 37.90 | -74.34 | 15:04:00 | 15:08:48 | 37.78 | -74.02 |
| 15:08:48 | 15:13:37 | 37.65 | -73.71 | 15:13:37 | 15:18:27 | 37.51 | -73.39 |
| 15:34:56 | 15:39:46 | 38.12 | -73.12 | 15:39:46 | 15:45:30 | 38.29 | -73.37 |
| 15:45:30 | 15:52:14 | 38.48 | -73.66 | | | | |
| 7 March 1991 | | | | | | | |
| 17:04:12 | 17:12:08 | 37.71 | -74.89 | 17:12:08 | 17:16:18 | 37.52 | -74.35 |
| 17:21:09 | 17:26:04 | 37.39 | -74.06 | 17:26:04 | 17:30:57 | 37.47 | -74.28 |
| 17:30:57 | 17:35:51 | 37.56 | -74.49 | 17:43:45 | 17:48:41 | 37.60 | -74.56 |
| 17:48:41 | 17:53:36 | 37.44 | -74.10 | 17:53:36 | 17:58:31 | 37.26 | -73.62 |
| 17:58:31 | 18:07:50 | 37.10 | -72.95 | 18:07:50 | 18:14:45 | 37.37 | -72.70 |
| 18:28:15 | 18:33:14 | 38.17 | -73.27 | 18:33:14 | 18:38:13 | 38.31 | -73.48 |
| 18:38:13 | 18:43:11 | 38.43 | -73.67 | 18:43:11 | 18:49:10 | 38.55 | -73.87 |
| 18:49:10 | 18:55:09 | 38.70 | -74.14 | 19:00:58 | 19:06:00 | 38.64 | -74.59 |
| 19:06:00 | 19:11:00 | 38.39 | -74.74 | 19:11:00 | 19:16:01 | 38.14 | -74.89 |

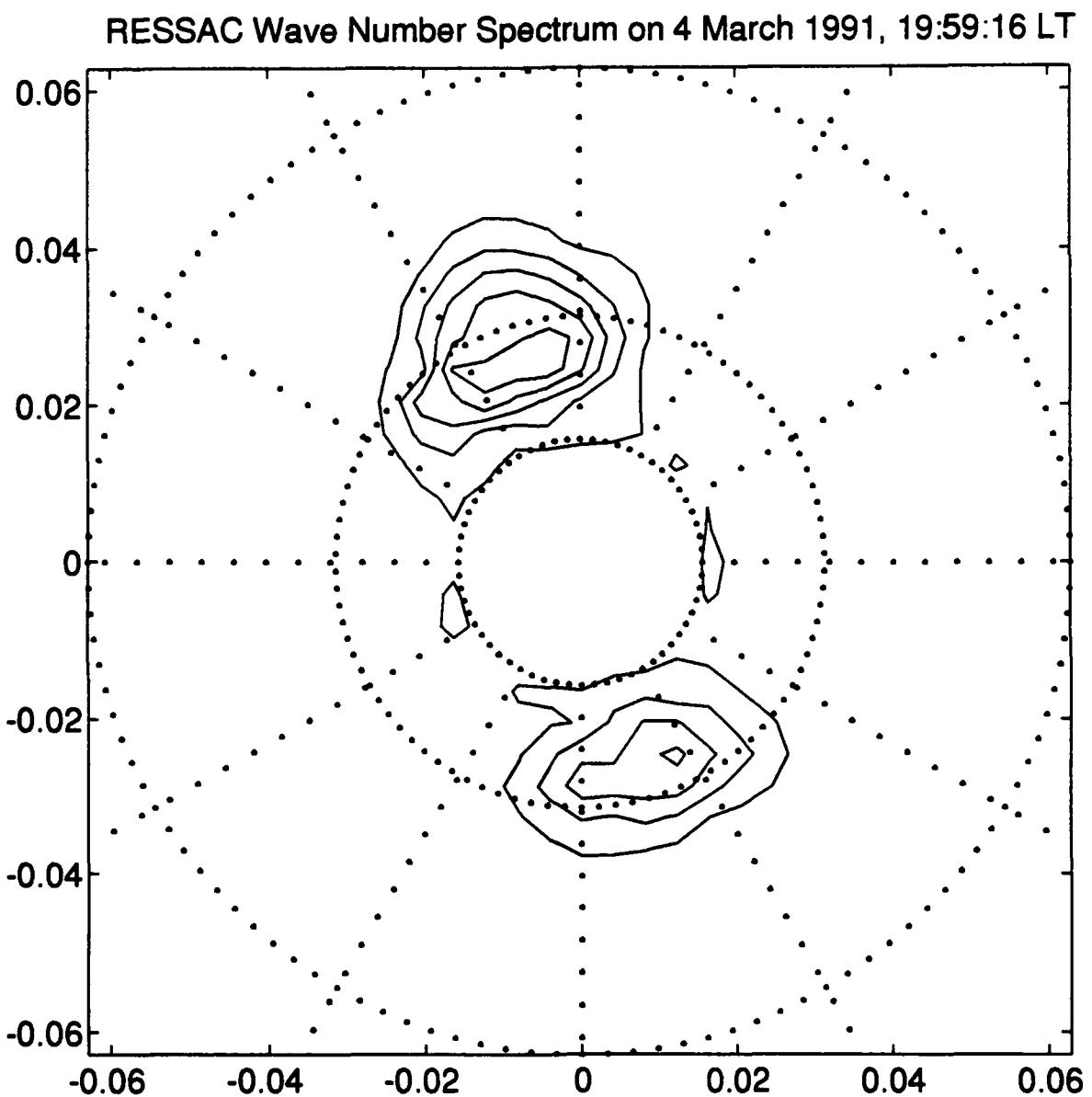


Figure 7: Wave number spectrum from RESSAC on 4 March 1991, 19:59:16 LT between buoys D-EAST and D-Central. Wavelength and direction at the spectral peak are 256 m and 335 deg, respectively. Associated wave height is 2.30 m. Circles correspond to wavelengths at 100, 200, and 400 m

and 1, 2, 4, 5 and 7 March 1991. The tracks also indicate the locations of directional wave measurements during these flights. Two examples of the directional wave number and corresponding frequency spectra are shown in Figure 9 from the flight on 5 March 1991.

Airborne expendable current profiler

During the IOP-3 in *SWADE* slow-fall Airborne eXpendable Current Profilers (AXCPs) and Airborne eXpendable BathyThermographs (AXBTs) were deployed during an SRA flight from the NASA NF-3A research aircraft on 5 March 1991. The AXCPs and AXBTs provided a high-resolution, three-dimensional snapshot of the ocean current and temperature structure in the vicinity of the Gulf Stream.

A total of 23 slow-fall AXCPs and 10 AXBTs were deployed at 30-km intervals in a star-like pattern skewed toward the warm side of the Gulf Stream (Figure 10). Of the 33 AXCPs and AXBTs deployed on this flight, oceanographic data were telemetered to the aircraft from 30 of the probes for a success rate of 90 percent (Table 6). Four of the AXCPs only provided data in the upper 70-90 m (instead of 250 m) and a few profiles contained noisy temperatures. The last AXCP was deployed within 2 km of the *Frederic G. Creed* and an ADCP current profile in the warm core ring located toward the northwest of the Gulf Stream. In Figure 11 the observed near-surface current vectors are displayed from the AXCP drops and ADCP on 5 March 1991. After removal of the depth-averaged flow from the ADCP profile, the comparison to the closest AXCP revealed correlations of 0.87 and 0.96 between the horizontal velocity components with *rms* errors of 2.3 and 2.7 cm s^{-1} (Shay 1993).

The AXCP is the airborne version of the XCP that senses the ocean's relative velocity by measuring the motion-induced voltage difference between two electrodes spaced 5 cm apart (Sanford et al. 1982). The XCP accurately samples the baroclinic current structure relative to an unknown, but depth-independent velocity with *rms* errors of 1-2 cm s^{-1} over 2- to 3-m depth intervals. Although the depth-independent component is not resolved by the AXCP, the barotropic flow is about 0.1-0.2 ms^{-1} in the Gulf Stream (Halkin and Rossby 1985) or at most 5-10 percent of the total baroclinic signal of 2 ms^{-1} . The AXCPs deployed in *SWADE* were modified to fall slowly at a rate of 2.2 ms^{-1} to resolve the upper ocean currents and temperatures (to 250 m), and the orbital velocities of the low-frequency surface wave components. A summary of the results from *SWADE* are described in Shay (1993).

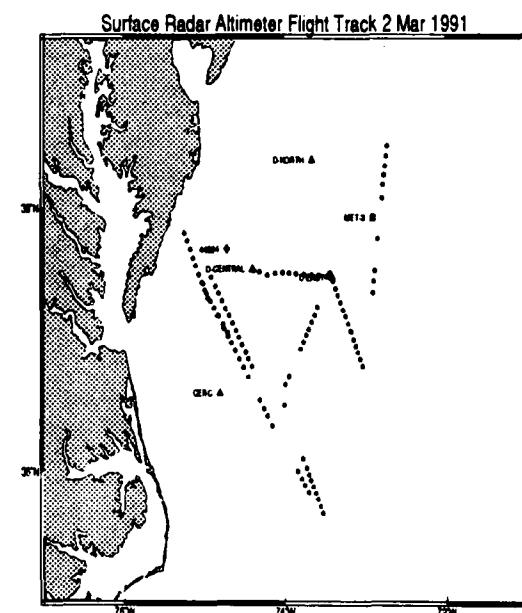
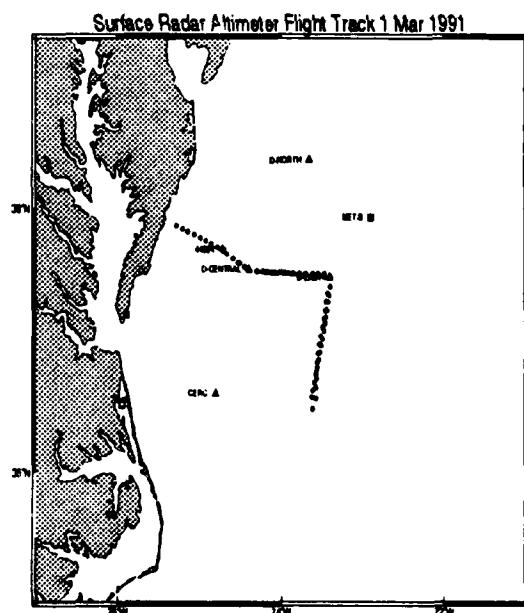
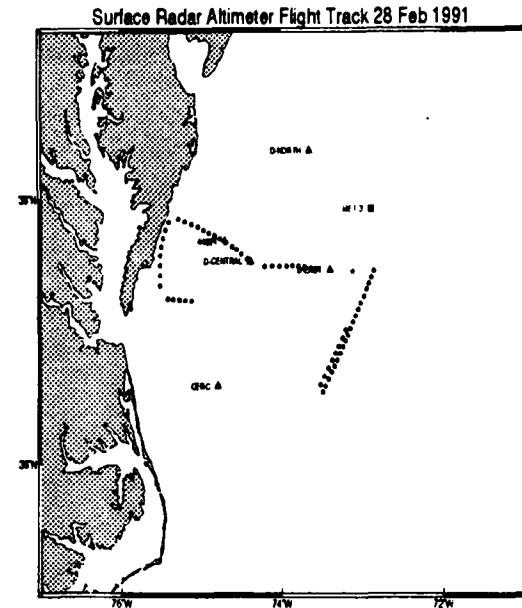
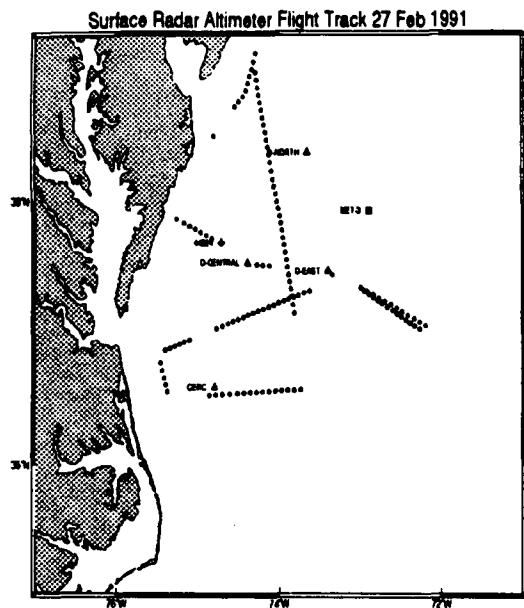


Figure 8: Flight tracks for the surface radar altimeter during IOP-3. Dots indicate locations where directional wave measurements were acquired (Continued)

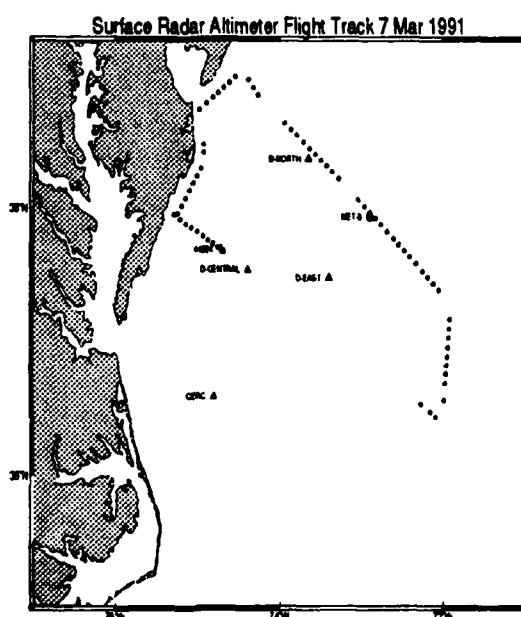
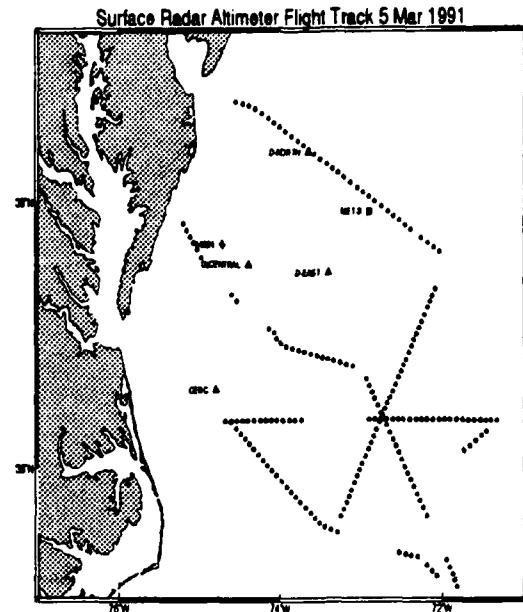
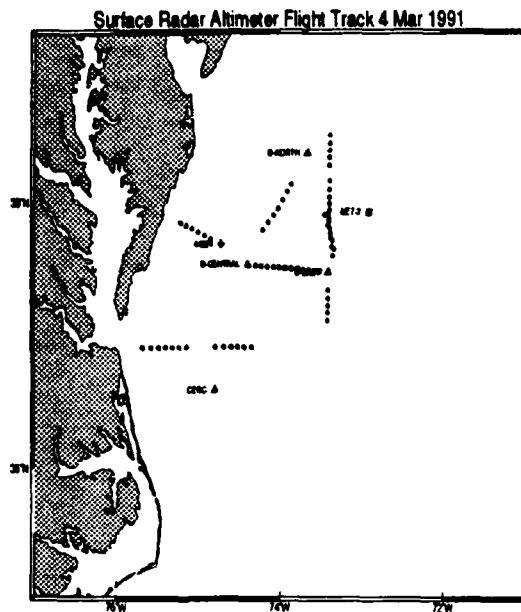


Figure 8: (Concluded)

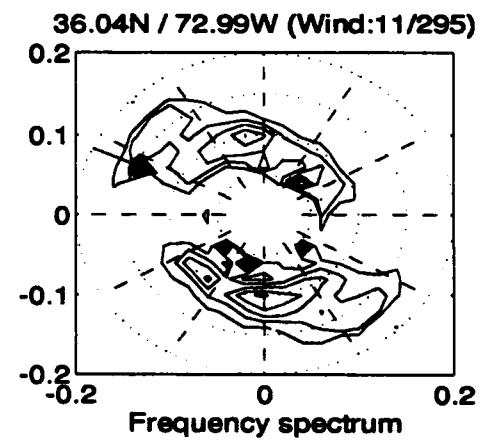
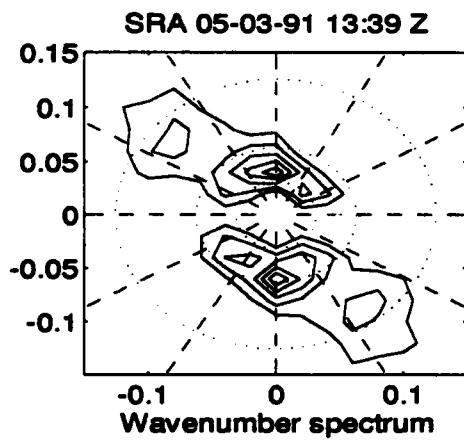
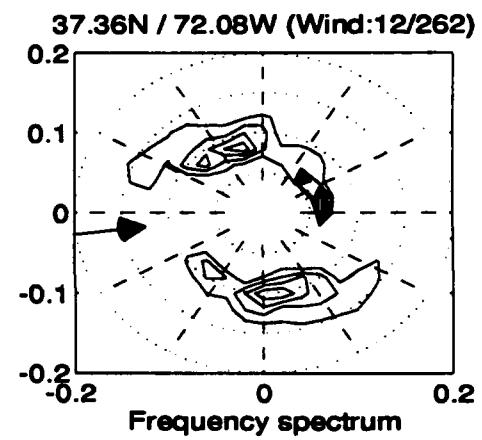
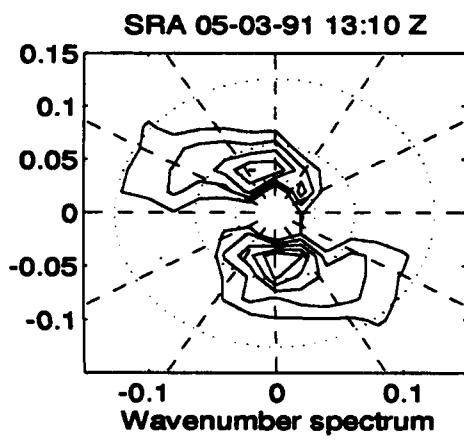
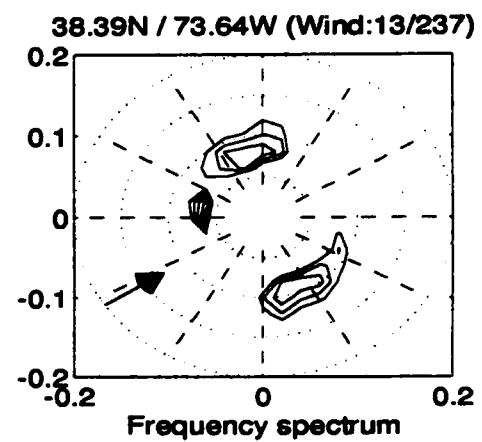
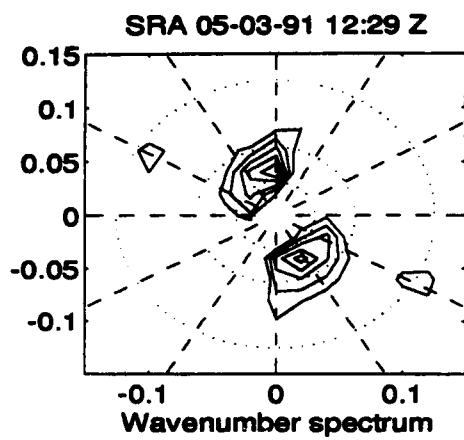


Figure 9: Directional wave number and frequency spectra from the surface radar altimeter on 5 March 1991. Circles in the wavenumber plots correspond to wavelengths at 50, 100 and 200 m

Table 6
Times and Positions of AXCPs (CP) and AXBTs (BT)
Deployed on 5 March 1991 from the NASA NP-3A

| Drop No. | Time UTC | LAT | LONG | Type | Comments |
|----------|----------|--------------|--------------|------|-------------------------|
| 01 | 1755 | 37° 34.70' N | 71° 53.60' W | CP | RF/AF Failures: No Data |
| 02 | 1813 | 37° 20.50' N | 72° 06.60' W | BT | |
| 03 | 1817 | 37° 05.30' N | 72° 17.00' W | CP | |
| 04 | 1824 | 36° 51.20' N | 72° 26.60' W | BT | |
| 05 | 1827 | 36° 37.40' N | 72° 36.20' W | CP | |
| 06 | 1837 | 36° 07.40' N | 72° 56.70' W | CP | 90 m |
| 07 | 1842 | 35° 53.10' N | 73° 06.80' W | CP | RF/AF Failures: No Data |
| 08 | 1847 | 35° 37.20' N | 73° 14.50' W | CP | Variable Rotation Rate |
| 09 | 1852 | 35° 24.30' N | 73° 24.20' W | CP | |
| 10 | 1859 | 35° 07.80' N | 73° 34.40' W | BT | |
| 11 | 2002 | 36° 21.80' N | 71° 25.30' W | CP | |
| 12 | 2007 | 36° 22.00' N | 71° 44.80' W | BT | |
| 13 | 2012 | 36° 22.40' N | 72° 05.20' W | CP | |
| 14 | 2017 | 36° 22.70' N | 72° 25.00' W | CP | |
| 15 | 2022 | 36° 22.70' N | 72° 44.80' W | CP | |
| 16 | 2027 | 36° 22.70' N | 73° 05.10' W | CP | |
| 17 | 2032 | 36° 22.50' N | 73° 25.10' W | CP | 75 m |
| 18 | 2037 | 36° 22.10' N | 73° 44.80' W | CP | |
| 19 | 2042 | 36° 21.70' N | 74° 05.20' W | BT | |
| 20 | 2047 | 36° 21.10' N | 74° 25.20' W | CP | |
| 21 | 2057 | 36° 22.20' N | 74° 42.70' W | BT | 85 m |
| 22 | 2120 | 35° 32.10' N | 73° 29.70' W | BT | |
| 23 | 2148 | 35° 07.40' N | 71° 54.90' W | BT | |
| 24 | 2153 | 35° 20.30' N | 72° 03.80' W | CP | |
| 25 | 2201 | 35° 34.80' N | 72° 14.10' W | BT | |
| 26 | 2204 | 35° 49.80' N | 72° 24.90' W | CP | T(z) Noisy |
| 27 | 2209 | 36° 04.10' N | 72° 35.30' W | CP | |
| 28 | 2219 | 36° 31.90' N | 72° 55.70' W | CP | |
| 29 | 2224 | 36° 44.40' N | 73° 07.50' W | CP | T(z) Noisy |
| 30 | 2230 | 36° 48.90' N | 73° 33.20' W | CP | T(z) Noisy |
| 31 | 2235 | 36° 52.60' N | 73° 53.00' W | CP | |
| 32 | 2241 | 36° 57.30' N | 74° 06.90' W | CP | |
| 33 | 2244 | 37° 07.20' N | 74° 23.80' W | BT | RF/AF Failures: No Data |

AXCP and AXBT DEPLOYMENTS

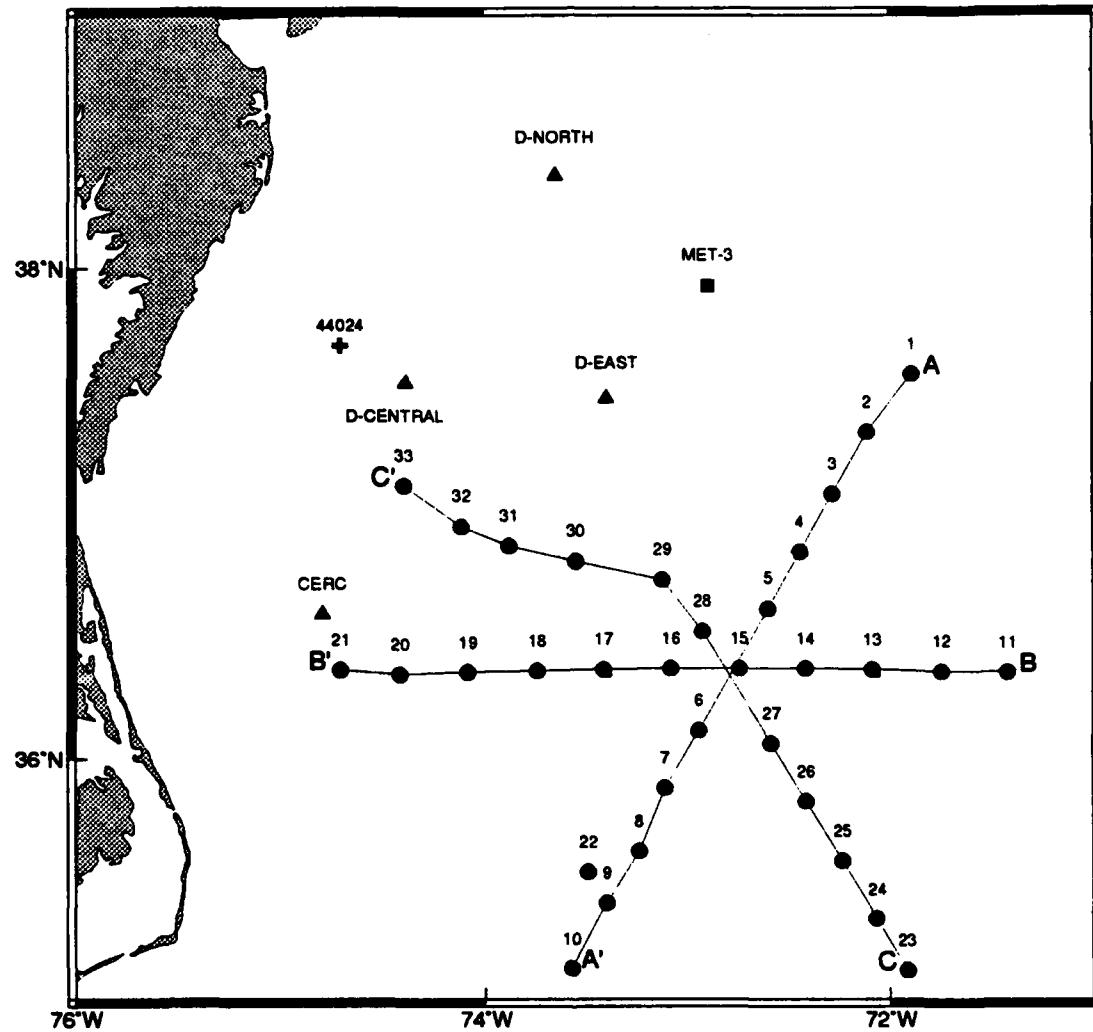


Figure 10: AXCP and AXBT deployments in a star-like pattern along three flight tracks of the NASA NP-3A at 30-km intervals along transects A-A', B-B' and C-C'

AXCP and ADCP Surface Currents on March 5, 1991

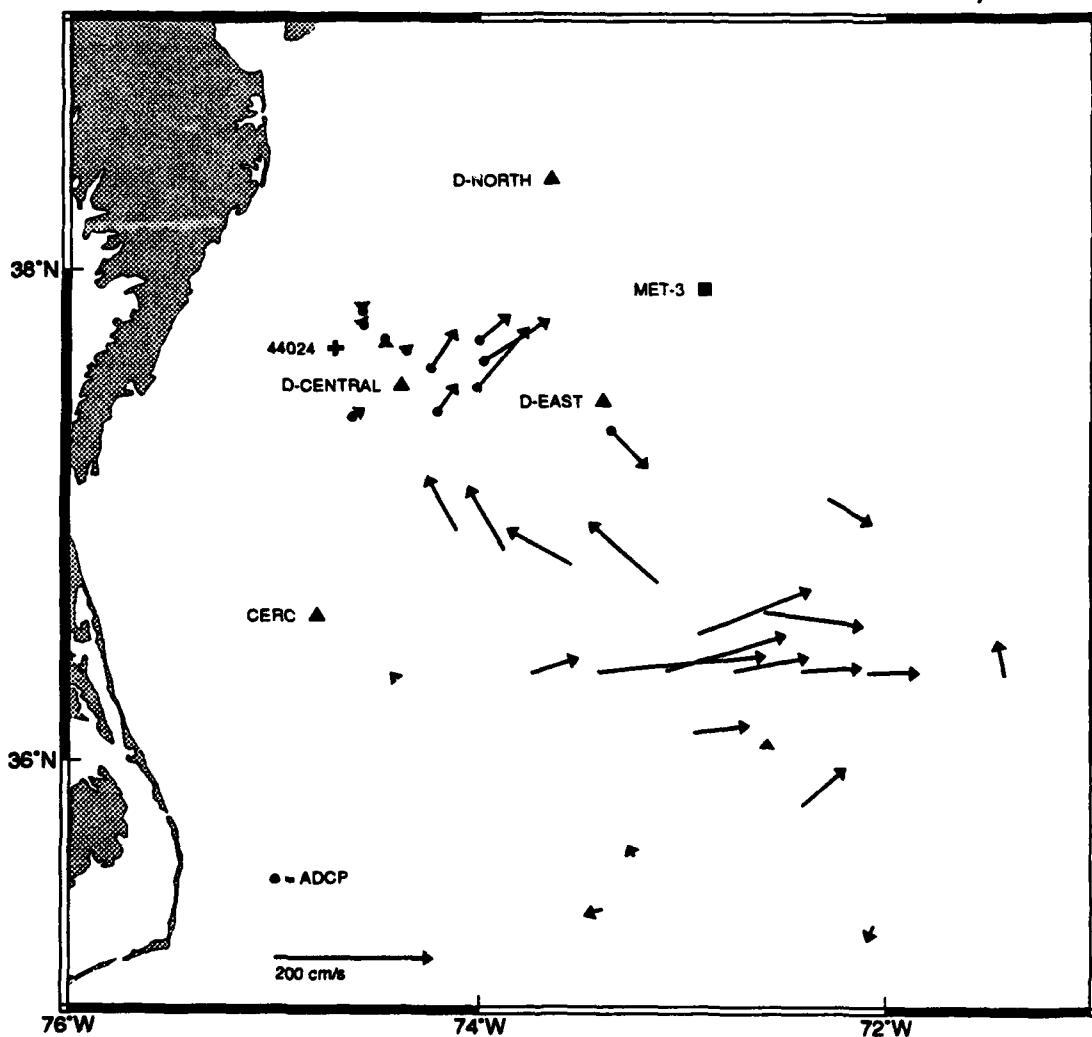


Figure 11: Current vectors from the AXCPs and ADCP deployed along all sections on 5 March 1991 (cf. Figure 8). Current vectors originating in a dot near Discus "Central" were obtained from the near-surface bin of the ADCP during the SWATH ship cruises (courtesy of Charles N. Flagg, Brookhaven National Laboratory, Upton, NY.)

Infrared imagery

Daily images of "sea surface temperature" were collected from the Advanced Very-High Resolution Radiometer (AVHRR) on board the National Oceanic and Atmospheric Administration (NOAA) satellites NOAA-10, -11, and -12. The full-resolution images (1024 × 1024 pixels) cover the U.S. east coast from about latitude 23°N to 48°N and longitude 52°W to 82°W on a Mercator projection with center latitude and longitude of 36.5°N and 67.0°W. Spatial and temperature resolution of the images are approximately 1 km and 0.125 °C, respectively, from pixel to pixel (Cornillon et al. 1988). There are several passes (ascending and descending) primarily from NOAA-10 per day over the SWADE experimental area. Some passes cover the area of interest only partially within the illuminated satellite field of view. For SWADE the optimal daily coverage typically occurred in the early morning and late afternoon hours.

Appendix E shows selected color images of sea surface temperature on mostly cloud-free days over the SWADE domain. The images are extracted from the full-resolution images and cover the SWADE domain from about latitude 32°N to 43°N and longitude 66°W to 80°W.

3 Ocean Wave Modelling and Grid Domains

Numerical modelling plays a complementary role in achieving the goals of *SWADE*. A particular objective is to examine the usefulness of a wave model as an analysis tool and a general objective is to validate wave models with the high quality wave data sets from *SWADE*. Furthermore, a comparison of measured and modelled source physics and the effect of incorporating wave-current interaction will provide additional evidence for refinement of numerical models.

The principal ocean wave prediction model used for these simulations is the third-generation WAM model (The WAMDI-Group 1988), which computes the directional wave spectrum by integration of the energy transport equation without prior specification of the spectral shape. There are 25 frequency bands from 0.0418 to 0.4114 Hz in logarithmic equally spaced increments and 24 directional bins at 15-deg intervals. Wind fields are internally interpolated onto the model grids and initially converted to friction velocities using the wind-speed-dependent drag coefficient described in Wu (1982). Growth and dissipation terms are computed based on a simple coupling of the air-sea dynamics following the wind-wave generation theory of Janssen (1989, 1991). The resulting growth rate depends on both the friction velocity and the roughness length produced by the waves themselves.

Several forecast (Jensen, Gruber, and Caruso 1991) and hindcast (Gruber, Caruso, and Jensen 1991) studies for the *SWADE* IOPs have been carried out with WAM *Cycles 2, 3, 3.5*, and most recently *4* (Günther, Hasselmann, and Janssen 1991), where the later versions include options for nested grids to specify proper boundary conditions as would arise in situations when swell is propagating into the model domain, and for time and spatially varying currents to study wave-current interactions. More detailed studies are presently under way by the *SWADE* modelling team to investigate (1) sources of errors attributed to wind field specification; (2) differences in source term physics and grid nesting; and (3) the inclusion of depth-dependent wave physics and the influence of wave-current interaction. Model output fields include maps of significant wave height, mean wave period, mean wave direction, swell wave height, swell period and swell direction. In addition, two-dimensional wave spectra are produced at selected output points near buoy stations within the *SWADE* experimental area.

A hierarchy of model grids was designed for *SWADE* to examine the wave physics at different spatial and temporal scales, and the usefulness of a nested system. Each grid fulfills a specific function and provides results that can be used to accomplish the goals of the experiment. Pictorials of the grids are shown in Caruso et al. (1993). The WAM model has been implemented in spherical coordinates on three grids described previously (Weller et al. 1991).

Atlantic Basin Model

The basin scale grid covers the entire North and South Atlantic Oceans and extends from latitude 63°S to 72°N and from longitude 100°W to 34°E in 1-deg increments. The primary purpose of this grid is to accurately simulate northward-propagating swell originating in the

southern ocean and provide boundary conditions for the regional scale model. Also, wave height maps provide some overview of storm activities in both Atlantic basins. Output results will show the quality of the synoptic scale forecast and provide some indication of subscale variability.

Western North Atlantic Model

This medium-resolution grid covers the Western North Atlantic from latitude 24°N to 48°N and from longitude 82°W to 52°W in 0.25-deg increments. The purpose of this model grid is to provide high quality wind and wave analyses for evaluation of SWADE scientific objectives and for assessing sources and magnitudes of errors in the wind field specification.

SWADE Model

This high-resolution grid was designed to simulate the small scale wave physics and to improve and verify the source term physics. The grid extends from latitude 35°N to 42°N and from land to longitude 70°W in 0.083-deg increments. The measured meteorology and various interpolation and assimilation schemes will be used to provide winds for these simulations.

4 Wind Fields

Six different wind field representations are available for this particular time period. Some preliminary results using a subset of these wind fields have been briefly discussed in Graber, Caruso, and Jensen (1991), and they indicate considerable differences in the representations of the atmospheric conditions. The set of wind fields includes analyses from operational numerical weather prediction models such as Fleet Numerical Oceanography Center (FNOC), European Centre for Medium-Range Weather Forecasts (ECMWF), and United Kingdom Meteorological Office (UKMO), objectively interpolated model results from National Meteorological Center (NMC) and NASA/GSFC and a manual kinematic analysis from Ocean-weather/Atmospheric Environment Service (OW/AES). A brief description of each of the wind fields is given below.

Appendix D includes two maps per day of wind vectors and the corresponding contours of significant wave height for the six wind field simulations on the regional grid for the entire IOP-3. The time period begins on 25 February 1991, 12:00 GMT and ends on 9 March 1991, 00:00 GMT.

FNOC

The FNOC has provided analyzed and forecast wind stress and 19.5-m neutrally stable wind fields derived from the Navy Operational Global Atmospheric Prediction System (NOGAPS) spectral forecast model (Hogan and Rosmond 1991). The predicted winds are computed with the (T80) model system, which uses 80 Fourier coefficients and 18 vertical layers from the surface to a pressure level at 10 mb. The fields are spectrally interpolated in the horizontal to 1.5 deg. The NOGAPS uses a planetary boundary-layer (PBL) model similar to that of the ECMWF (Louis, Tiedtke, and Geleyn 1982), but with a major modification for the computation of surface fluxes when the PBL is conditionally unstable. The 19.5-m neutrally stable winds are directly computed from the wind stress fields at each local grid point taking into account atmospheric stability effects. A final, linear interpolation is done onto a spherical grid with a spatial resolution of 1.25° in latitude and longitude. The time interval of wind and wind stress fields is every 6 hr starting at 00:00.

ECMWF

Analyzed 10-m wind fields from the ECMWF generated by their operational atmospheric general circulation model are available for the entire SWADE period. These analyzed winds are from the ECMWF/TOGA (Tropical Ocean-Global Atmosphere) advanced operational analysis surface and diagnostic fields data set. Geometrical coverage is specified on a (N80) Gaussian grid with a spatial resolution of 1.125° in latitude and longitude. The time interval of wind fields is every 6 hr beginning at 00:00. Analyzed surface pressure fields and surface temperature fields are also available with the same spatial and temporal resolution.

NMC/GSFC

Two additional wind field products are available from the NMC and NASA/GSFC. Both wind fields were derived from the first-guess fields of NMC's coarse ($2.5^\circ \times 2.5^\circ$) large-scale analysis. In each case the observed data are reinserted into a high-resolution grid where grid points with data remain unaltered, whereas non-data points are computed using a "conditional" relaxation procedure.

The NMC model winds are generated with an *objective interpolation* scheme, which corrects the nearest grid point according to the data value and relaxes all non-data points. The method includes a check on gross errors. The fidelity of the wind field is determined by withholding one piece of ship data at a time. This is repeated about 10 times. The resulting wind fields are regredded covering the regional model domain with a resolution of 0.3° in latitude and 0.5° in longitude. The time interval between wind fields is 6 hr.

The GSFC model winds are determined with the *successive correction method*, which uses seven sweeps over the model domain and successively reduces the area of influence in each pass from 500 km to 120 km. Consistency checks and error minimization are only performed at buoy locations. No additional quality checks are made by withholding individual buoy measurements. The final output is a spatially high-resolution wind field on a 0.25- by 0.25-deg grid. The time interval between successive wind fields is every 3 hr.

Both methods make a final check of the wind fields for consistency and the goodness of these winds is evaluated with root mean square error statistics.

OW/AES

High-resolution wind fields were developed by OW/AES over a limited domain, coinciding approximately with the fine-mesh *SWADE* grid. These wind fields were produced with a manual kinematic analysis, originally described in Cardone et al. (1980), from pressure fields, air and sea surface temperature fields, ship and buoy data. All data are carefully screened for inconsistencies and measured winds are adjusted in height and corrected with a stability-dependent surface layer model to effective neutral 20-m-height hourly averages. Hourly averages of wind speed and direction are computed from three consecutive hourly buoy observations with weights of 0.25, 0.5, and 0.25, respectively. Detailed hand analyses of the pressure and temperature fields carefully preserves temporal and spatial continuity of low pressure centers and frontal boundaries. Outside of the limited domain, the effective neutral winds are calculated with the marine boundary layer model of Cardone (1969). Time histories of measured and modelled and standard statistical measures of difference are used to evaluate the quality of the final wind fields.

The resulting high-resolution winds are gridded onto a 0.5- by 0.5-deg grid over the regional model domain and are available hourly to simulate accurately the temporal evolution of the storm centers and frontal systems passing over the *SWADE* domain.

UKMO

These wind fields are computed from the coarse-mesh, 11-layer general atmospheric circulation model in operational use at the UKMO (Bell and Dickinson 1986). Global coverage is implemented on a mesh with grid lengths of 1.5° in latitude and 1.875° in longitude. A 6-hr data assimilation cycle is employed, and physical and subgrid-scale processes are also included in the model (Gilchrist and White 1982). Analyzed winds at the 19.5-m height are available every 2 hr beginning at 00:00.

Winds from the limited-area fine-mesh model are also available at hourly intervals. While the resolution of the fine-mesh model is twice that of the coarse mesh model (*i.e.*, $\Delta\phi = 0.75\text{-deg}$ and $\Delta\lambda = 0.9375\text{-deg}$), its North Atlantic coverage extends only as far south as 30° N, which is not sufficient for the Western North Atlantic regional model grid domain.

5 Surface Currents

Analyzed surface current fields obtained from Fleet Numerical Oceanography Center (FNOC) were generated from their regional-scale circulation model DART (Data Assimilation Research and Transition), which uses two active layers for the Gulf Stream region. DART is initialized from the dynamic height field derived from daily Gulf Stream temperature (AVHRR infrared imagery) and salinity products. The currents are given in terms of the U and V components [cm s^{-1}]. Geometrical coverage is specified on a spherical grid domain with a spatial resolution of 0.20° in latitude and longitude and is limited to the Western North Atlantic and the Gulf Stream regions. Physical dimensions of the grid are from latitude 26.2°N to 46.0°N and from longitude 50.0°W to 79.8°W . The time interval of the surface current fields is every 6 hr beginning at 00:00.

Daily maps of the surface currents within the fine-mesh SWADE model grid for IOP-3 are shown in Appendix C from 25 February 1991, 00:00 GMT to 9 March 1991, 00:00 GMT.

6 Summary

This report provides a summary of wind, wave, current, and meteorological measurements during the third intensive observation period (IOP-3) of the *SWADE*. The time series of wind, wave, and meteorological parameters provide a guide to the availability of the numerous observations during IOP-3 and a first look at the temporal and spatial variability of Gulf Stream and eddy dynamics impinging on the *SWADE* array and the passage of two cold air outbreaks. Hindcast results from the third-generation ocean wave model (WAM) with six different wind fields are intended to show the diverse representation of the steady southwesterly flow and the frontal passages as well as a description of the larger scale meteorological and sea state conditions during IOP-3.

Two complementary reports describe general observations on the meteorological and oceanographic conditions for IOP-1 (Caruso et al. 1993) and IOP-2 (Caruso et al. (in preparation)).

References

Anctil, F., M.A. Donelan, W.M. Drennan and H.C. Graber, 1993: Eddy correlation measurements of air-sea fluxes from a discus buoy. *J. Atmos. Ocean. Technol.*, (In press).

Bell, R.S. and A. Dickinson, 1986: The Meteorological Office operational numerical weather prediction system. *Sci. Pap., Meteorol. Off.* No. 41, Her Majesty's Stationery Office, London, 61pp.

Cardone, V.J., 1969: Specification of the wind distribution in the marine boundary layer for wave forecasting. Report TR-69-01, Geophys. Sciences Lab., New York University, 137pp.

Cardone, V.J., A.J. Broccoli, C.V. Greenwood and J.A. Greenwood, 1980: Error characteristics of extratropical storm wind fields specified from historical data. *J. Petrol. Tech.*, **32**, 873-880.

Caruso, M.J., H.C. Graber, R.E. Jensen, and M.A. Donelan, 1993: Observations and modelling of winds and waves during the surface wave dynamics experiment. Intensive Observation Period IOP-1: 20 - 31 October 1990. Tech. Rep. CERC-93-6, US Army Engineer Waterways Experiment Station, Vicksburg, MS, 203pp.

Caruso, M.J., H.C. Graber, R.E. Jensen, and M.A. Donelan, (in preparation): Observations and modelling of winds and waves during the surface wave dynamics experiment. Intensive Observation Period IOP-2: 14 - 25 January 1991.

Cornillon, P., D. Evans, O.B. Brown, R. Evans, P. Eden and J. Brown, 1988: Processing, compression and transmission of satellite IR data for near-real-time use at sea. *J. Atmos. Ocean. Technol.*, **5**, 320-327.

Donelan, M.A., W.M. Drennan, N. Madsen, K.B. Katsaros, E.A. Terray and C.N. Flagg, 1992: Directional wave spectra from the Swath ship in SWADE. NWRI report 92-11, National Water Research Institute, Burlington, Ont., Canada, 51pp.

Drennan, W.M., M.A. Donelan, N. Madsen, K.B. Katsaros, E.A. Terray and C.N. Flagg, 1994: Directional wave spectra from a Swath ship at sea. *J. Atmos. Ocean. Technol.*. (In press).

Drennan, W.M., H.C. Graber and M.A. Donelan, (in preparation): On the measurement of directional wave spectra from pitch-roll and acceleration buoys.

Gilchrist, A. and P.W. White, 1982: The development of the Meteorological Office new operational forecasting system. *Meteorol. Mag.*, **111**, 161-179.

Graber, H.C., M.J. Caruso and R.E. Jensen, 1991: Surface wave simulations during the October storm in SWADE. *Proc. MTS '91 Conf.*, Marine Technology Society, New Orleans, LA, 159-164

Günther, H., S. Hasselmann and P.A.E.M. Janssen, 1991: Wamodel Cycle 4. Tech. Rept. 4, Deutsches Klimarechenzentrum, Hamburg, 91pp.

Halkin, D., and T. Rossby, 1985: The structure and transport of the Gulf Stream at 73°W. *J. Phys. Oceanogr.*, **15**, 1439-1452.

Hauser, D., G. Caudal, G.J. Rijckenberg, D. Vidal-Madjar, G. Laurent, and P. Lancelin, 1992: RESSAC: A new airborne FM/CW radar ocean wave spectrometer. *IEEE Trans. Geosci. Remote Sensing*, **30**(5), 981-995.

Hauser, D., Caudal G., and L.K. Shay, 1993: Behaviour of the ocean radar cross-section at low incidence, observed in the vicinity of the Gulf Stream. Submitted to *IEEE Trans. on Geosci. Remote Sensing*.

Hogan, T.F. and T.E. Rosmond, 1991: The description of Navy operational global atmospheric prediction system's spectral forecast model. *Mon. Wea. Rev.*, **119**, 1786-1815.

Howard, K.M., 1993: Characteristics and evolution of the marine boundary layer during the Surface Wave Dynamics Experiment. M.Sc. thesis, Dept. of Atmospheric Science, University of Washington, Seattle.

Janssen, P.A.E.M., 1989: On the interaction of wind and waves. *Phil. Trans. R. Soc. Lond.*, **A 329**, 289-301.

_____, 1991: Quasi-linear theory for wind-wave generation applied to wave forecasting. *J. Phys. Oceanogr.*, **21**, 1631-1642.

Jensen, R.E., Graber, H.C., and M.J. Caruso, 1991: A Wind-Wave Forecast for the Surface Wave Dynamics Experiment. *Proc. MTS '91 Conf.*, Marine Technology Society, New Orleans, LA, 147-153.

Katsaros, K.B., M.A. Donelan and W.M. Drennan, 1993: Flux measurements from a Swath ship in SWADE. *J. Mar. Sys.* **4**, 117-132.

Louis, J.F., M. Tiedtke and J.F. Geleyn, 1982: A short history of the operational PBL parameterization at ECMWF. *Workshop on Planetary Boundary Layer Parametrization*, ECMWF, Reading, Shinfield Park, England, 59-79.

Oberholtzer, D. and M.A. Donelan, 1993: SWADE data guide. NASA Report, (In preparation).

Parsons, C., and E. J. Walsh, 1989: Off-nadir radar altimetry. *IEEE Trans. Geosci. Remote Sens.*, **27**, 215-224.

Sanford, T.B., R.G. Drever, J.H. Dunlap, and E.A. D'Asaro, 1982: Design, operation and performance of an expendable temperature and velocity profiler (XTVP). Report **APL-UW 8110**, Applied Physics Lab., University of Washington, 83pp.

Shay, L.K., 1993: Airborne expendable current profiling in the Surface Wave Dynamics experiment. *RSMAS Technical Report 93-001*, Rosenstiel School of Marine and Atmospheric Science, University of Miami, 46pp.

Steele, K.E., C.-C. Teng and D.W.C. Wang, 1992: Wave direction measurements using pitch-roll buoys. *Ocean Engng.*, **19** (4), 349-375.

Walsh, E.J., D.W. Hancock III, D.E. Hines, R.N. Swift, and J.F. Scott, 1985: Directional wave spectra measured with the surface contour radar. *J. Phys. Oceanogr.*, **15**, 566-592.

Walsh, E.J., D.W. Hancock III, D.E. Hines, R.N. Swift, and J.F. Scott, 1989: An observation of the directional wave spectrum evolution from shoreline to fully developed sea. *J. Phys. Oceanogr.*, **19**, 670-690.

The WAMDI-Group, 1988: The WAM model - a third generation ocean wave prediction model. *J. Phys. Oceanogr.*, **18**, 1775-1810.

Weller, R.A., M.A. Donelan, M.G. Briscoe and N.E. Huang, 1991: Riding the crest: A tale of two wave experiments. *Bull. Amer. Met. Soc.*, **72**, No. 2, 163-183.

Wu, J., 1982: Wind-stress coefficients over sea surface from breeze to hurricane. *J. Geophys. Res.*, **87**, 9704-9706.

Appendix A: Time Series from SWADE and NDBC Buoys

Time series plots of the observed data are presented in this appendix in the following sequence:

1. Directional Wave Buoys

- Discus Buoy "North" (44001)
- Discus Buoy "East" (44015)
- Discus Buoy "Central" (44023)
- Discus Buoy "CERC" (44014)

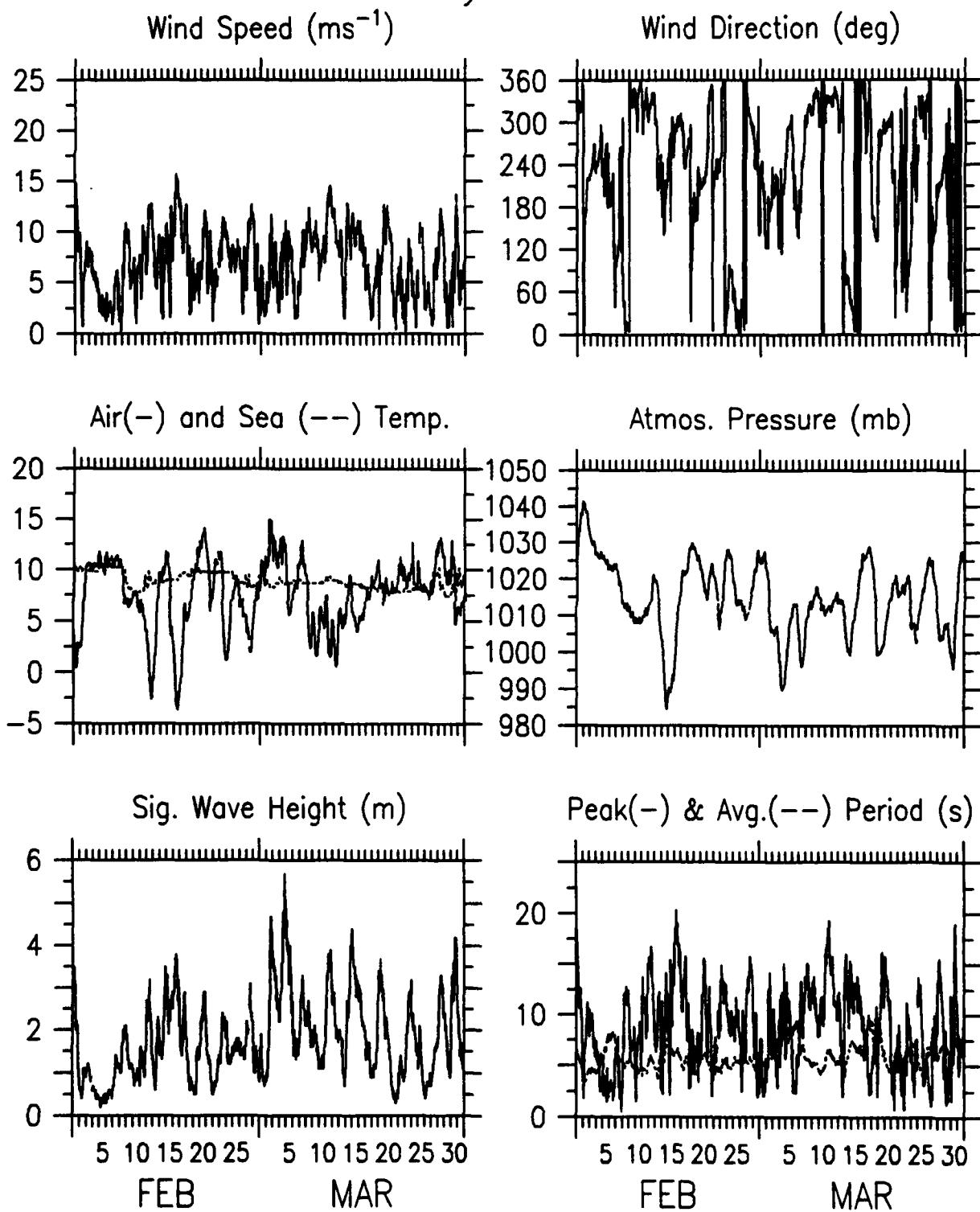
2. Non-directional Buoys and C-MAN Stations

- Buoy 41001
- Buoy 44004
- Buoy 44008
- Buoy 44009
- Buoy 44011
- Buoy 44012
- C-MAN Station DSLN7
- C-MAN Station CHLV2
- C-MAN Station BUZM3

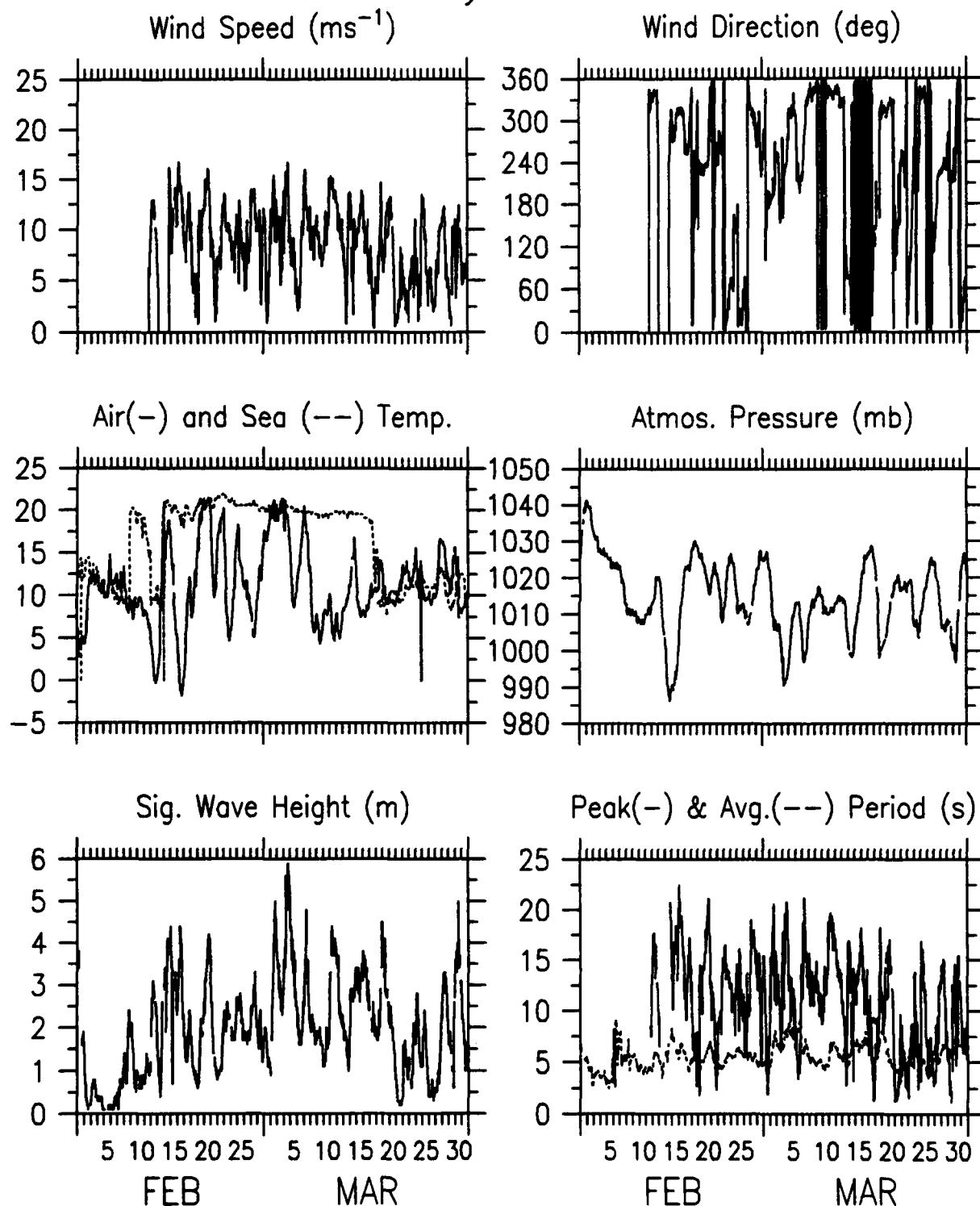
3. MiniMet Buoys

- Station MET-1
- Station MET-3

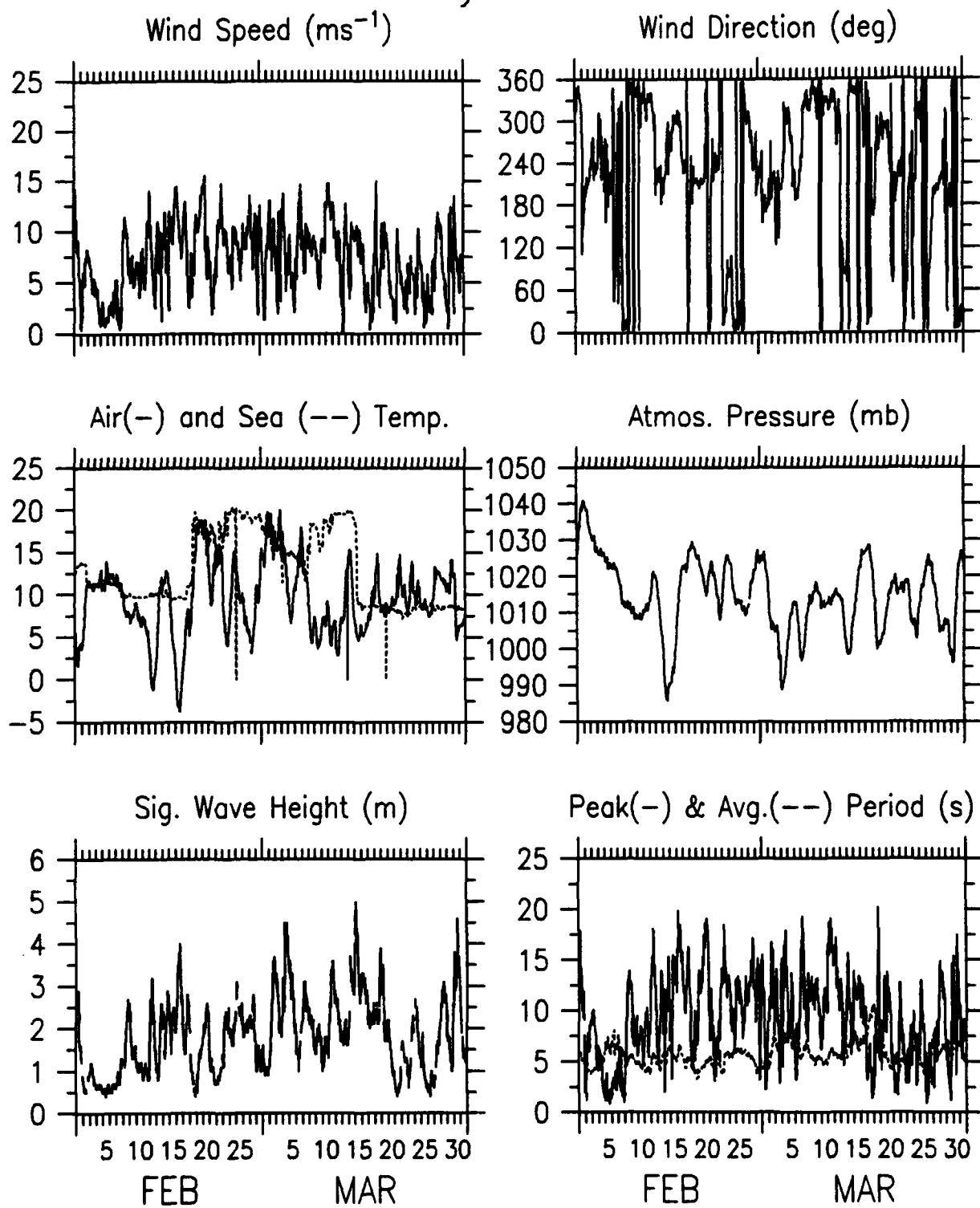
Buoy 44001



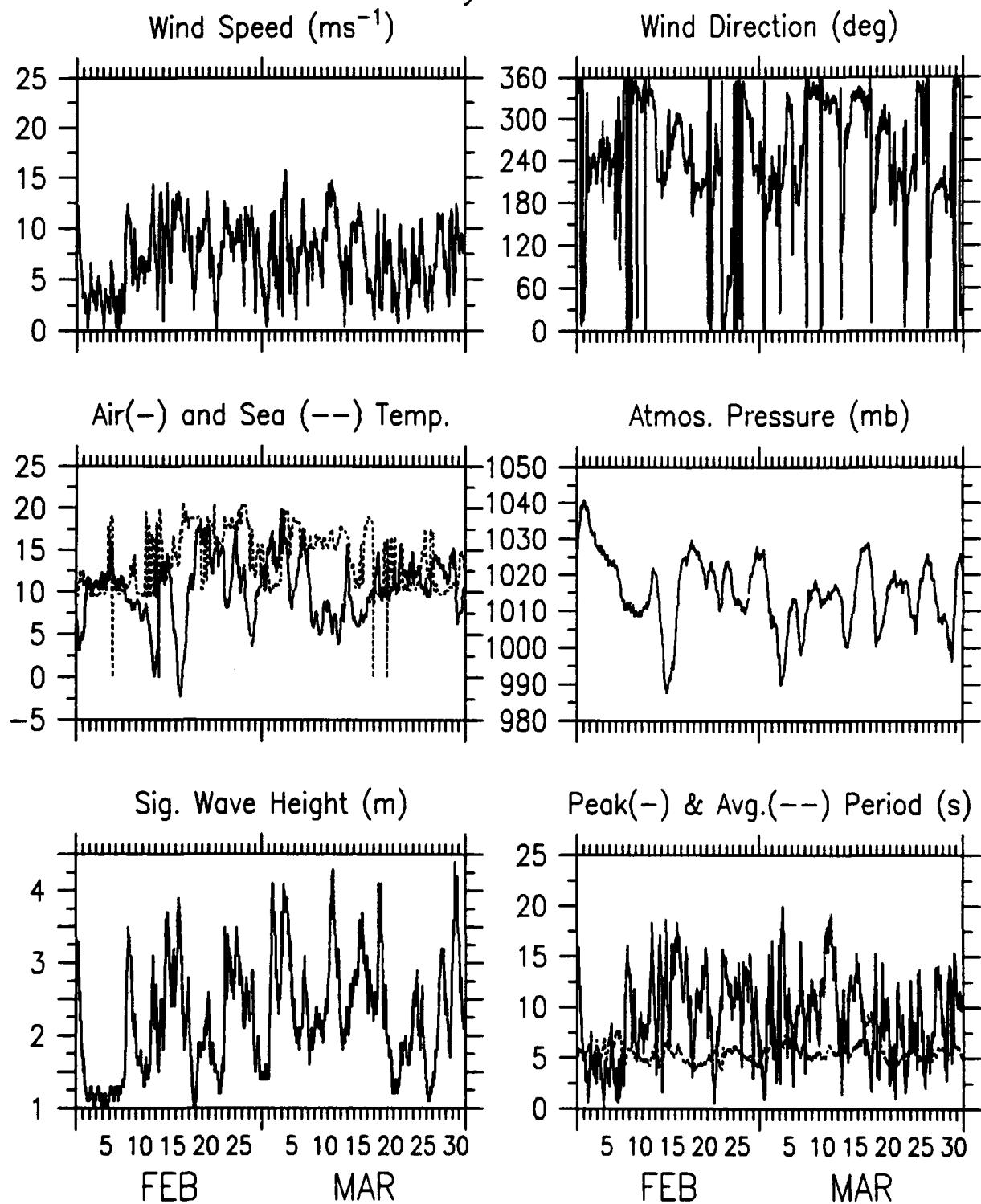
Buoy 44015



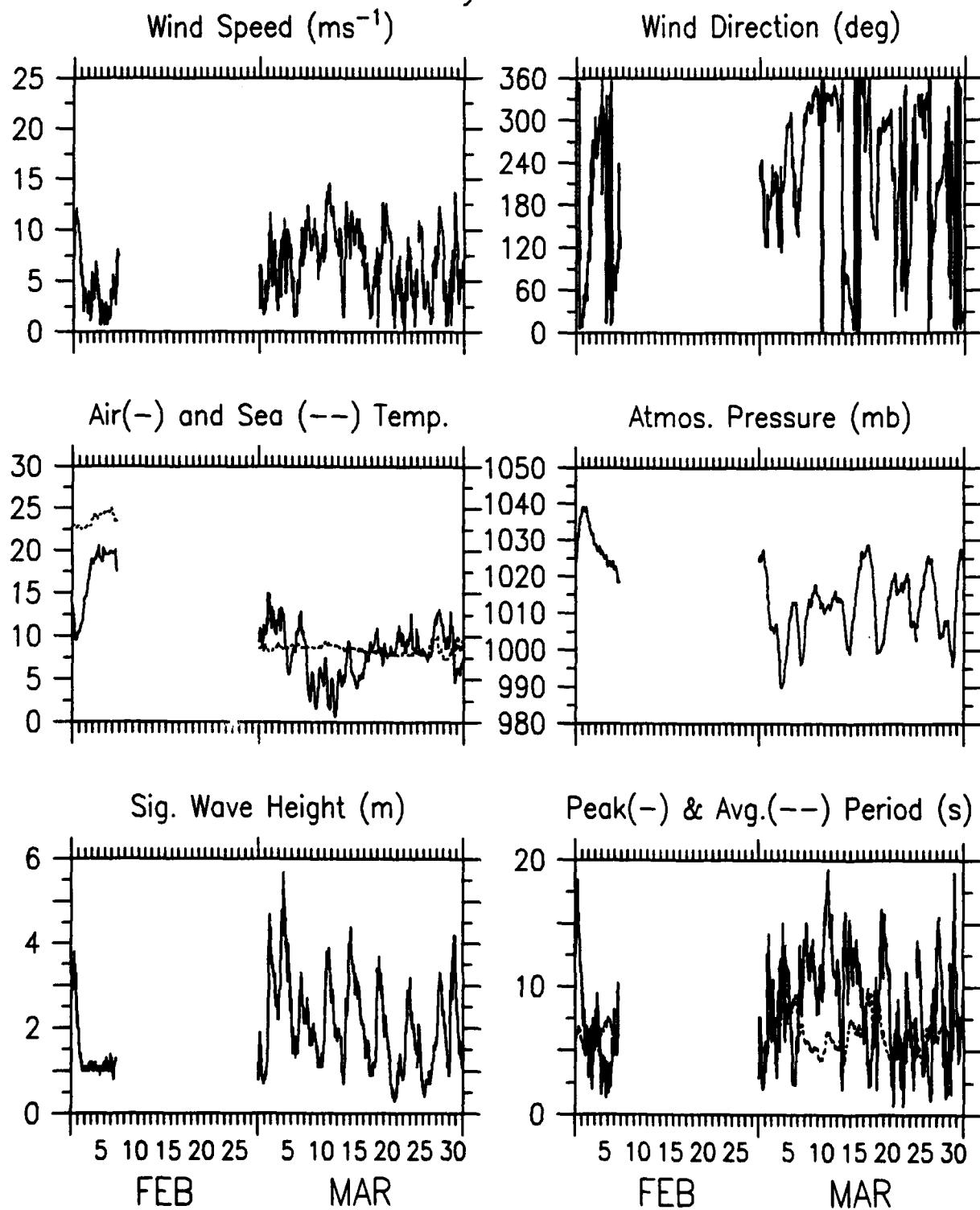
Buoy 44023



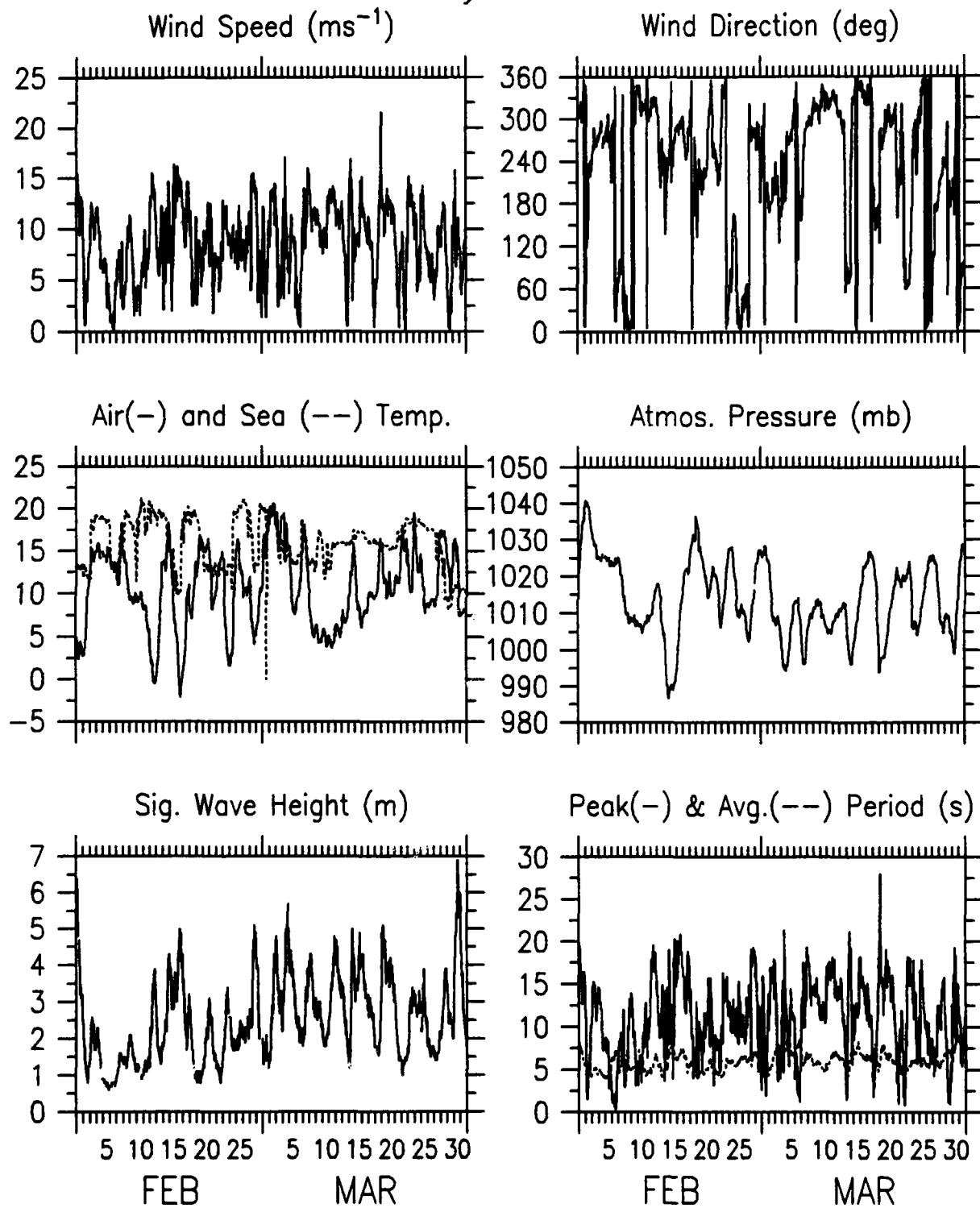
Buoy 44014



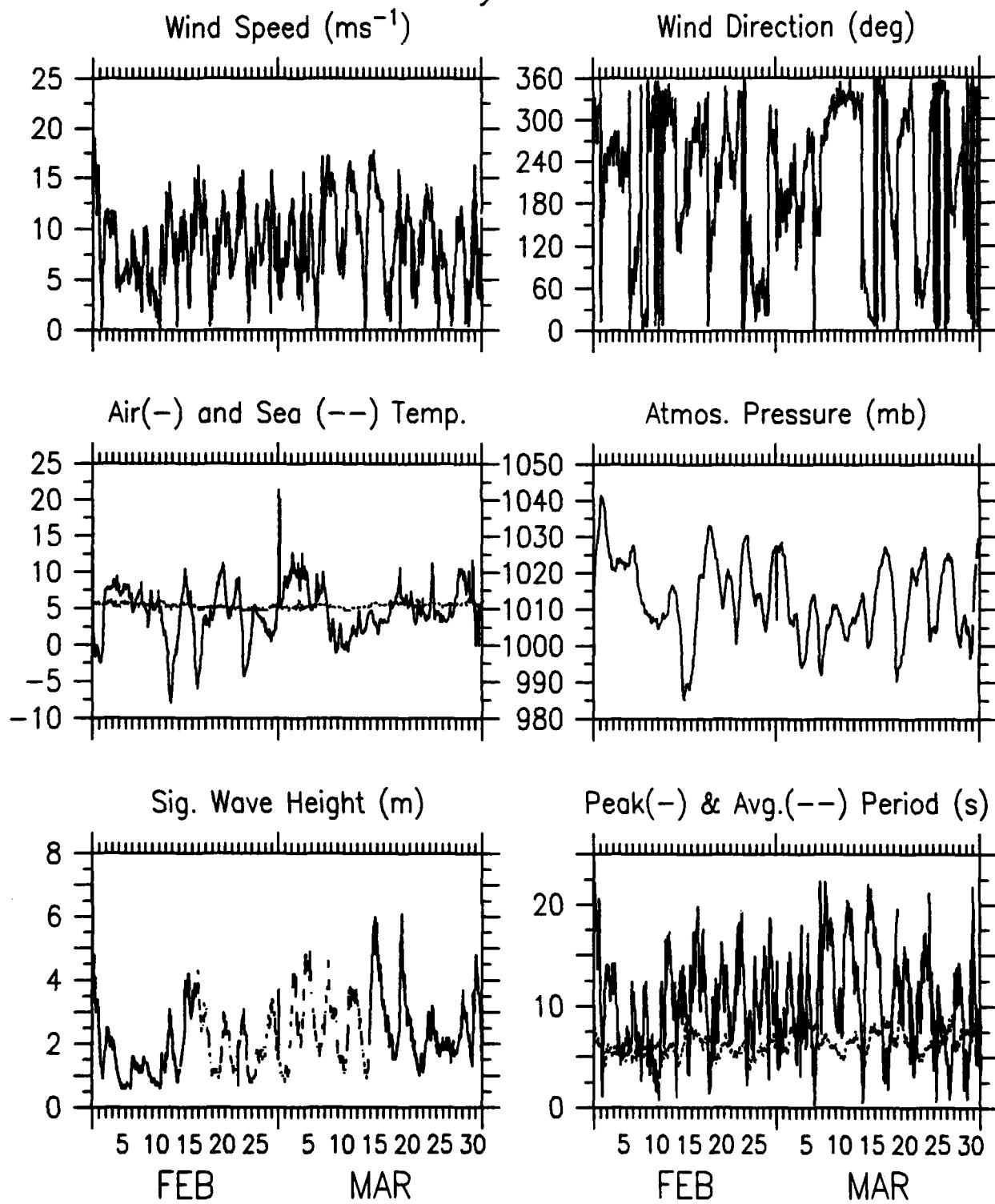
Buoy 41001



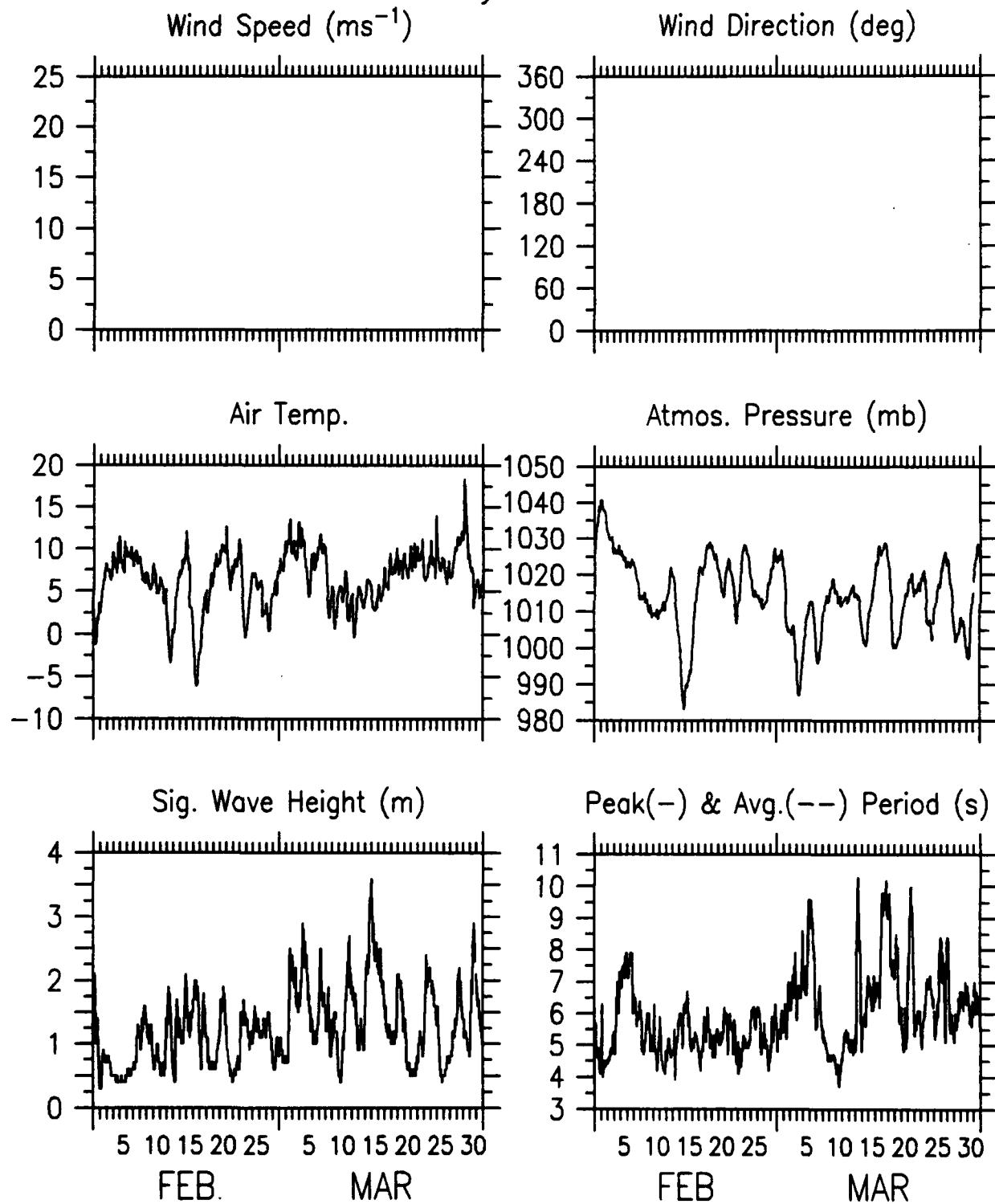
Buoy 44004



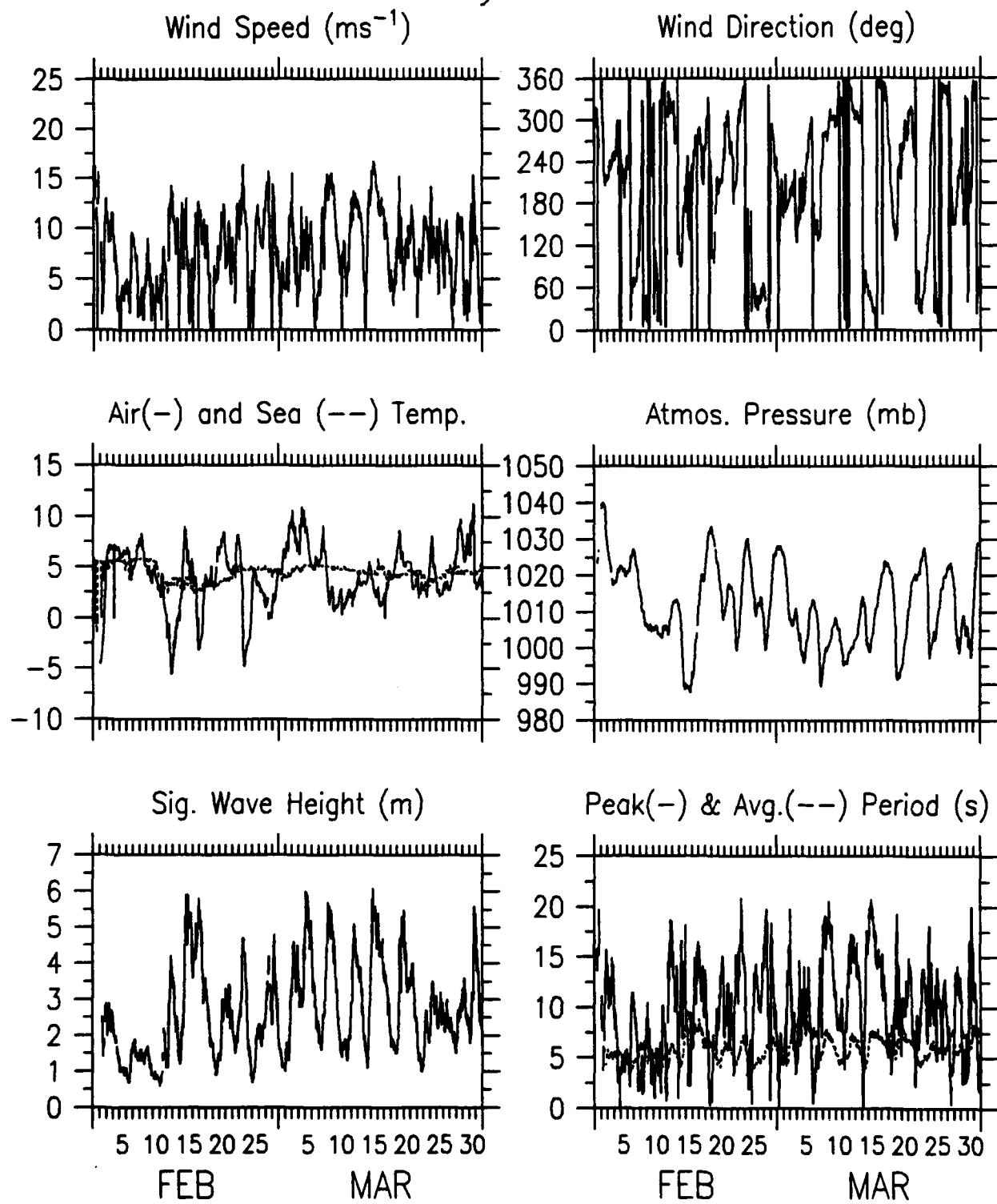
Buoy 44008



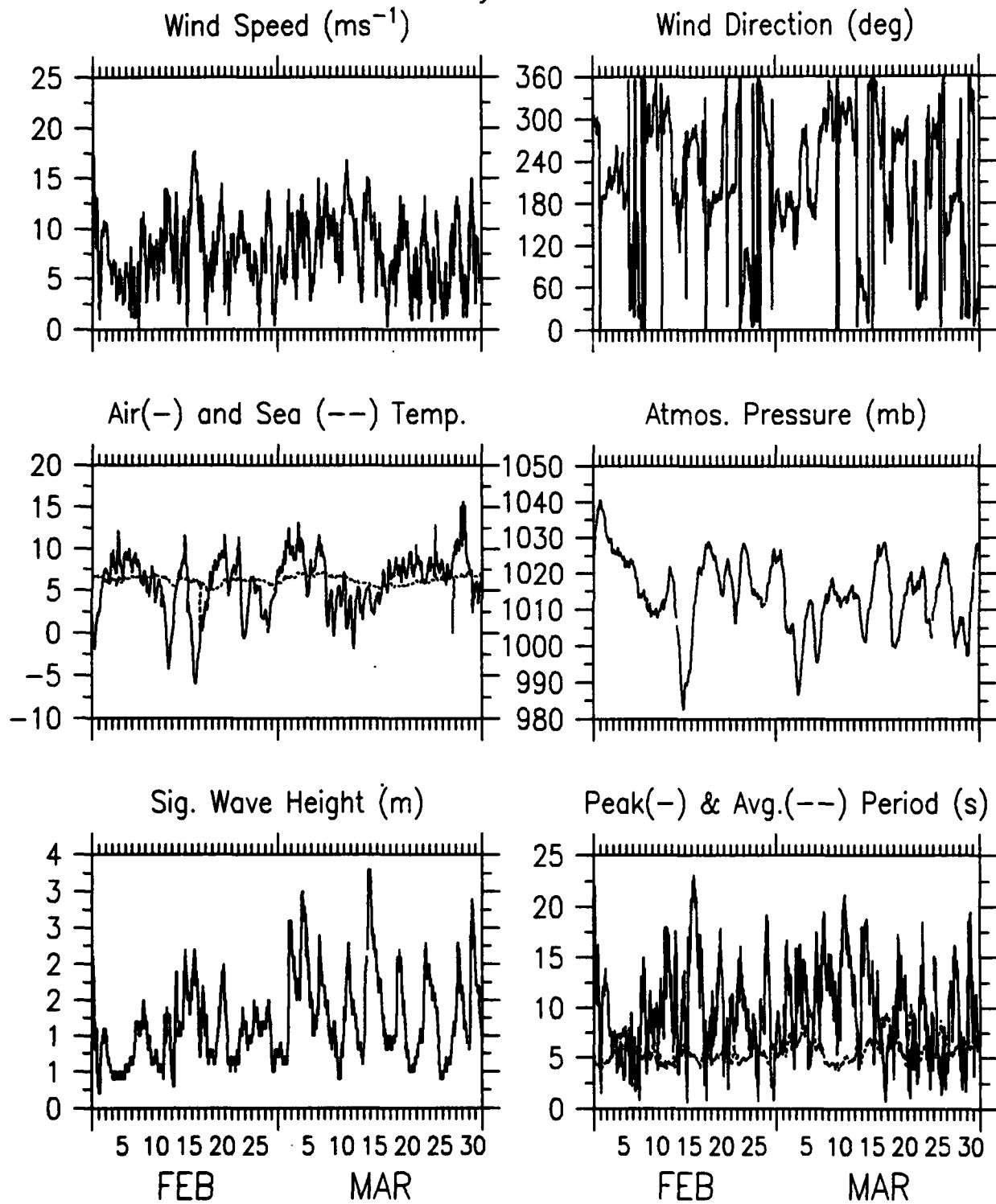
Buoy 44009



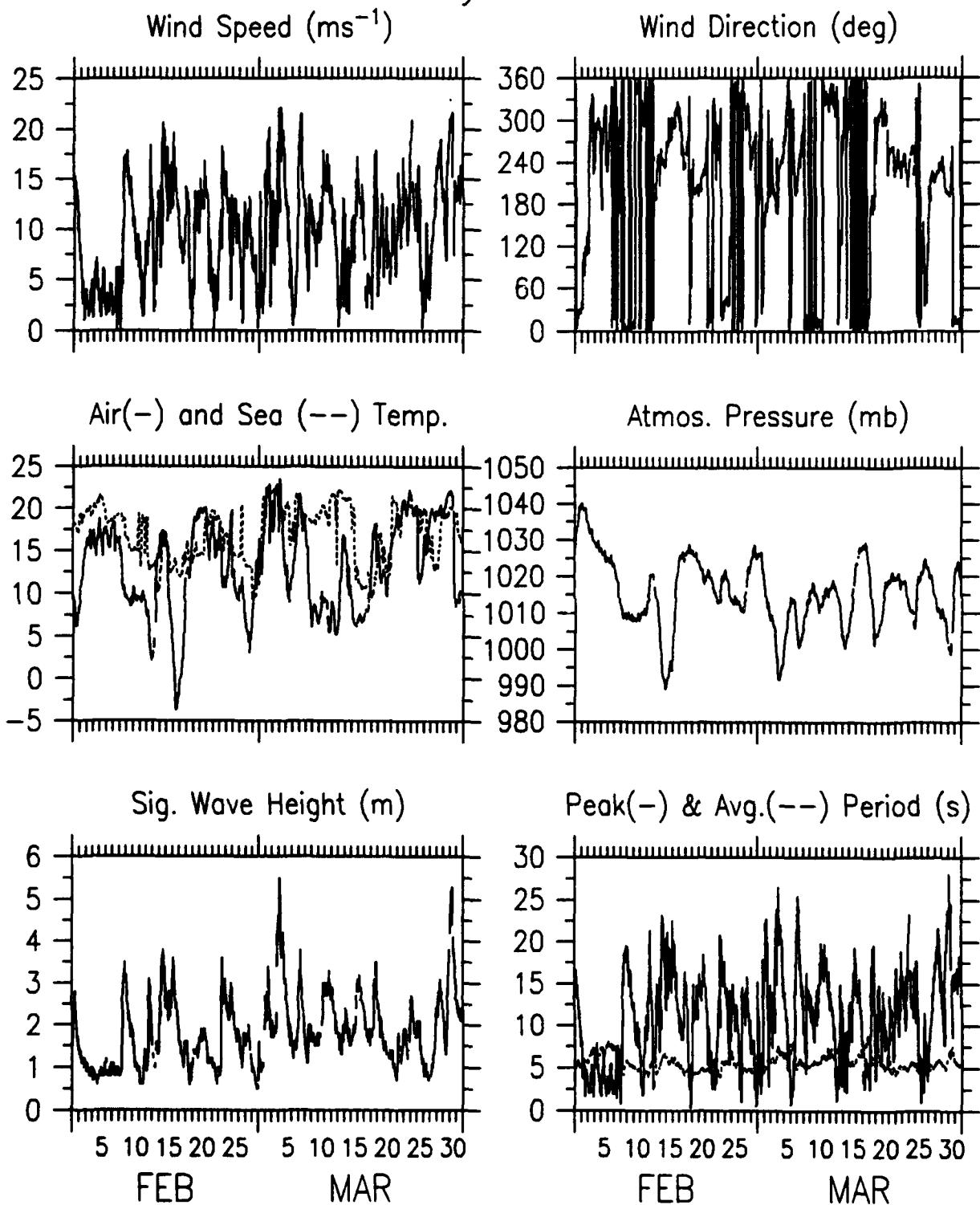
Buoy 44011



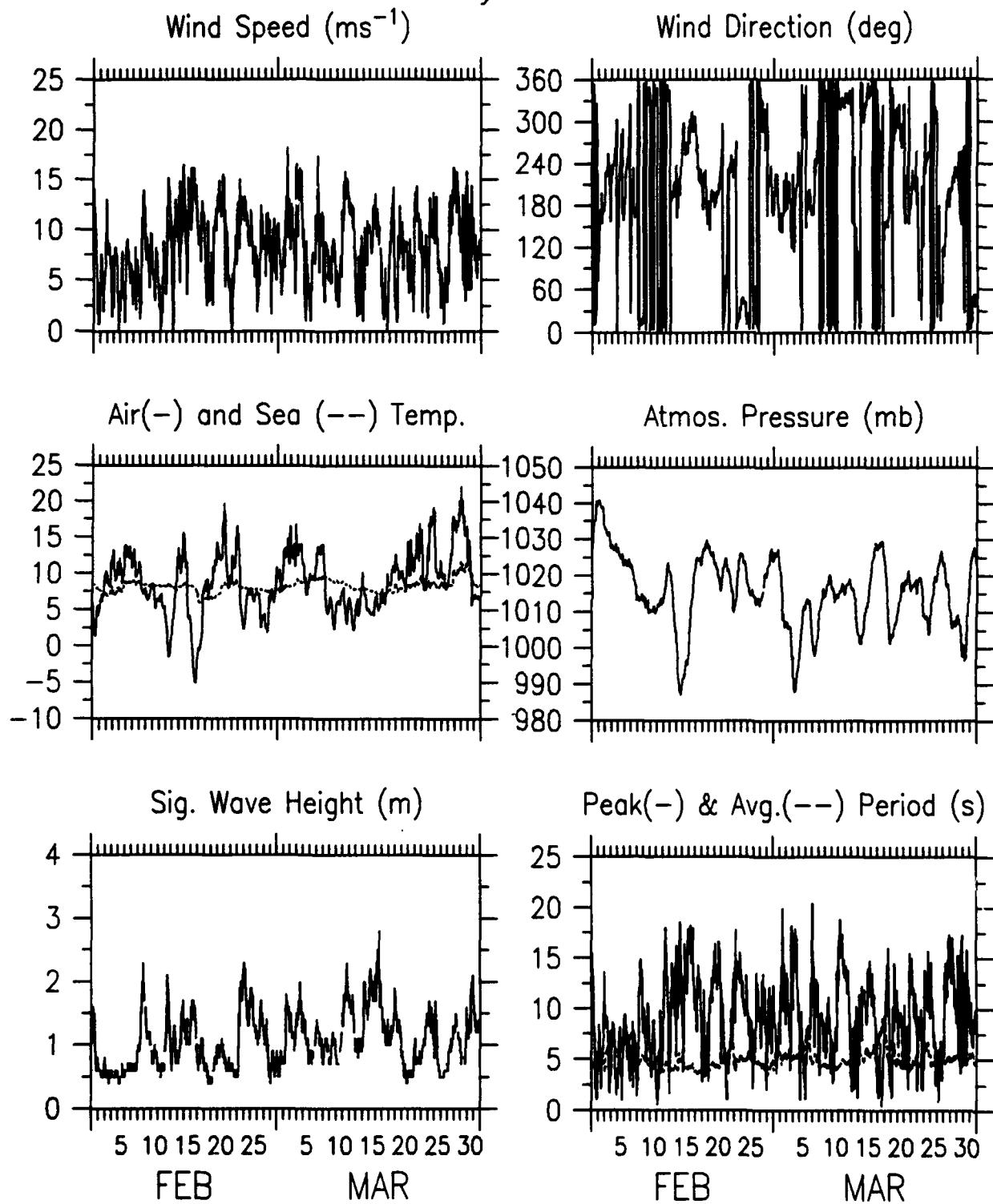
Buoy 44012



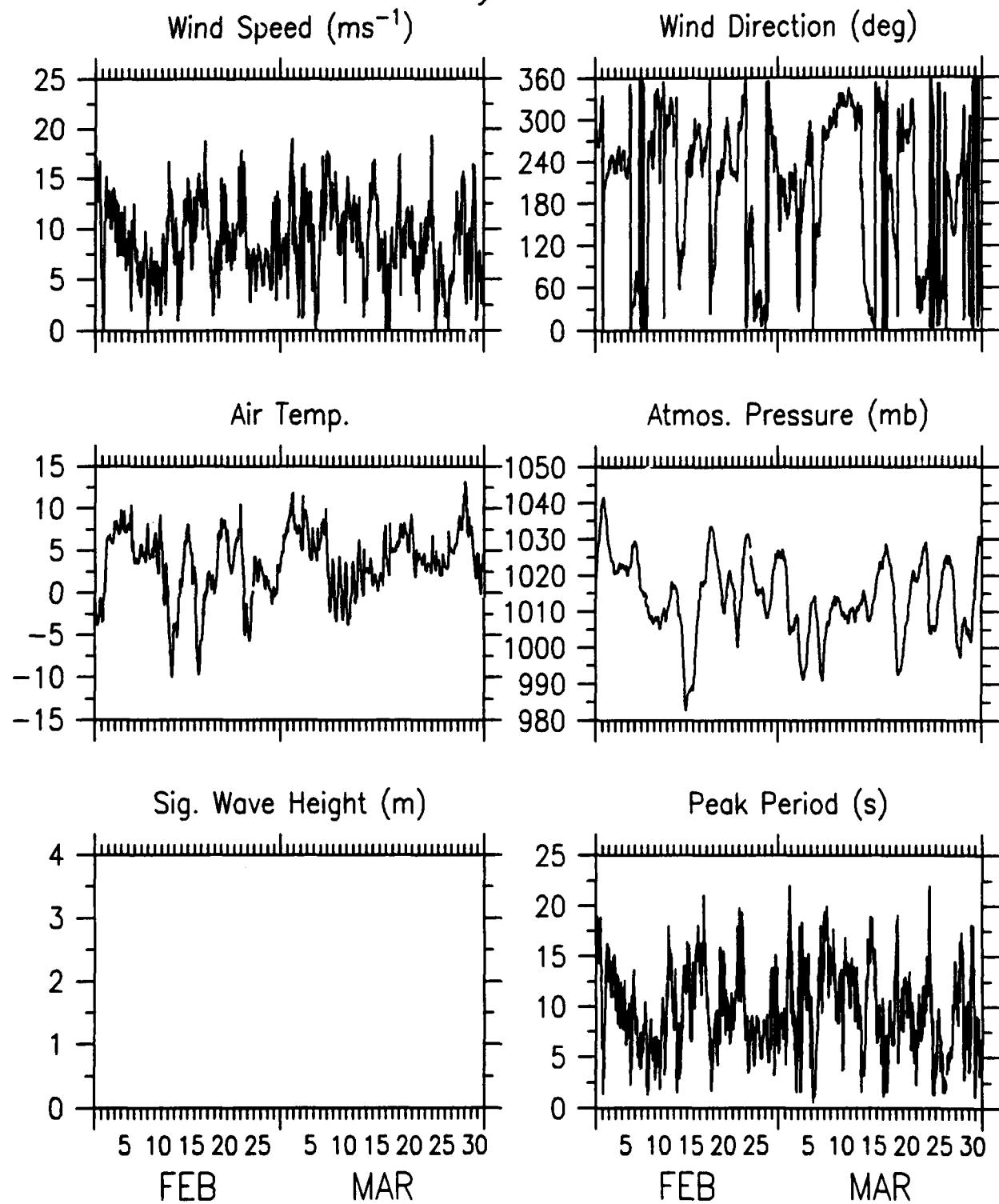
Buoy DSLN7



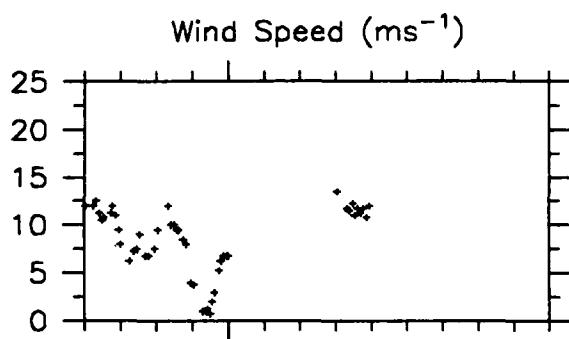
Buoy CHLV2



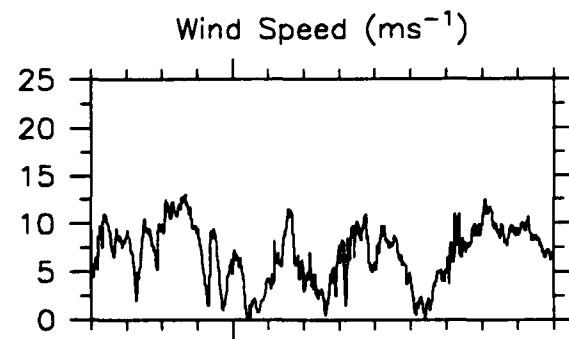
Buoy BUZM3



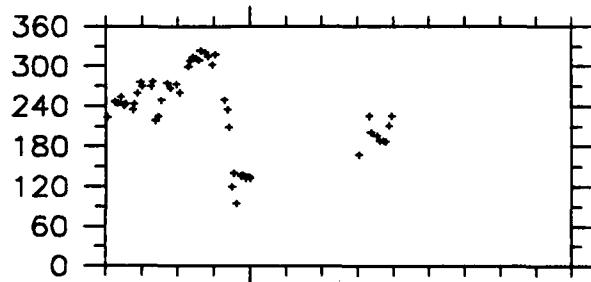
Buoy Met-1



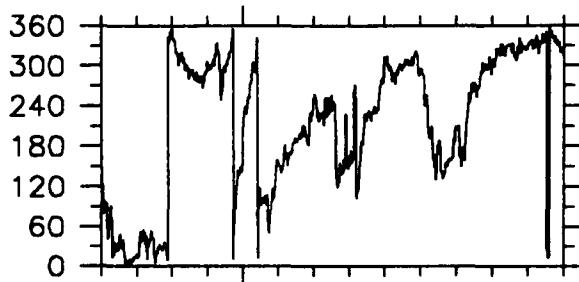
Buoy Met-3



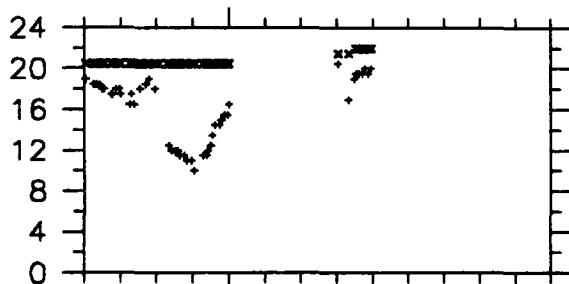
Wind Direction (deg)



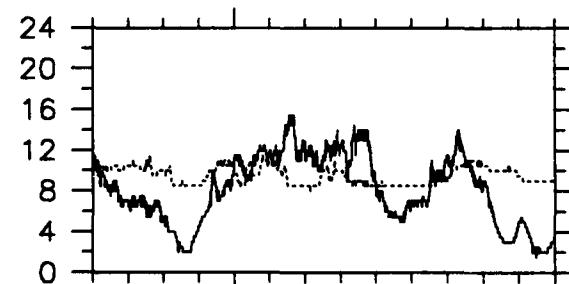
Wind Direction (deg)



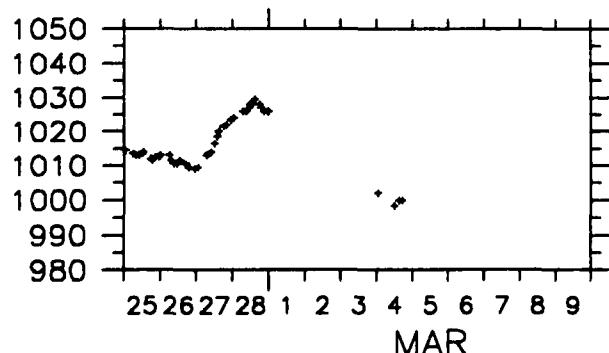
Air(+) and Sea (x) Temp.



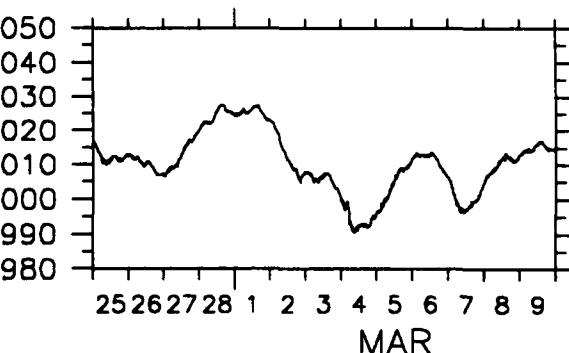
Air(--) and Sea (--) Temp.



Atmos. Pressure (mb)



Atmos. Pressure (mb)

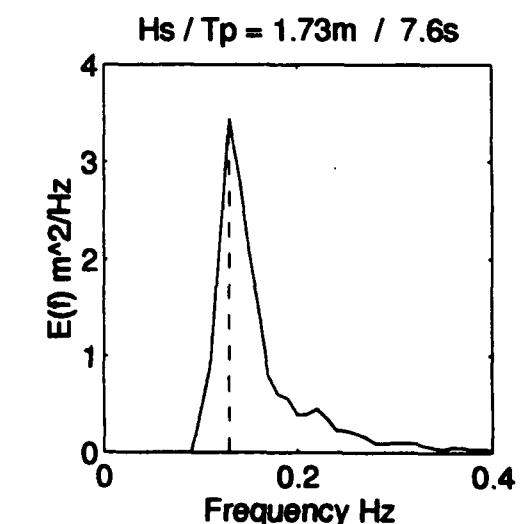
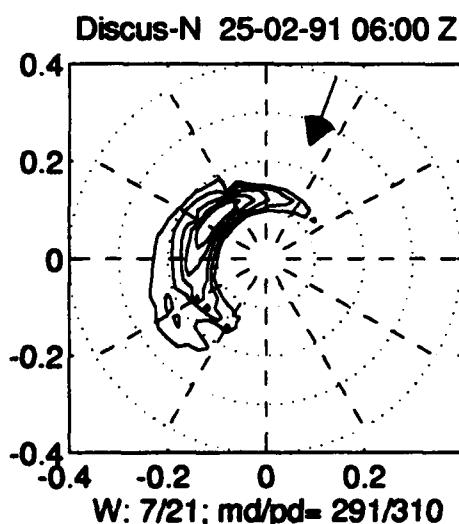
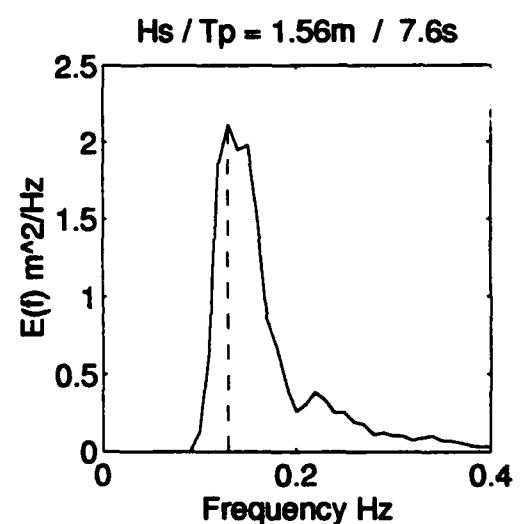
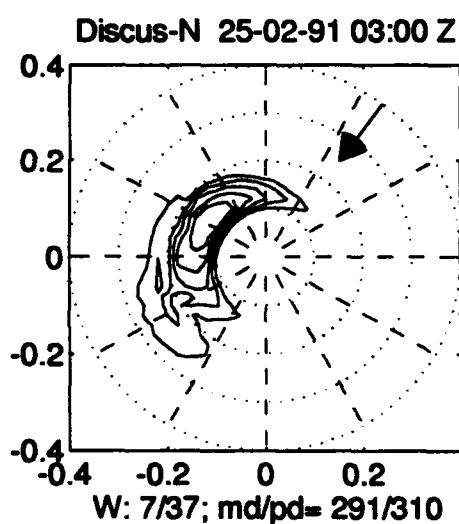
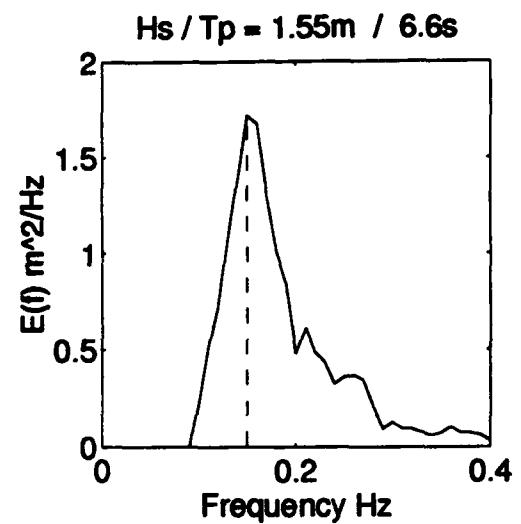
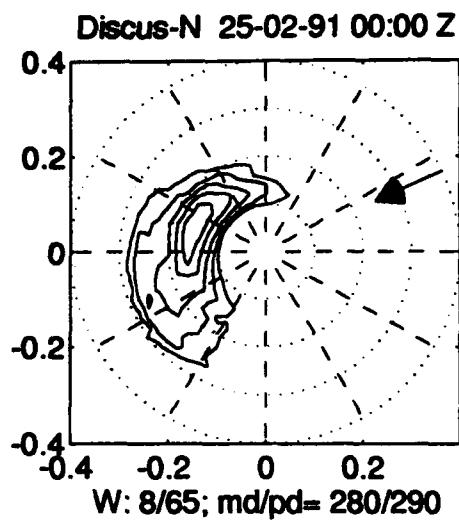


Appendix B: Directional Wave Spectra from SWADE Buoys

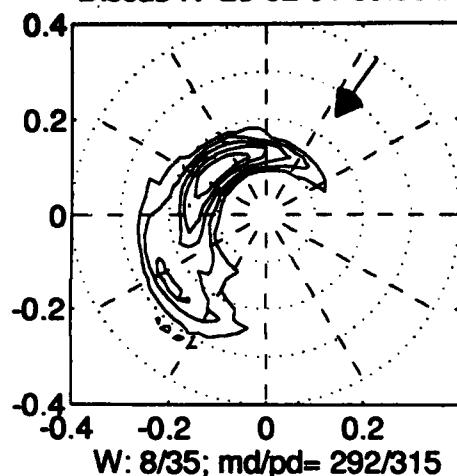
Plots of the directional wave spectra and the corresponding one-dimensional frequency spectra are presented in this appendix for buoys D-North, D-East, D-Central, and CERC (44014) every 3 hr from 25 February 1990, 00:00 GMT to 9 March 1991, 00:00 GMT.

Two-dimensional wave spectra are plotted in polar coordinates with five equally spaced contours between the maximum of $\log[F(f, \theta)]$ and $\log[F(f, \theta)] = -1.25$. Each plot presents a directional wave spectrum, its corresponding one-dimensional frequency spectrum, $E(f) = \int F(f, \theta) d\theta$ and a vector of the prevailing wind direction. The frequency axis ranges from 0 to 0.4 Hz with concentric circles every 0.1 Hz. The top header of the directional wave spectral plot identifies the buoy station, date and time in GMT. The bottom header provides the wind speed and wind direction (from) measured clockwise from north, as well as the mean and peak wave directions (towards). The header of the frequency spectrum provides the significant wave height and the peak period which is also marked (dashed line) on the plot.

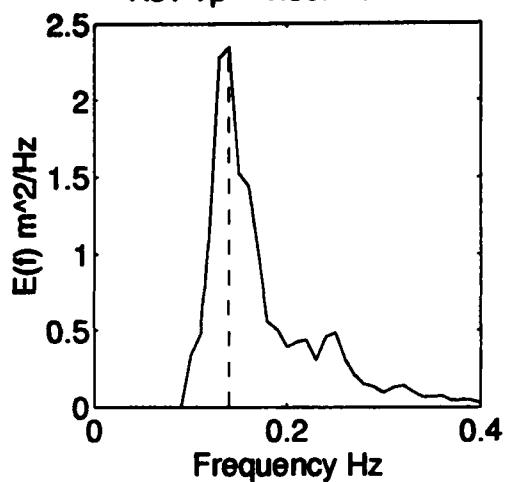
B.1: Discus Buoy “North”



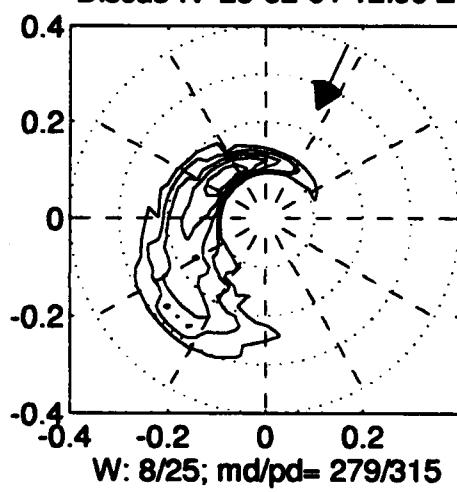
Discus-N 25-02-91 09:00 Z



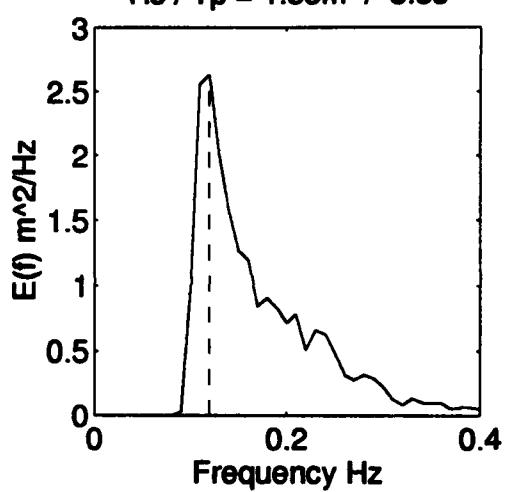
Hs / Tp = 1.59m / 7.1s



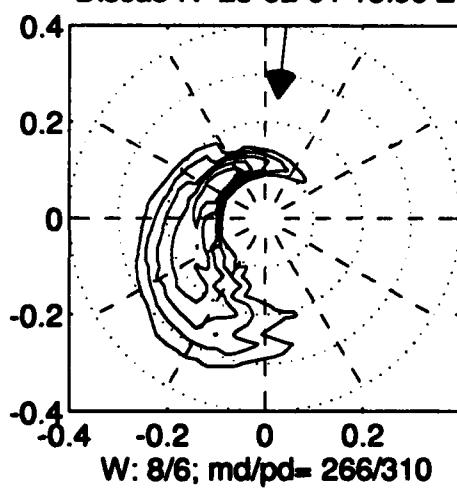
Discus-N 25-02-91 12:00 Z



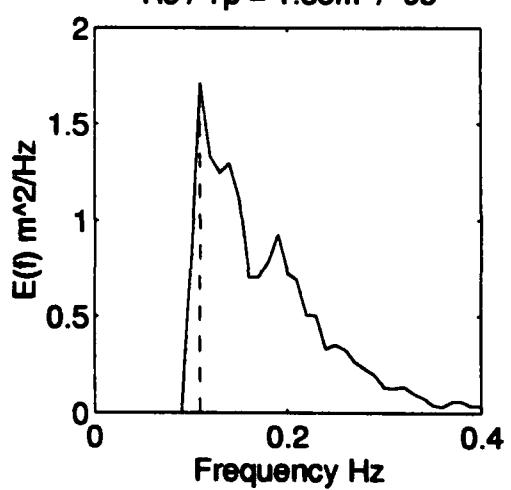
Hs / Tp = 1.83m / 8.3s

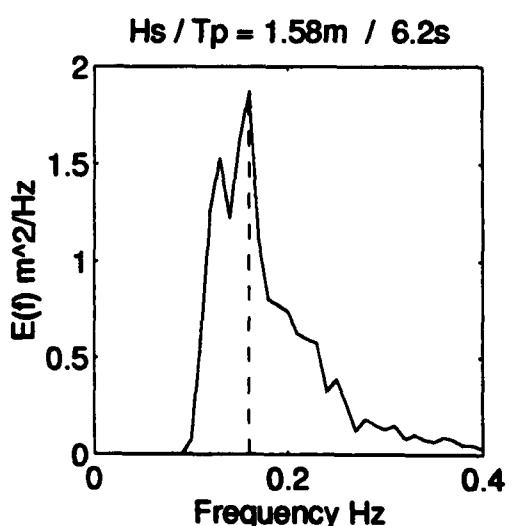
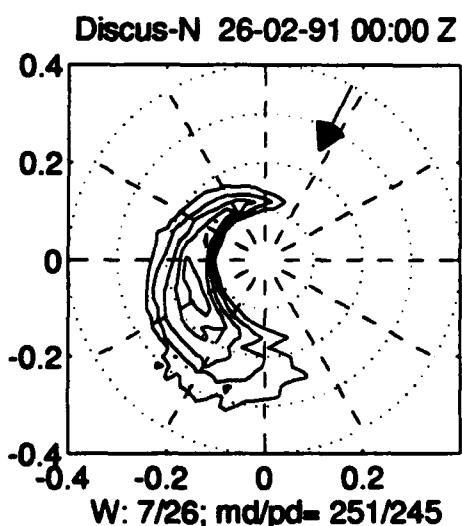
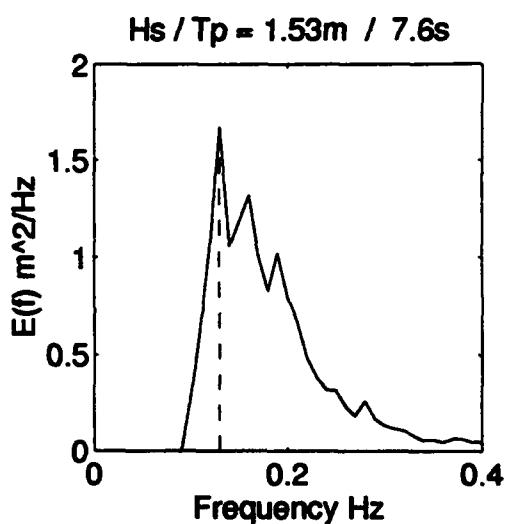
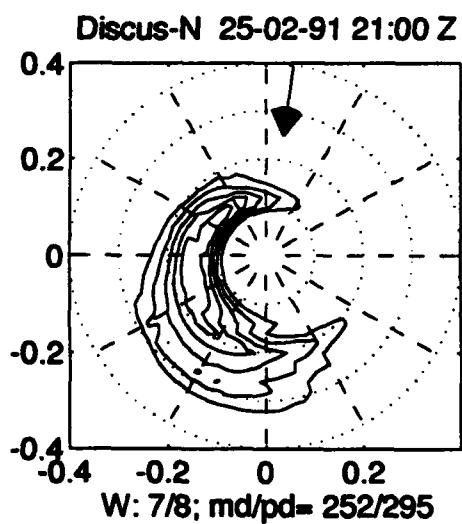
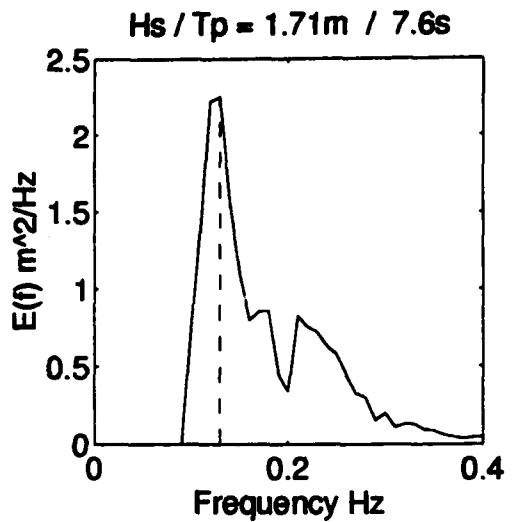
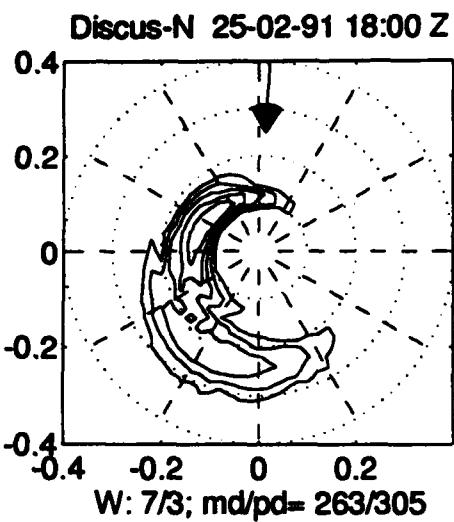


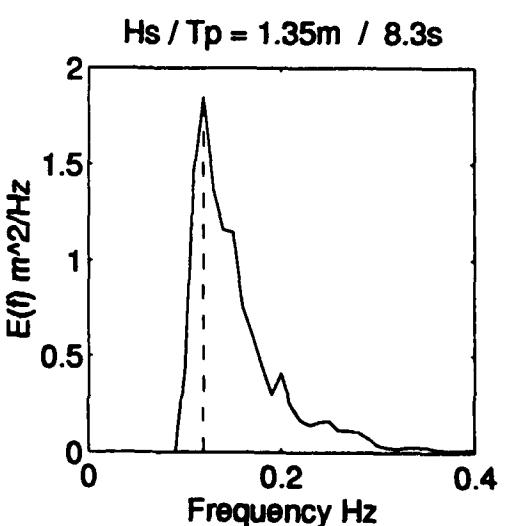
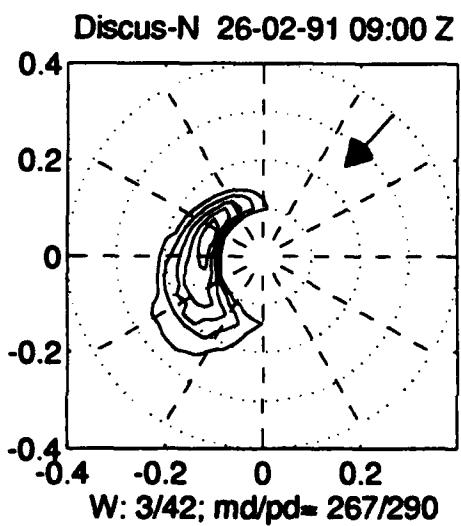
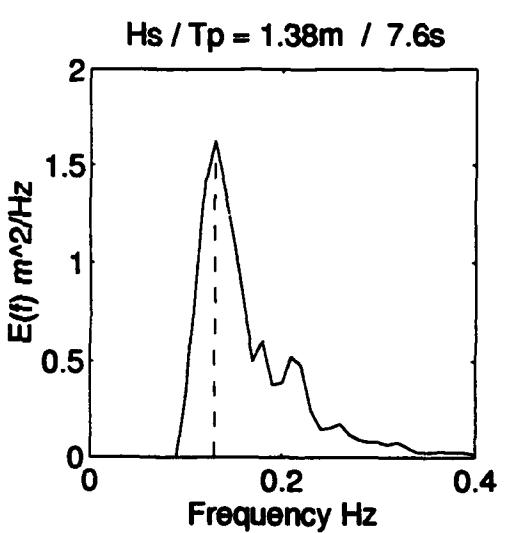
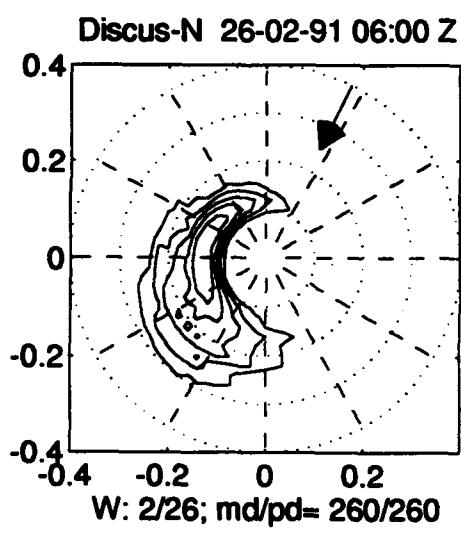
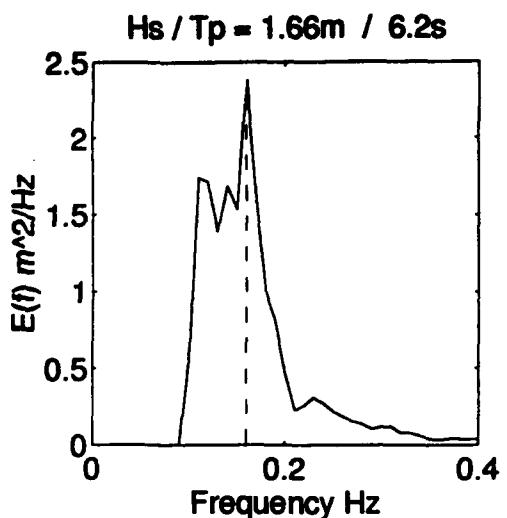
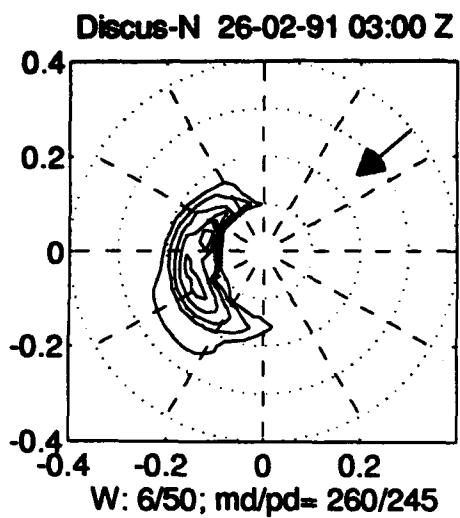
Discus-N 25-02-91 15:00 Z

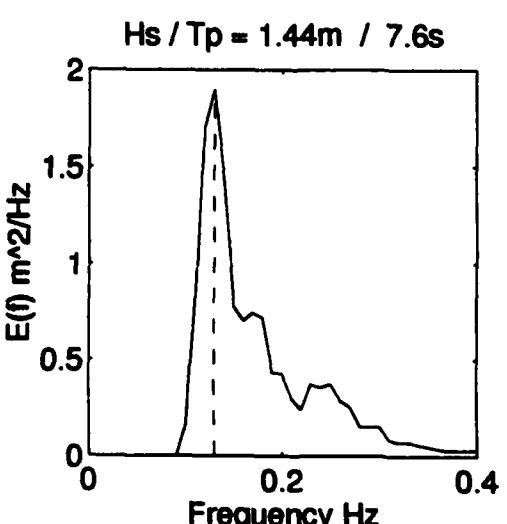
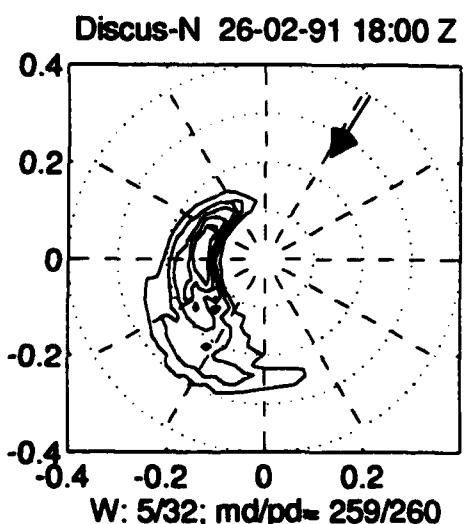
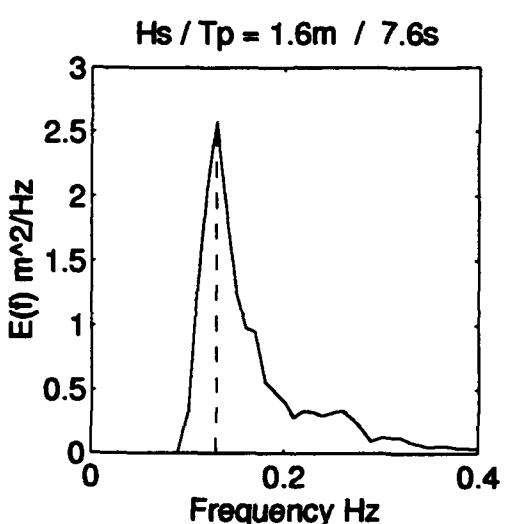
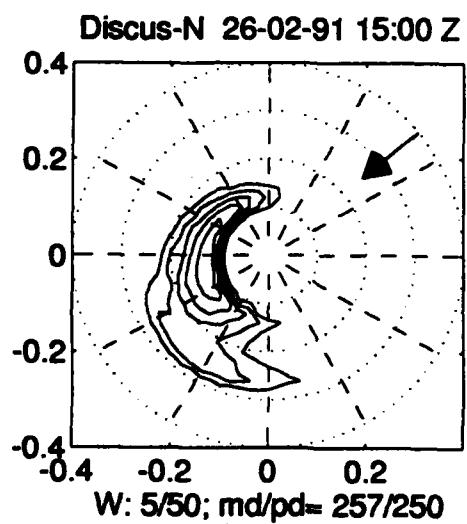
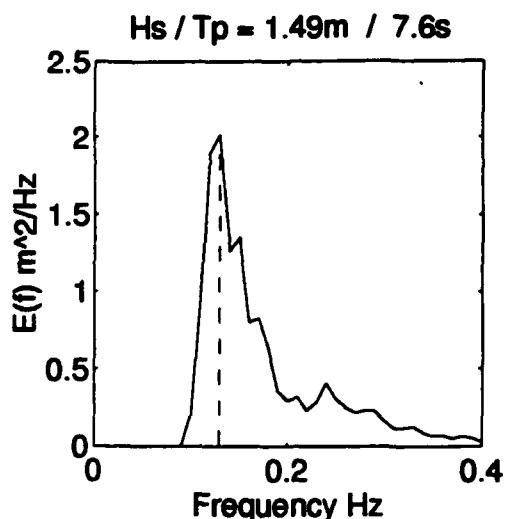
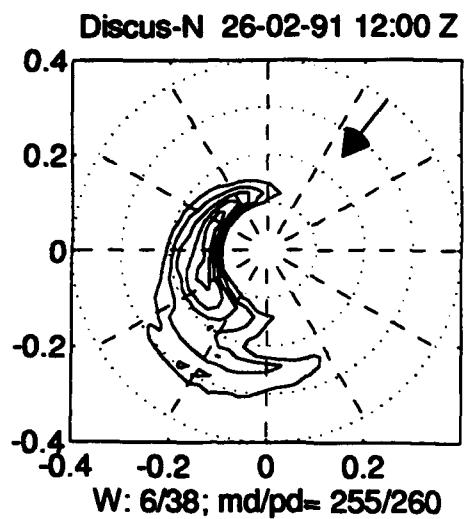


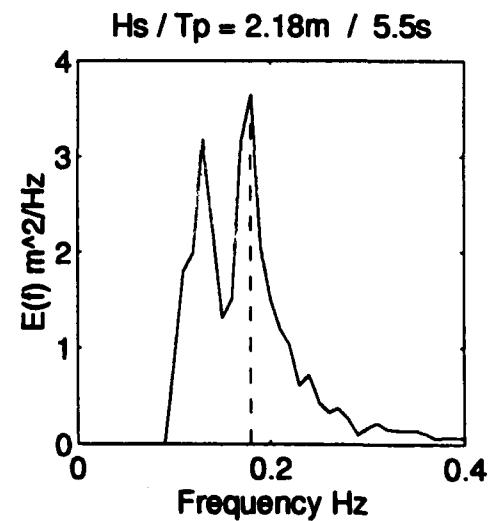
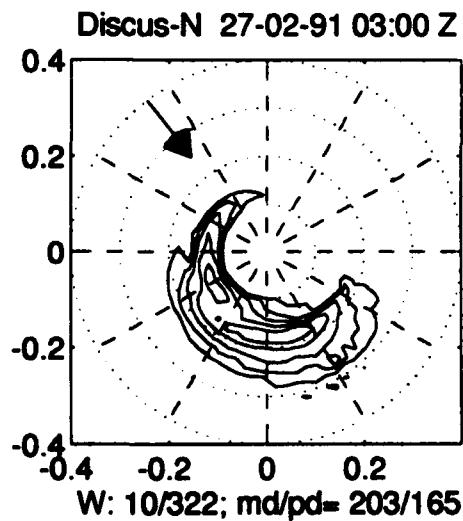
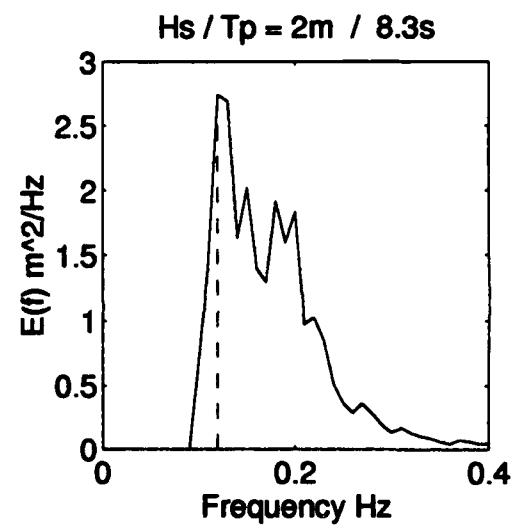
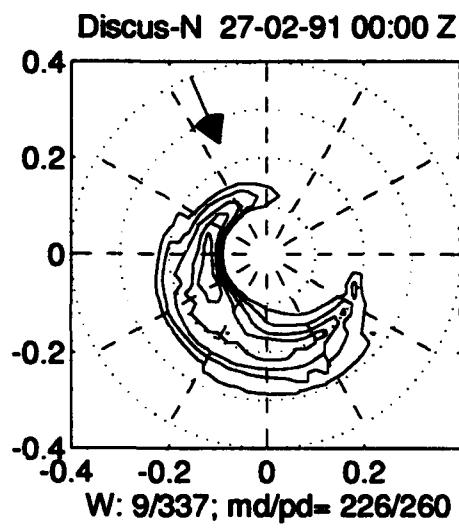
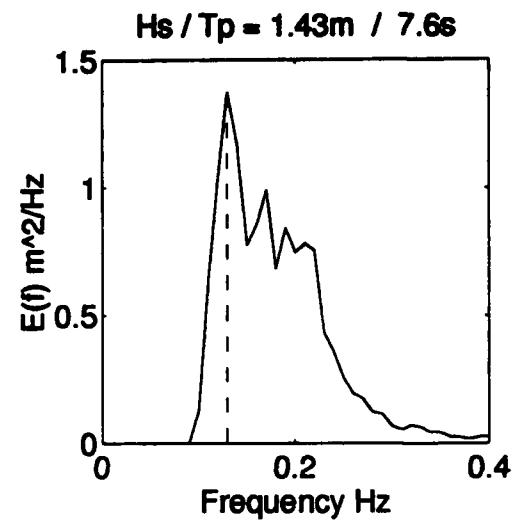
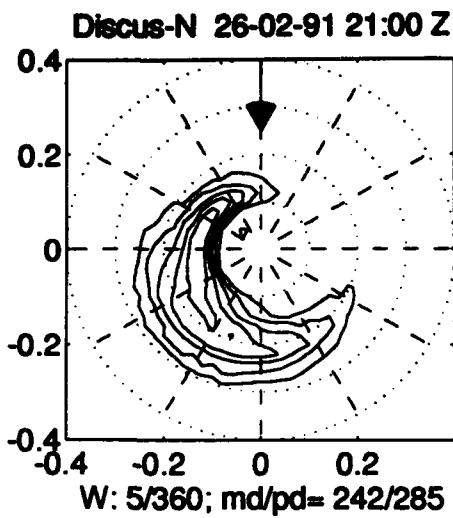
Hs / Tp = 1.58m / 9s

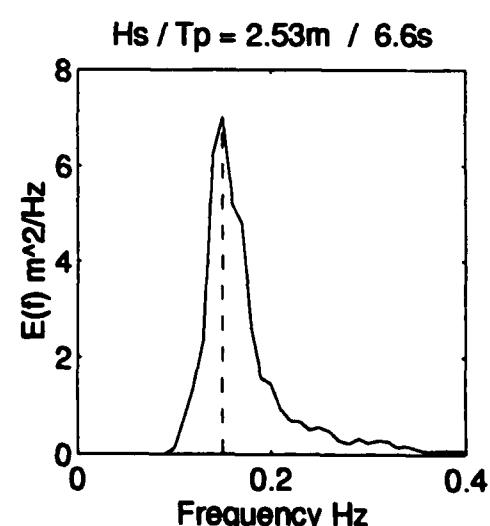
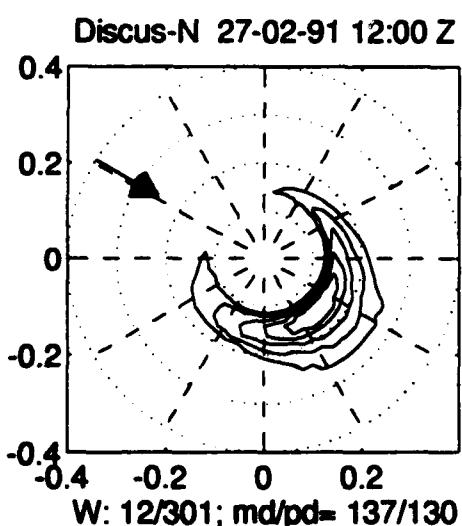
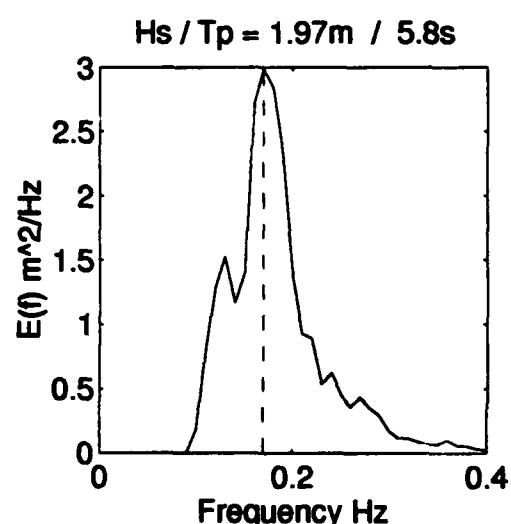
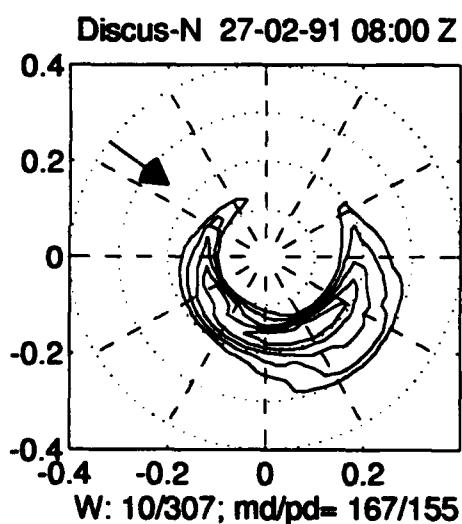
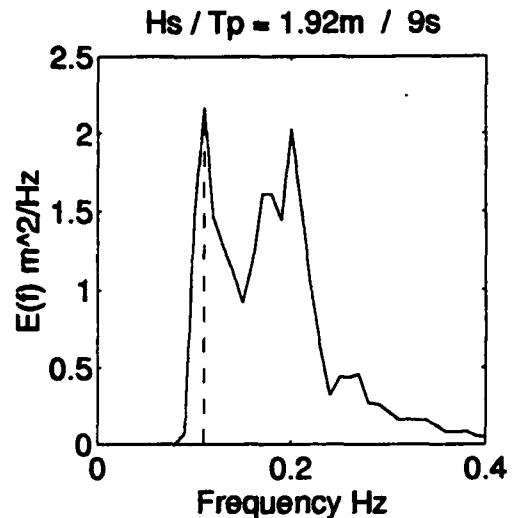
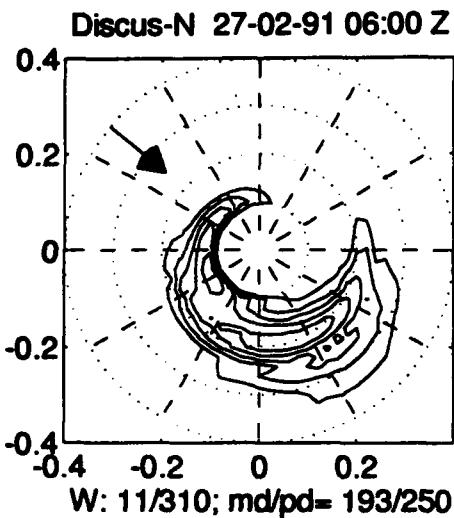


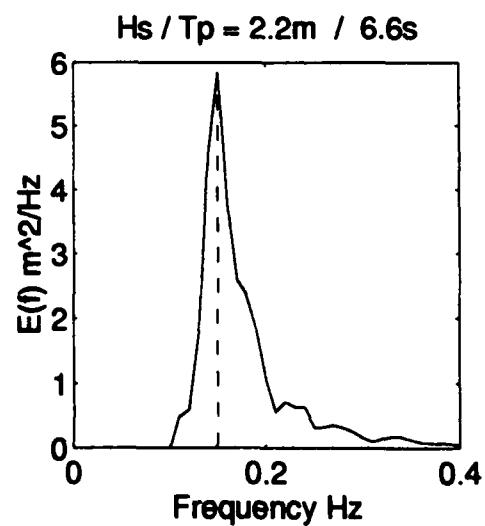
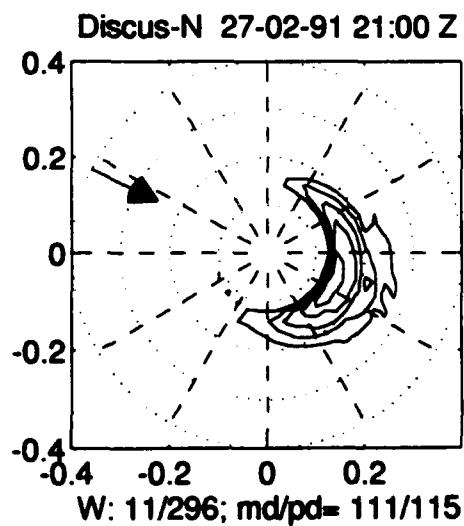
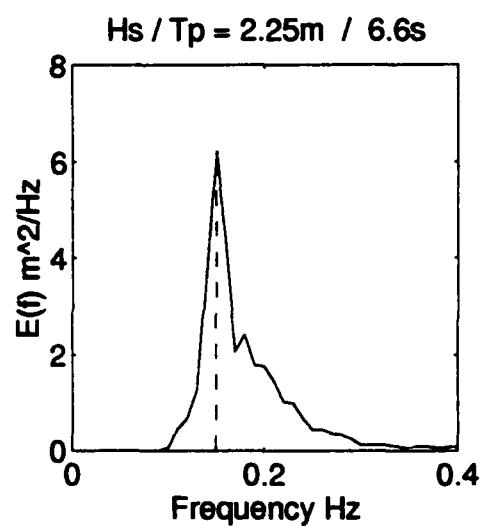
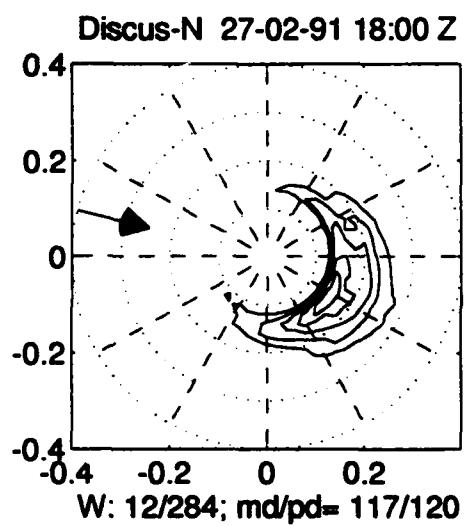
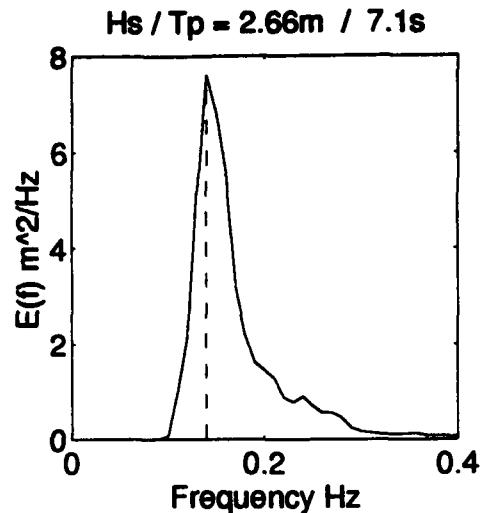
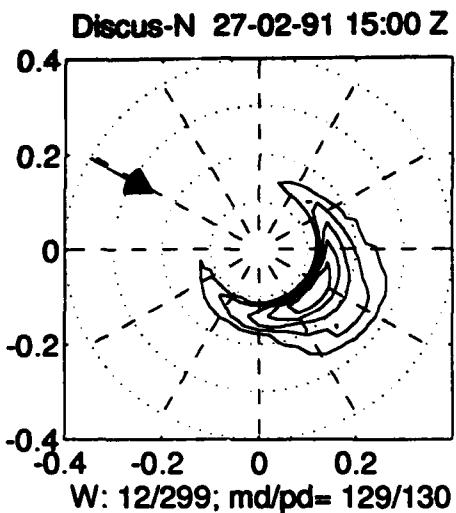


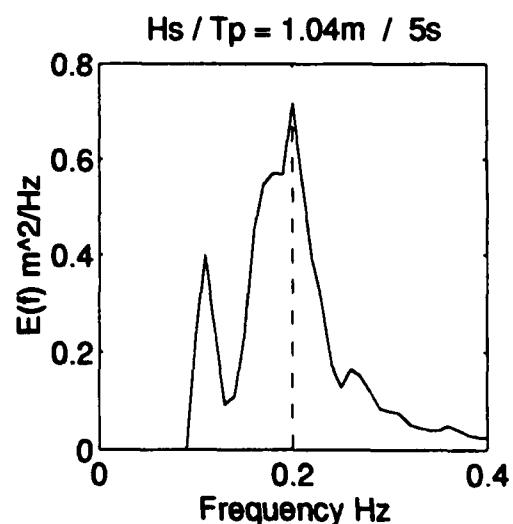
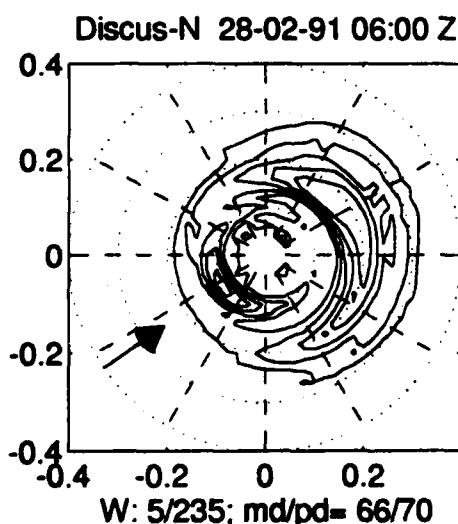
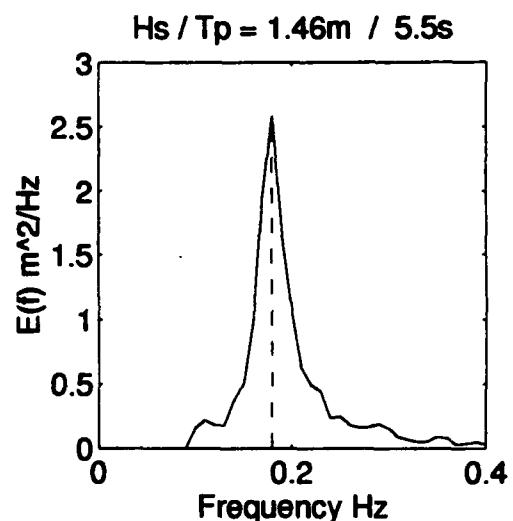
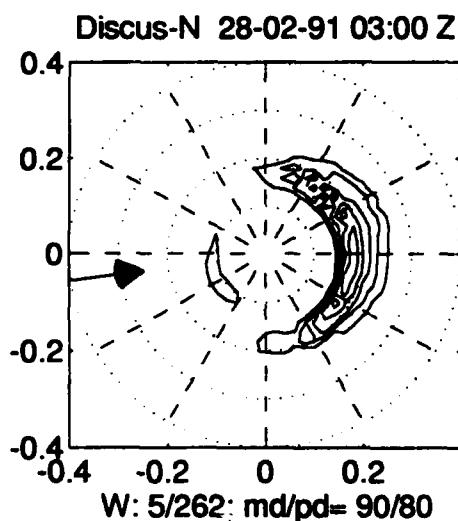
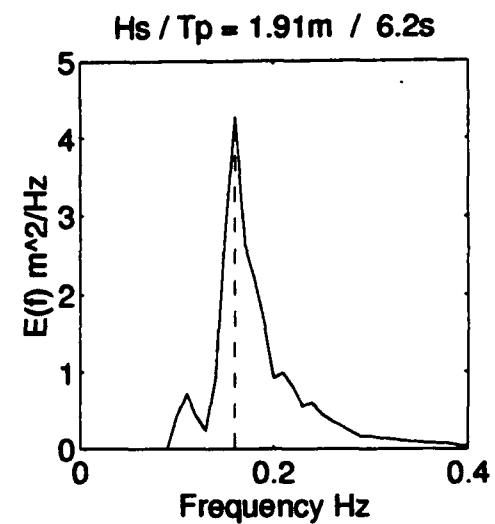
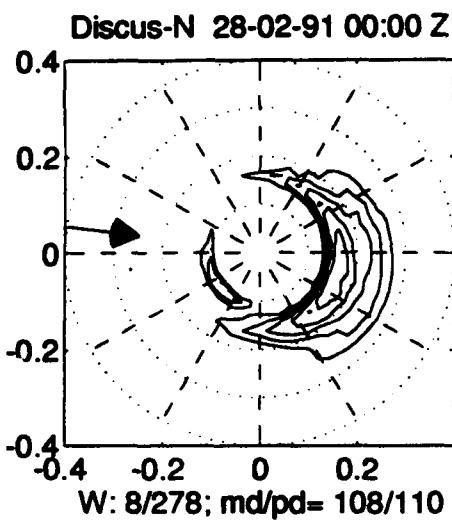


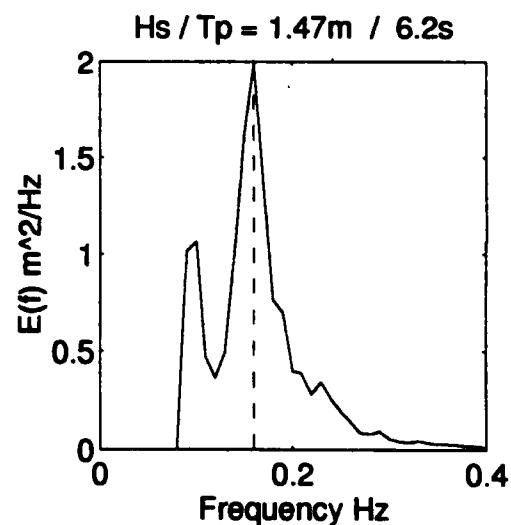
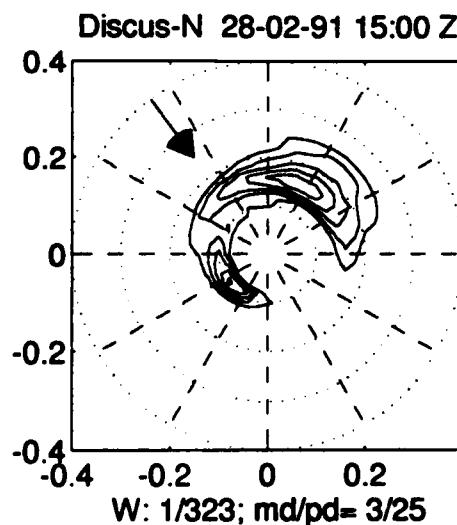
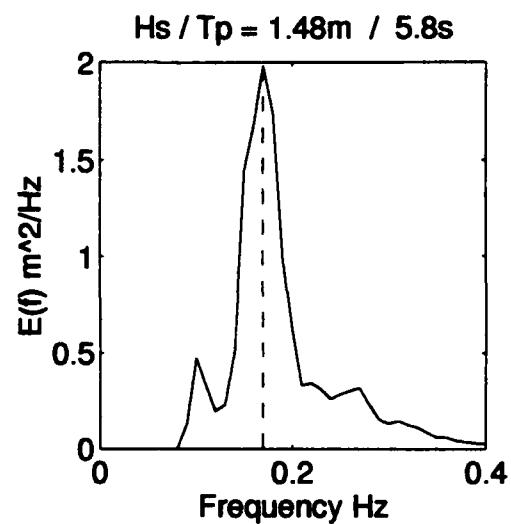
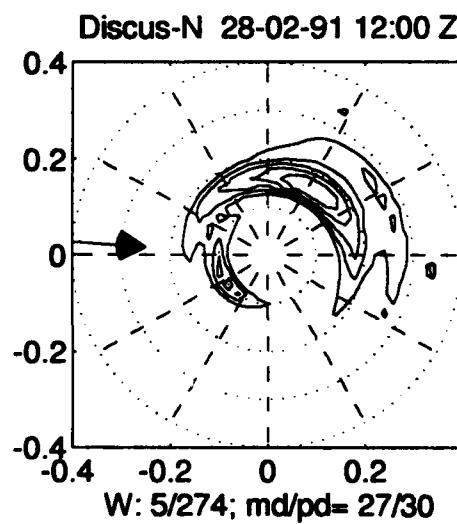
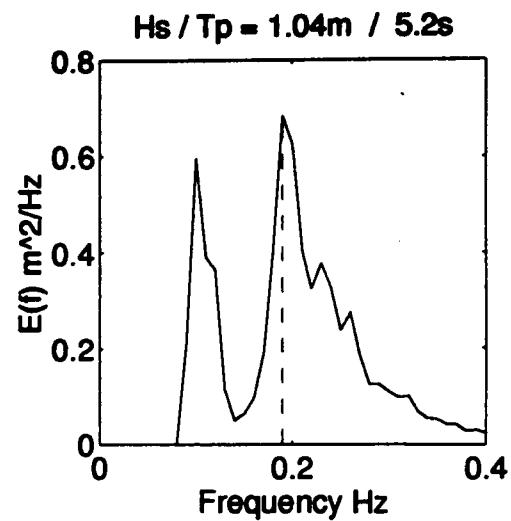
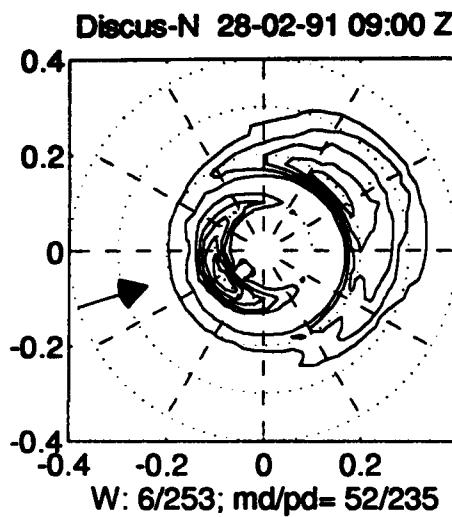


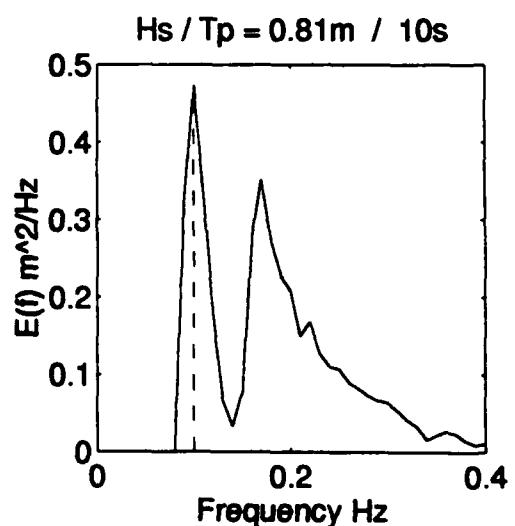
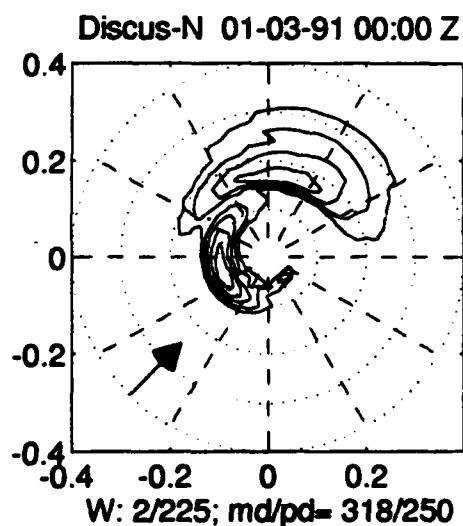
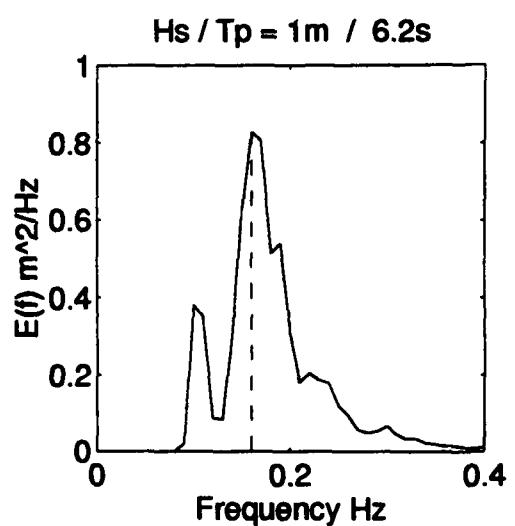
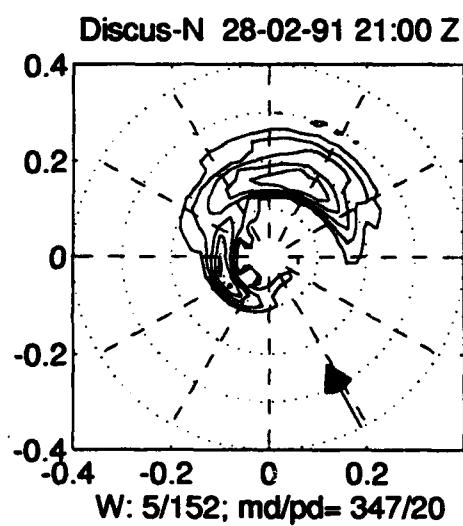
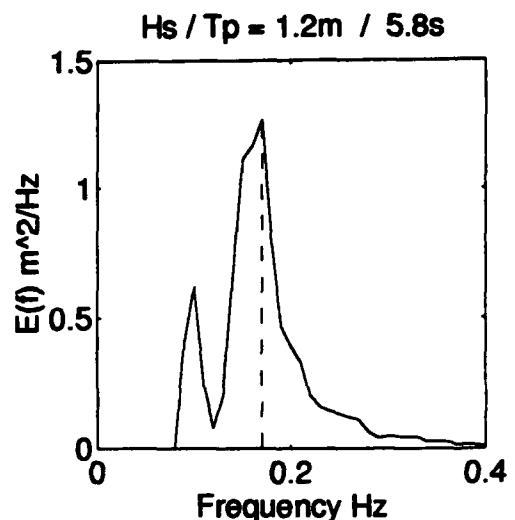
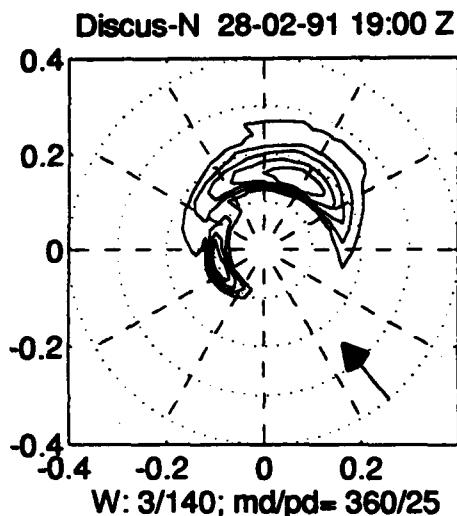


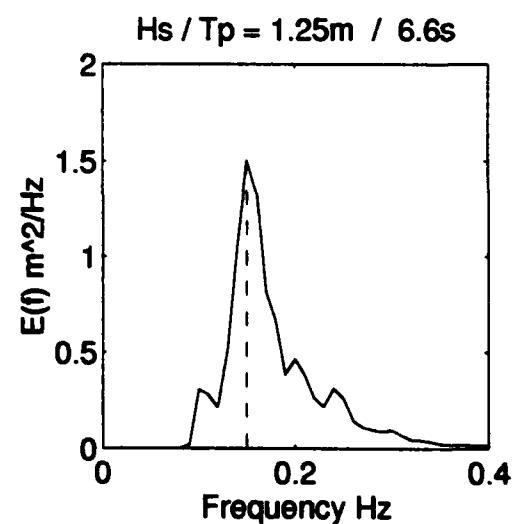
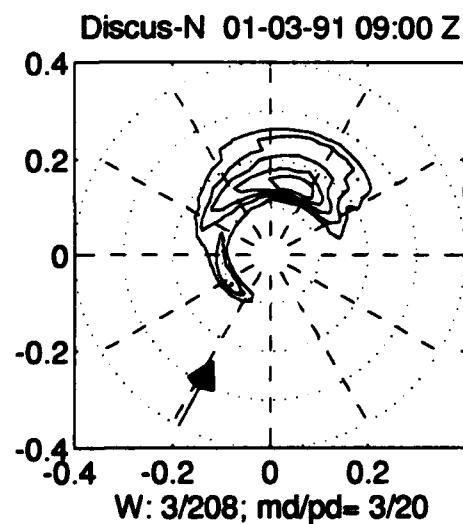
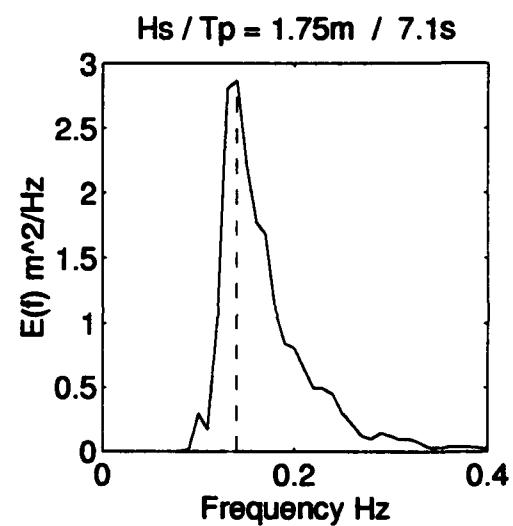
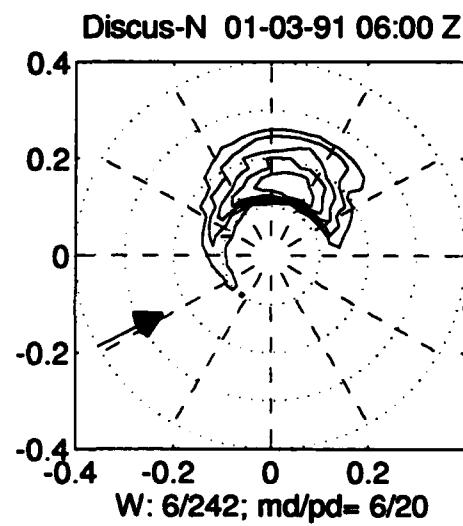
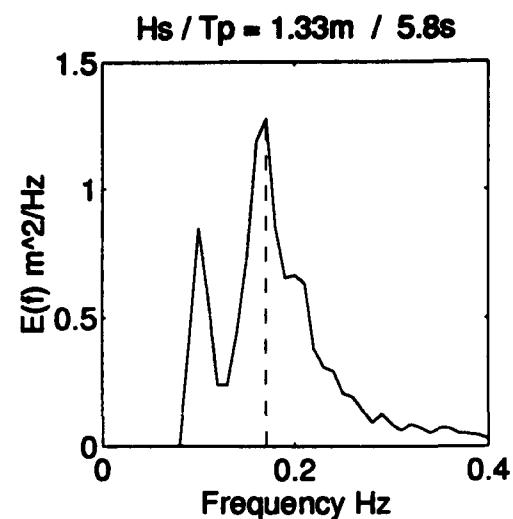
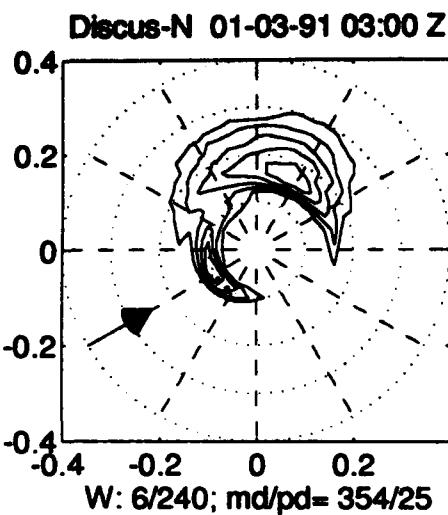


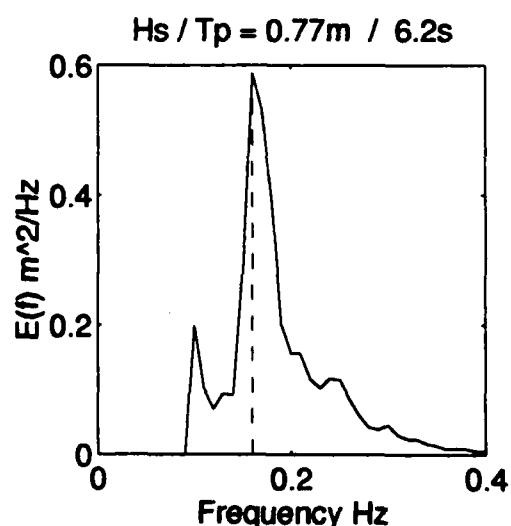
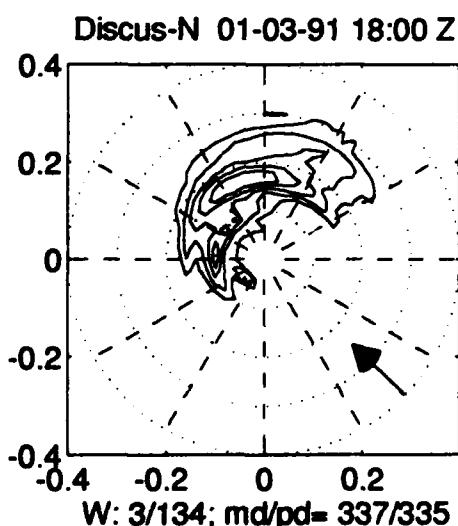
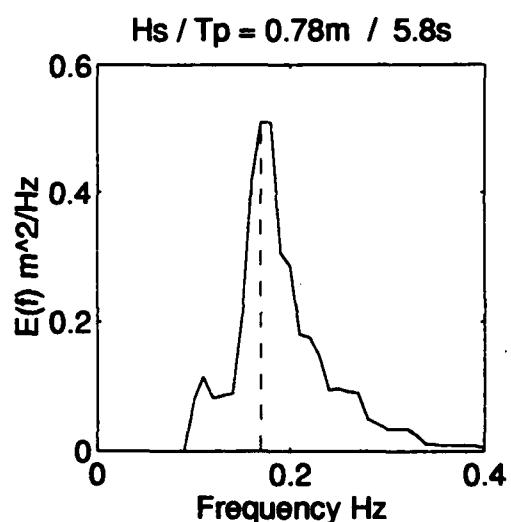
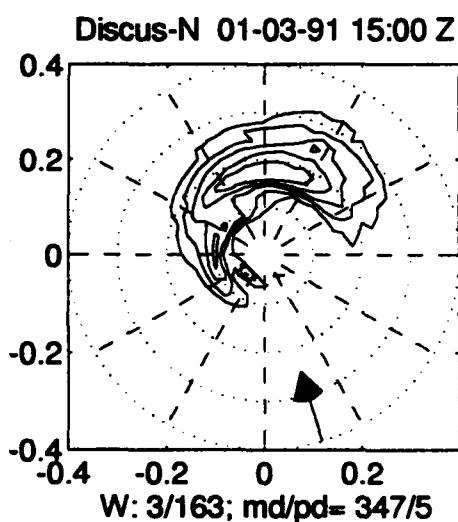
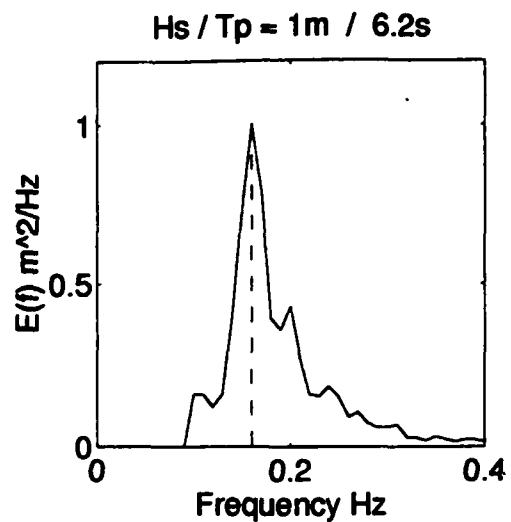
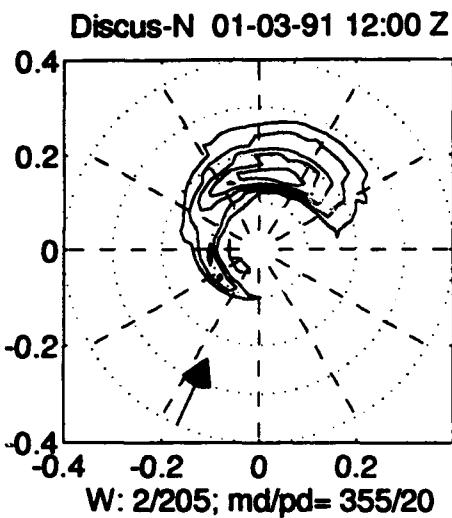


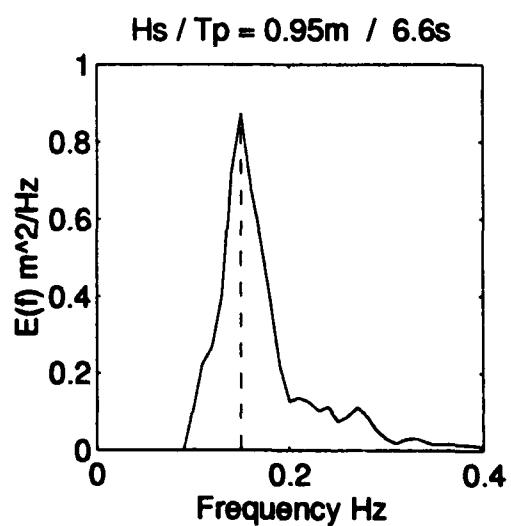
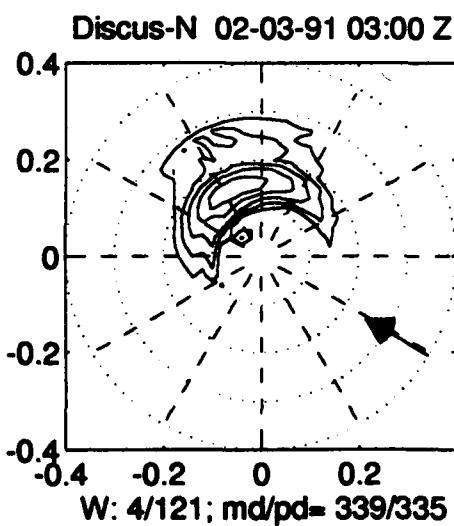
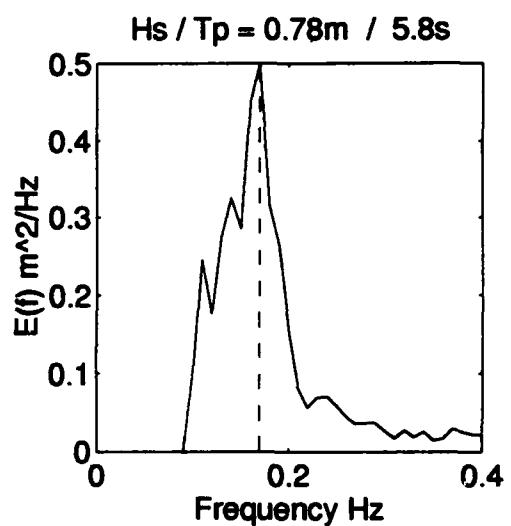
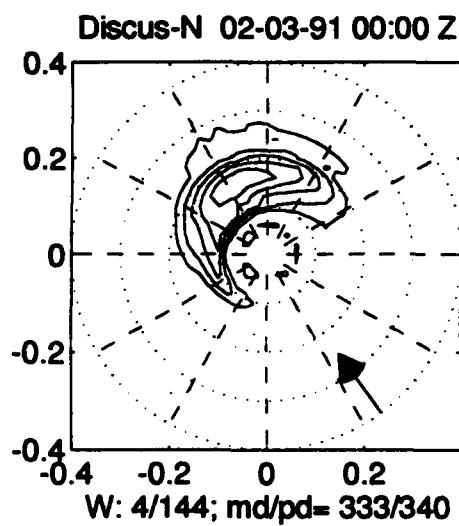
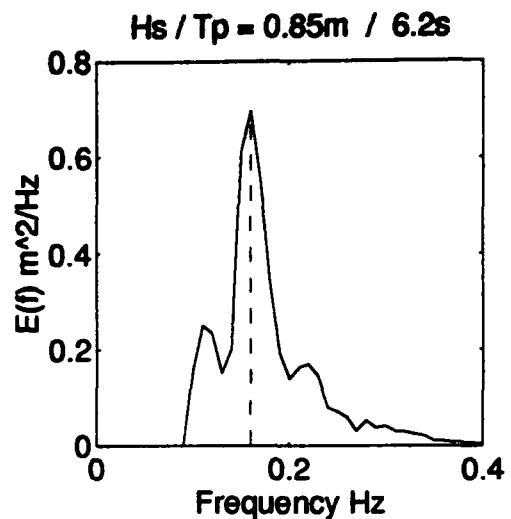
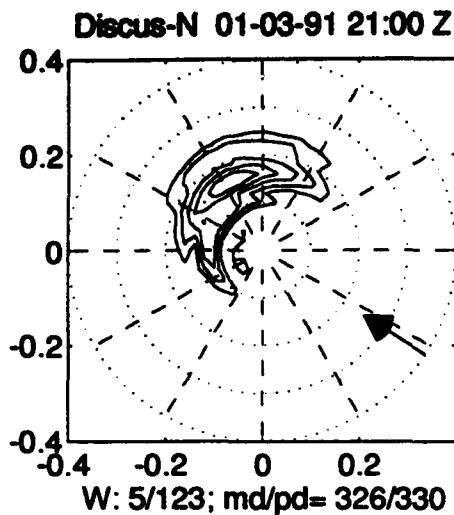


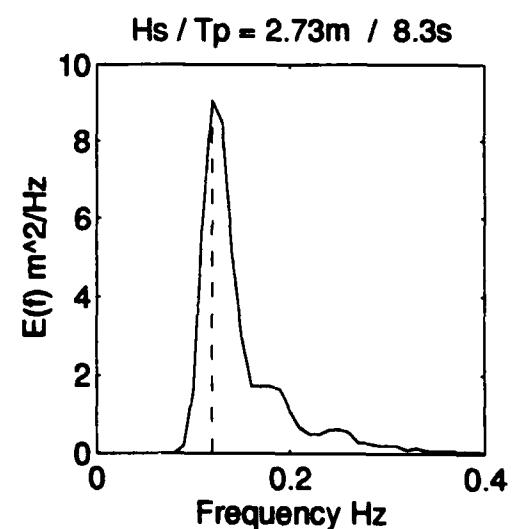
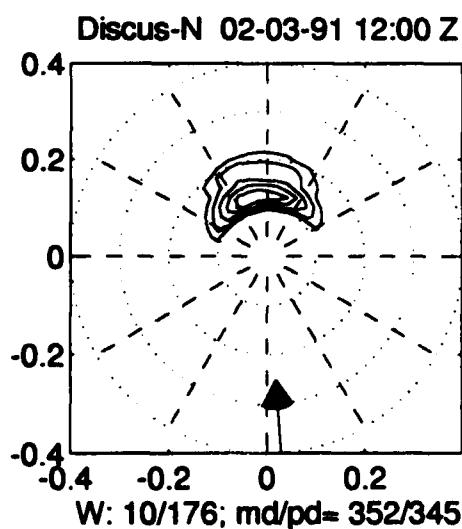
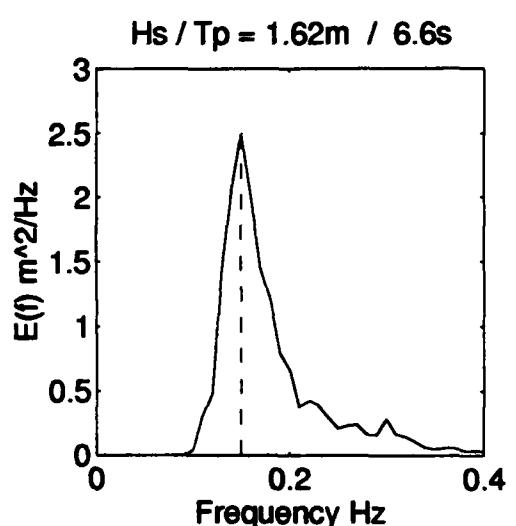
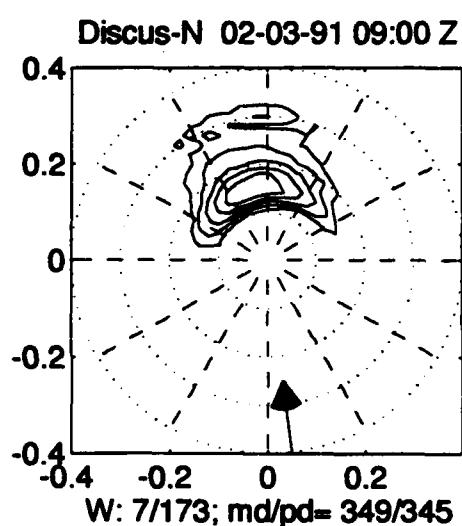
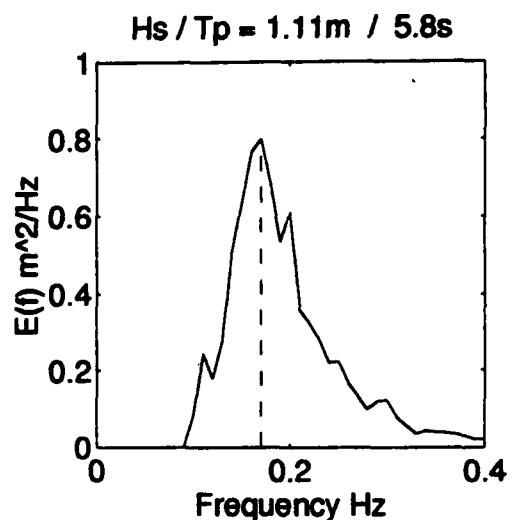
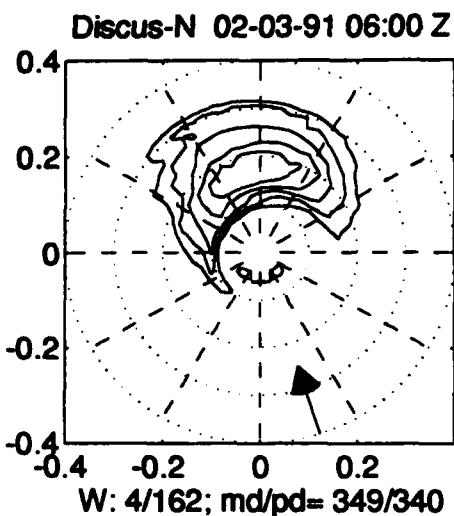


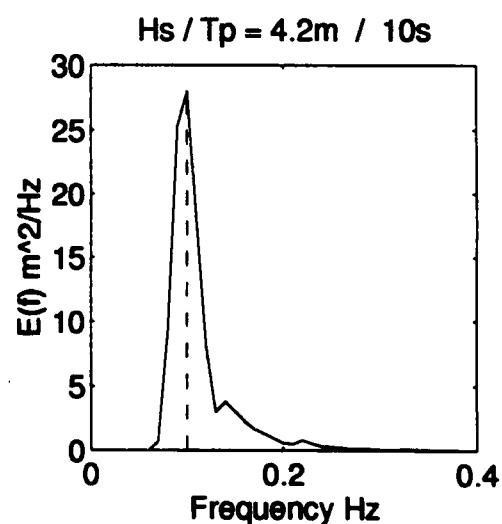
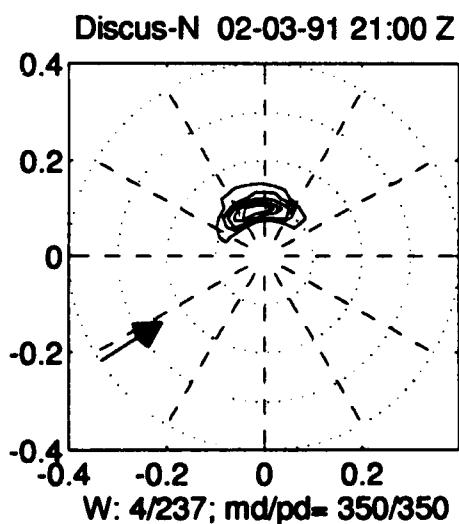
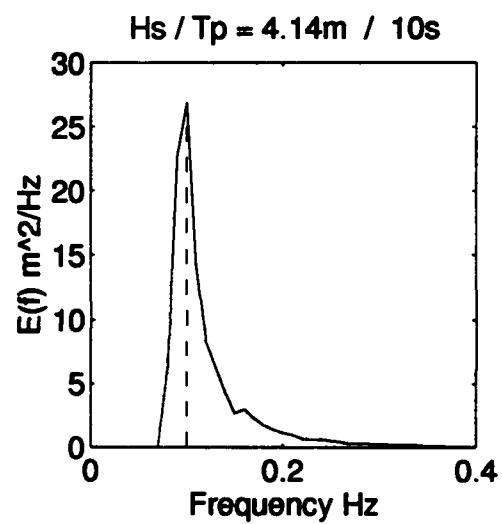
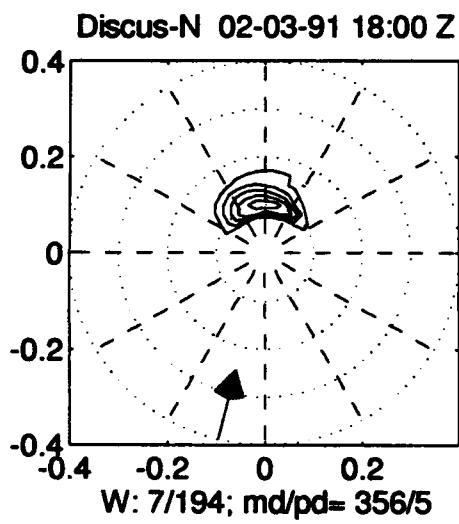
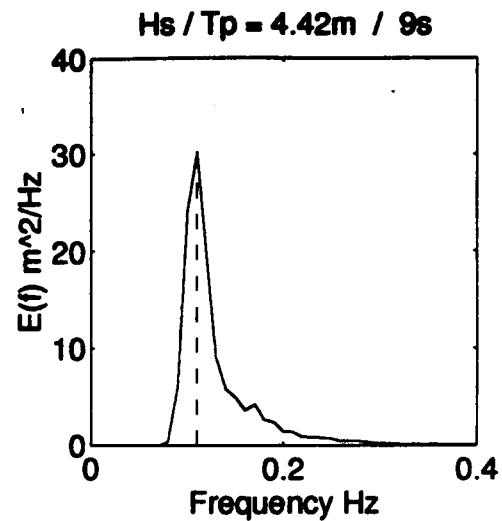
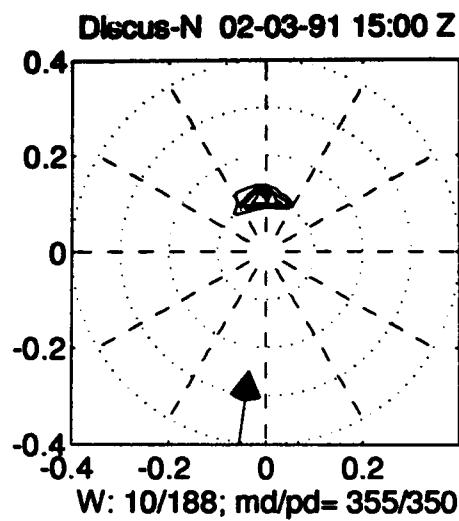


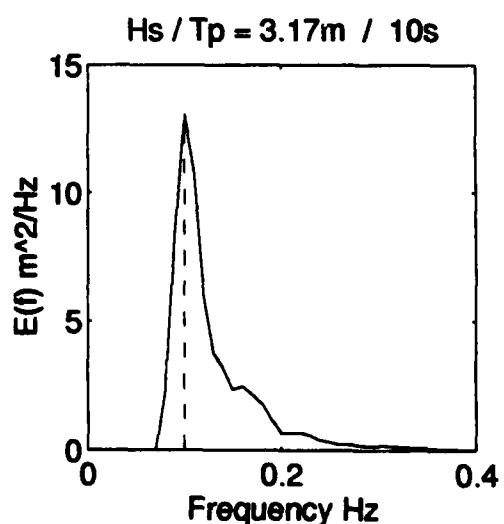
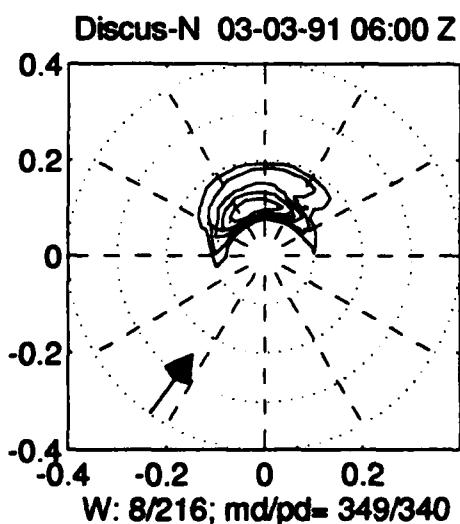
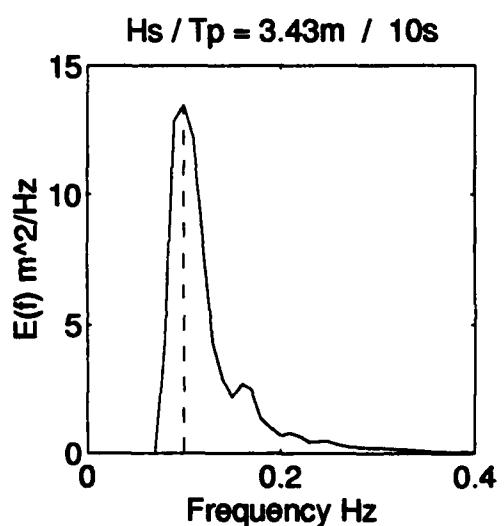
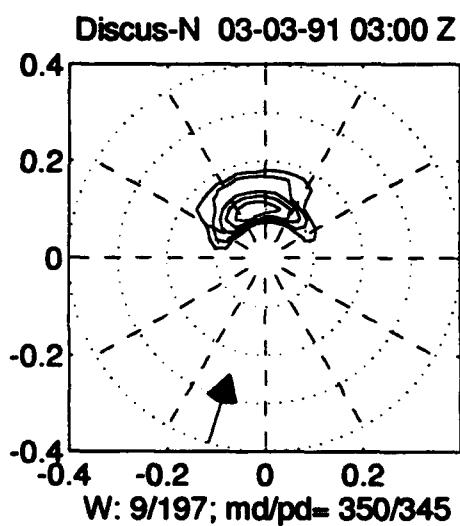
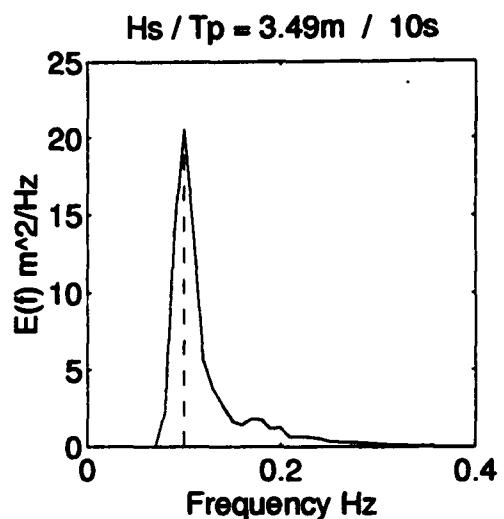
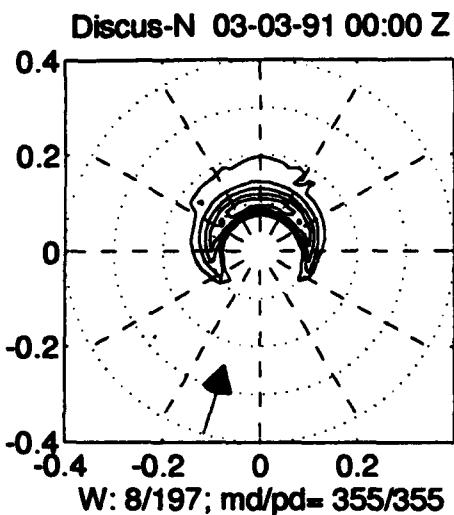


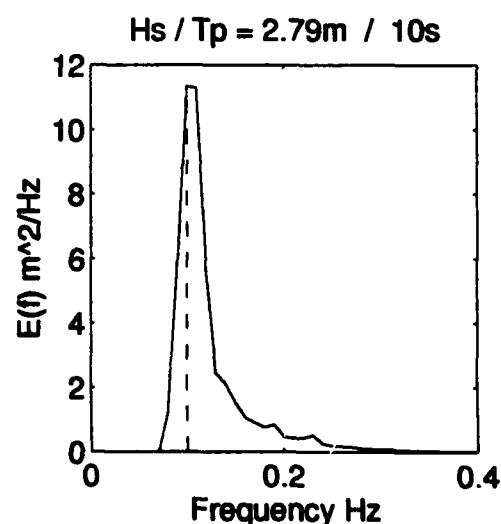
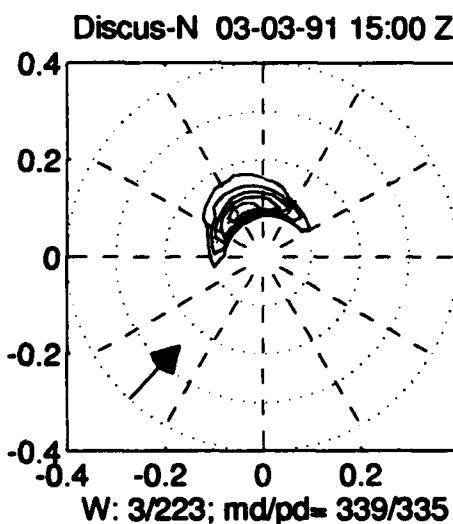
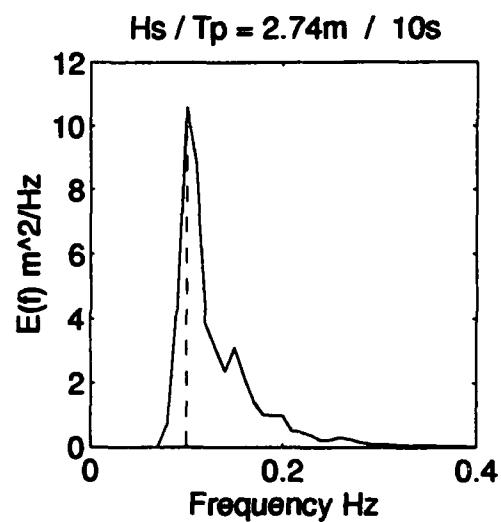
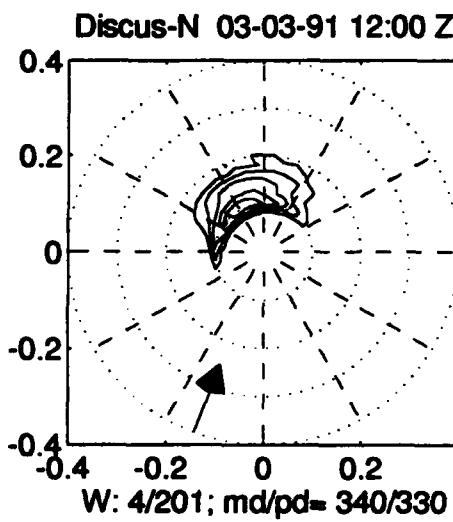
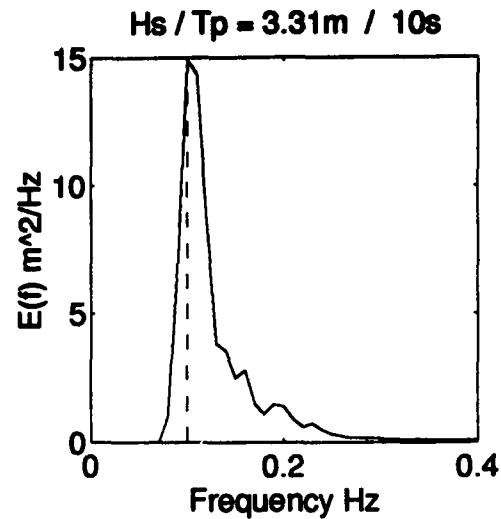
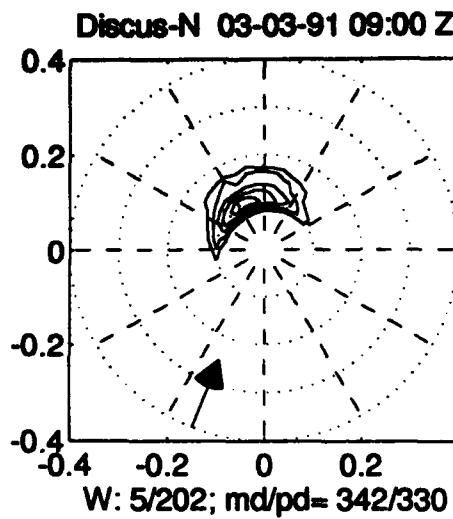


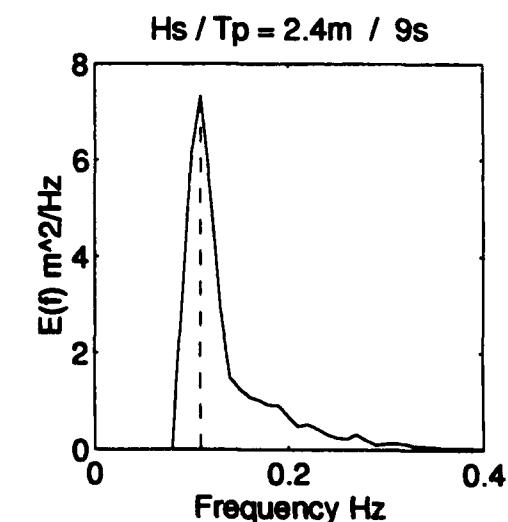
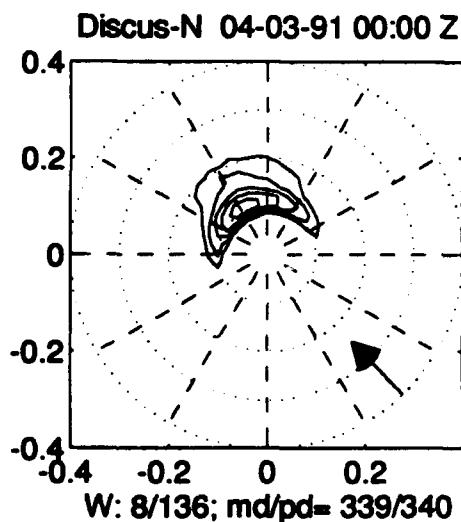
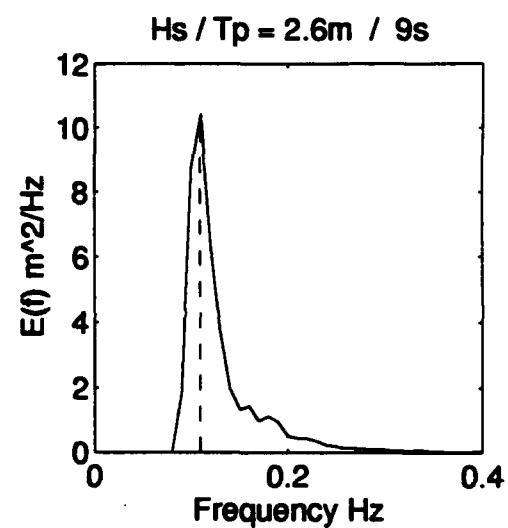
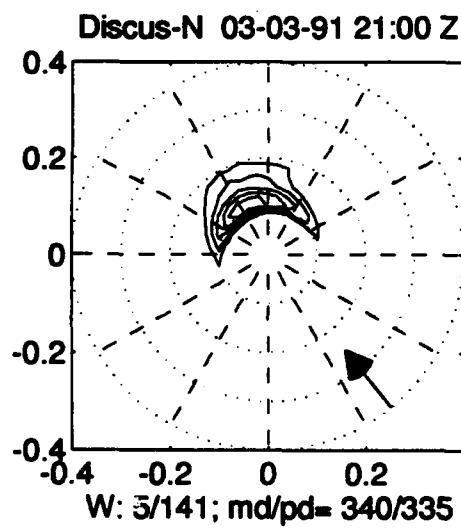
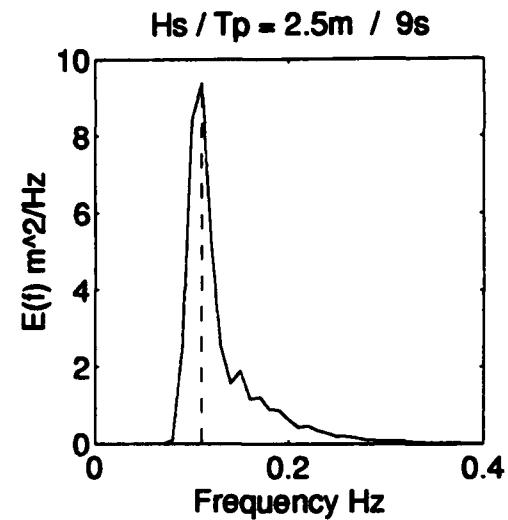
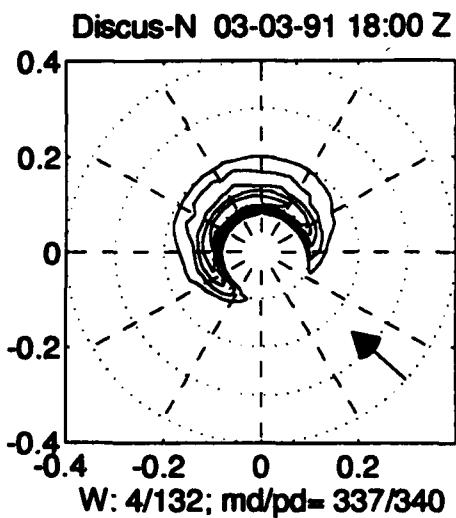


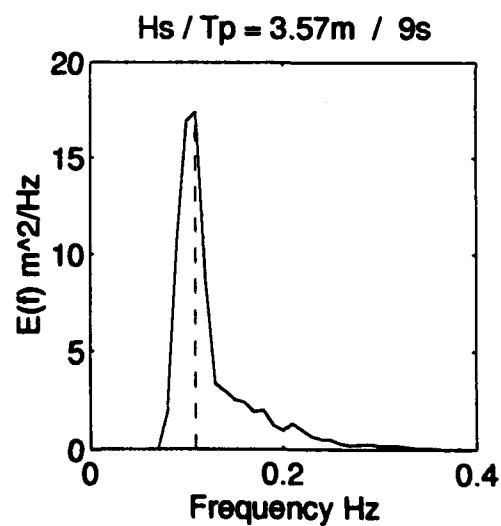
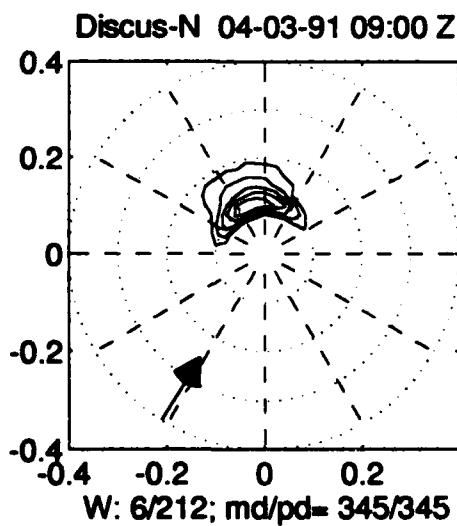
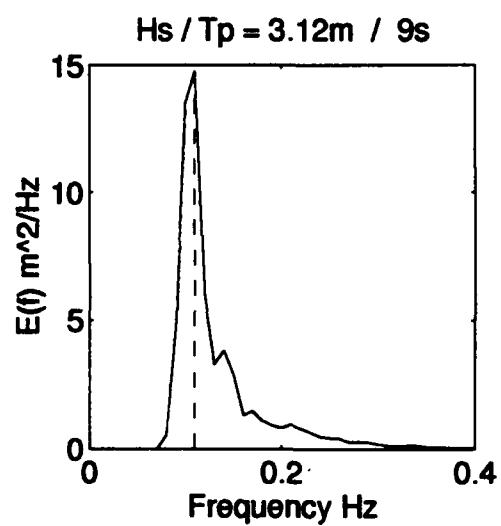
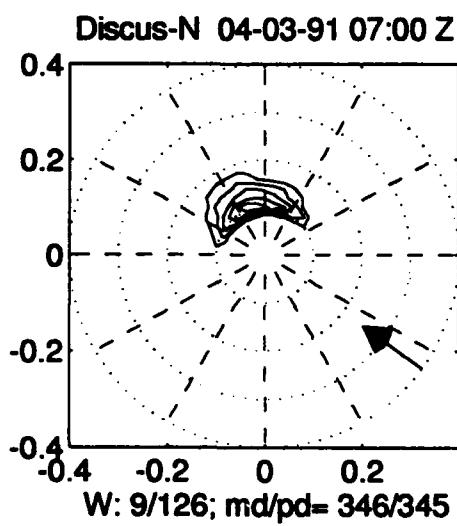
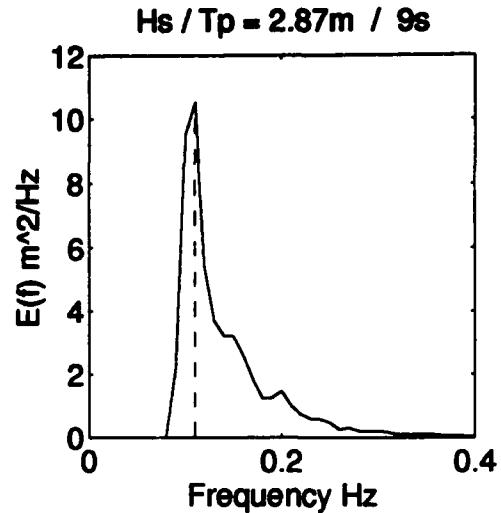
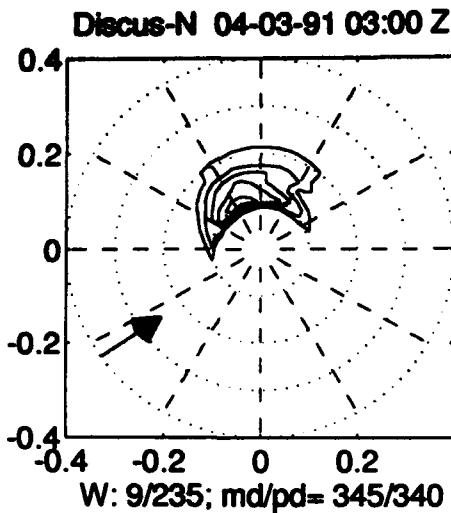


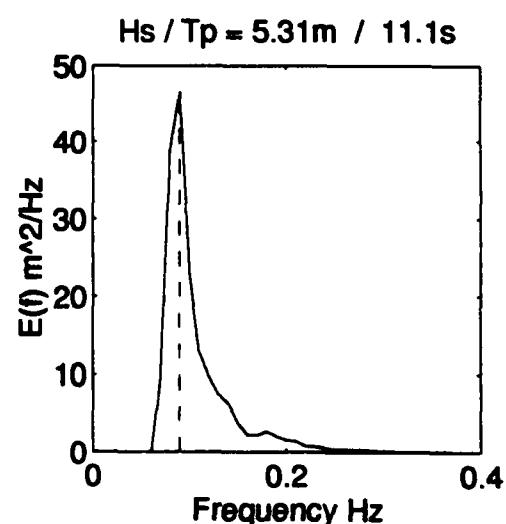
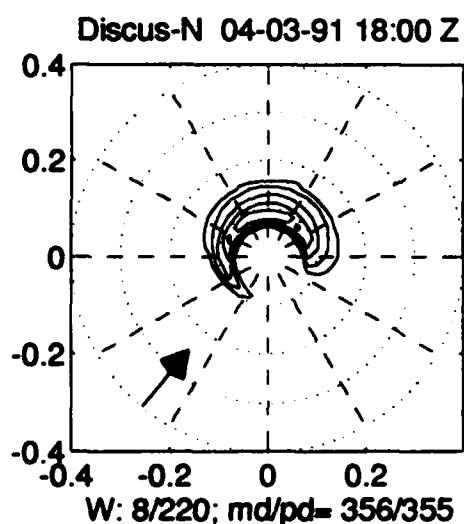
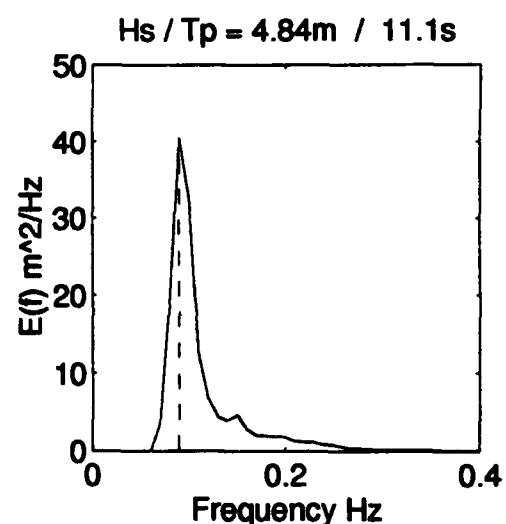
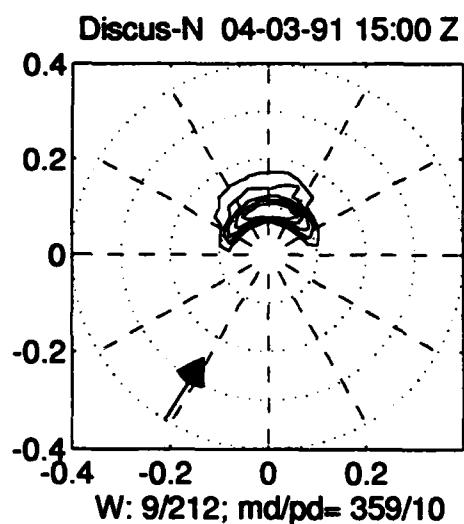
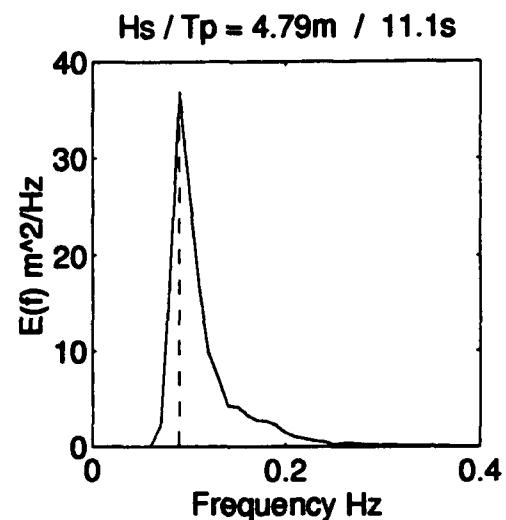
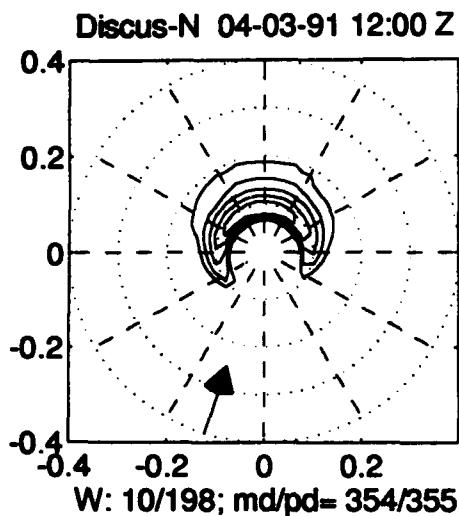




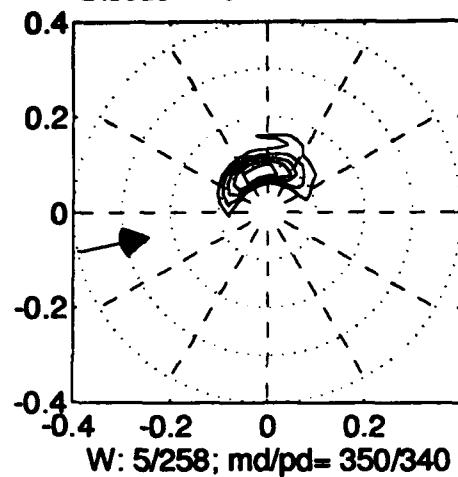




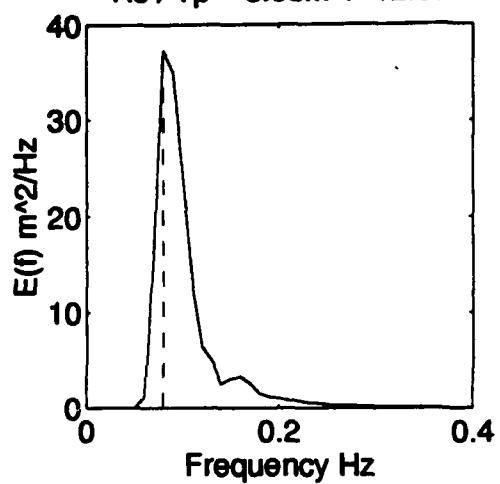




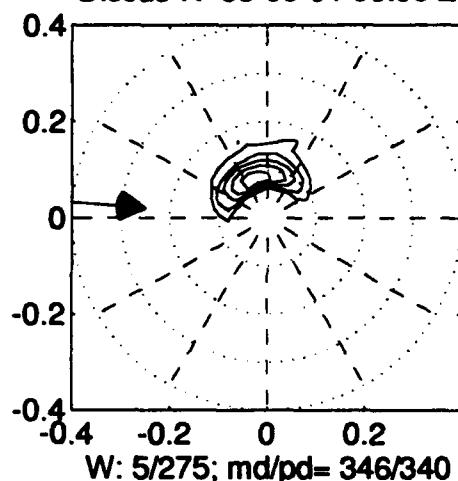
Discus-N 04-03-91 21:00 Z



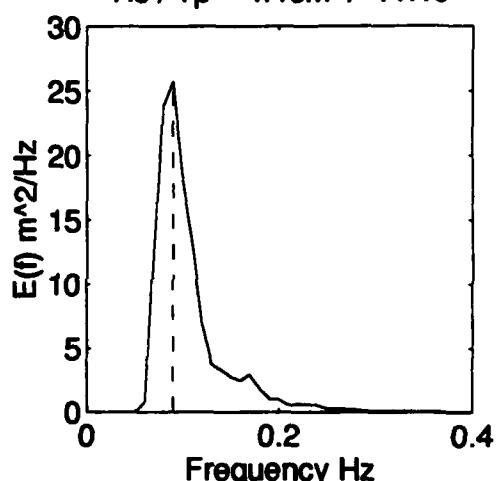
Hs / Tp = 5.05m / 12.5s



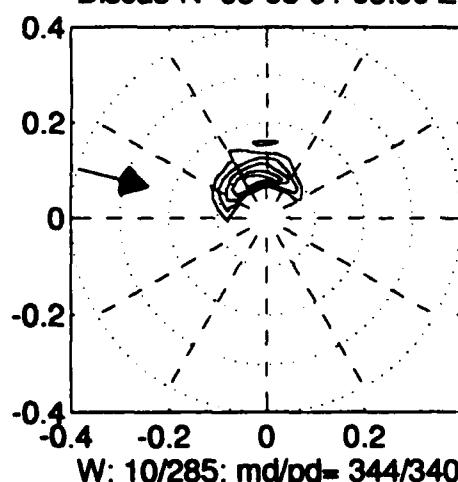
Discus-N 05-03-91 00:00 Z



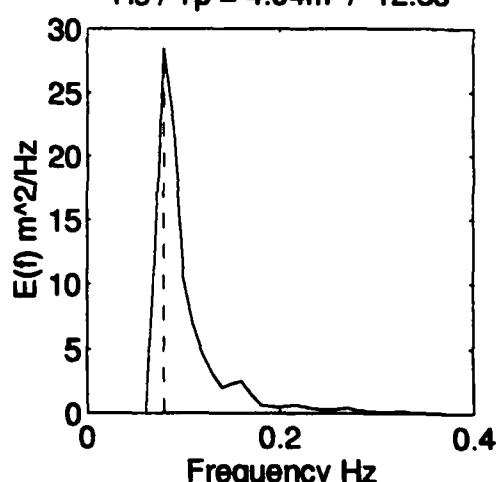
Hs / Tp = 4.46m / 11.1s

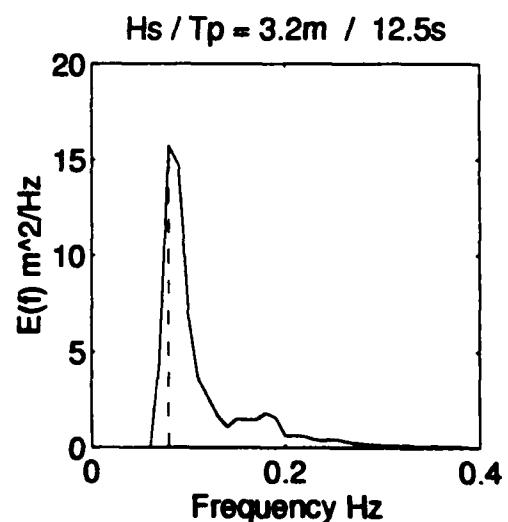
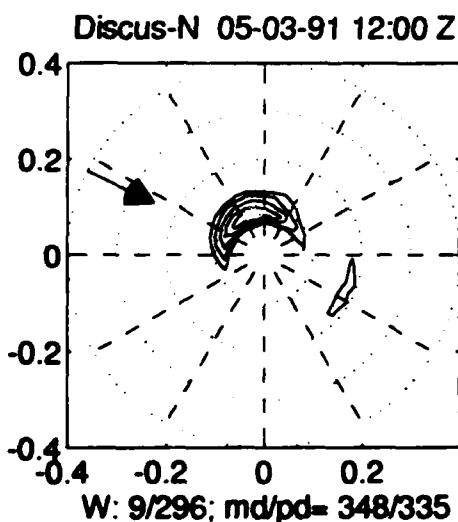
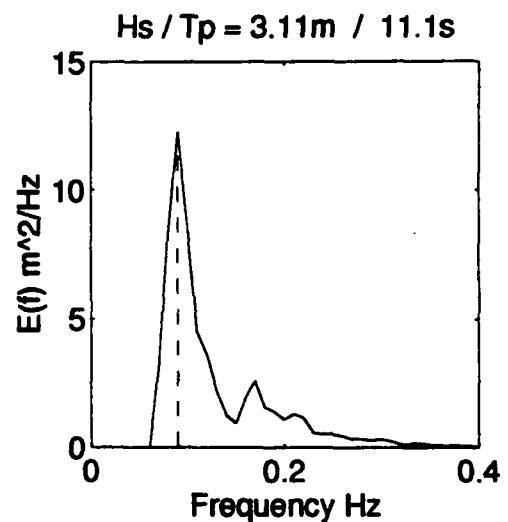
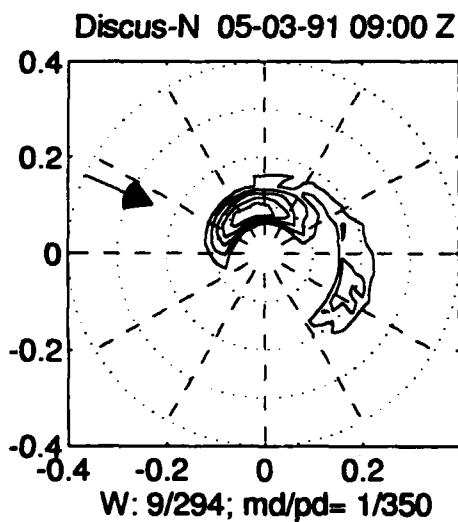
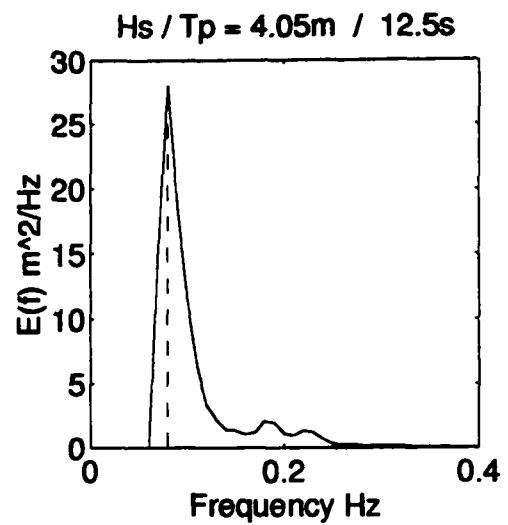
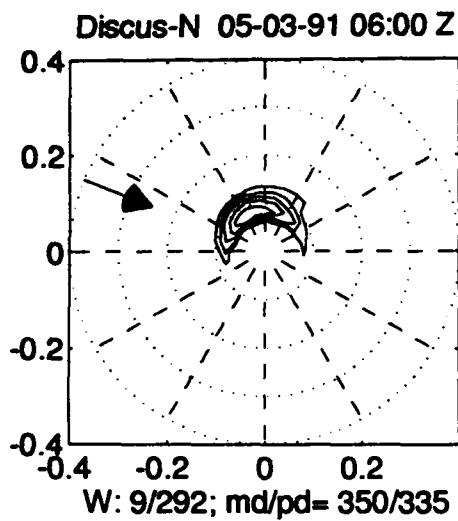


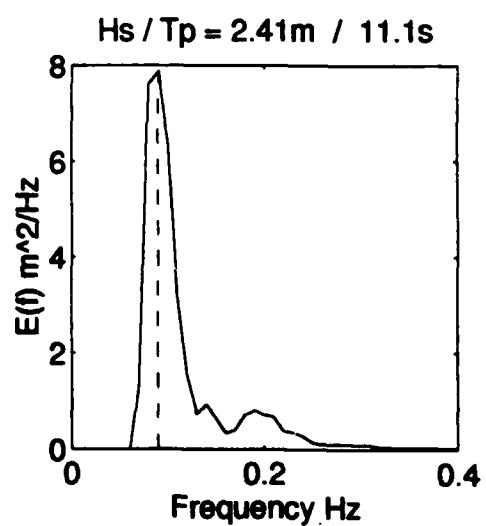
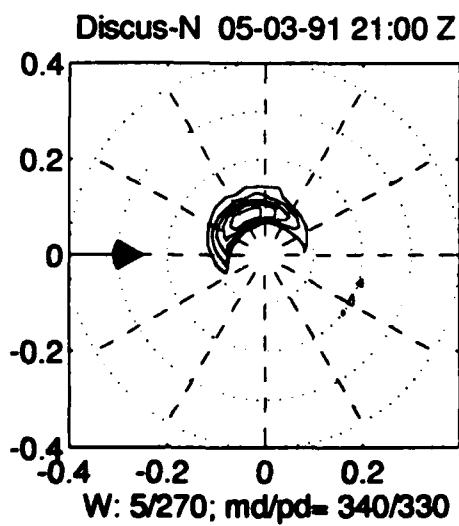
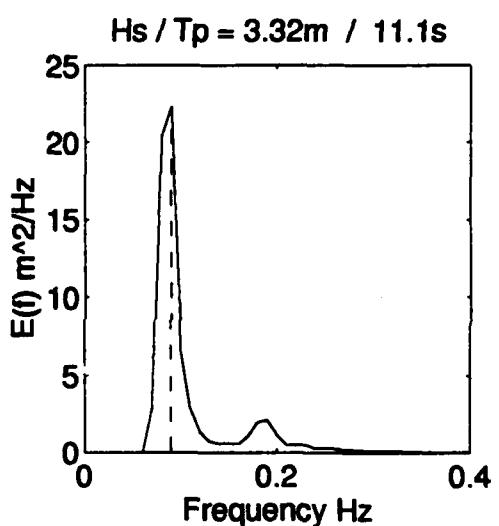
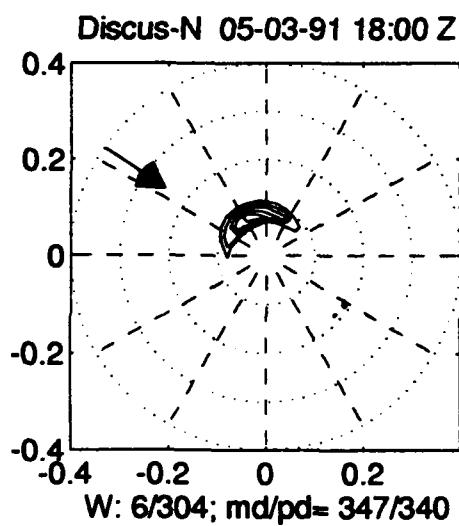
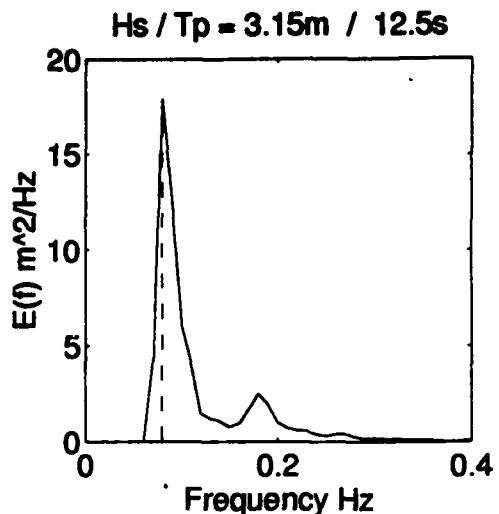
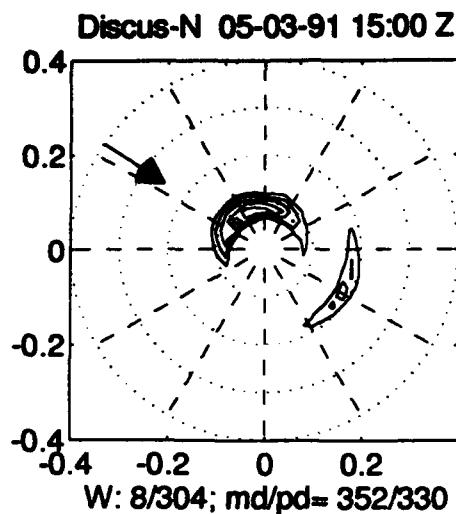
Discus-N 05-03-91 03:00 Z

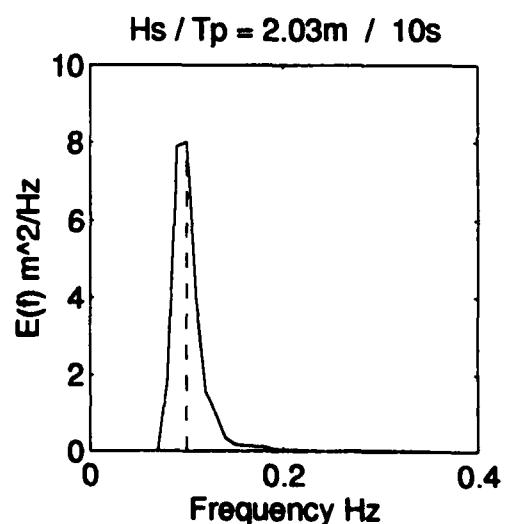
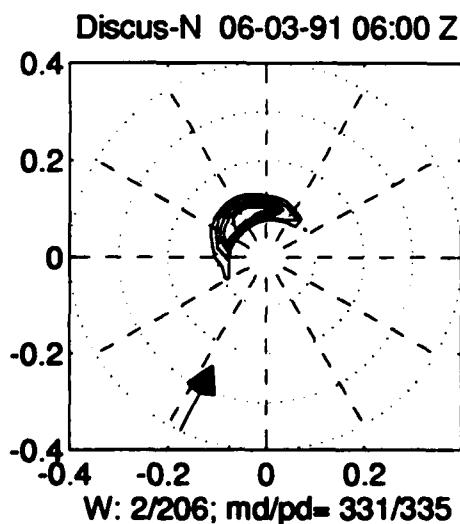
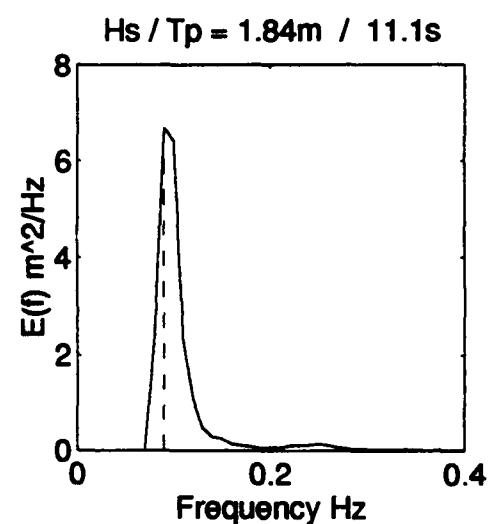
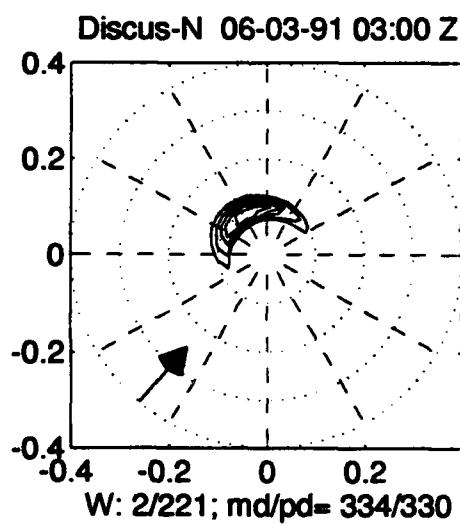
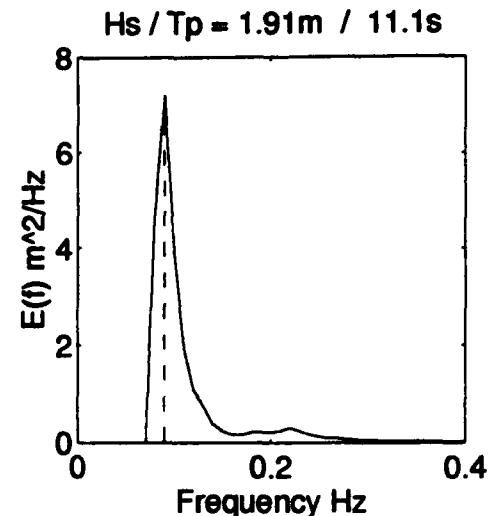
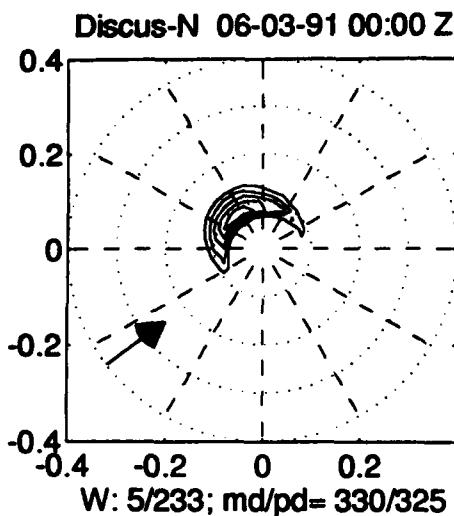


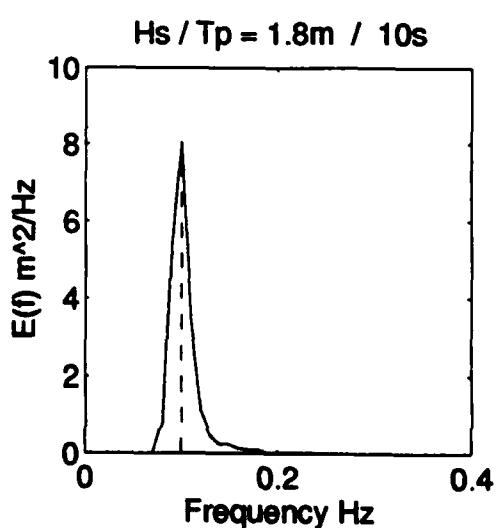
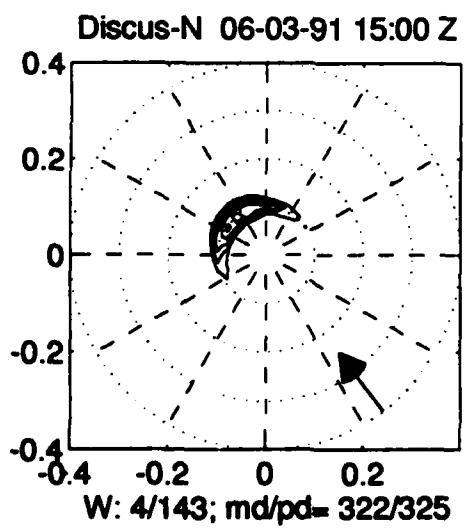
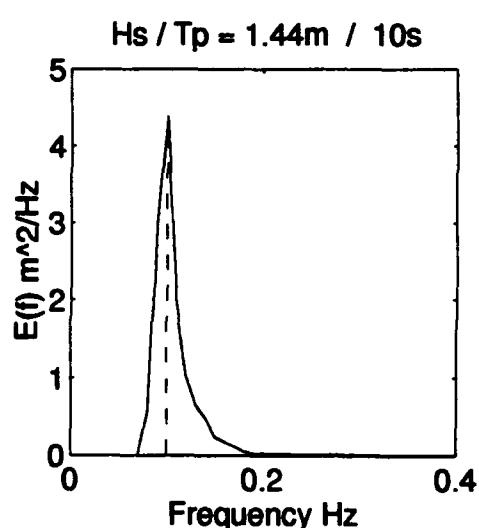
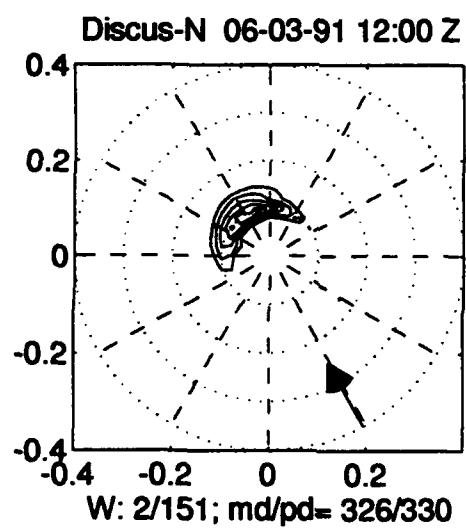
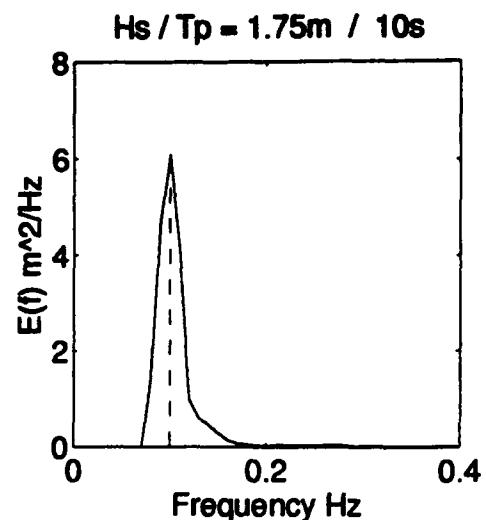
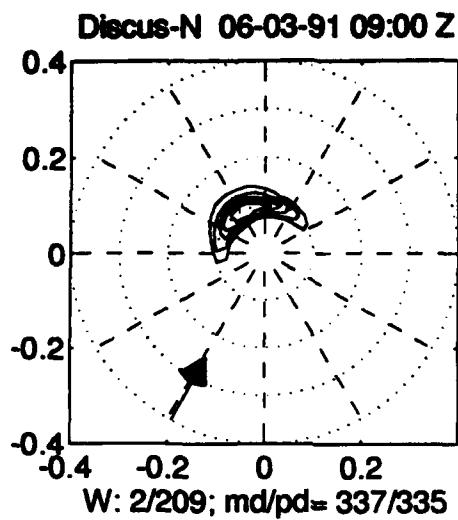
Hs / Tp = 4.04m / 12.5s

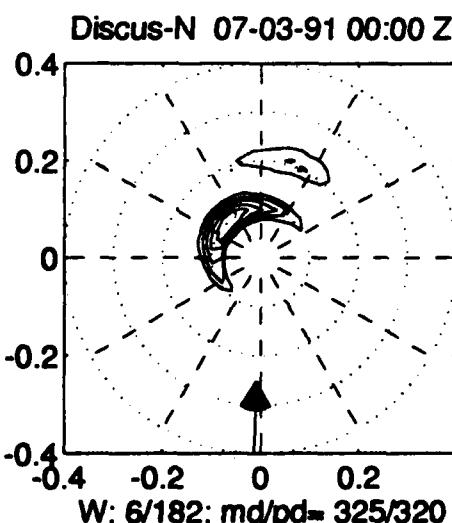
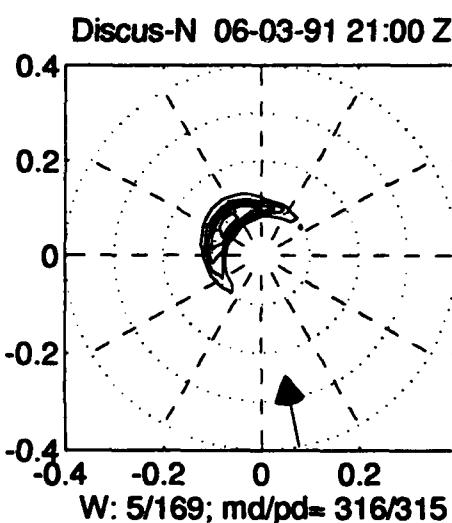
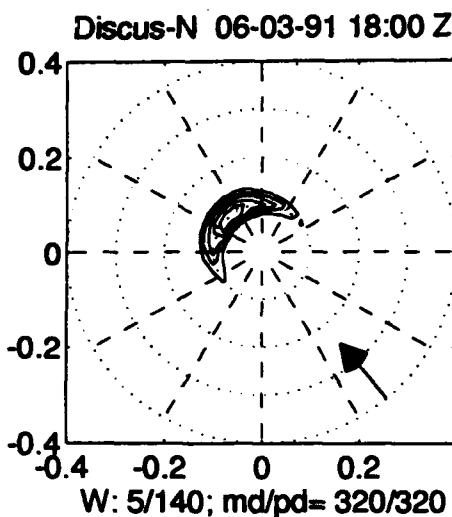


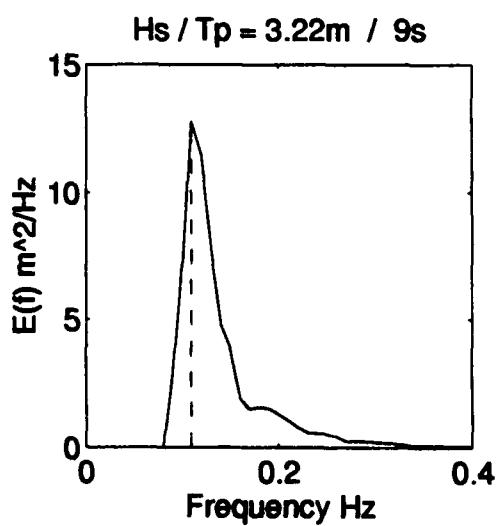
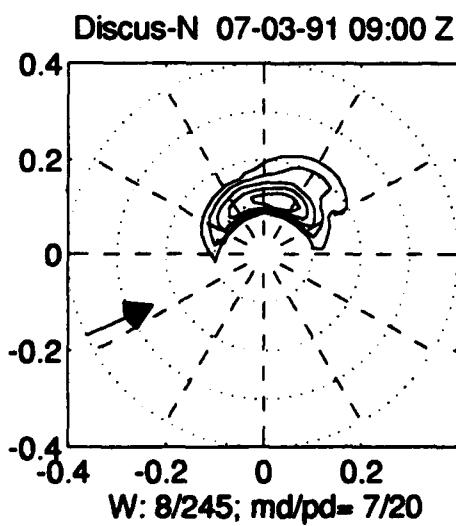
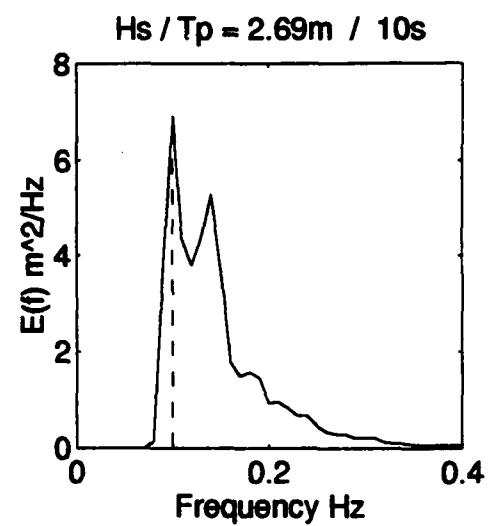
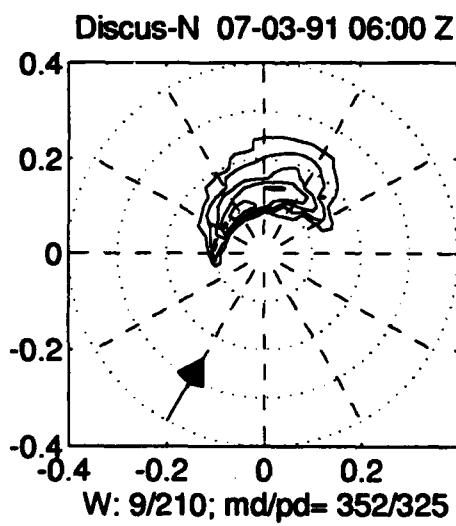
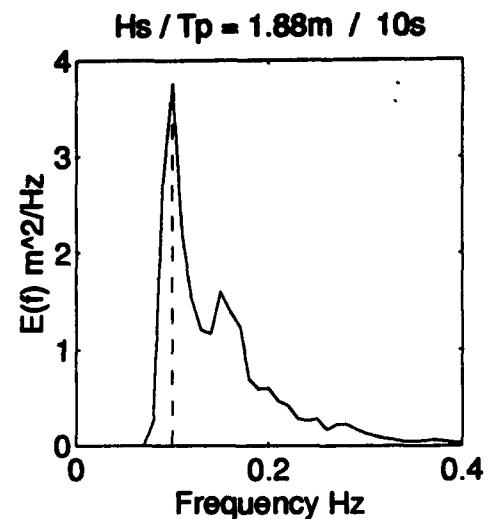
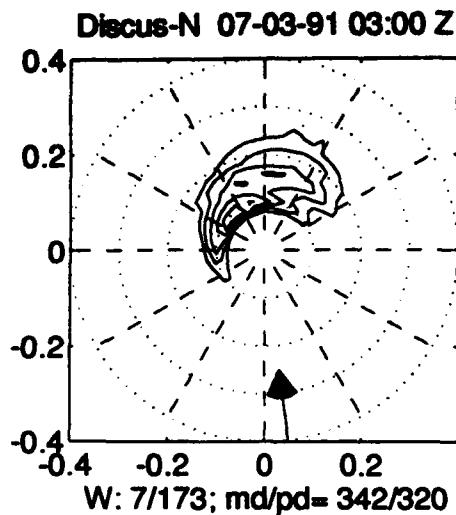


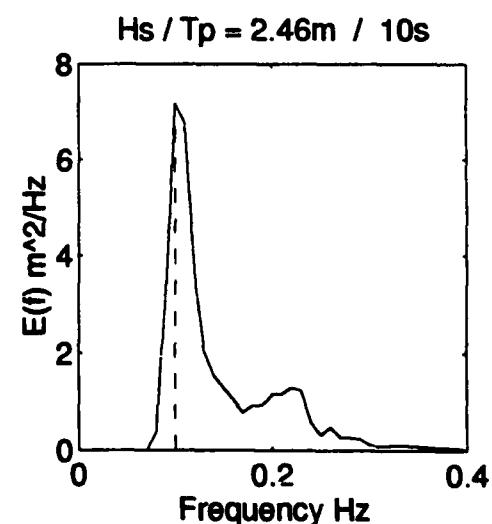
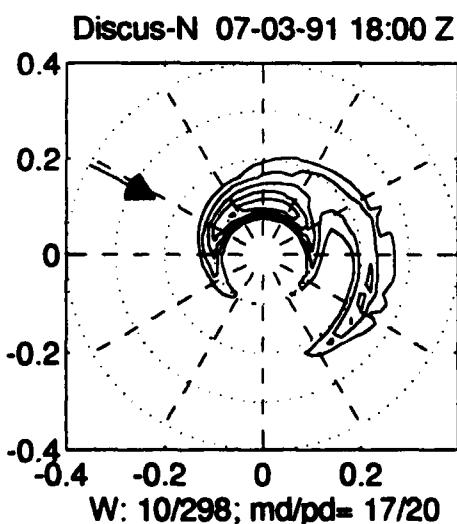
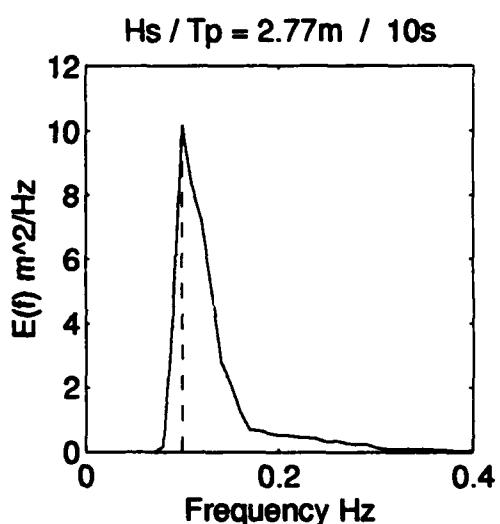
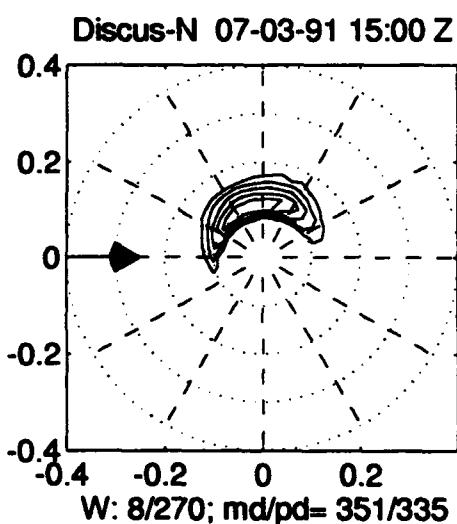
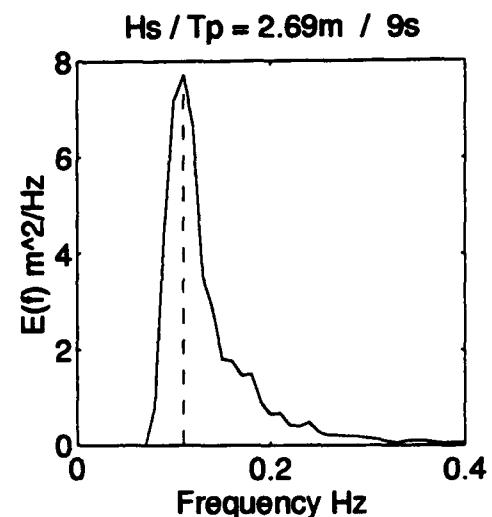
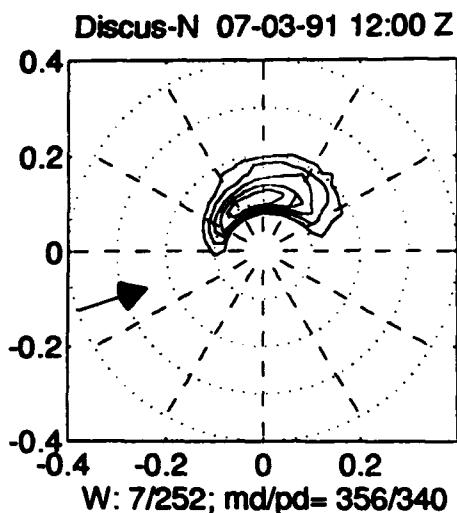


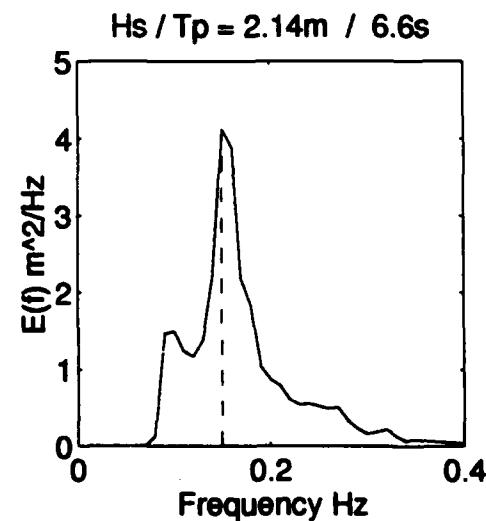
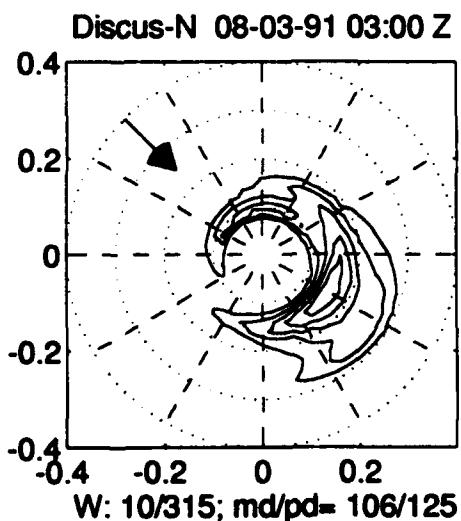
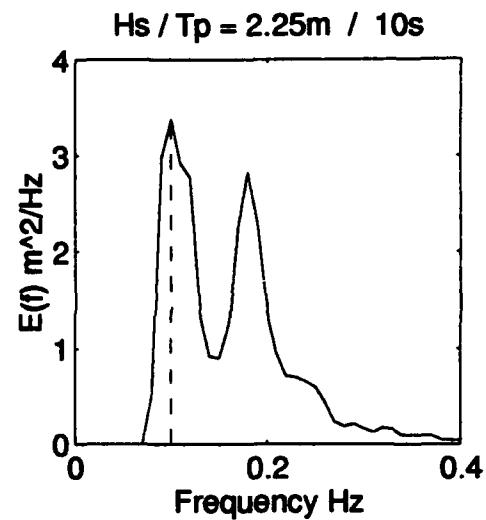
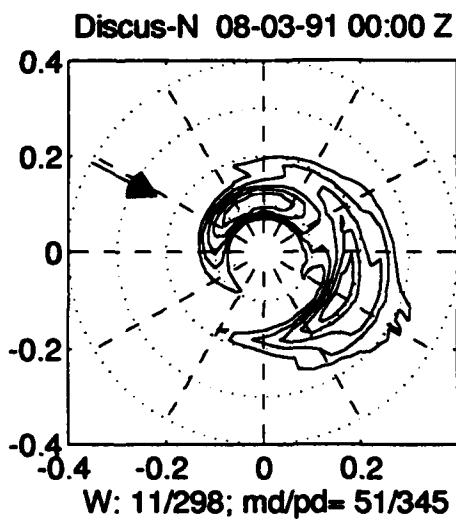
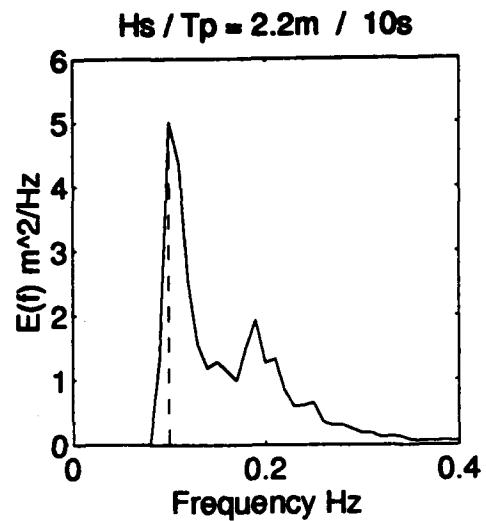
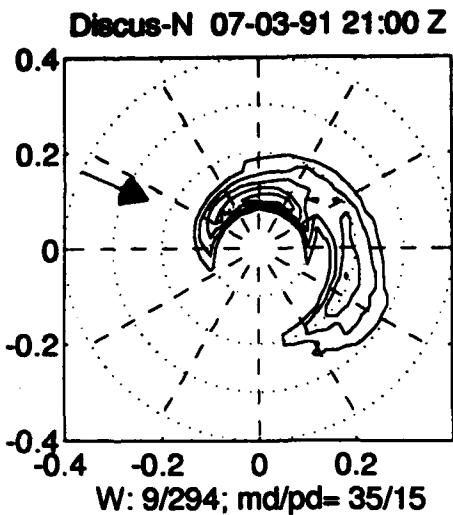


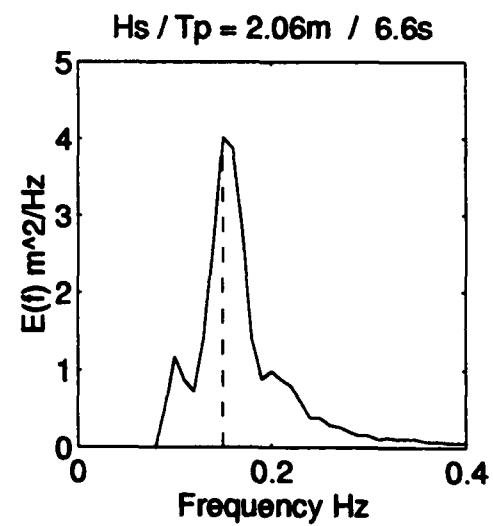
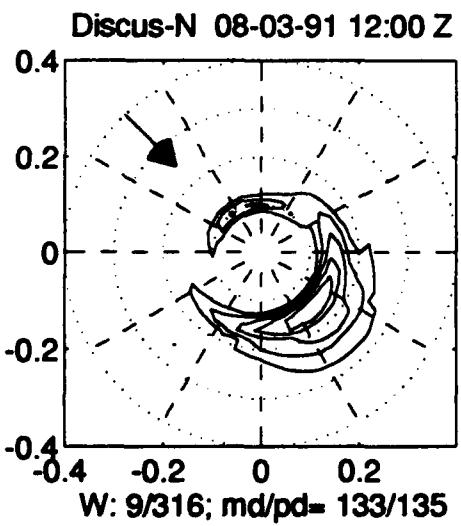
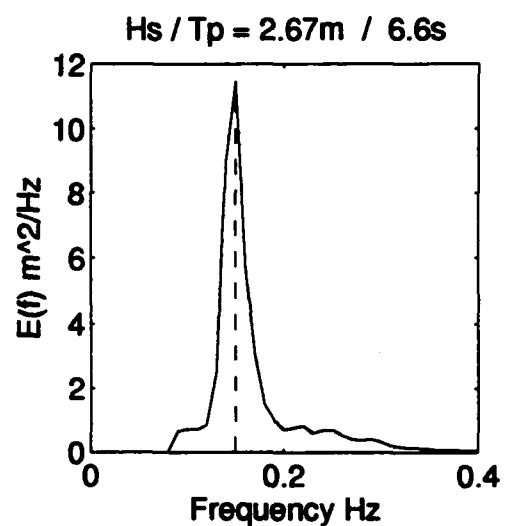
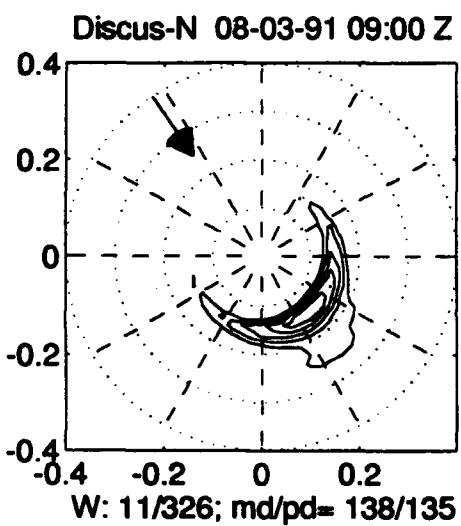
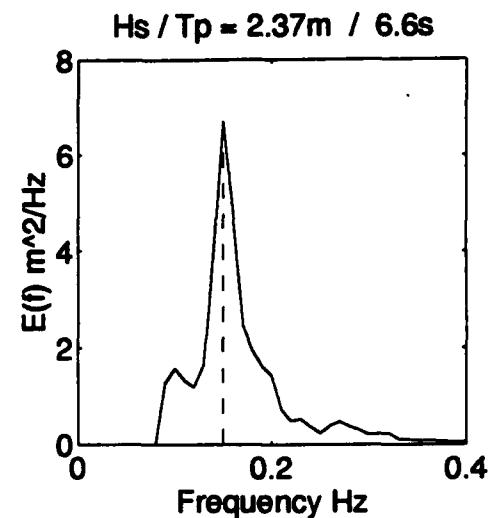
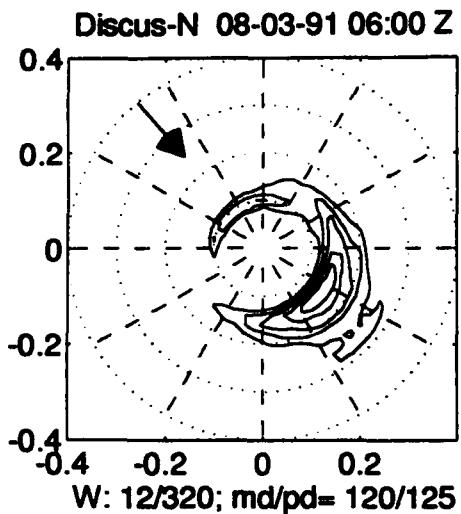


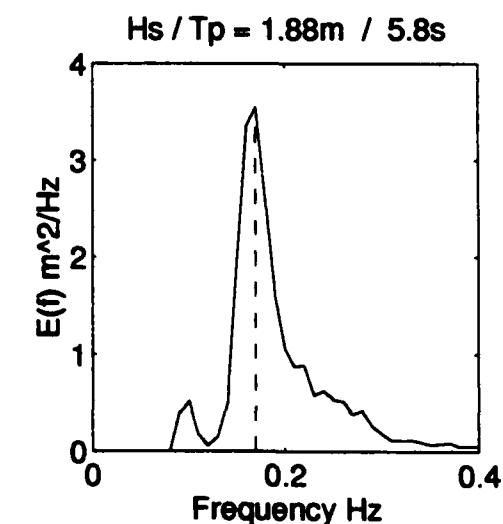
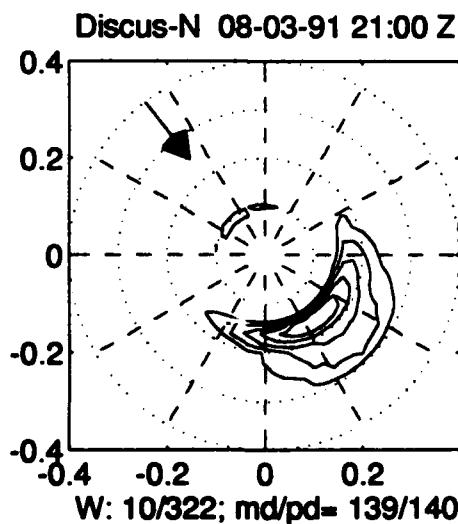
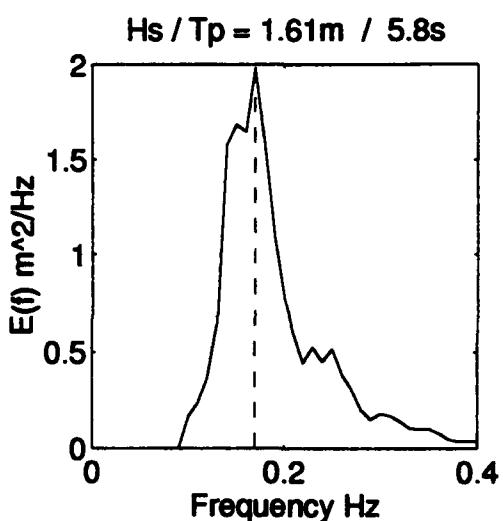
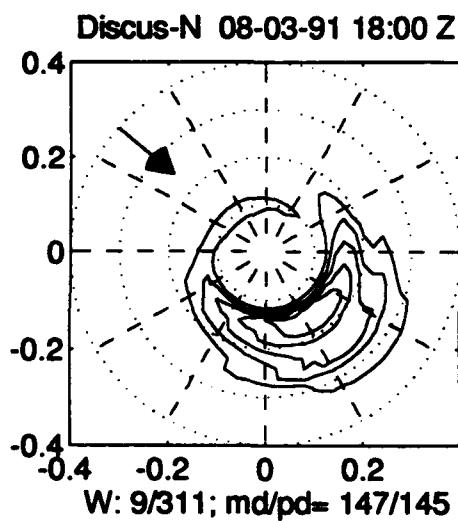
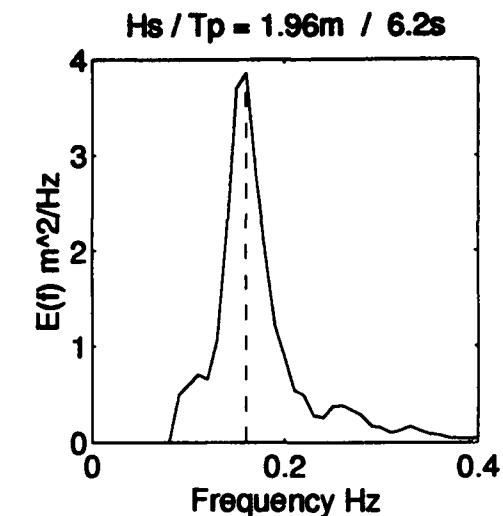
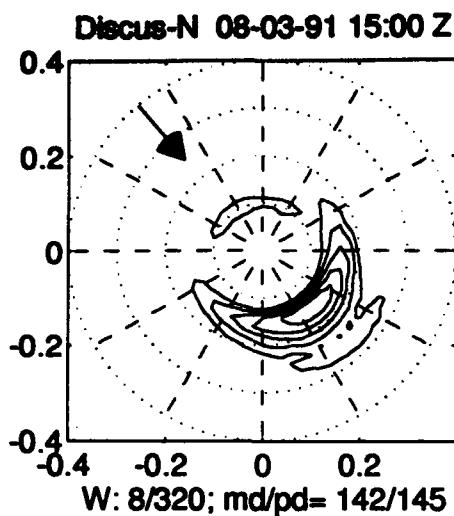


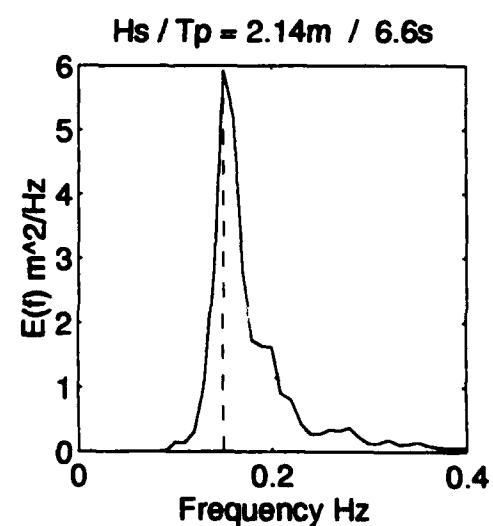
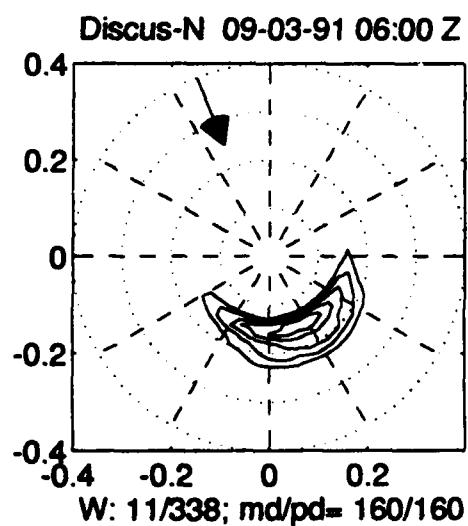
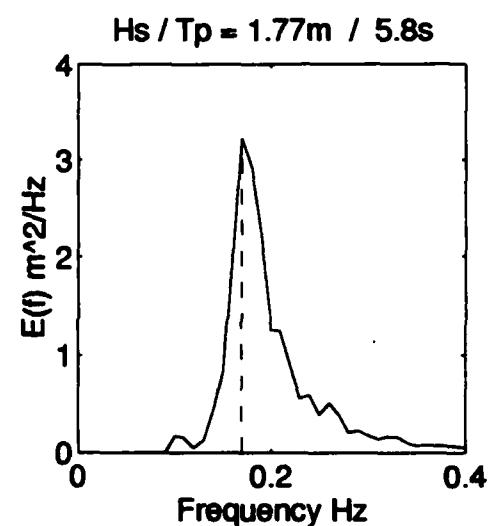
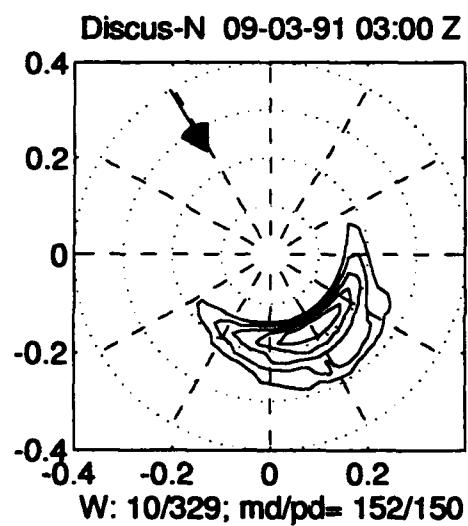
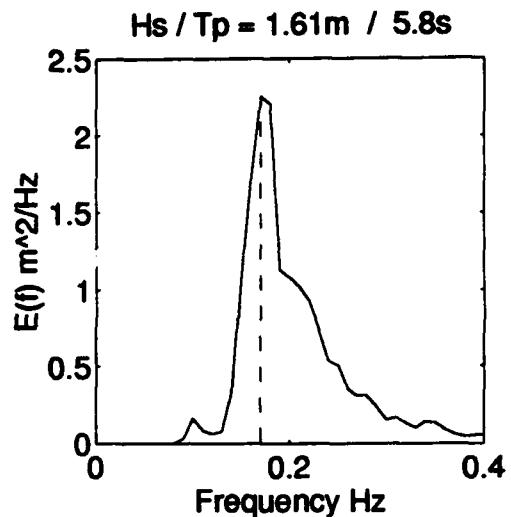
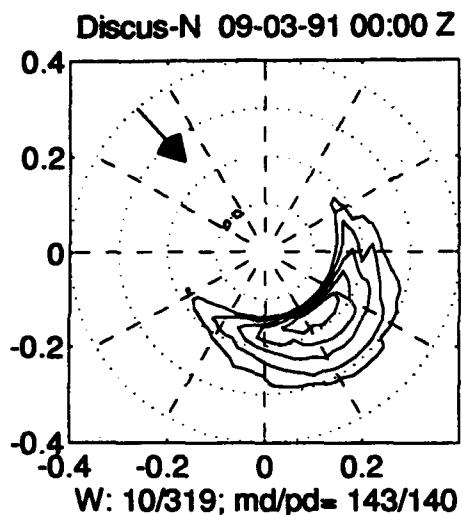




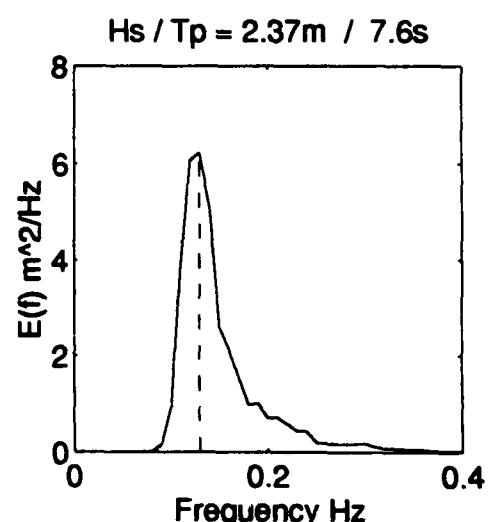
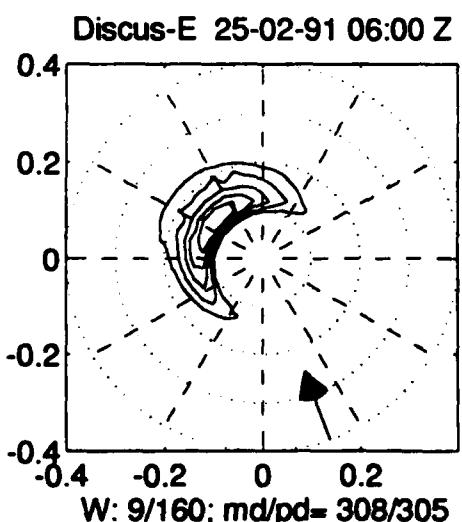
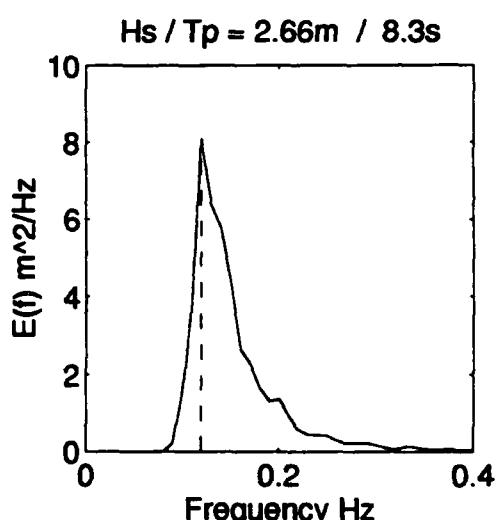
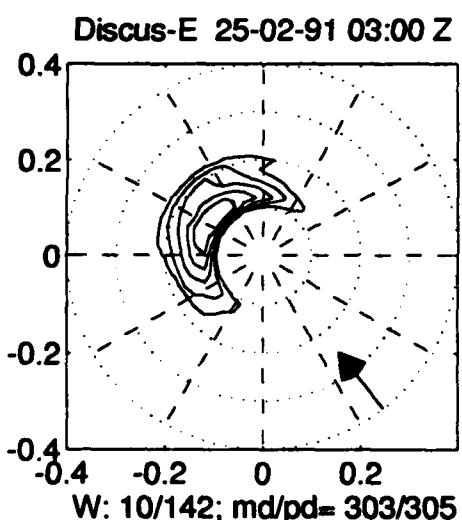
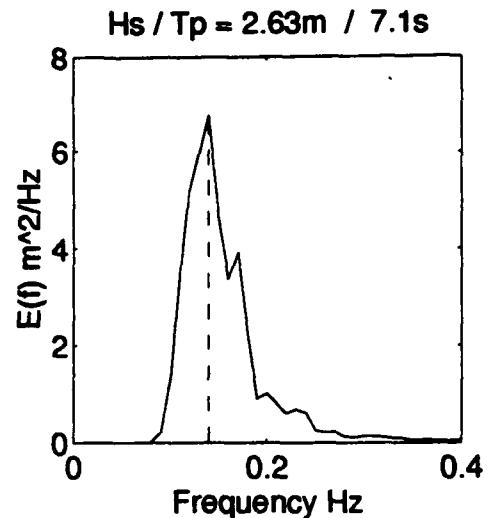
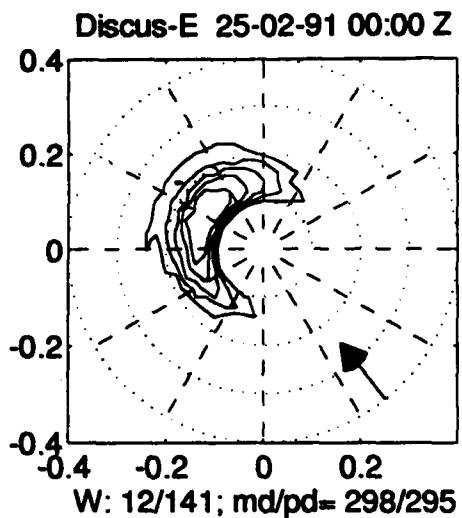


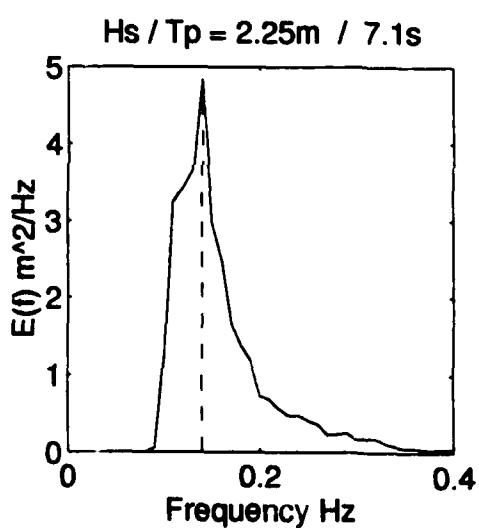
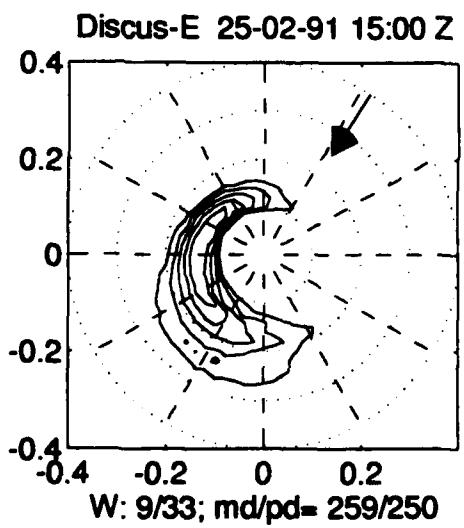
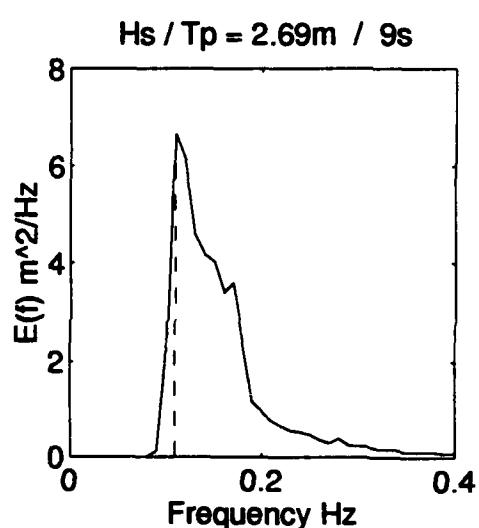
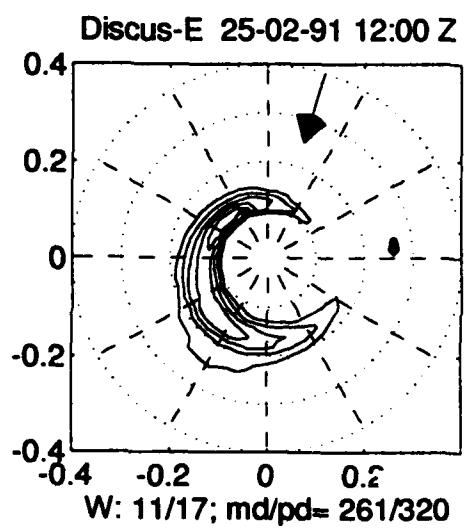
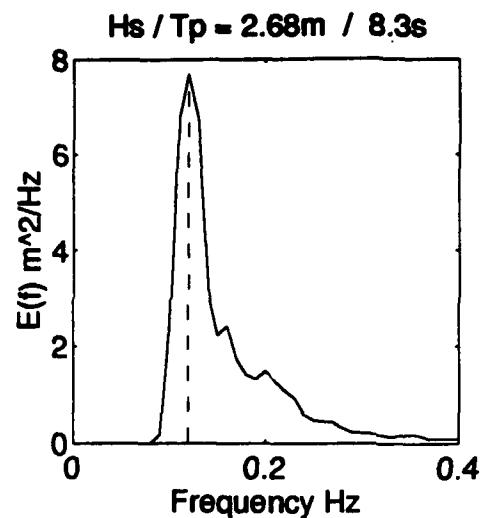
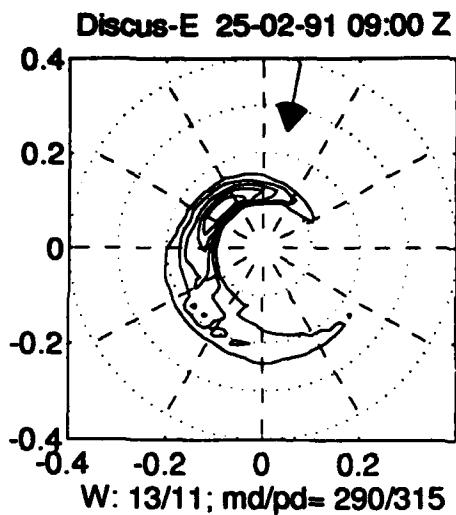


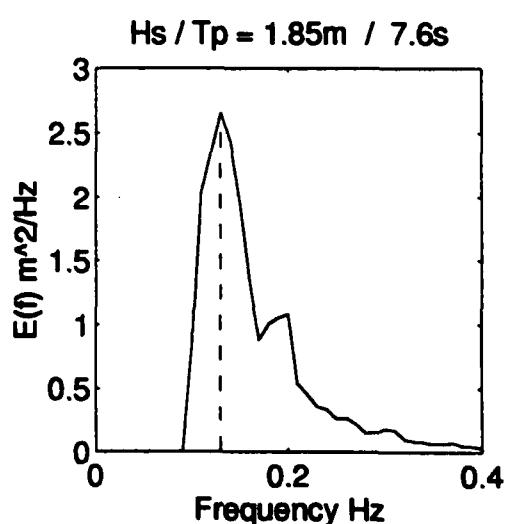
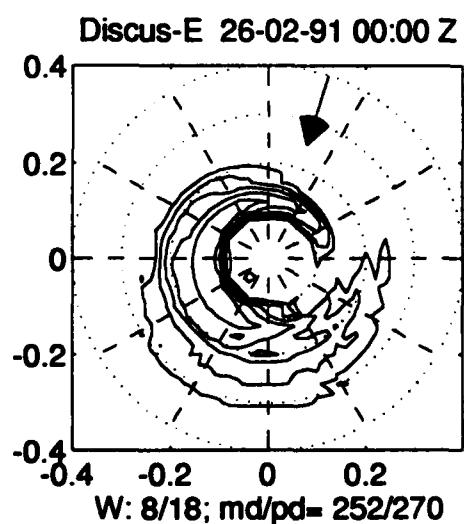
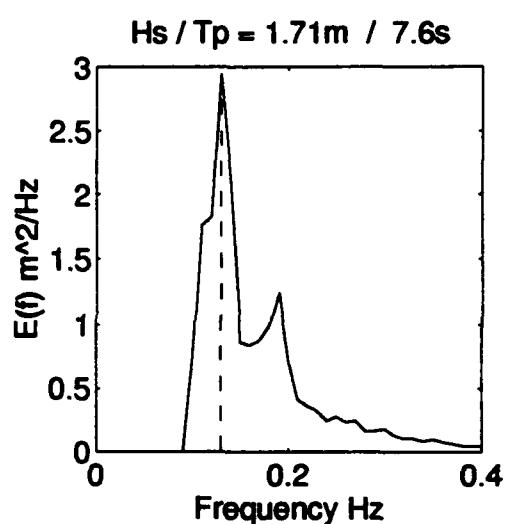
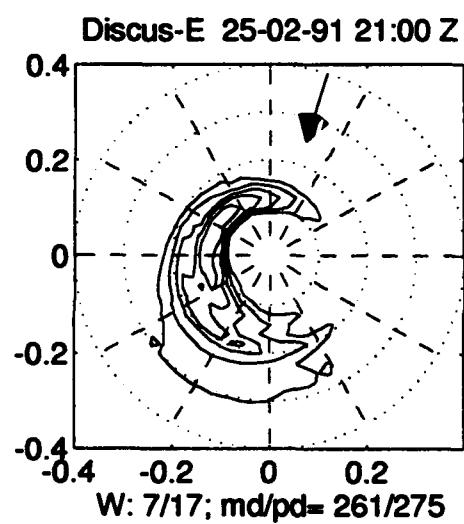
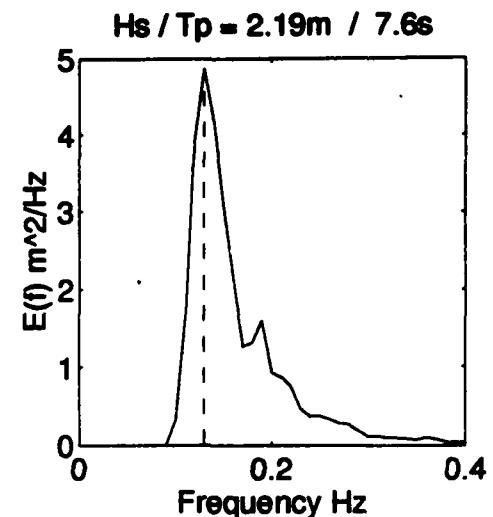
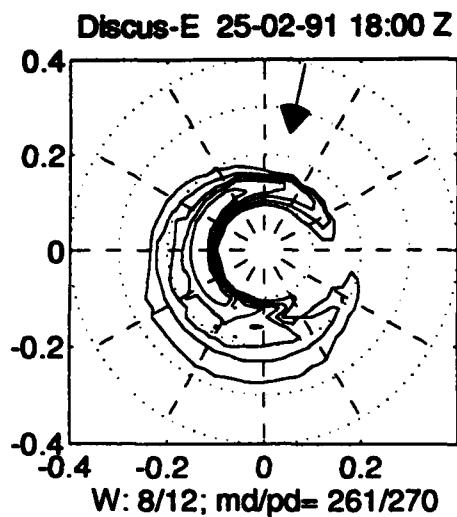


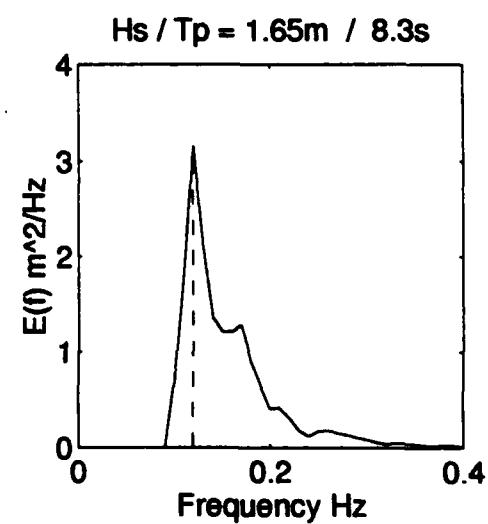
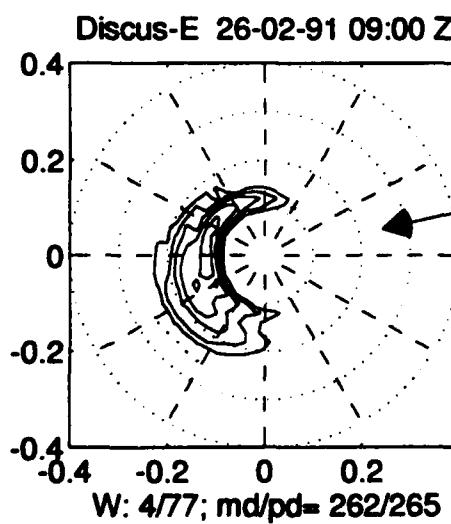
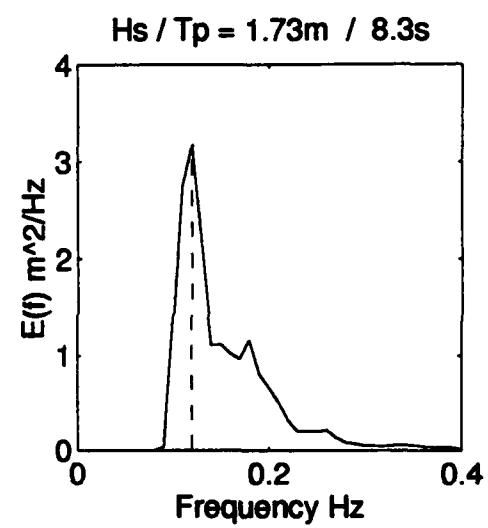
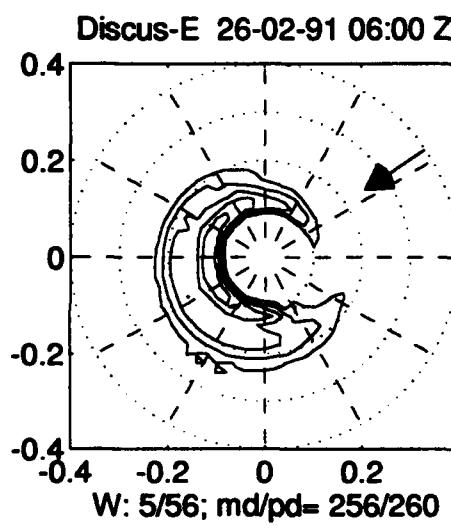
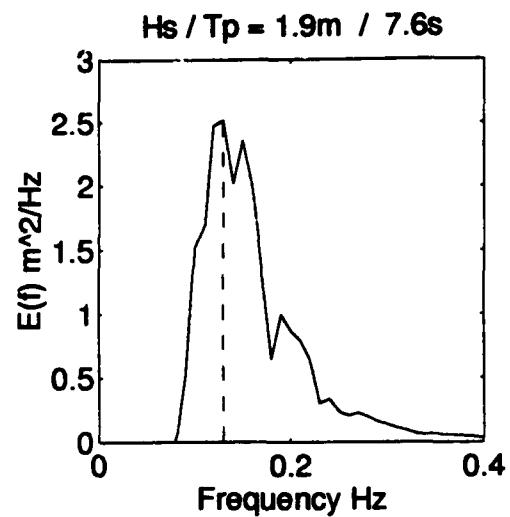
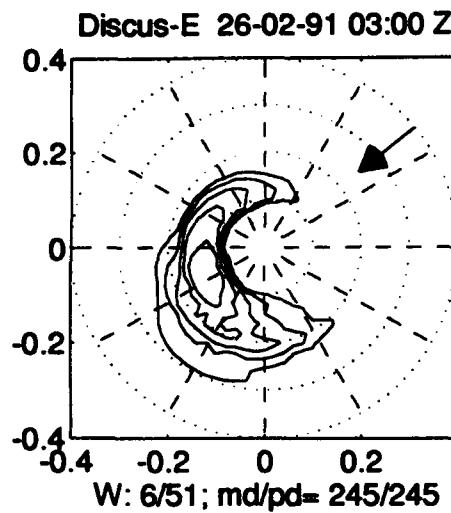


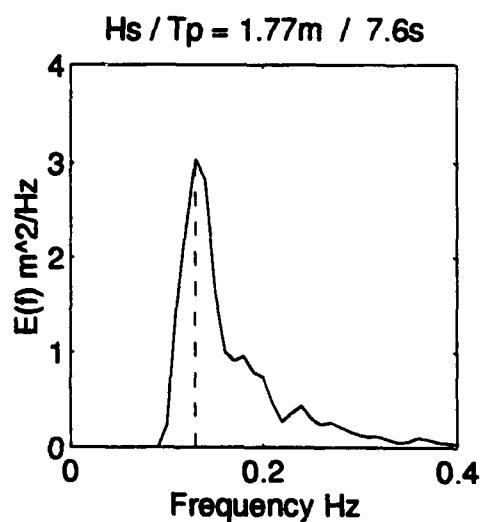
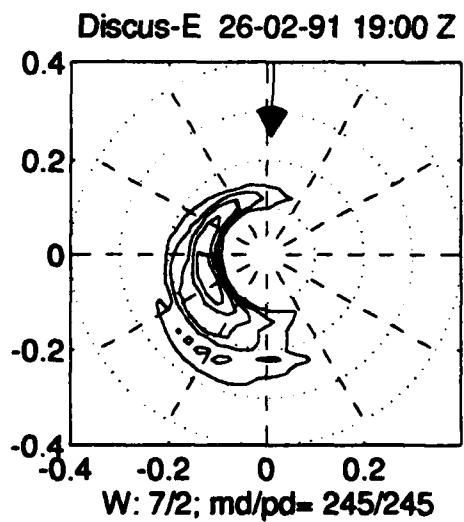
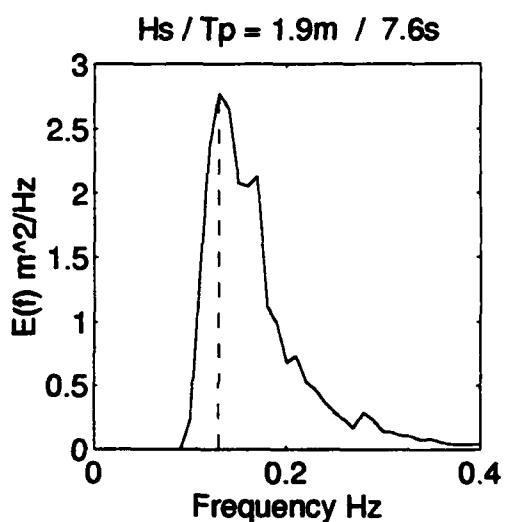
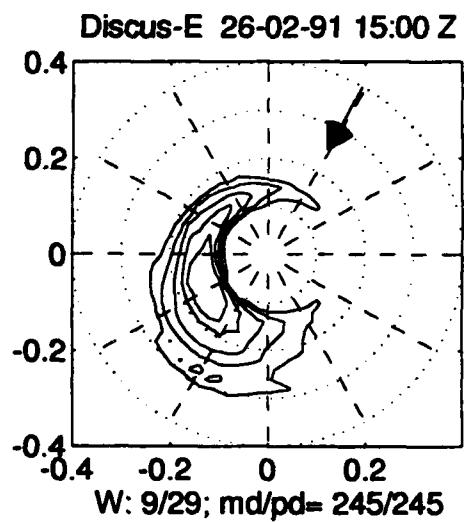
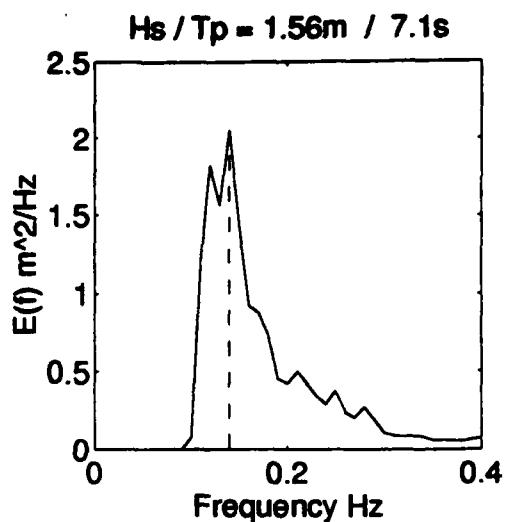
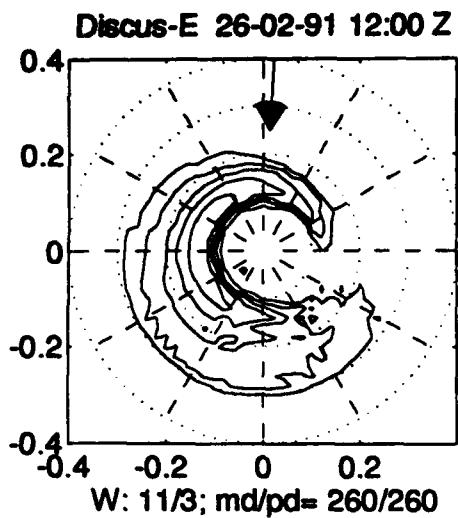
B.2: Discus Buoy "East"

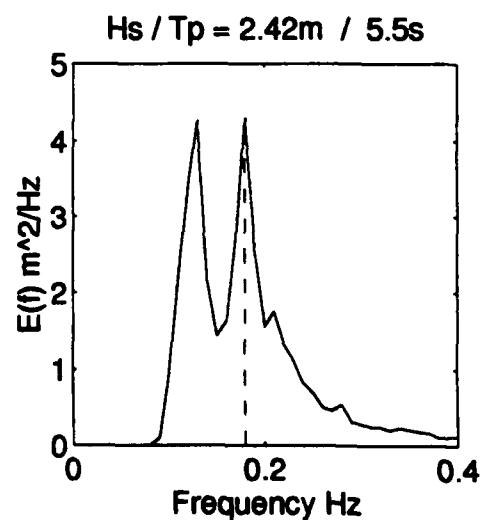
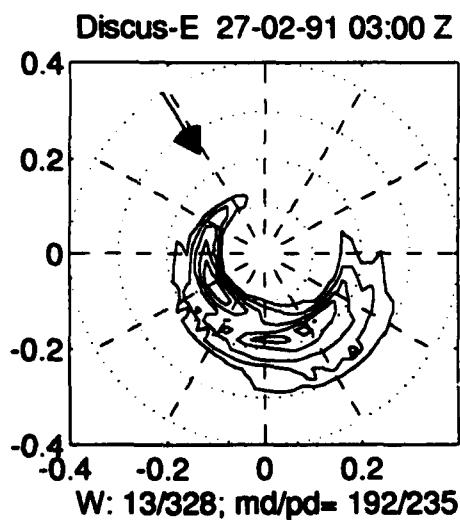
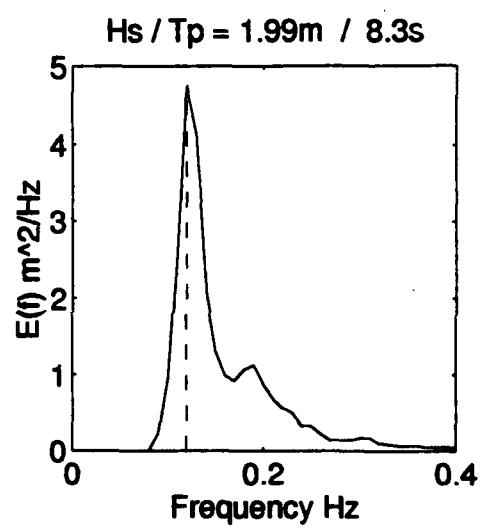
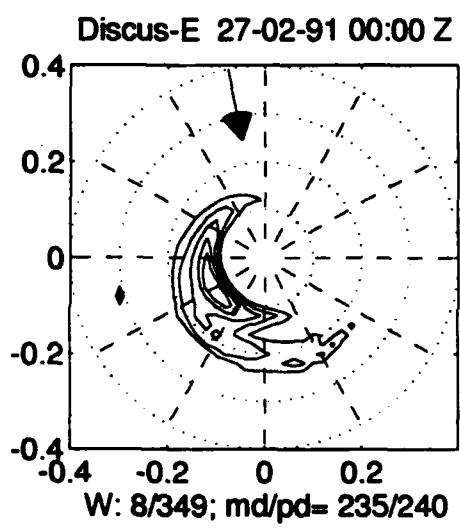
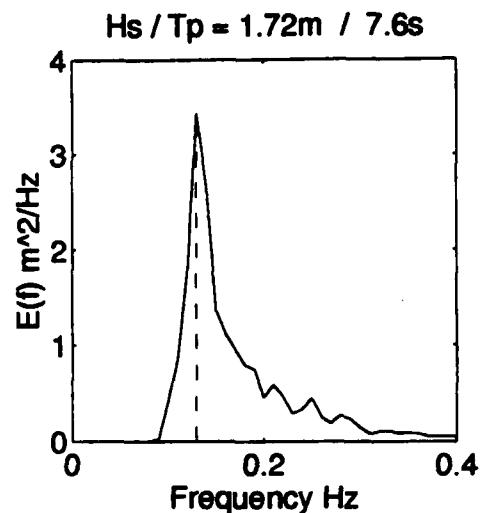
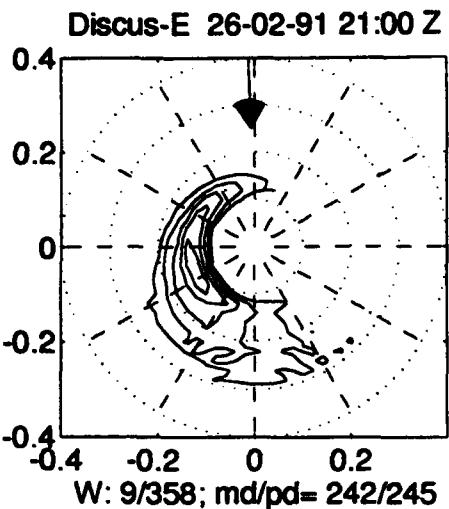


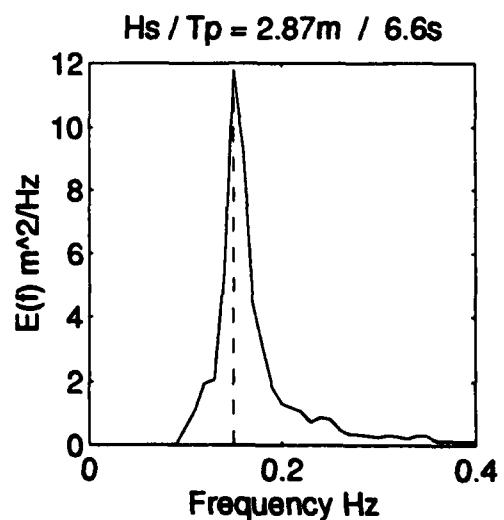
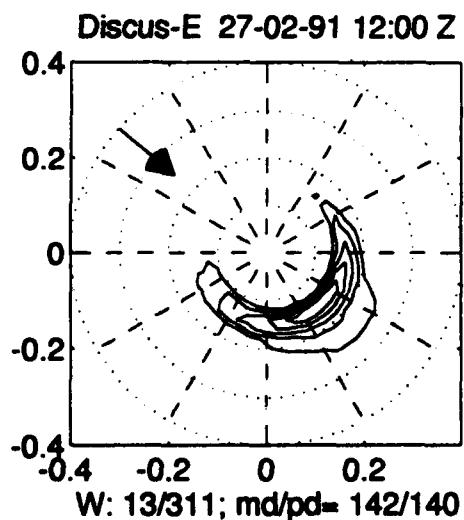
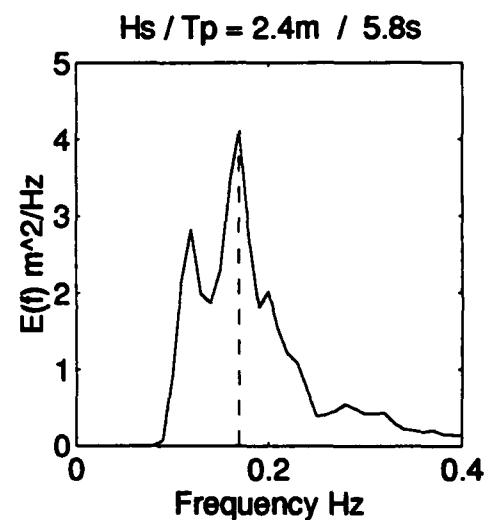
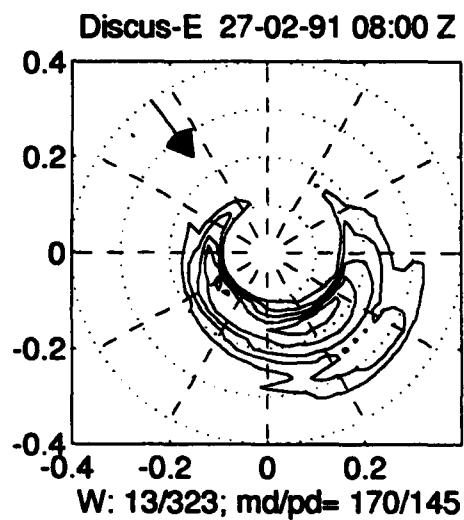
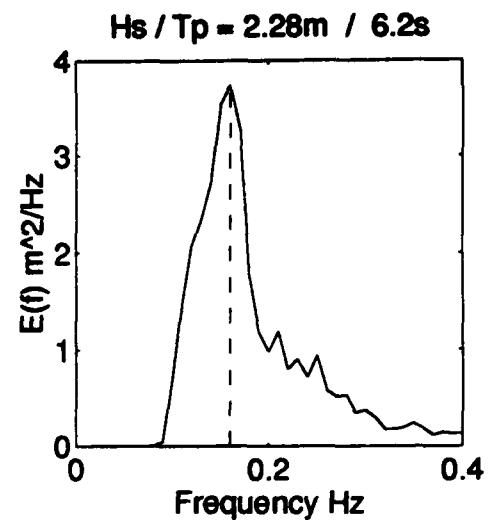
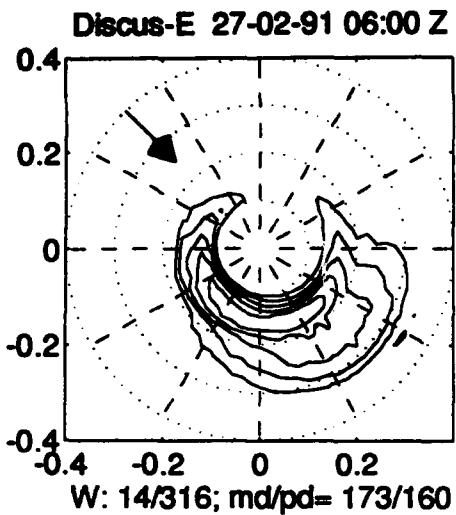


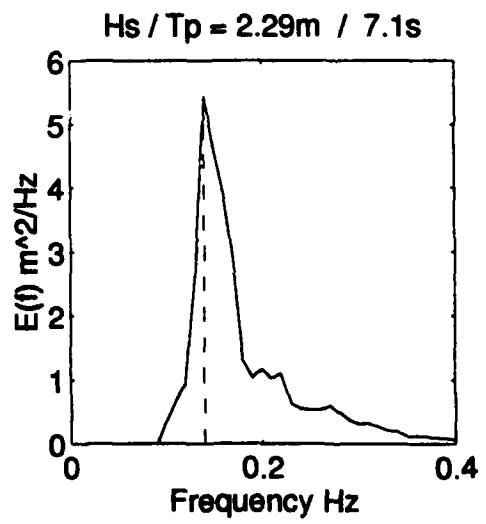
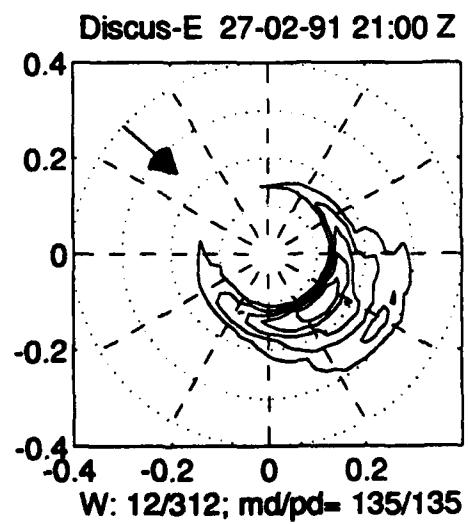
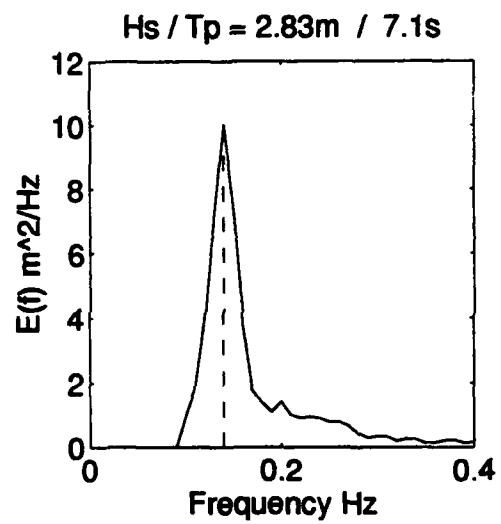
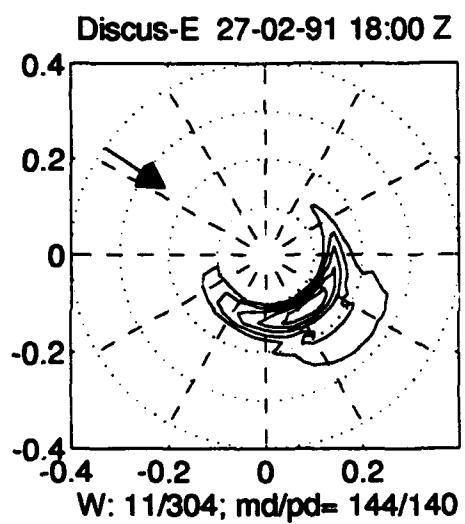
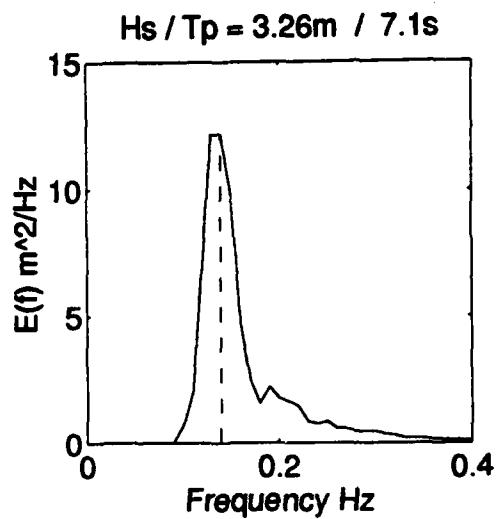
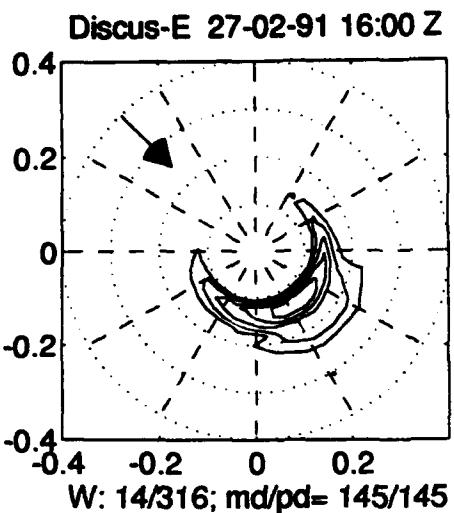


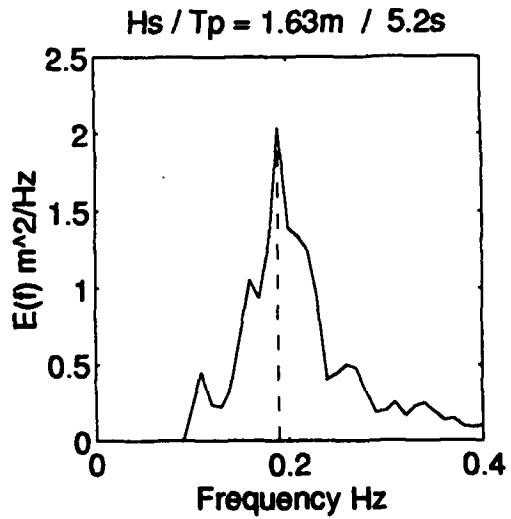
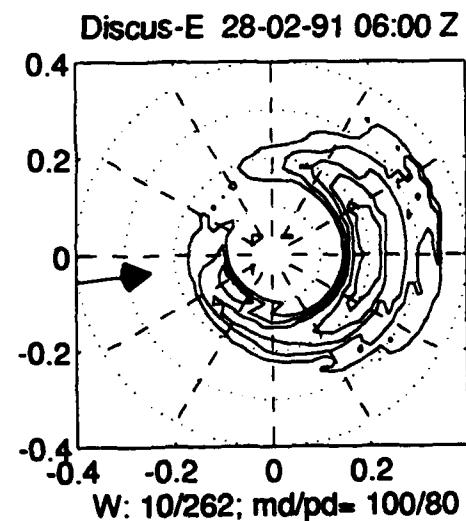
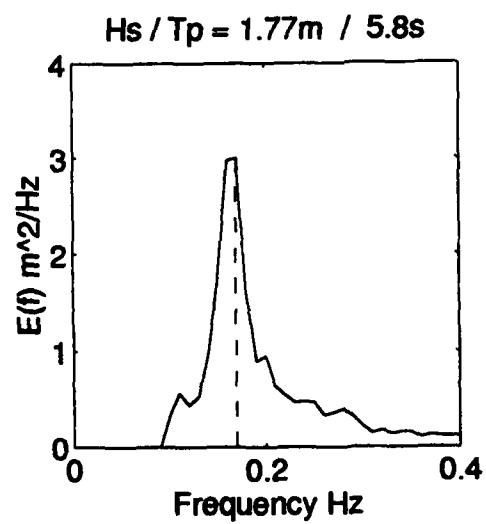
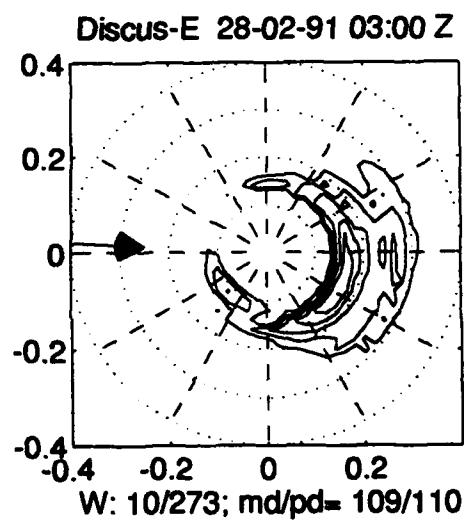
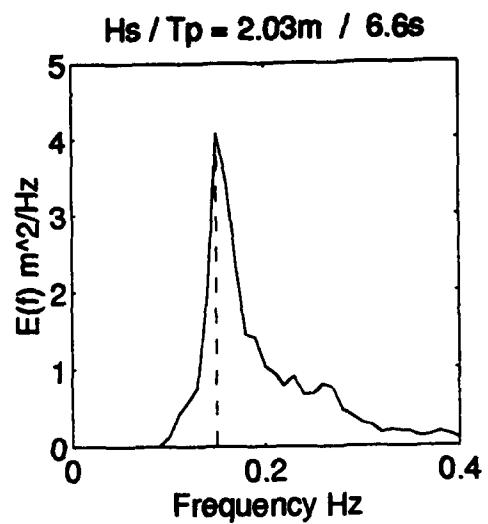
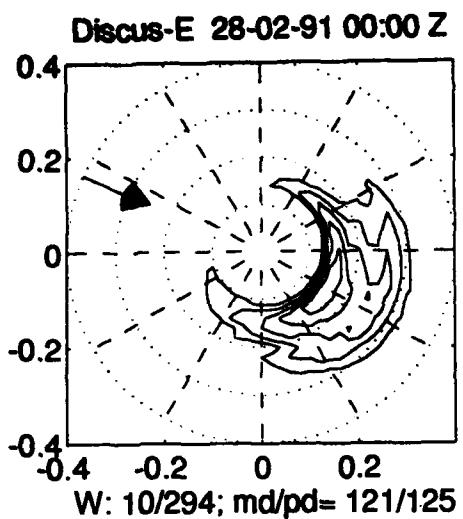


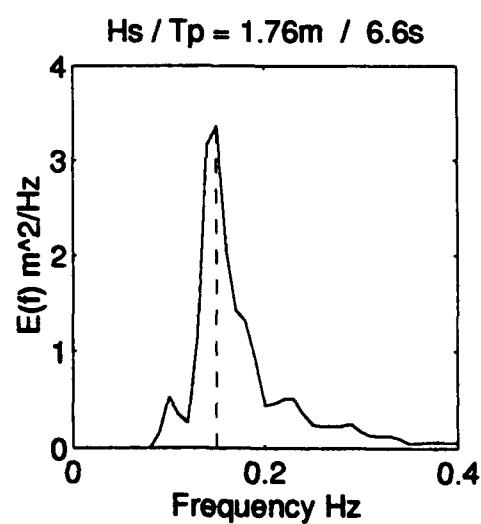
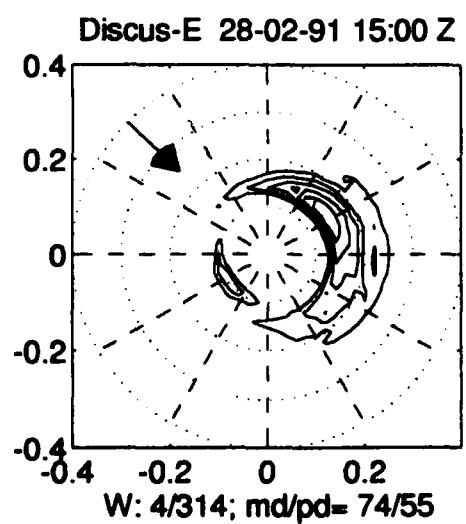
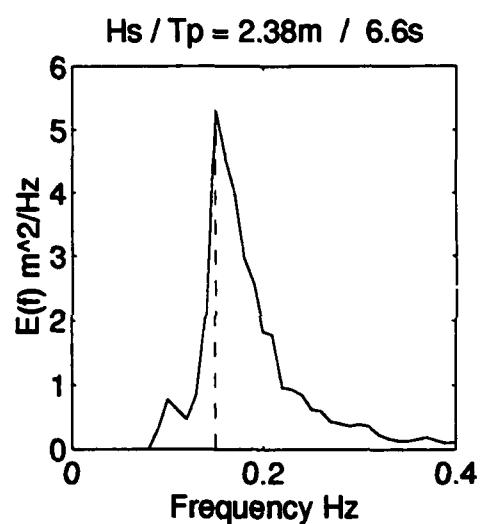
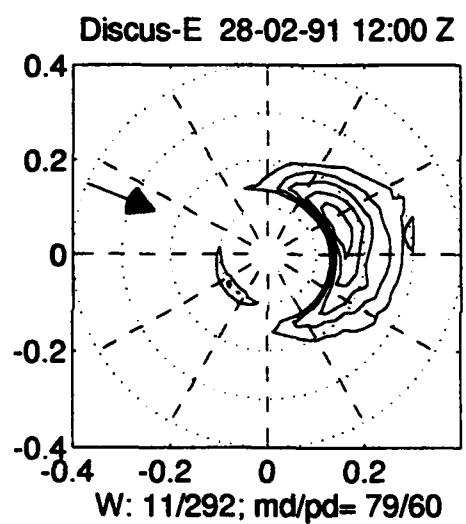
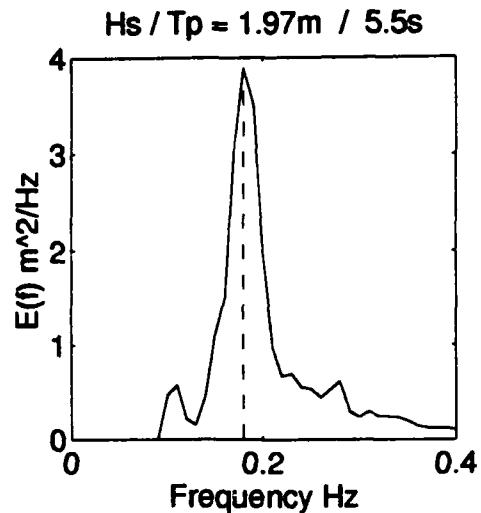
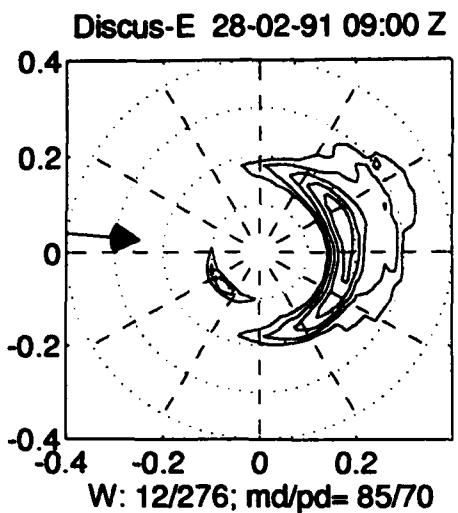


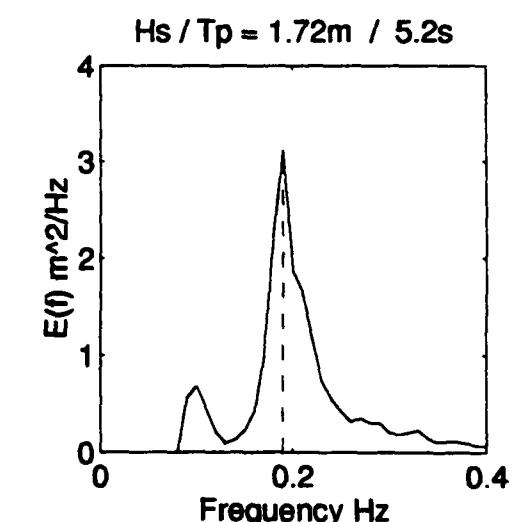
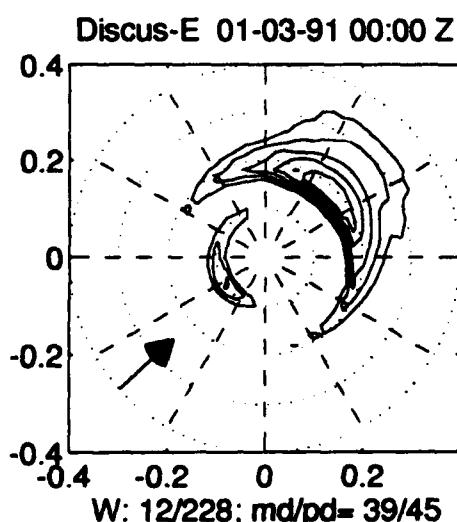
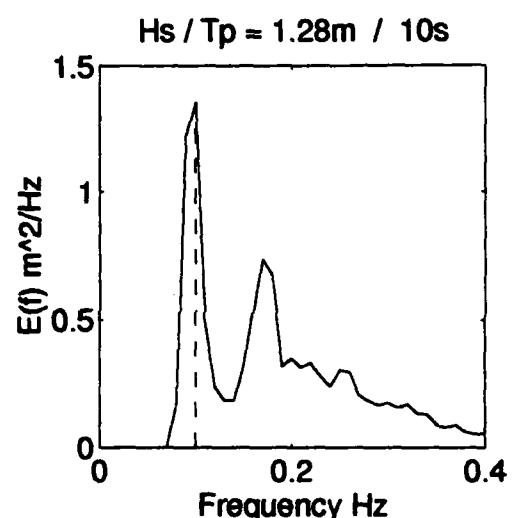
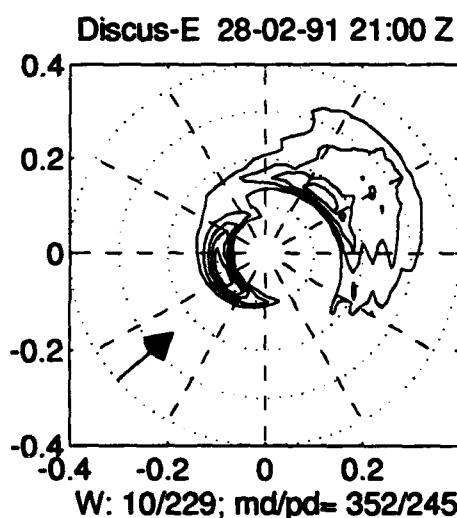
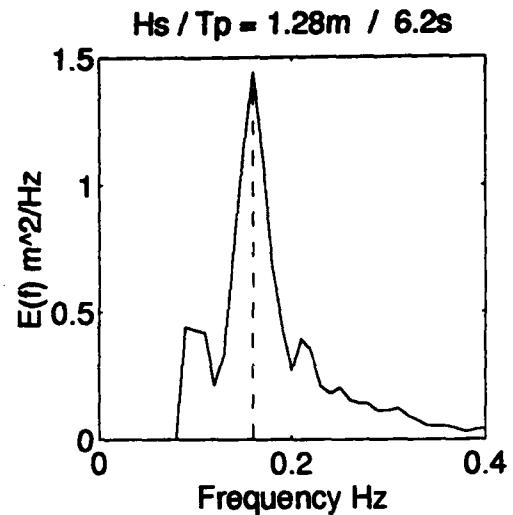
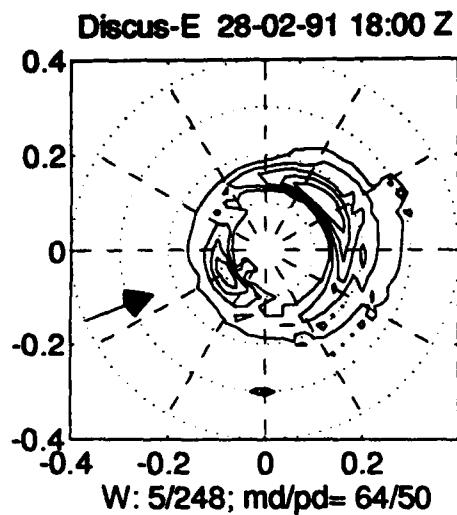


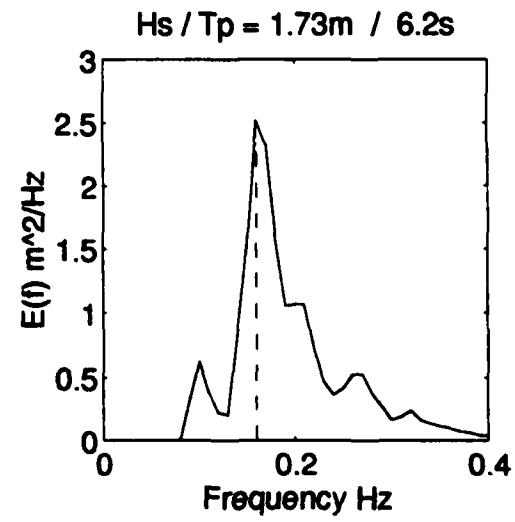
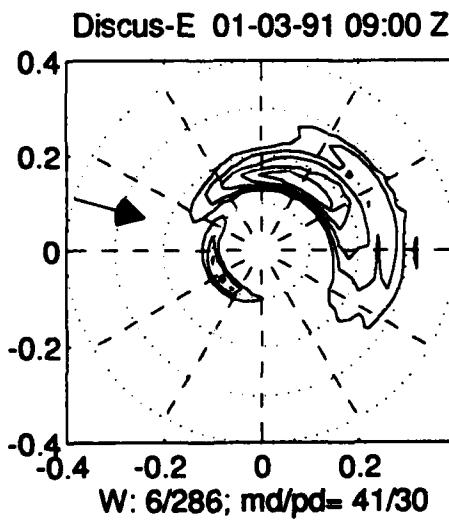
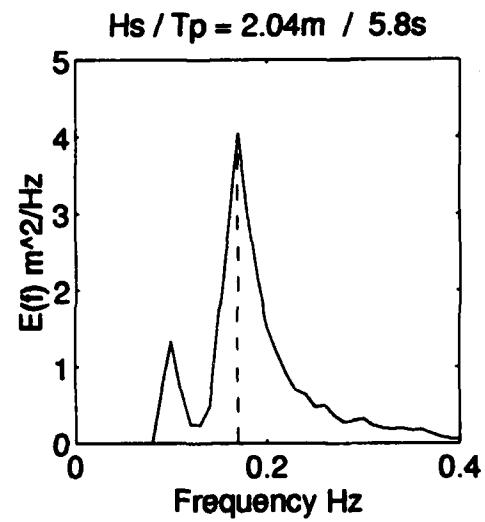
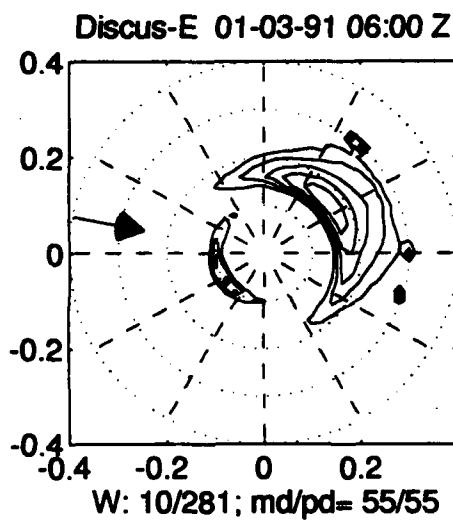
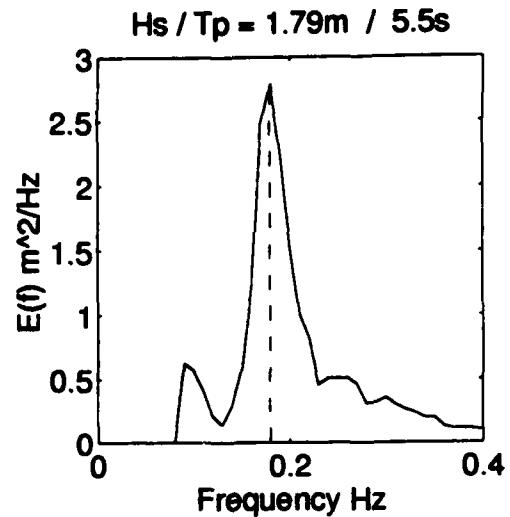
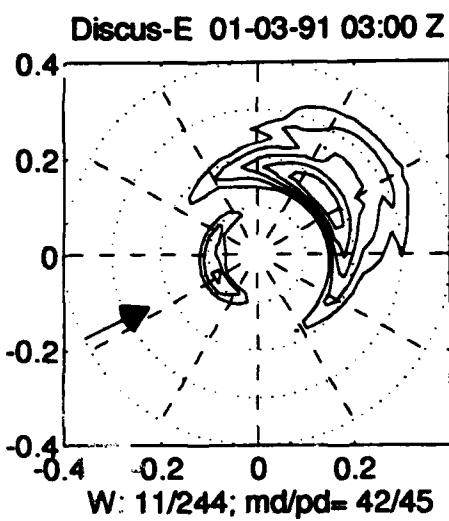


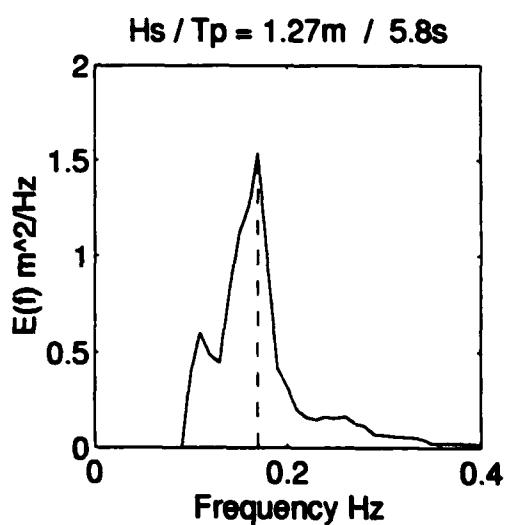
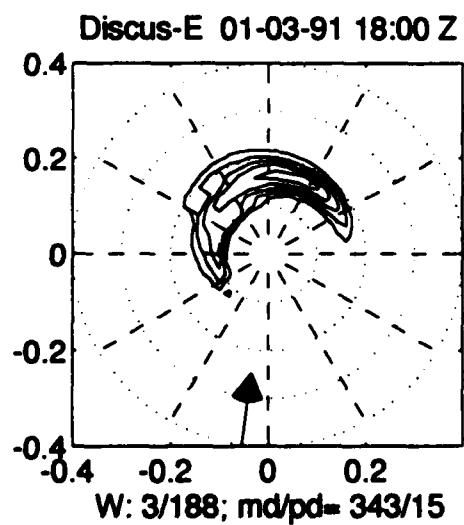
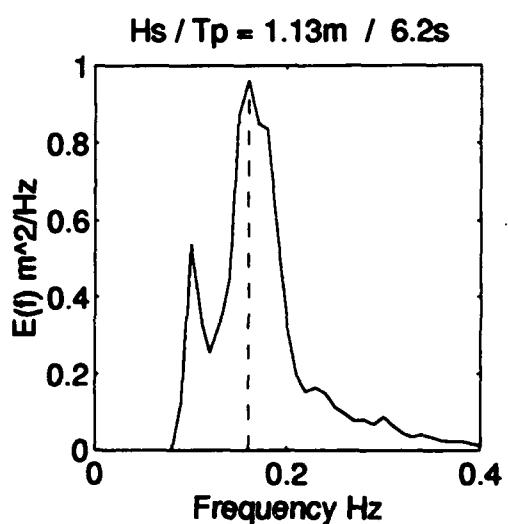
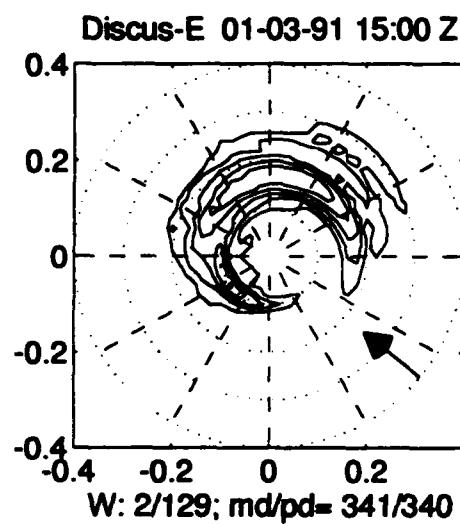
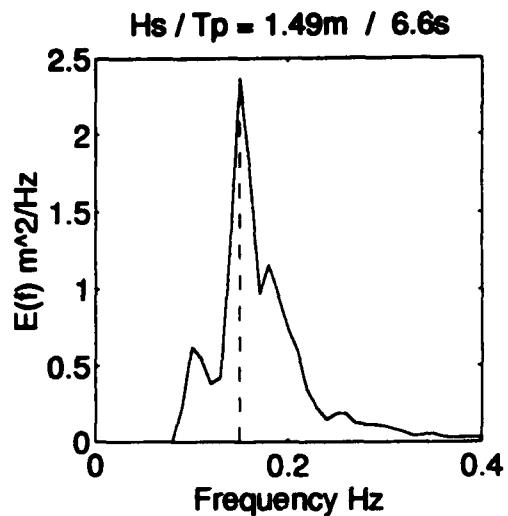
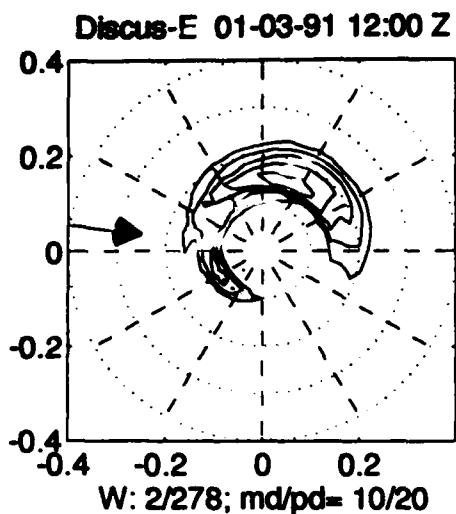


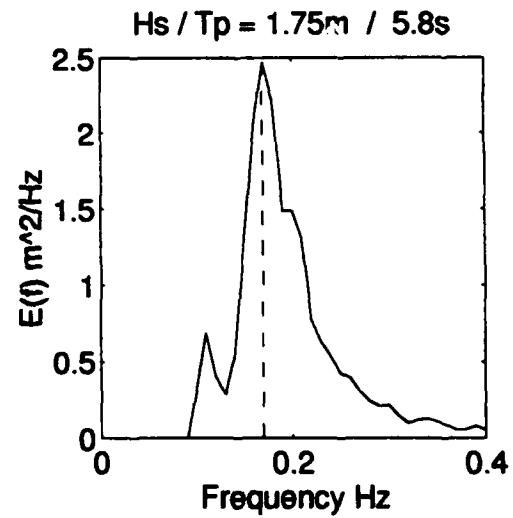
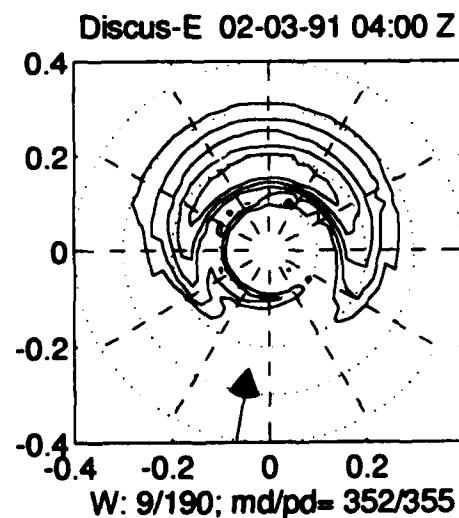
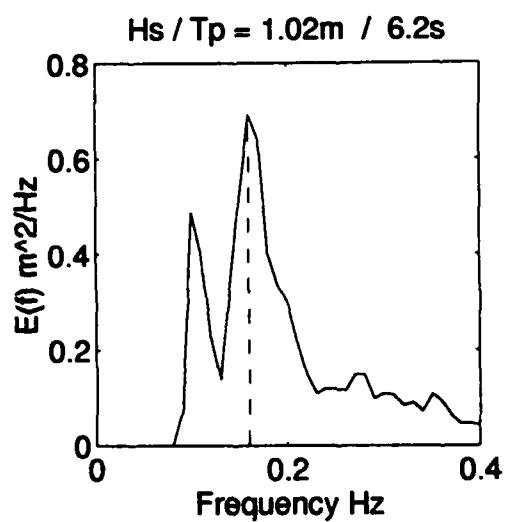
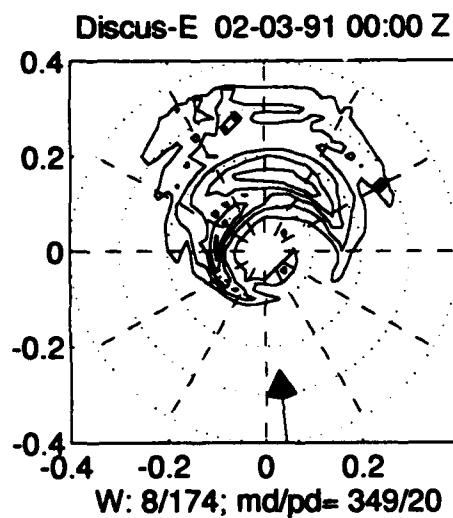
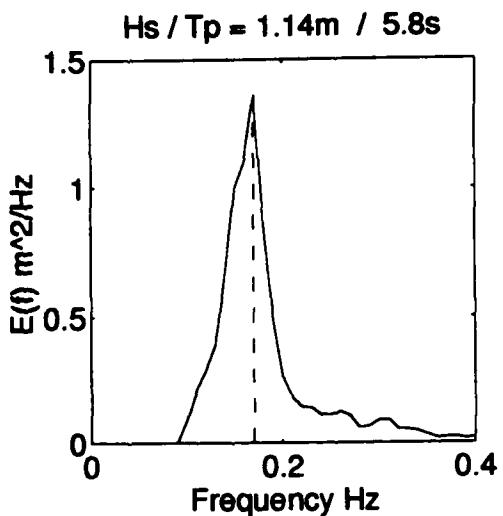
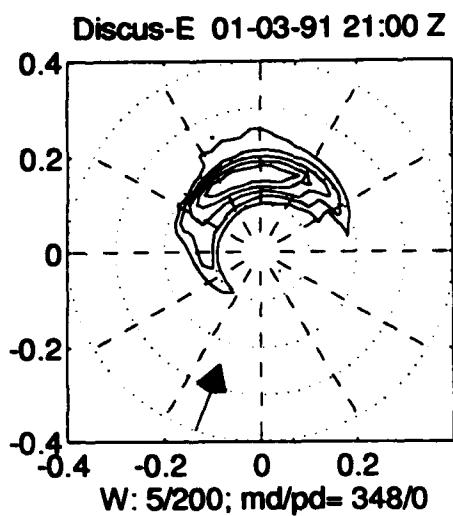


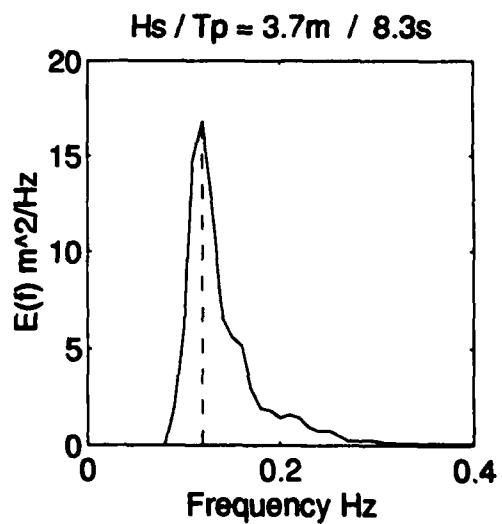
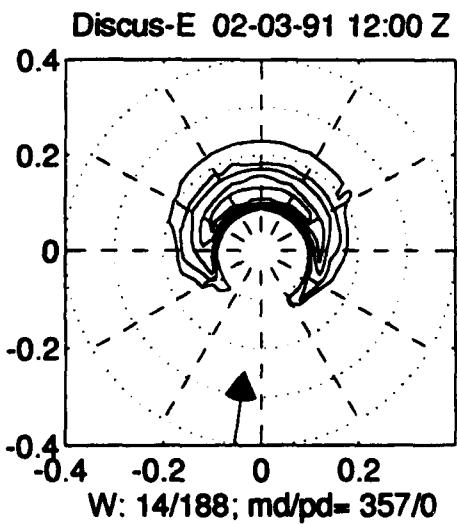
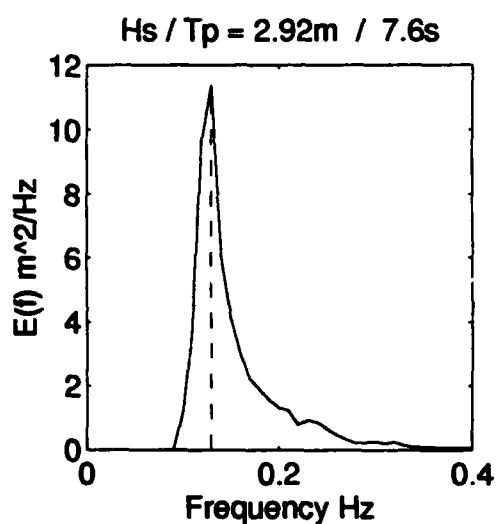
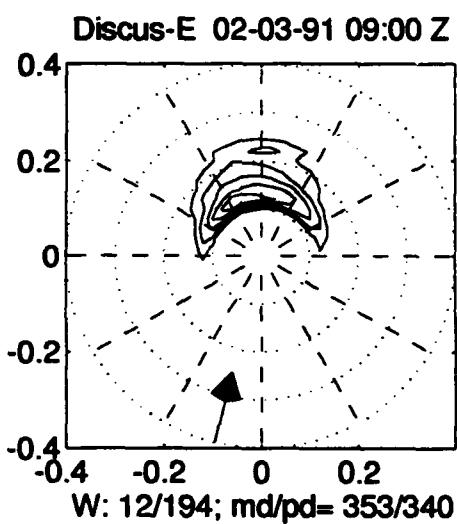
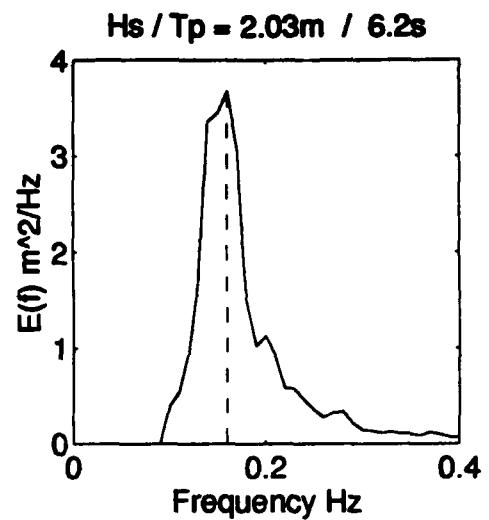
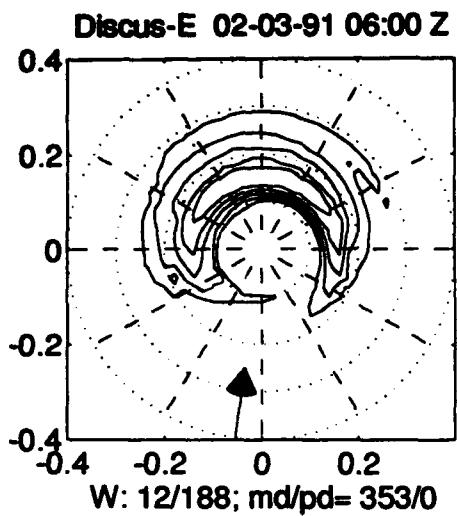


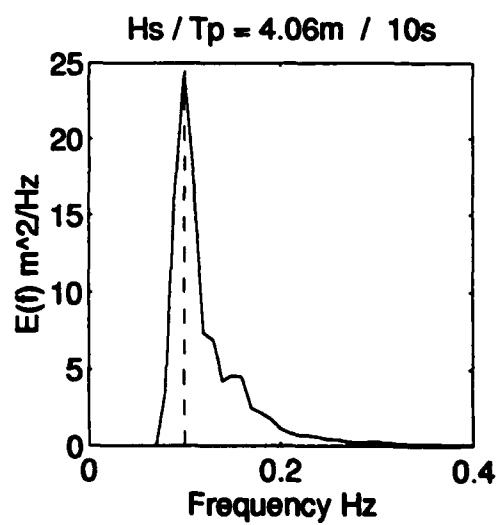
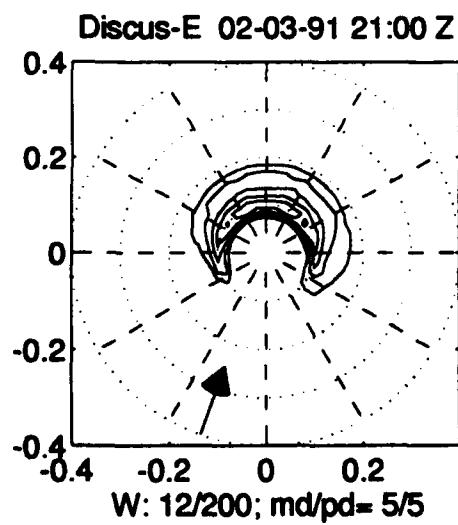
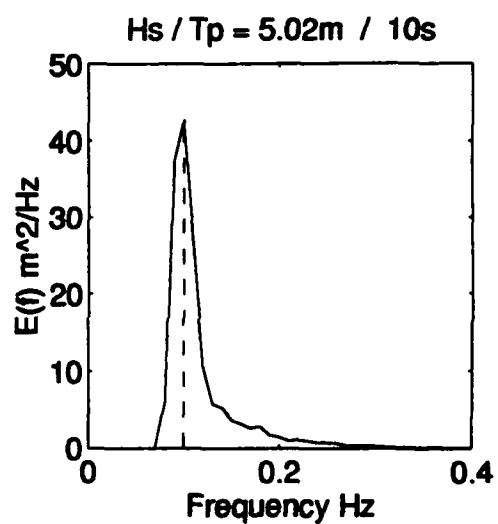
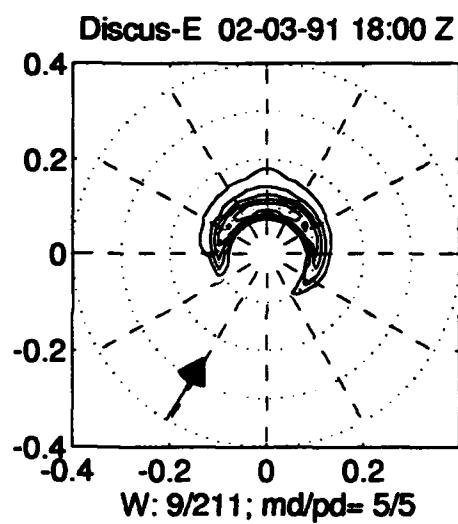
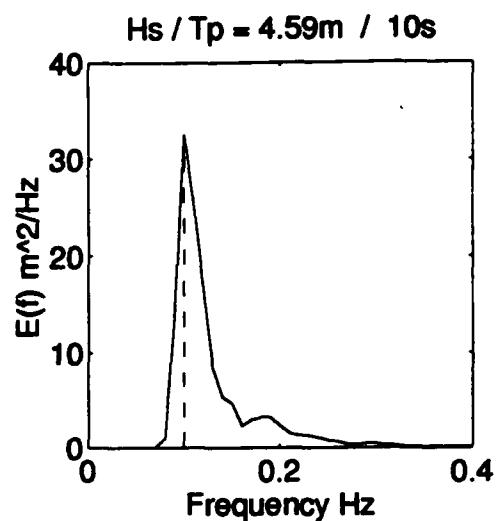
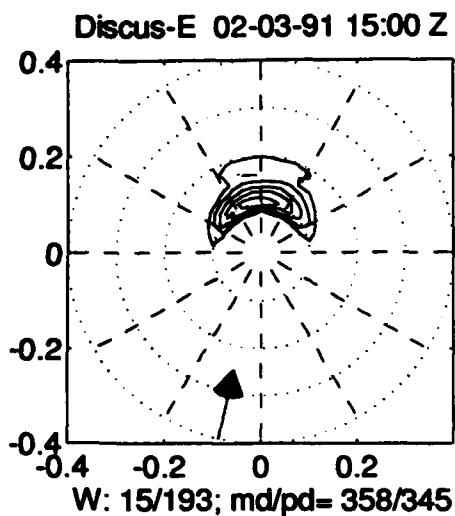


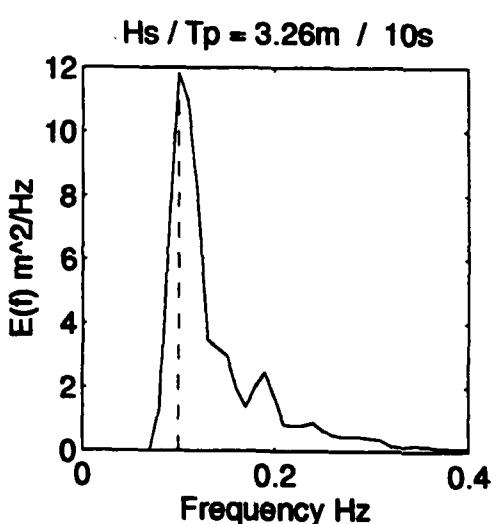
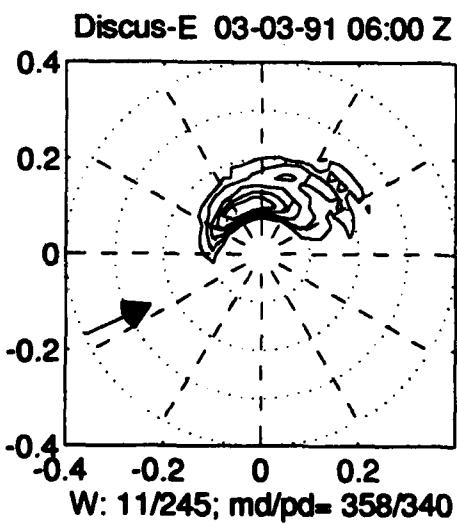
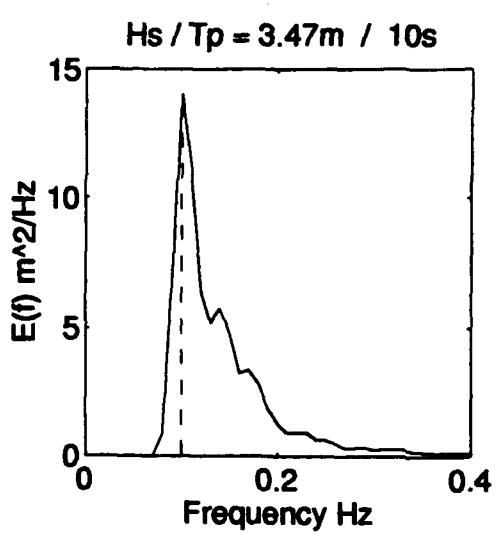
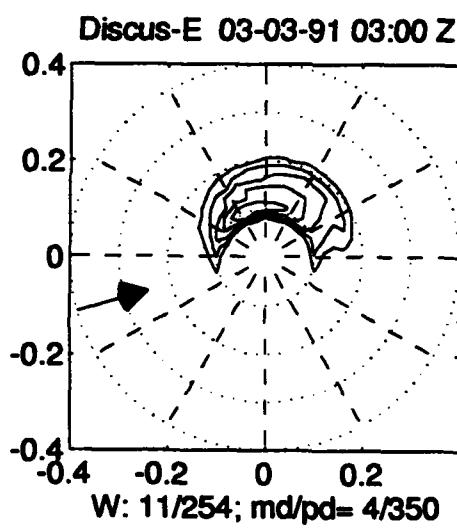
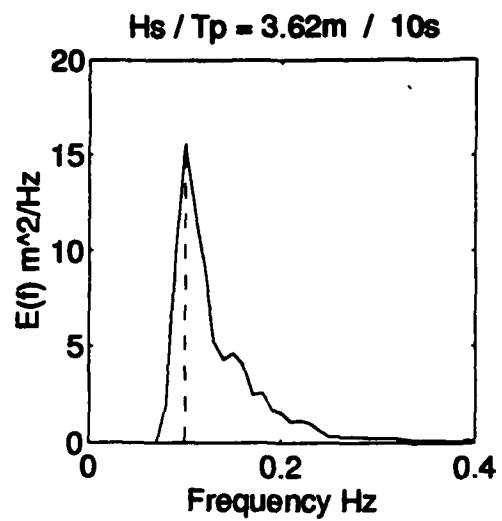
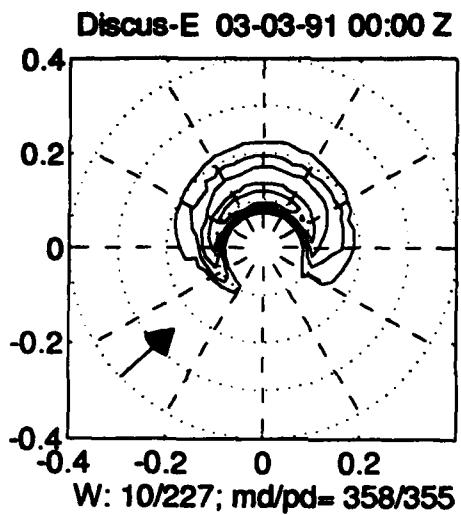


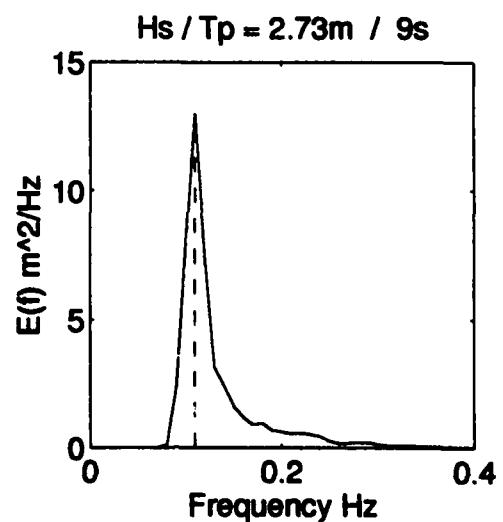
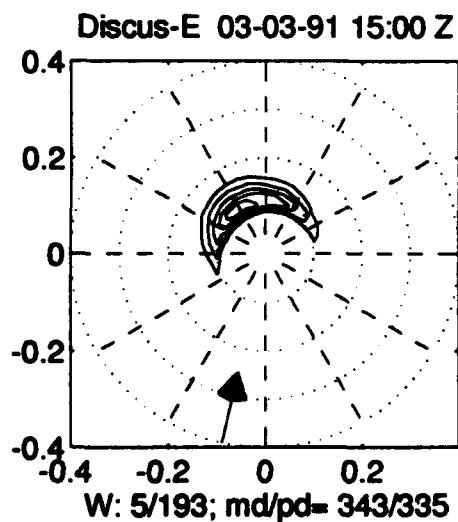
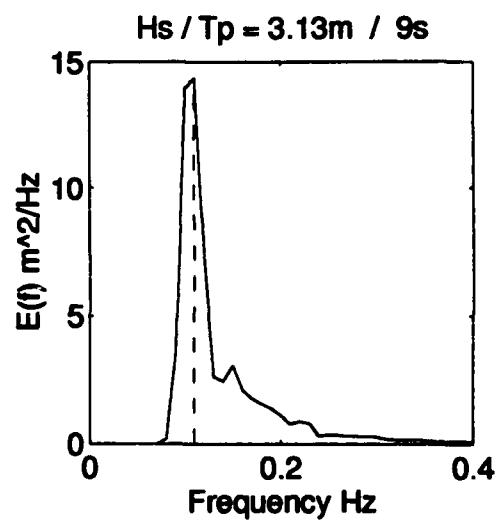
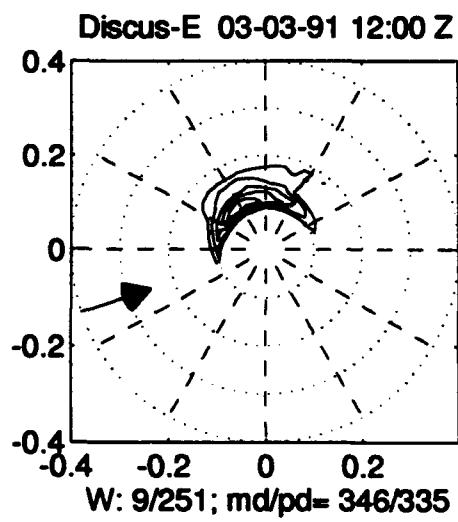
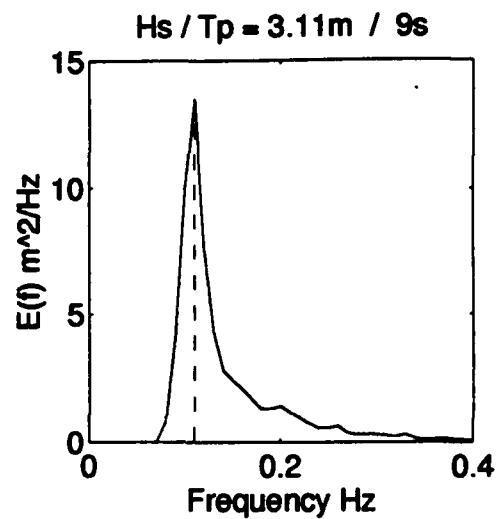
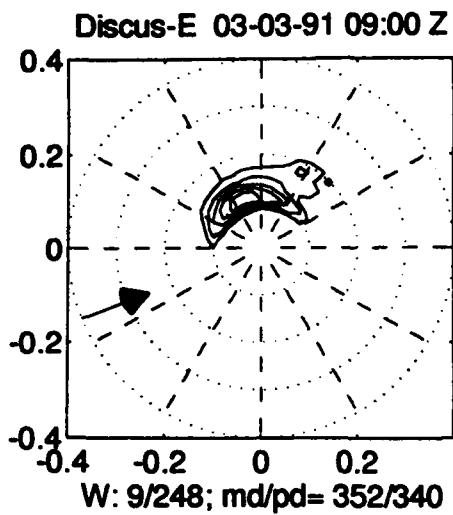


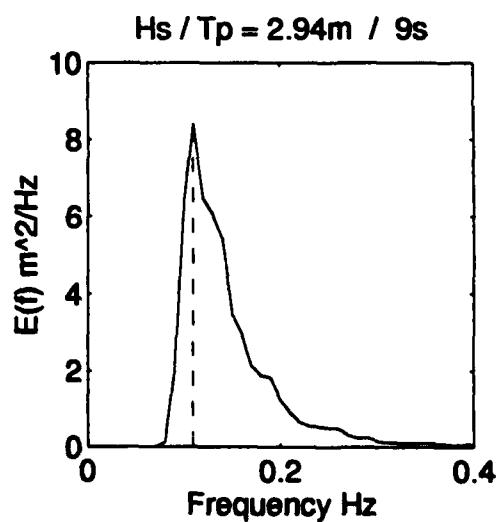
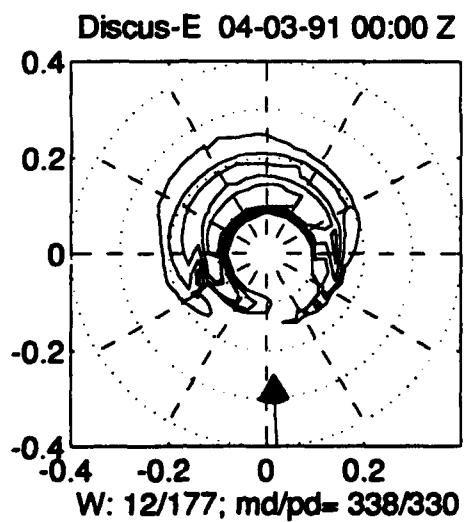
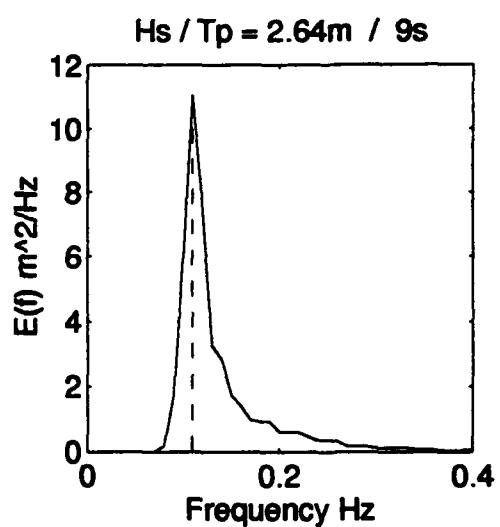
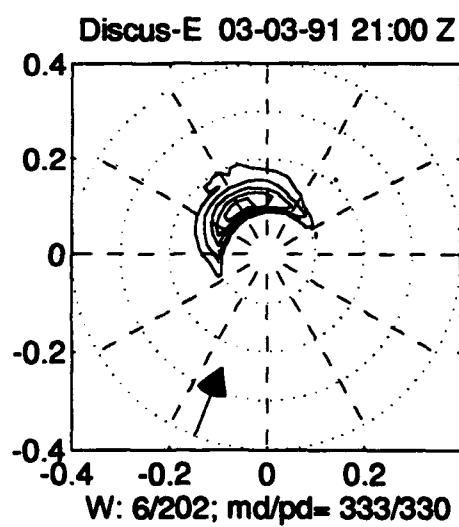
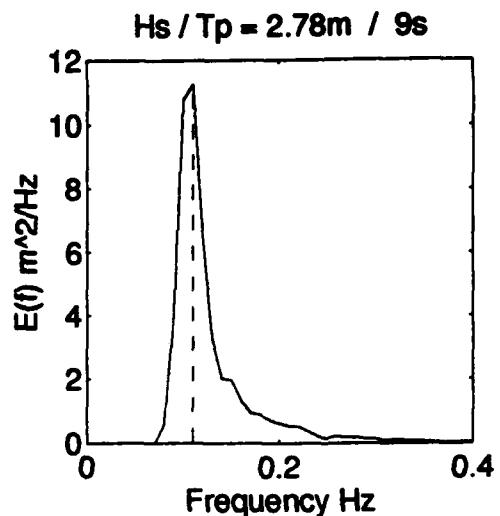
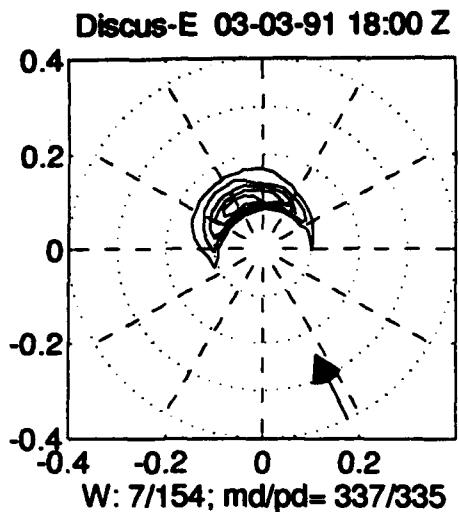


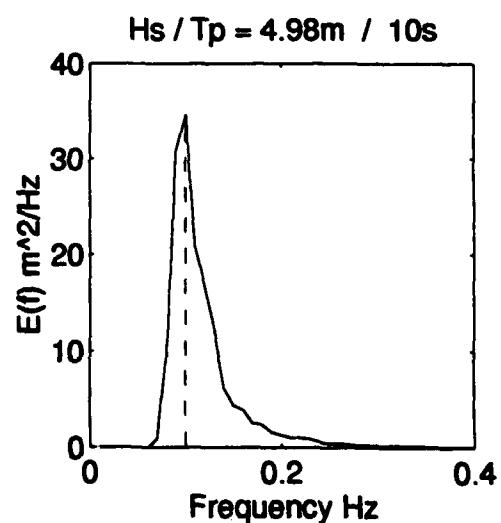
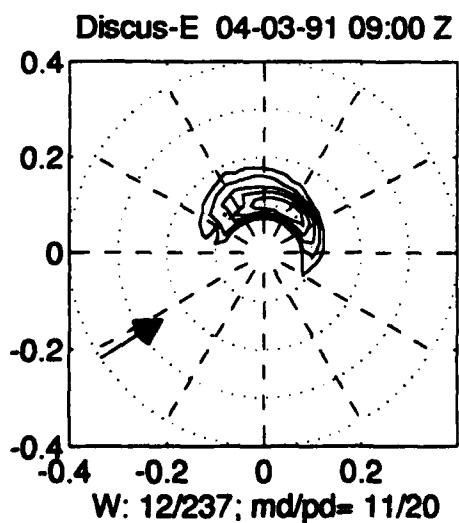
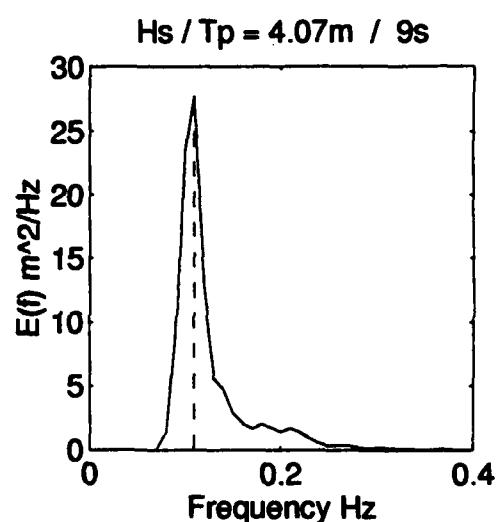
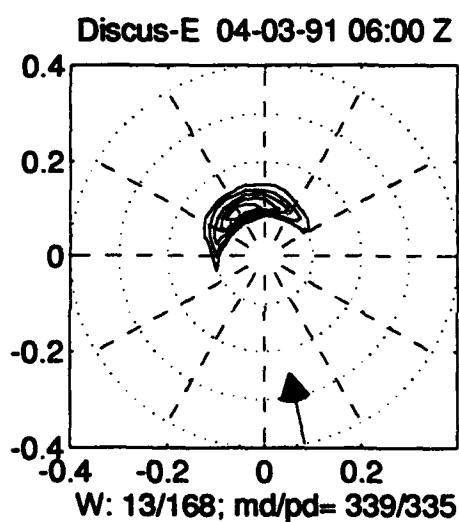
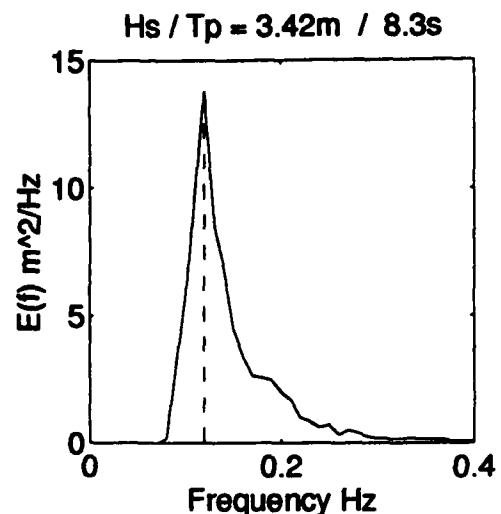
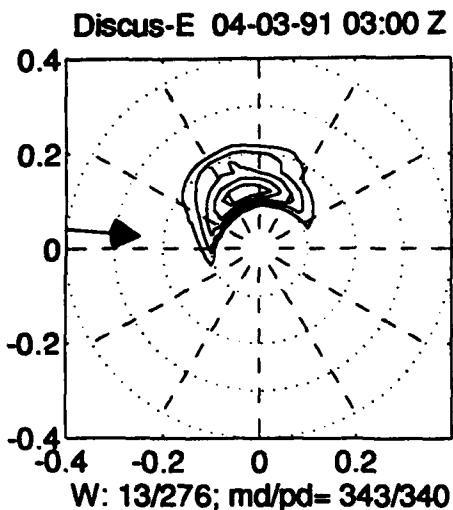


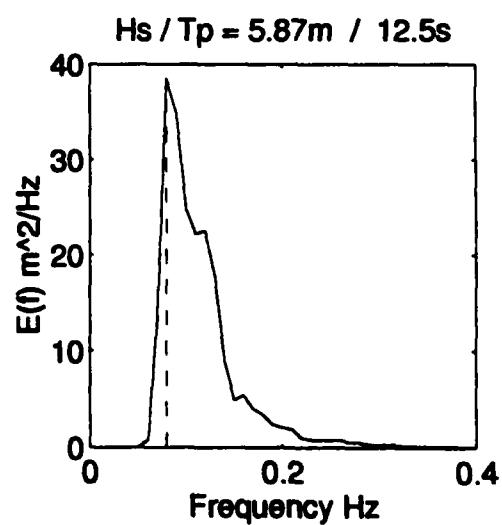
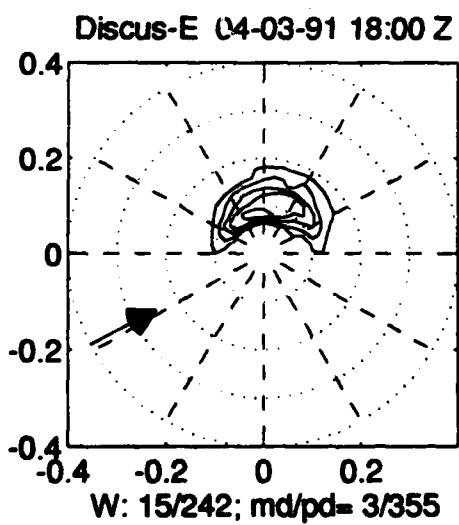
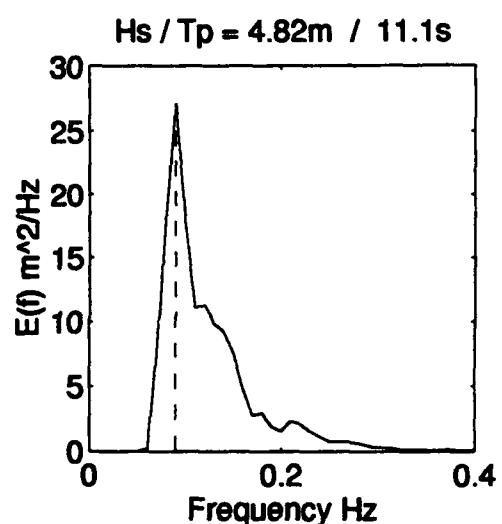
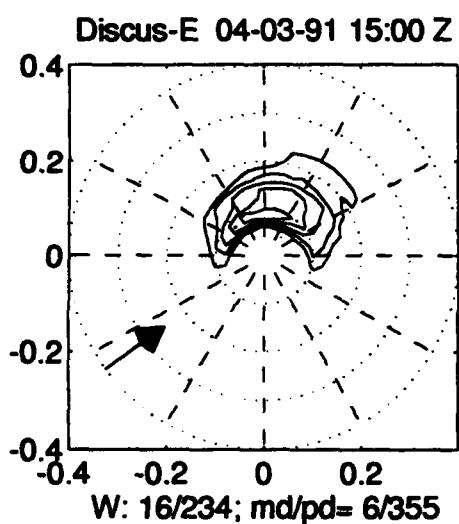
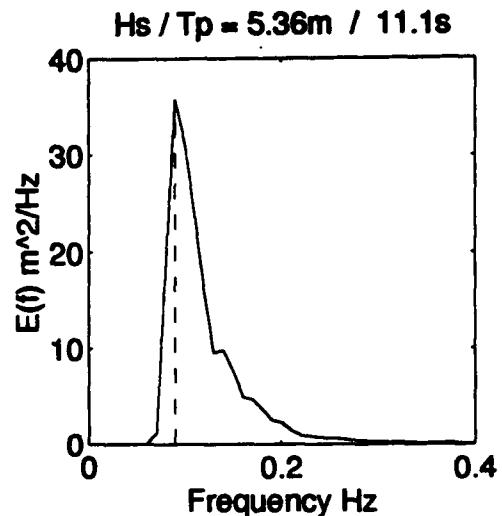
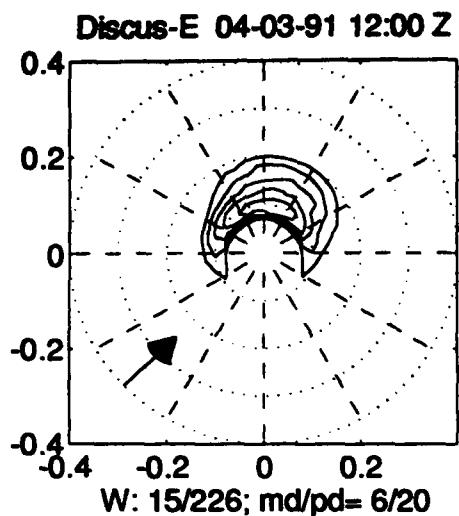


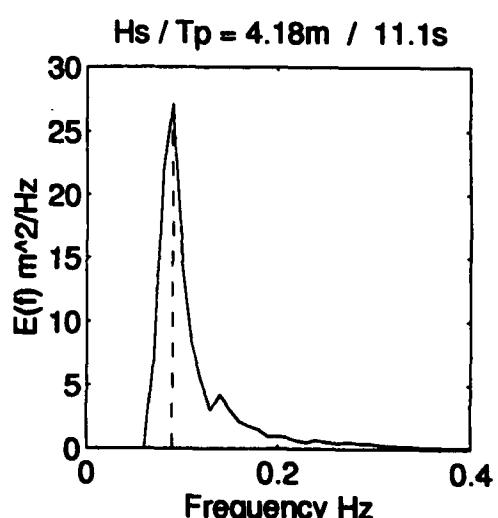
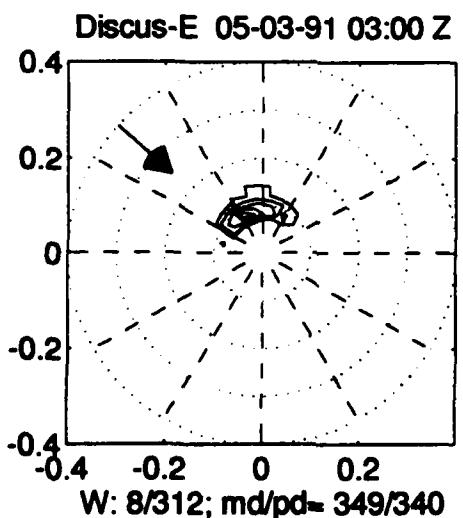
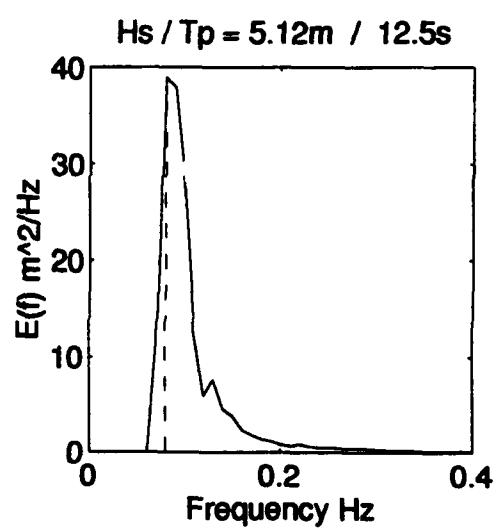
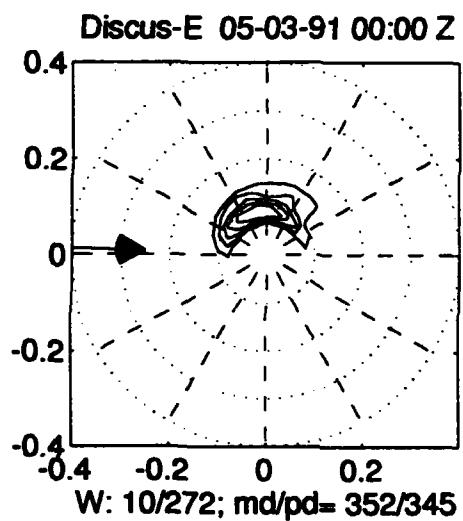
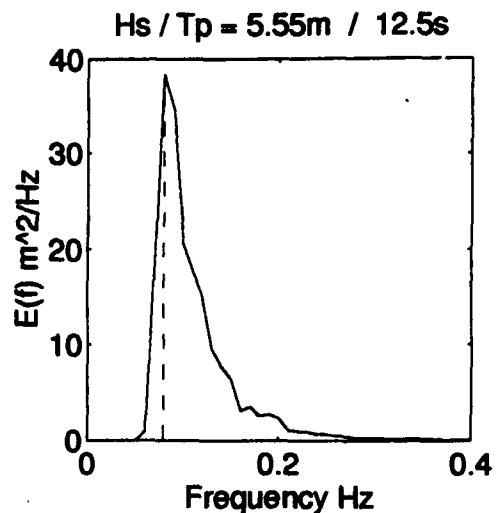
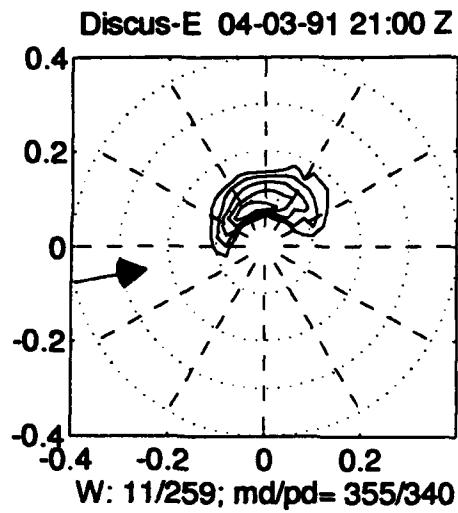


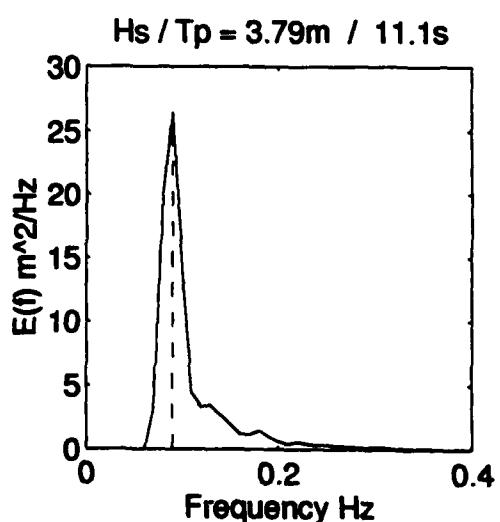
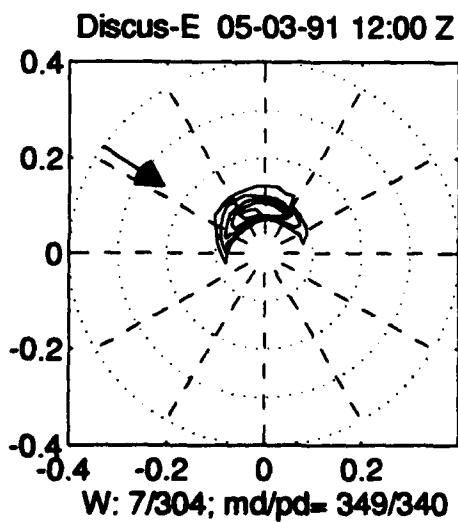
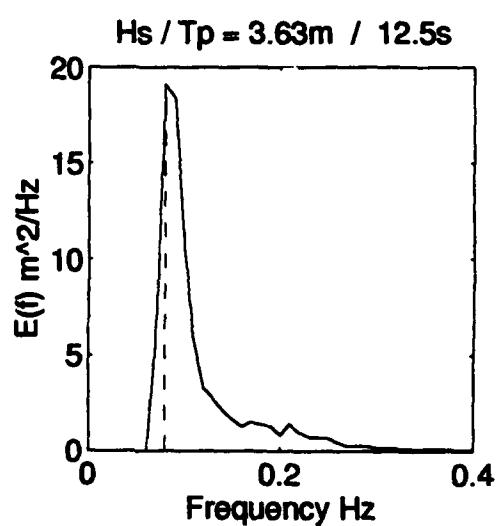
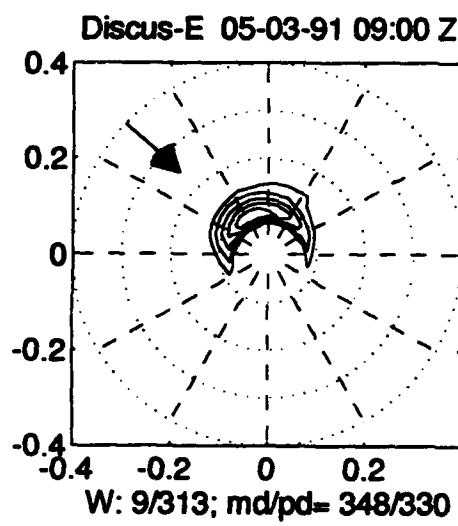
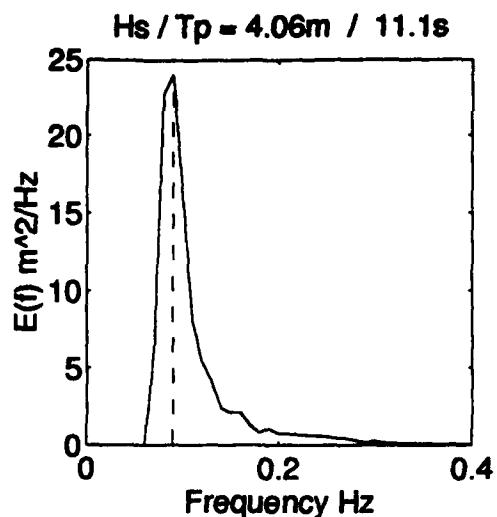
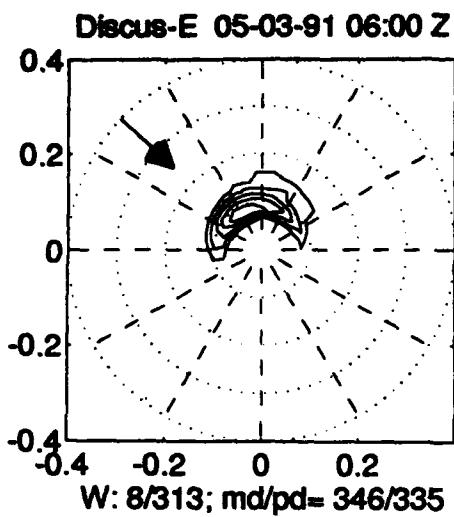


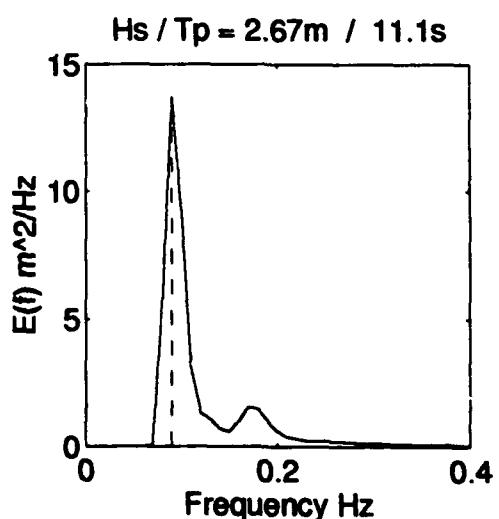
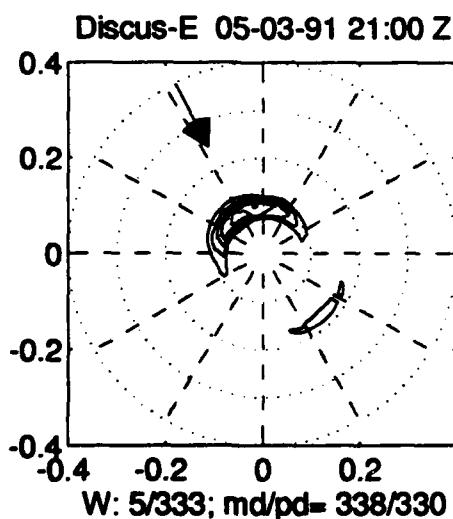
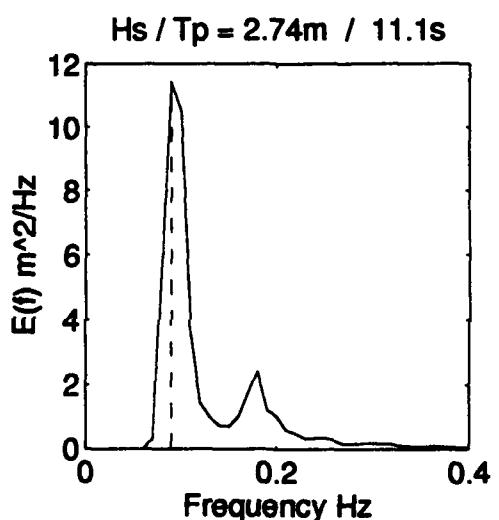
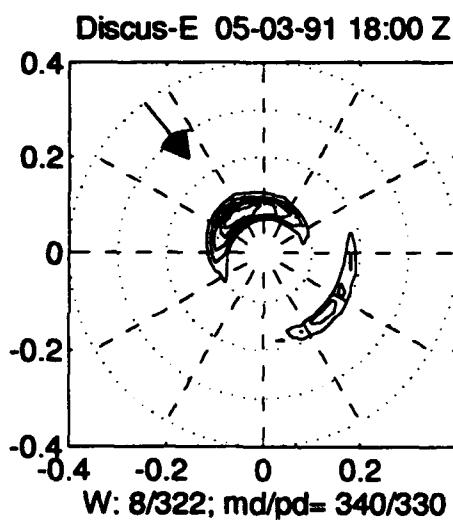
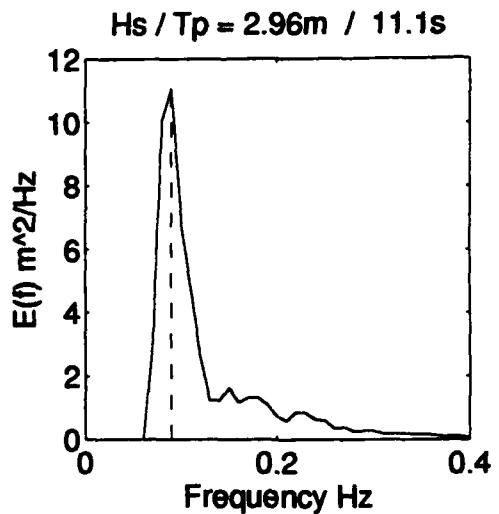
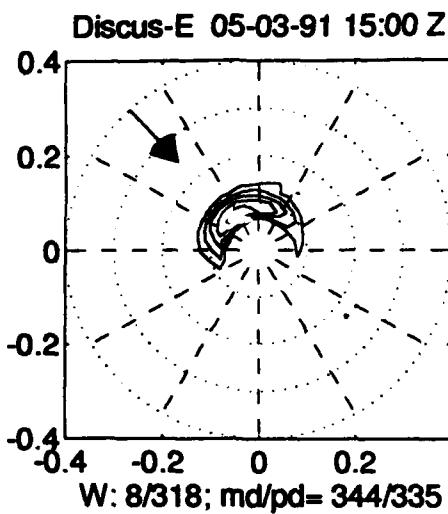


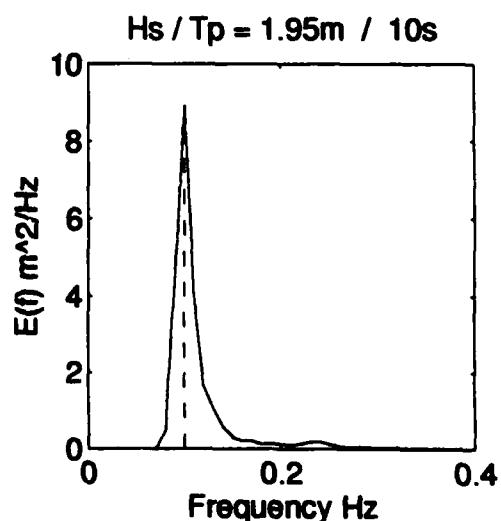
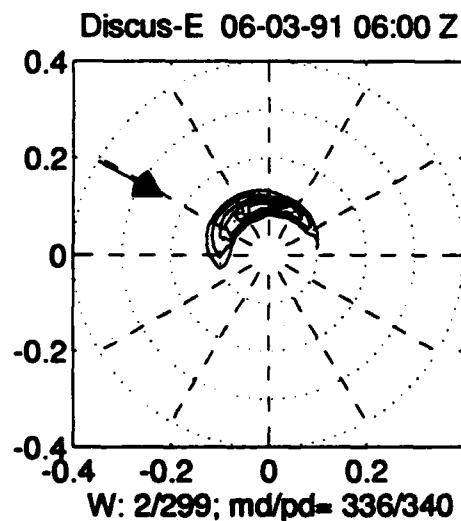
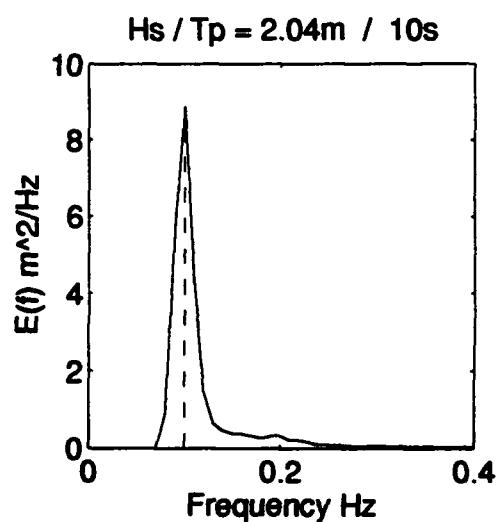
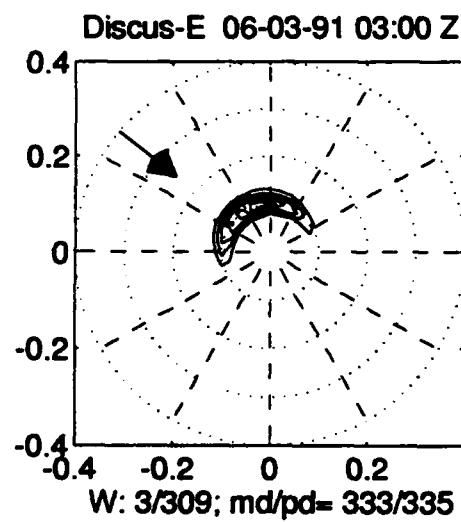
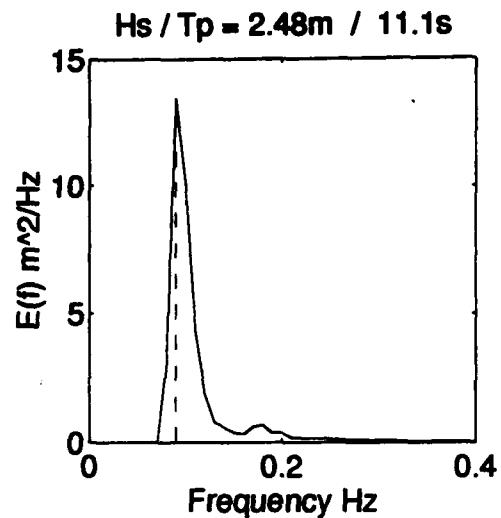
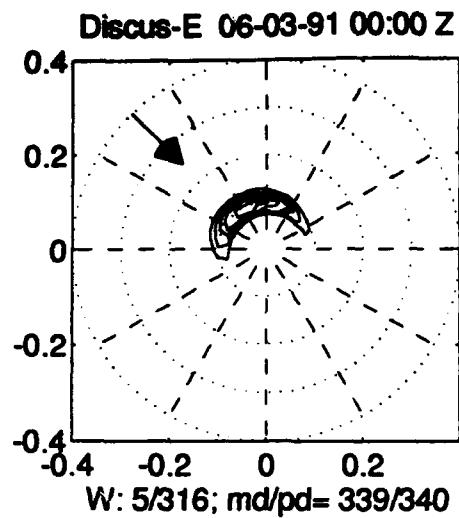


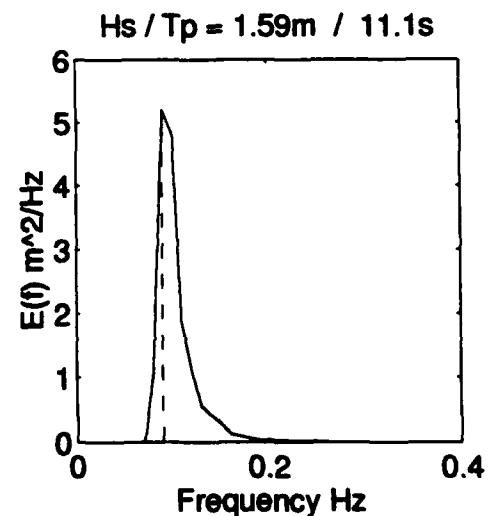
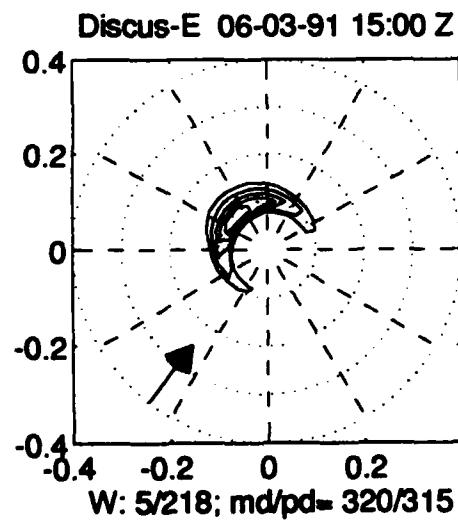
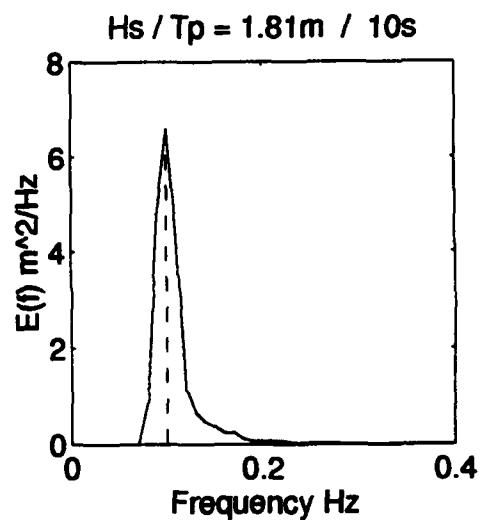
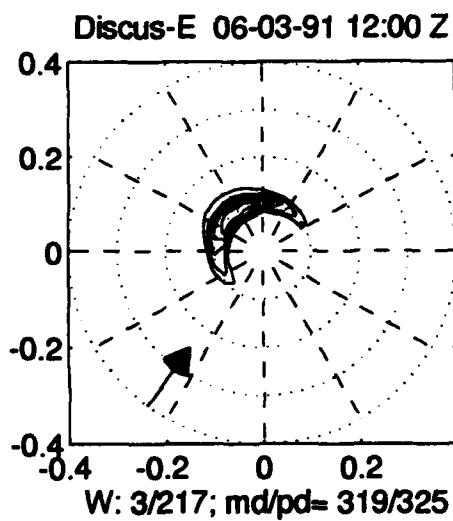
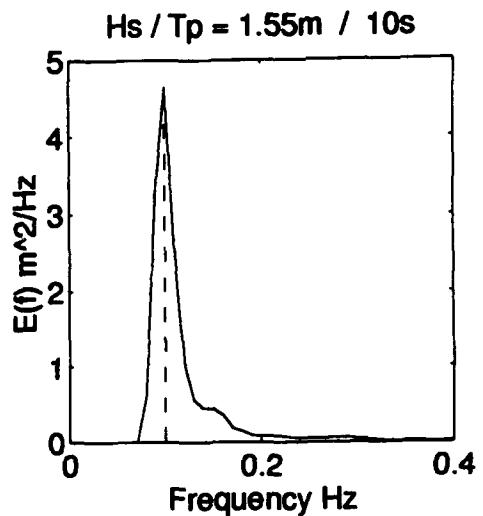
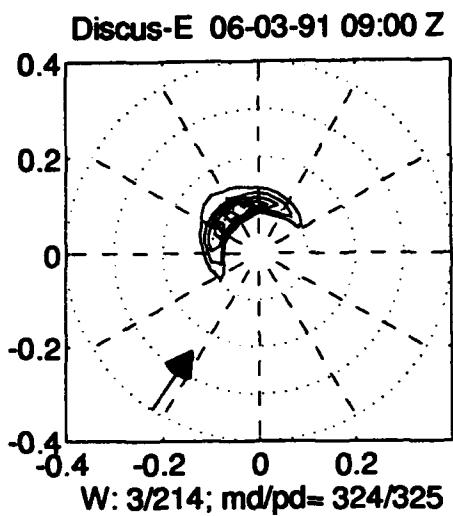


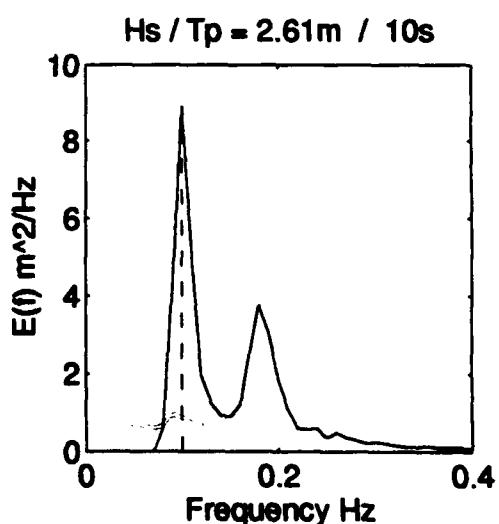
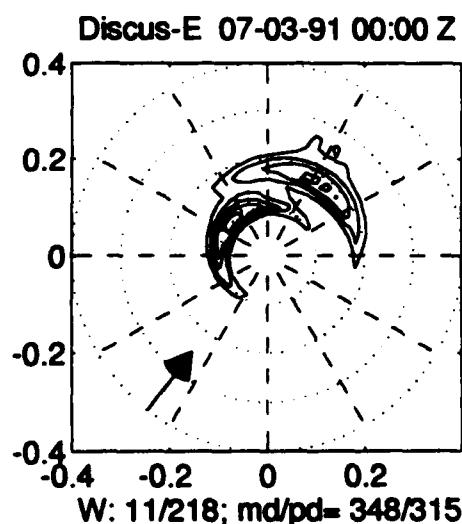
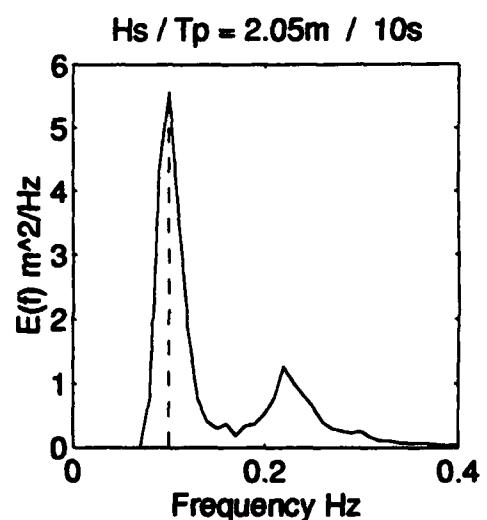
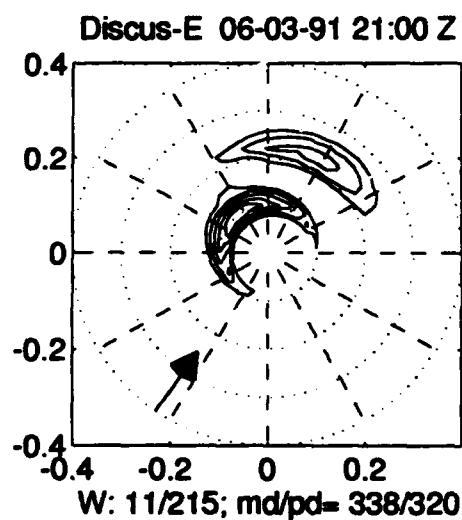
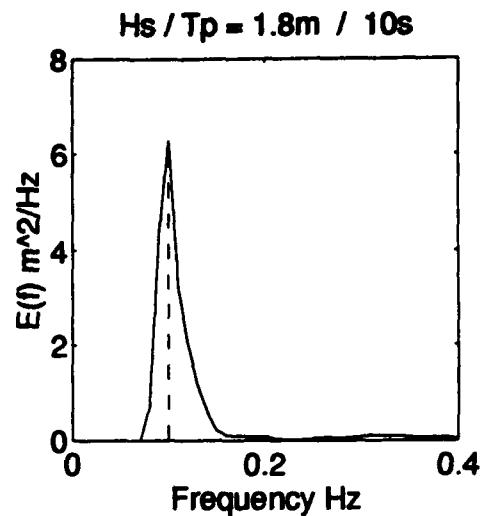
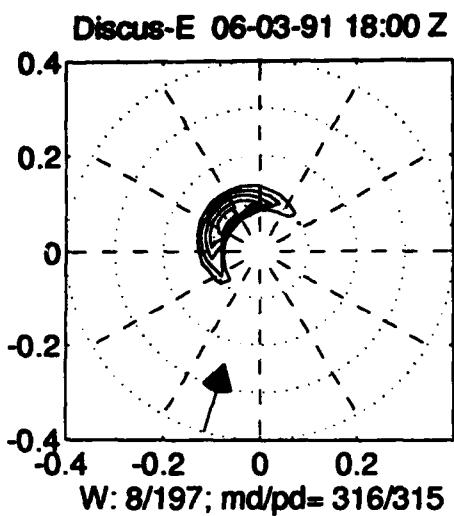


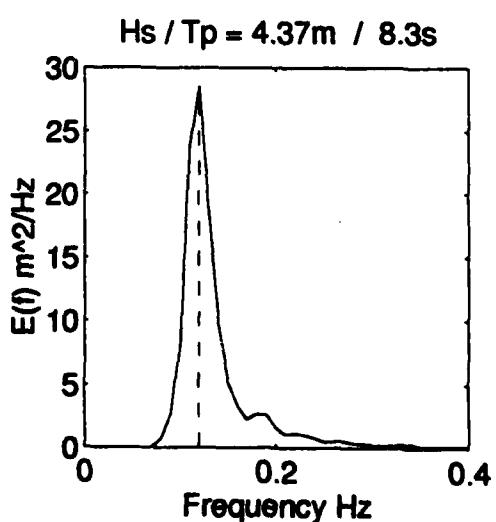
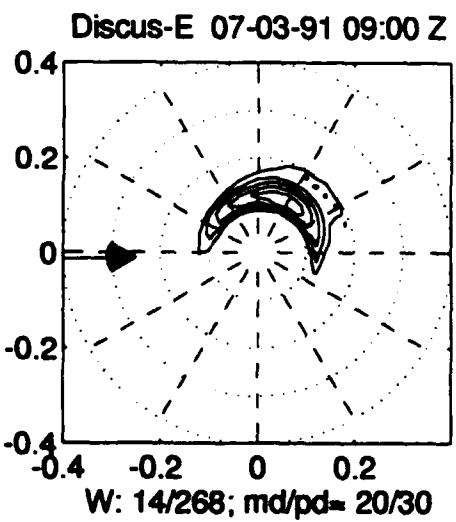
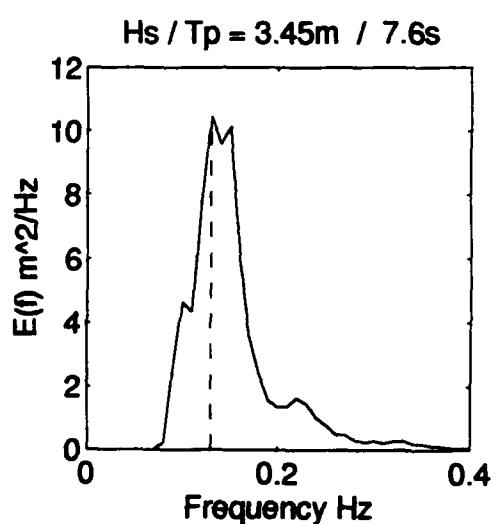
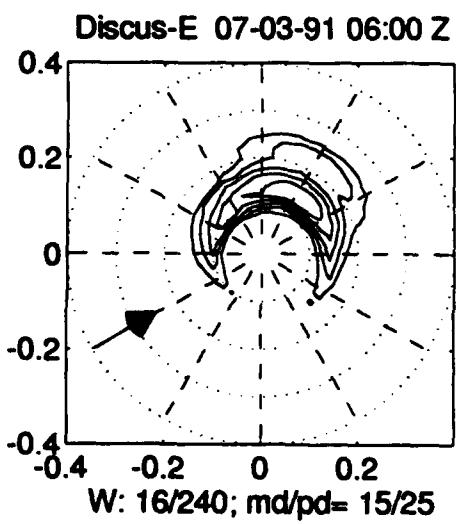
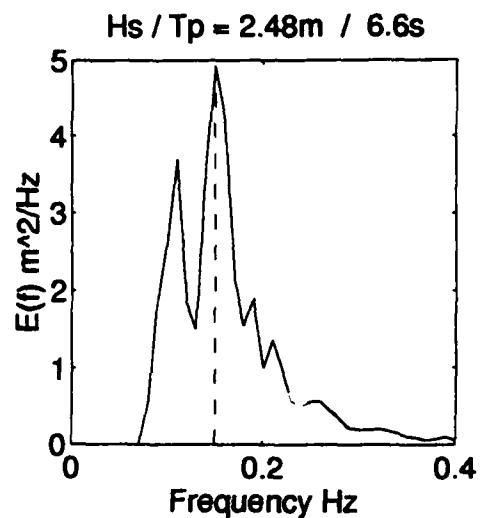
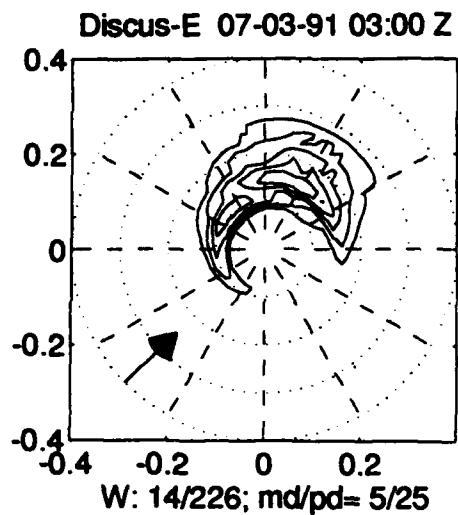


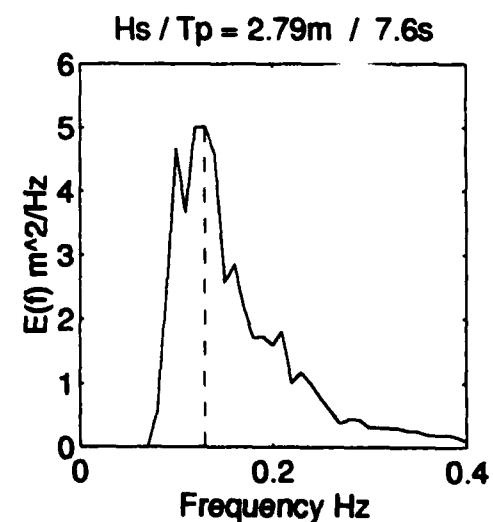
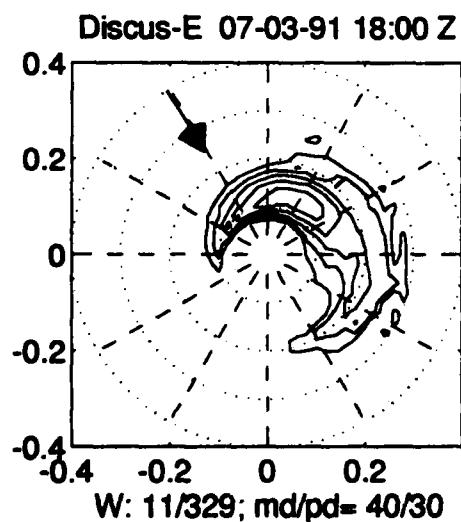
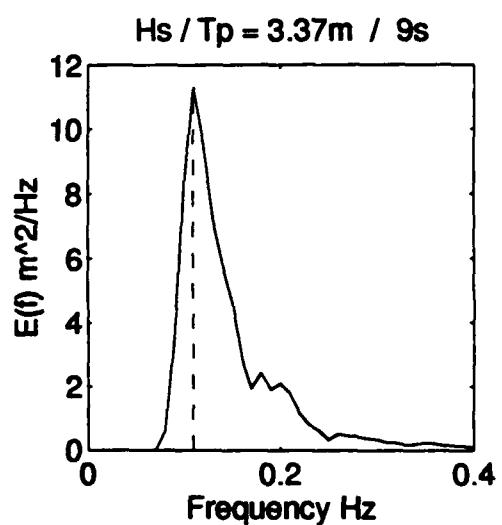
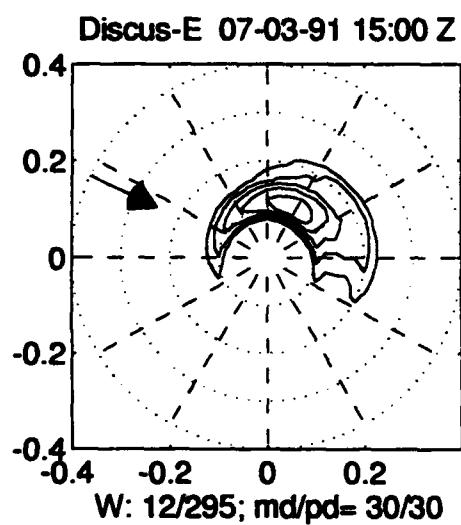
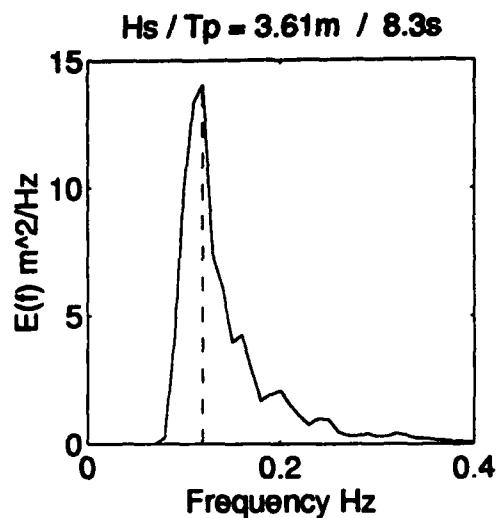
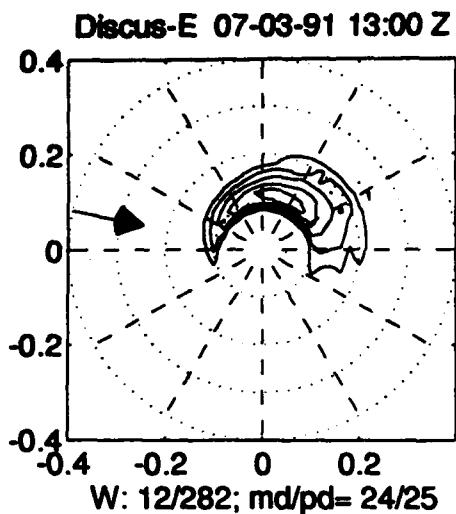


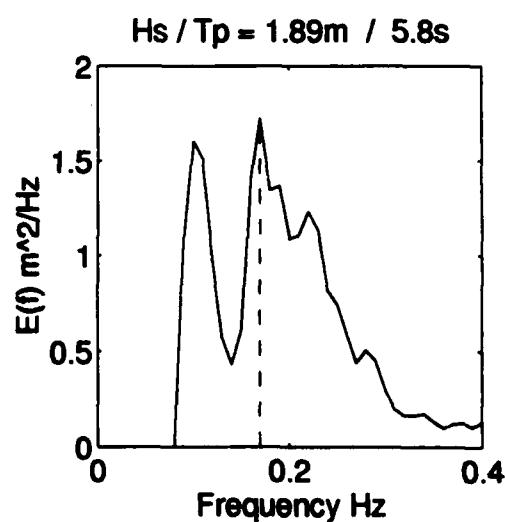
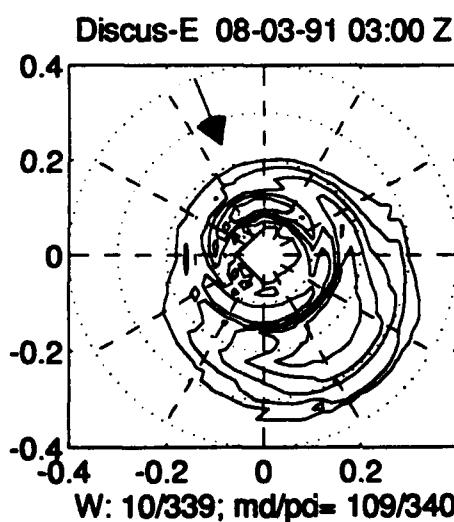
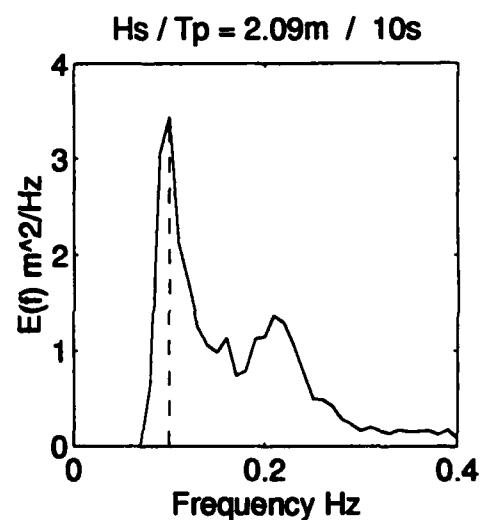
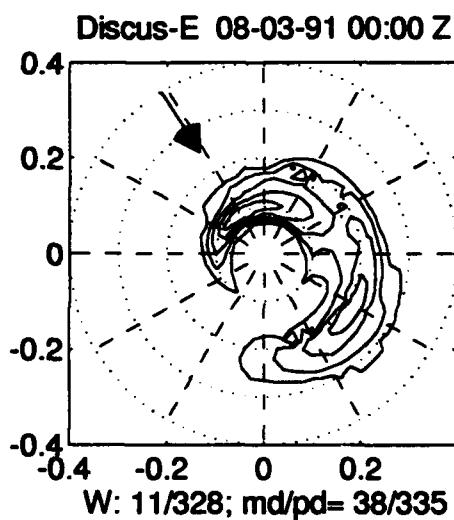
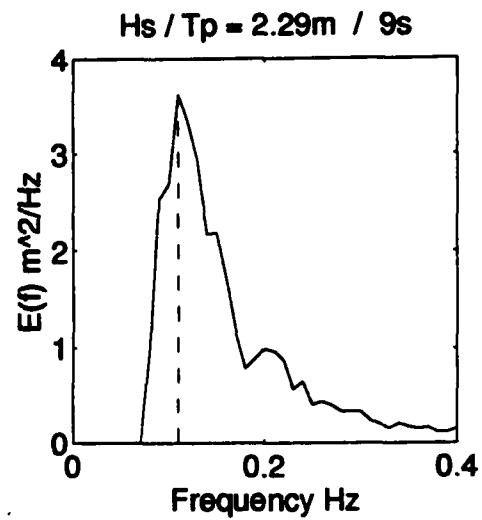
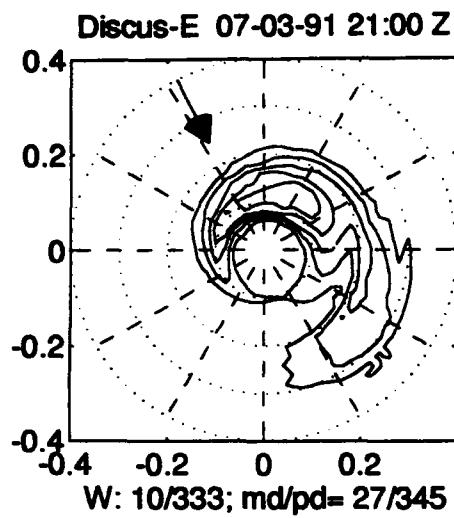


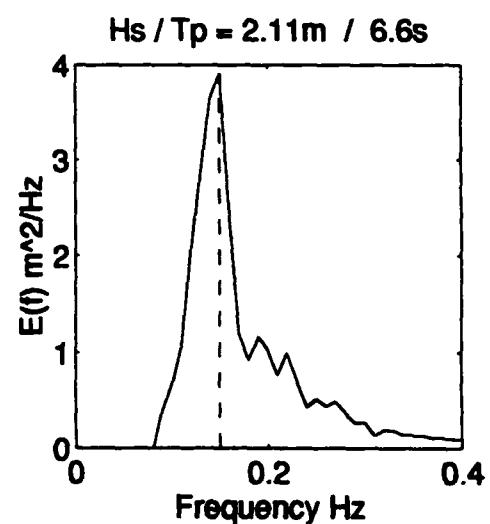
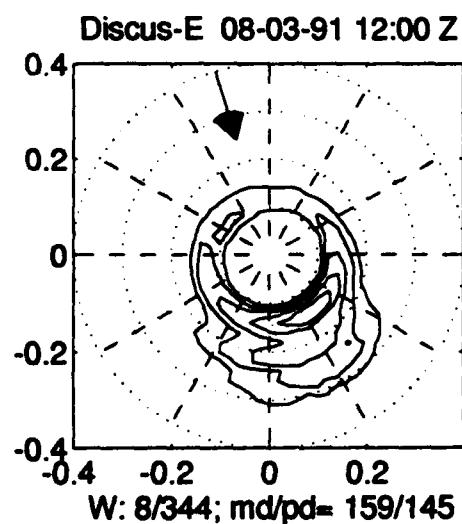
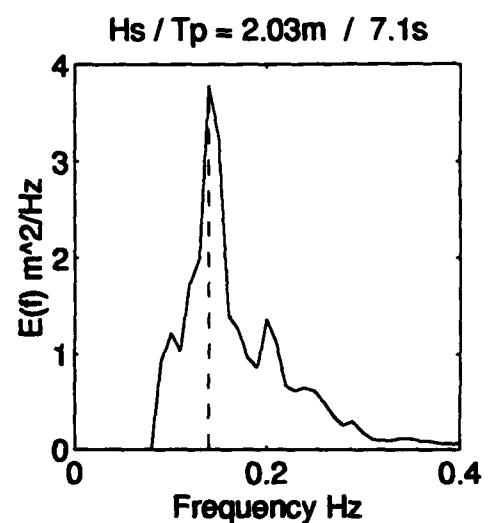
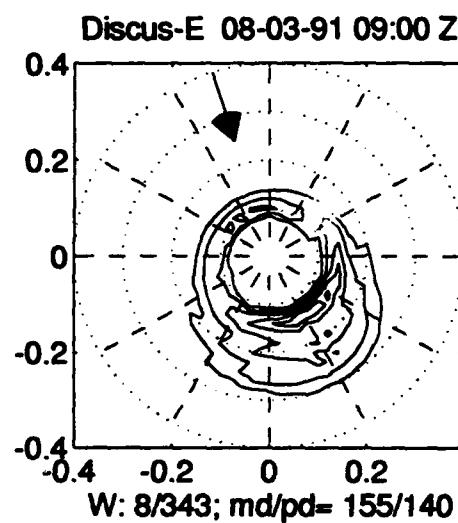
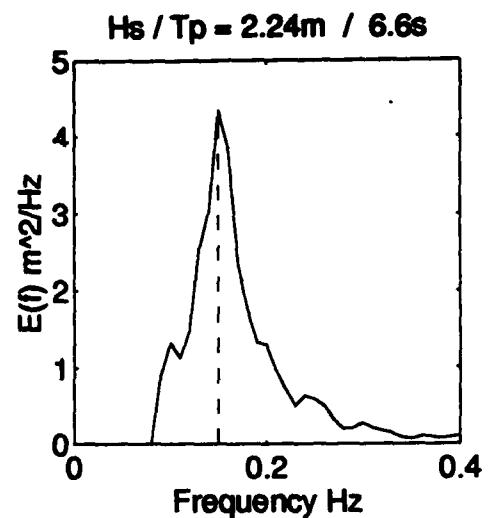
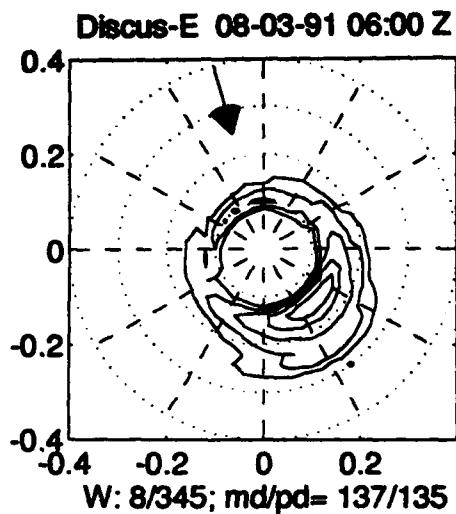


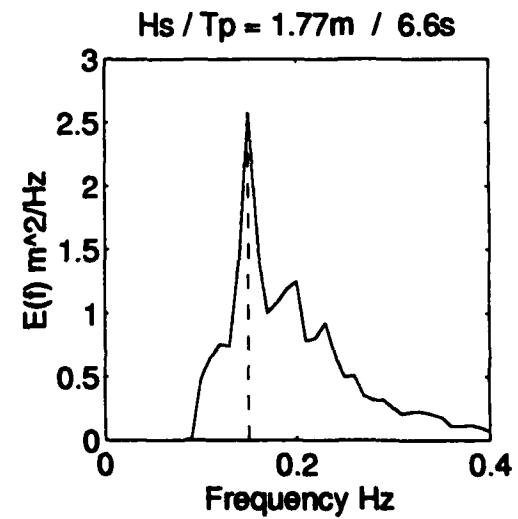
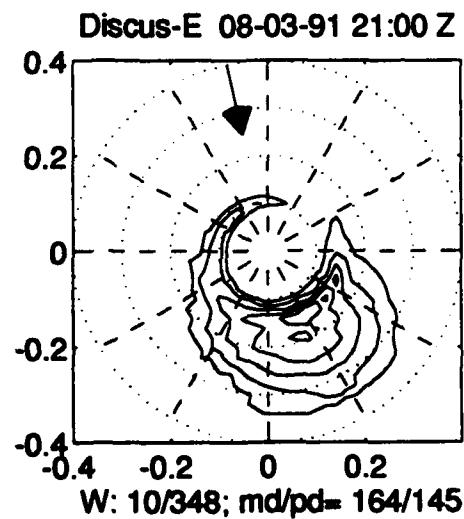
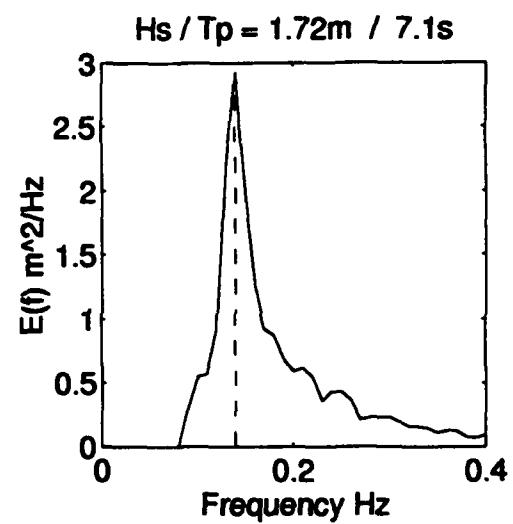
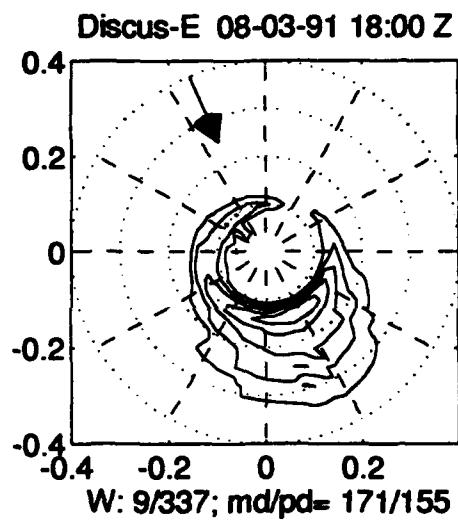
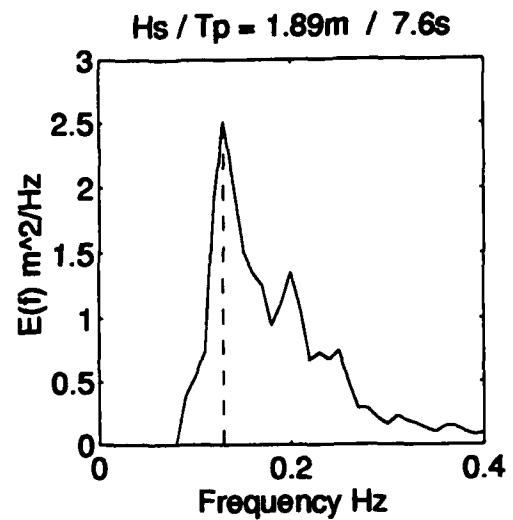
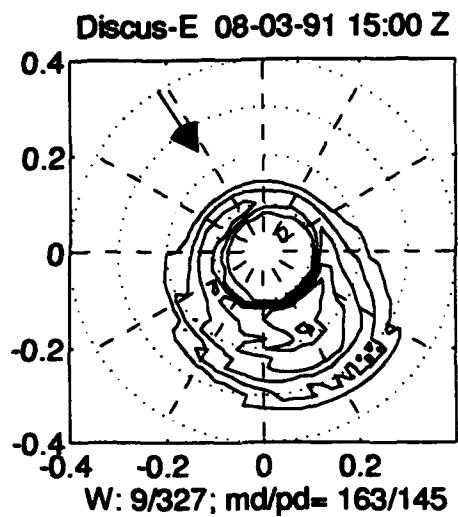


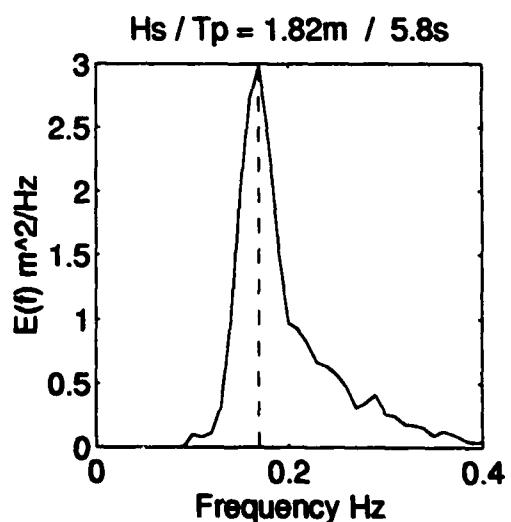
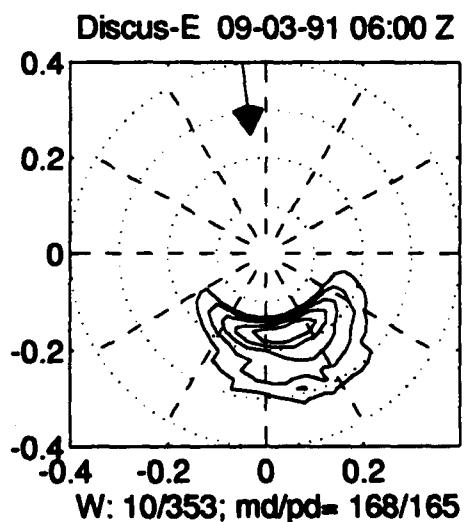
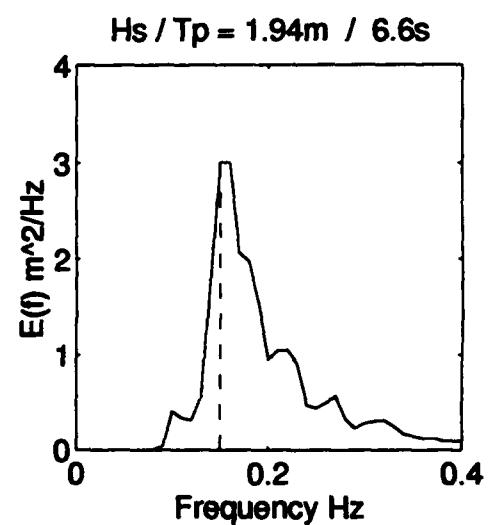
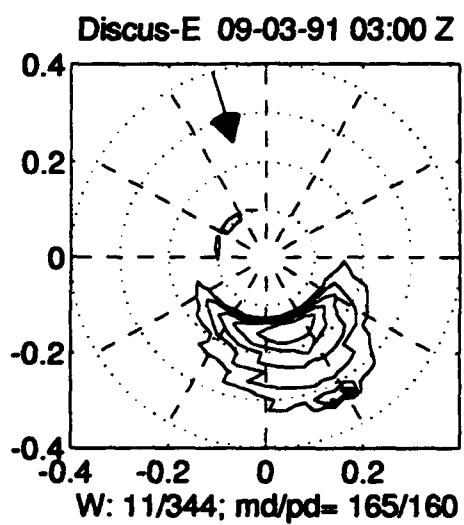
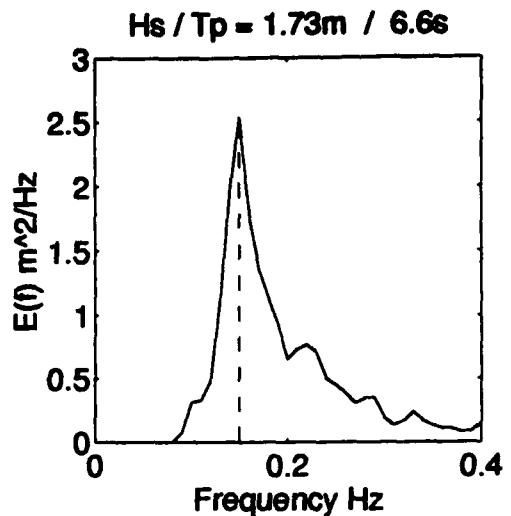
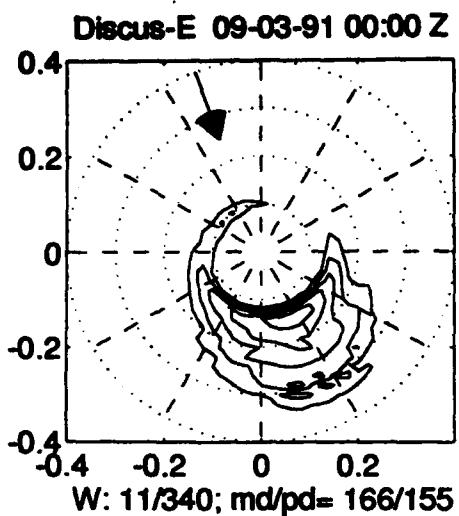




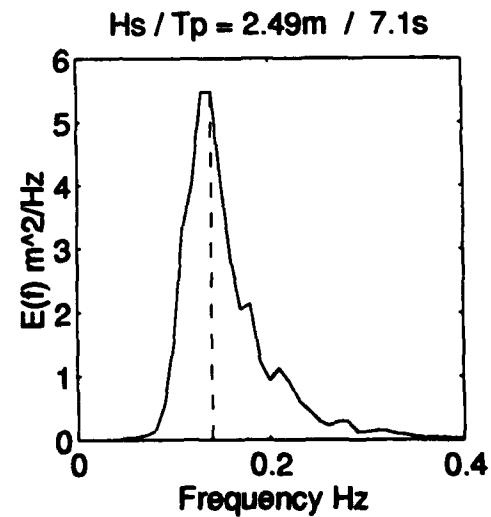
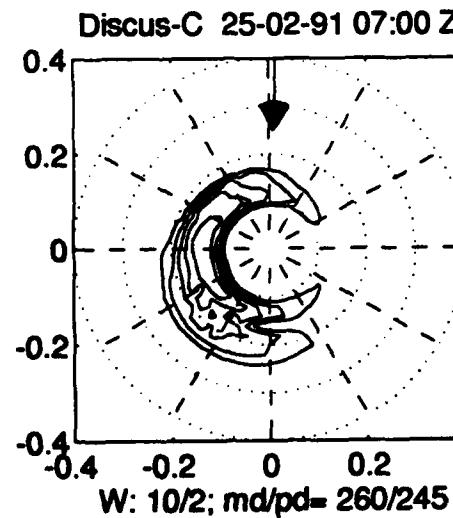
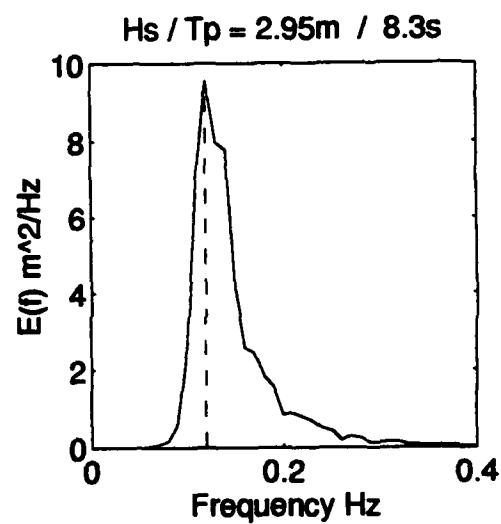
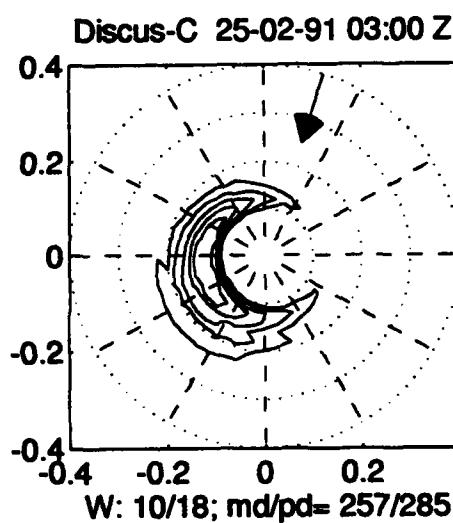
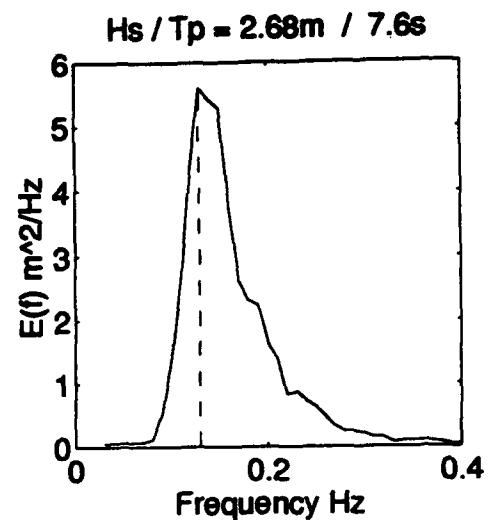
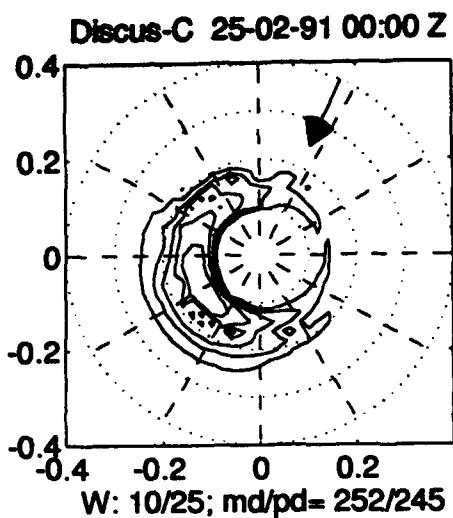


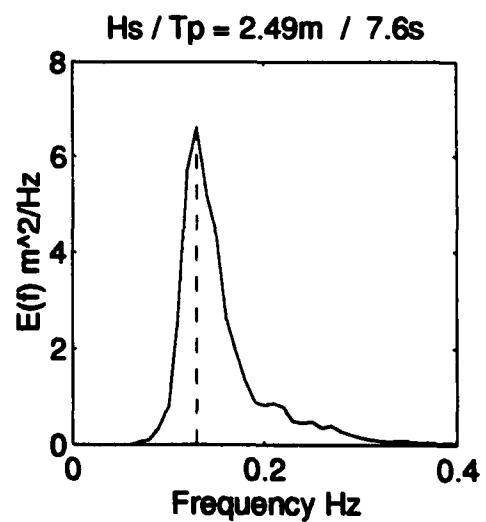
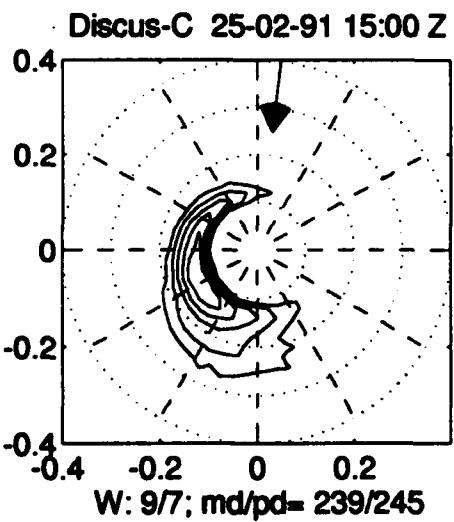
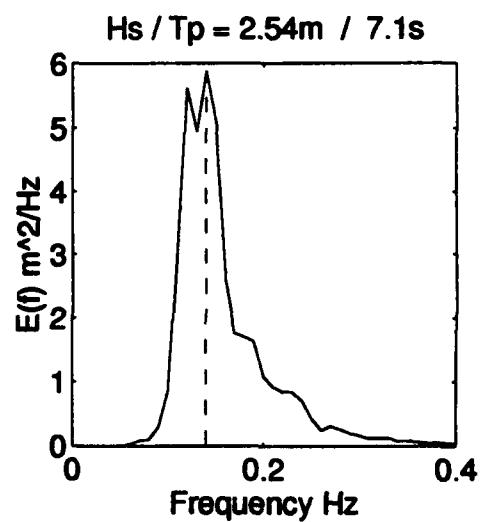
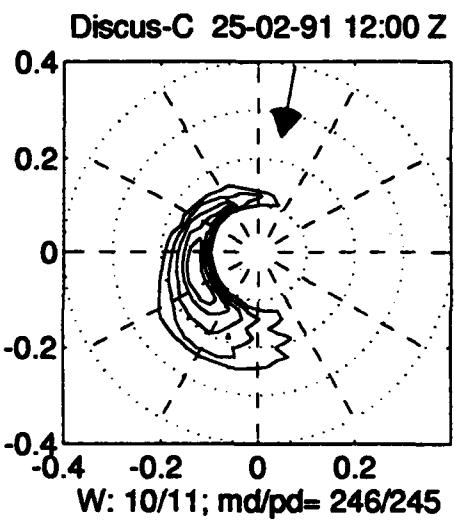
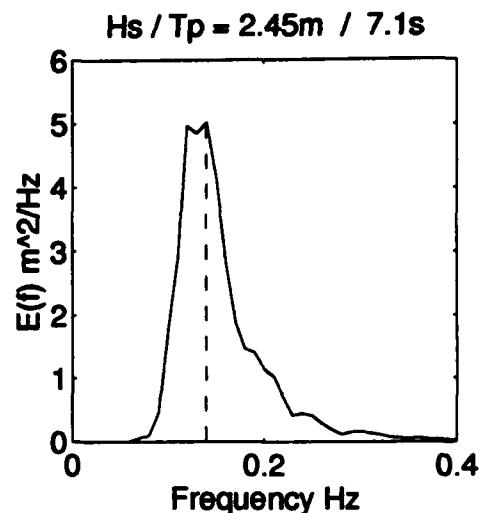
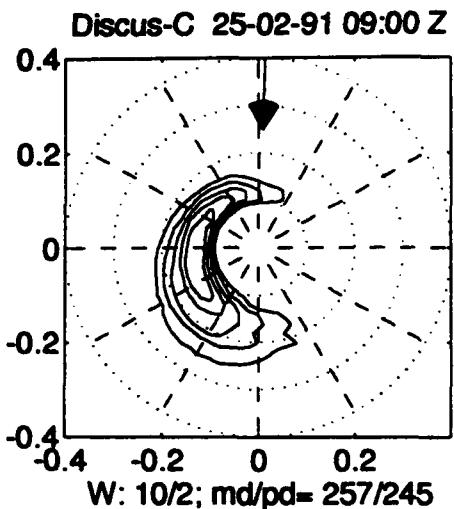


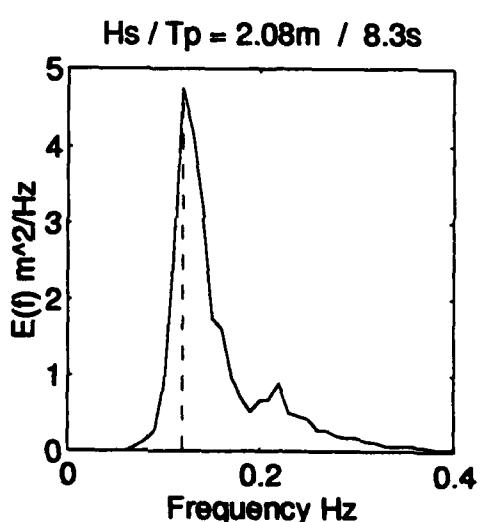
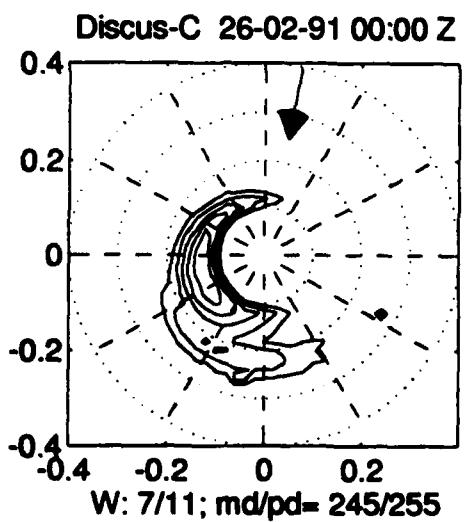
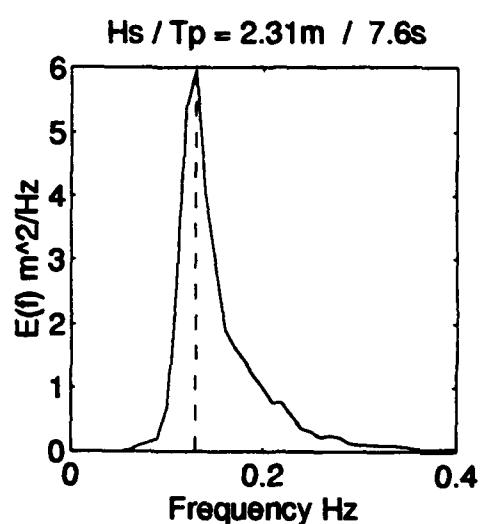
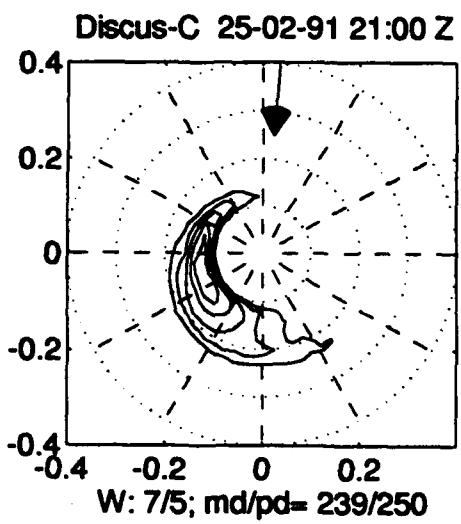
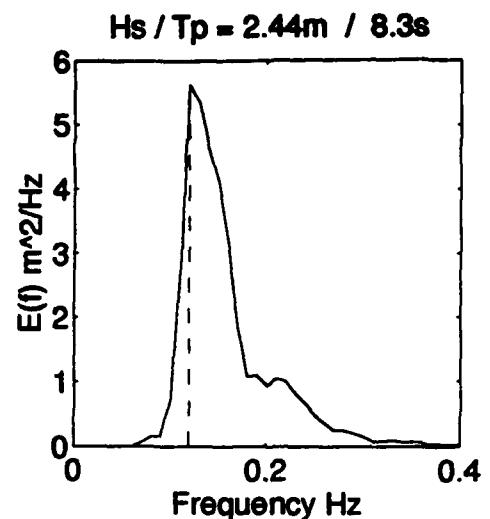
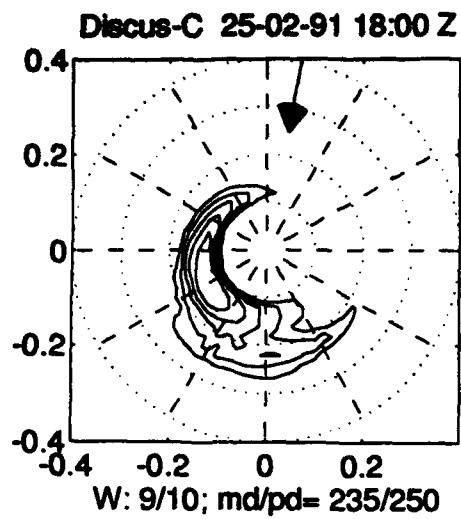


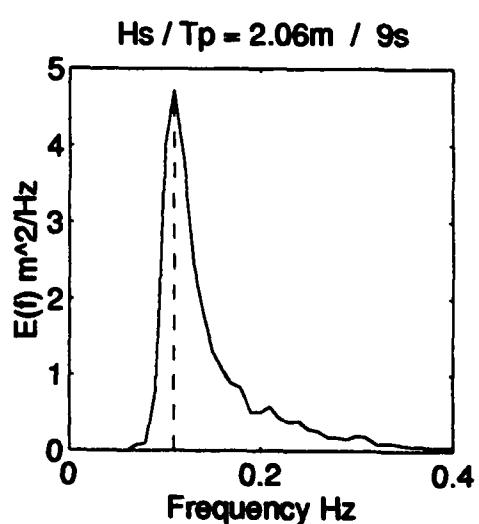
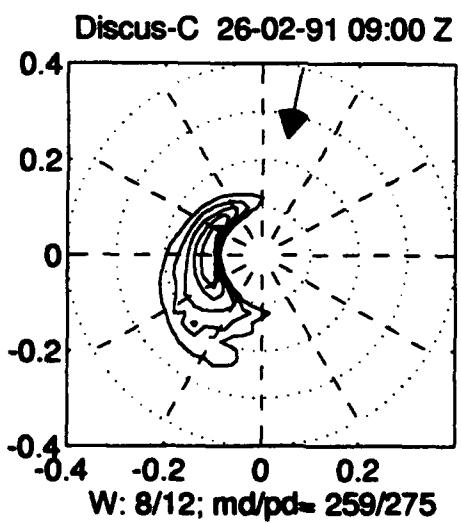
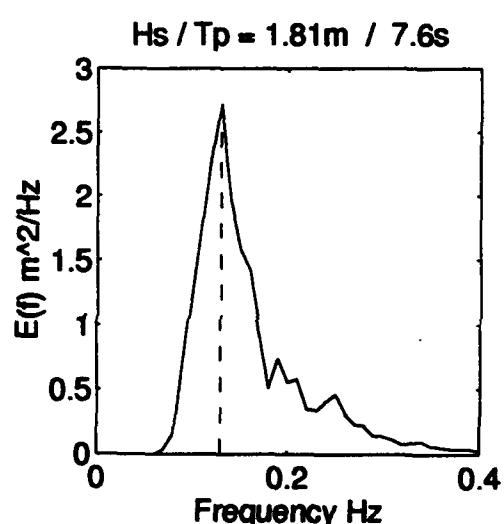
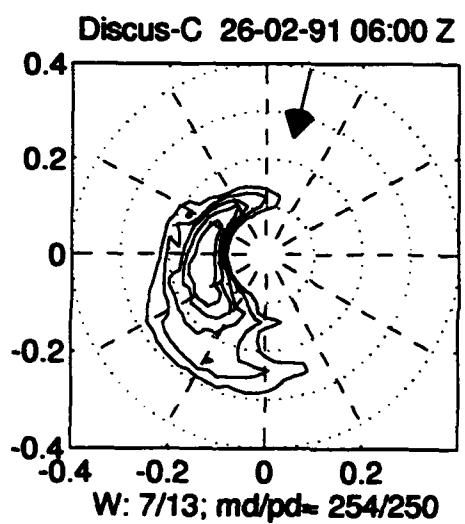
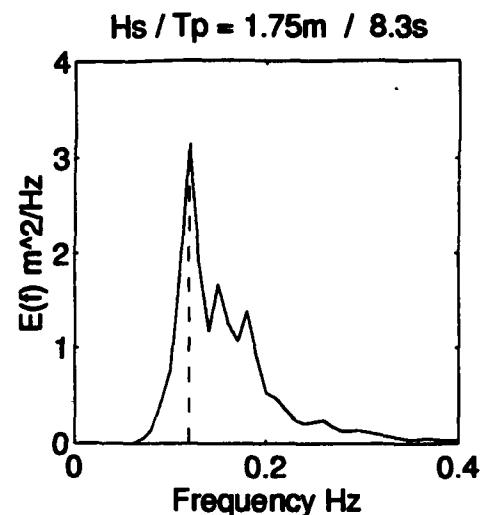
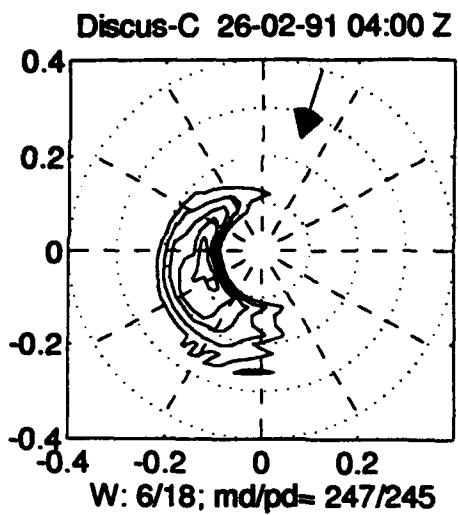


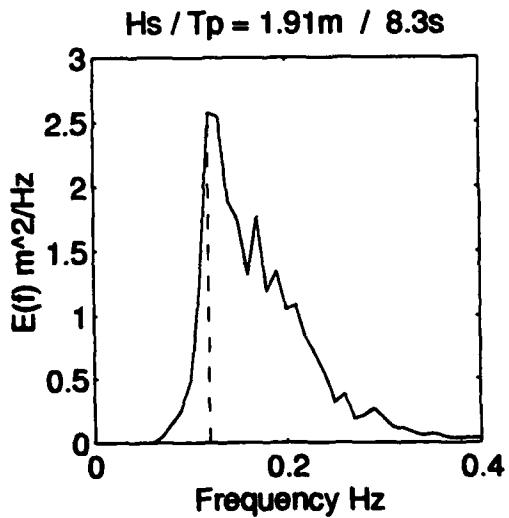
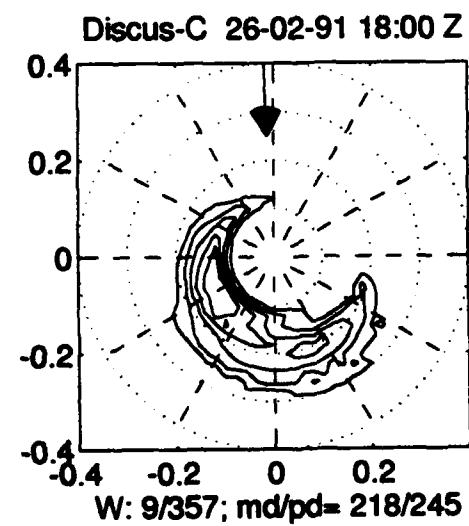
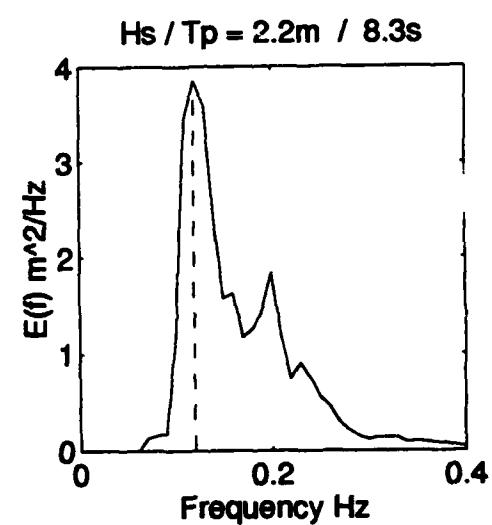
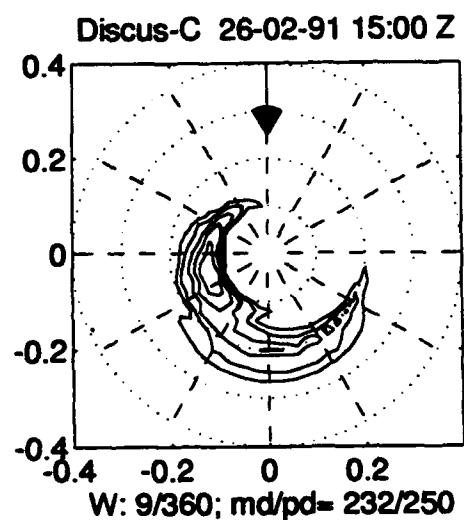
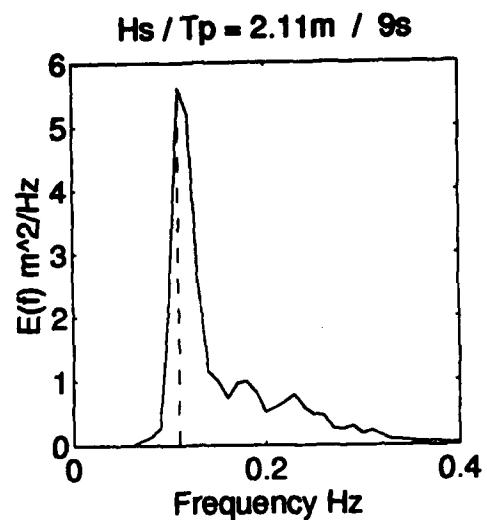
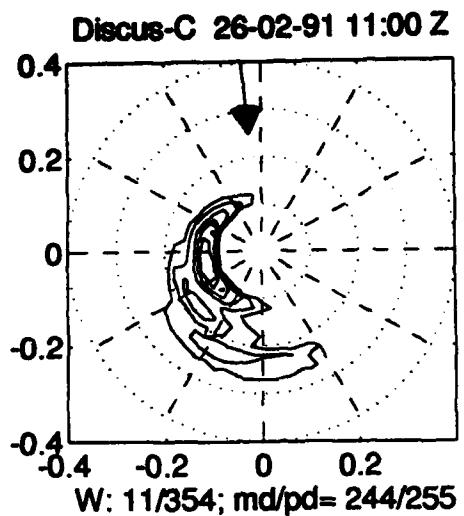
B.3: Discus Buoy "Central"

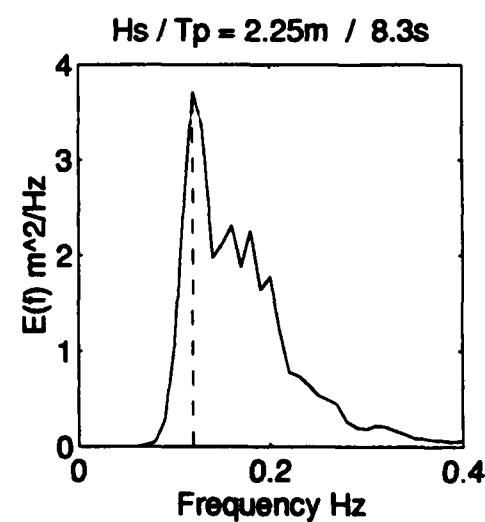
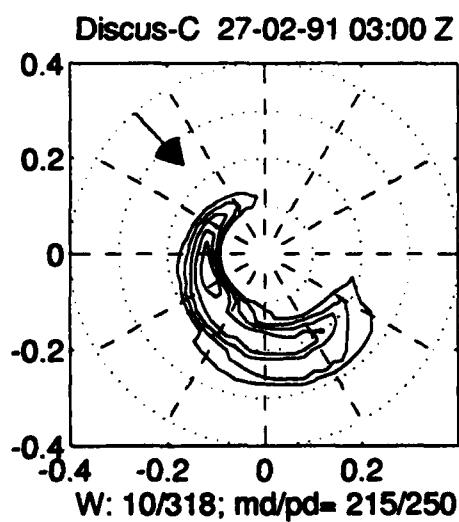
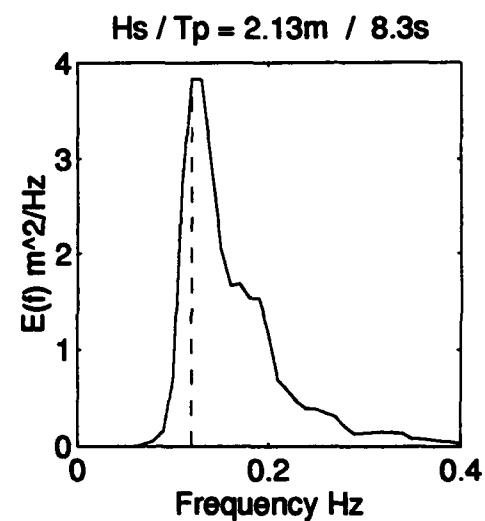
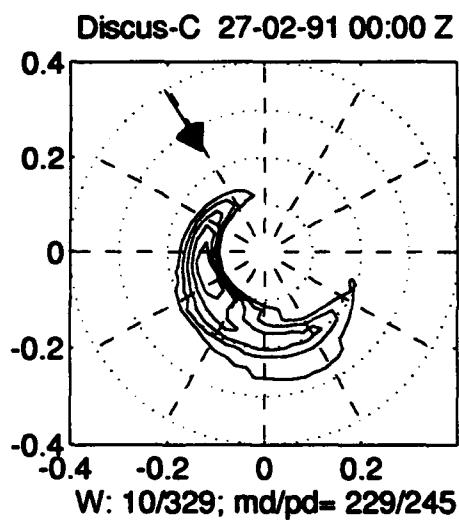
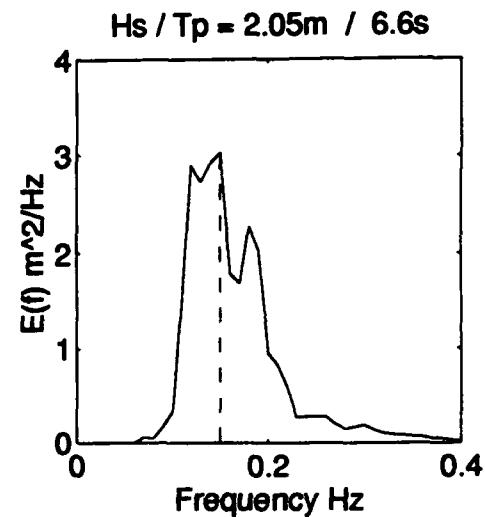
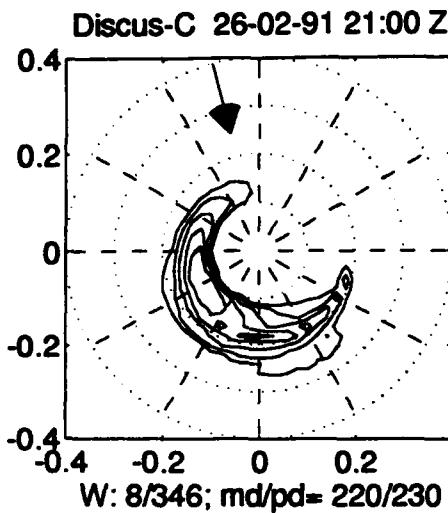


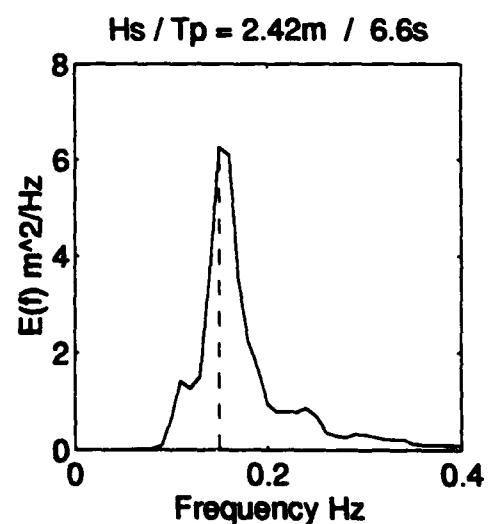
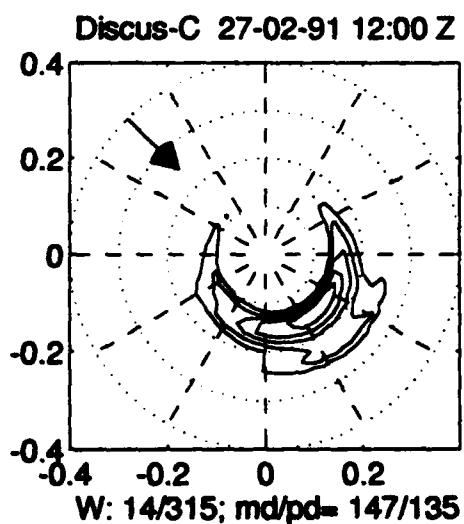
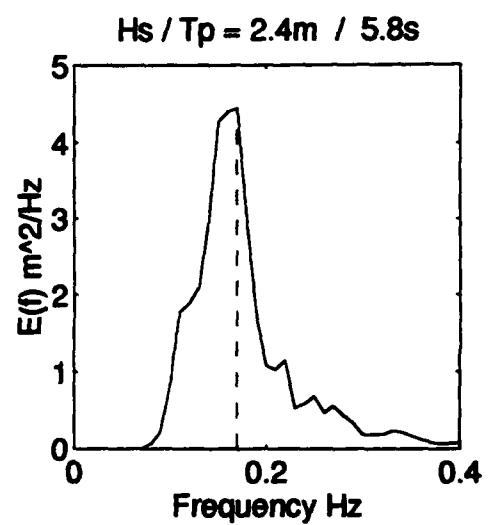
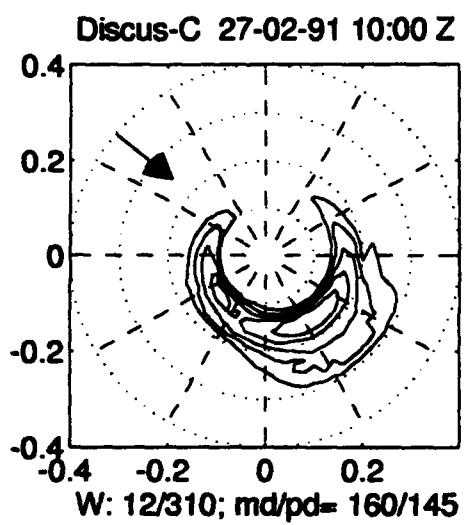
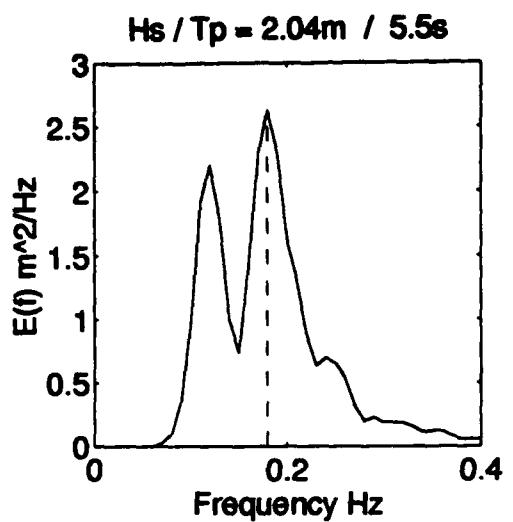
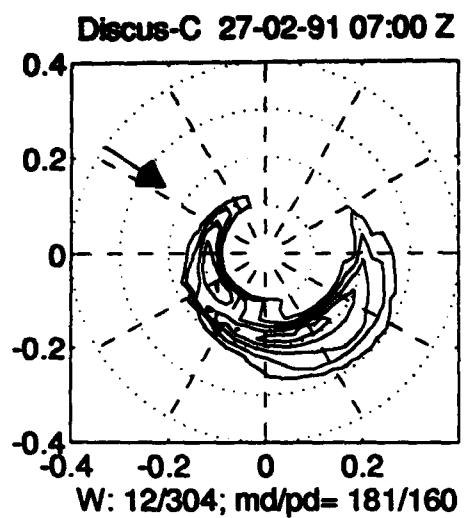


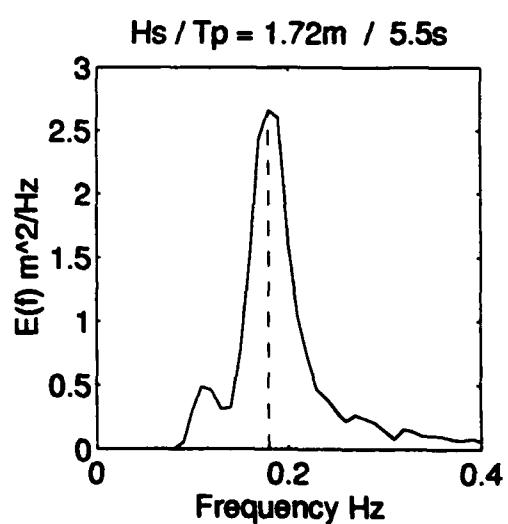
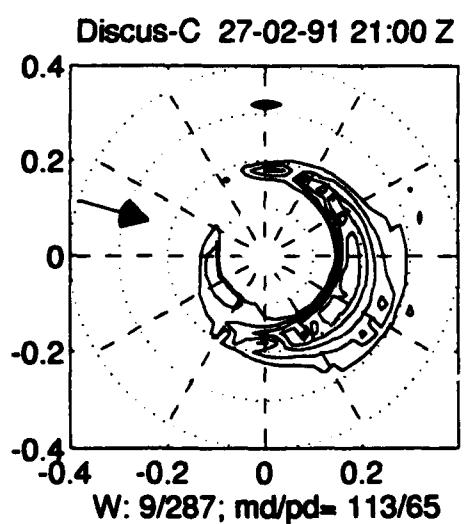
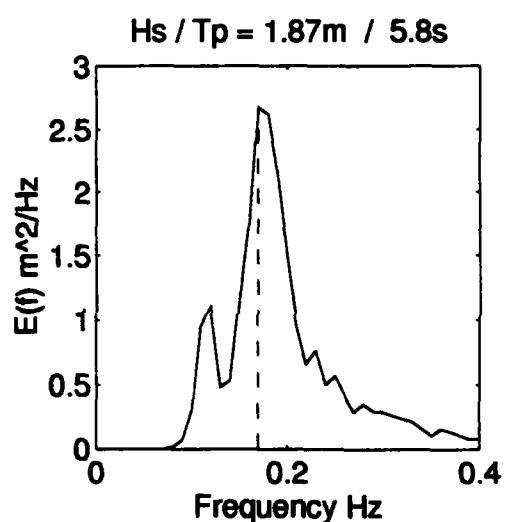
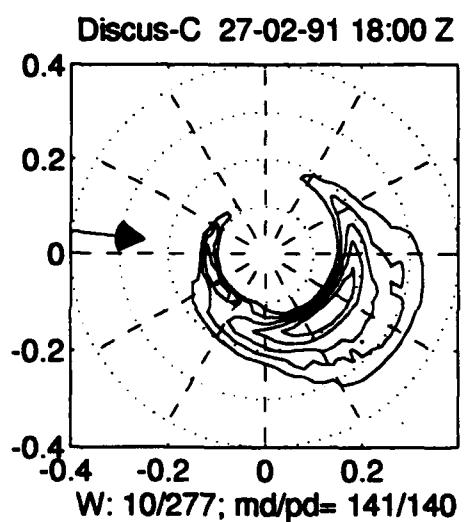
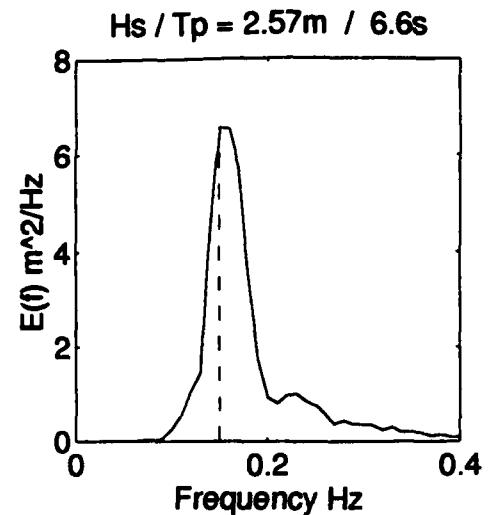
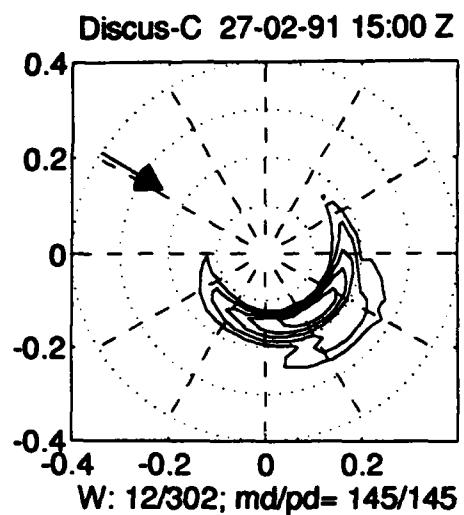


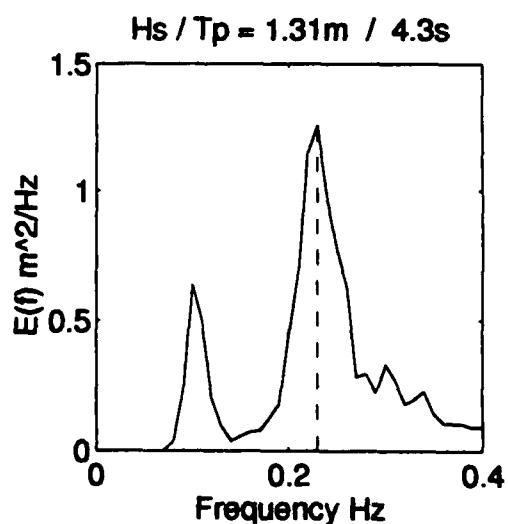
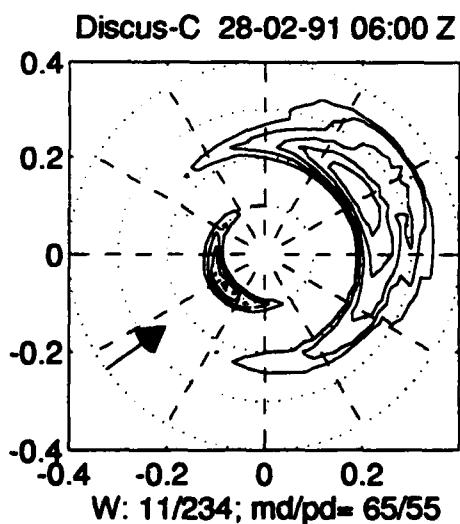
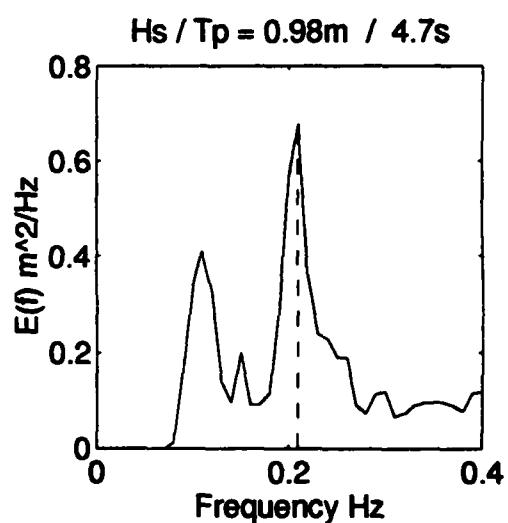
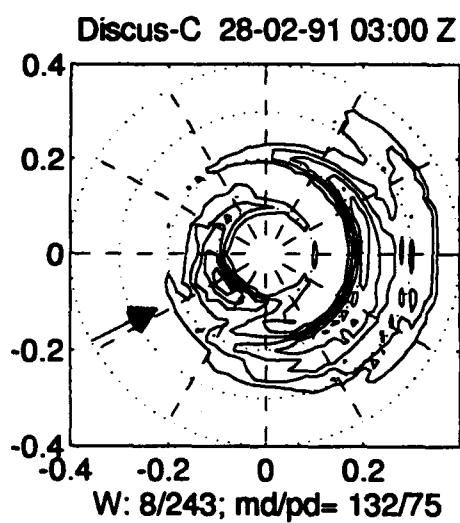
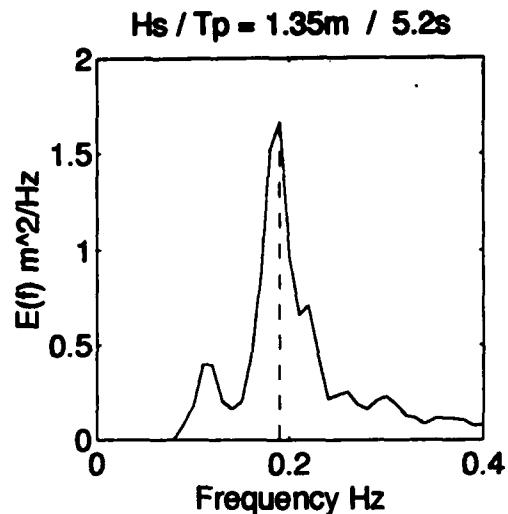
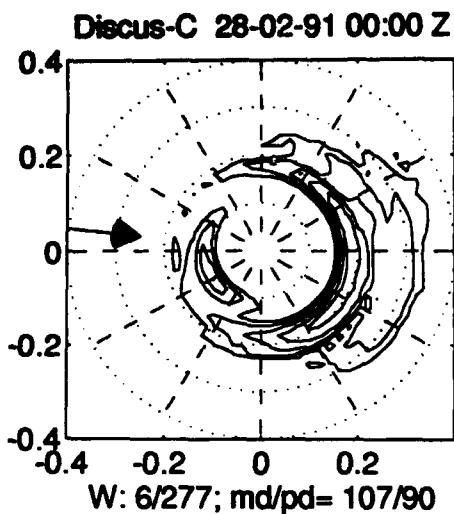


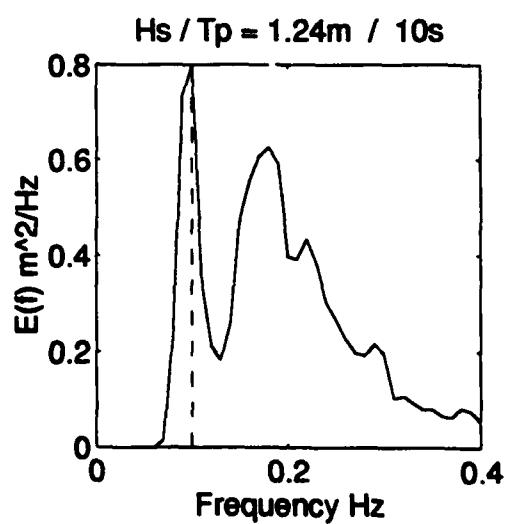
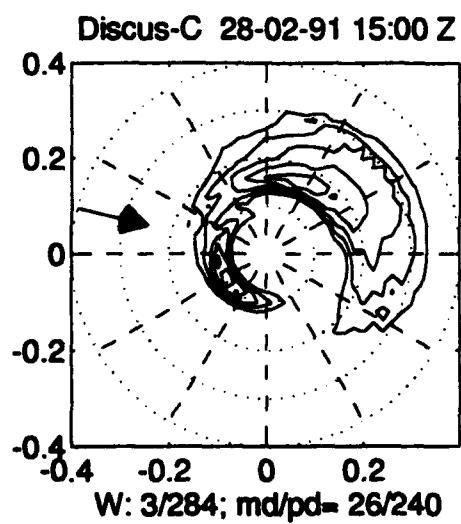
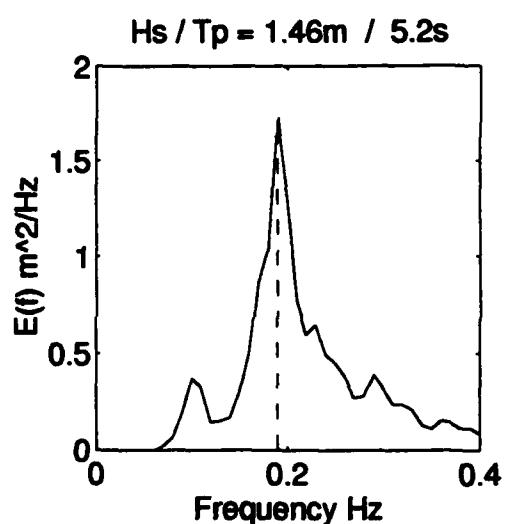
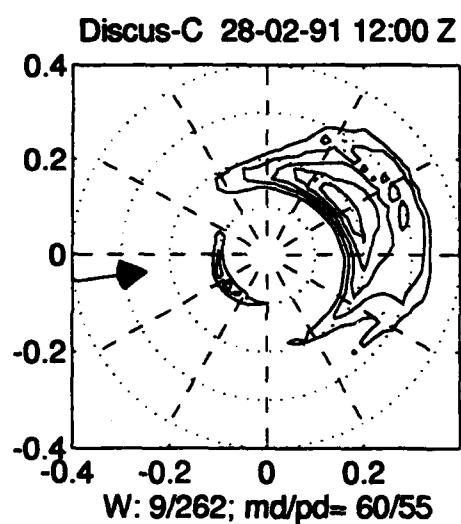
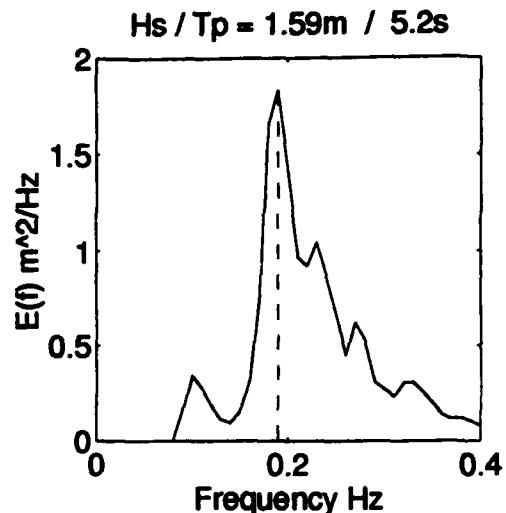
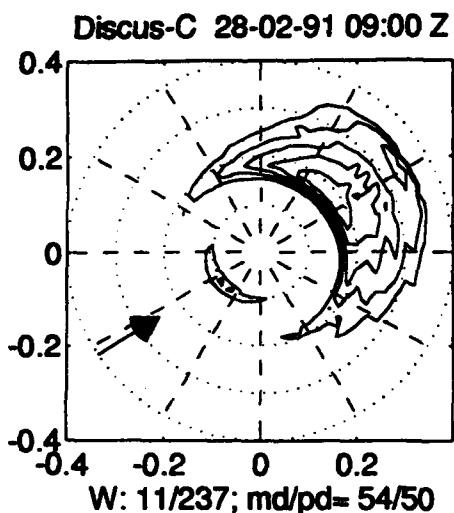


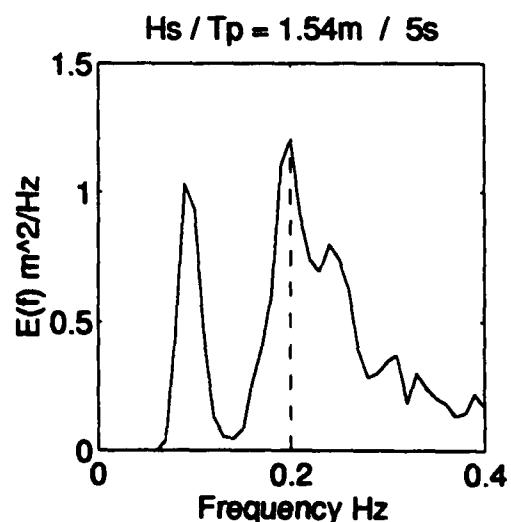
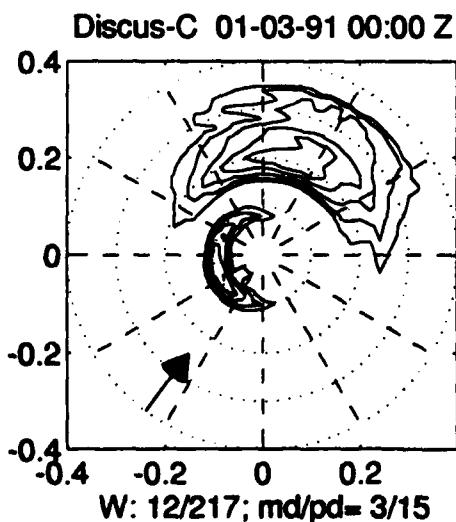
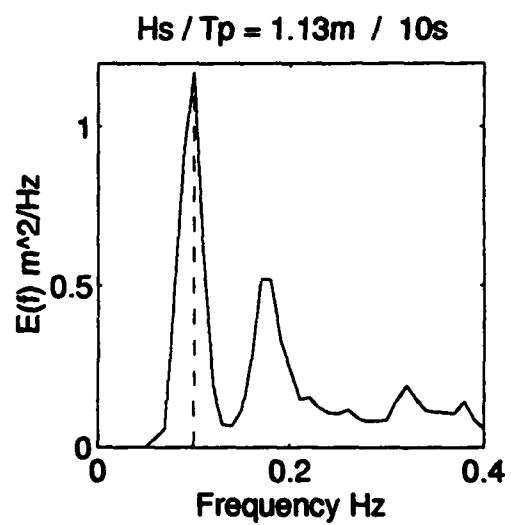
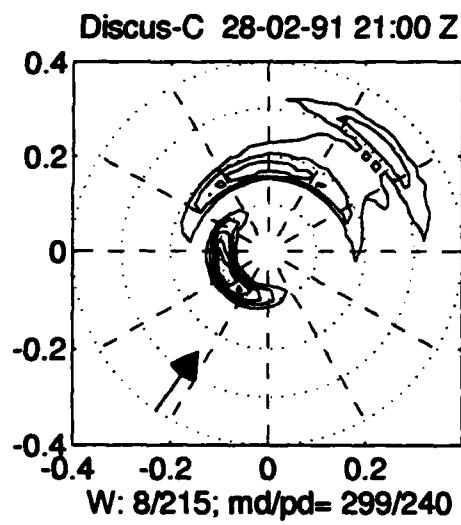
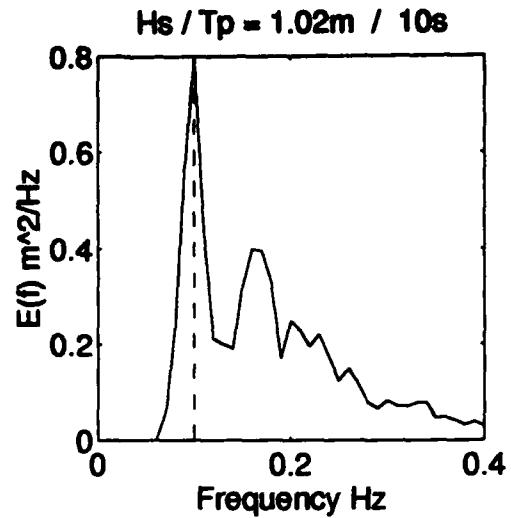
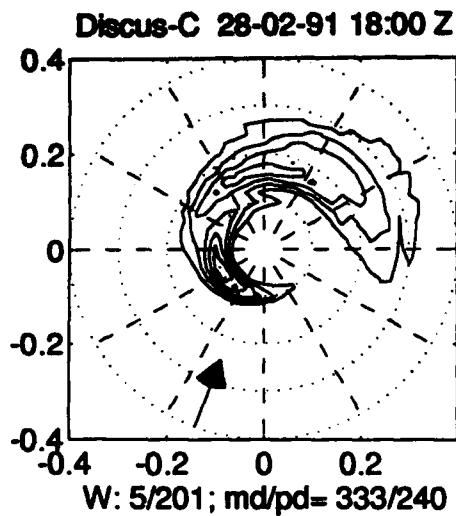


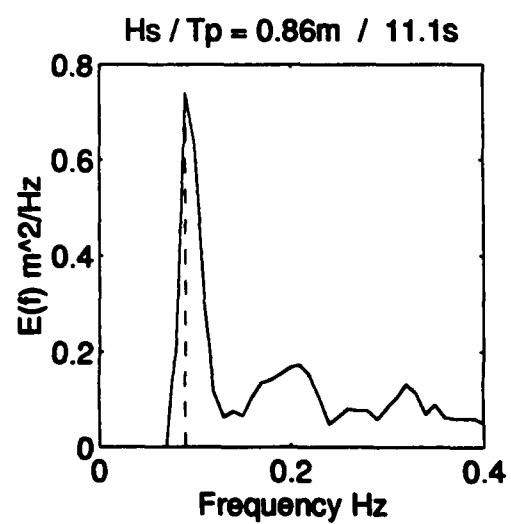
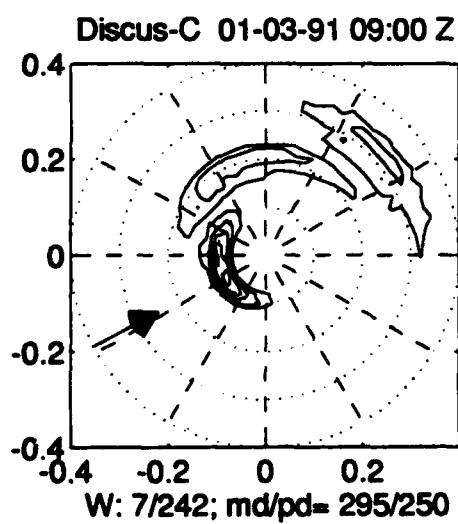
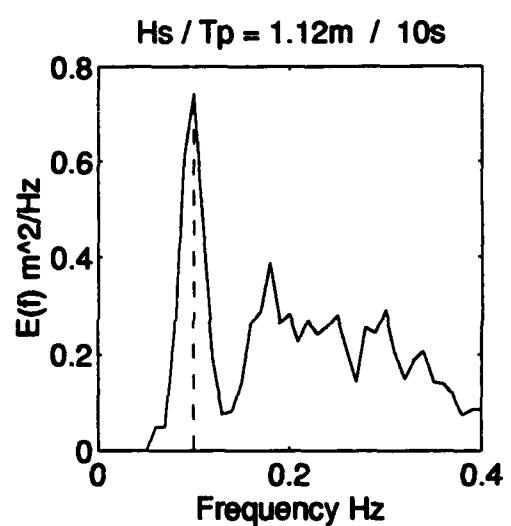
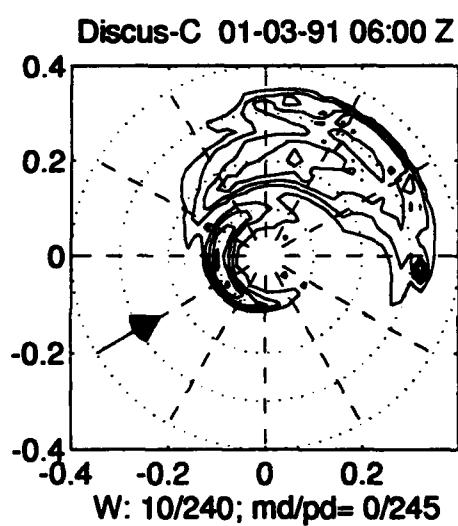
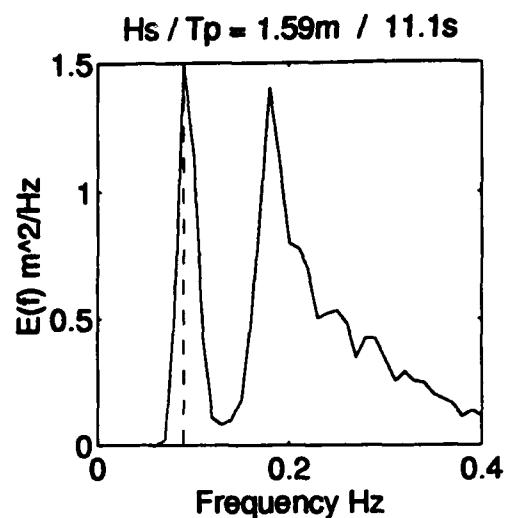
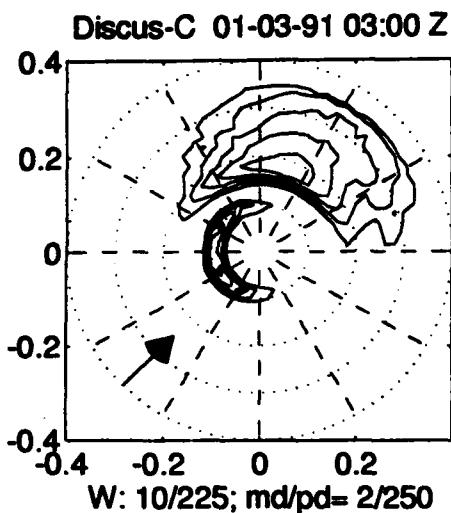


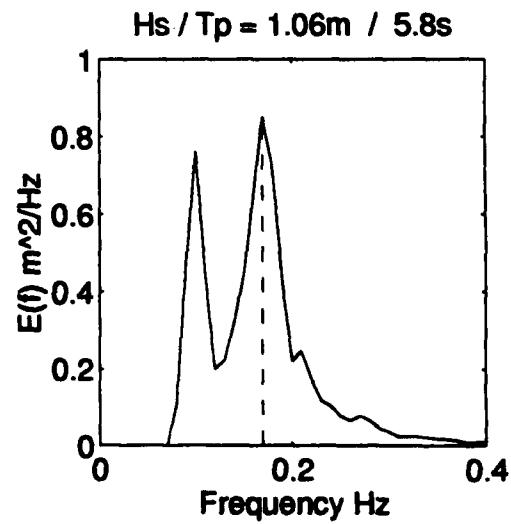
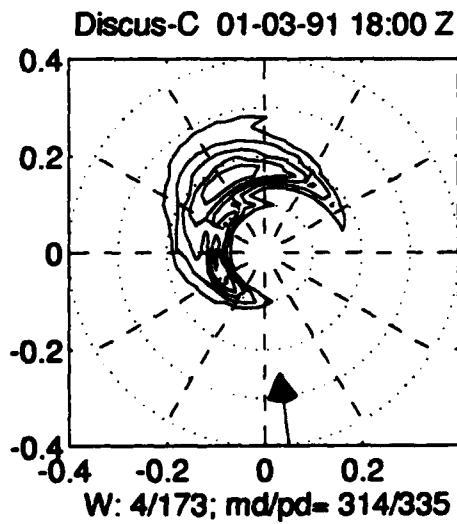
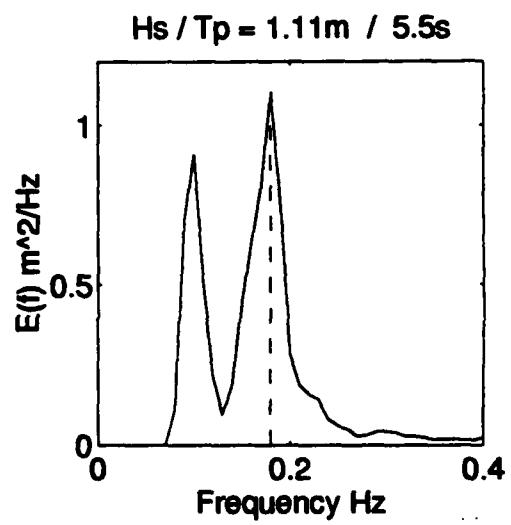
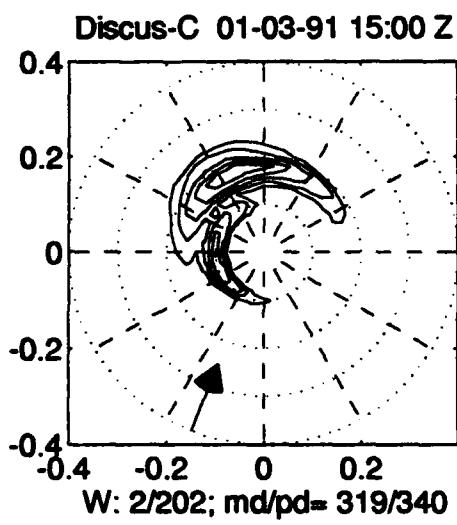
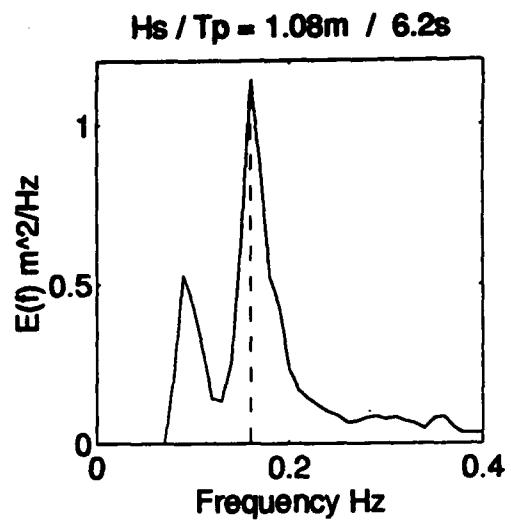
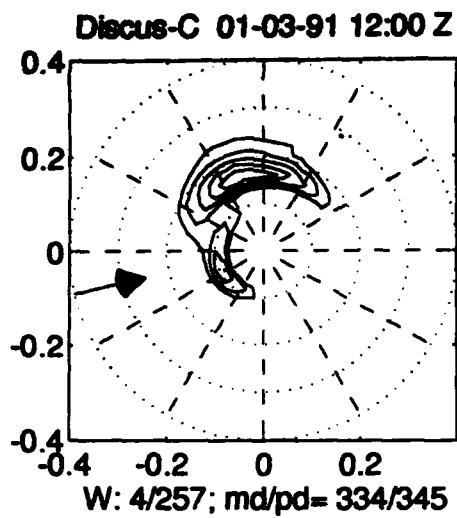


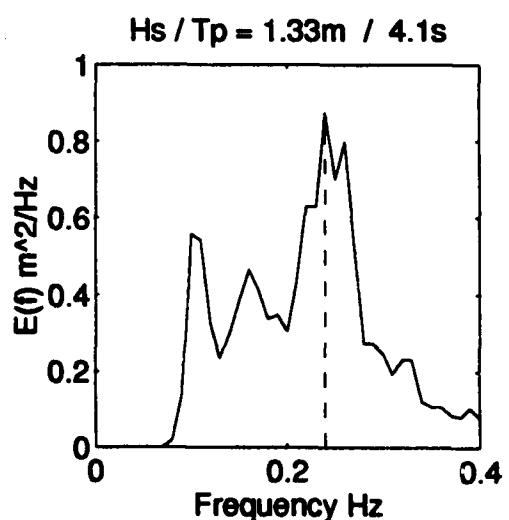
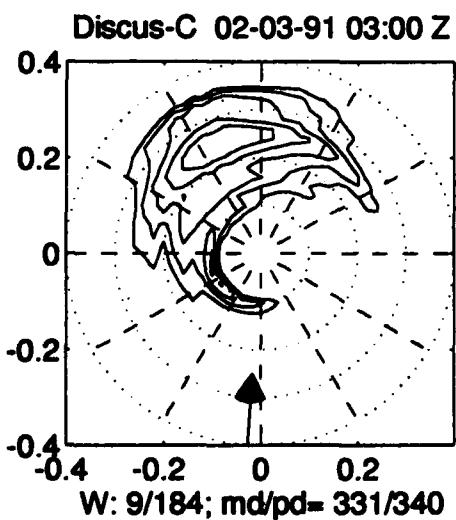
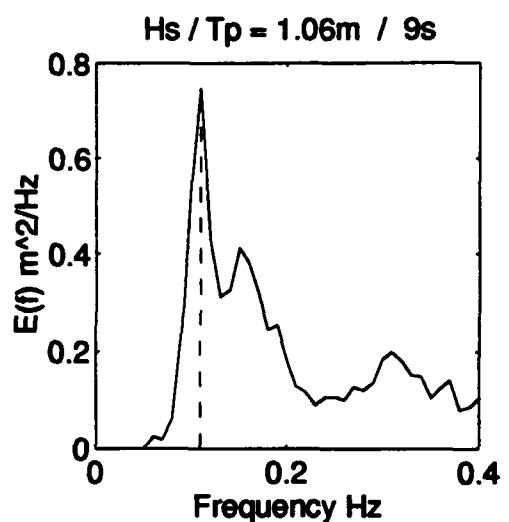
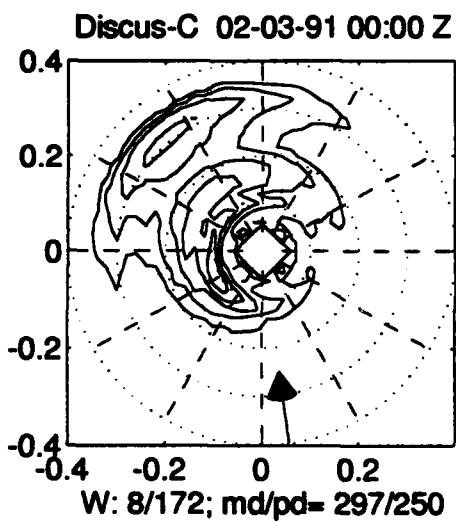
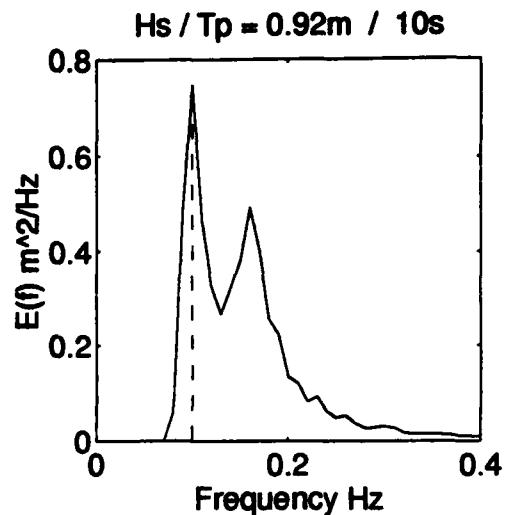
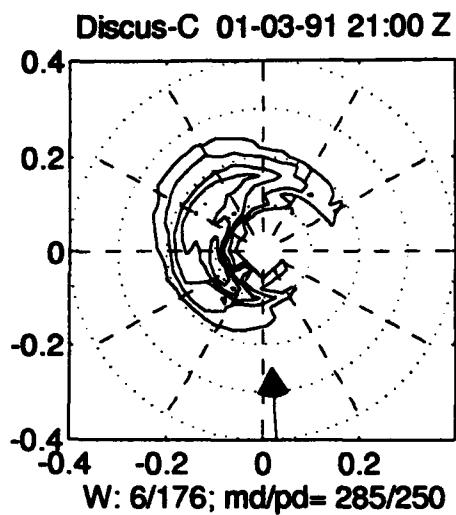




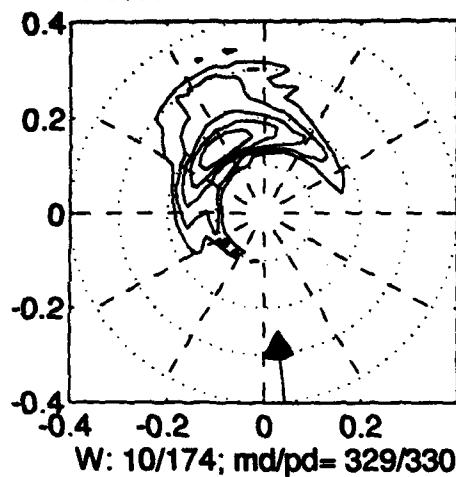




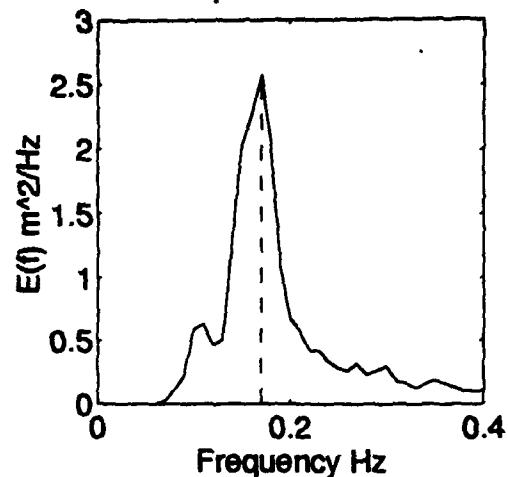




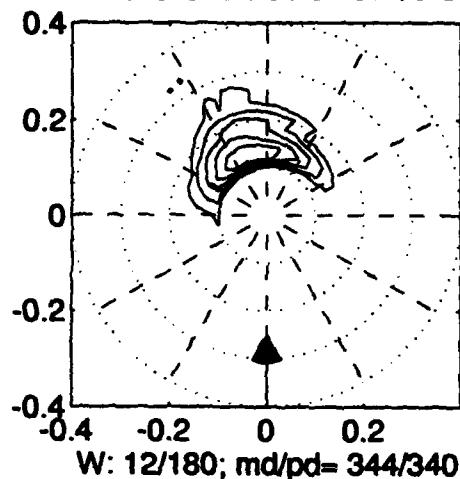
Discus-C 02-03-91 06:00 Z



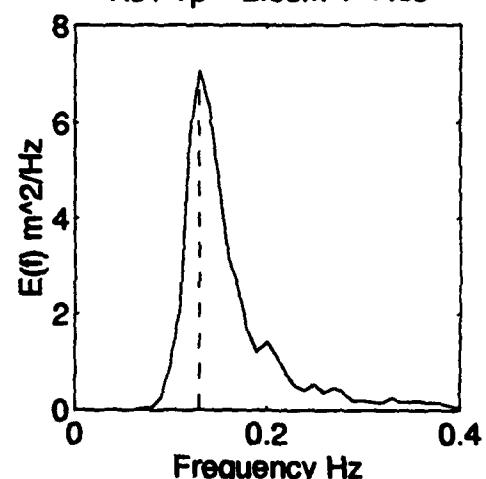
Hs / Tp = 1.75m / 5.8s



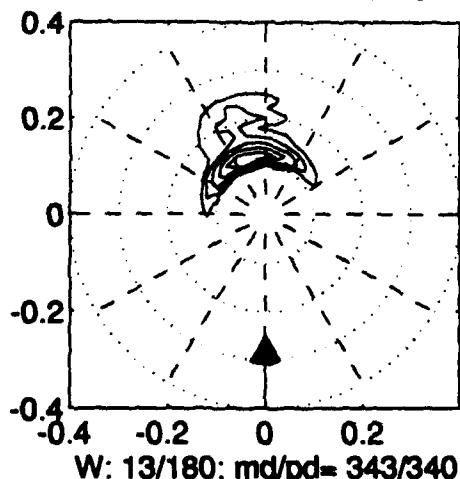
Discus-C 02-03-91 09:00 Z



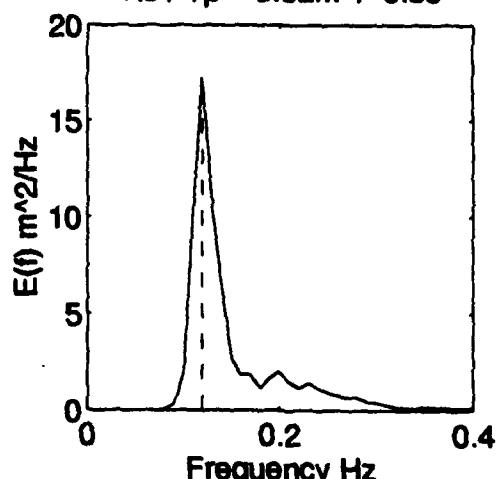
Hs / Tp = 2.65m / 7.6s

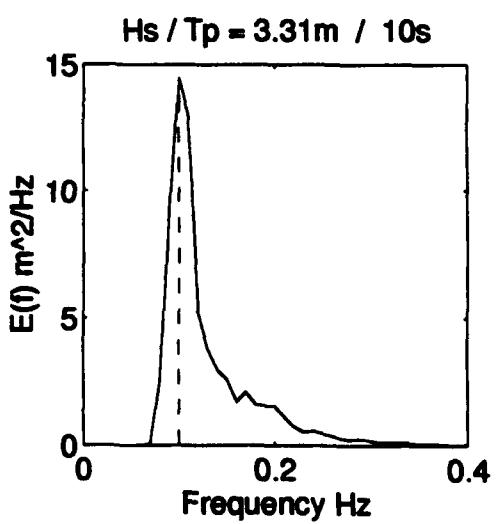
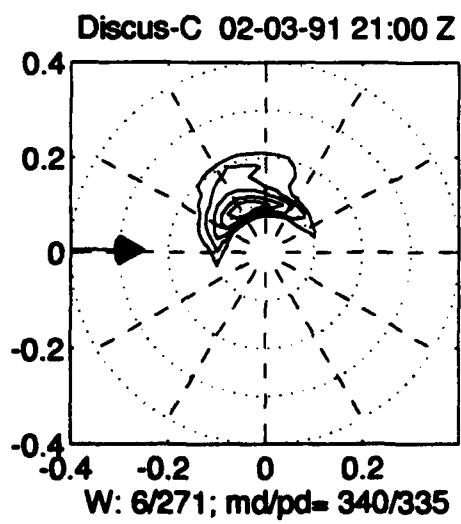
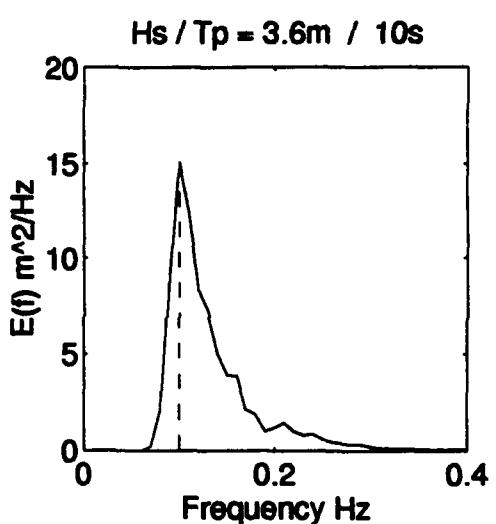
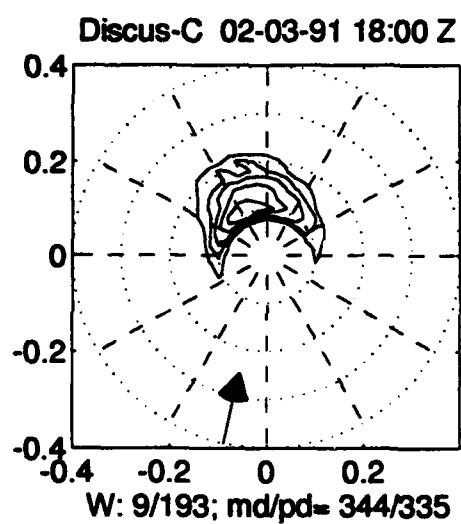
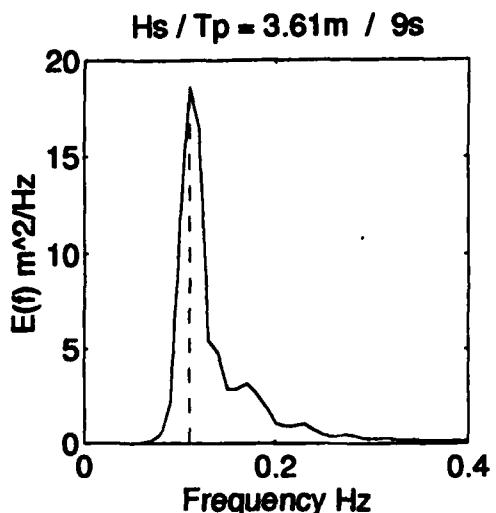
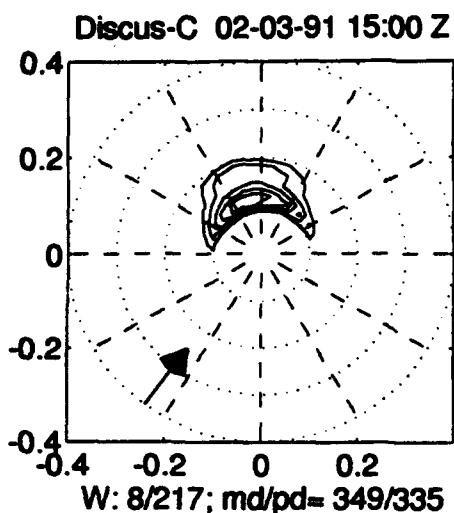


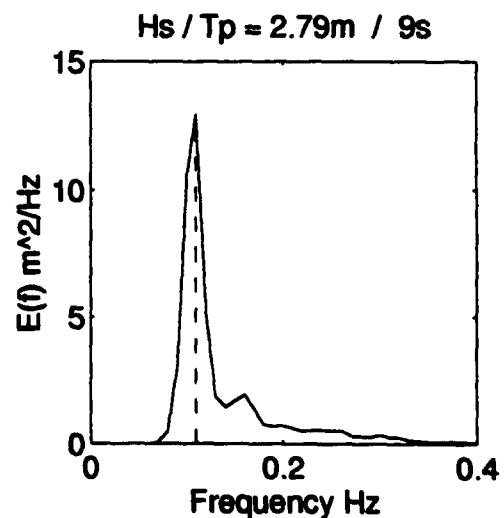
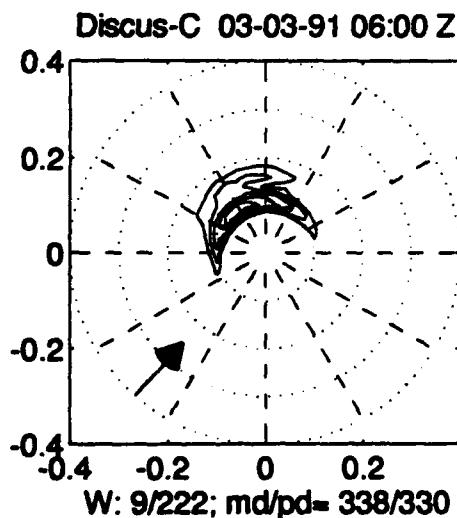
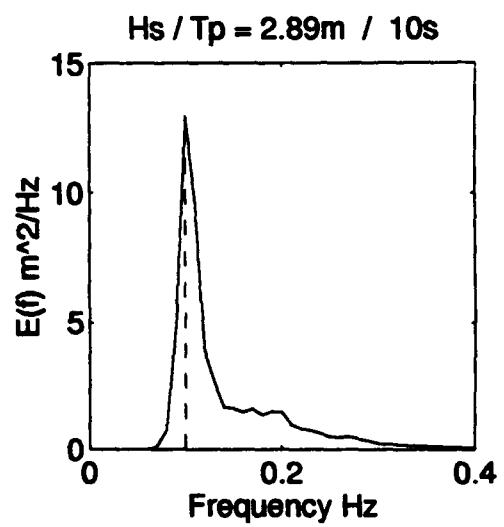
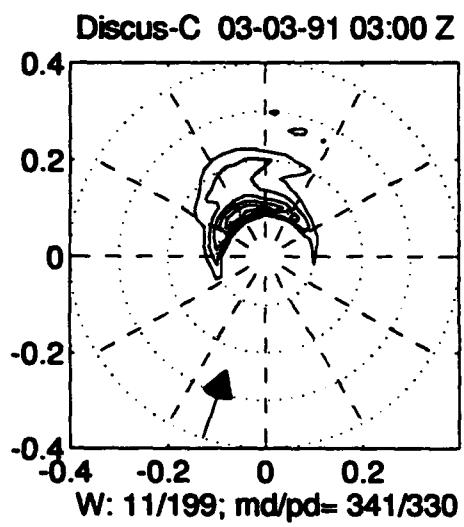
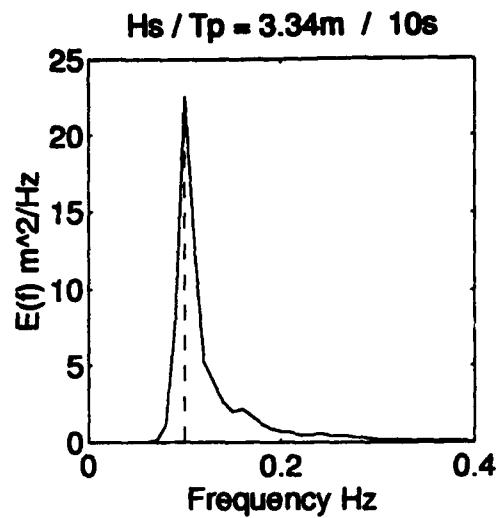
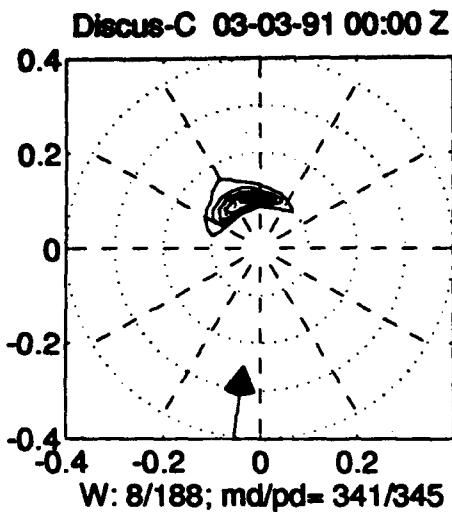
Discus-C 02-03-91 12:00 Z

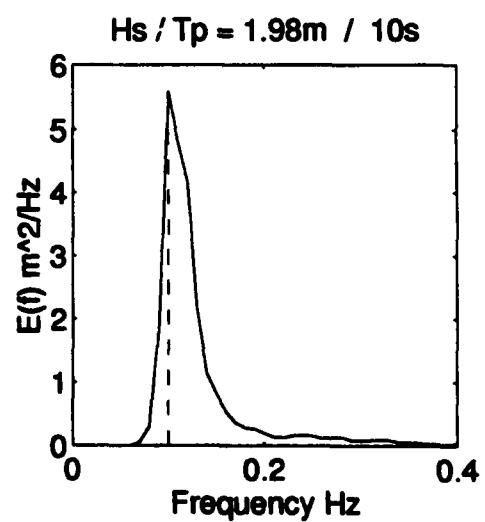
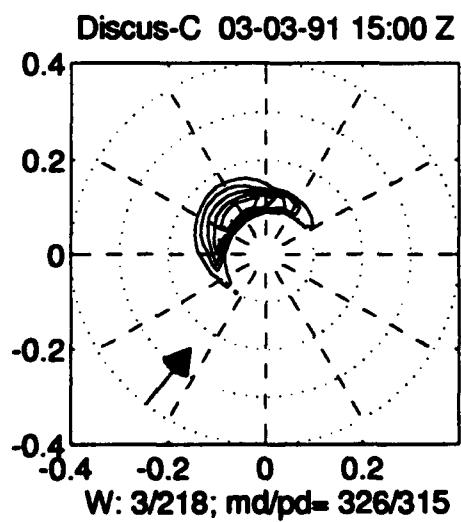
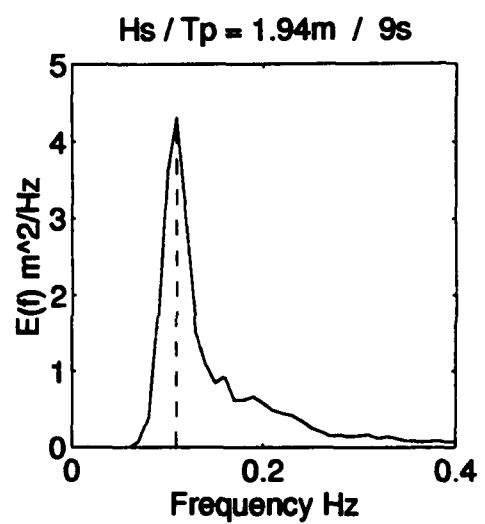
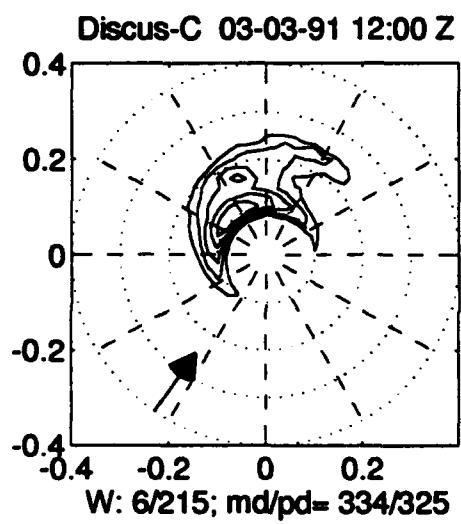
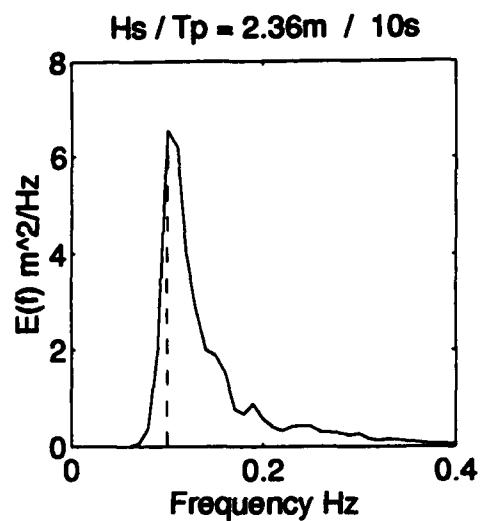
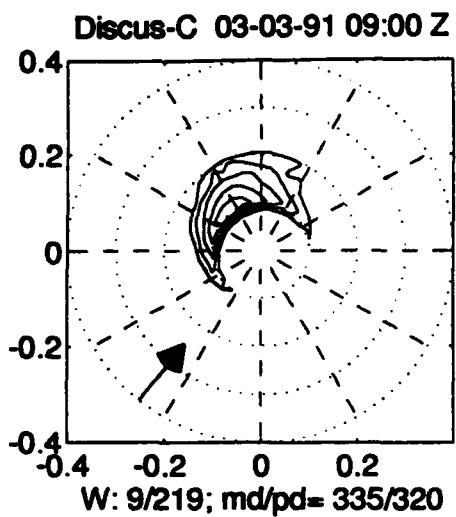


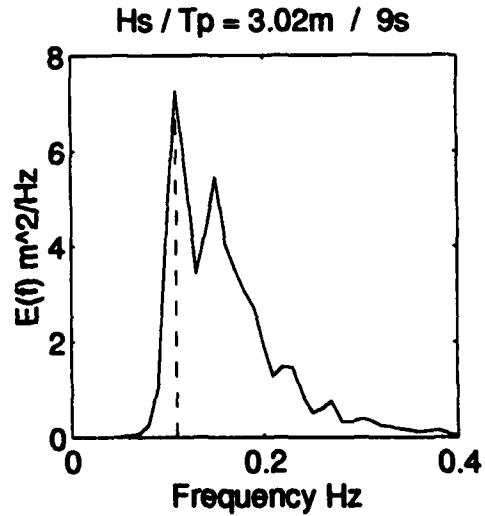
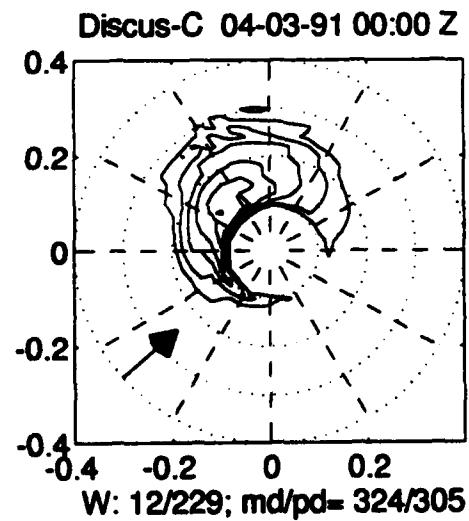
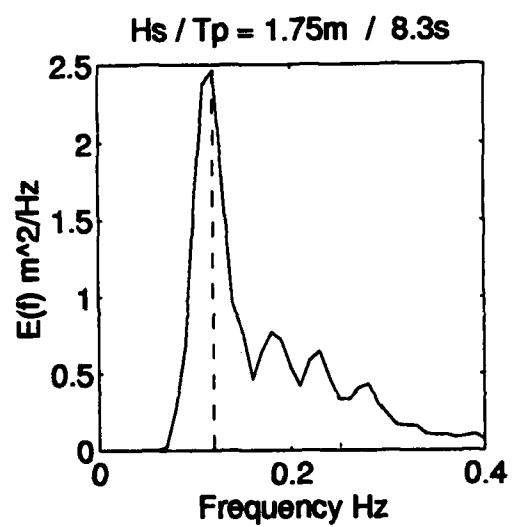
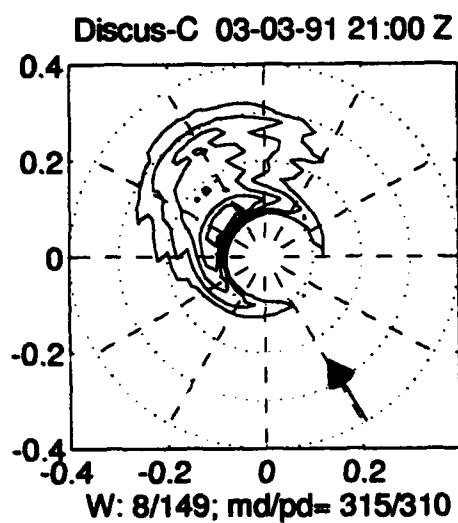
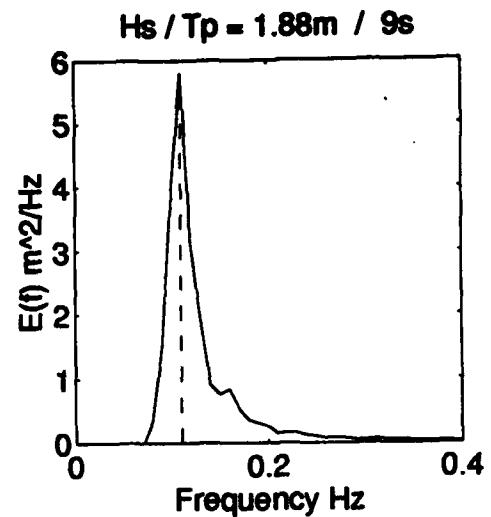
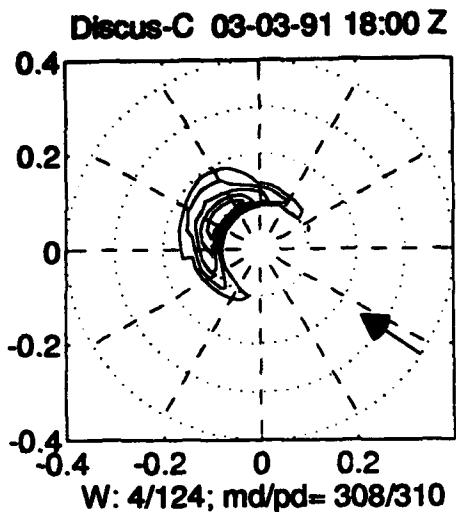
Hs / Tp = 3.32m / 8.3s

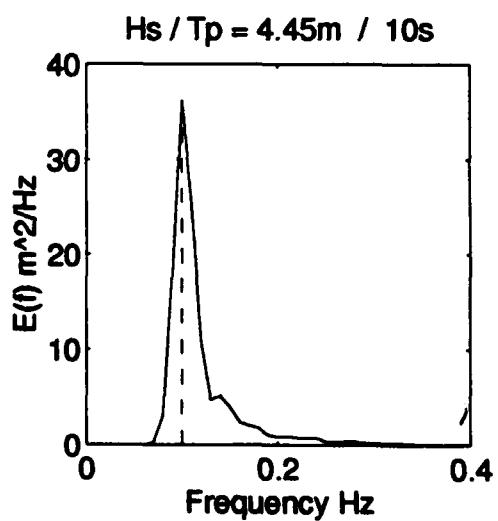
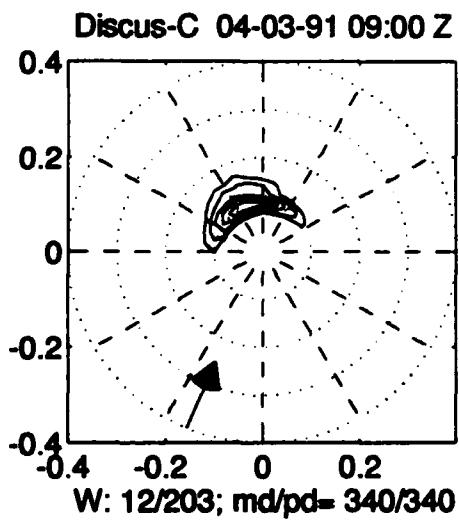
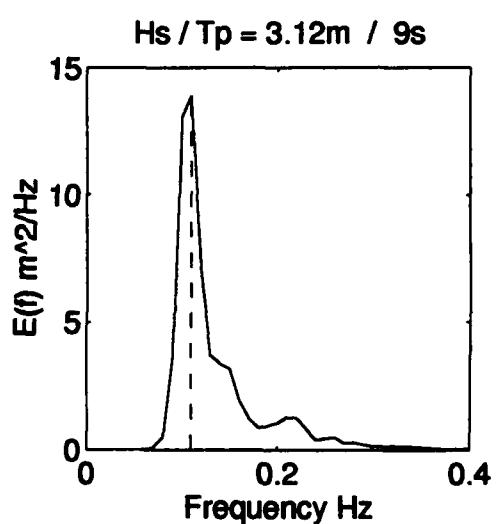
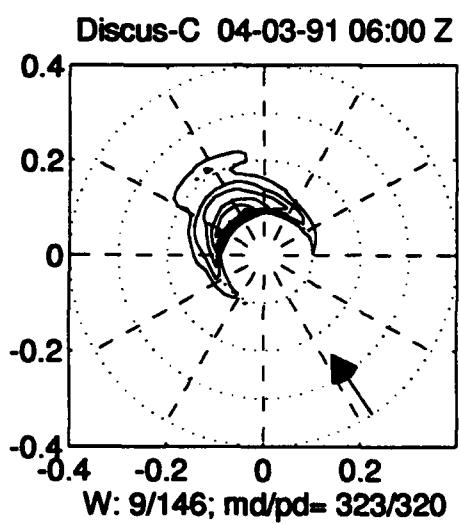
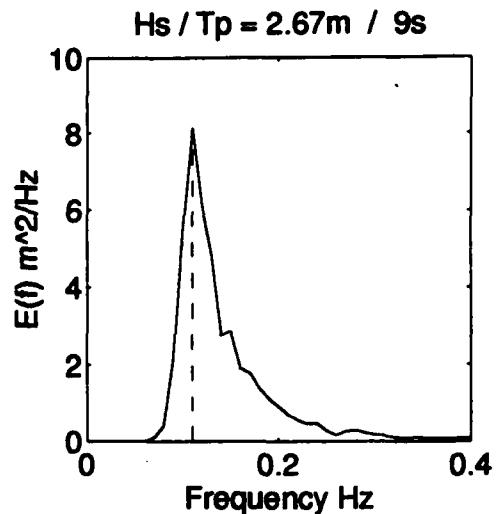
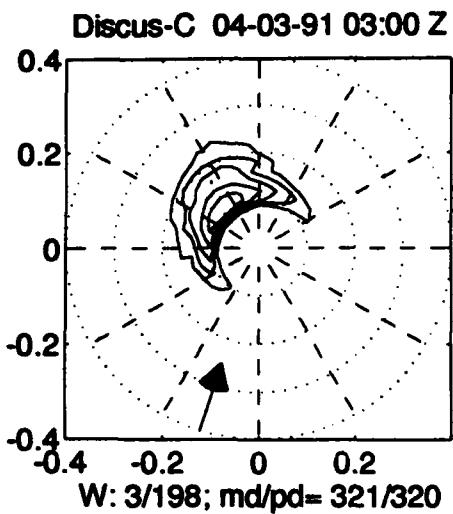


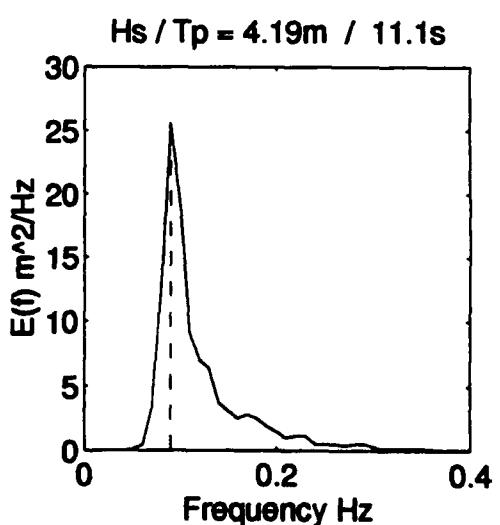
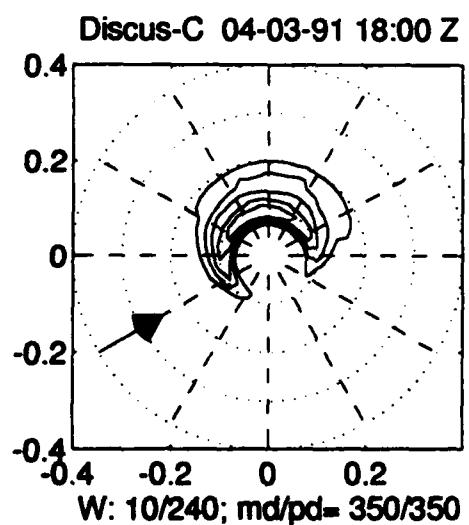
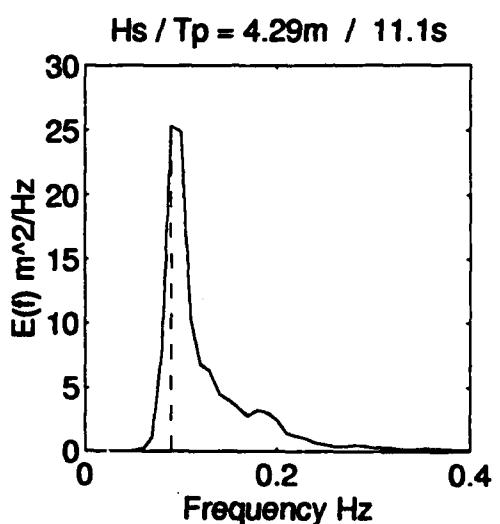
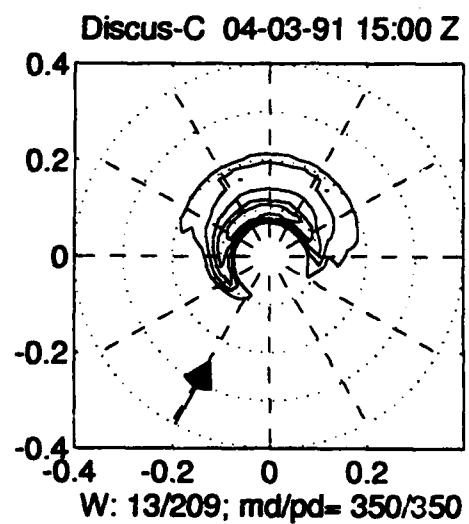
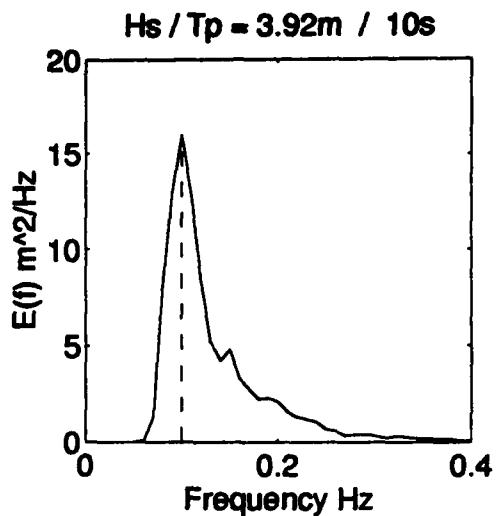
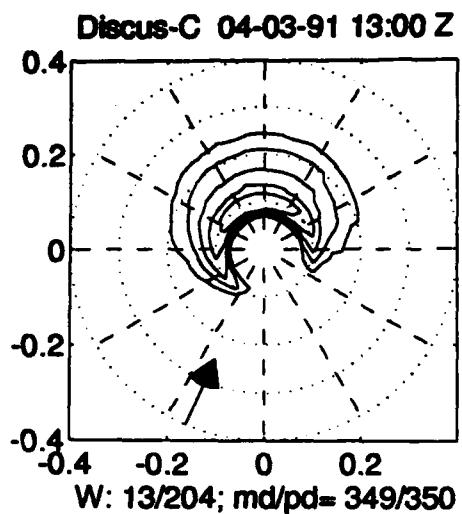


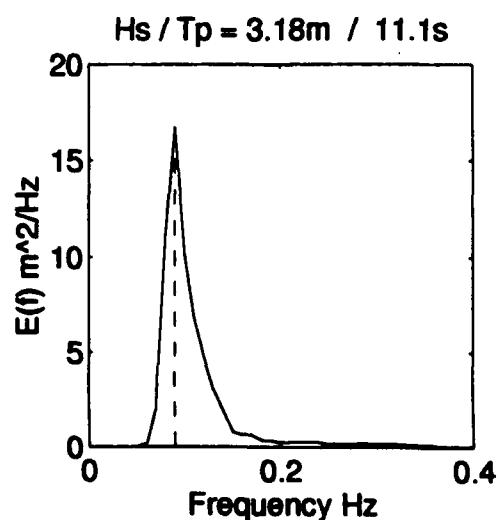
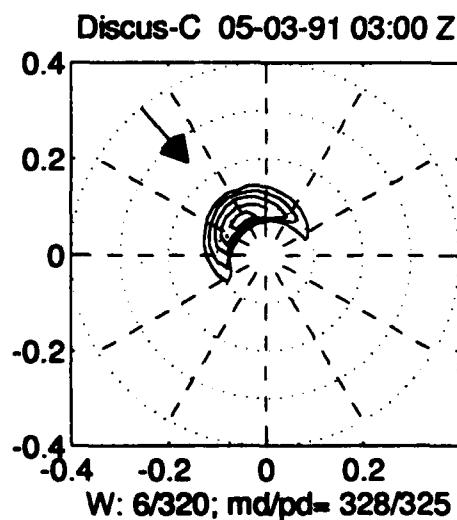
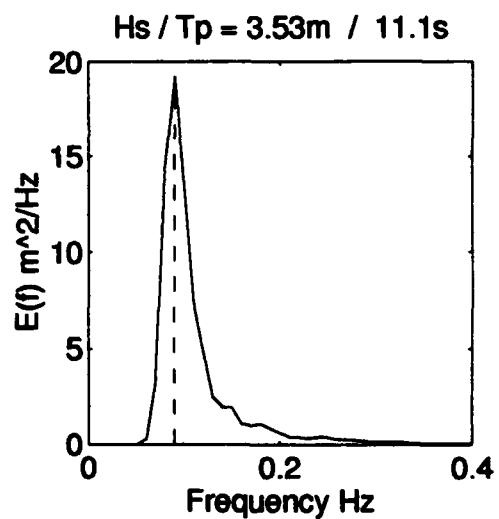
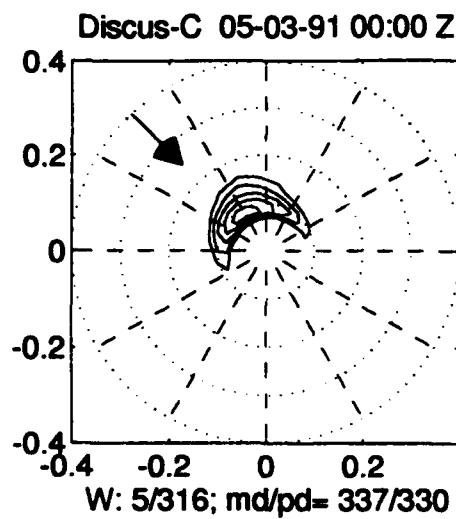
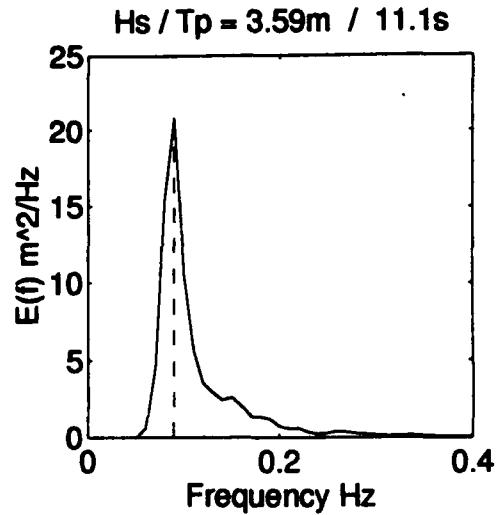
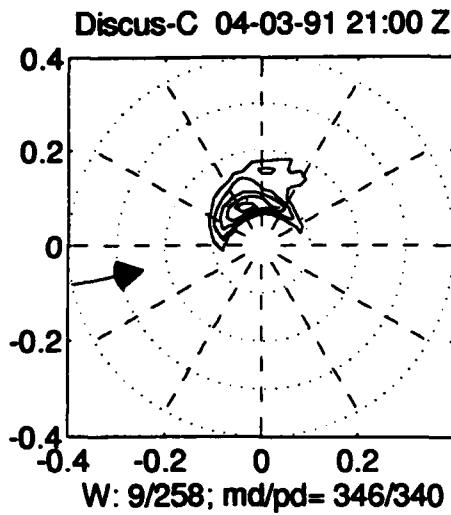


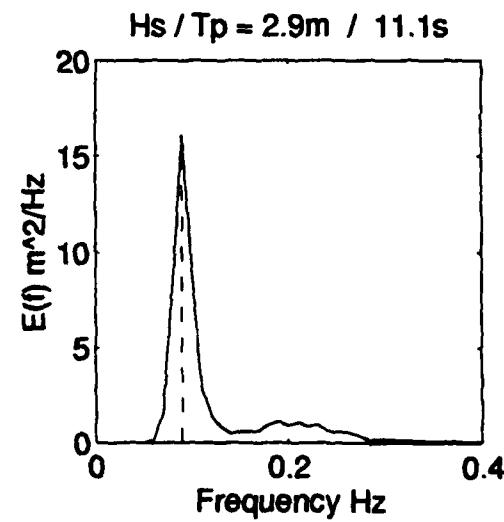
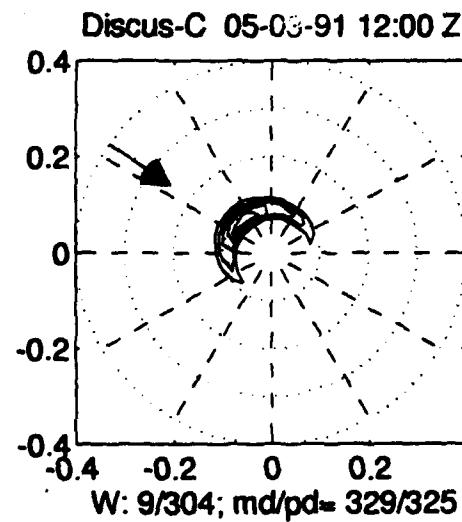
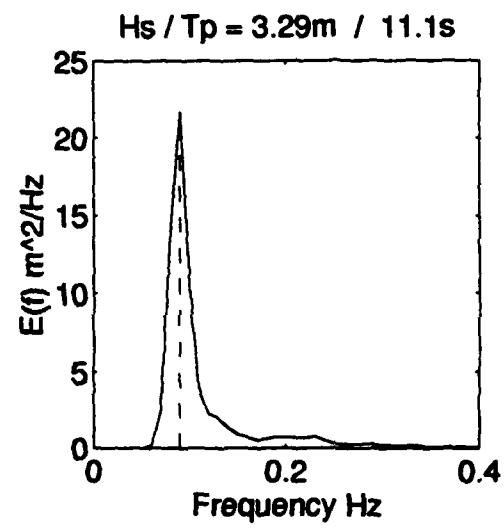
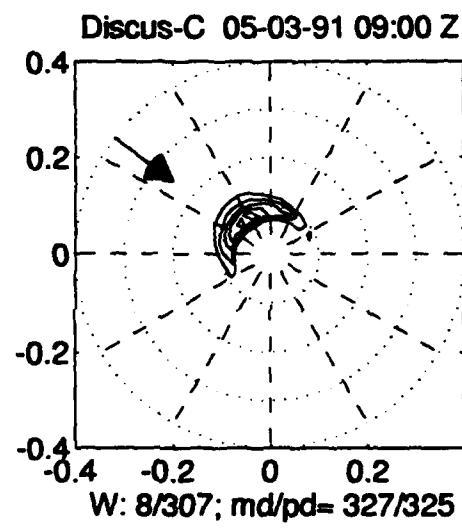
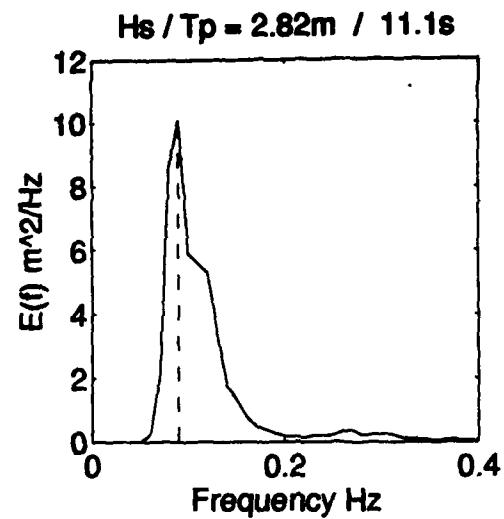
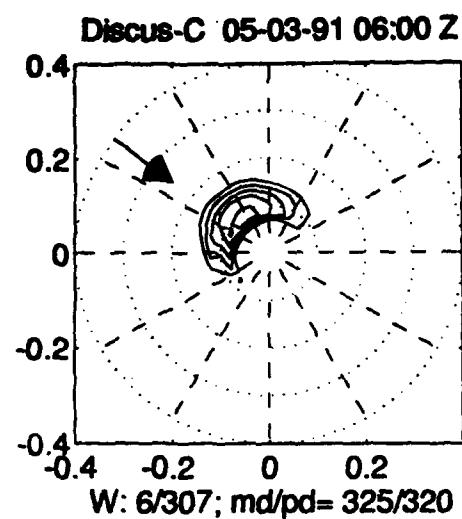


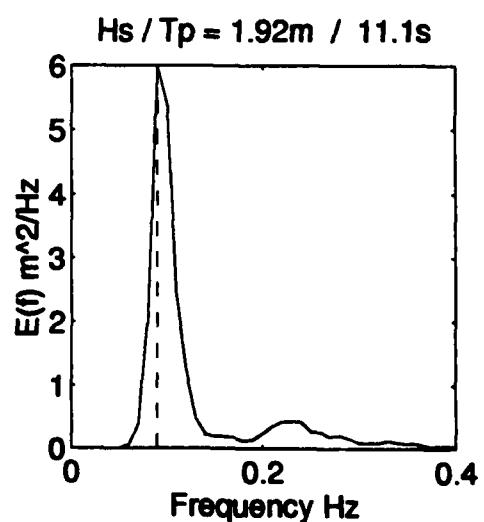
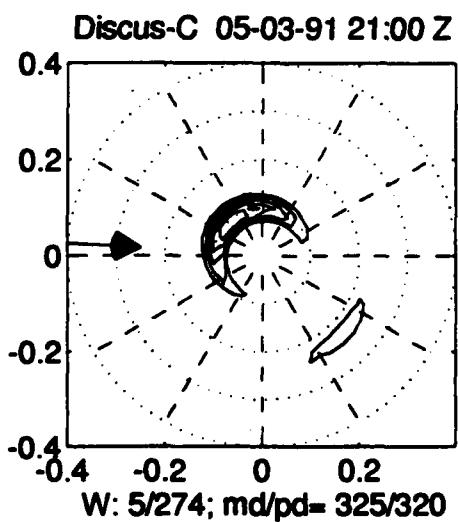
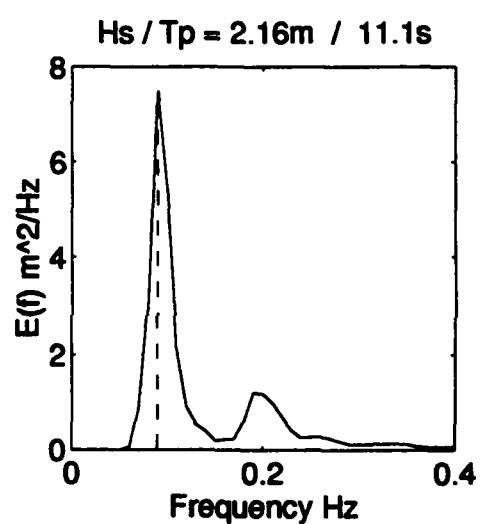
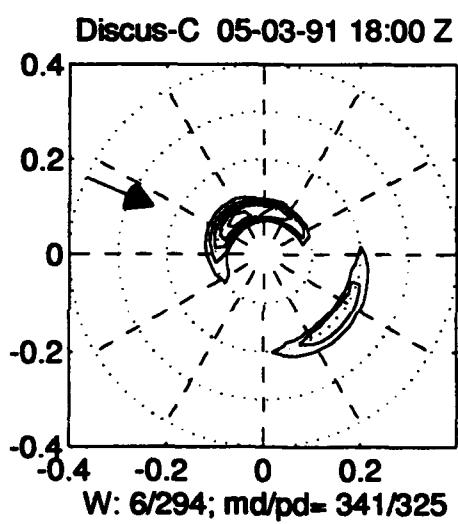
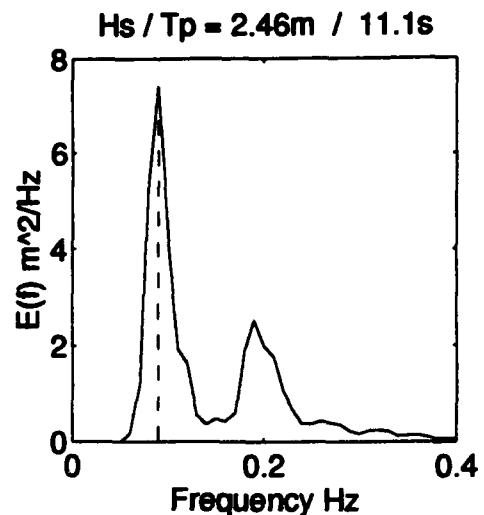
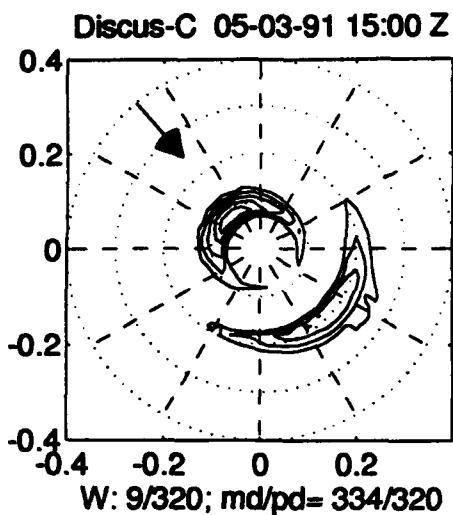


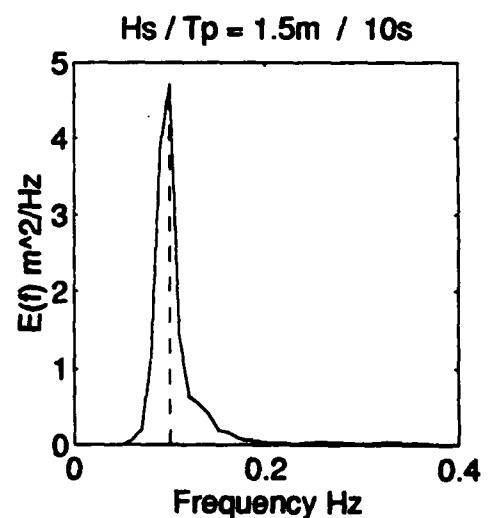
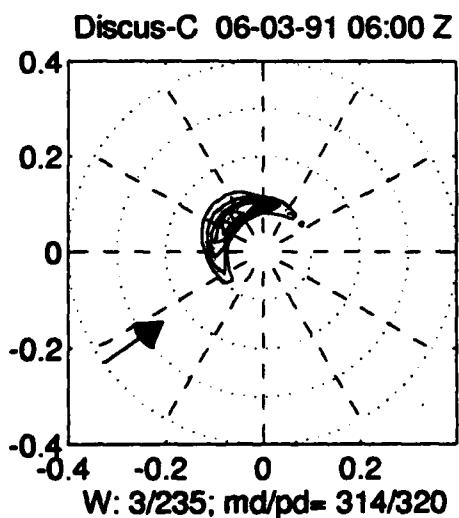
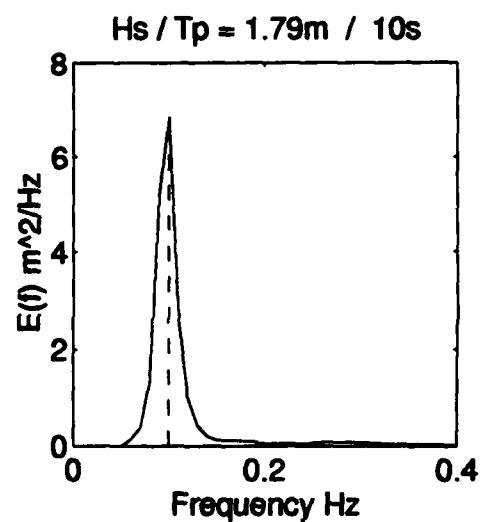
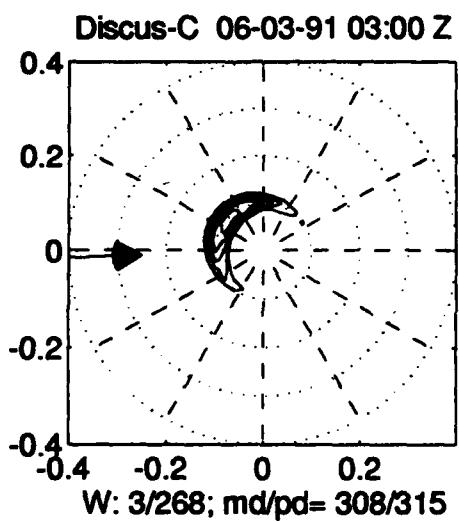
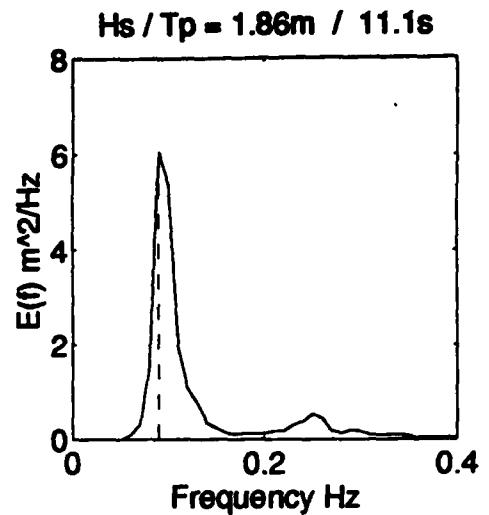
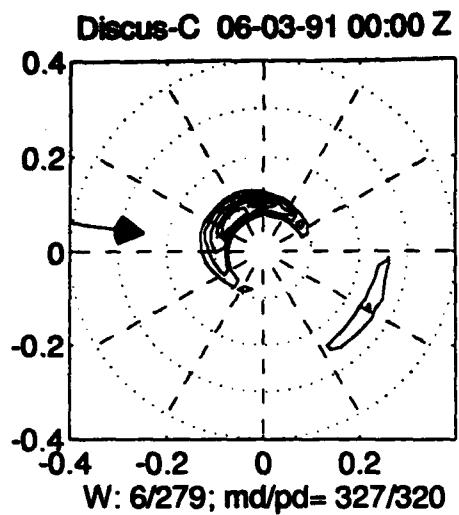


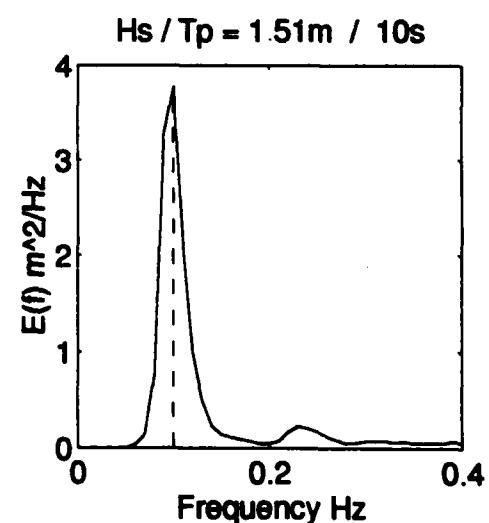
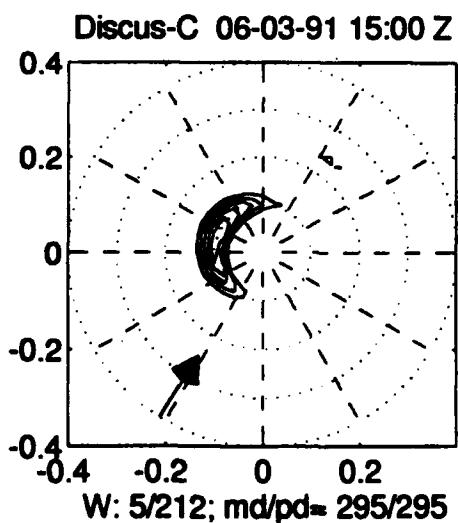
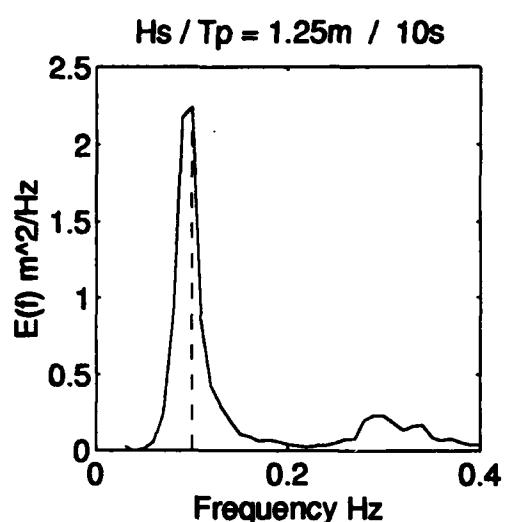
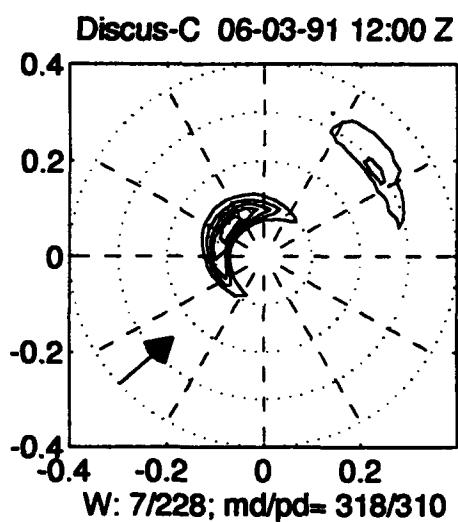
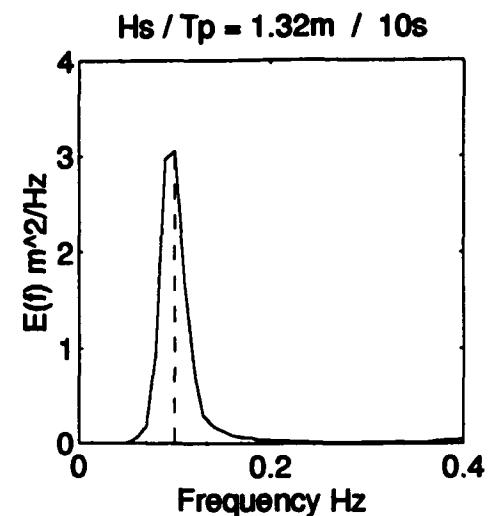
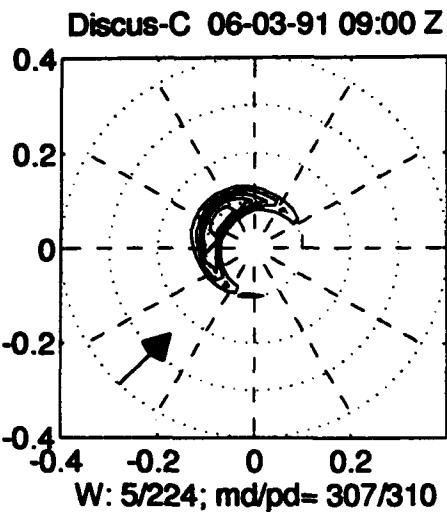


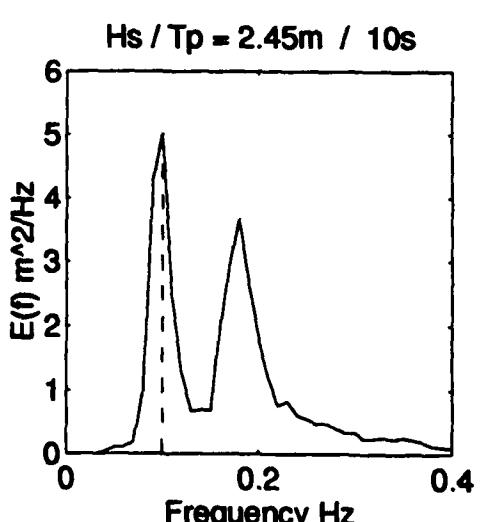
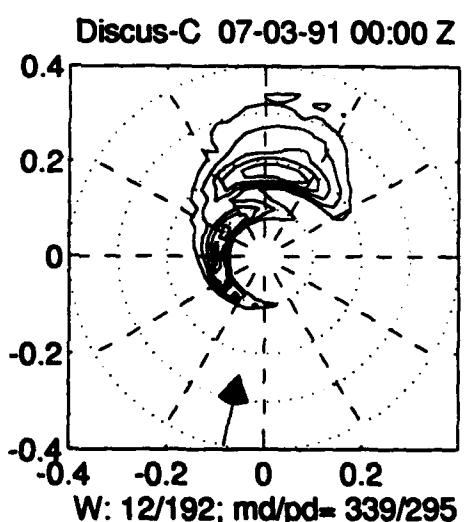
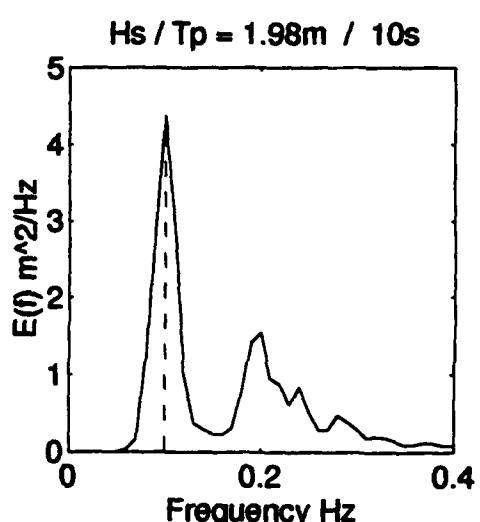
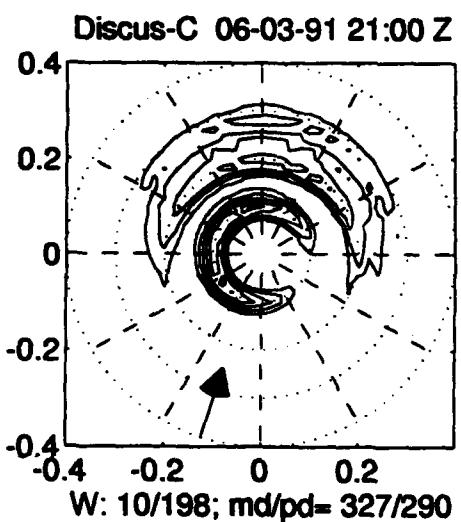
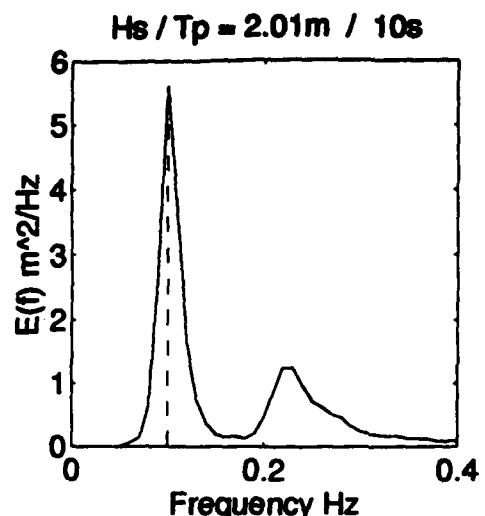
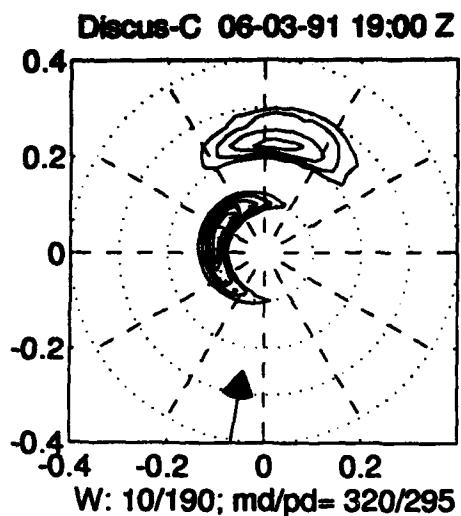


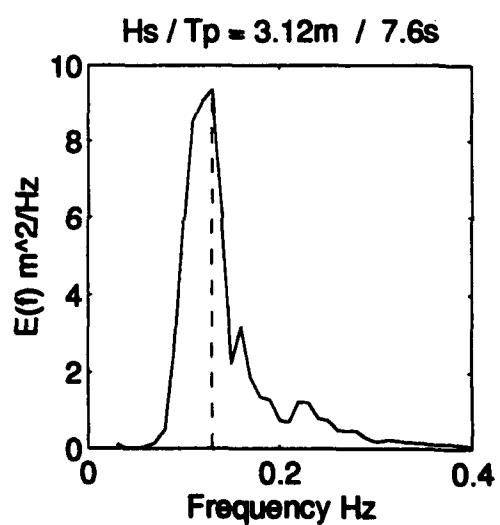
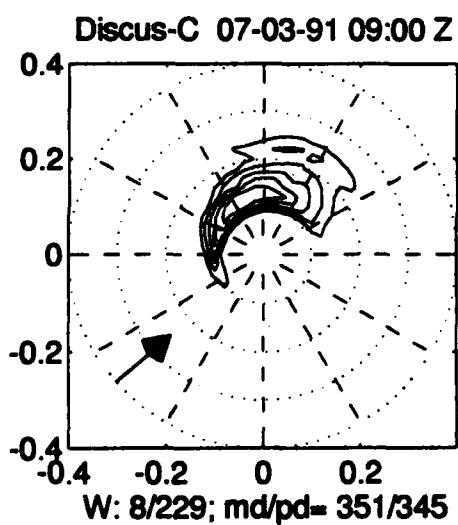
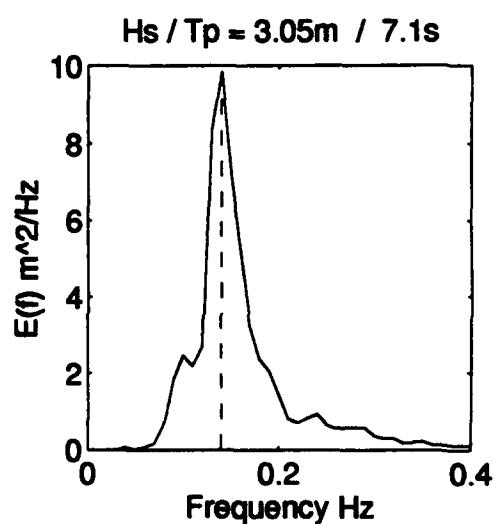
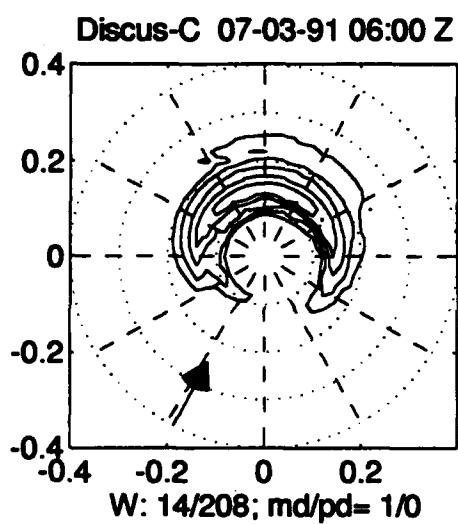
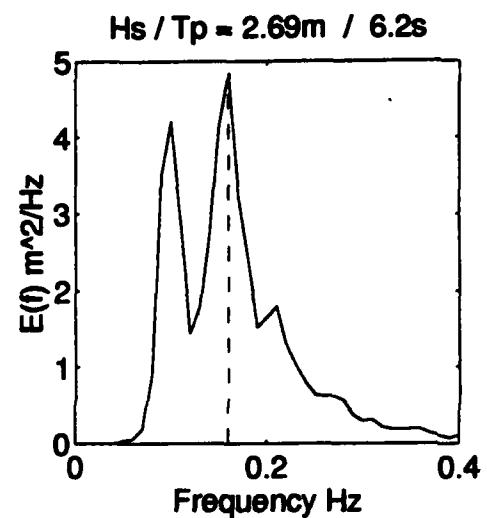
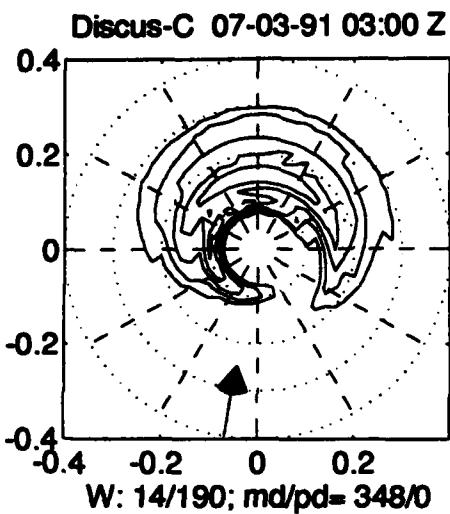


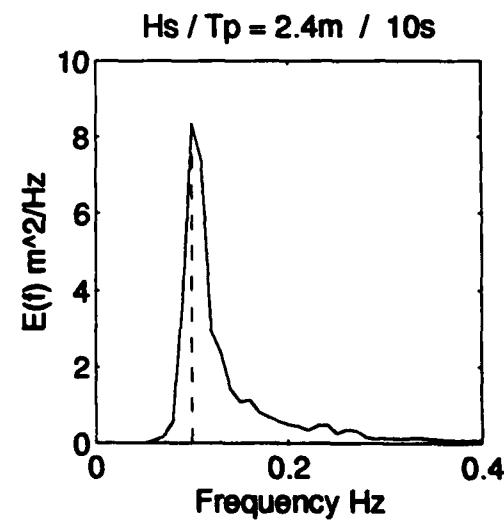
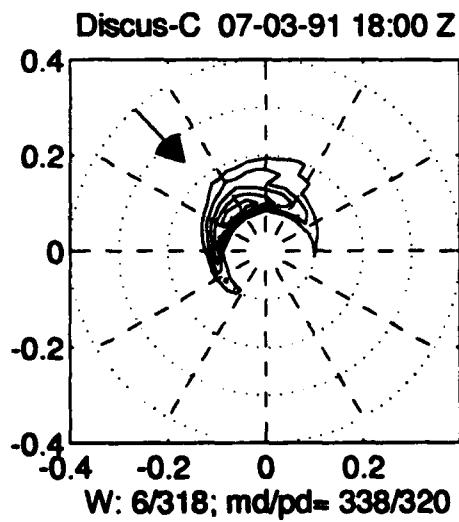
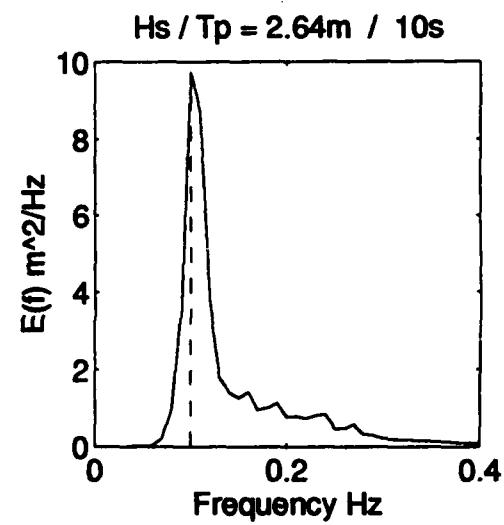
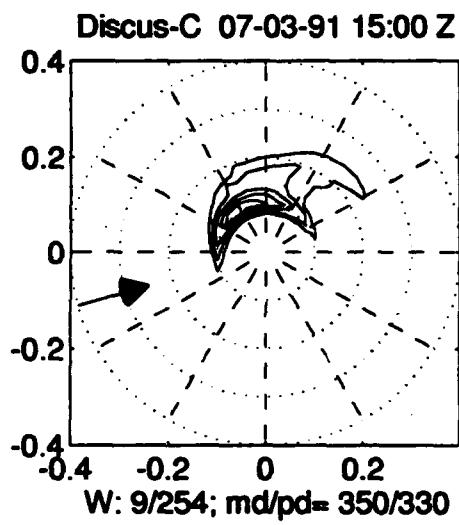
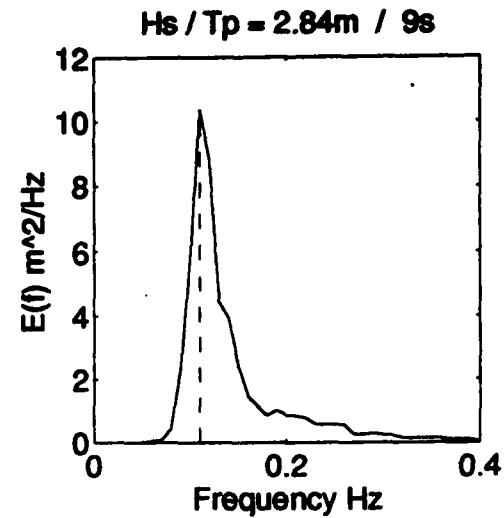
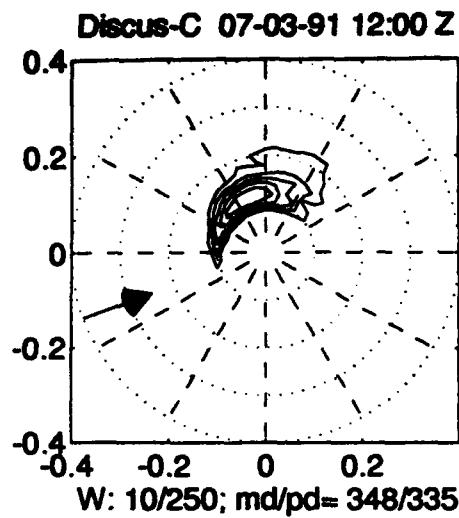


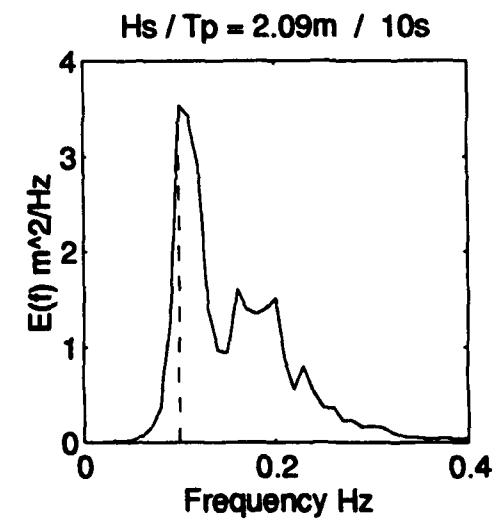
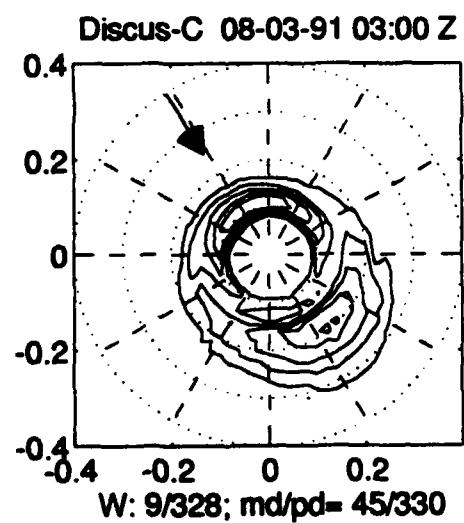
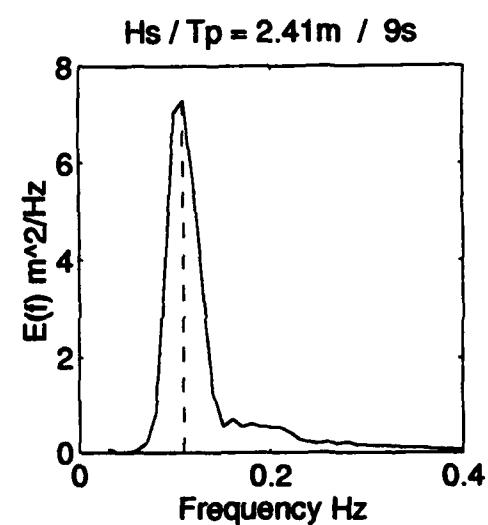
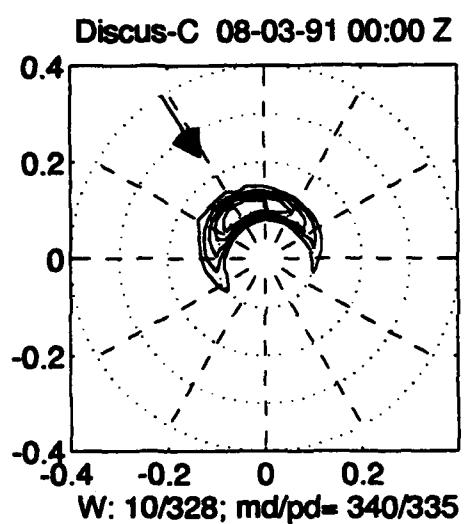
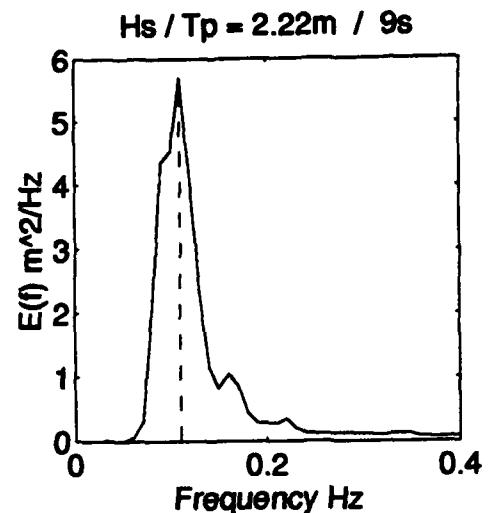
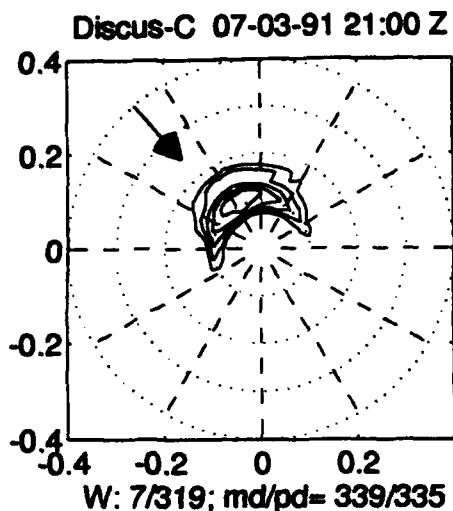


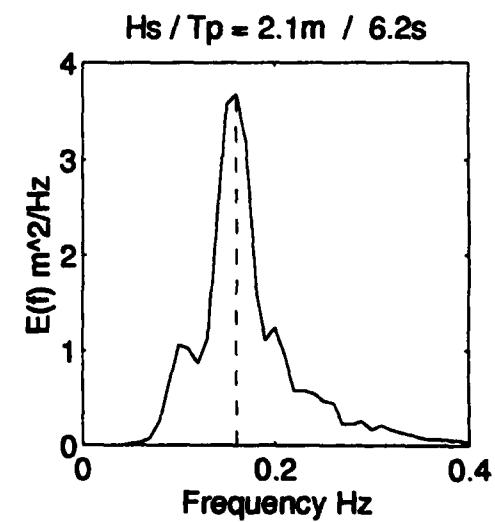
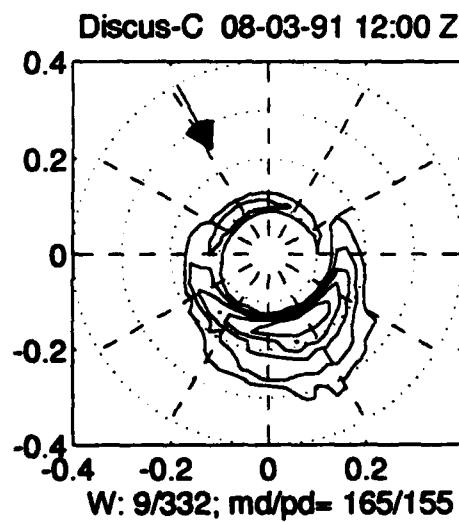
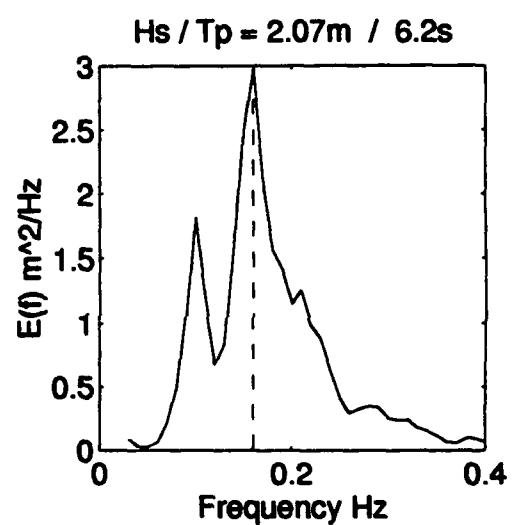
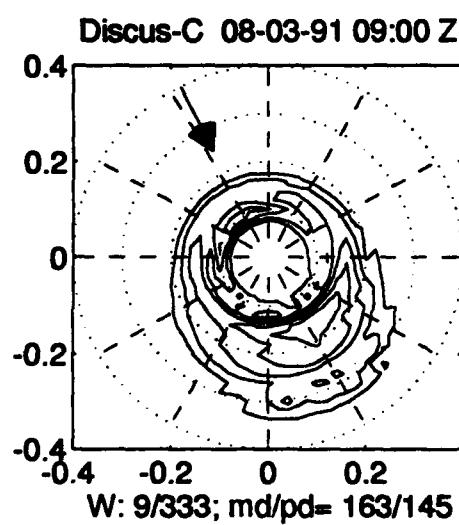
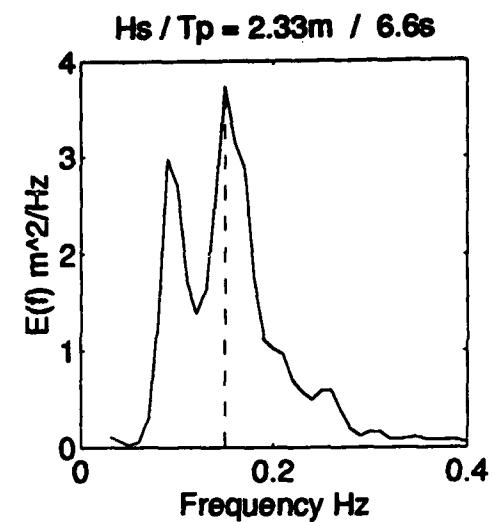
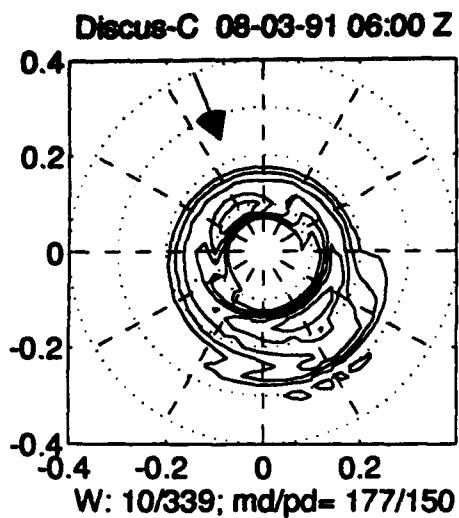


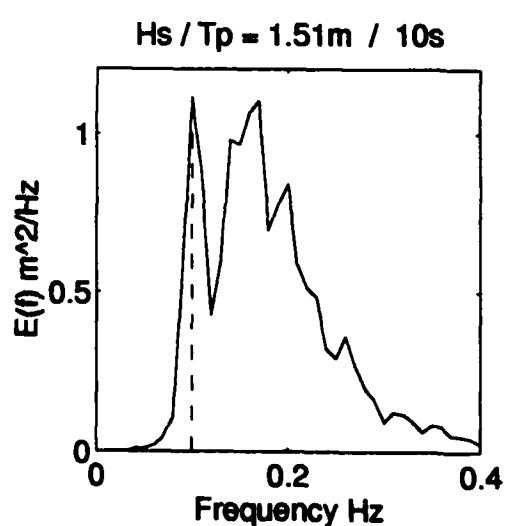
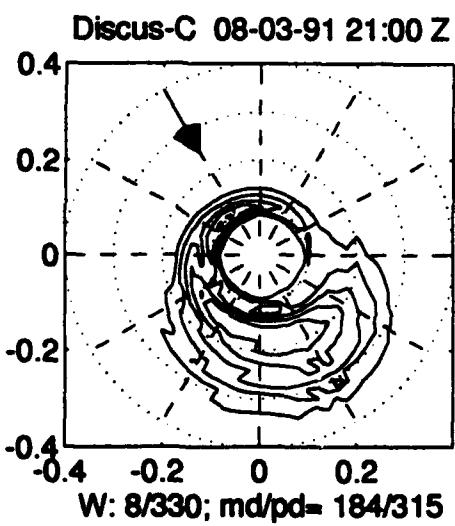
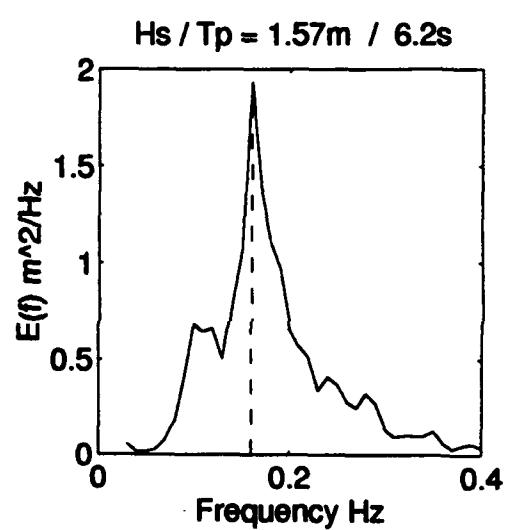
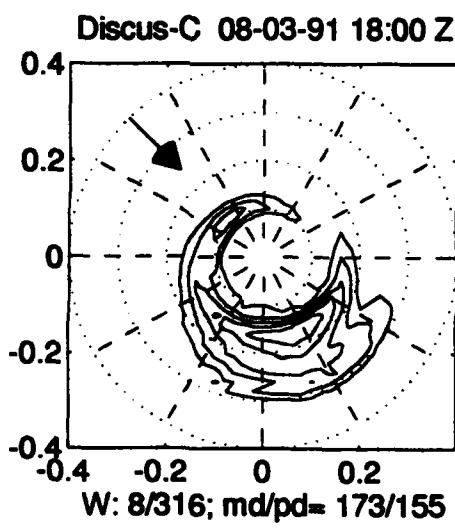
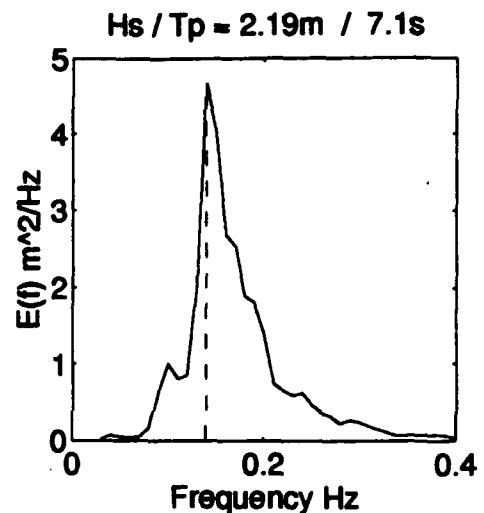
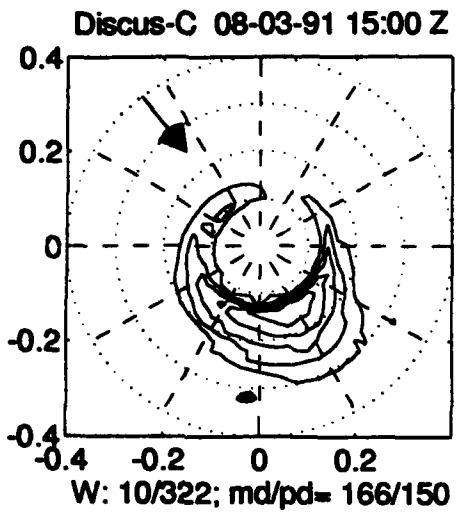


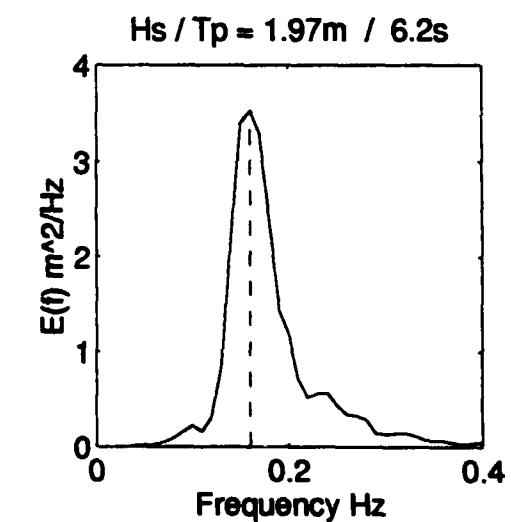
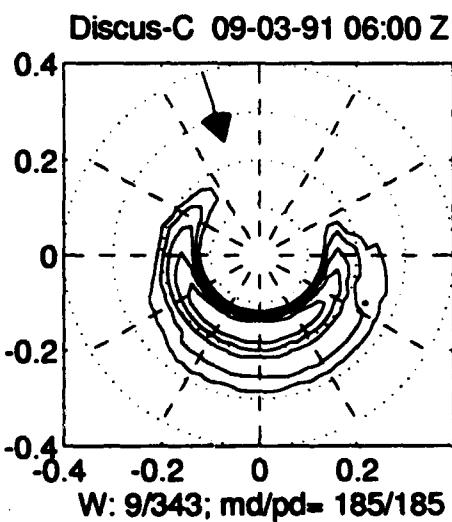
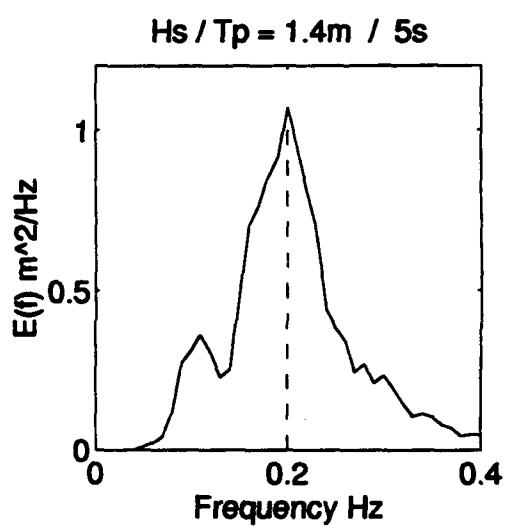
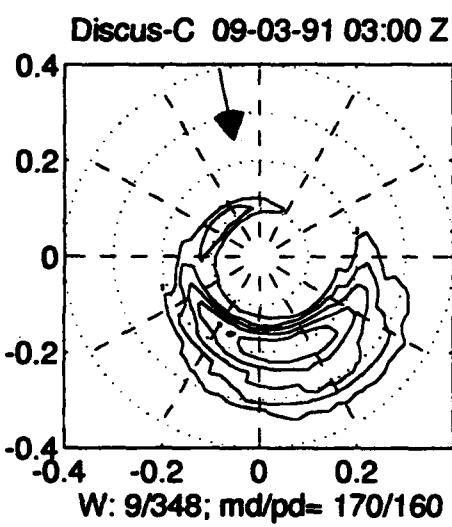
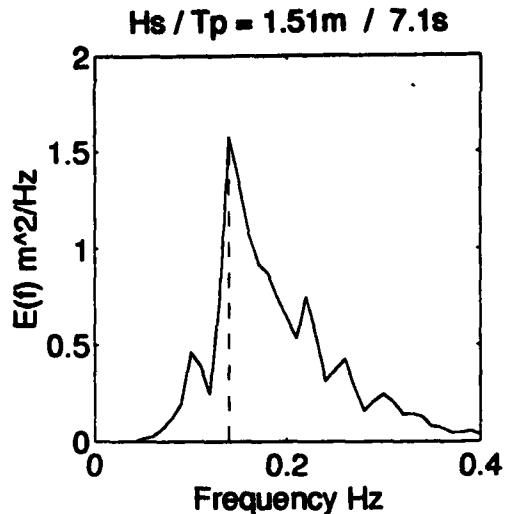
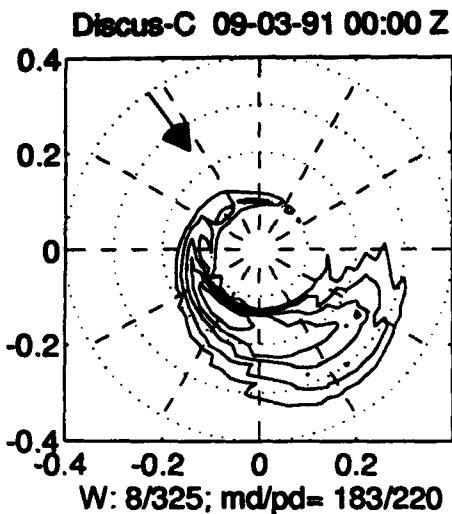




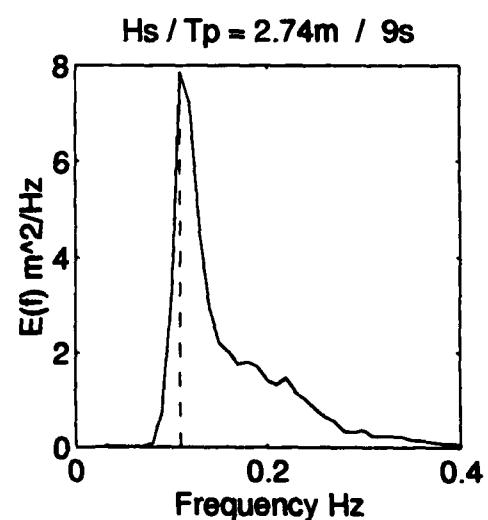
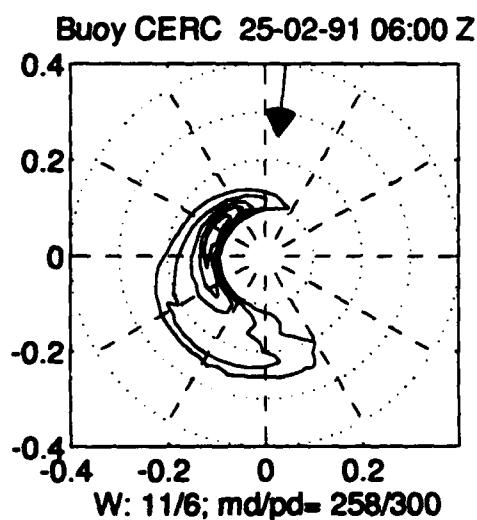
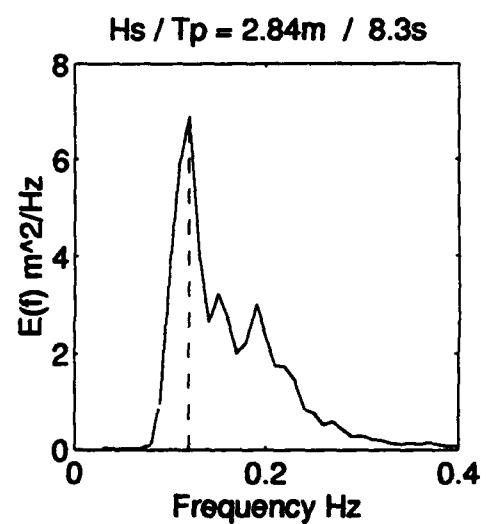
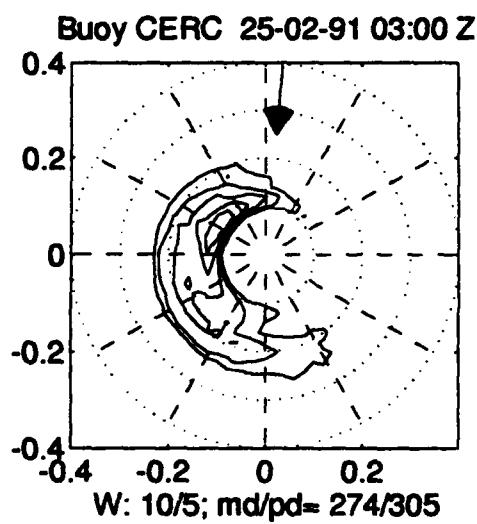
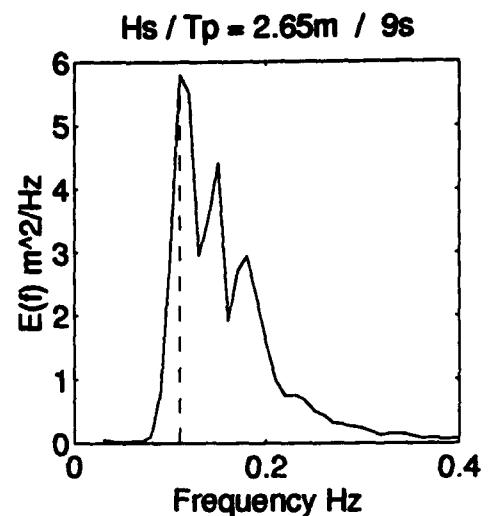
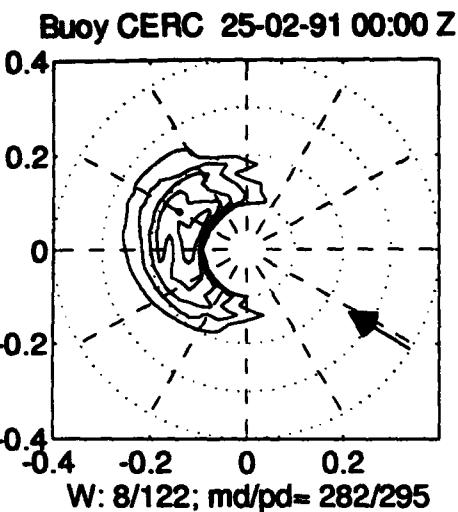


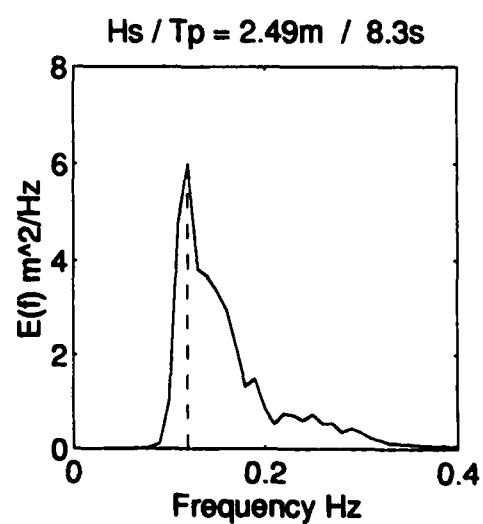
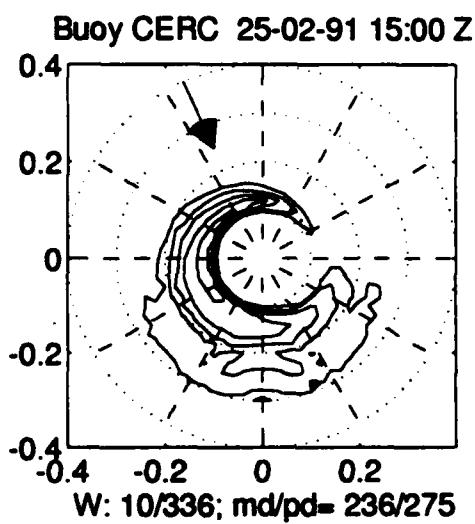
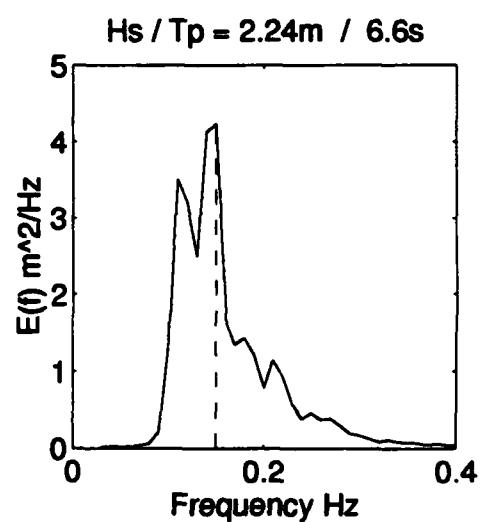
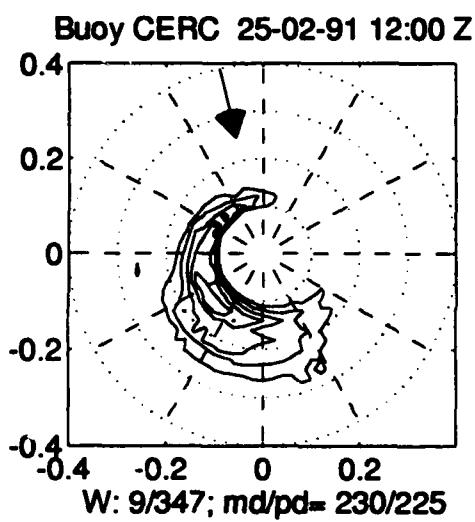
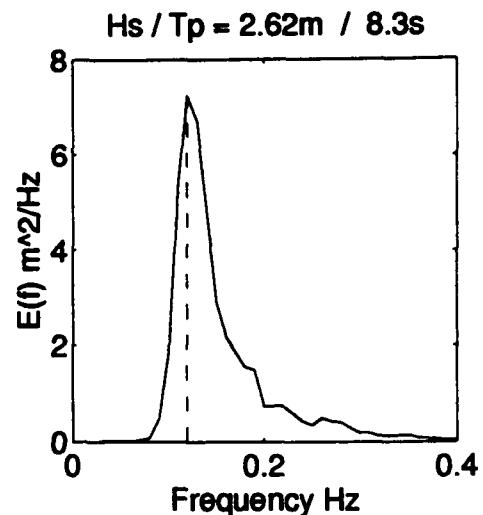
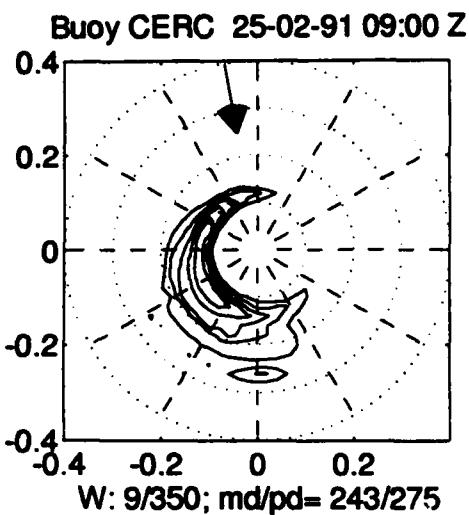


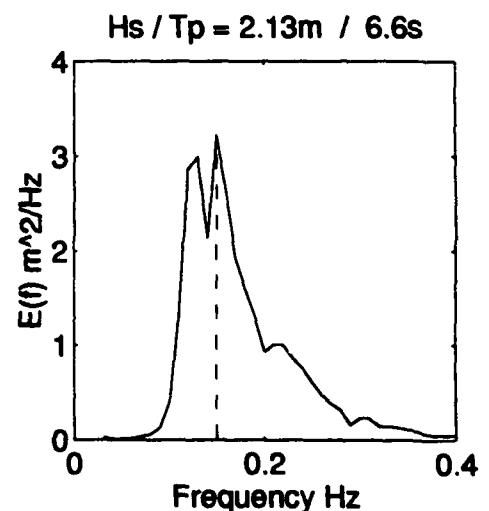
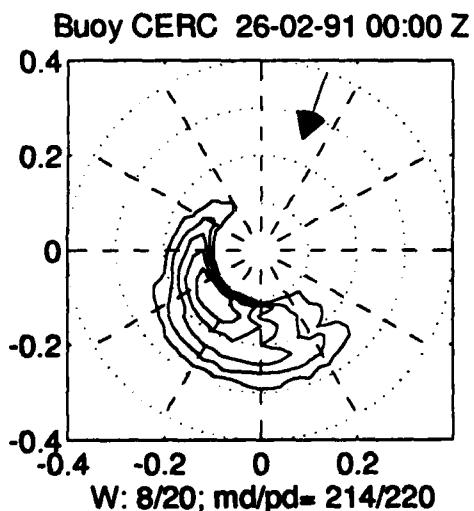
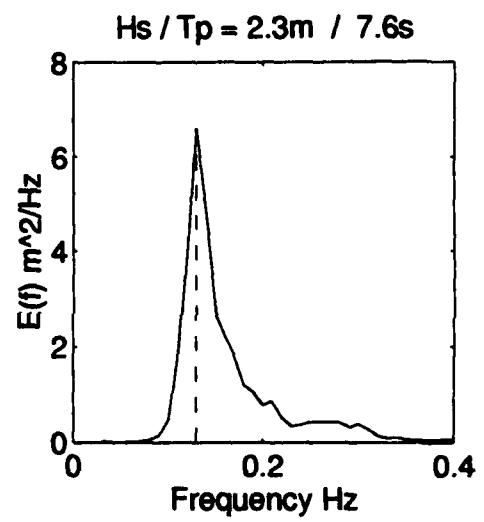
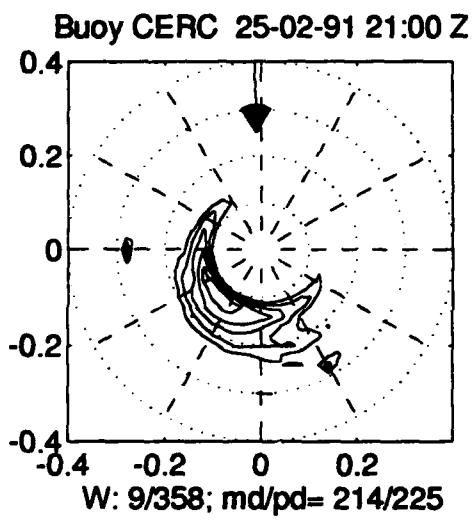
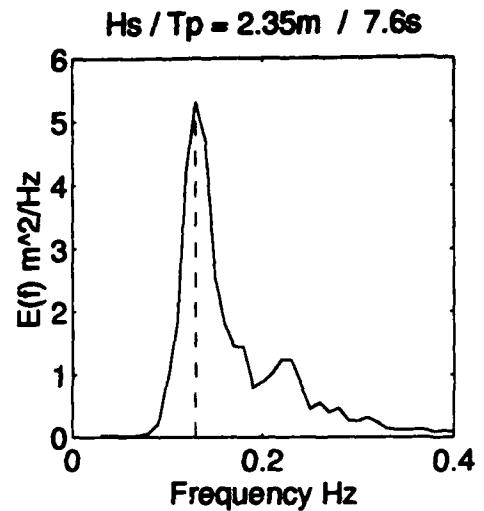
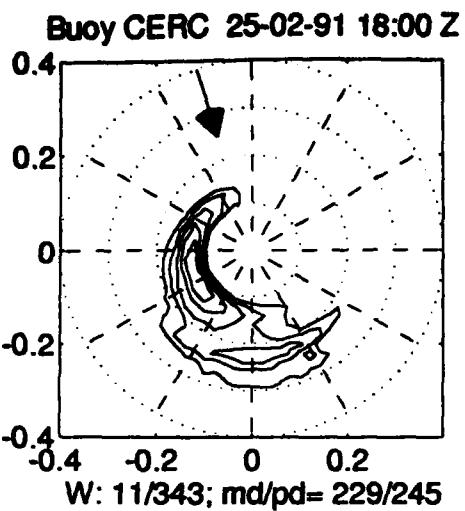


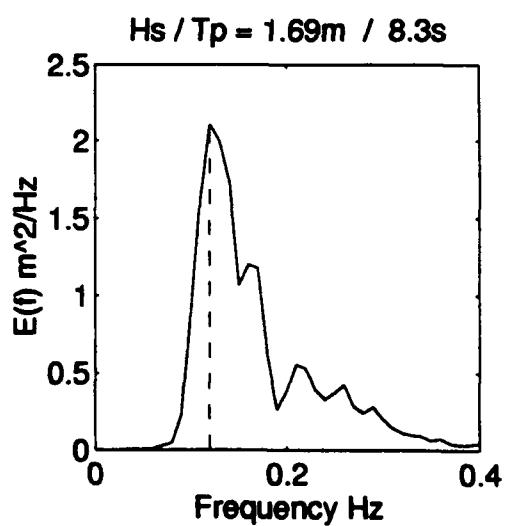
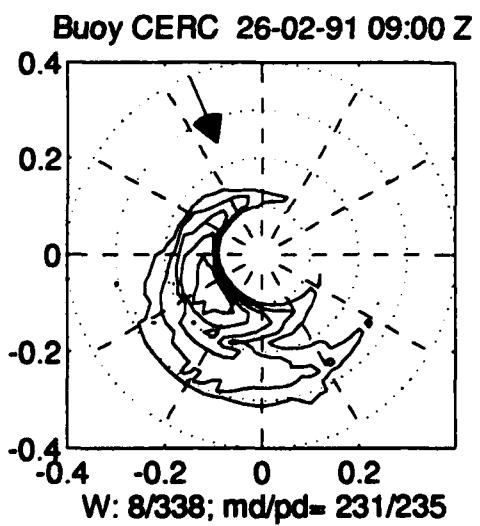
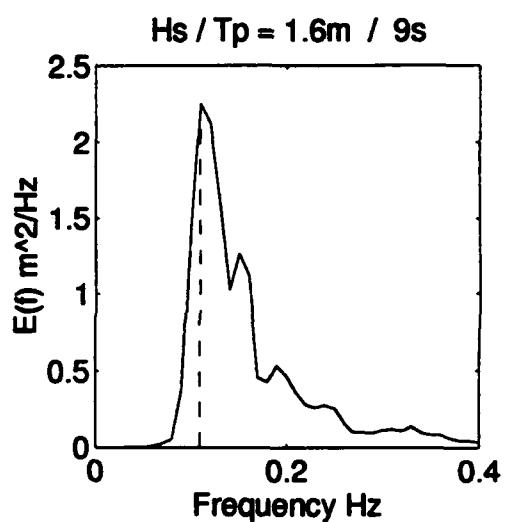
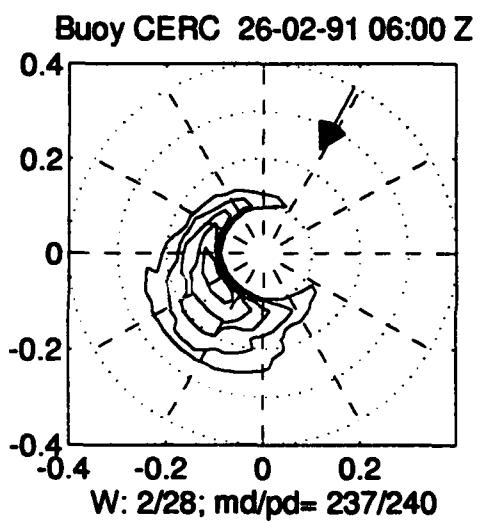
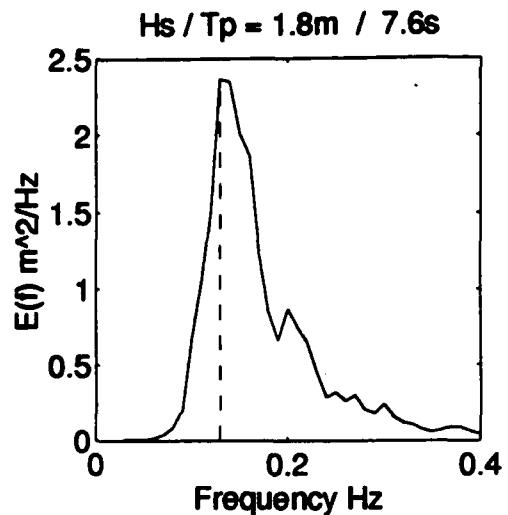
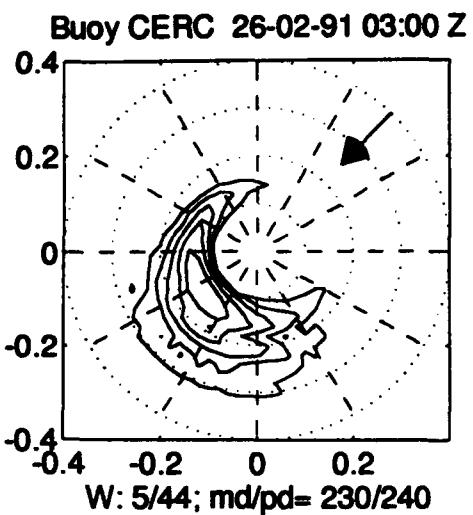


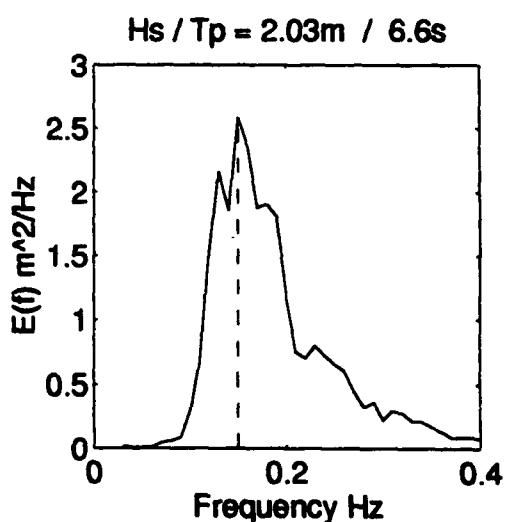
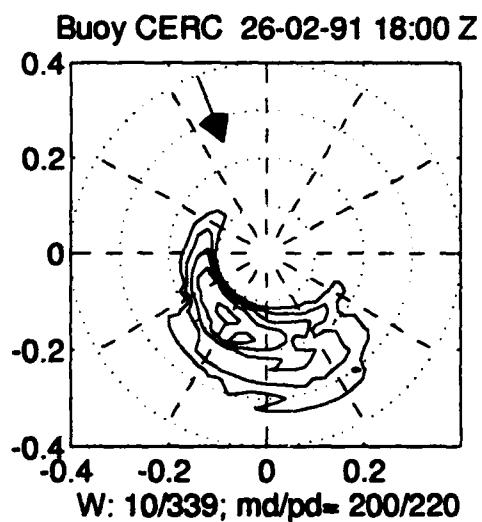
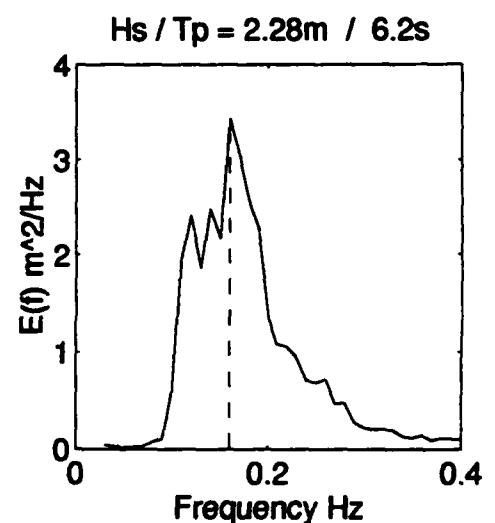
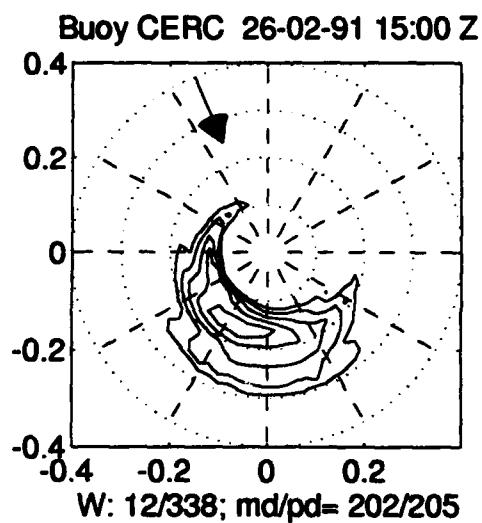
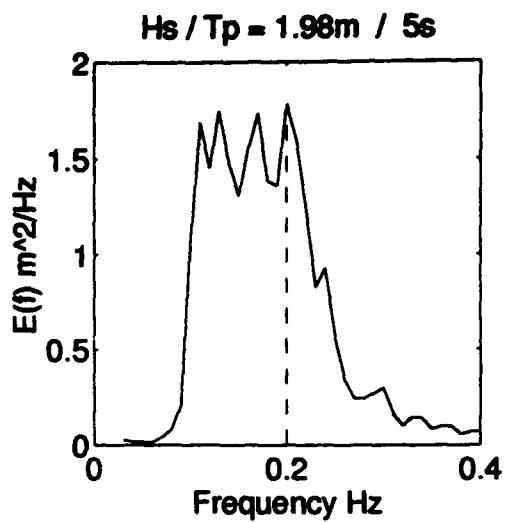
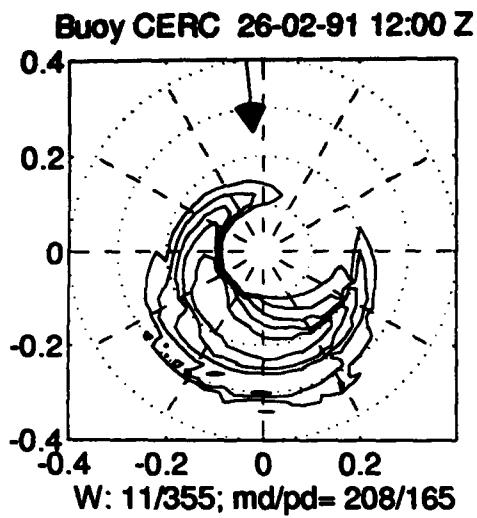
B.4: Discus Buoy "CERC"

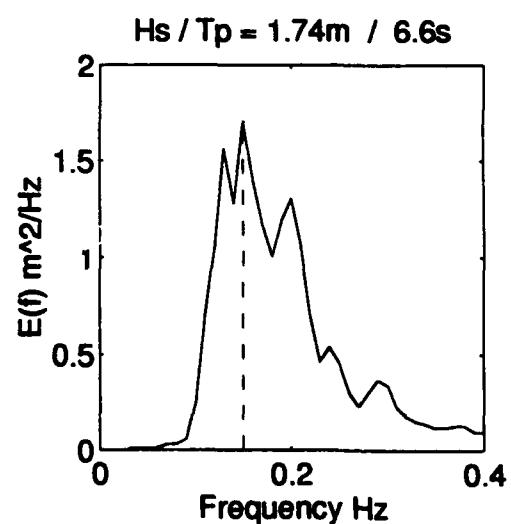
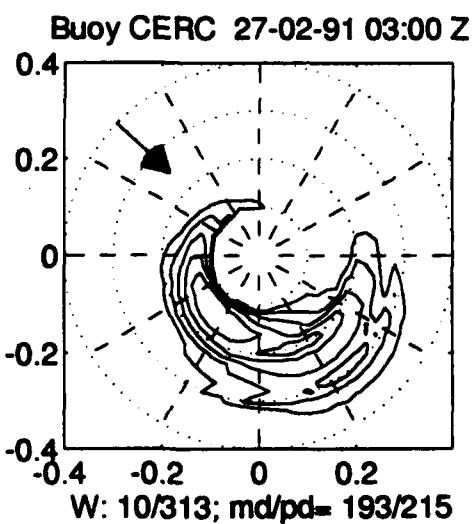
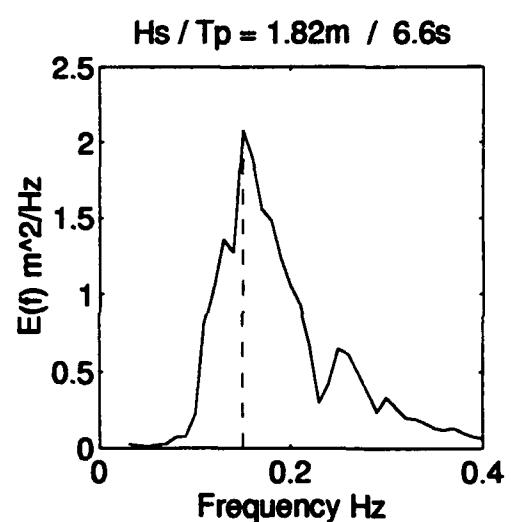
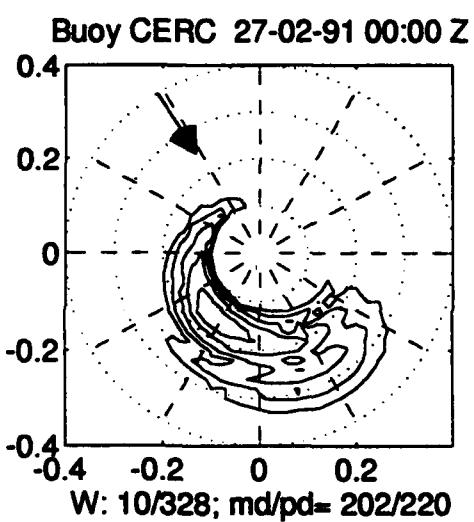
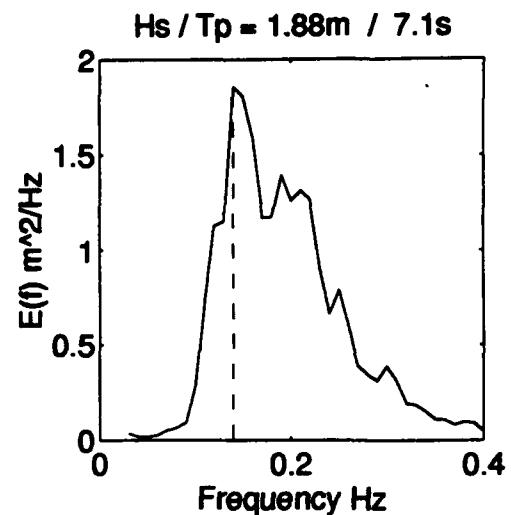
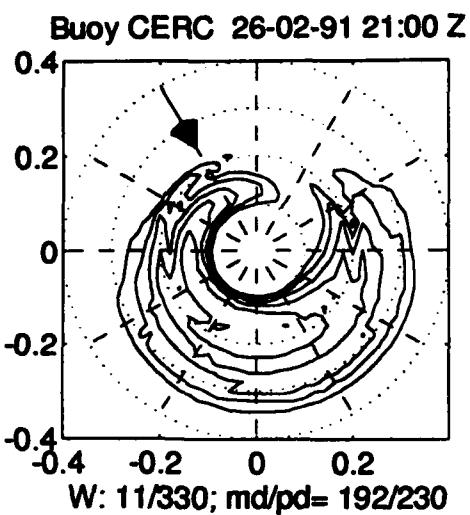


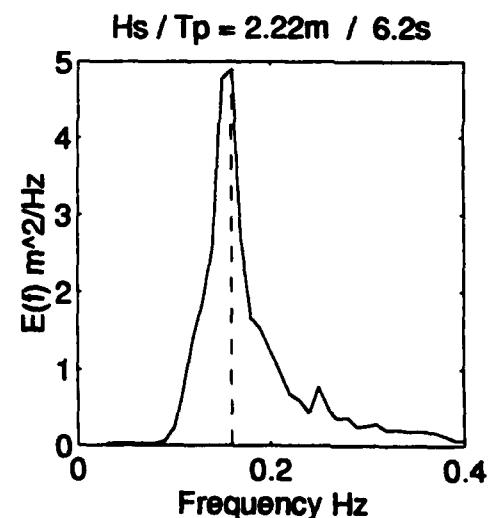
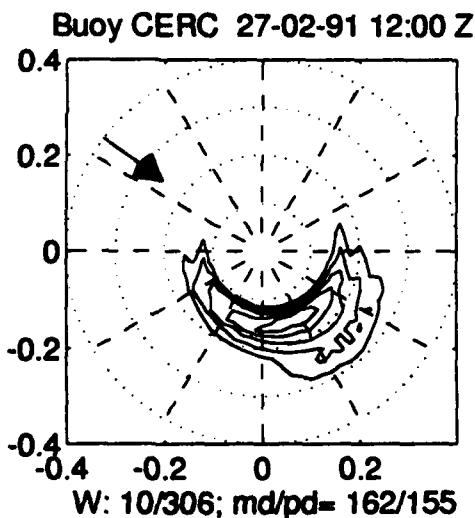
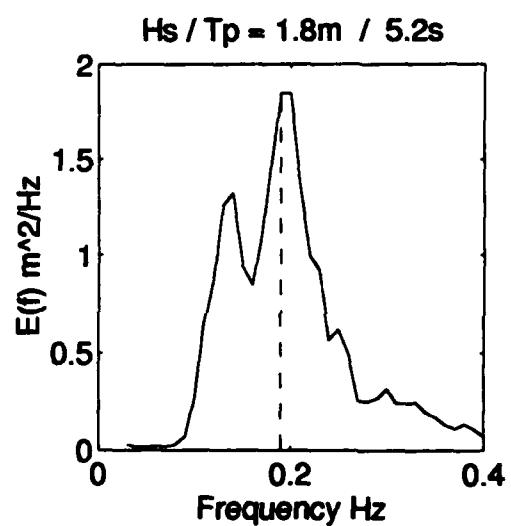
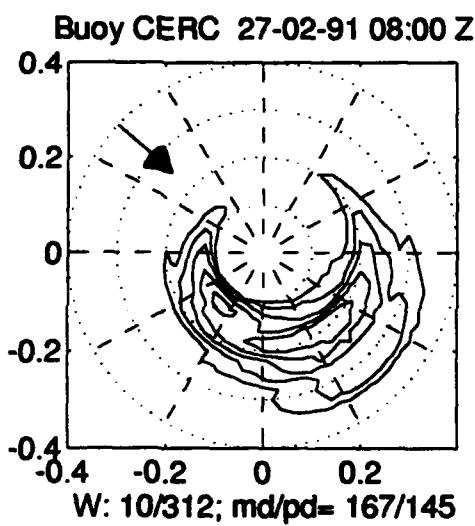
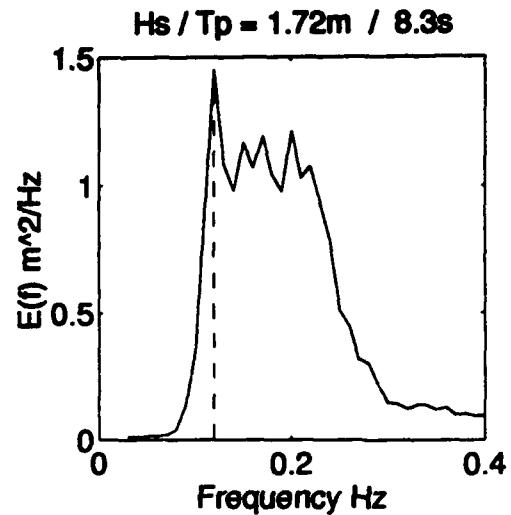
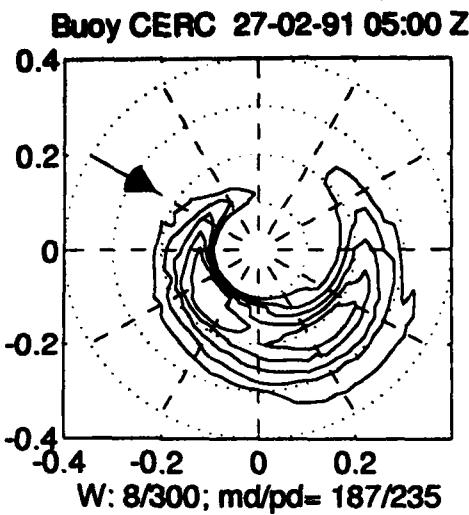


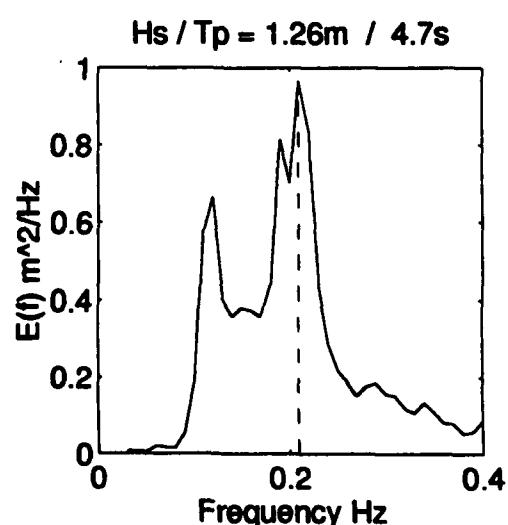
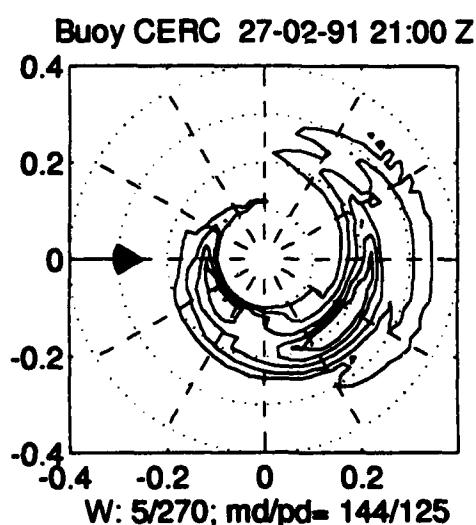
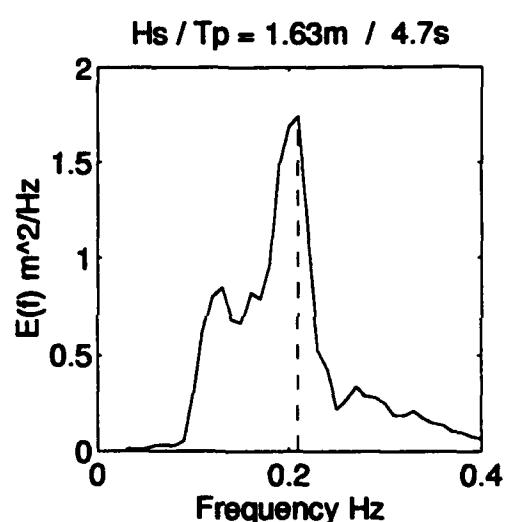
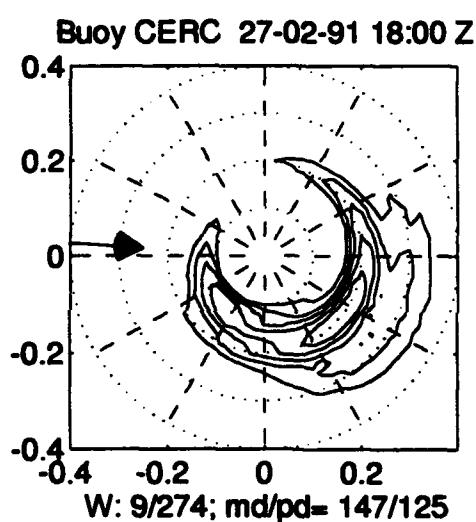
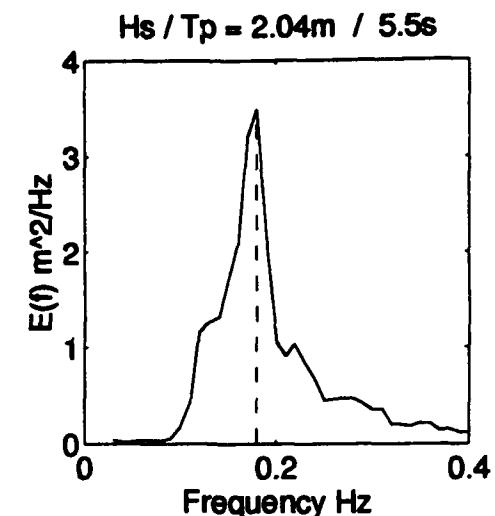
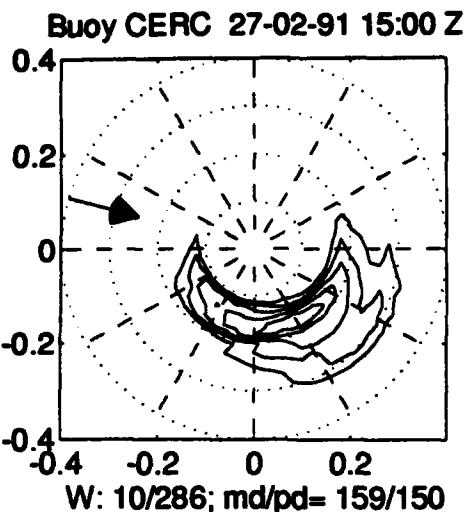


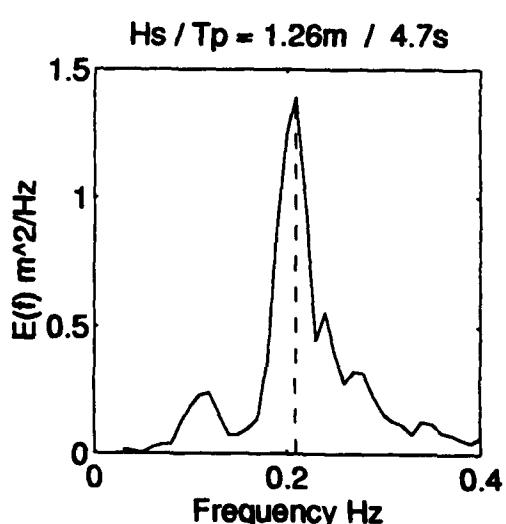
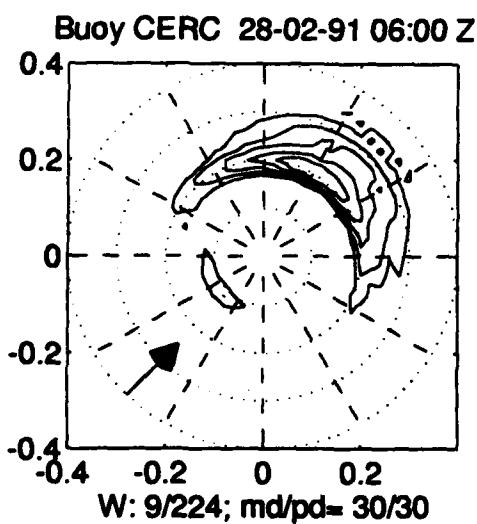
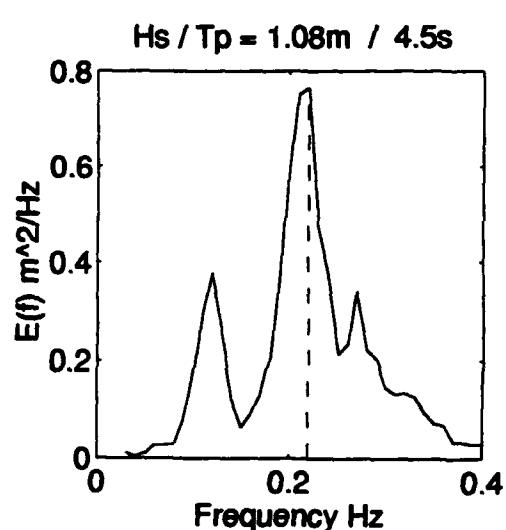
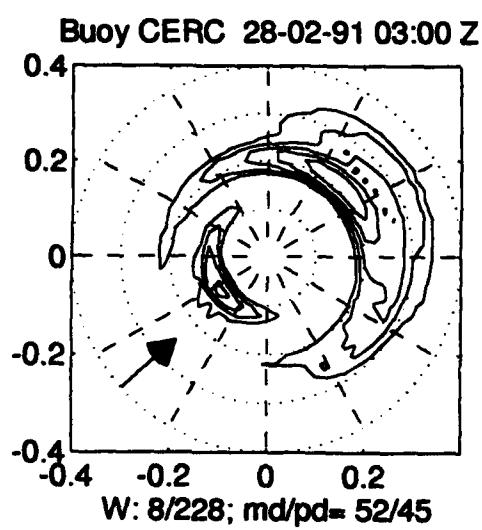
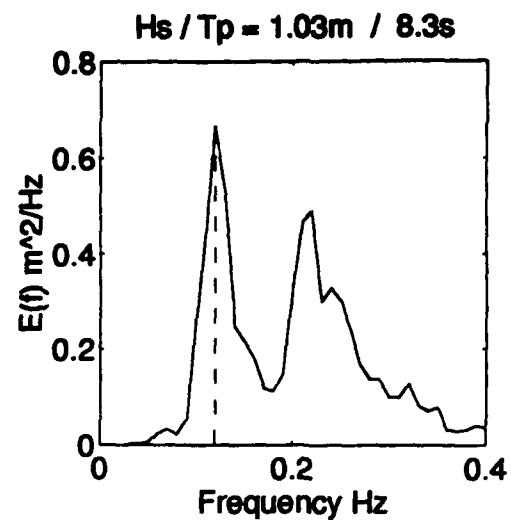
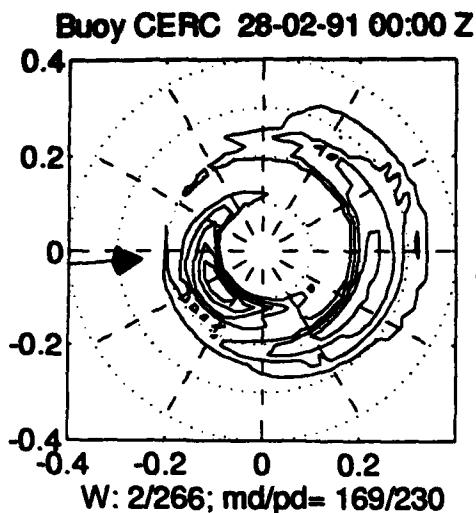


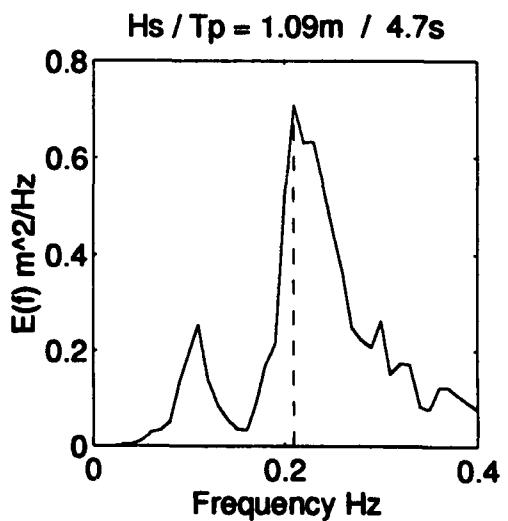
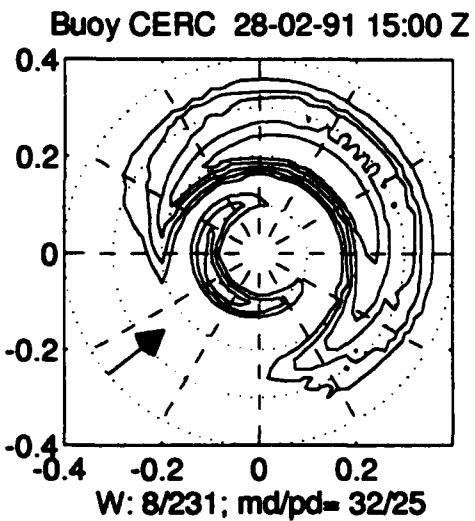
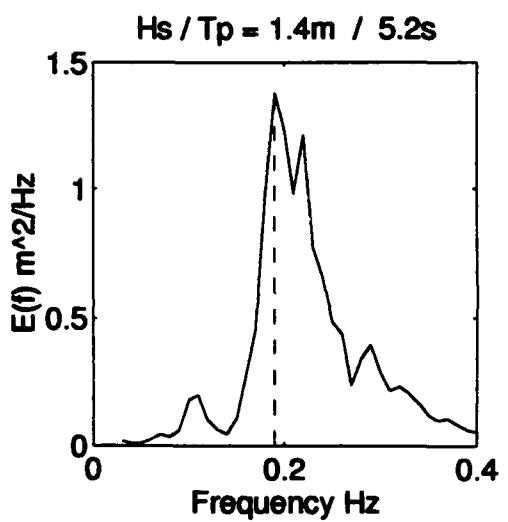
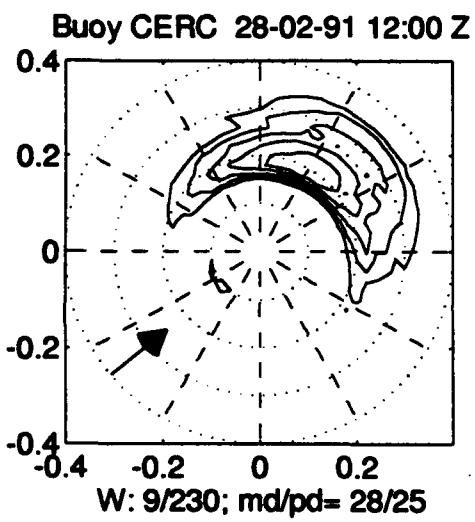
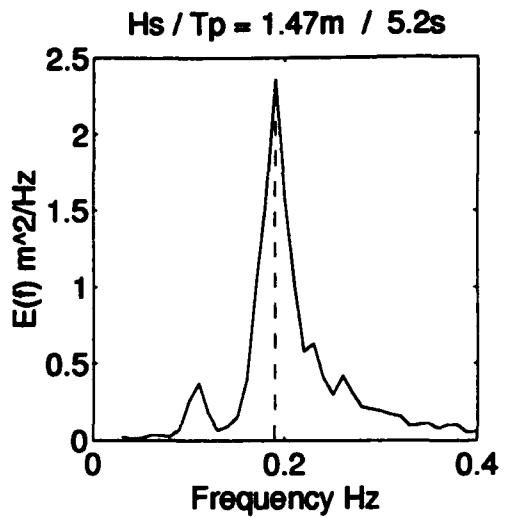
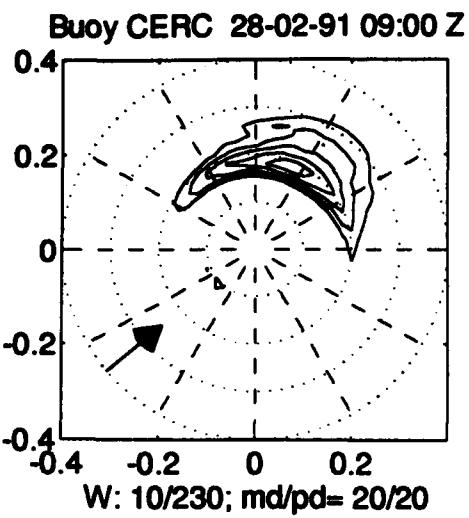


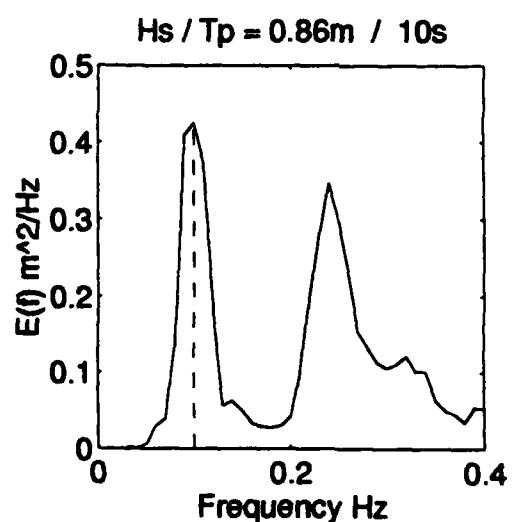
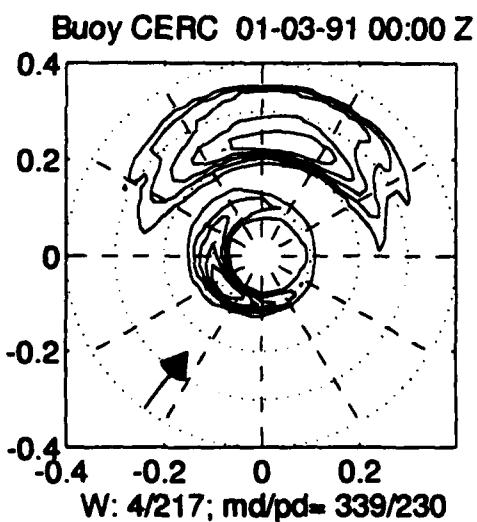
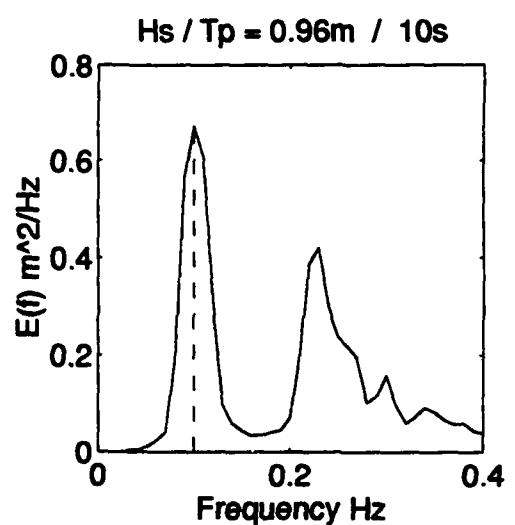
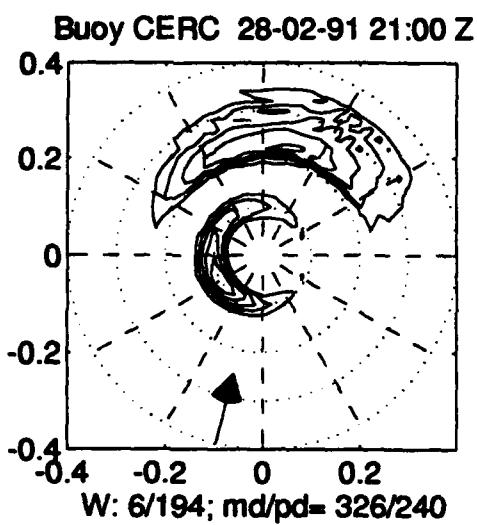
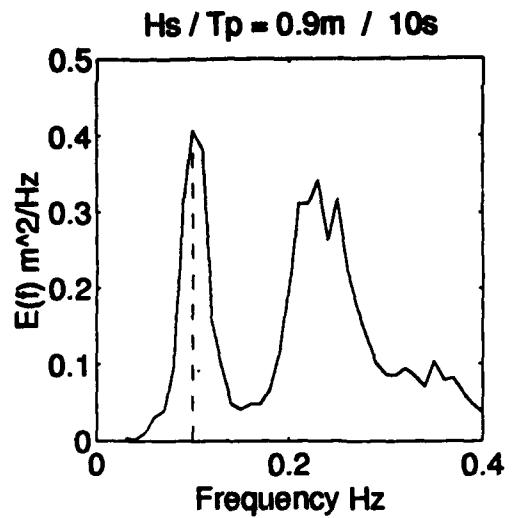
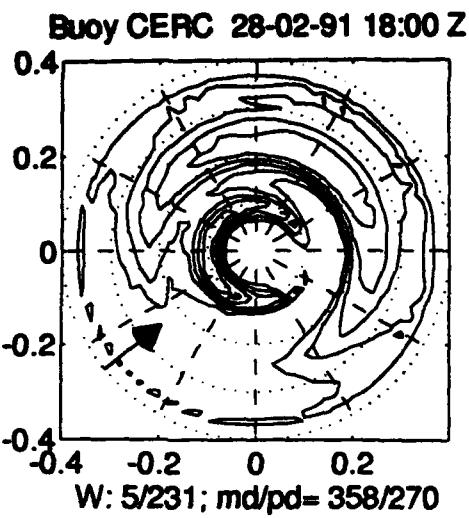


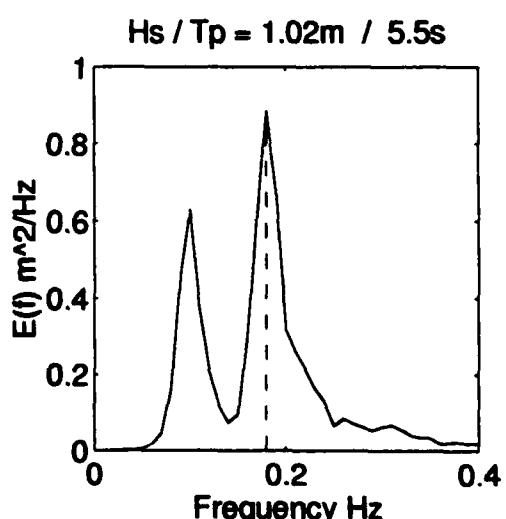
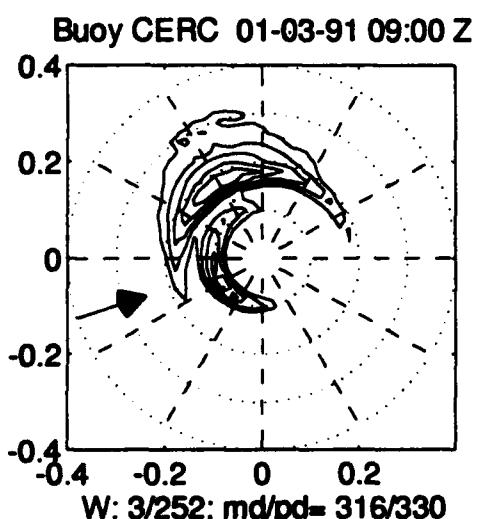
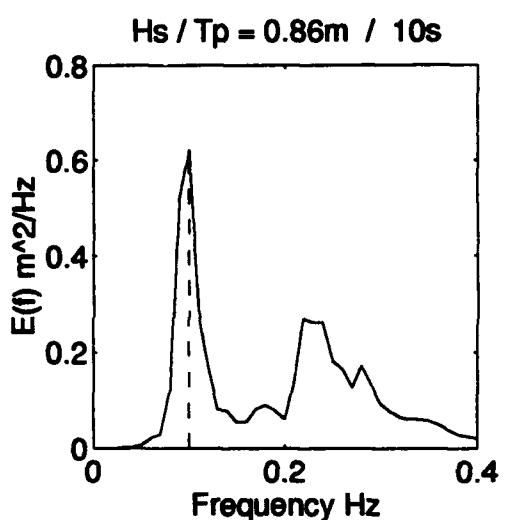
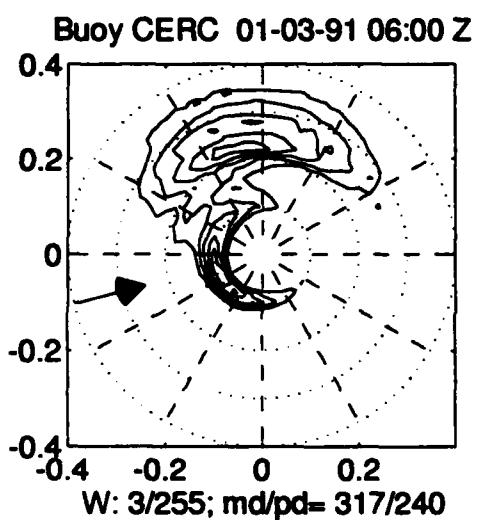
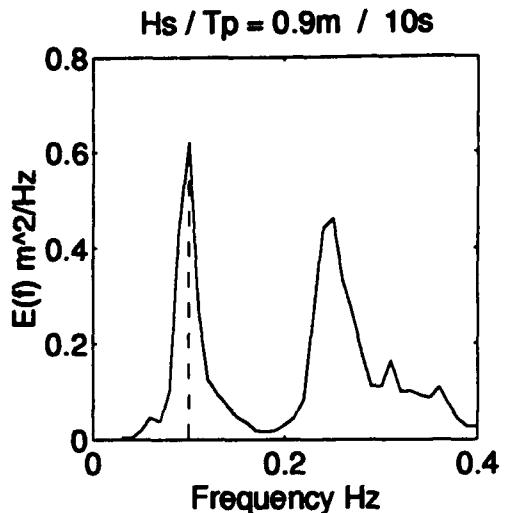
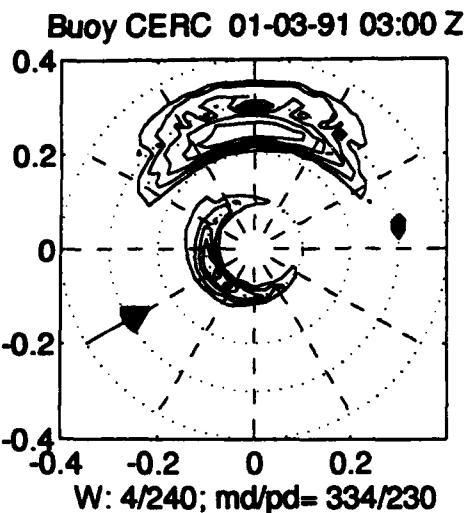


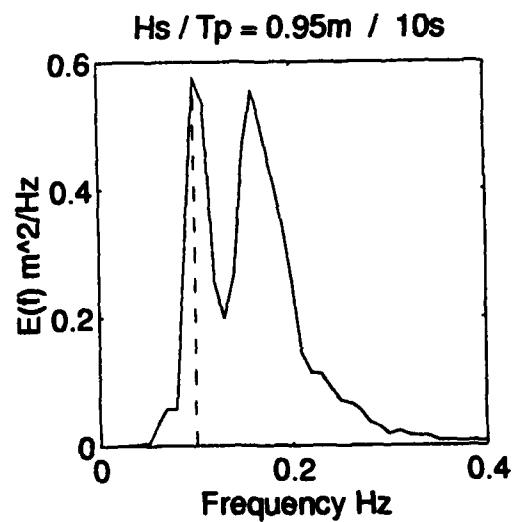
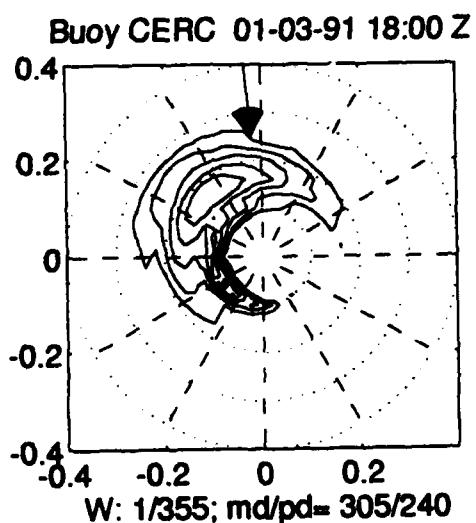
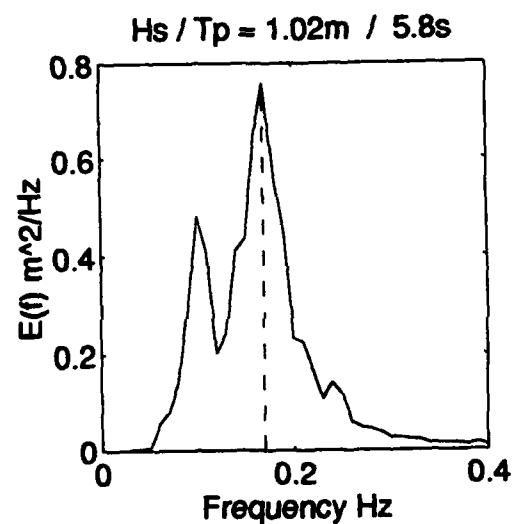
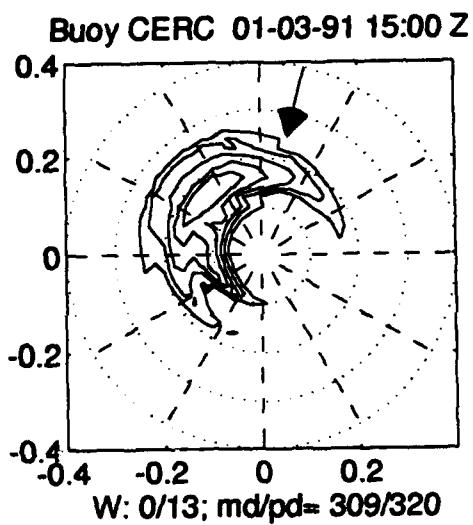
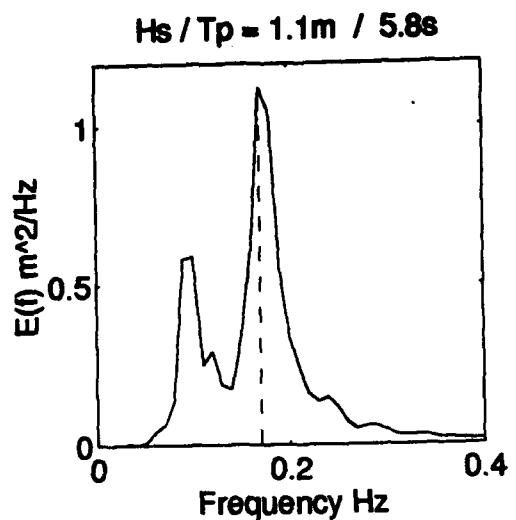
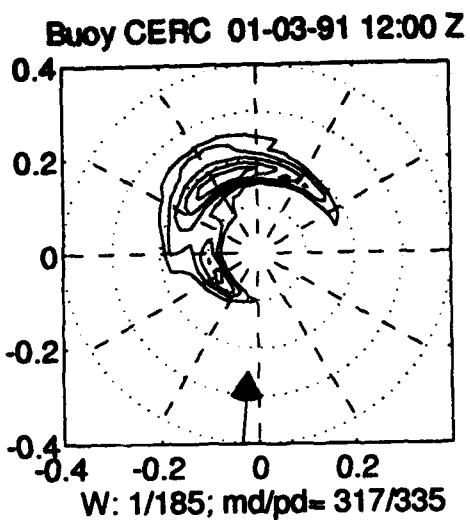


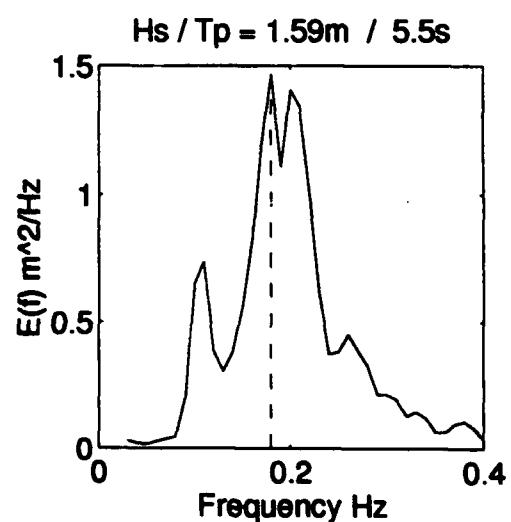
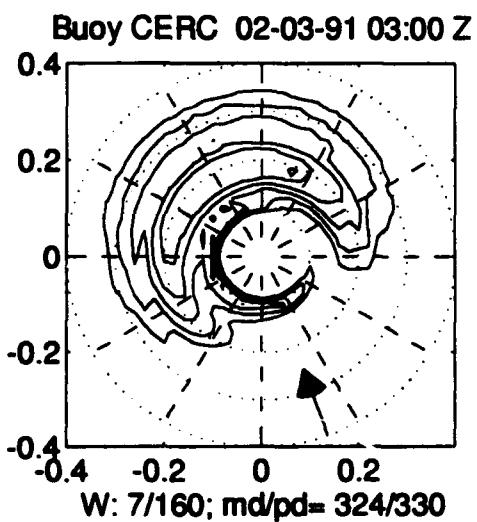
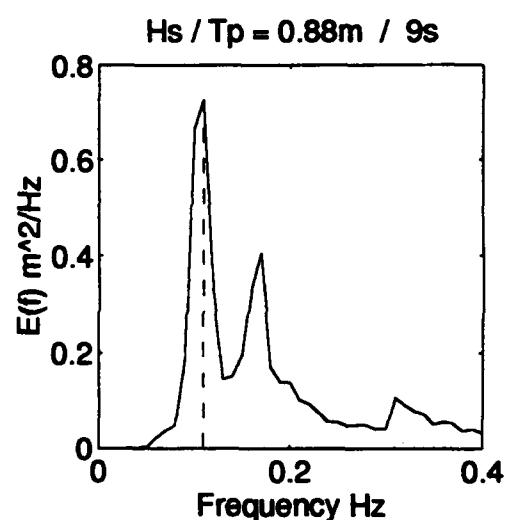
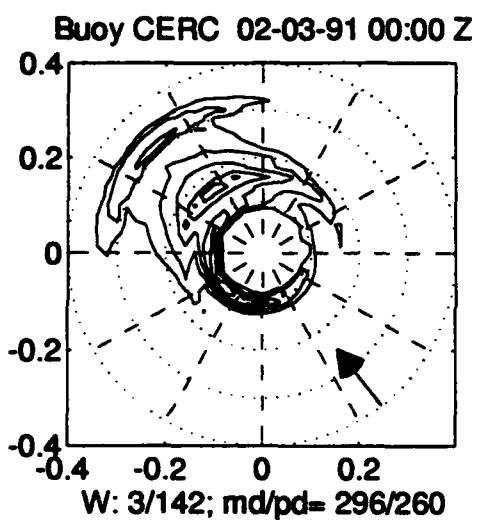
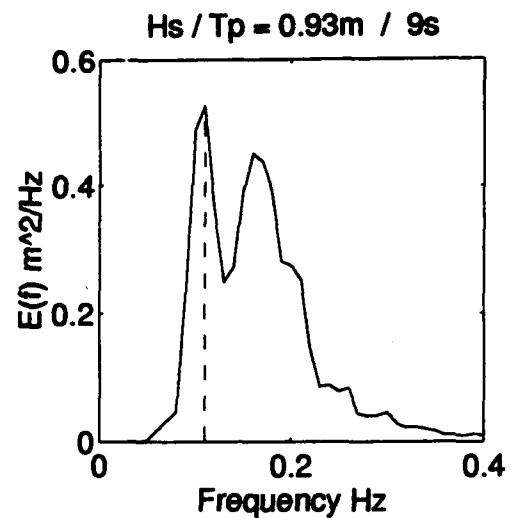
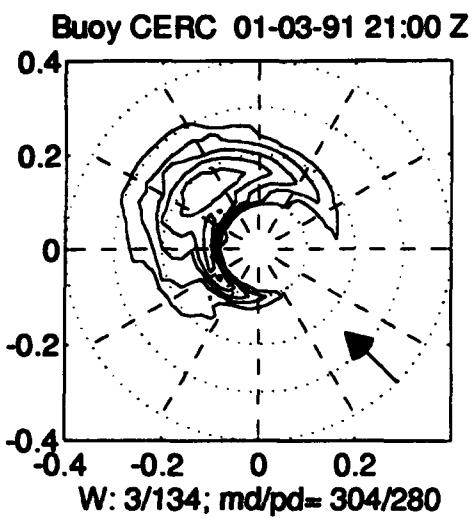


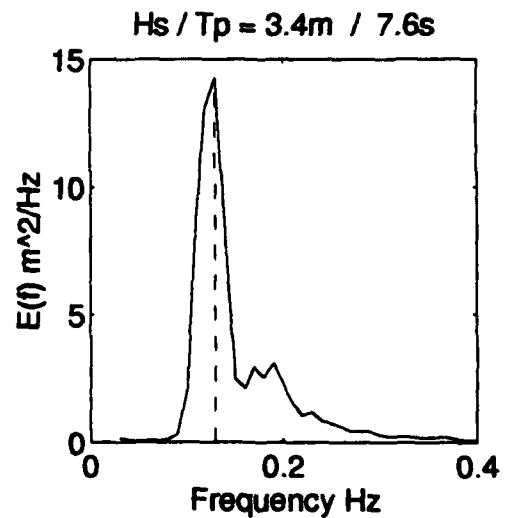
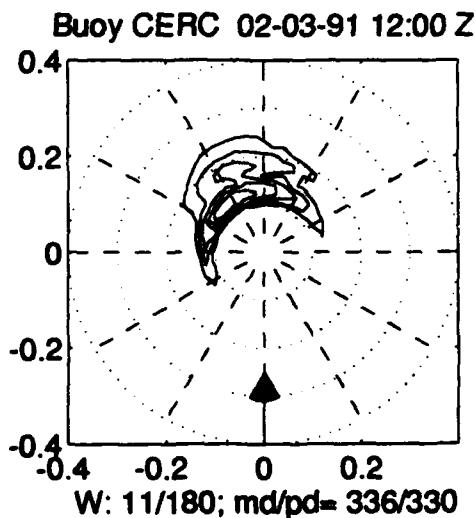
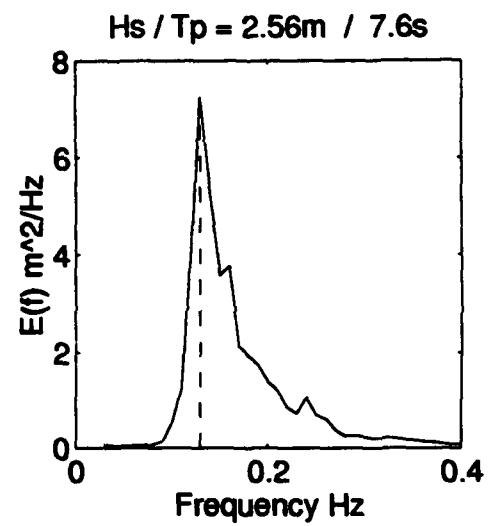
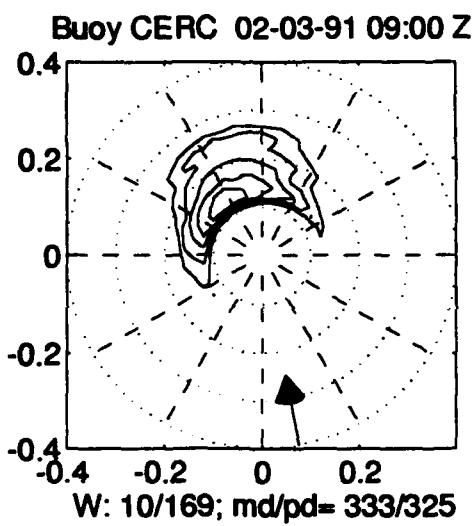
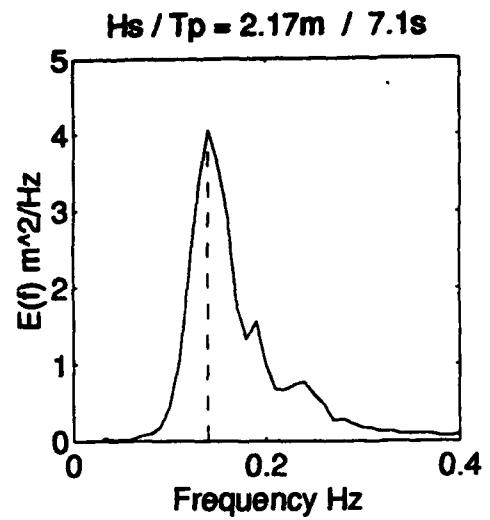
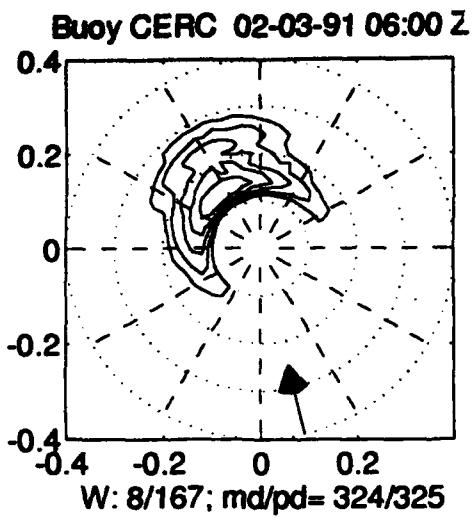


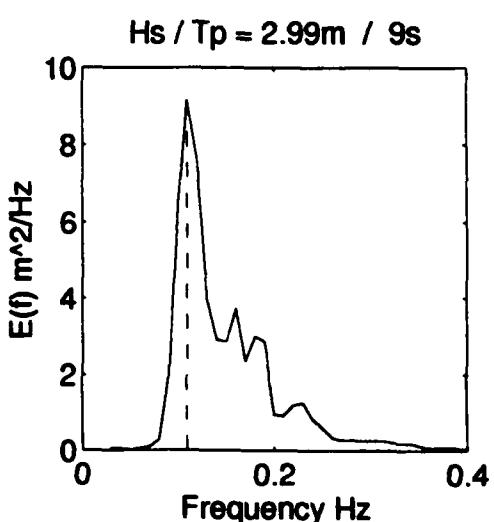
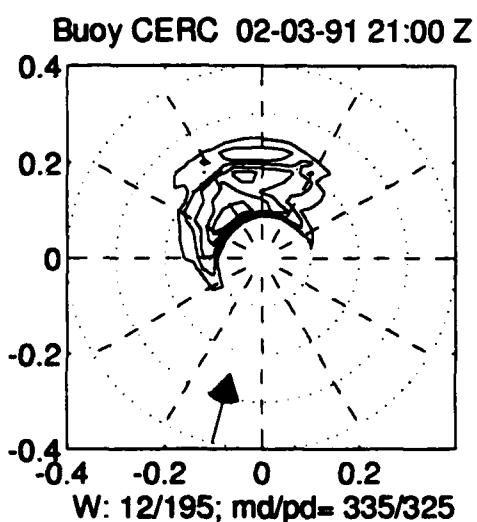
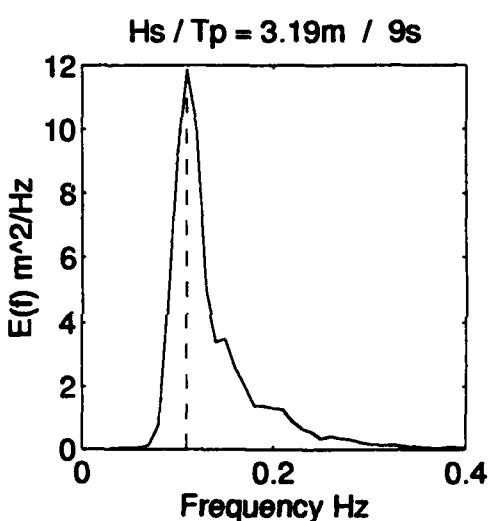
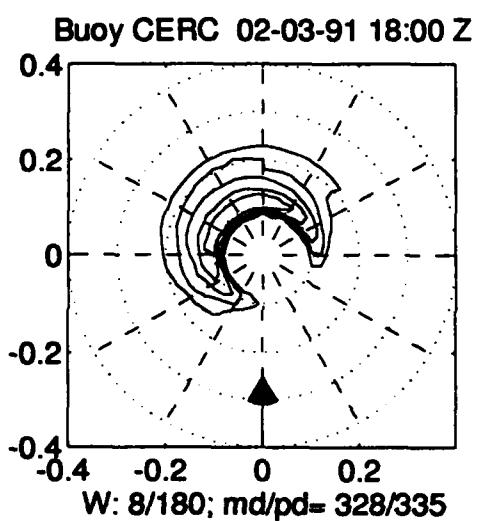
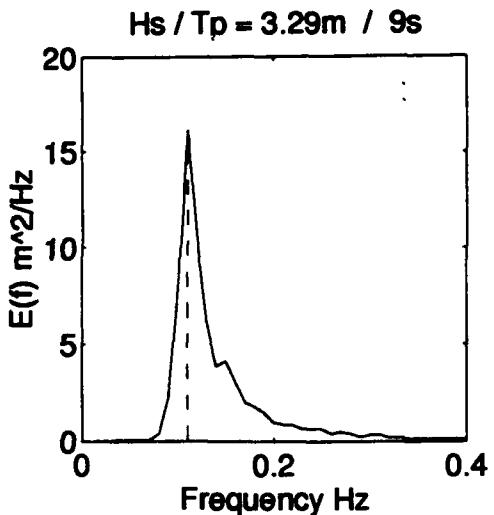
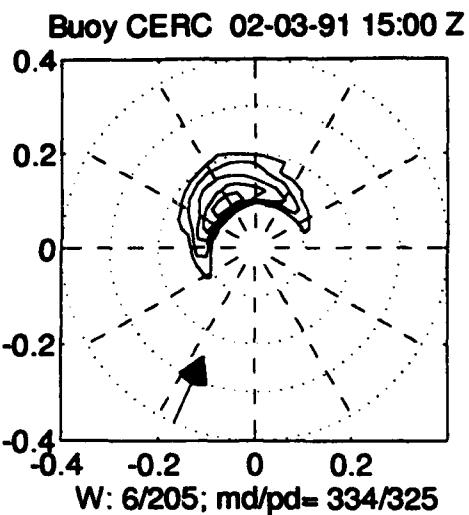


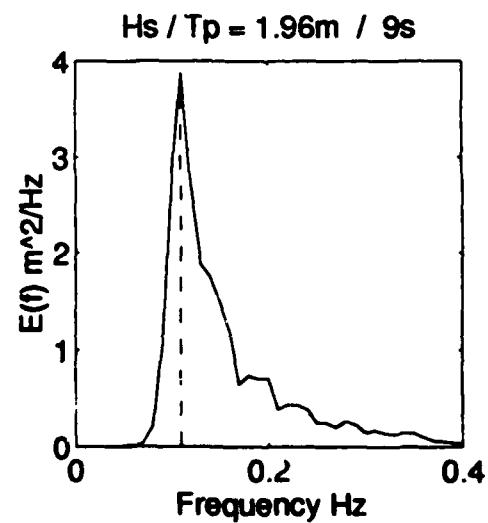
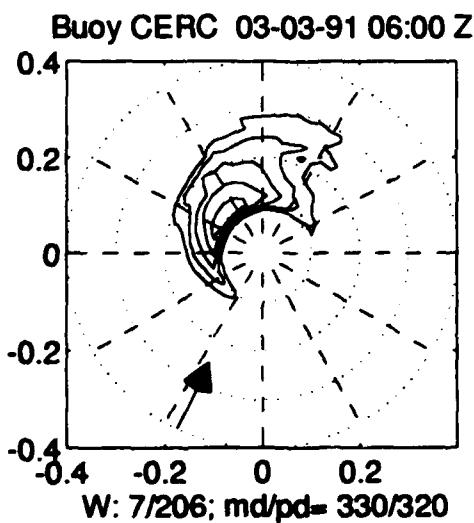
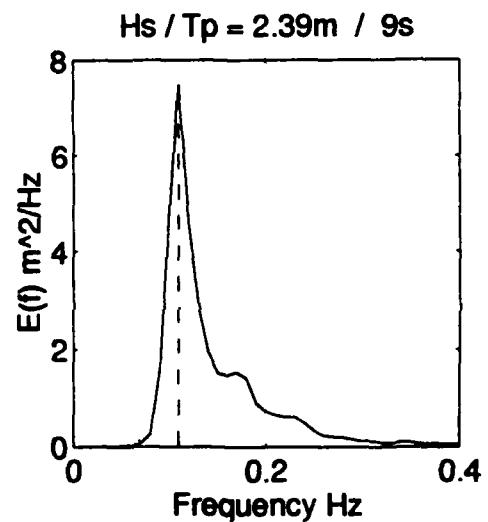
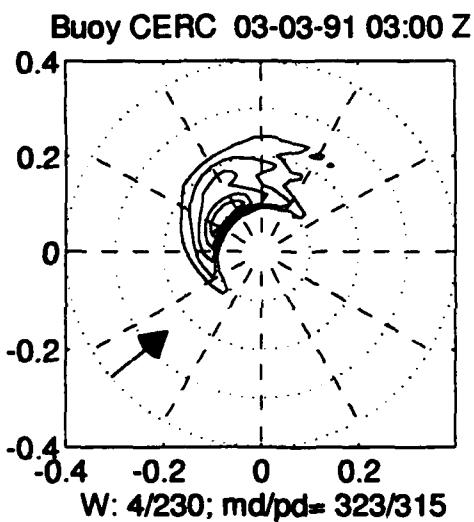
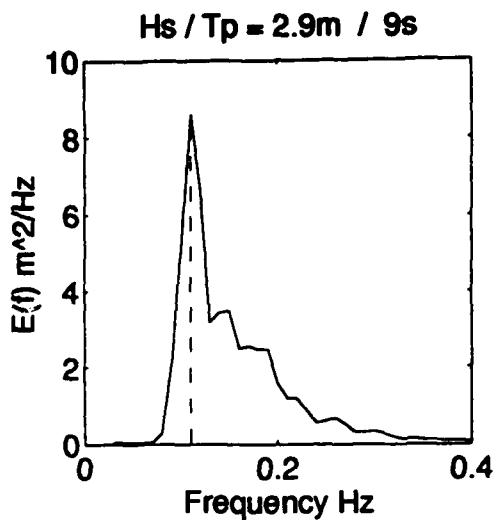
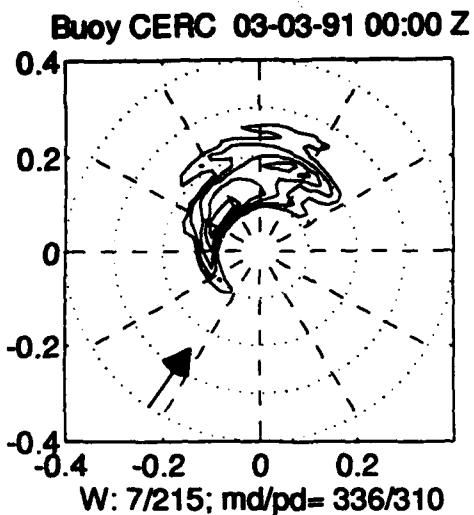


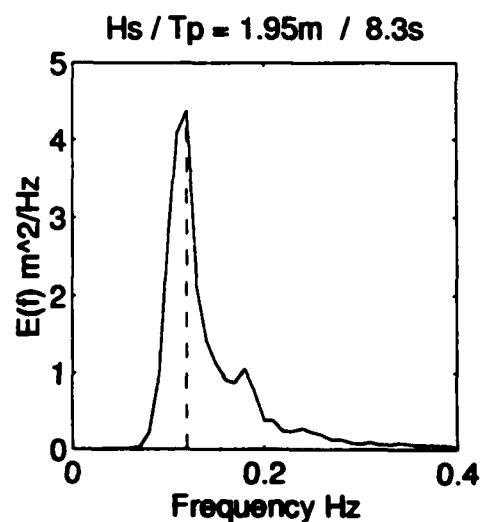
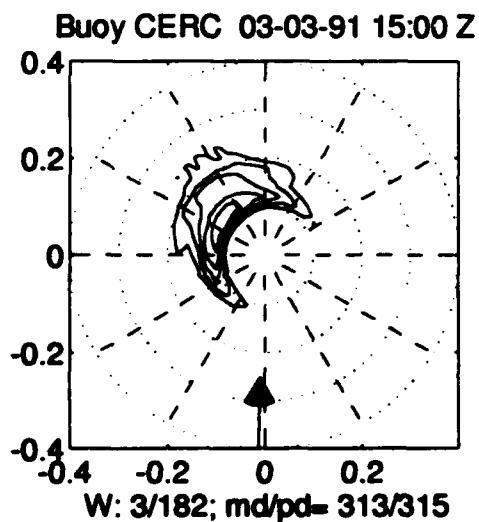
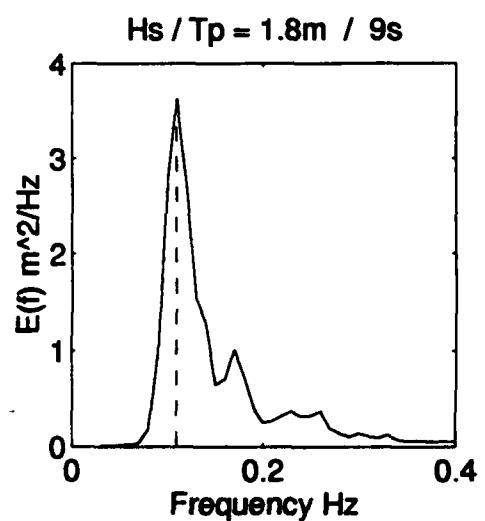
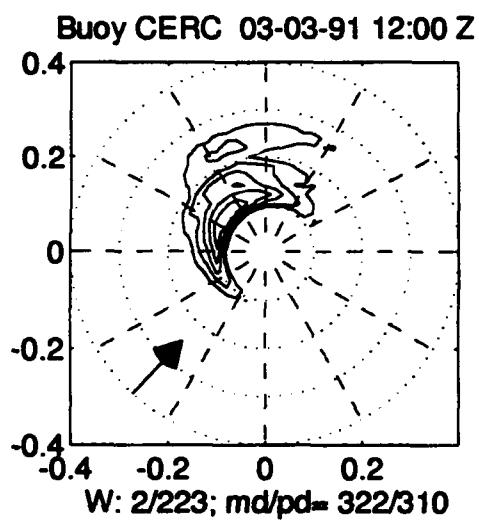
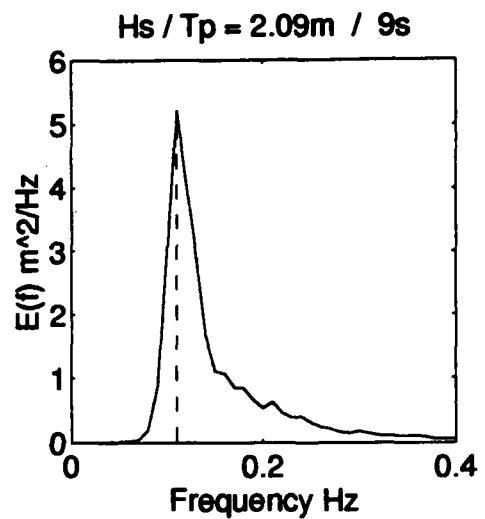
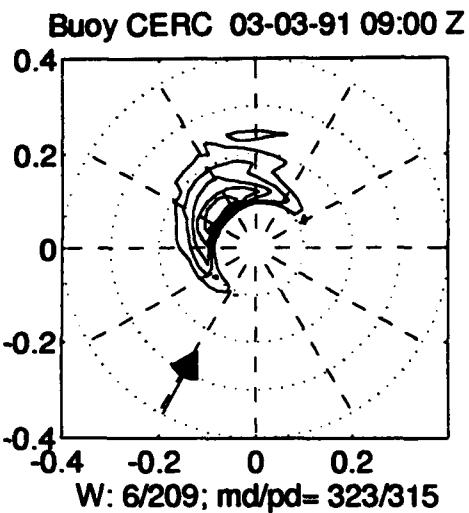


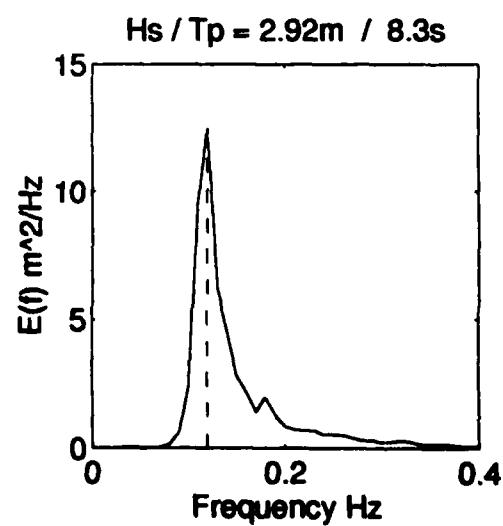
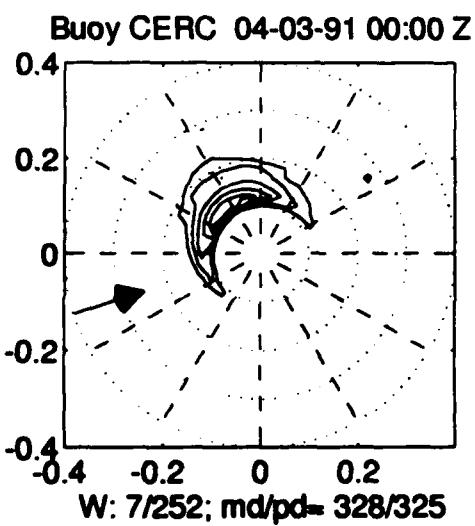
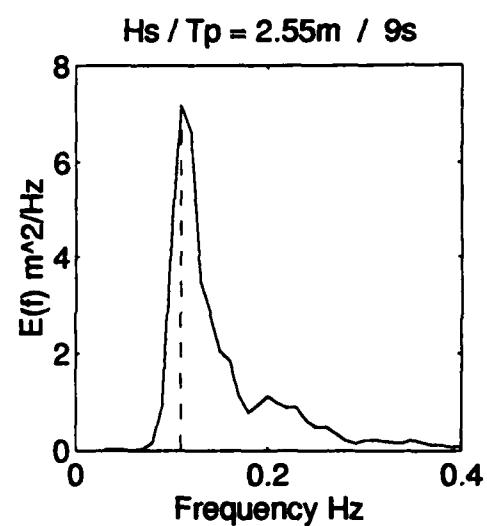
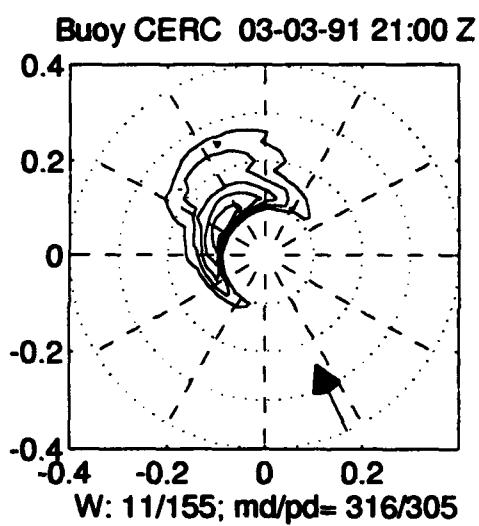
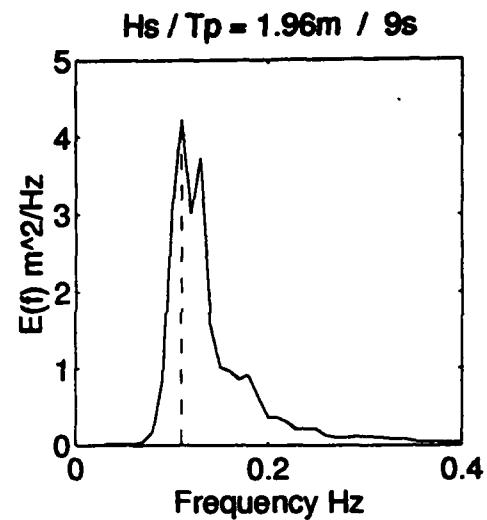
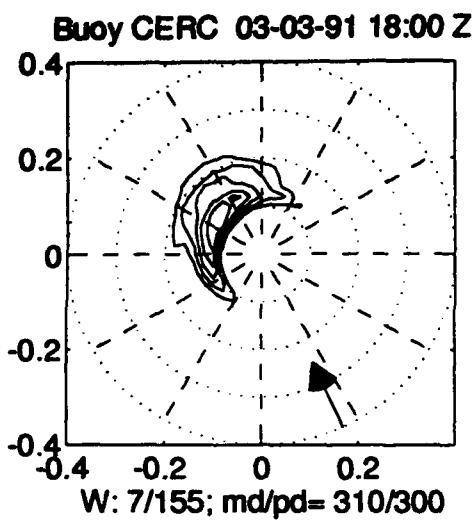


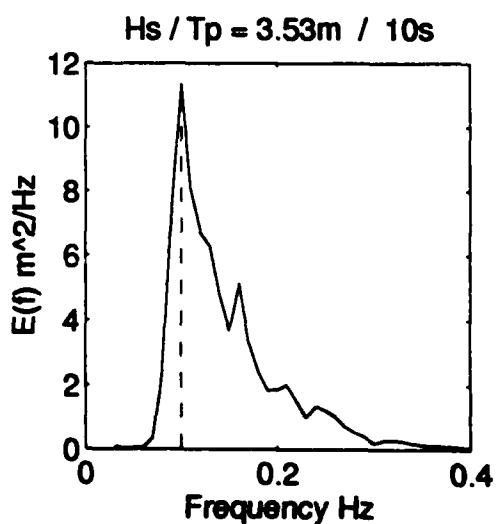
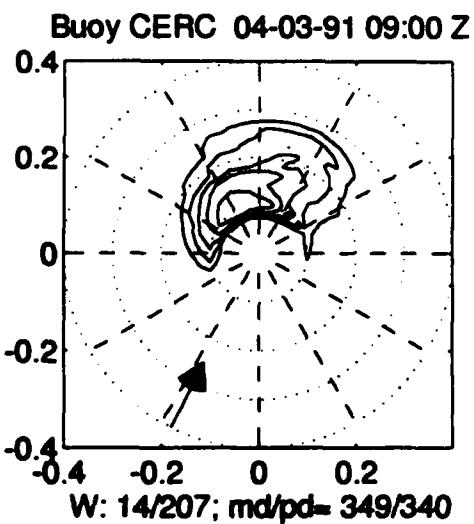
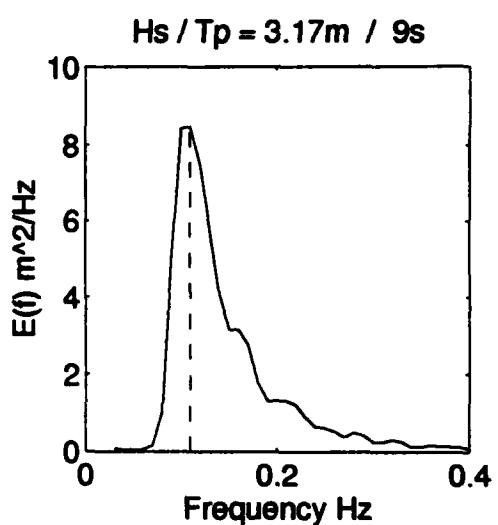
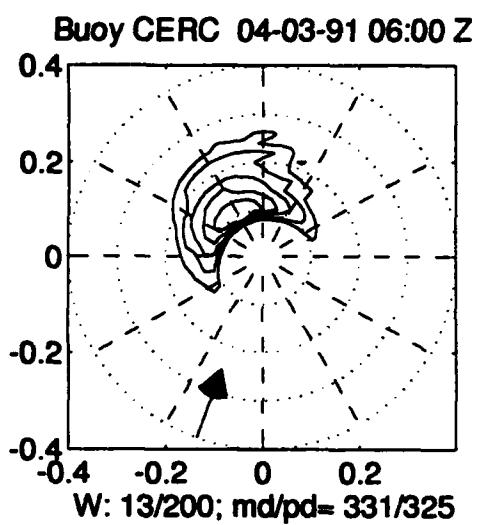
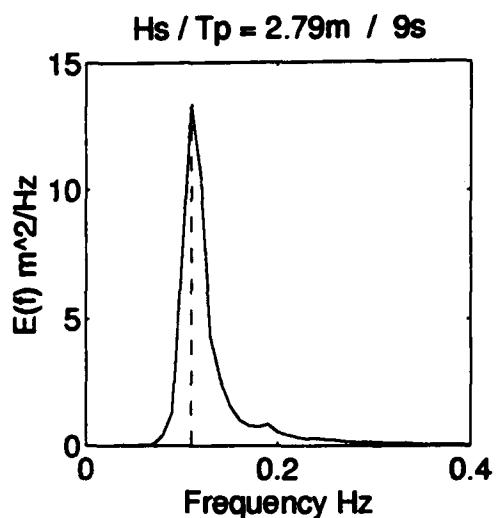
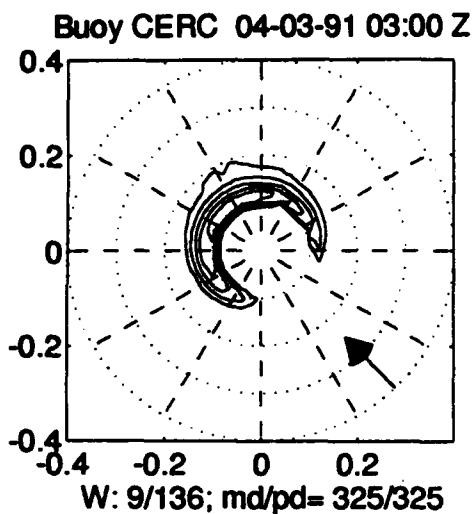


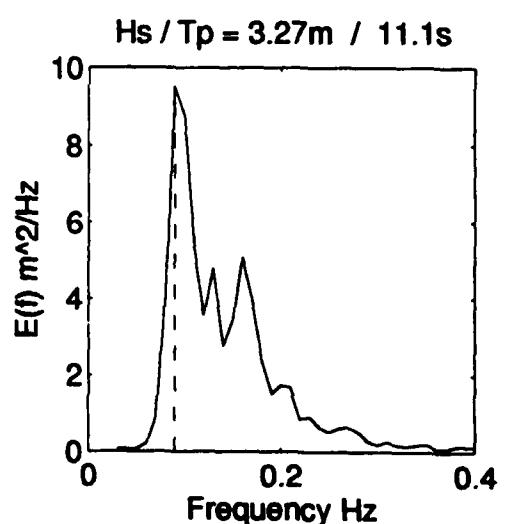
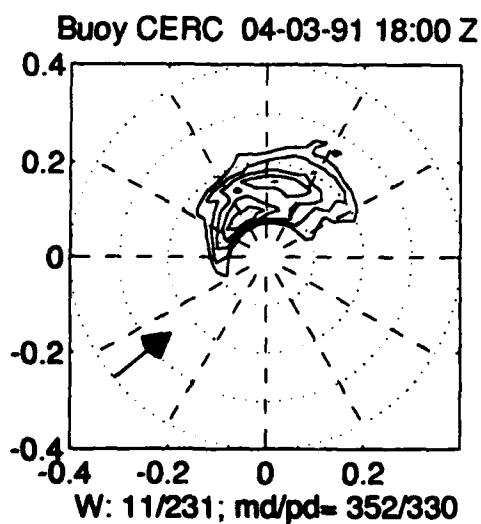
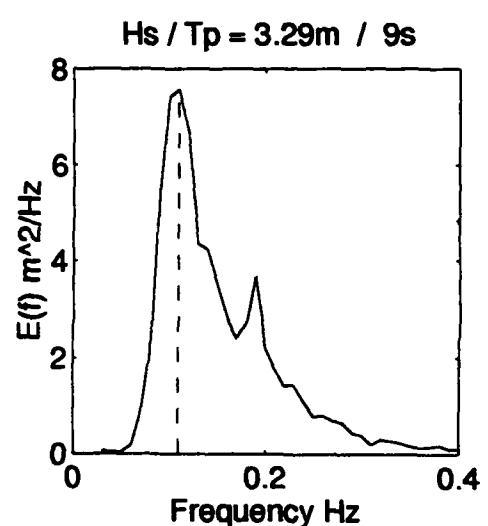
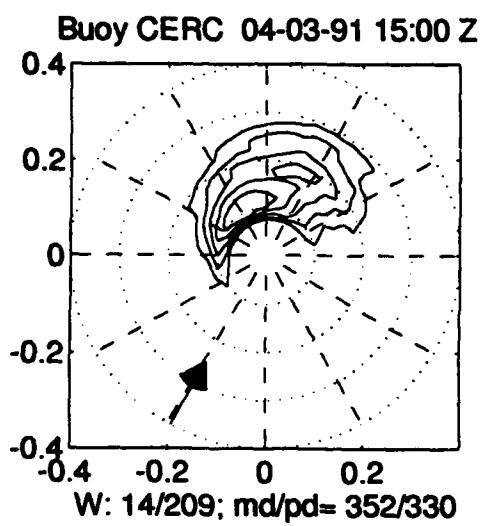
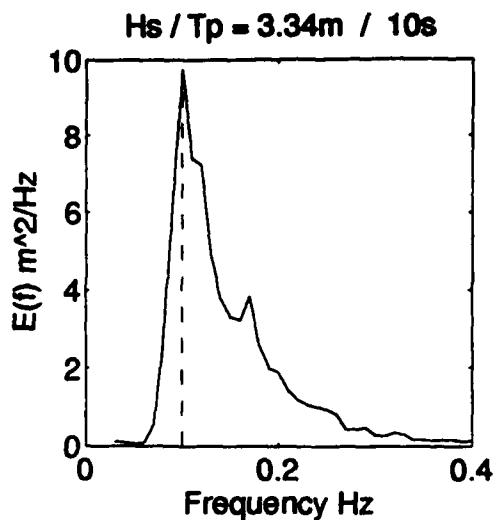
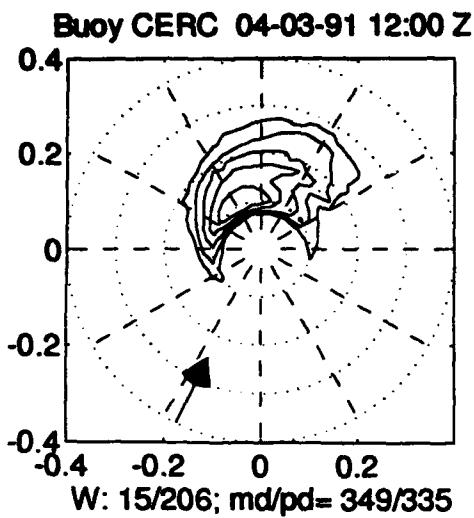


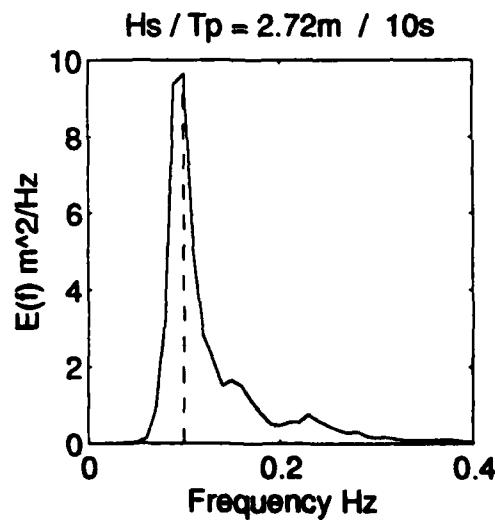
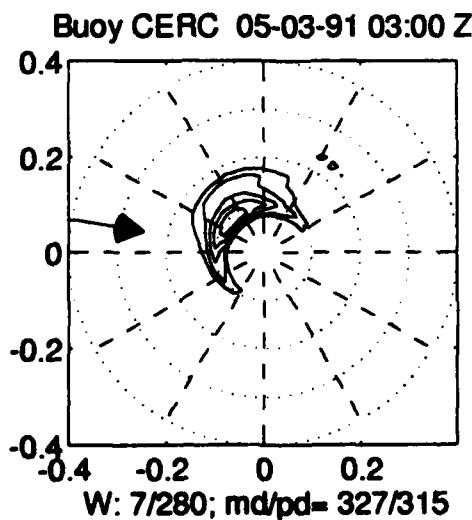
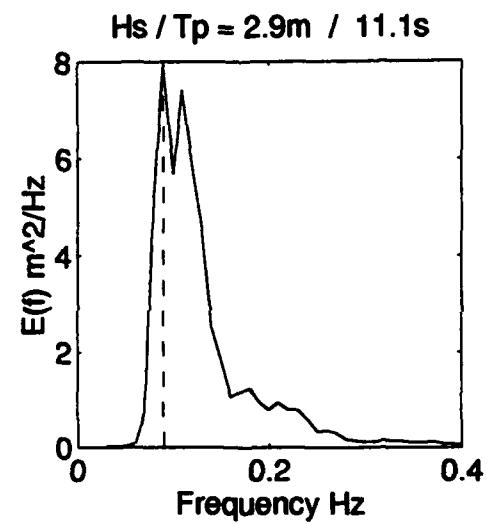
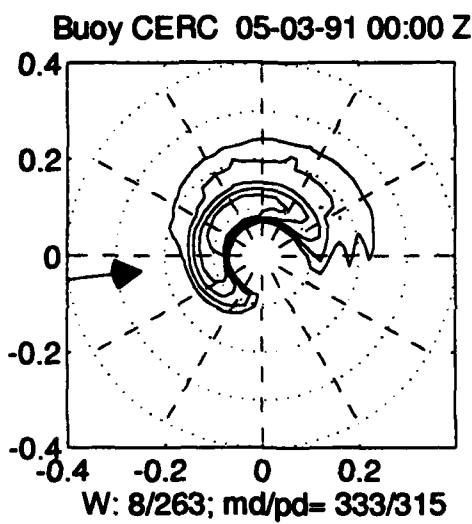
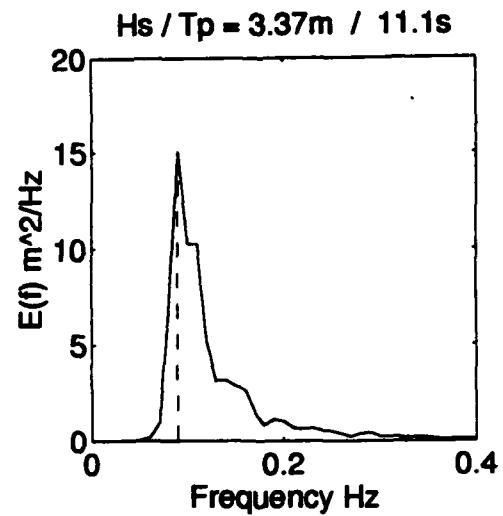
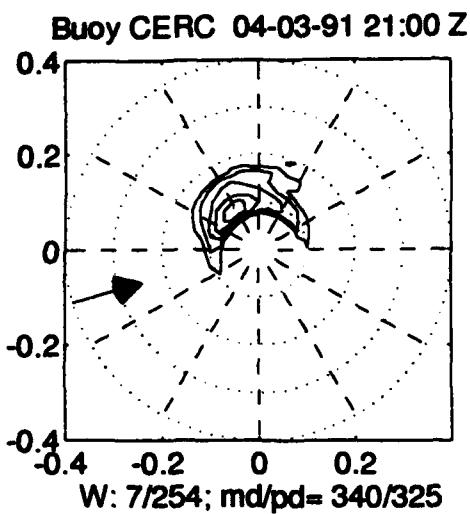


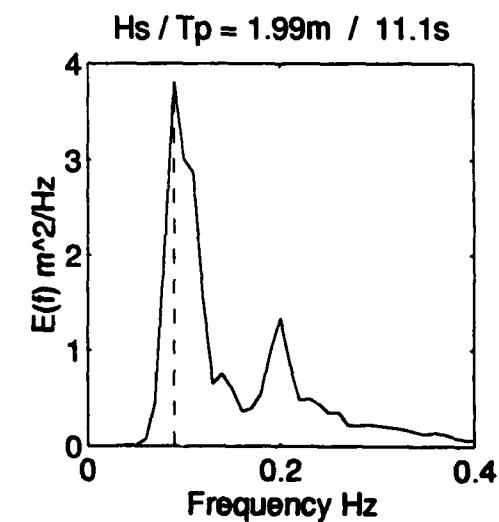
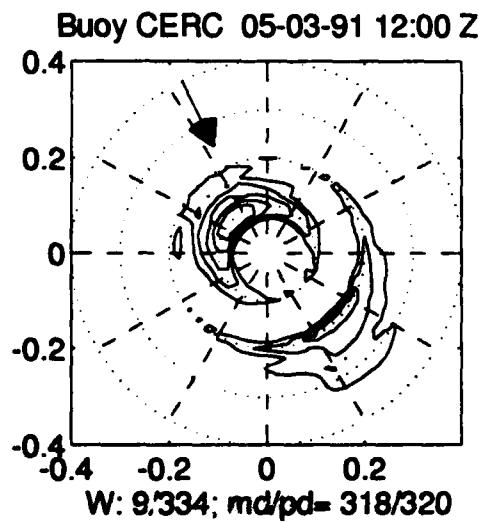
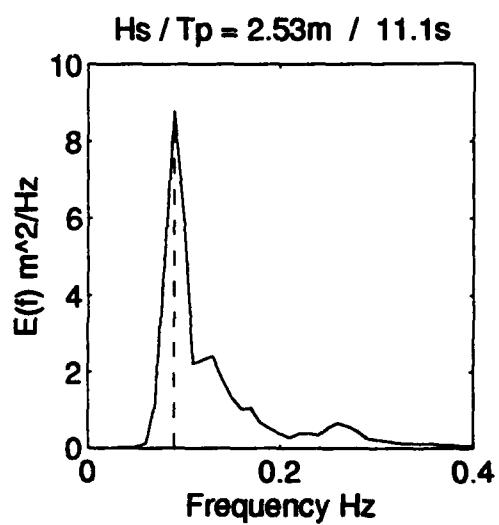
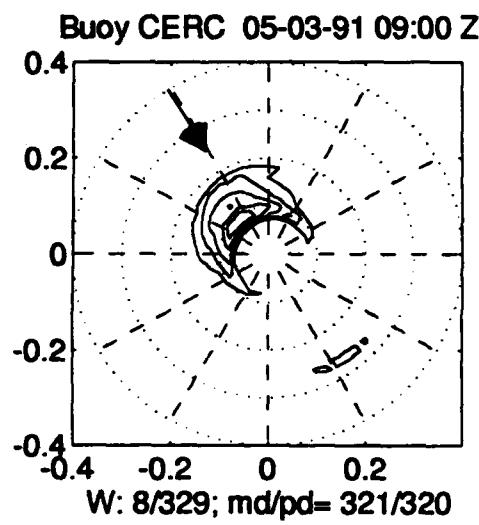
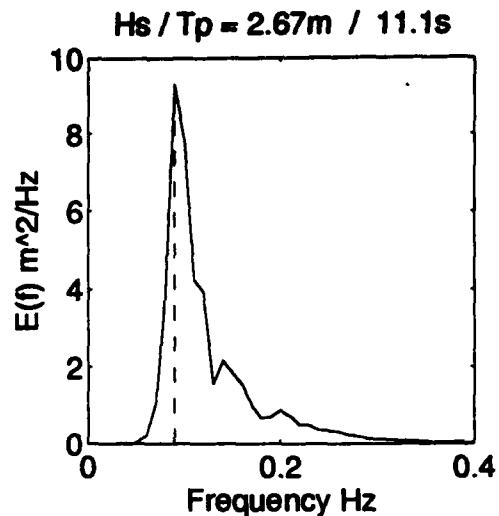
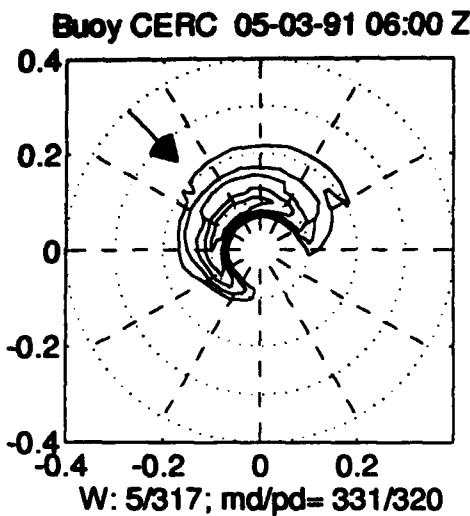


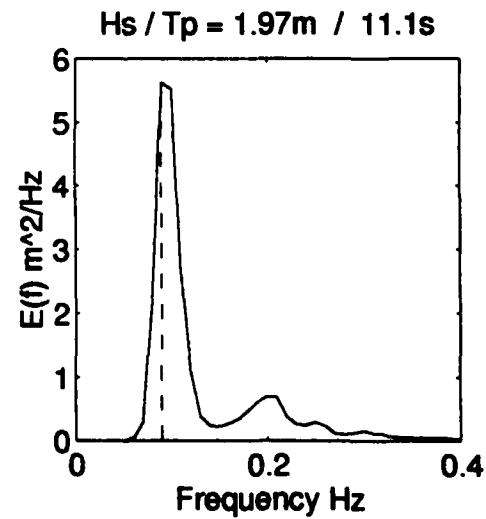
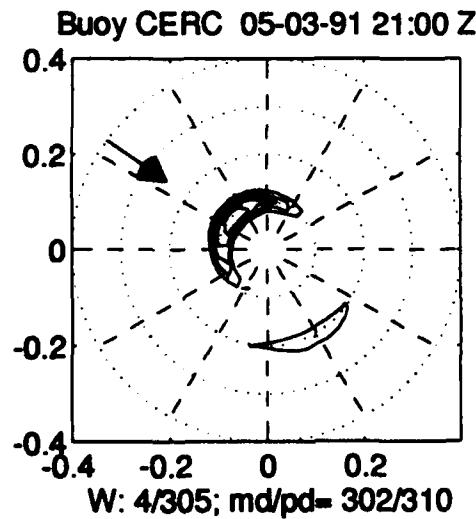
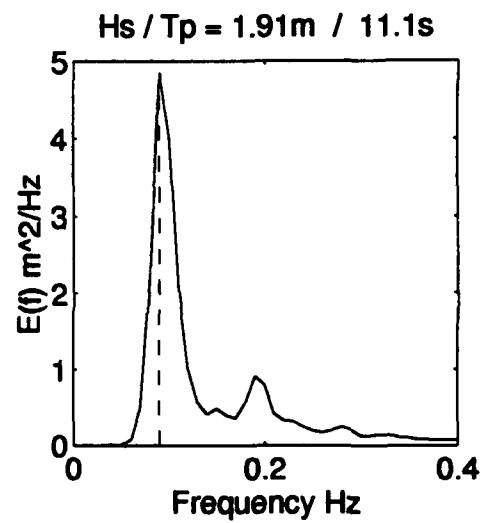
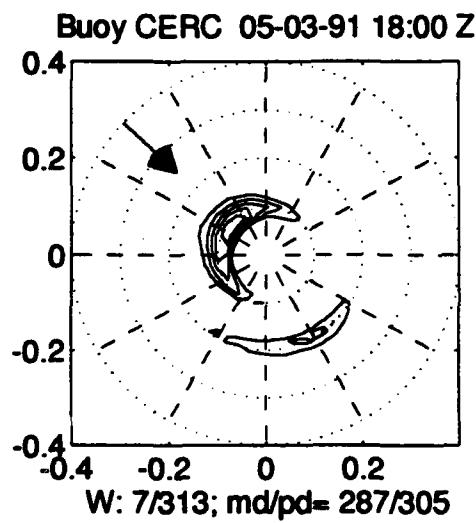
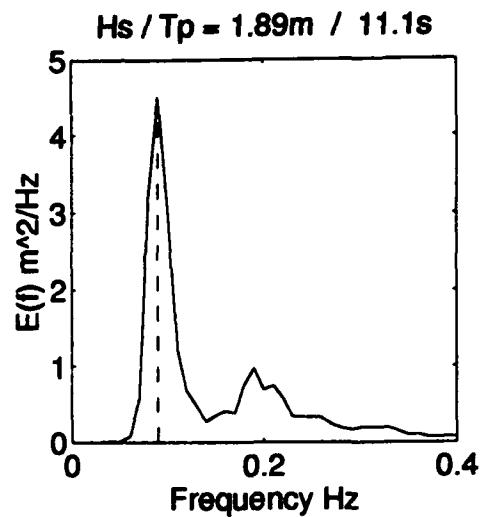
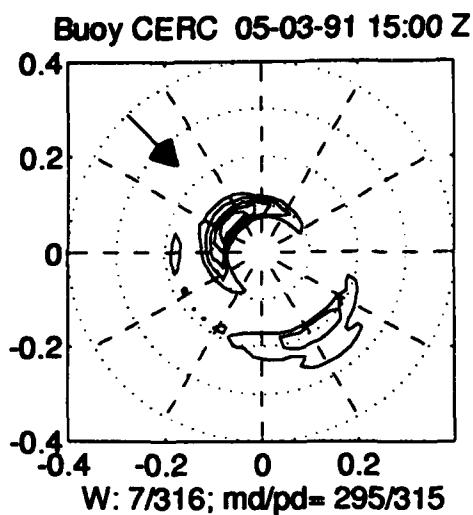


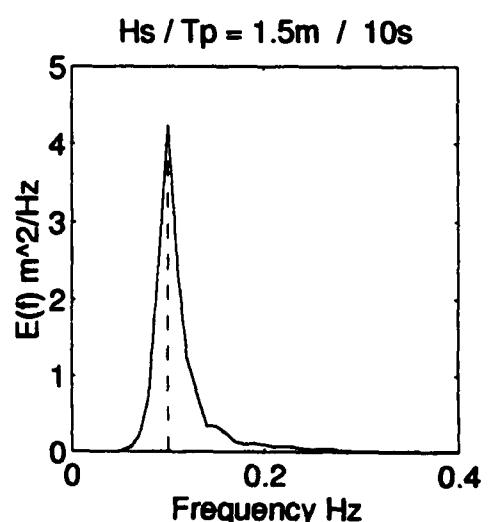
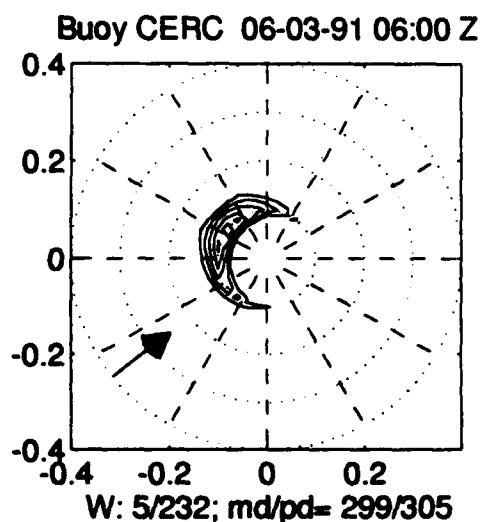
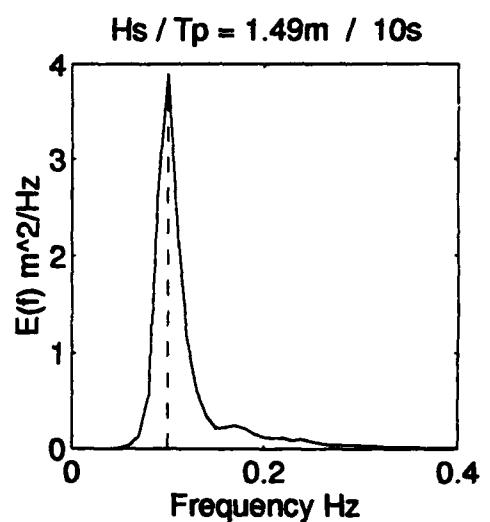
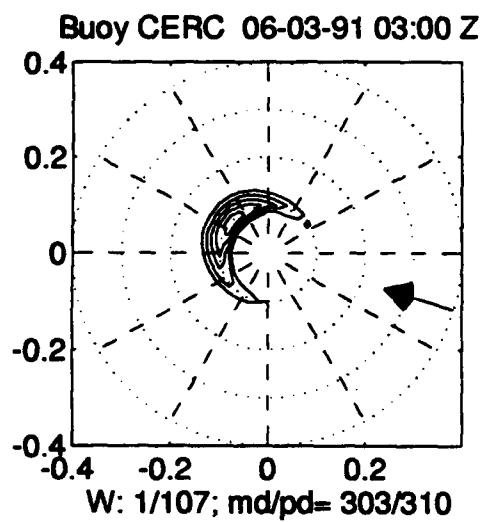
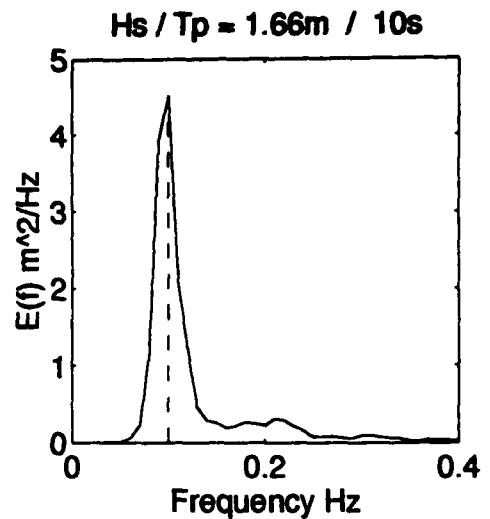
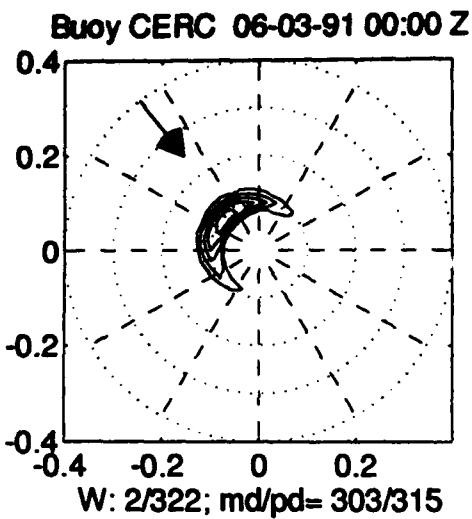


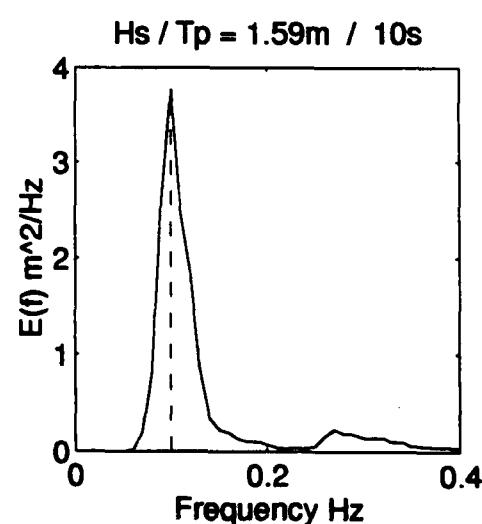
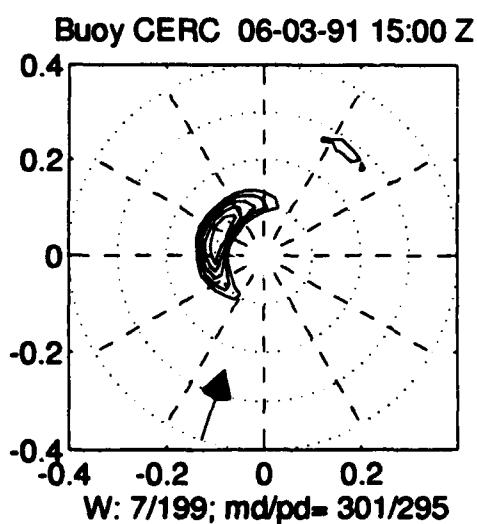
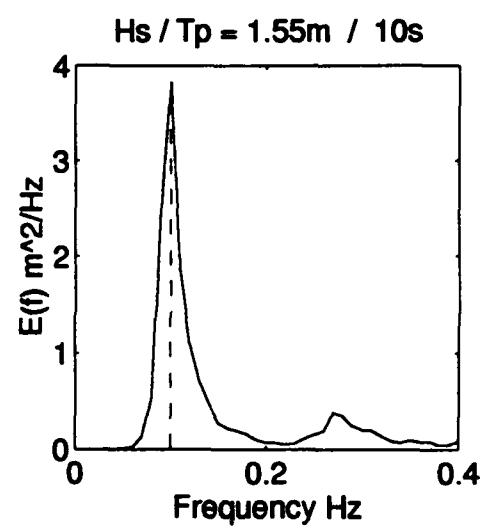
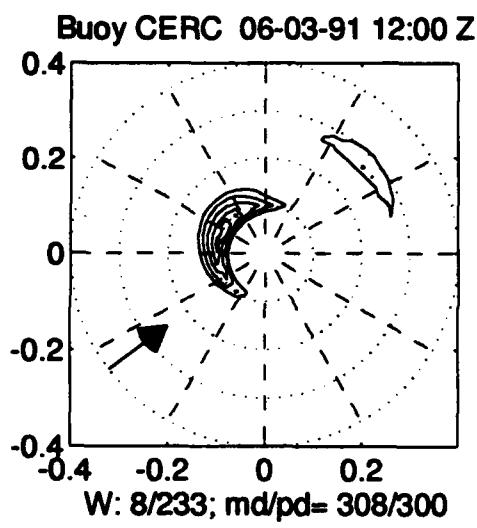
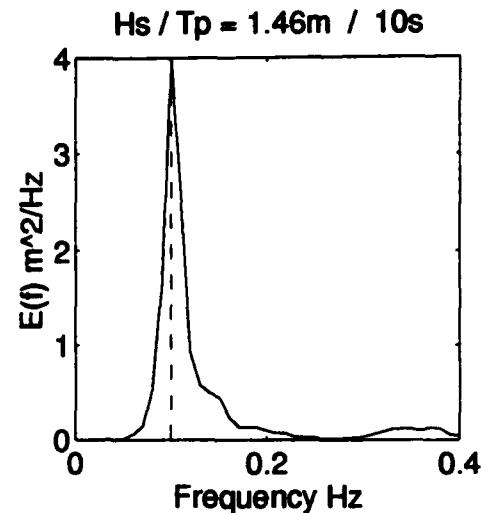
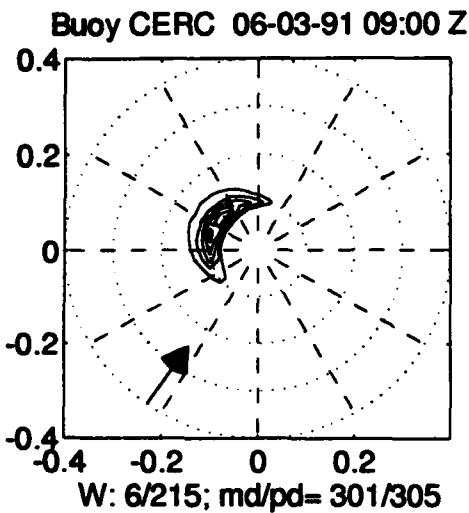


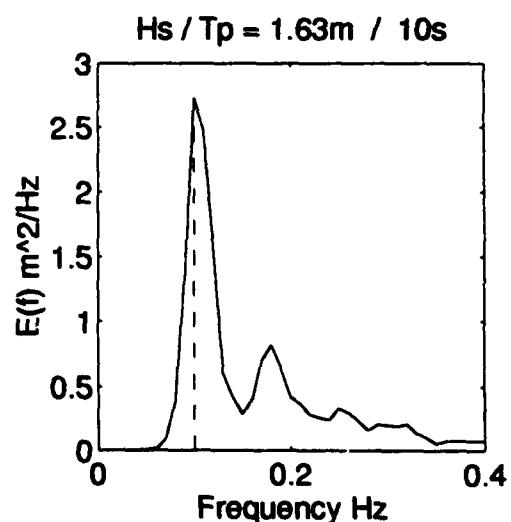
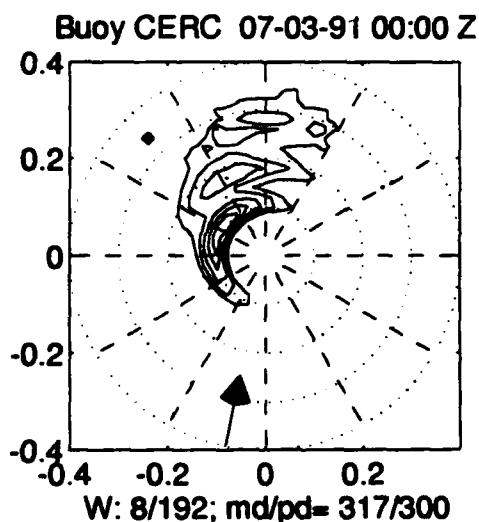
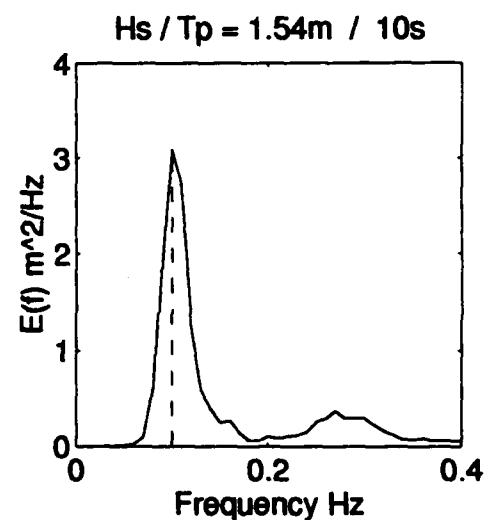
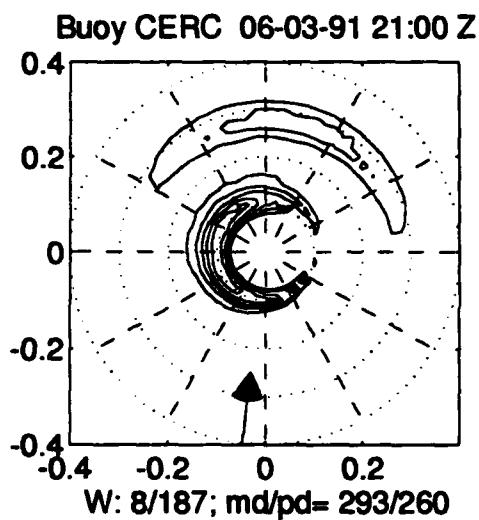
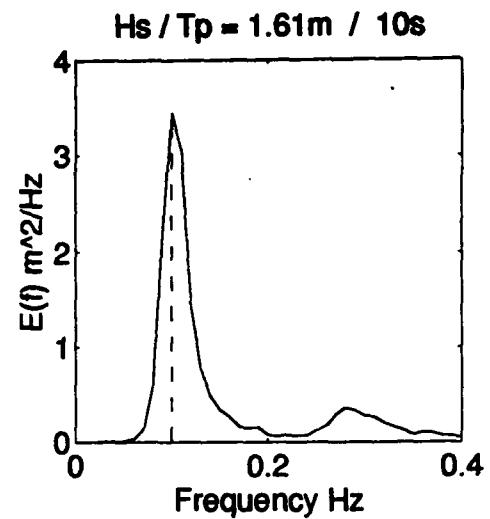
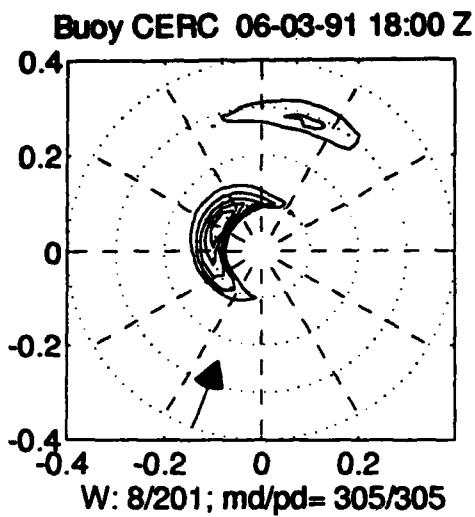


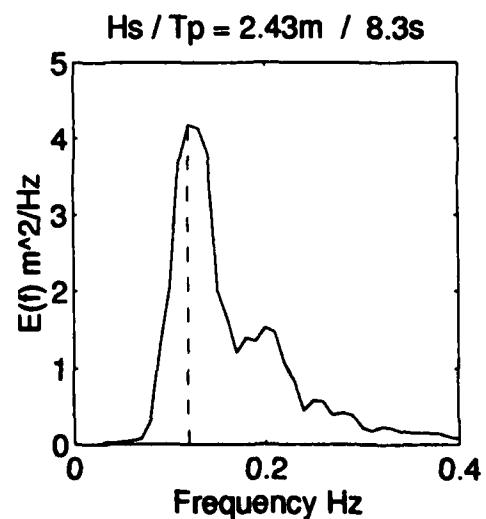
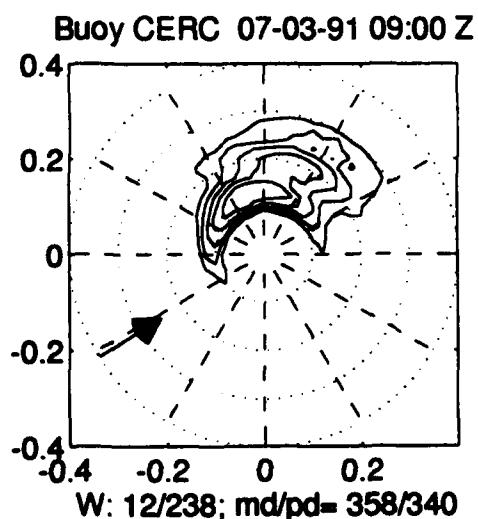
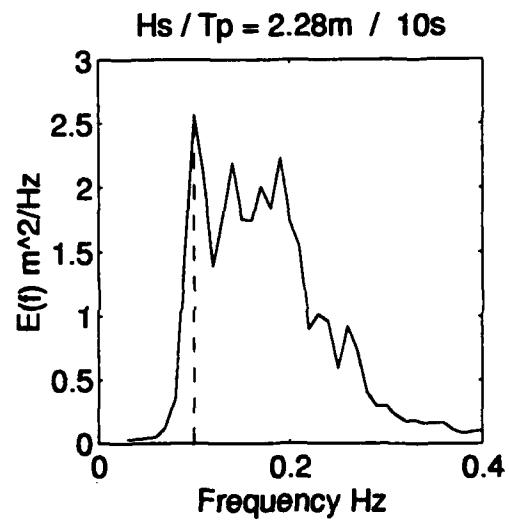
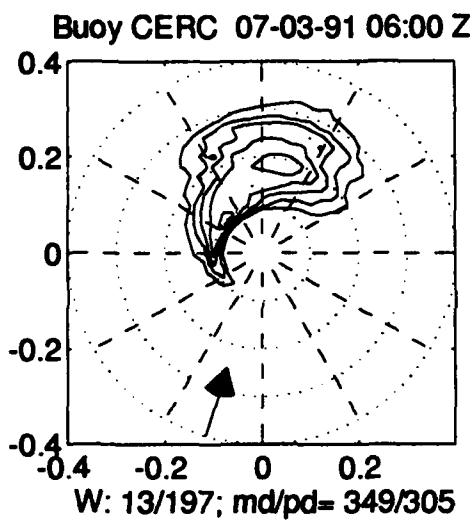
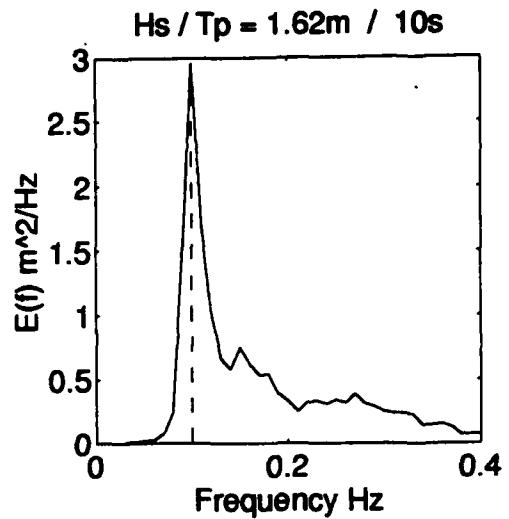
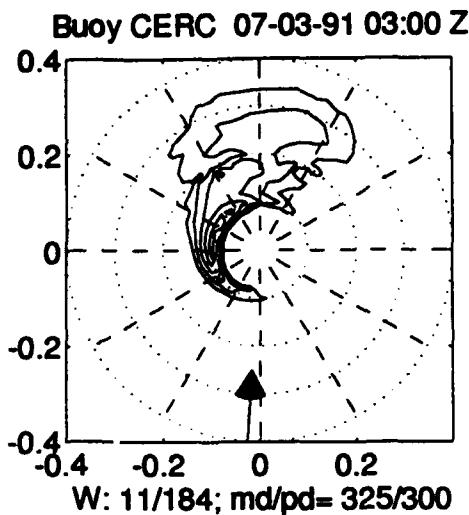


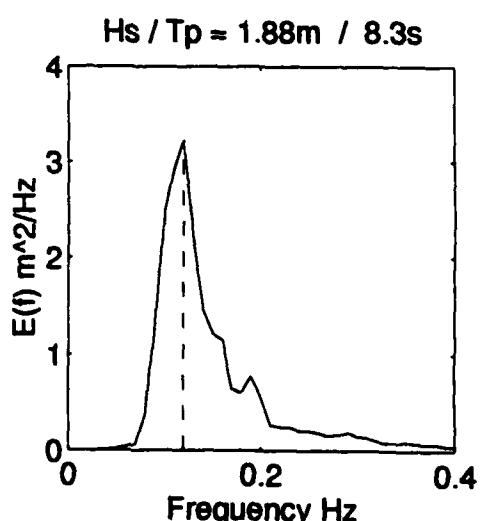
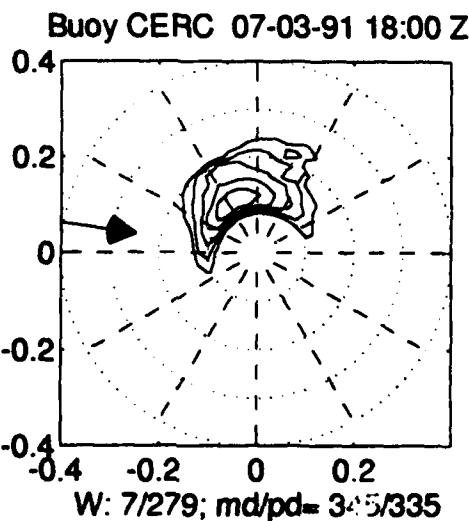
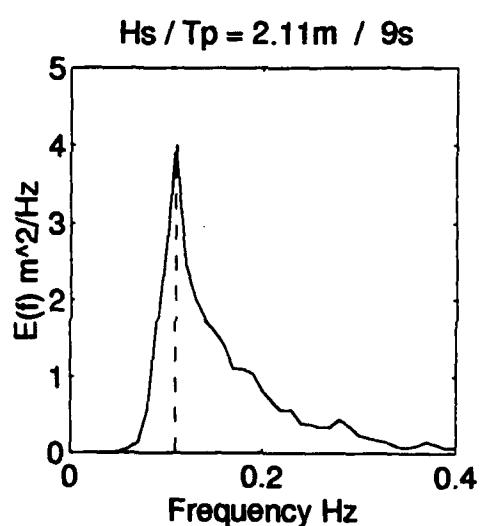
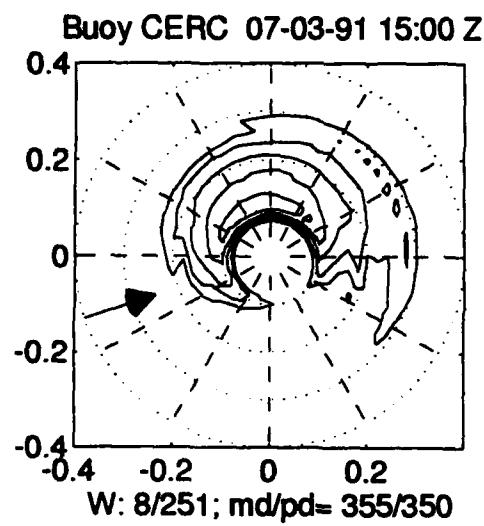
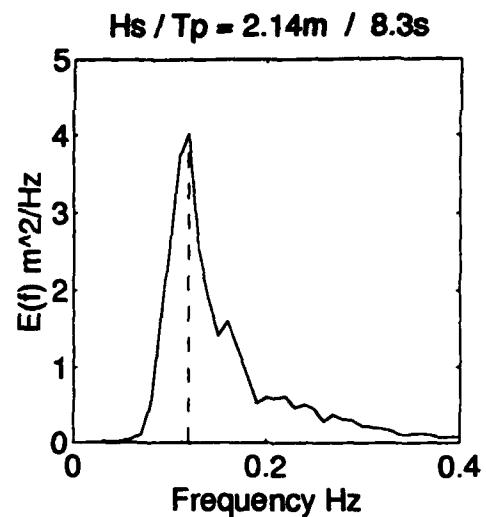
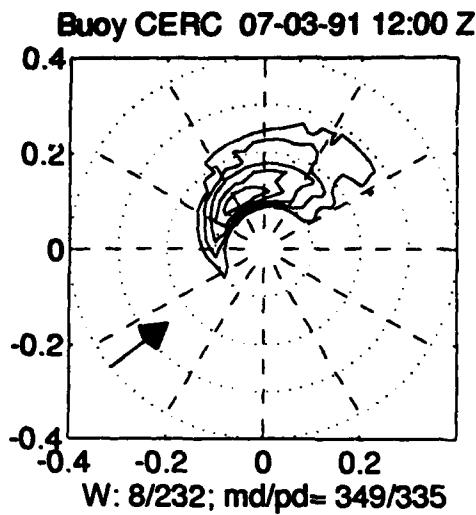


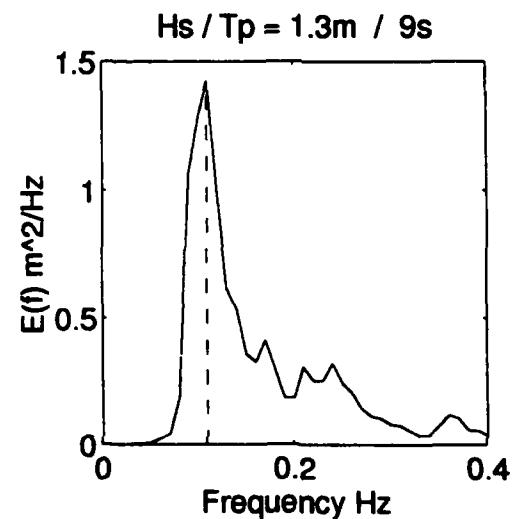
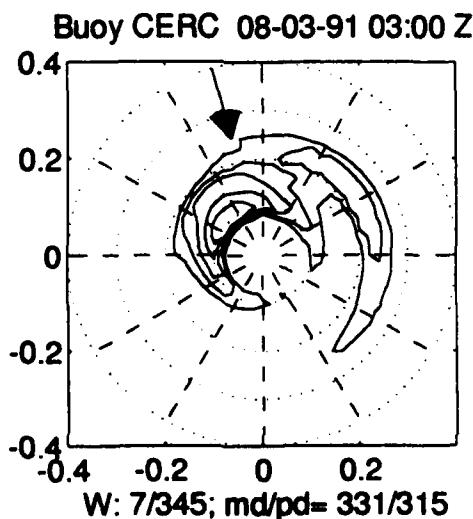
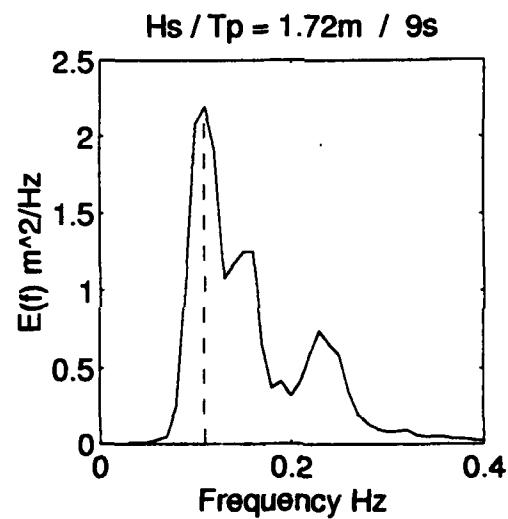
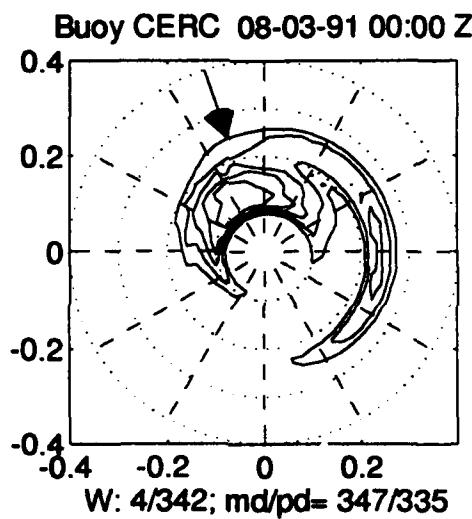
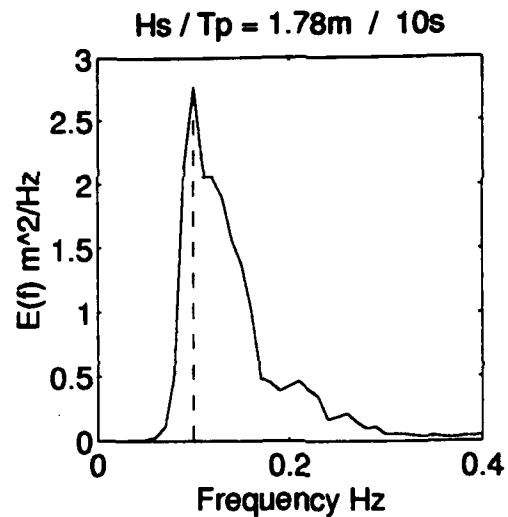
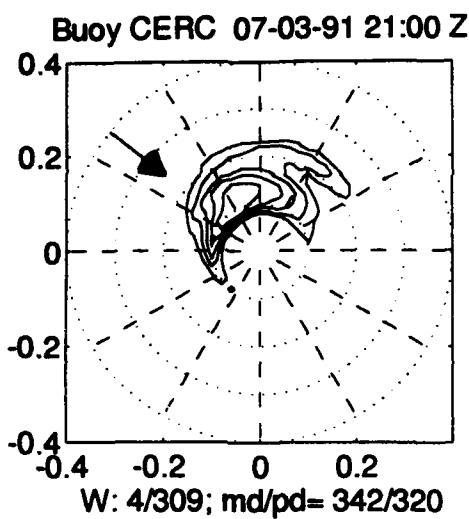


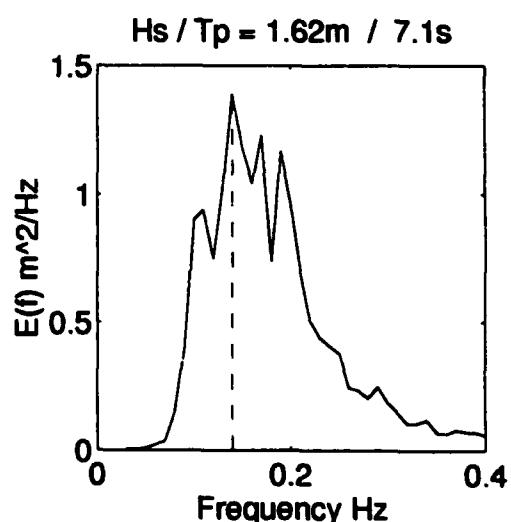
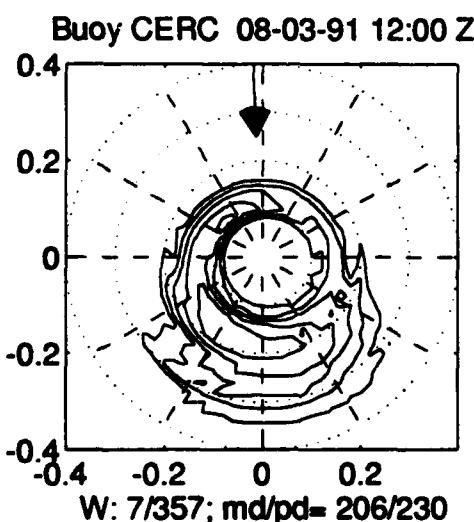
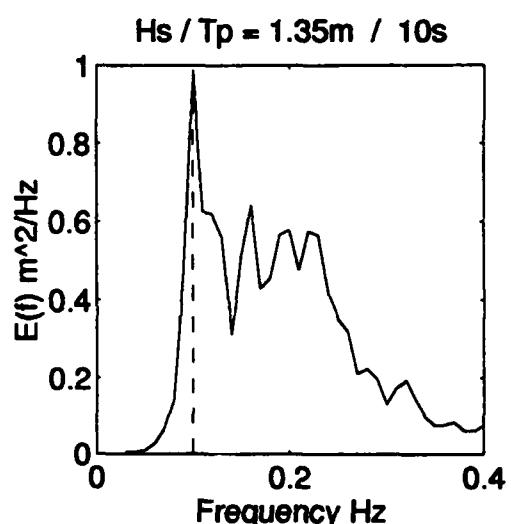
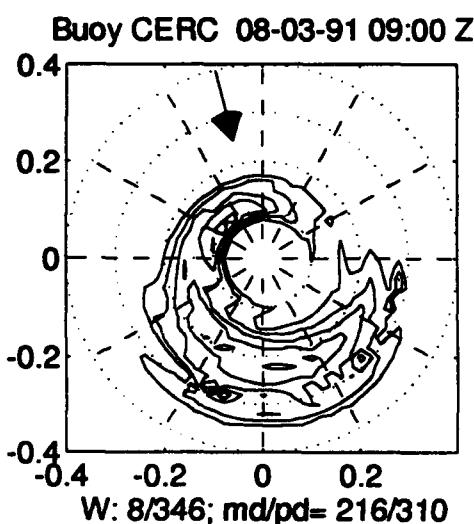
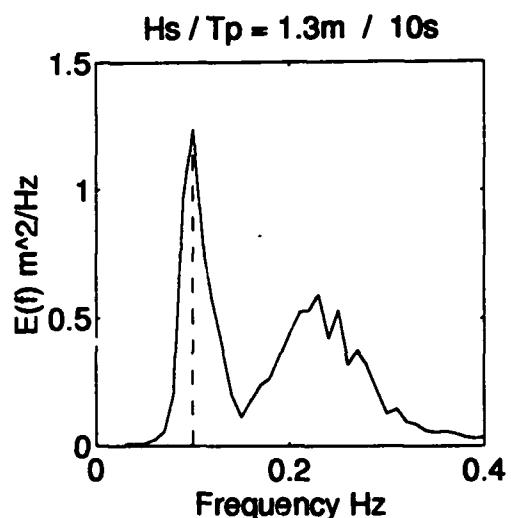
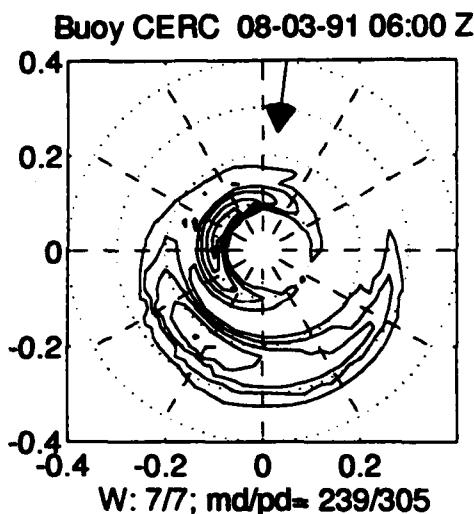


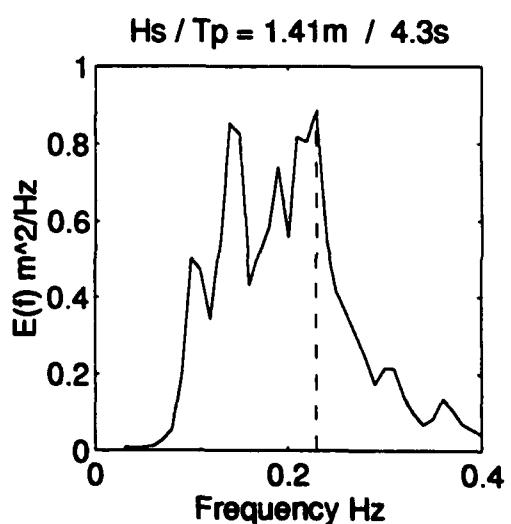
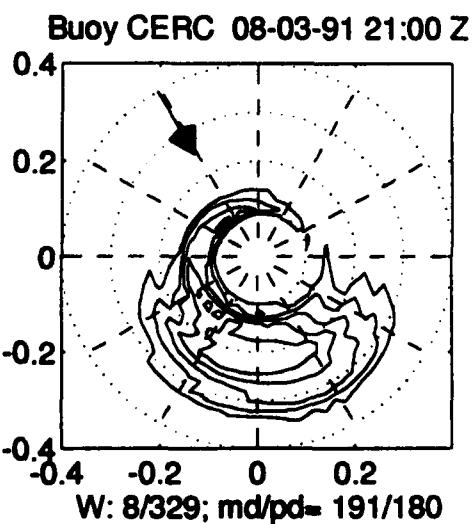
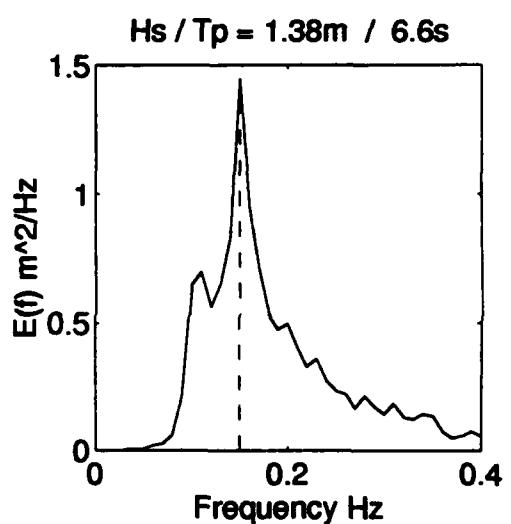
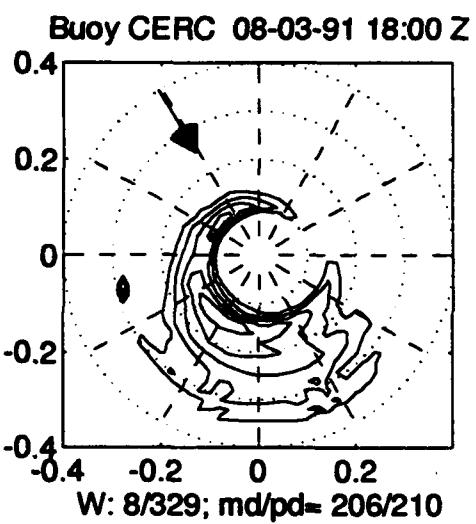
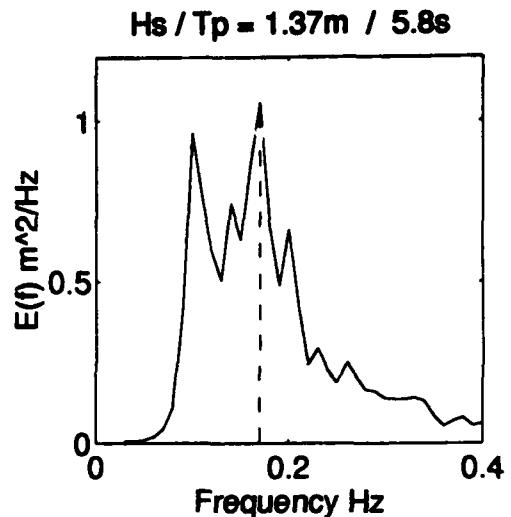
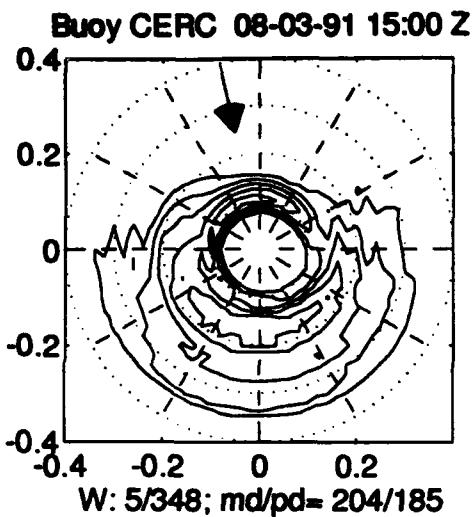


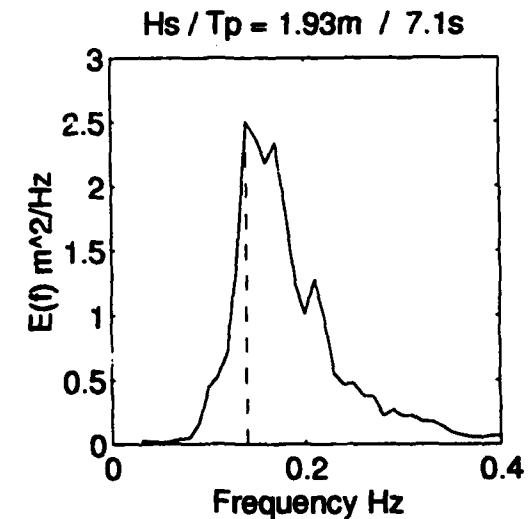
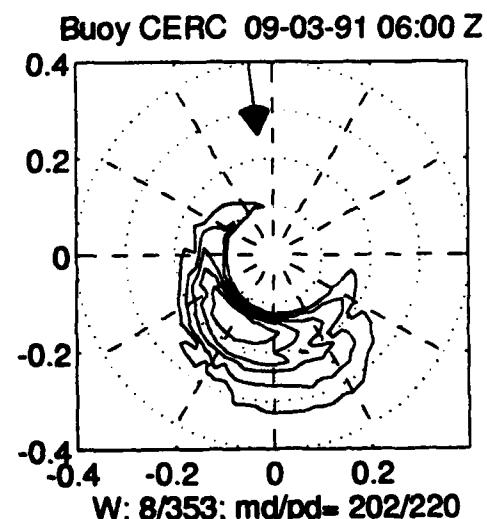
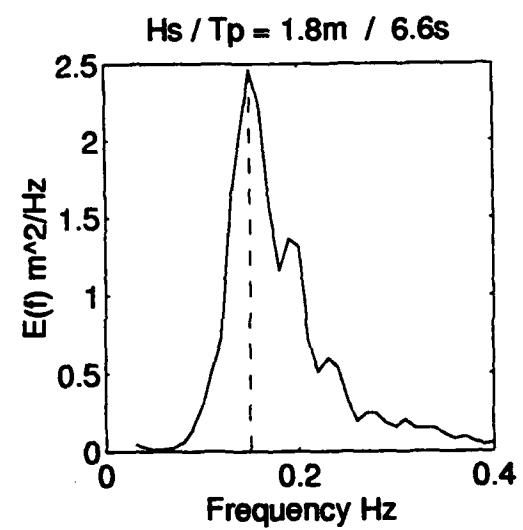
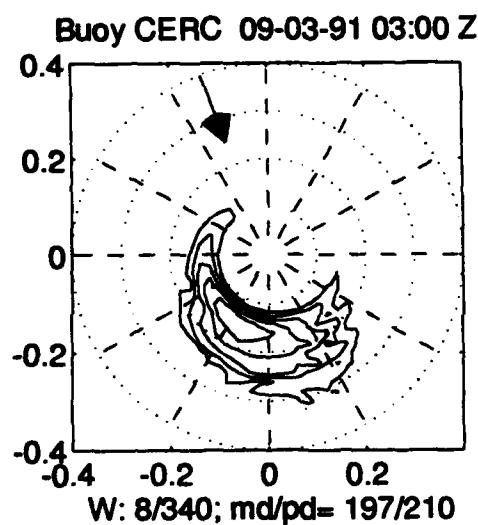
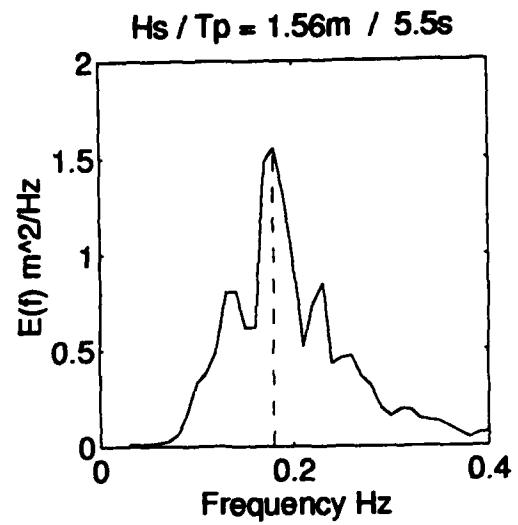
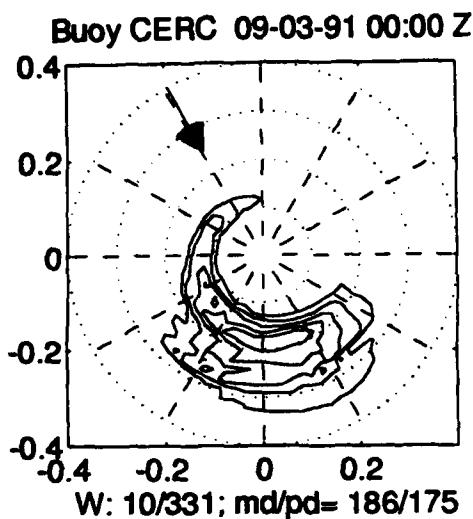






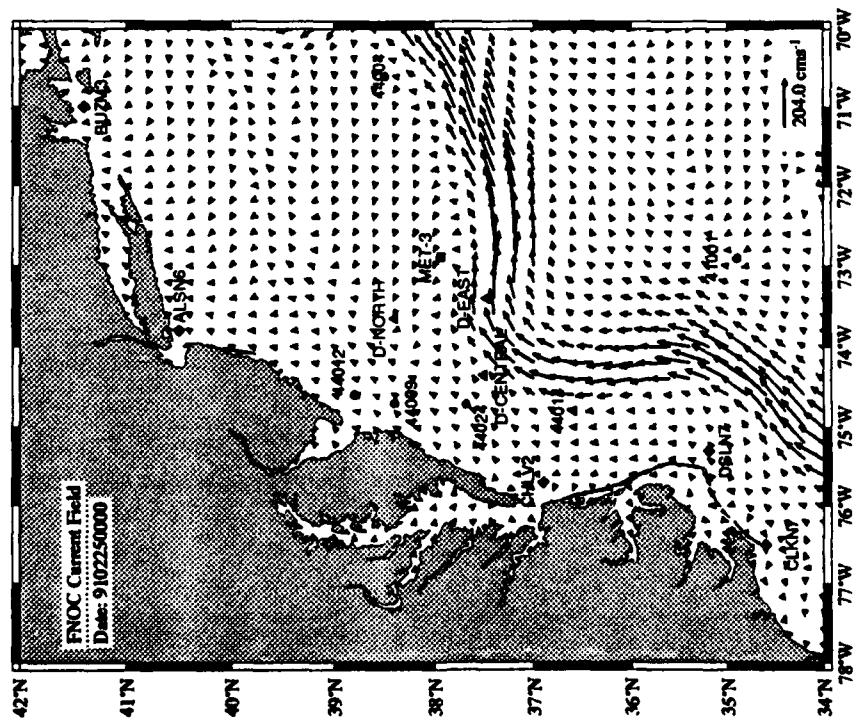
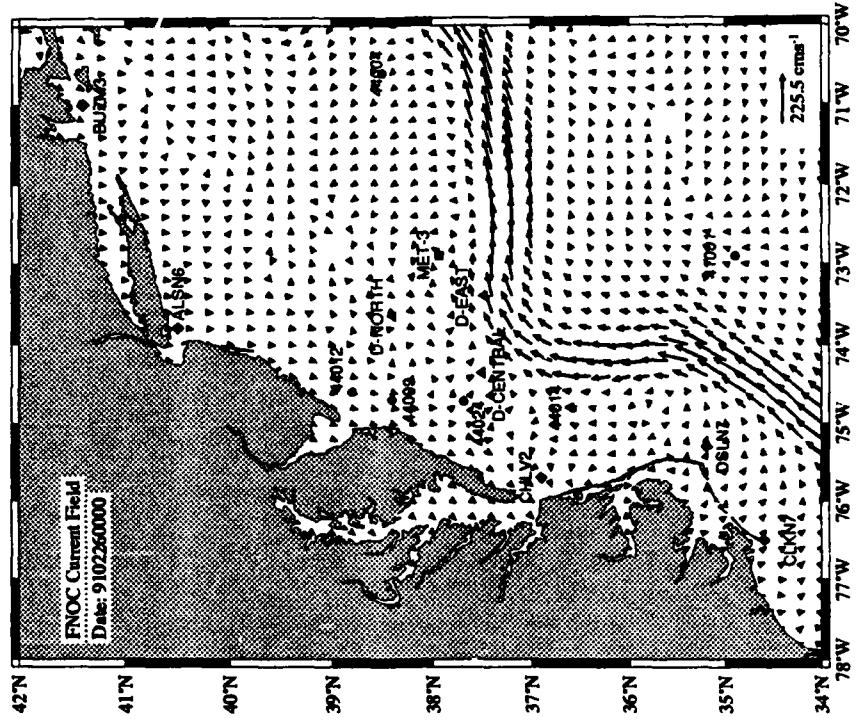


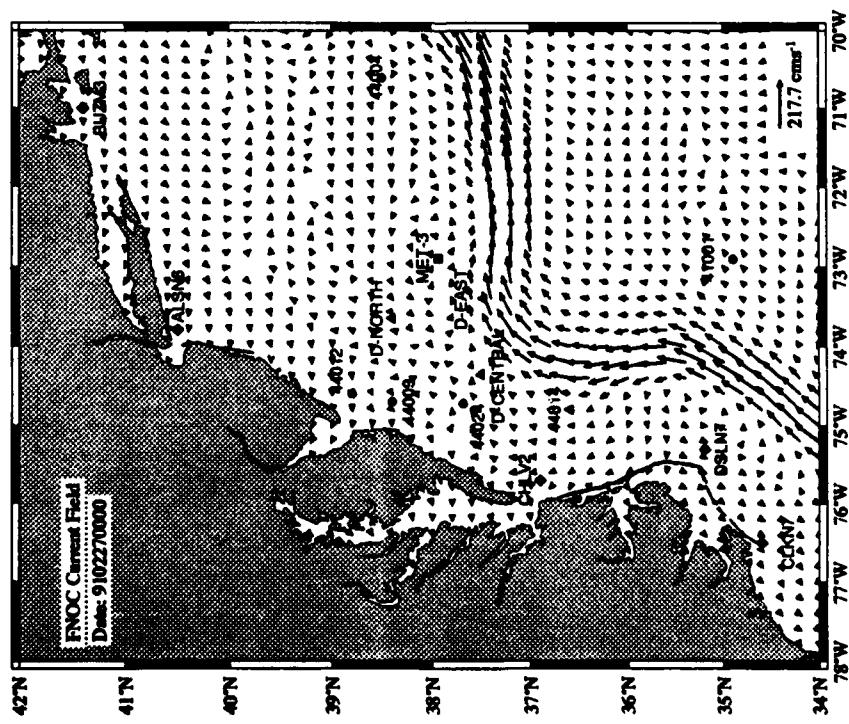
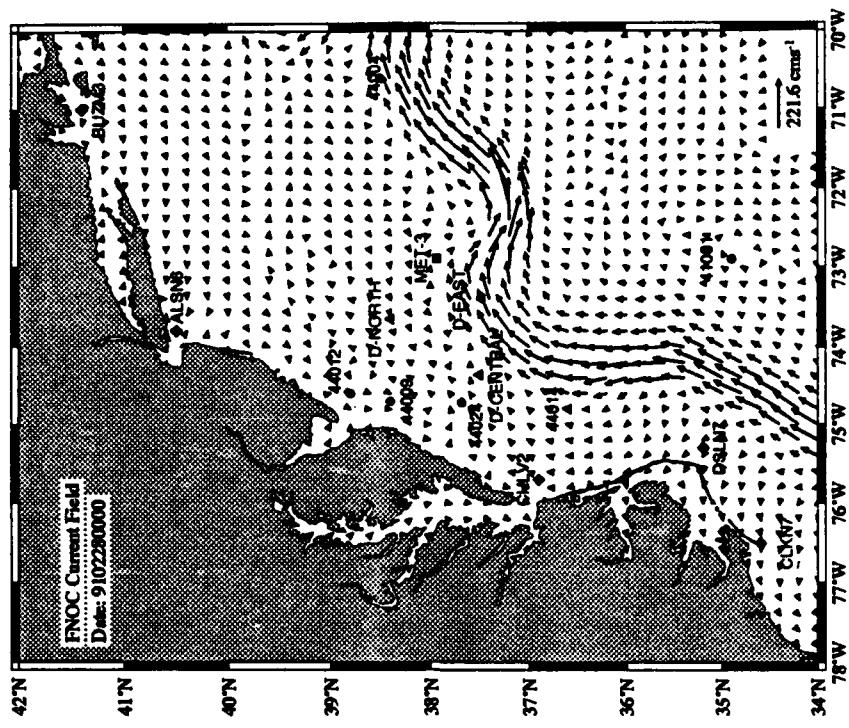


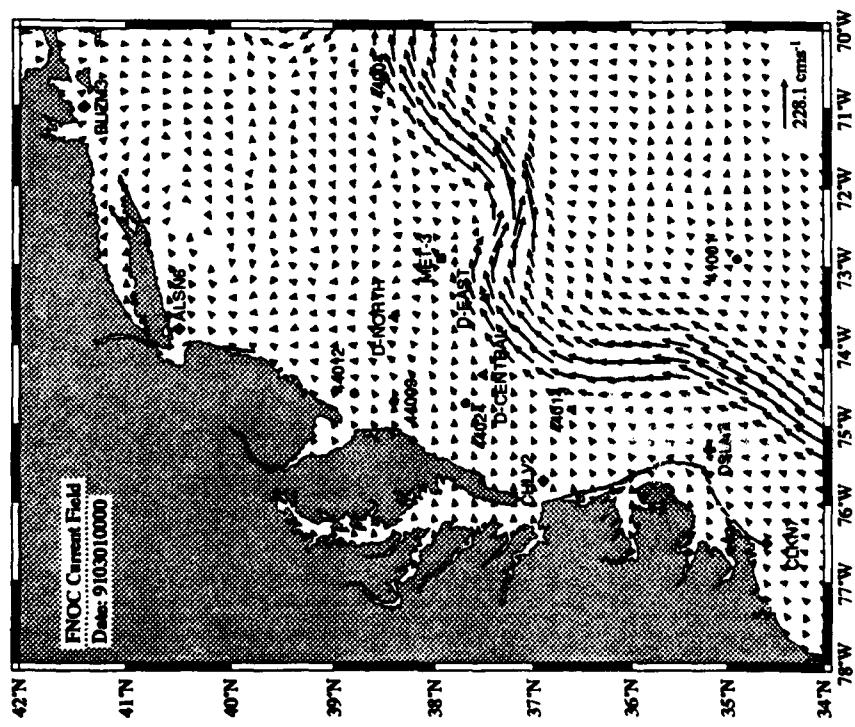
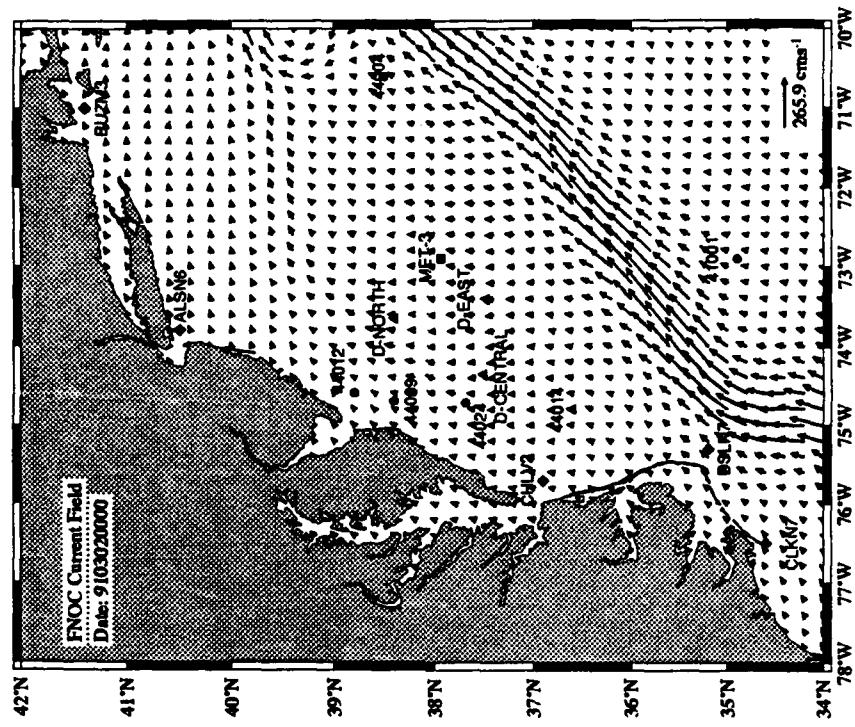


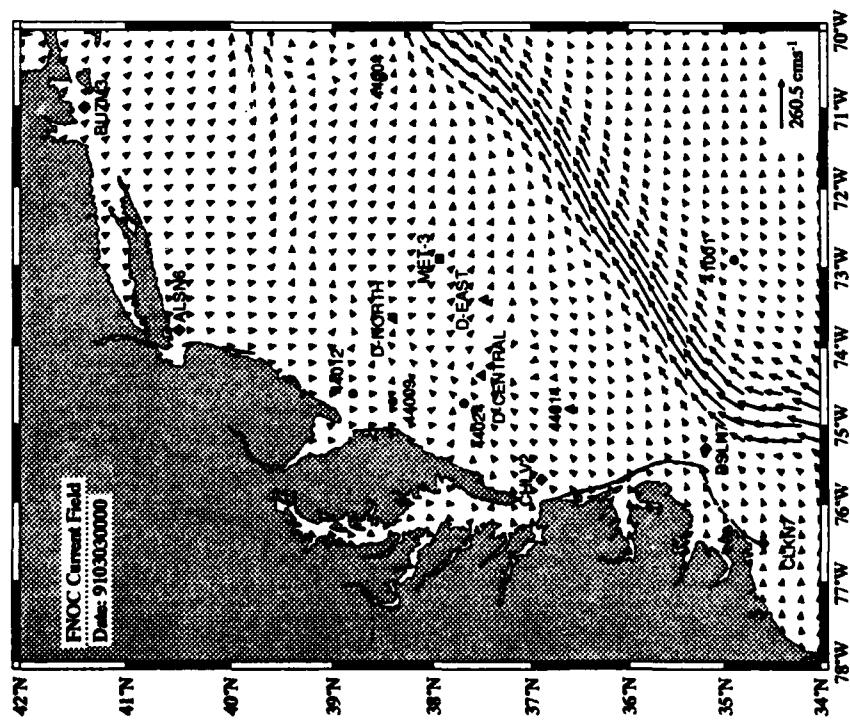
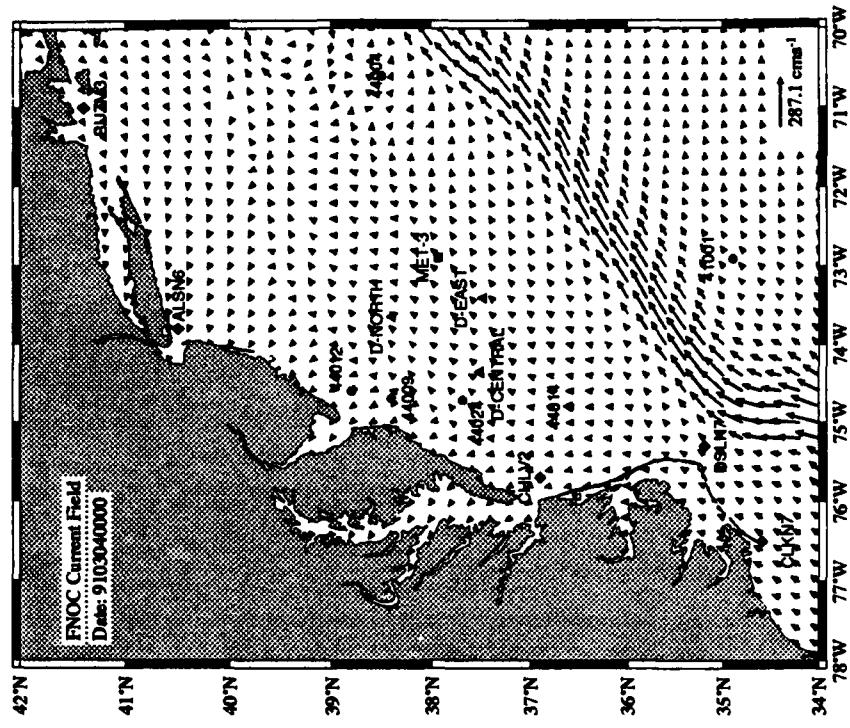
Appendix C: Custer Diagrams of Surface Current Fields

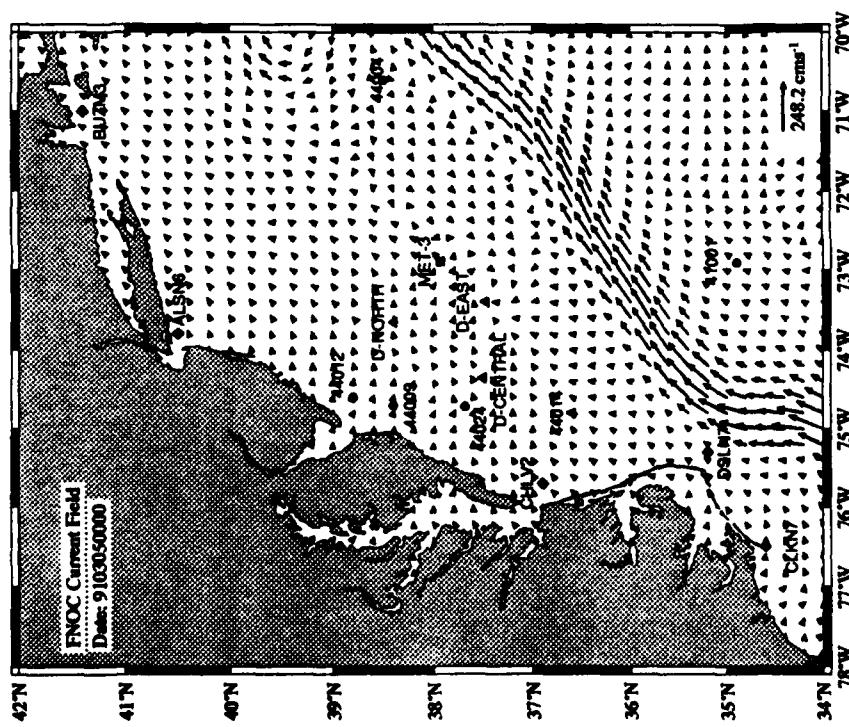
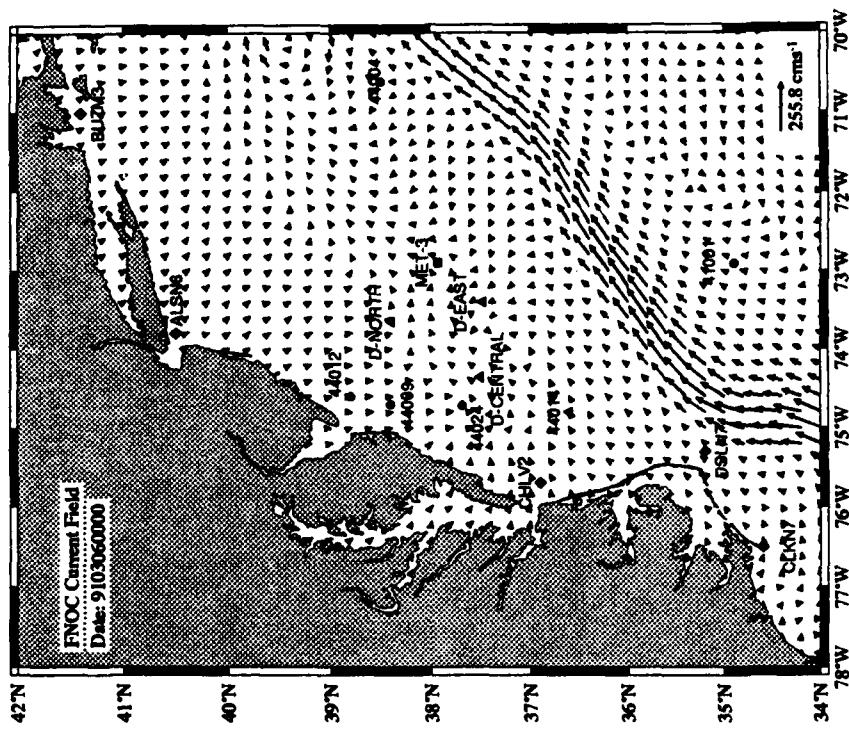
Daily maps of the surface current fields from FNOC are presented in this appendix beginning at 25 February 1991, 00:00 GMT to 9 March 1991, 00:00 GMT. Note that the fields on 8 March 1991 were not available and therefore were linearly interpolated.

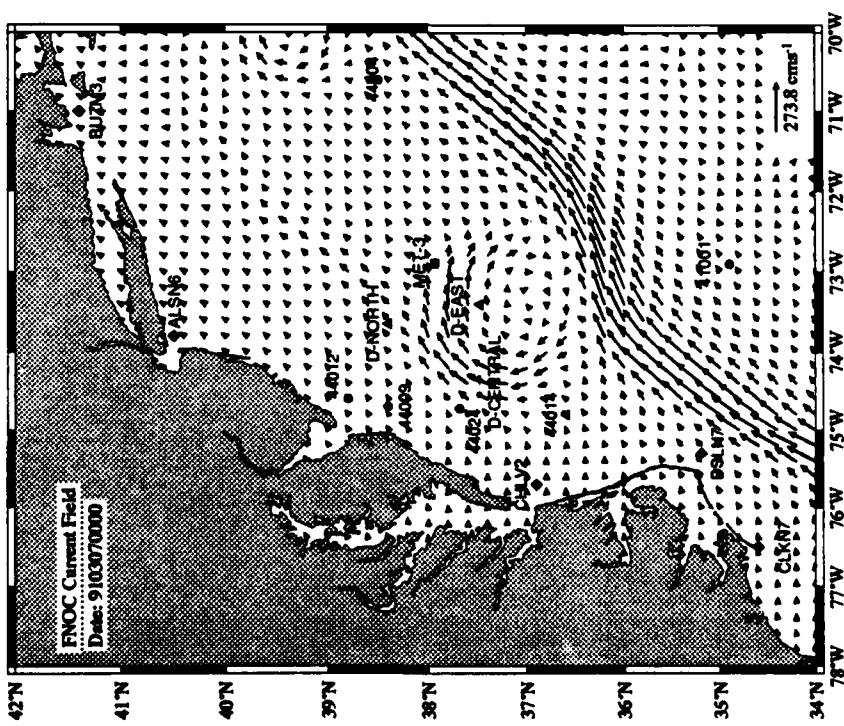
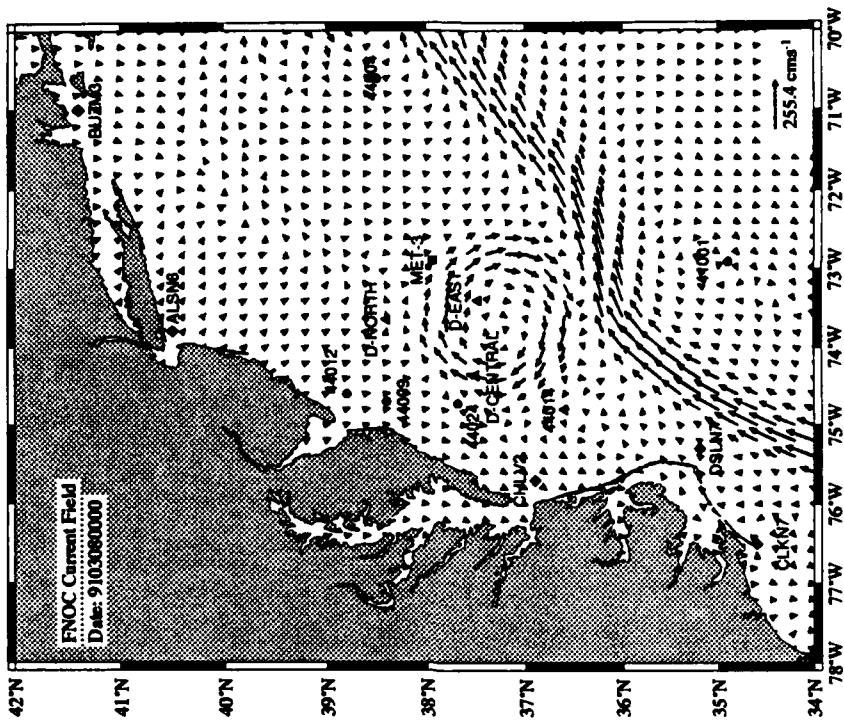


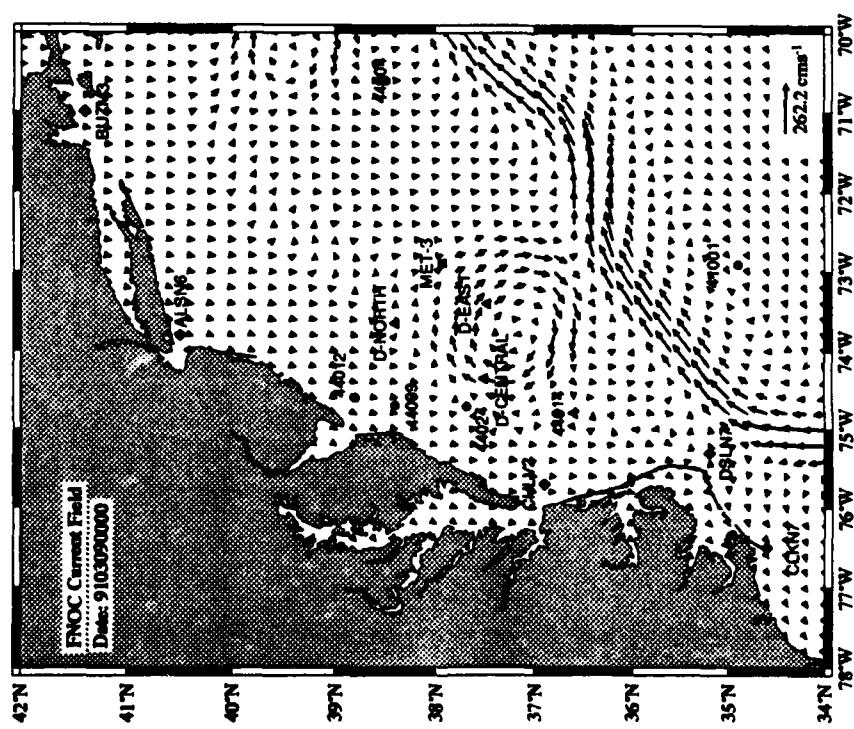










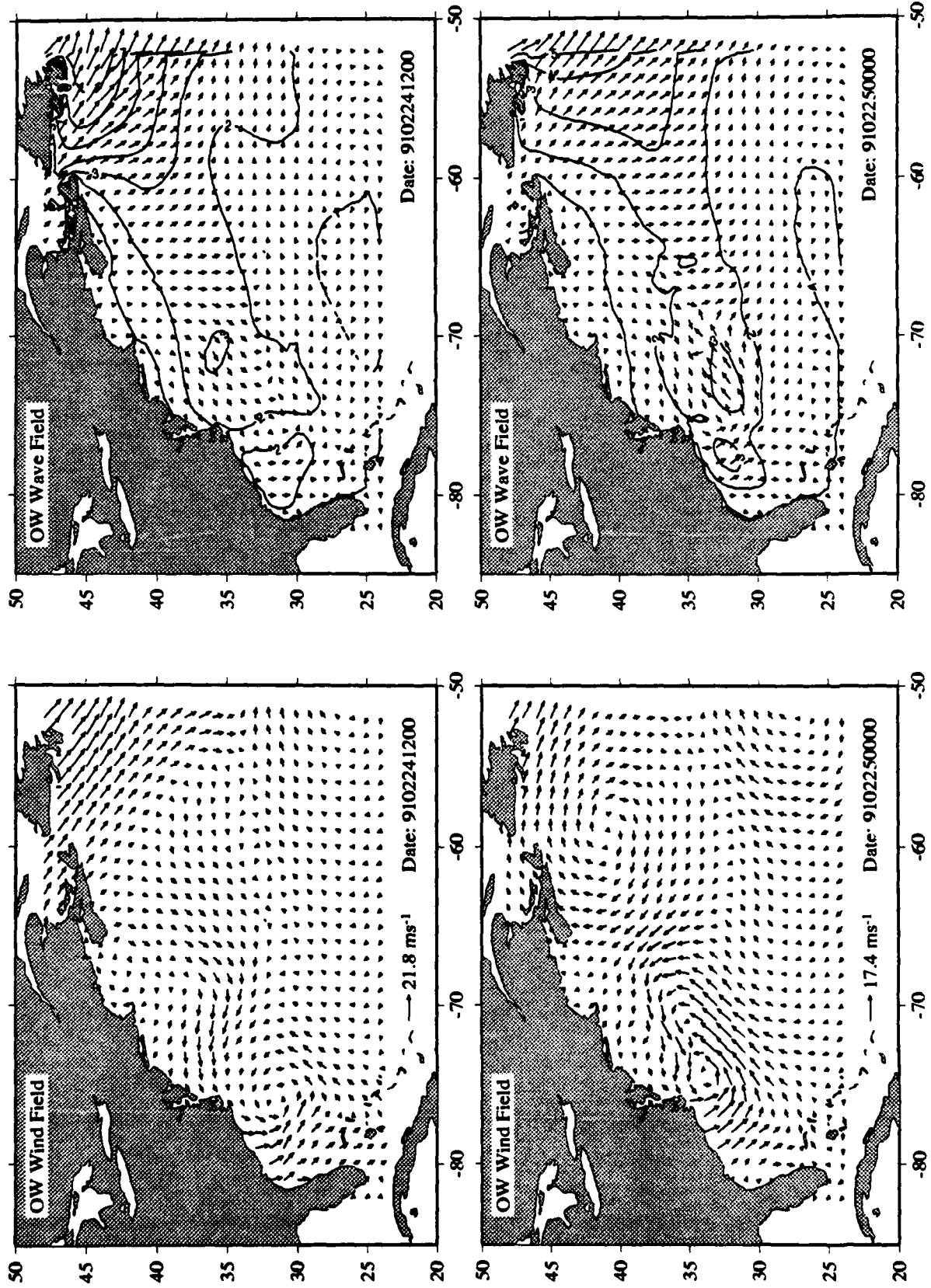


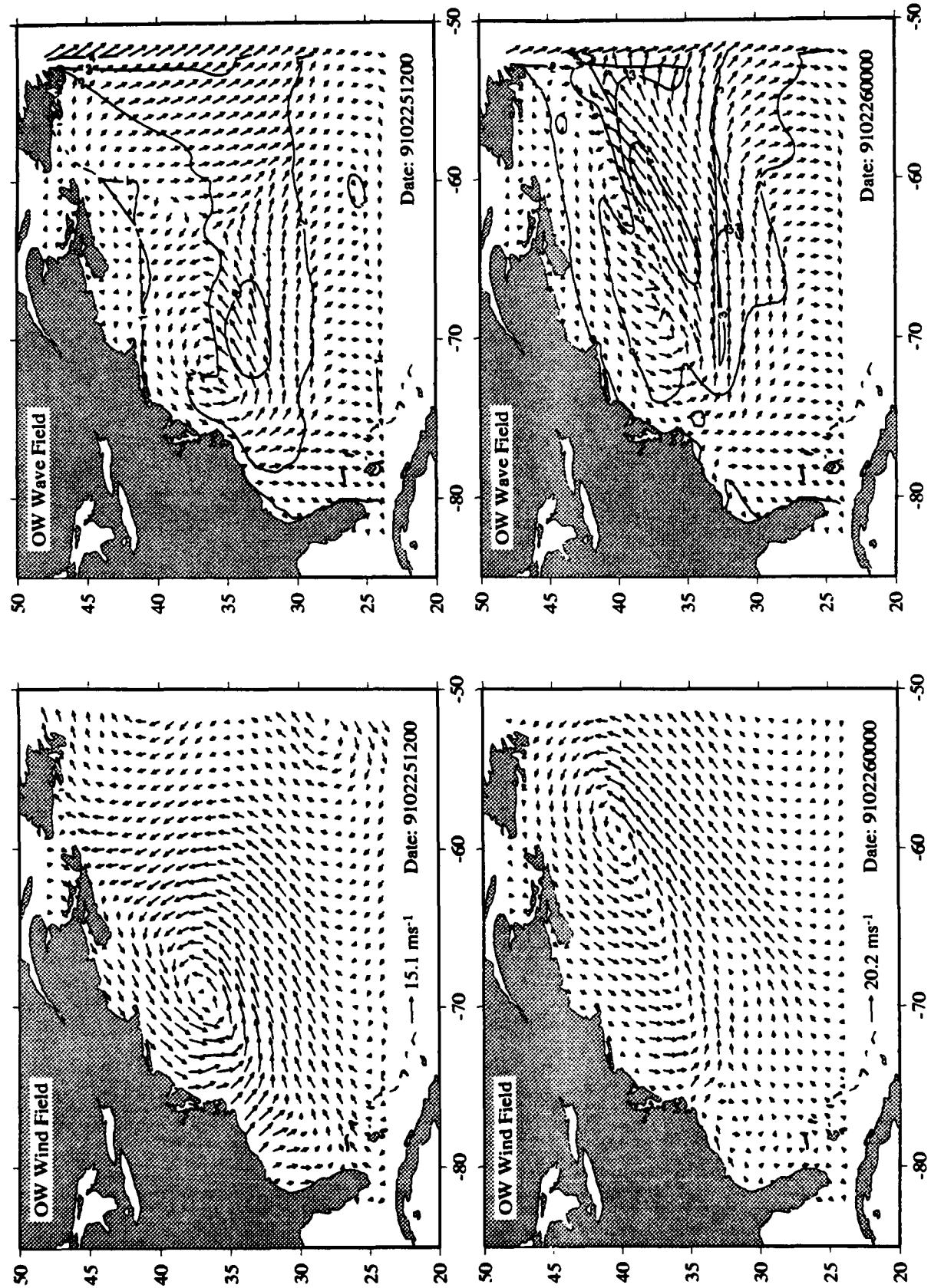
Appendix D: Custer Diagrams of Wind Fields and Wave Hindcasts

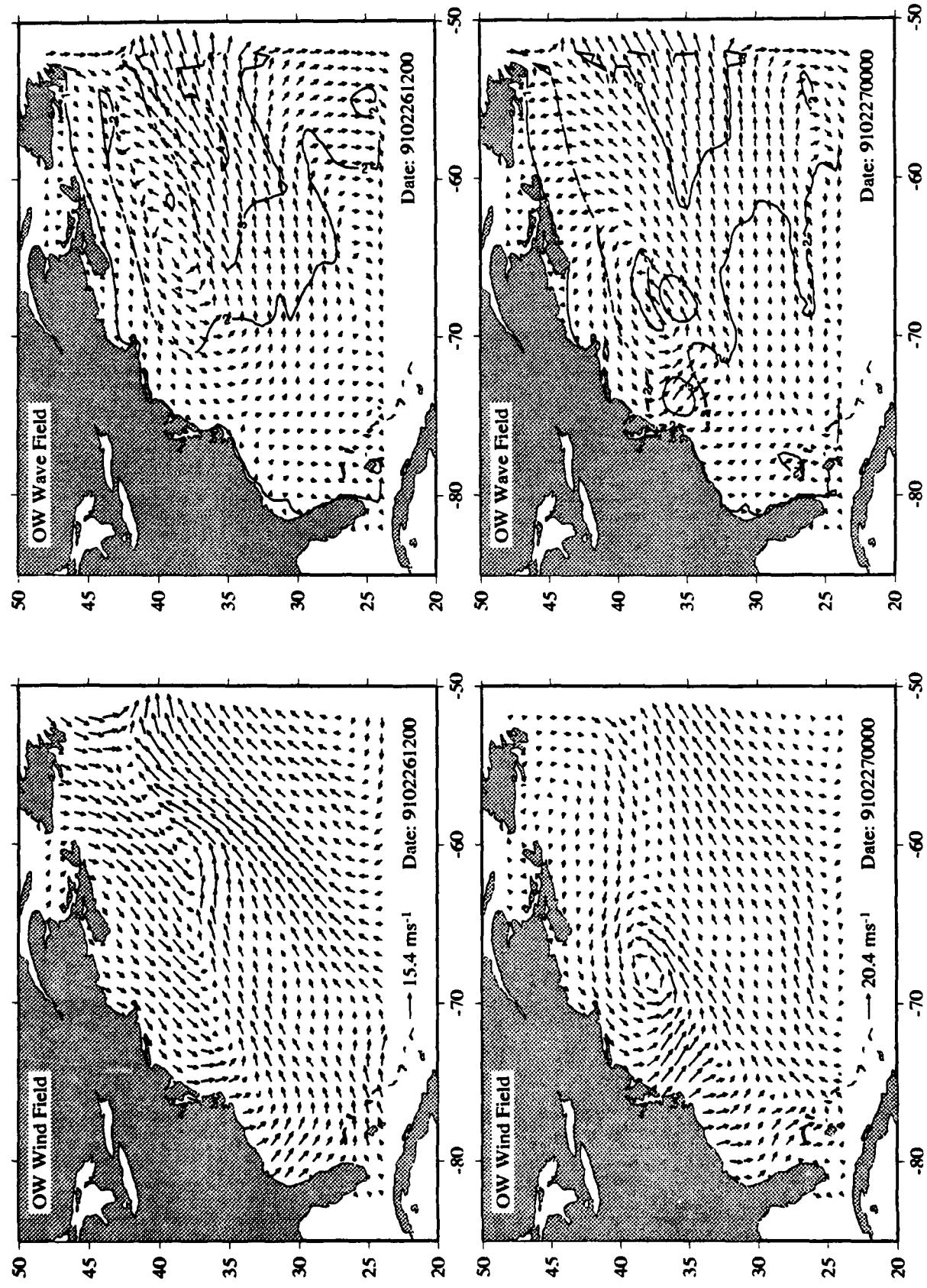
Maps of the wind vector fields (Custer diagrams) and corresponding wave height hindcasts with the ocean wave model "WAM" are presented in this appendix for six different wind field specifications. Each wind field Custer diagram presents the maximum wind speed for this time. The vectors of the wave height Custer diagram correspond to mean wave direction as computed by the WAM model. Contours of the wave heights are given in meters.

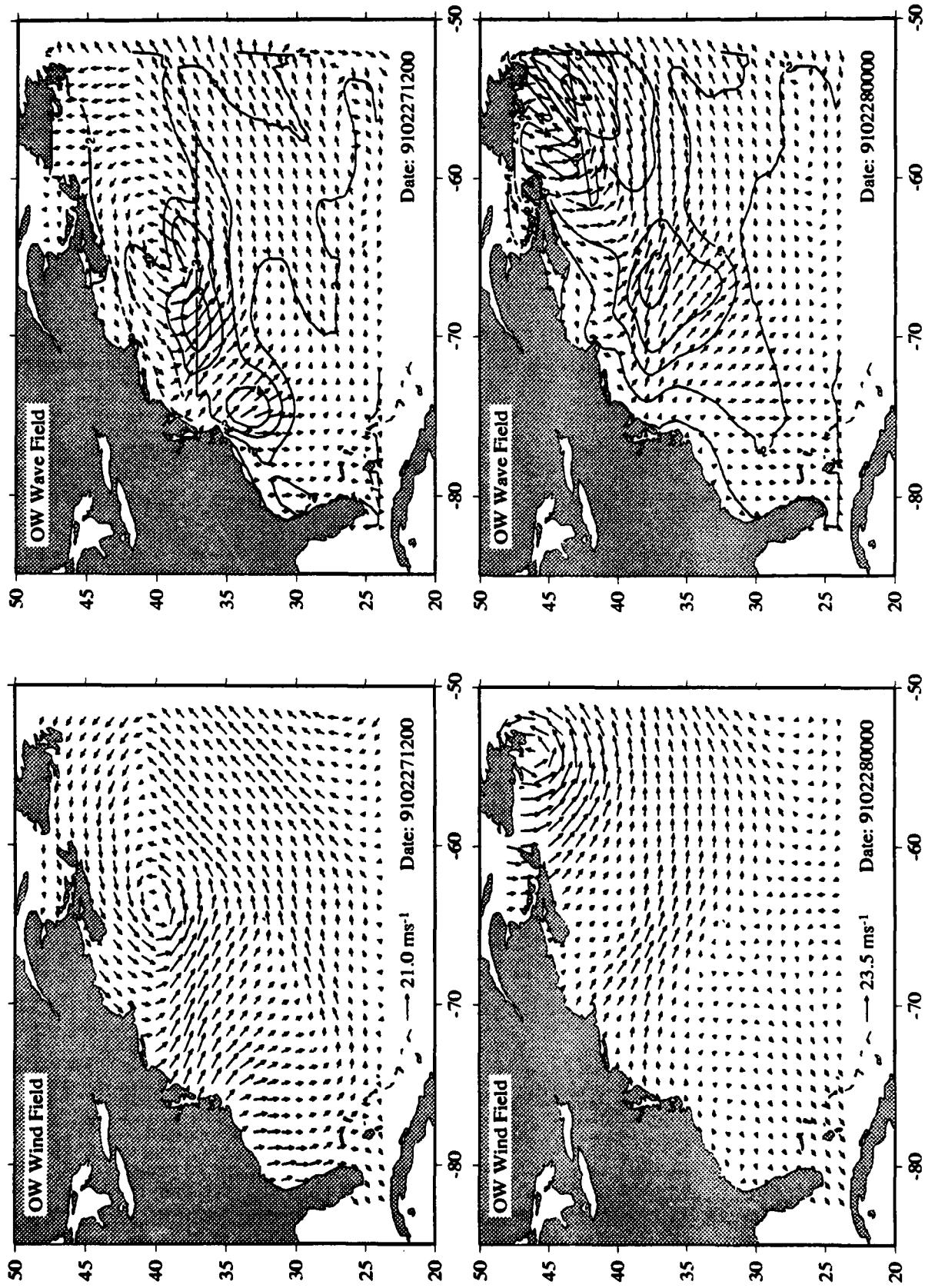
D.1: Oceanweather/Atmospheric Environment Service (OW/AES)

Custer diagrams are presented for the time period from 24 February 1991, 12:00 GMT to 9 March 1991, 00:00 GMT of the wind fields and corresponding wave hindcasts.

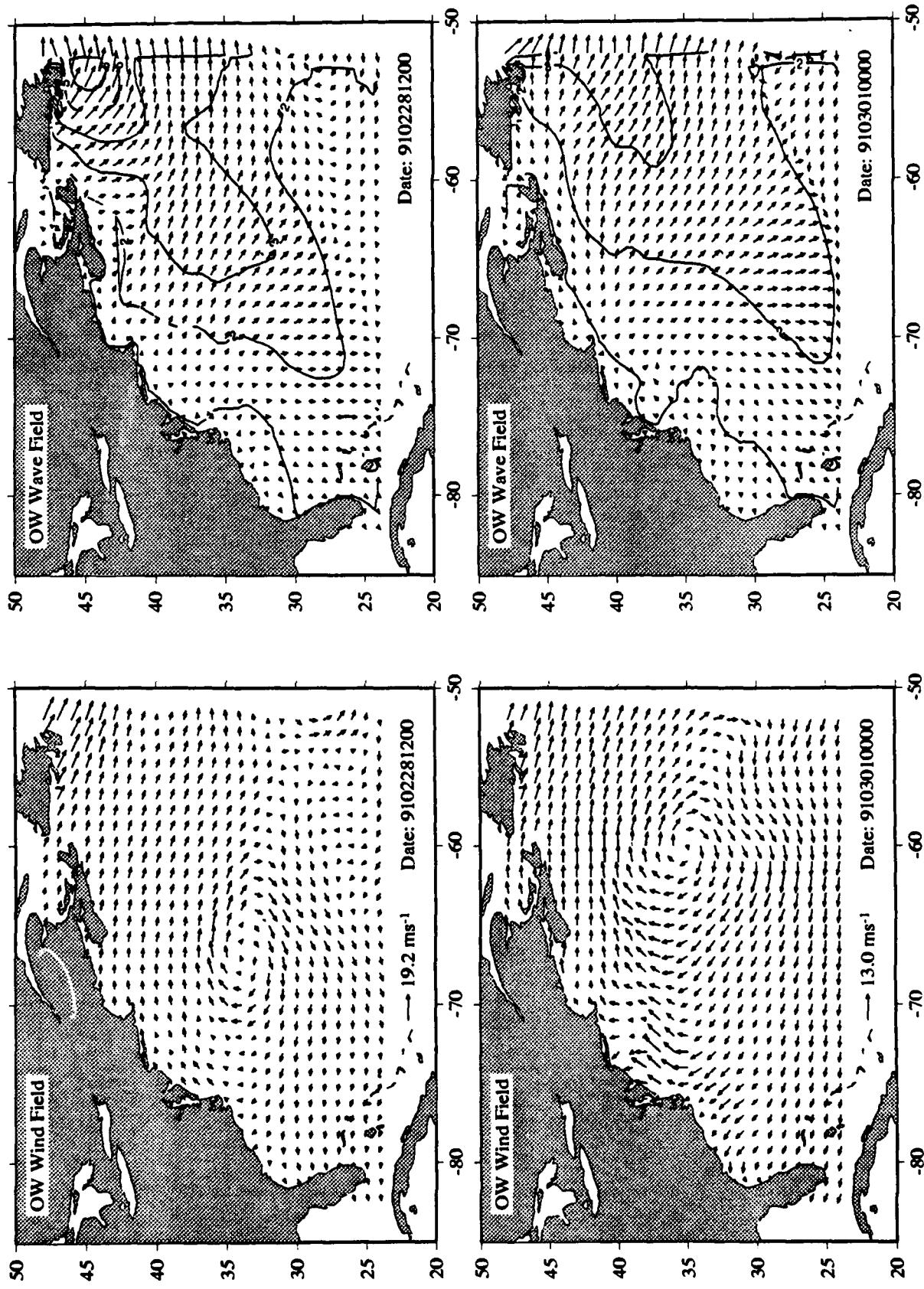


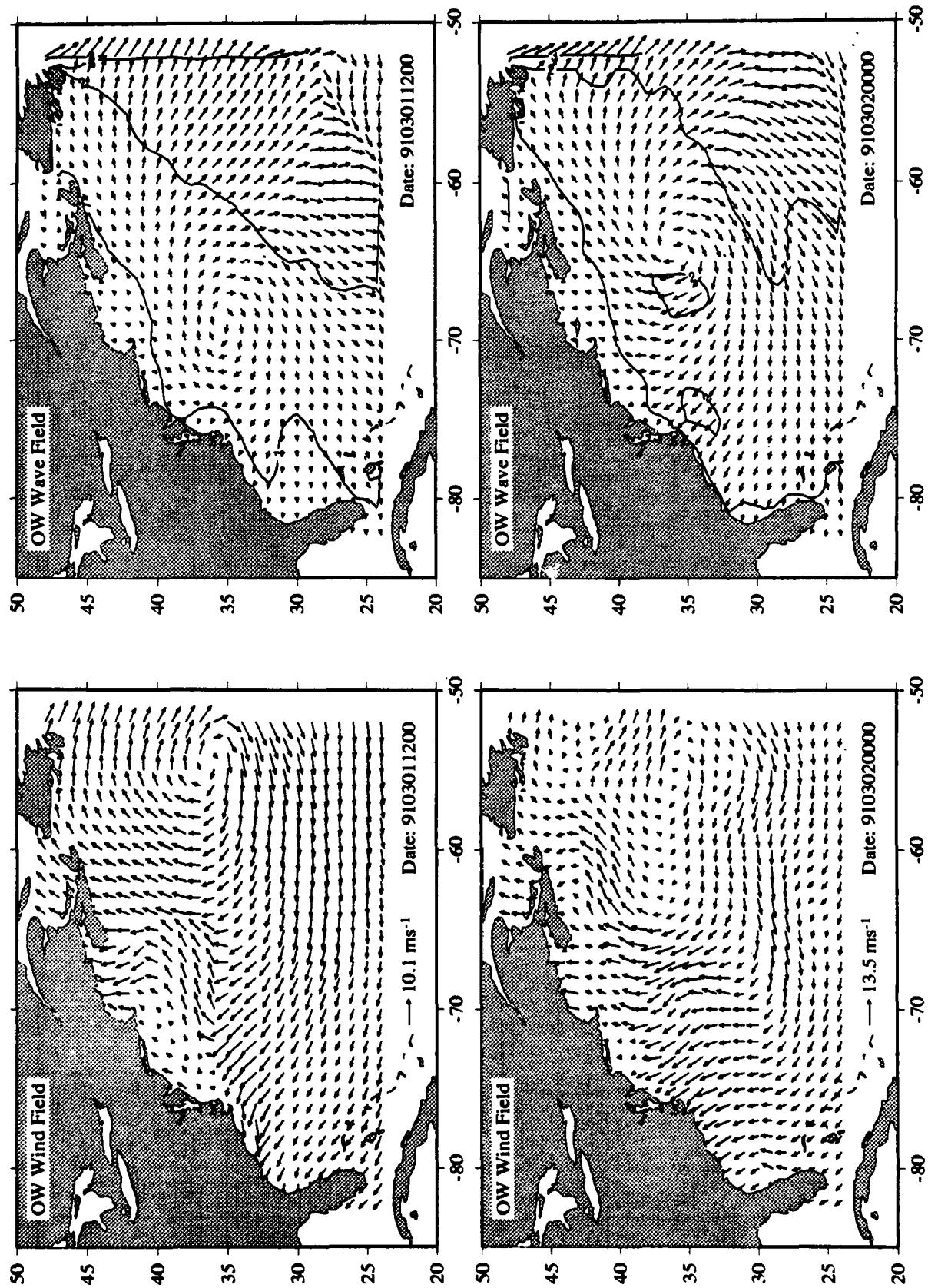




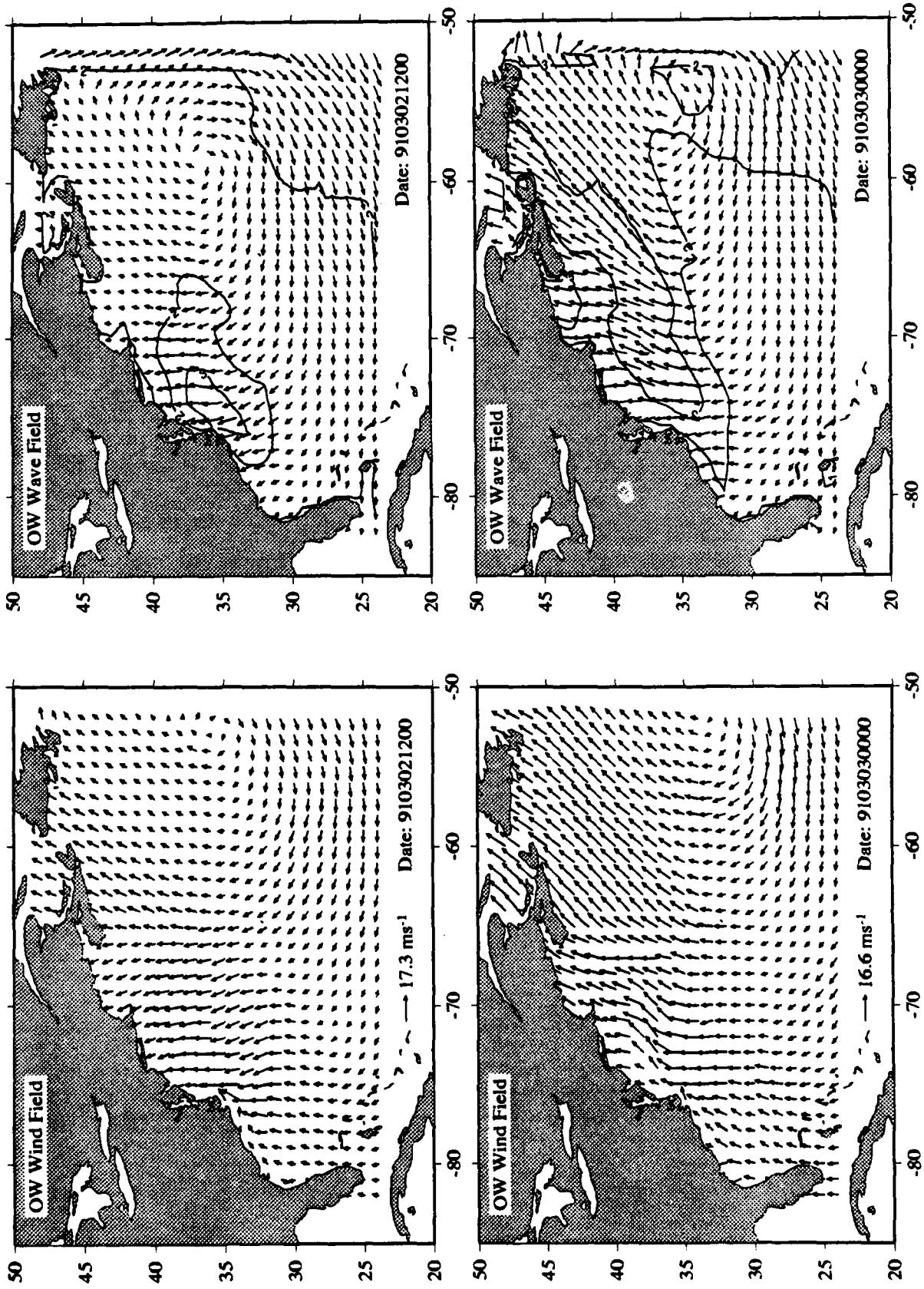


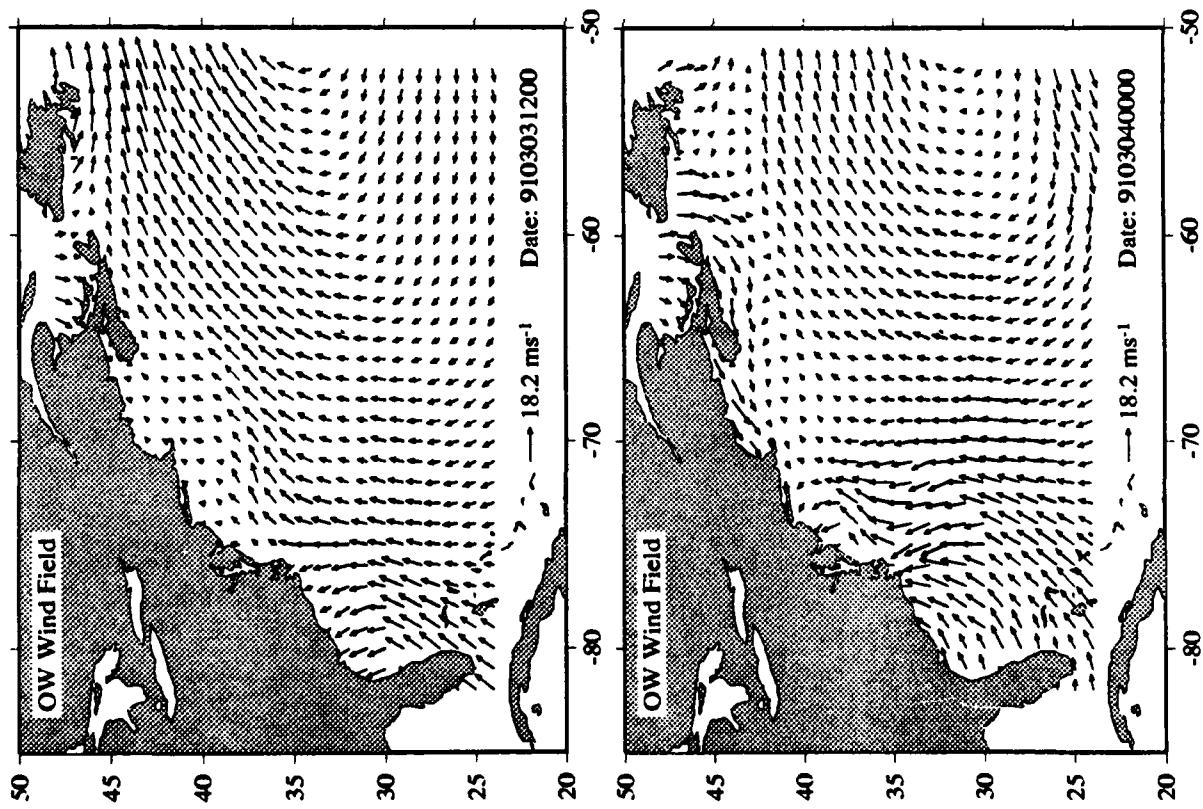
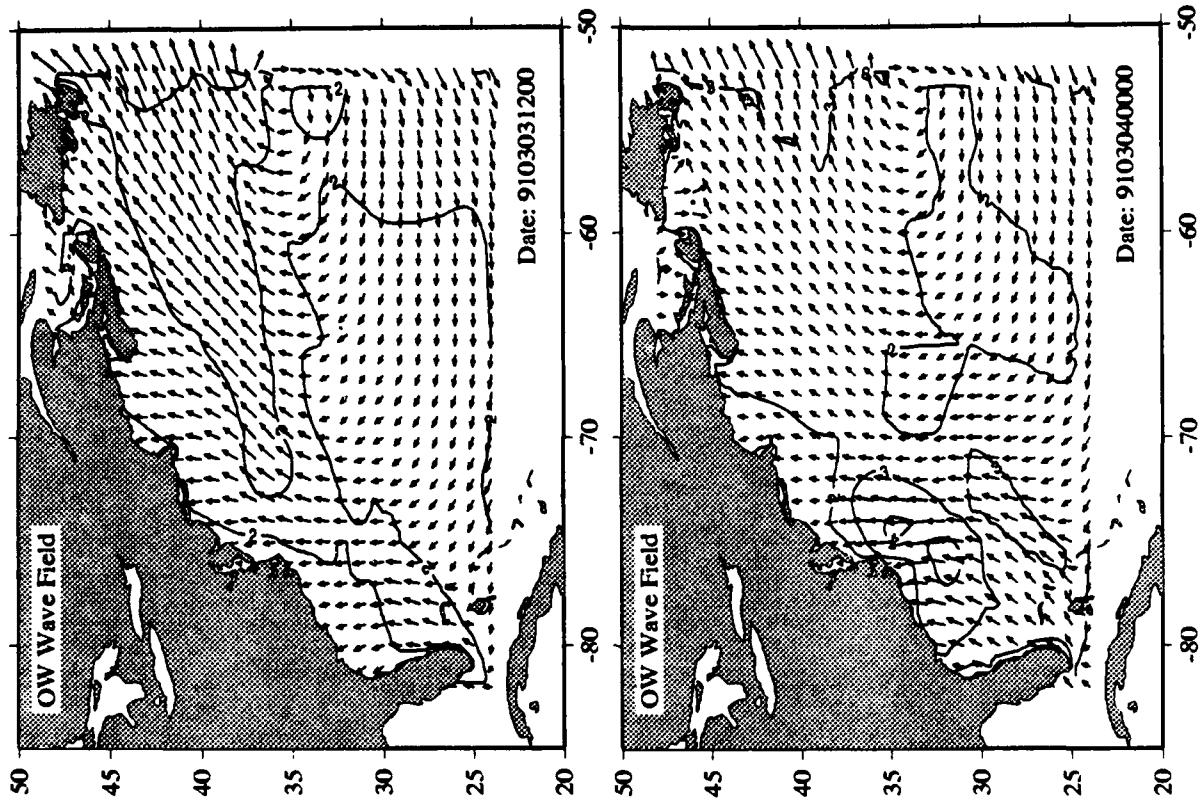
Appendix D Cluster Diagrams of Wind fields and Wave Hindcasts

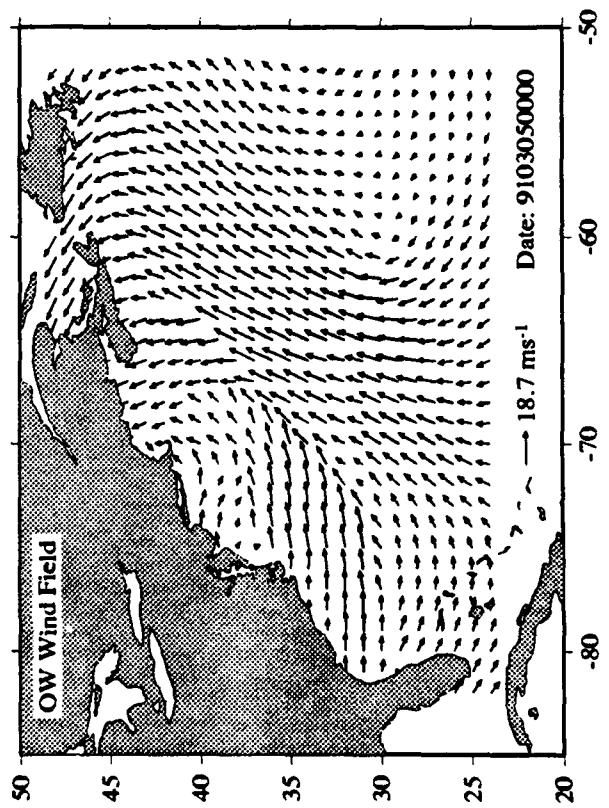
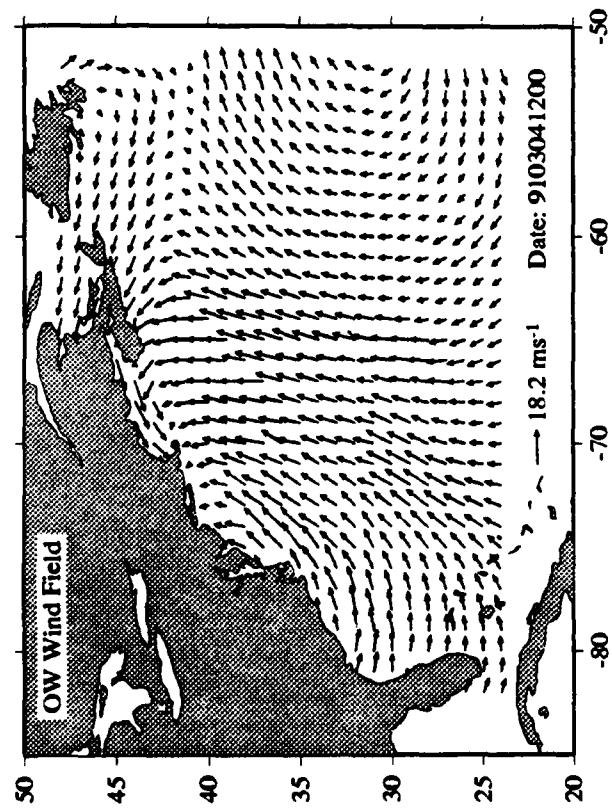
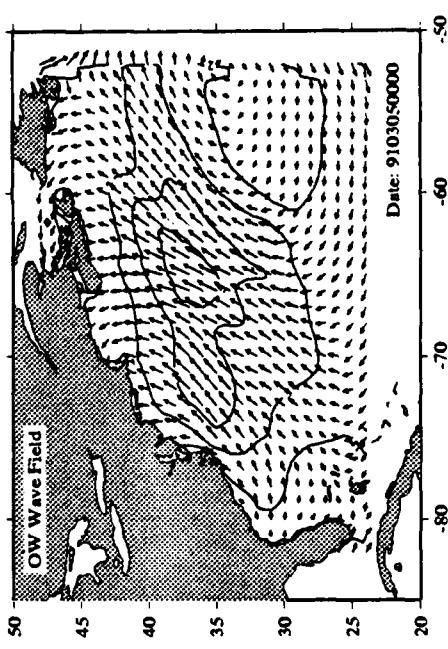
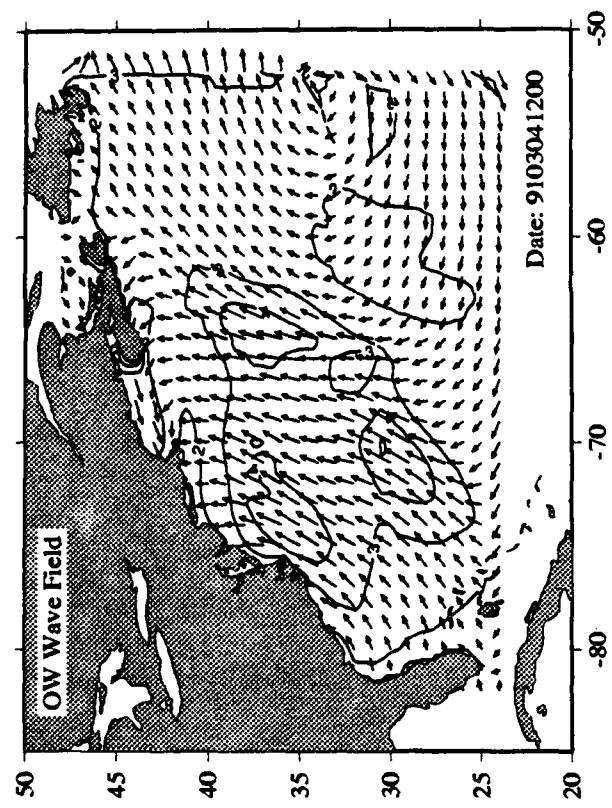


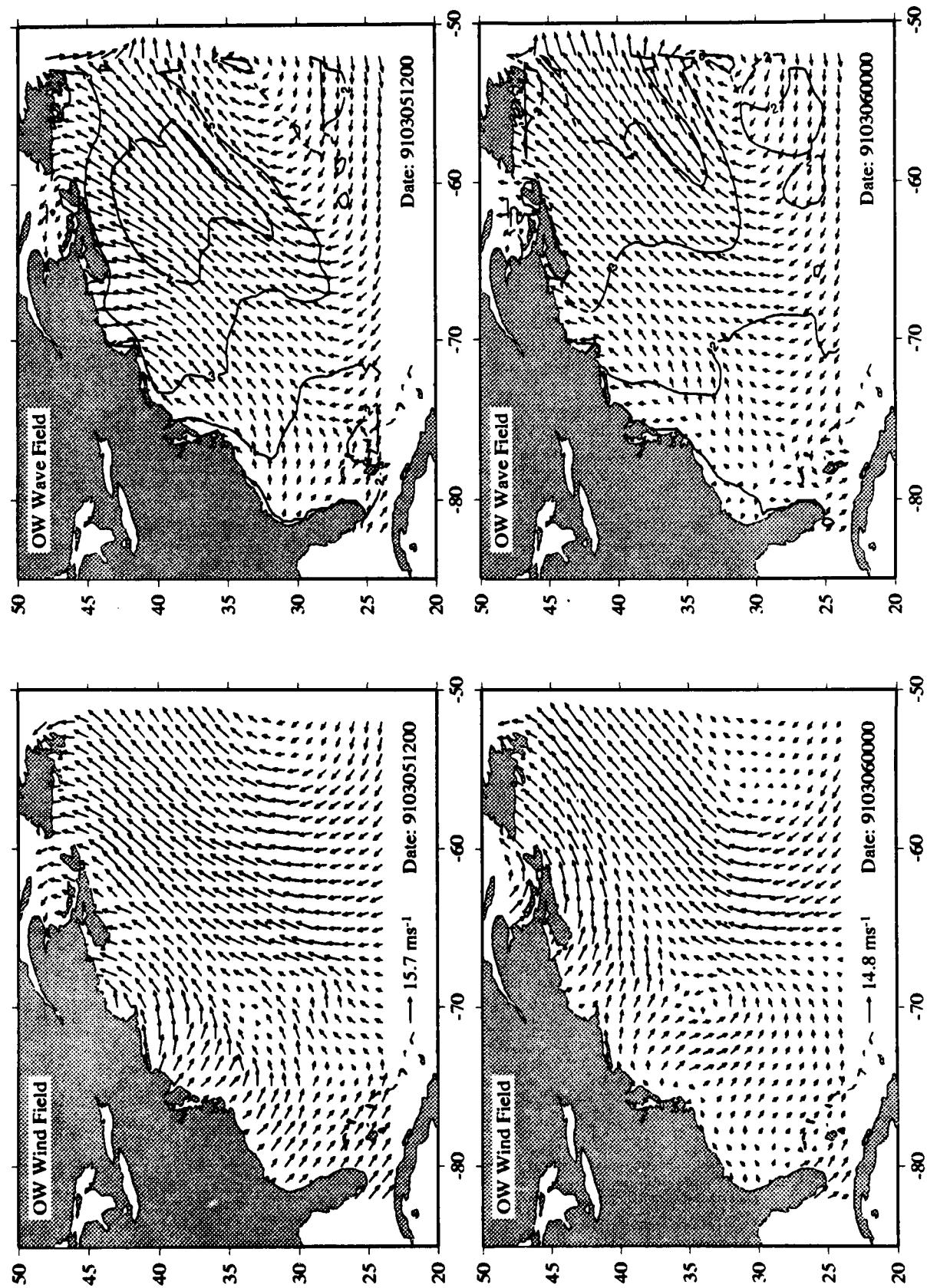


Appendix D Custer Diagrams of Wind fields and Wave Hindcasts

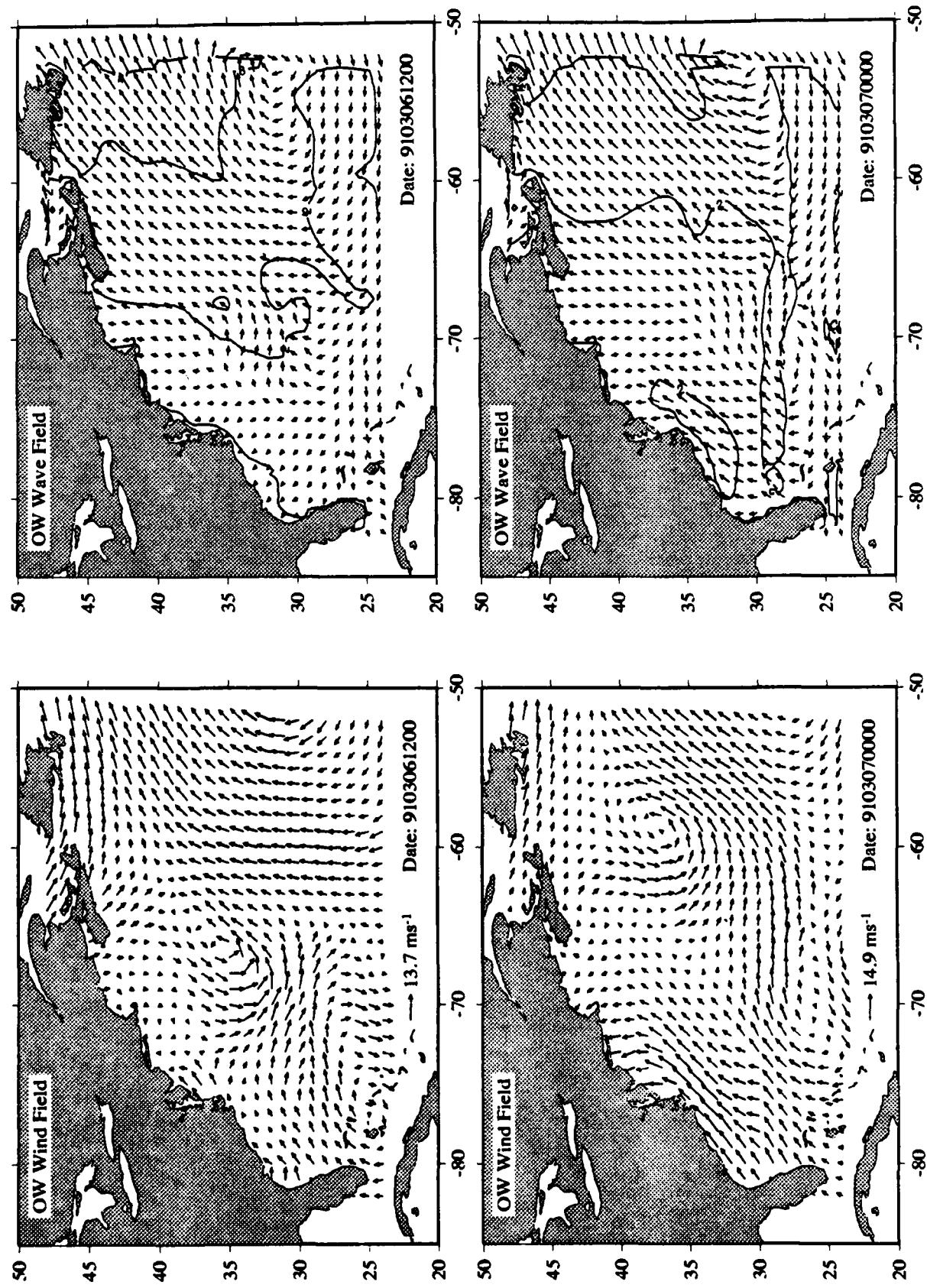


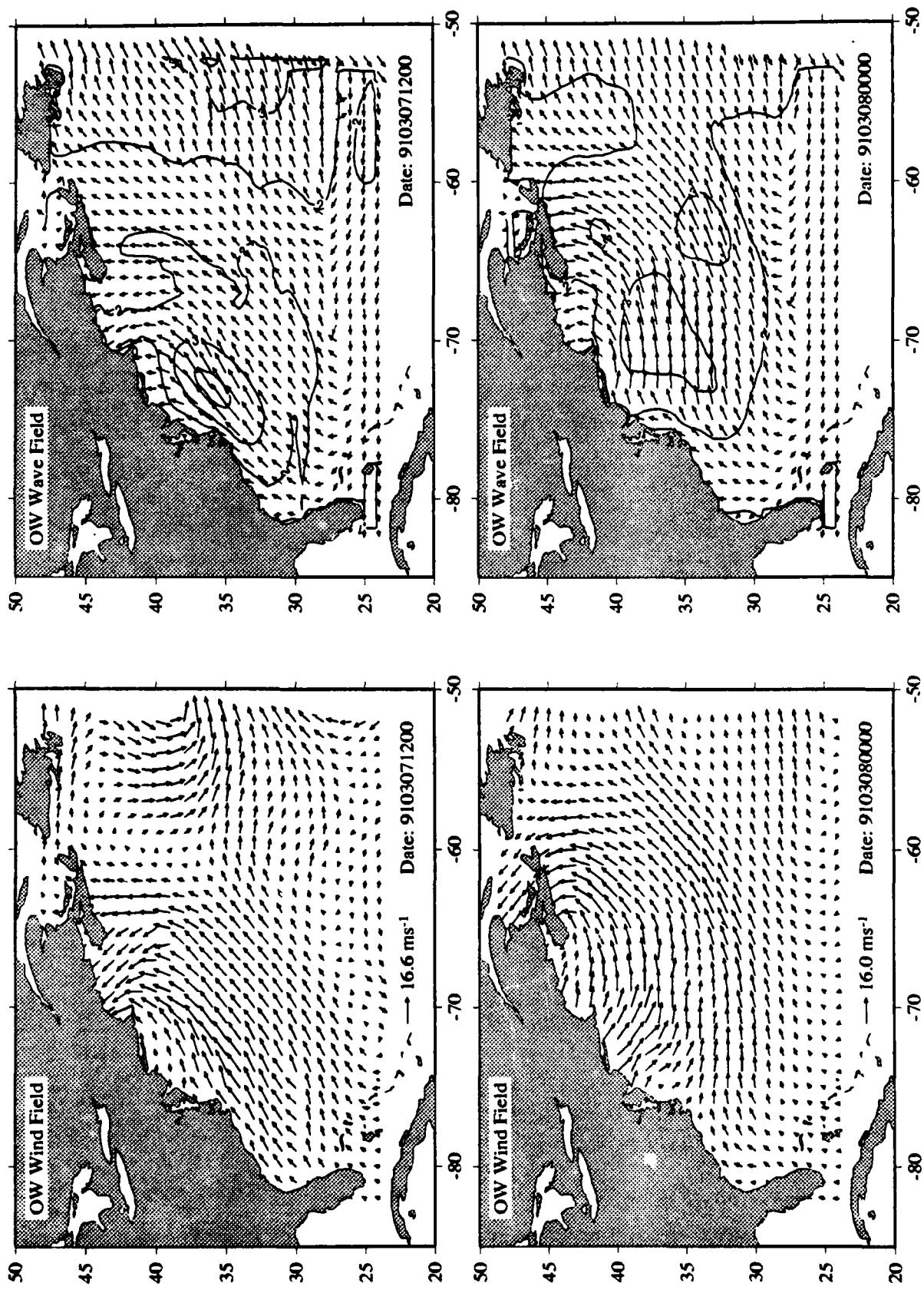


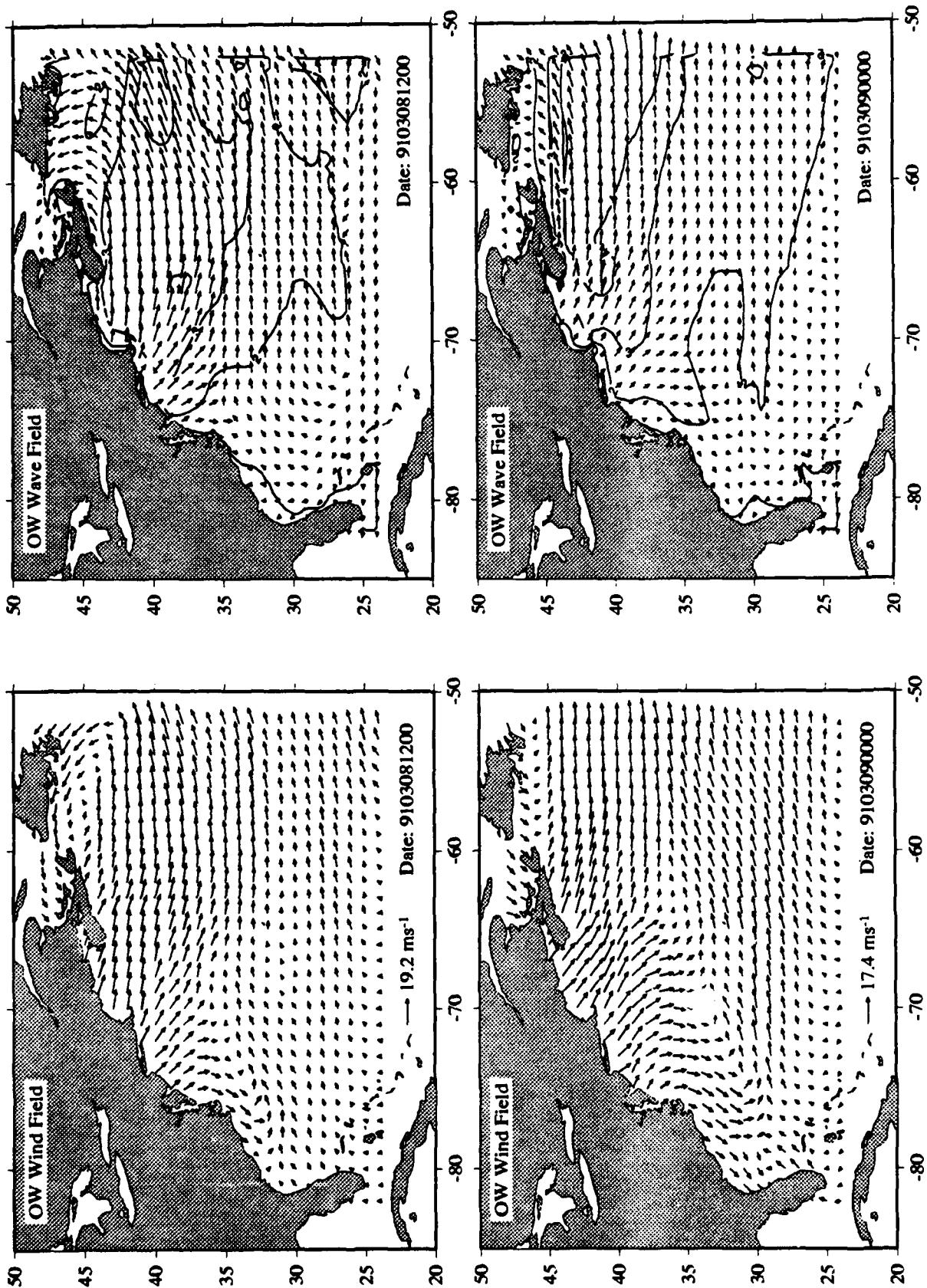




Appendix D Cluster Diagrams of Wind fields and Wave Hindcasts

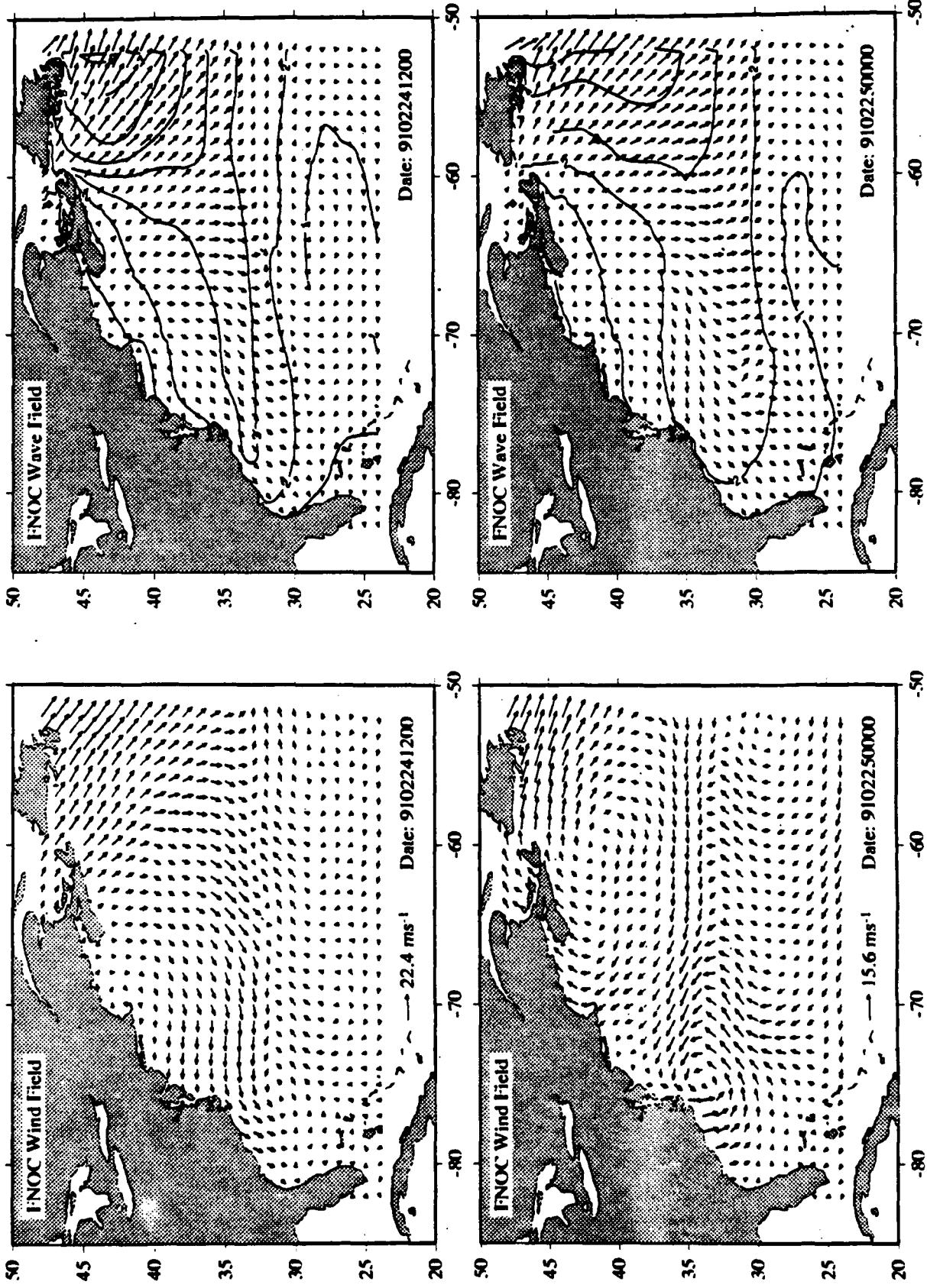


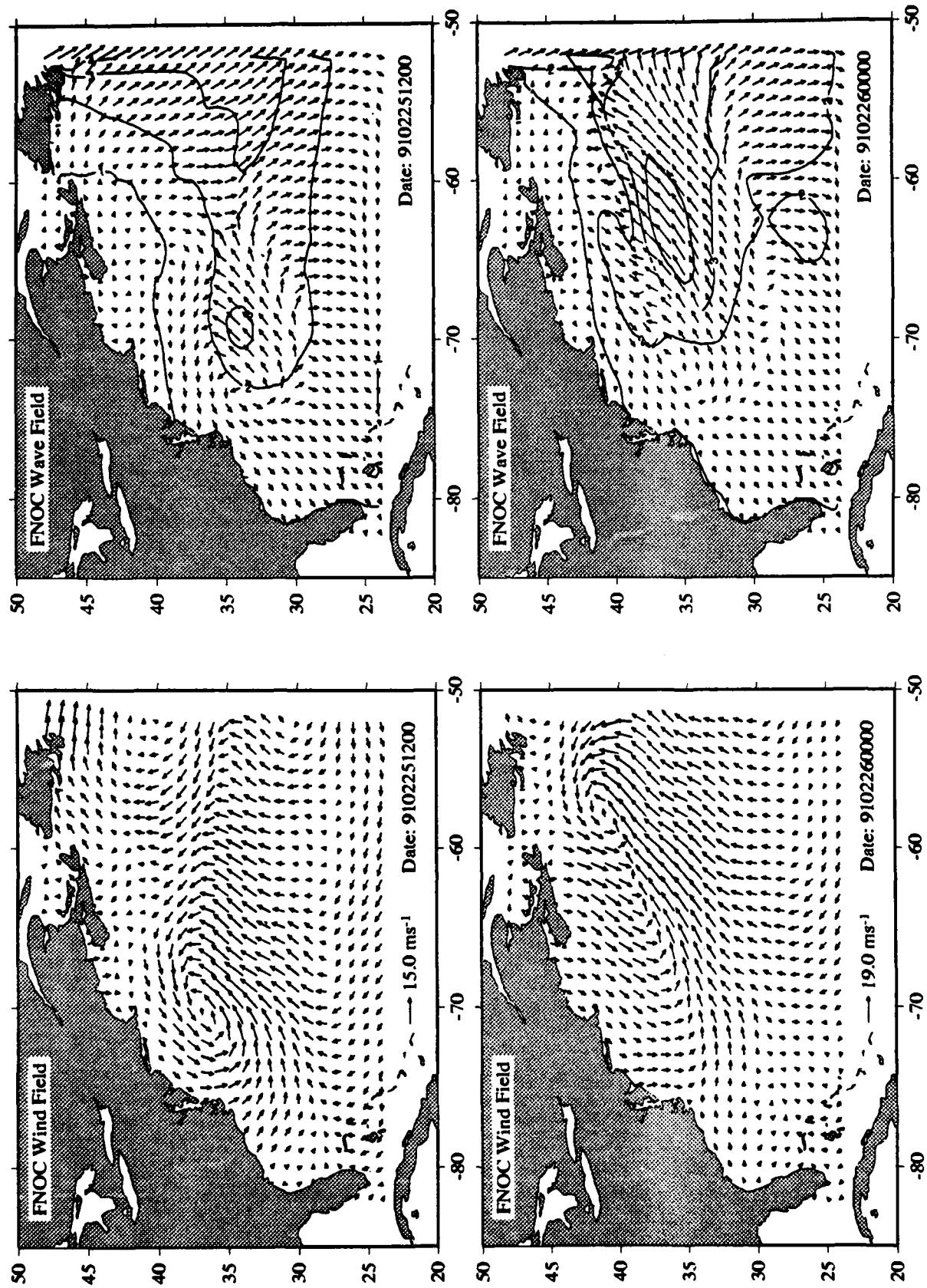




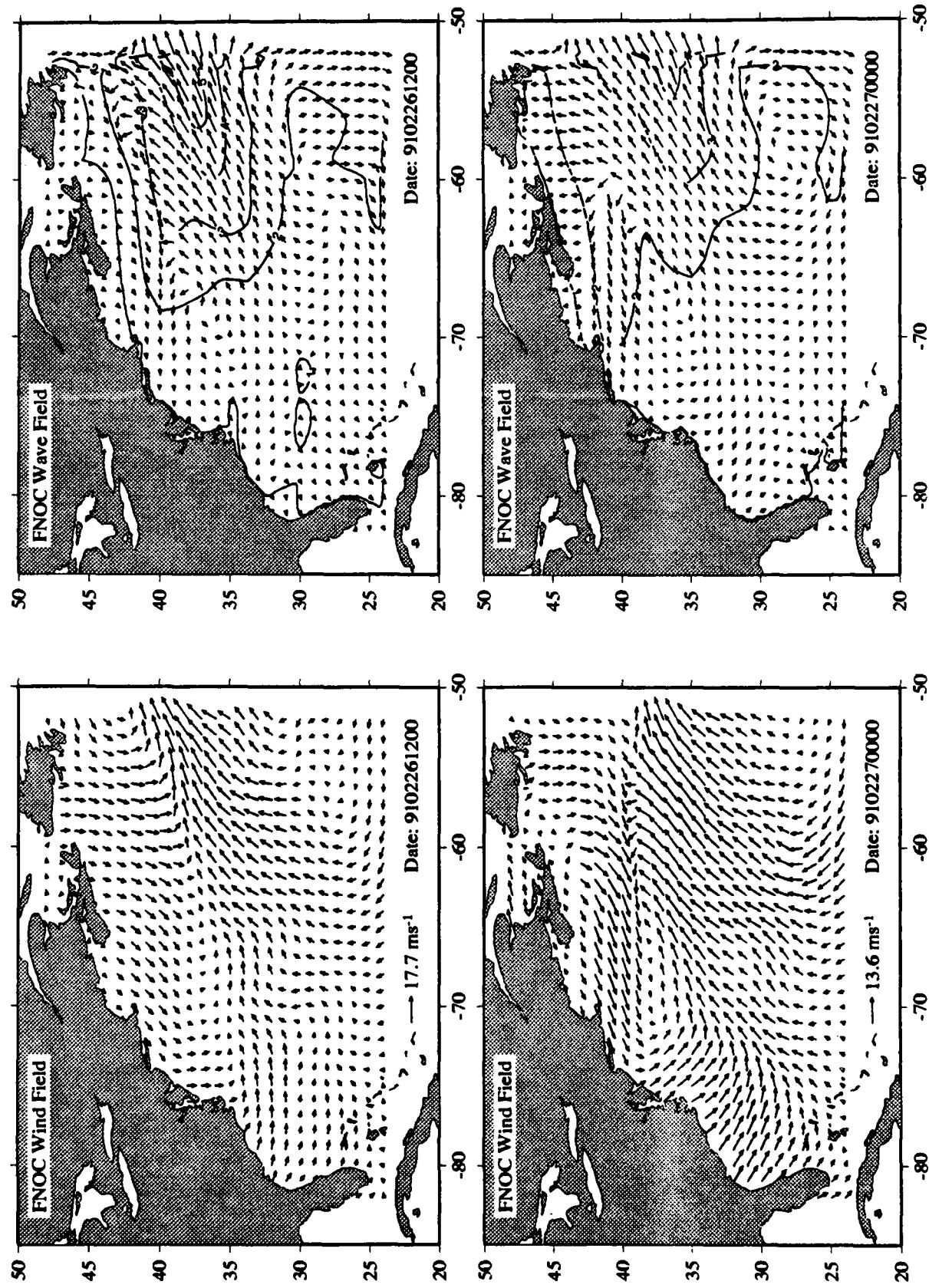
D.2: Fleet Numerical Oceanography Center (FNOC)

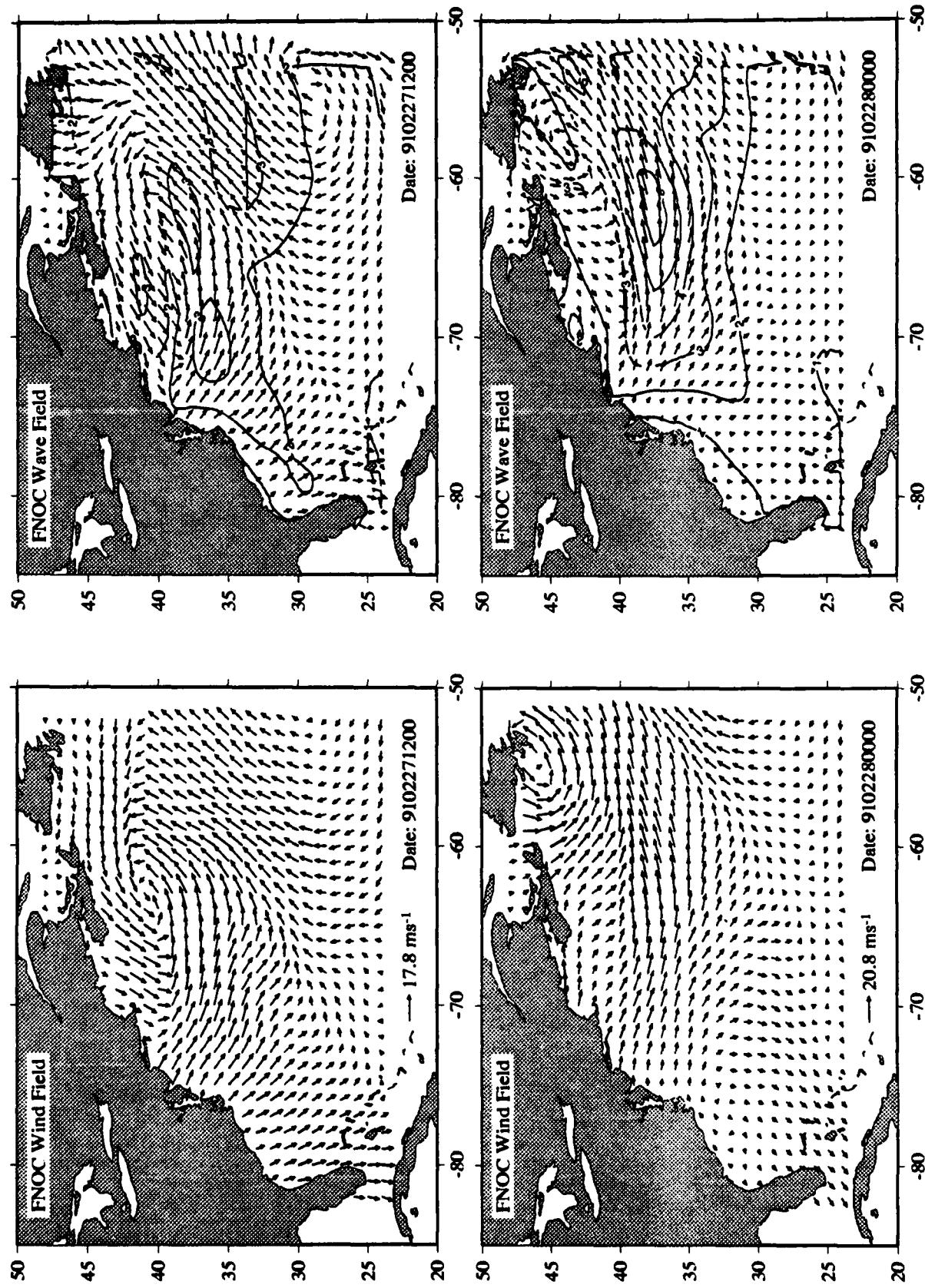
Custer diagrams are presented for the time period from 24 February 1991, 12:00 GMT to 9 March 1991, 00:00 GMT of the wind field and corresponding wave hindcasts.

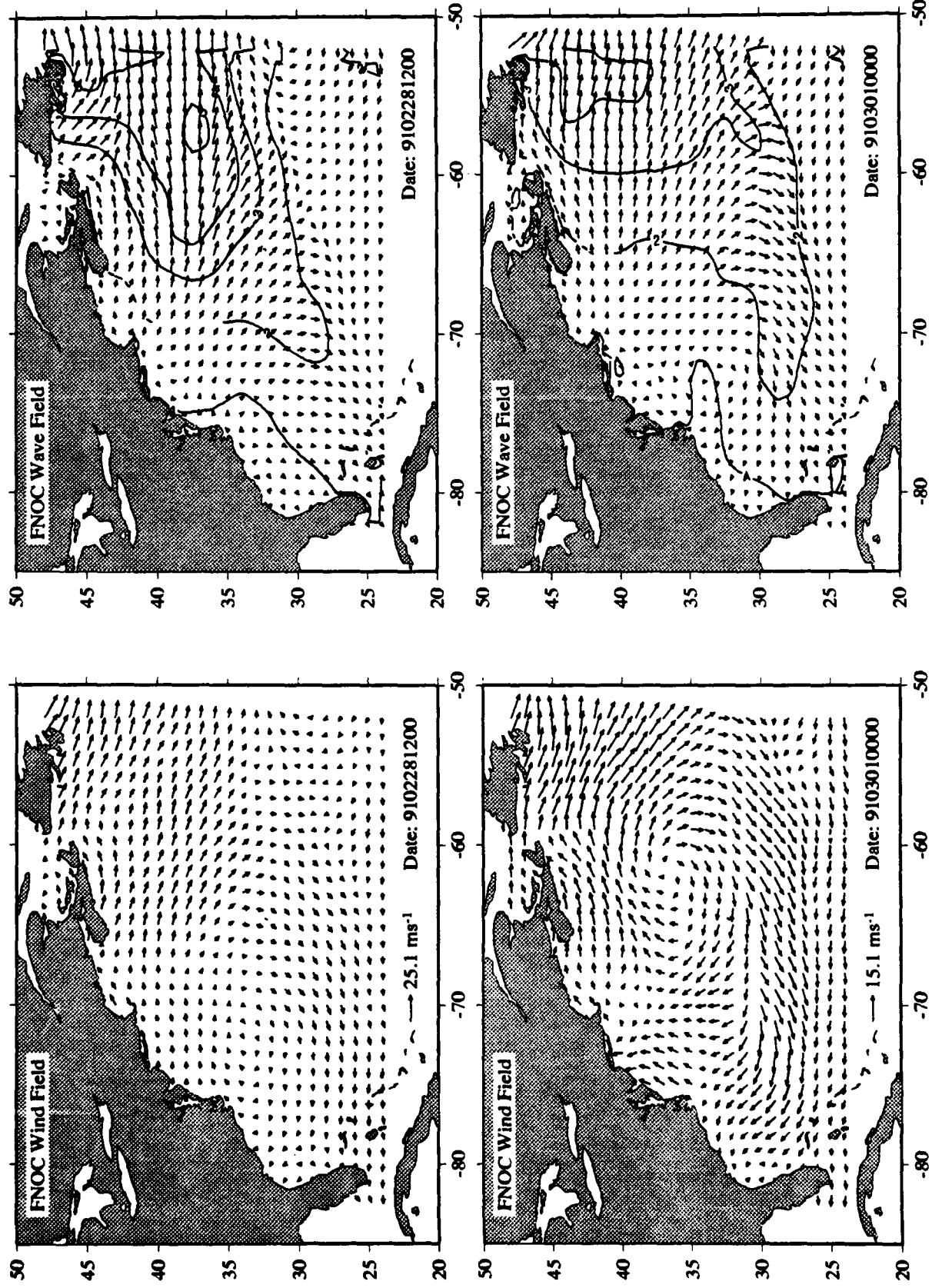


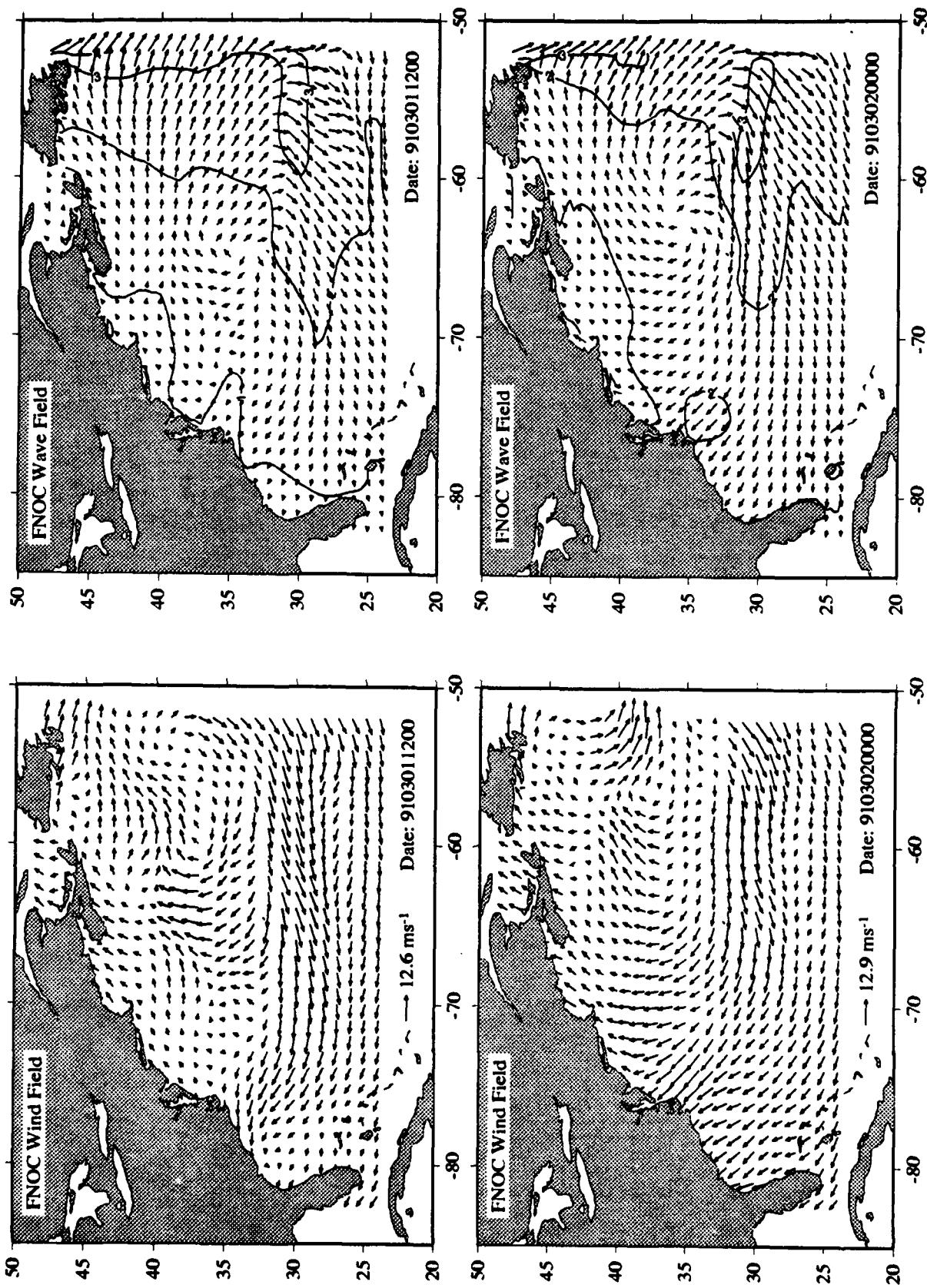


Appendix D Cluster Diagrams of Wind fields and Wave Hindcasts

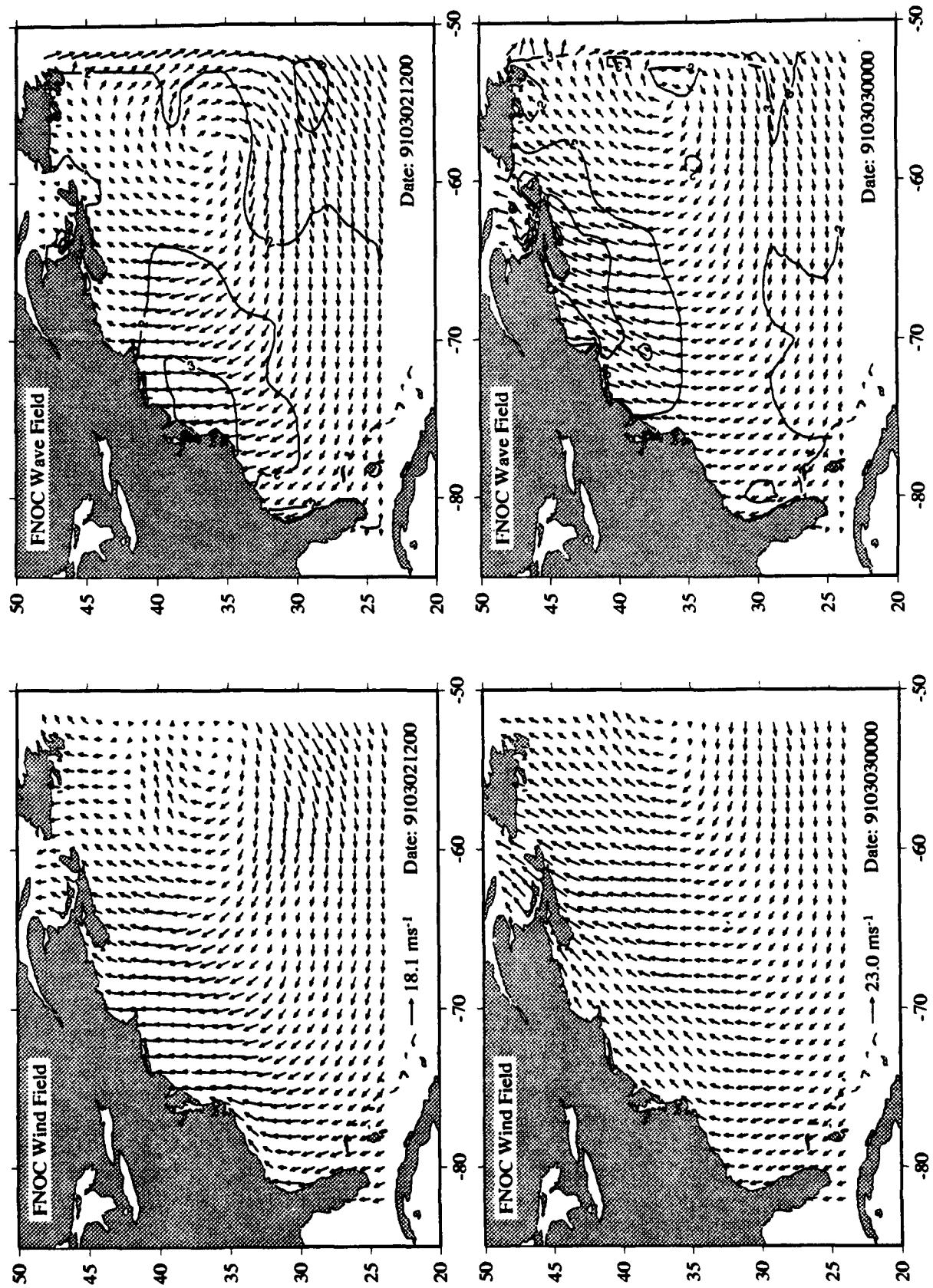


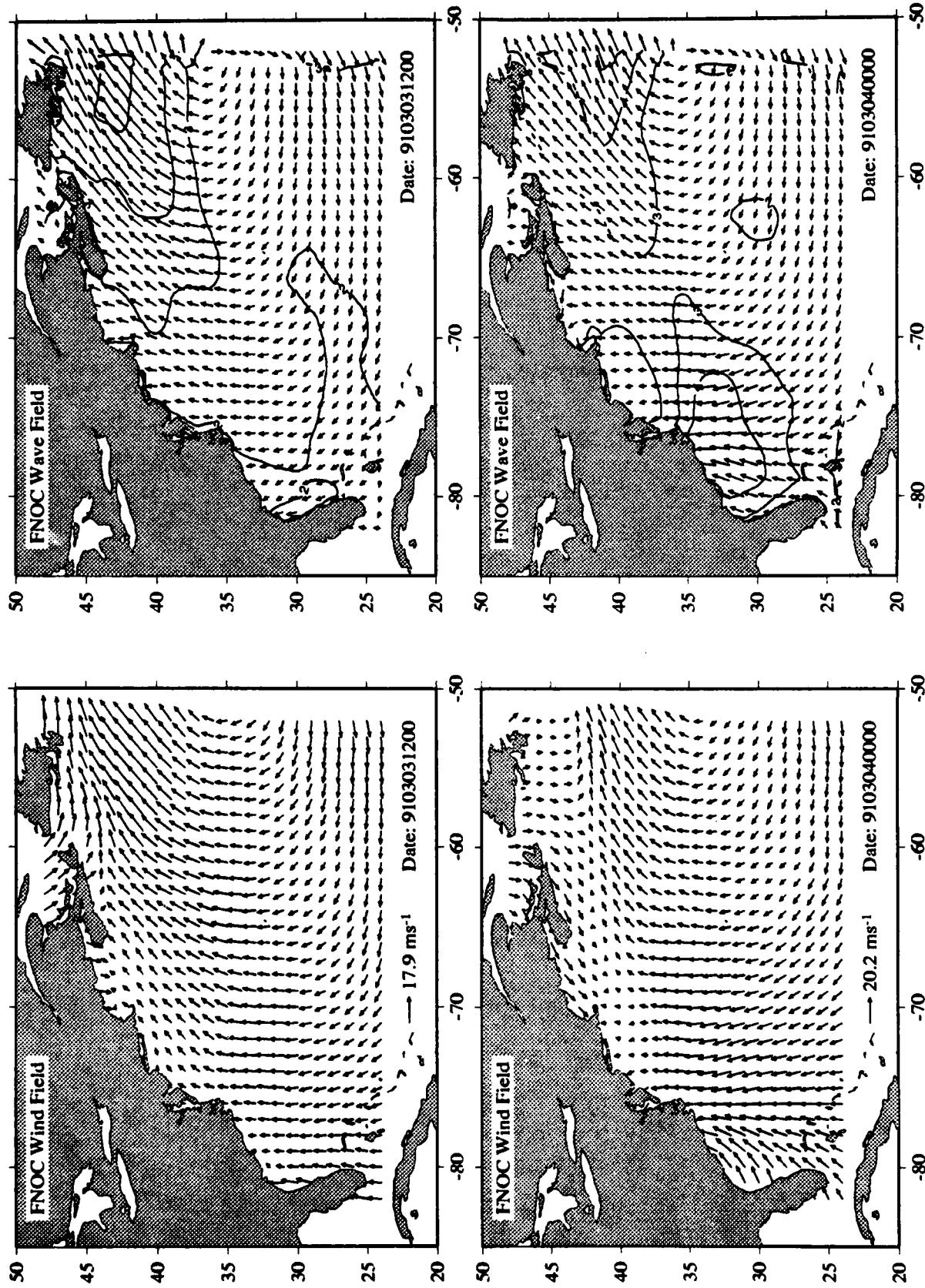


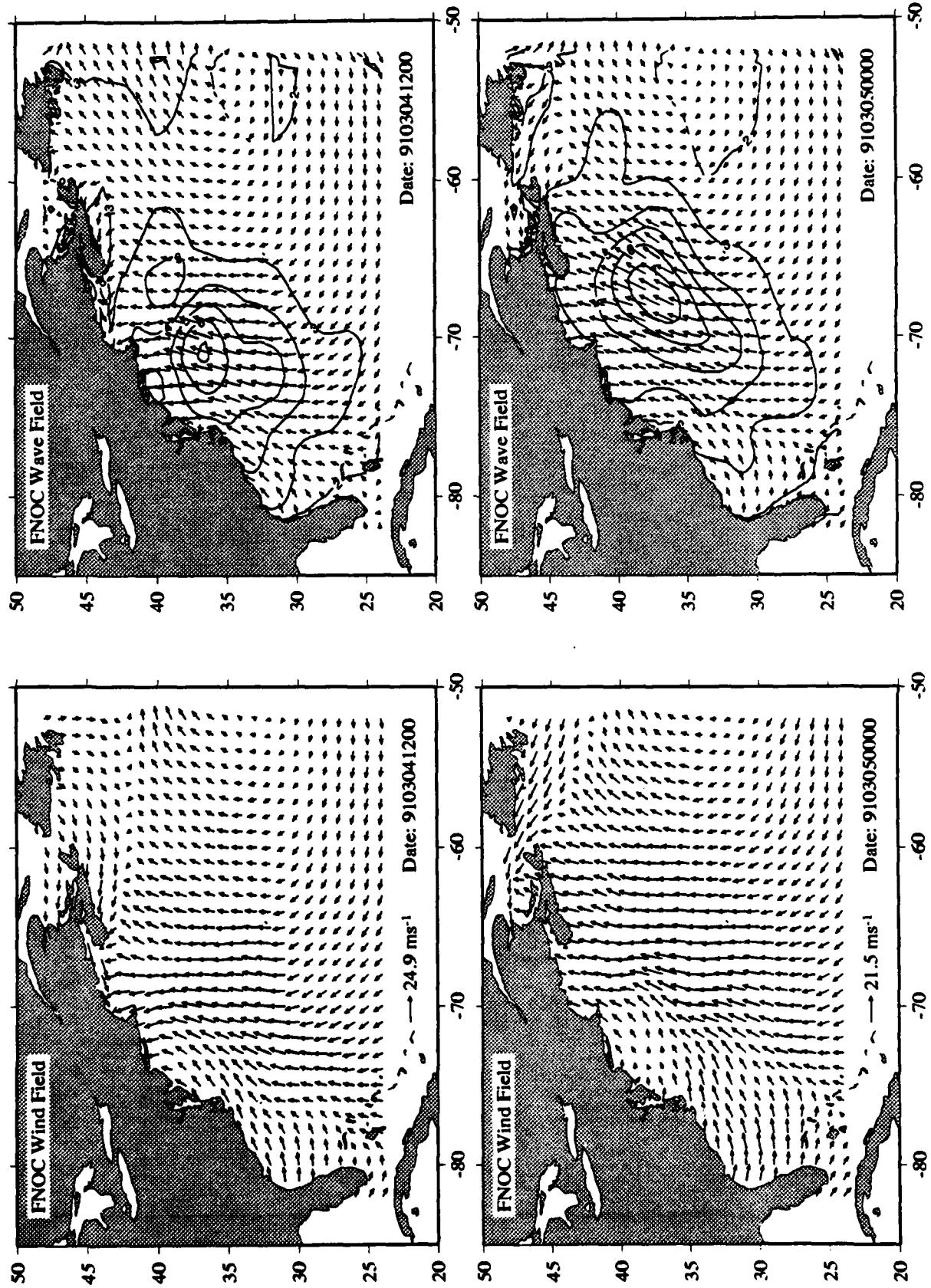


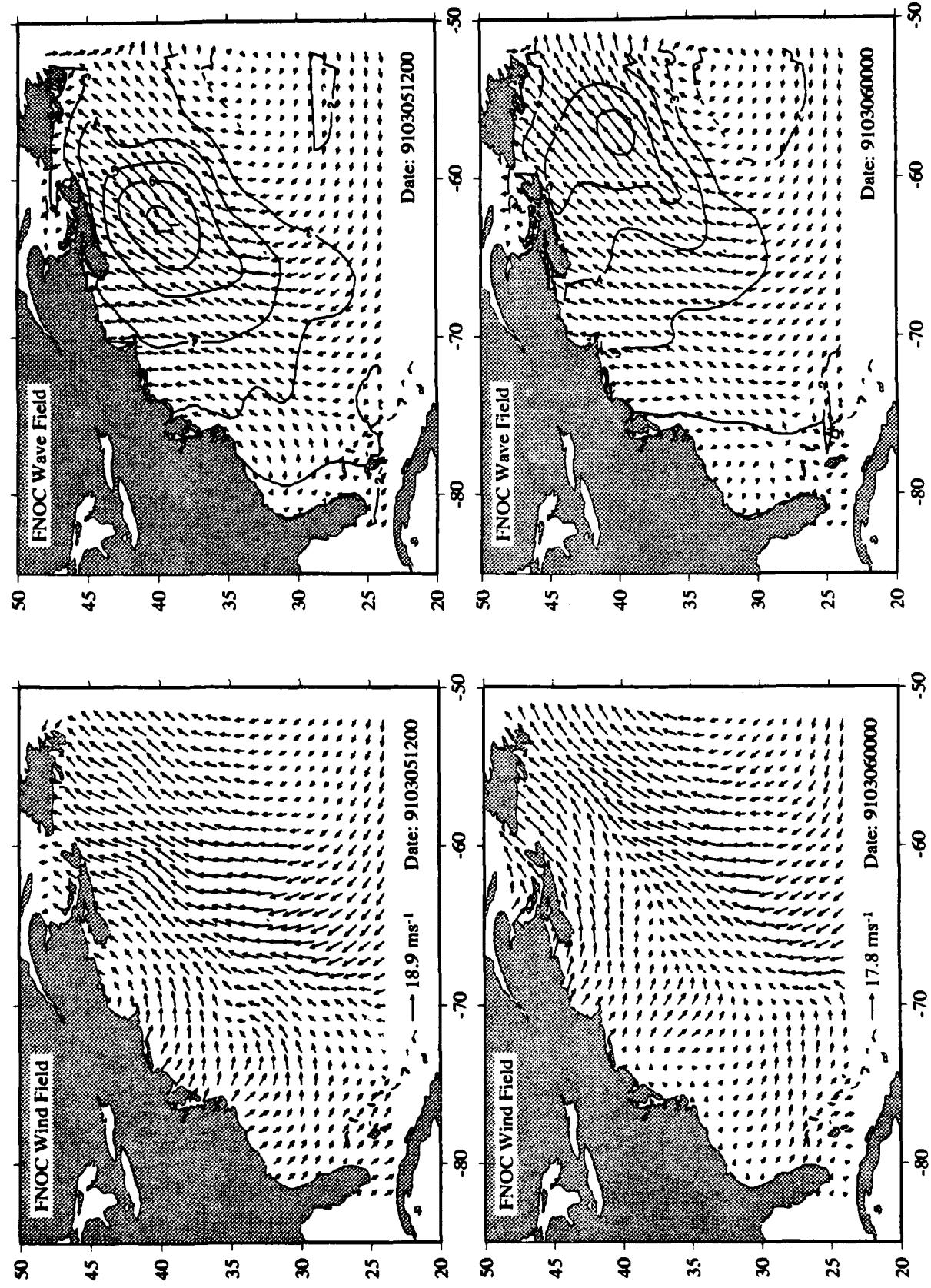


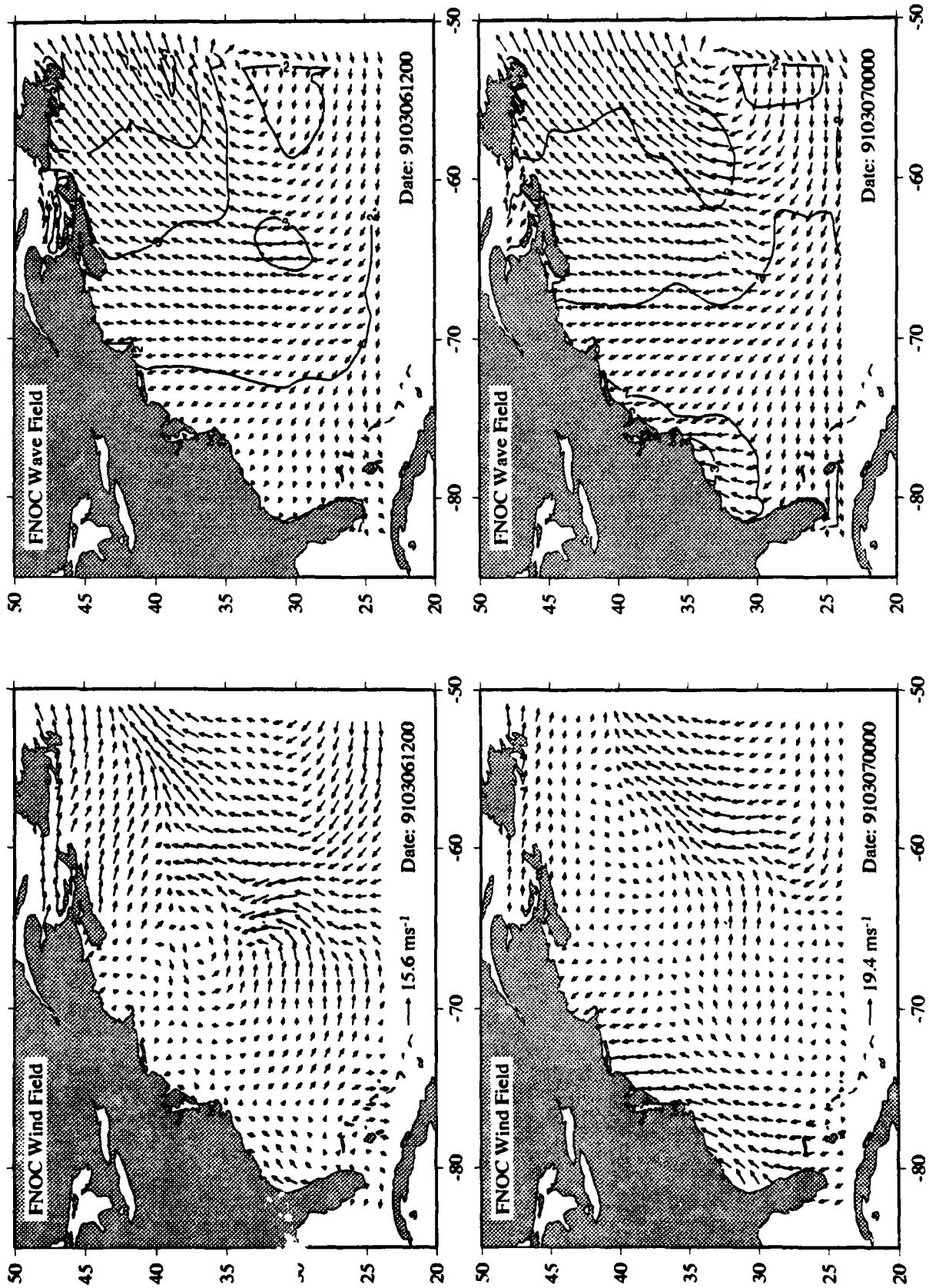
Appendix D Cluster Diagrams of Wind fields and Wave Hindcasts

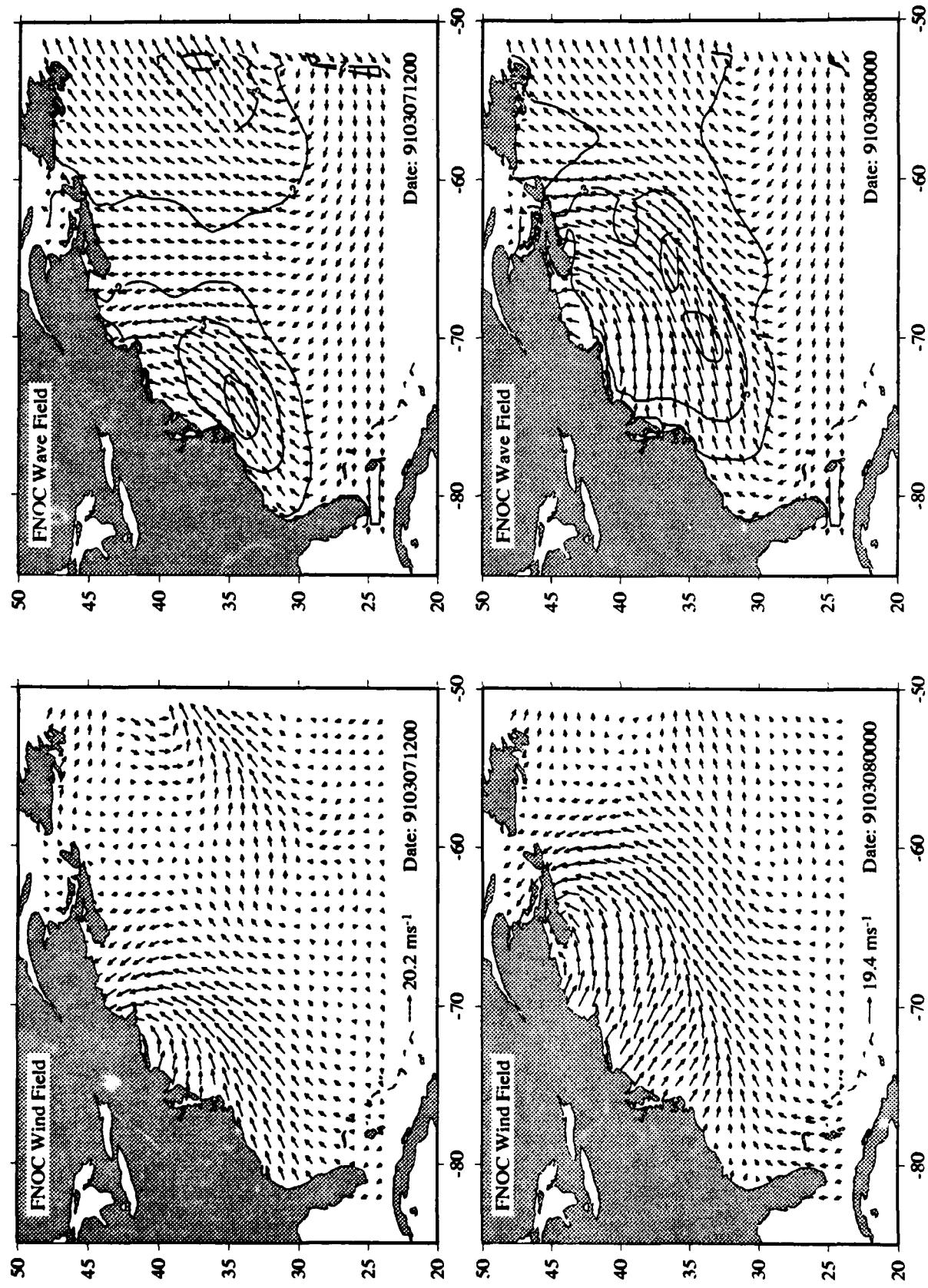


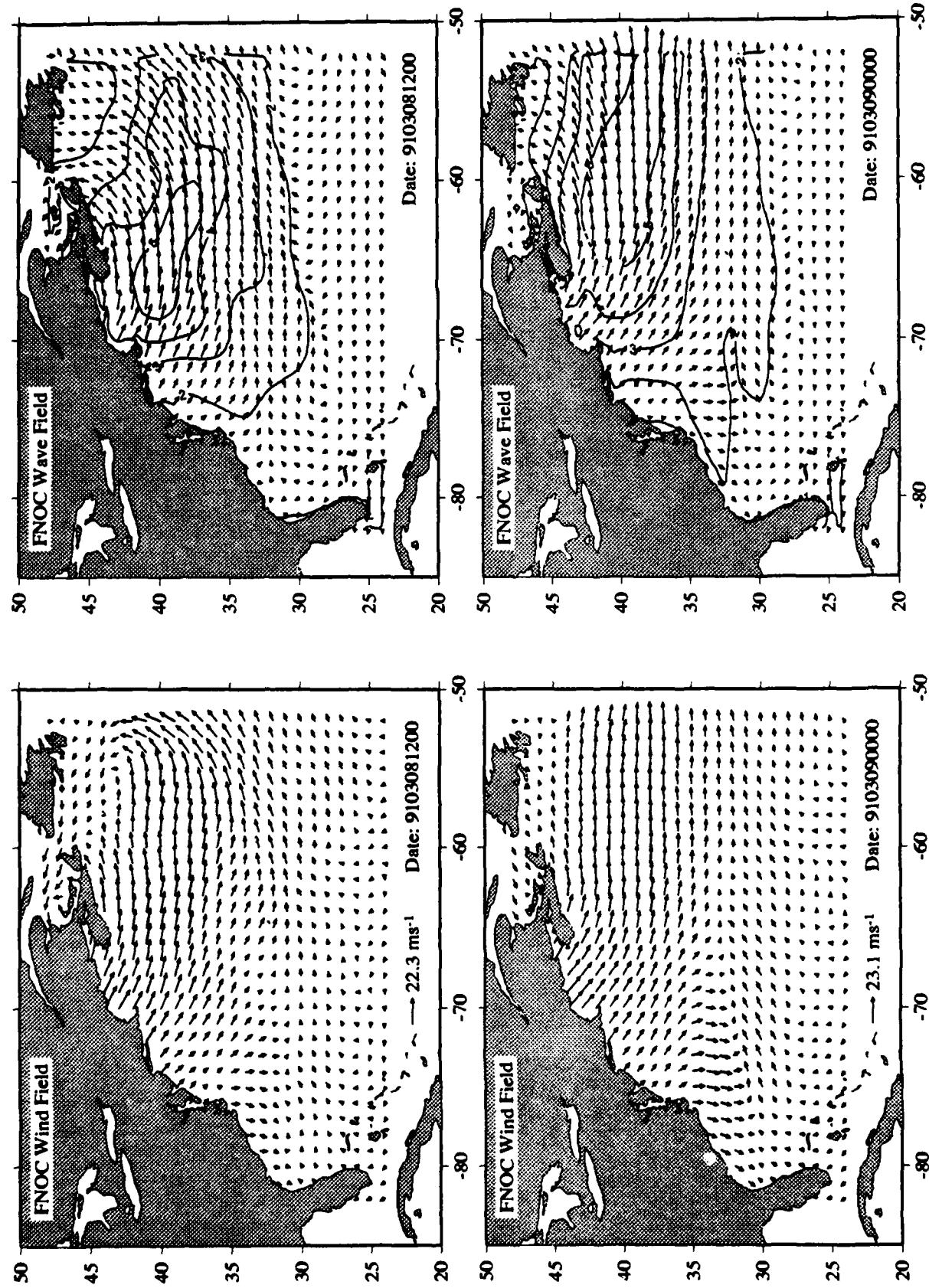






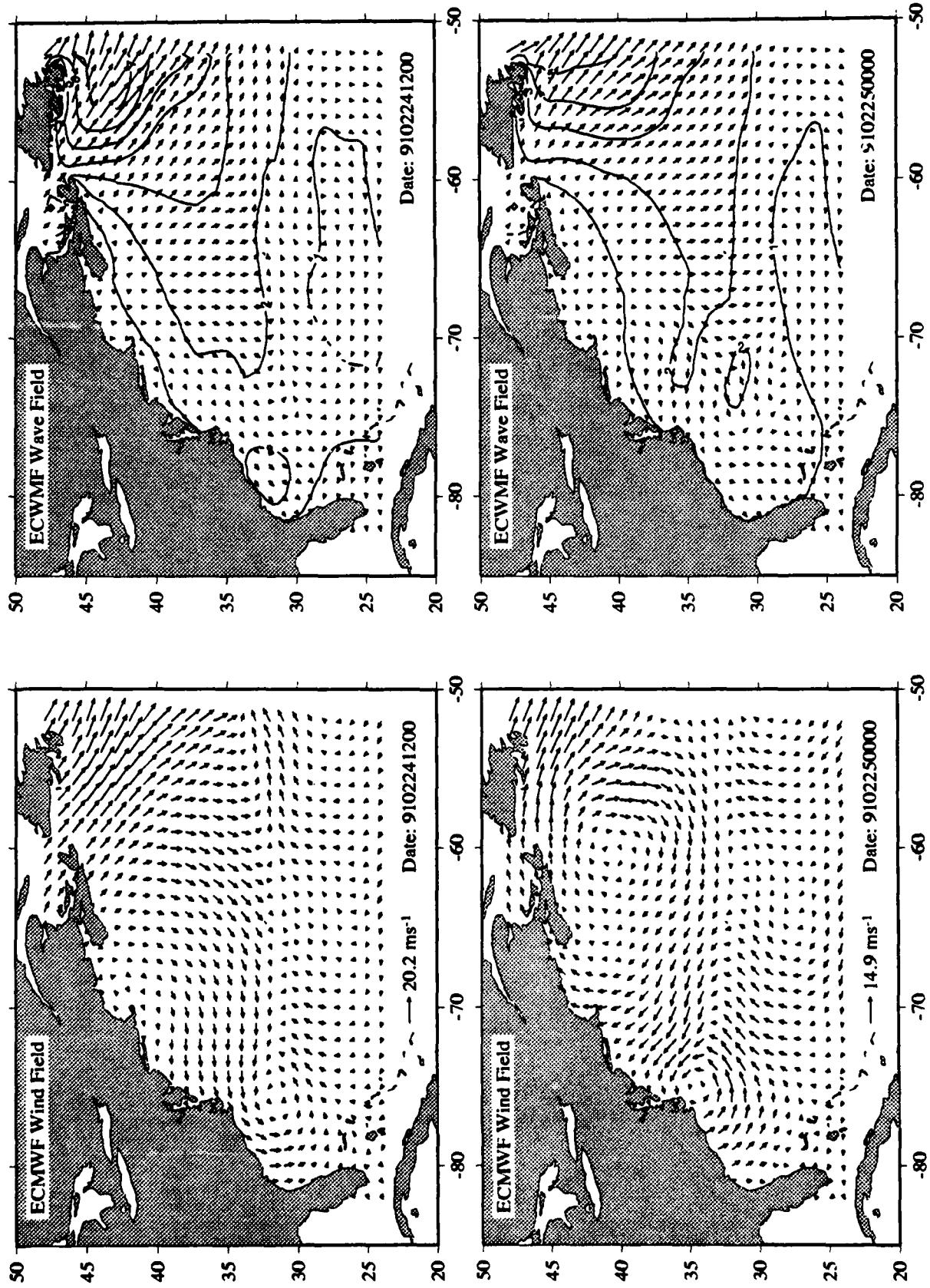


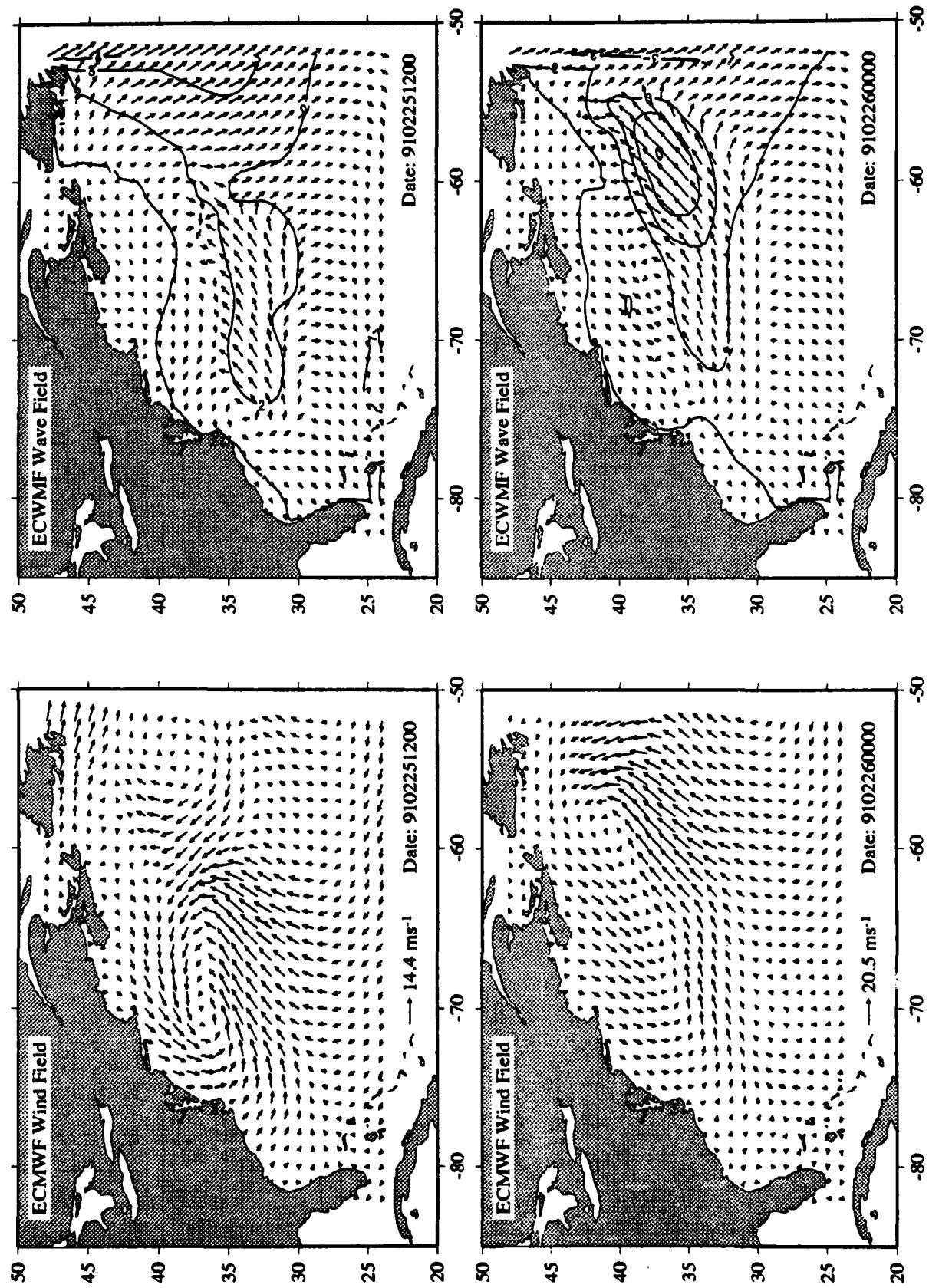


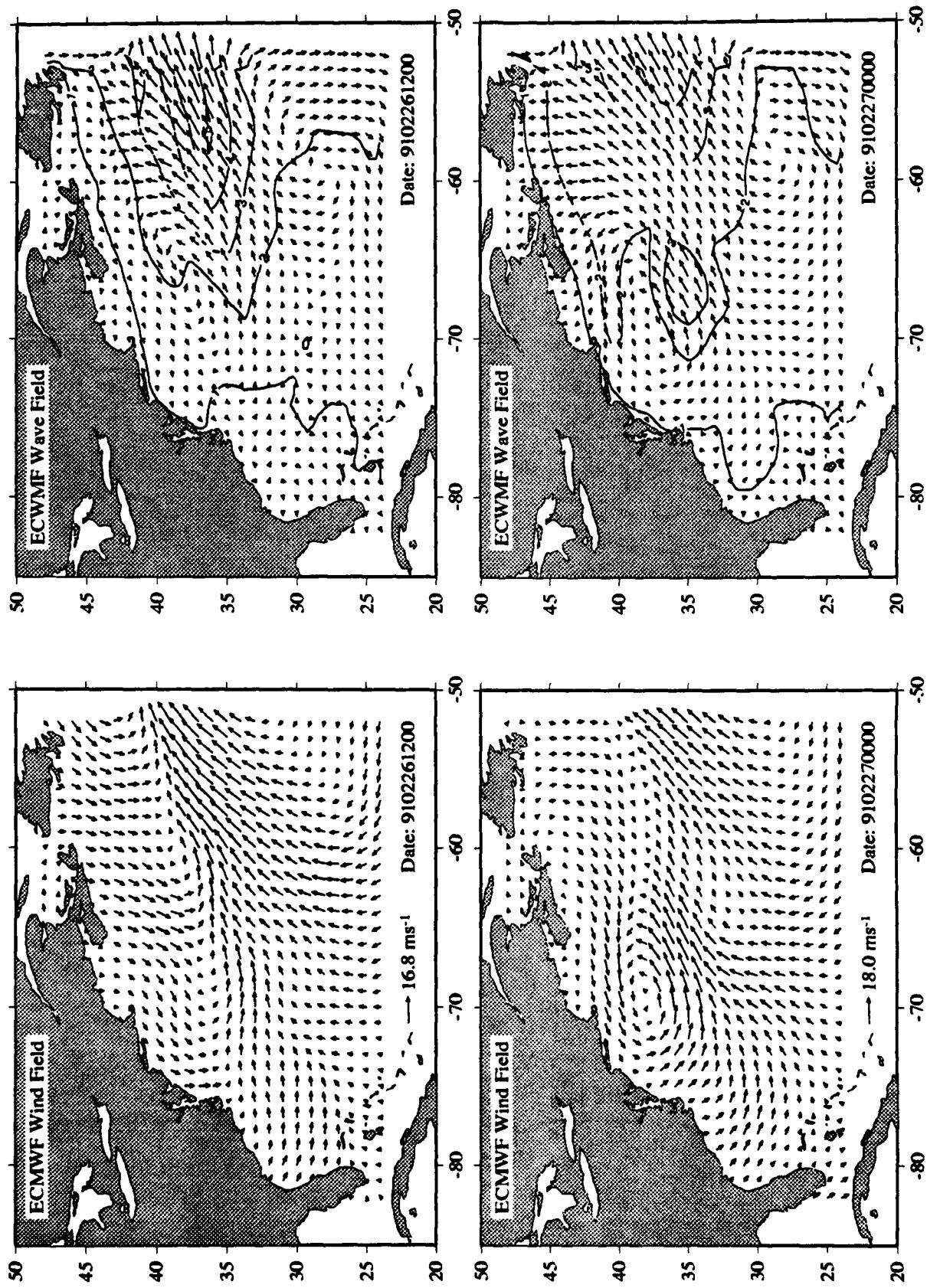


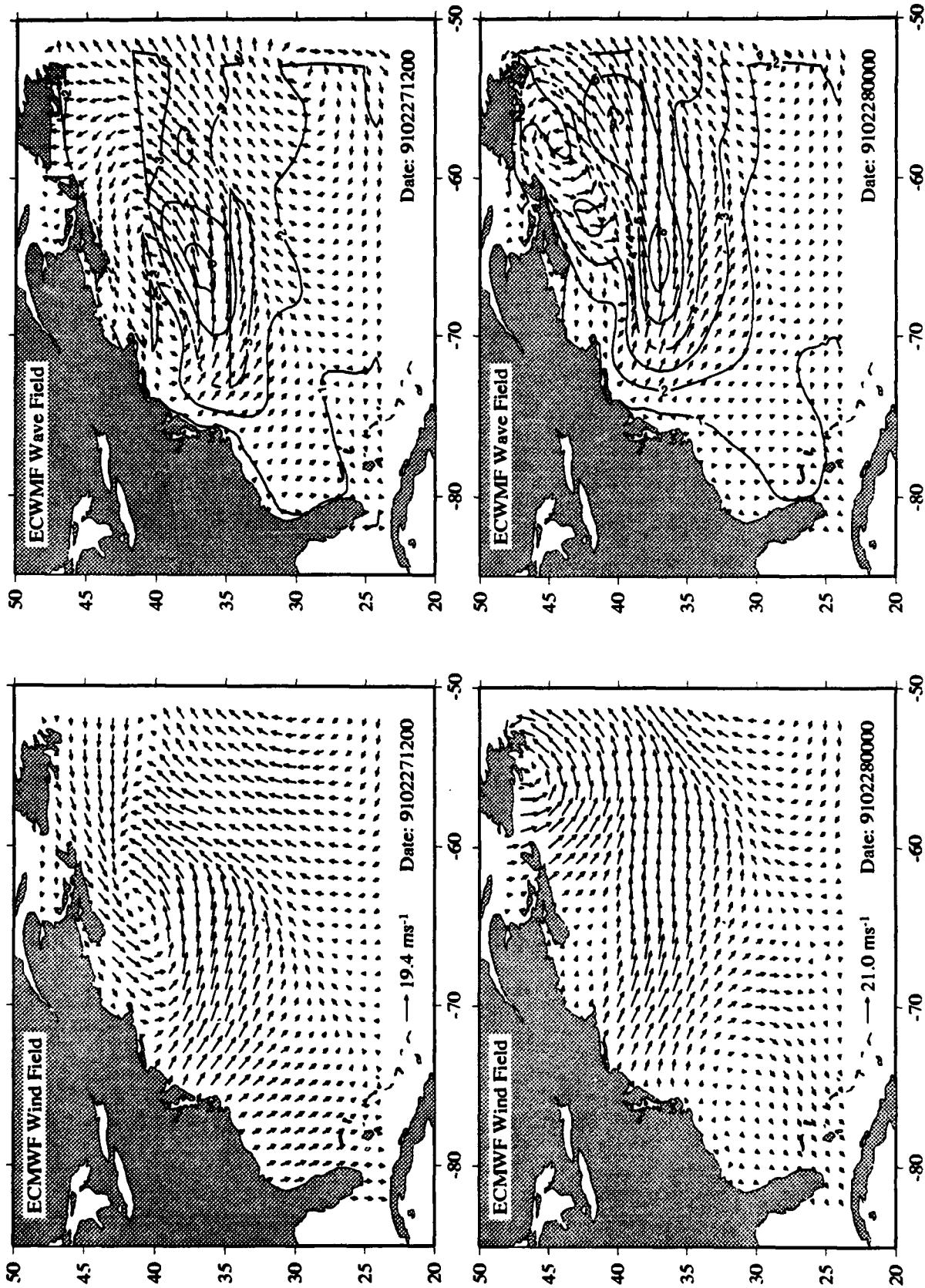
D.3: European Centre for Medium-Range Weather Forecasts (ECMWF)

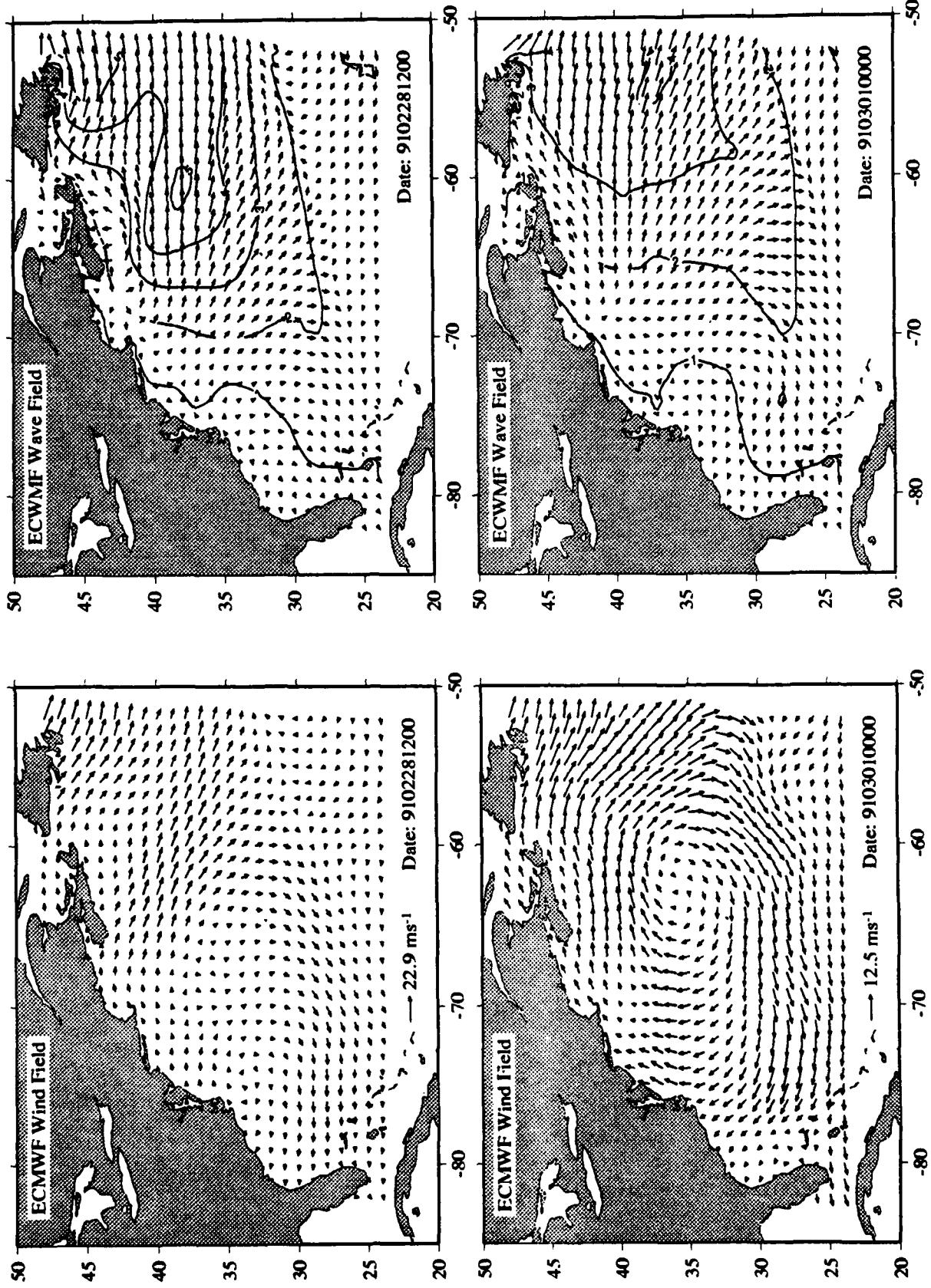
Custer diagrams are presented for the time period from 24 February 1991, 12:00 GMT to 9 March 1991, 00:00 GMT of the wind field and corresponding wave hindcasts.

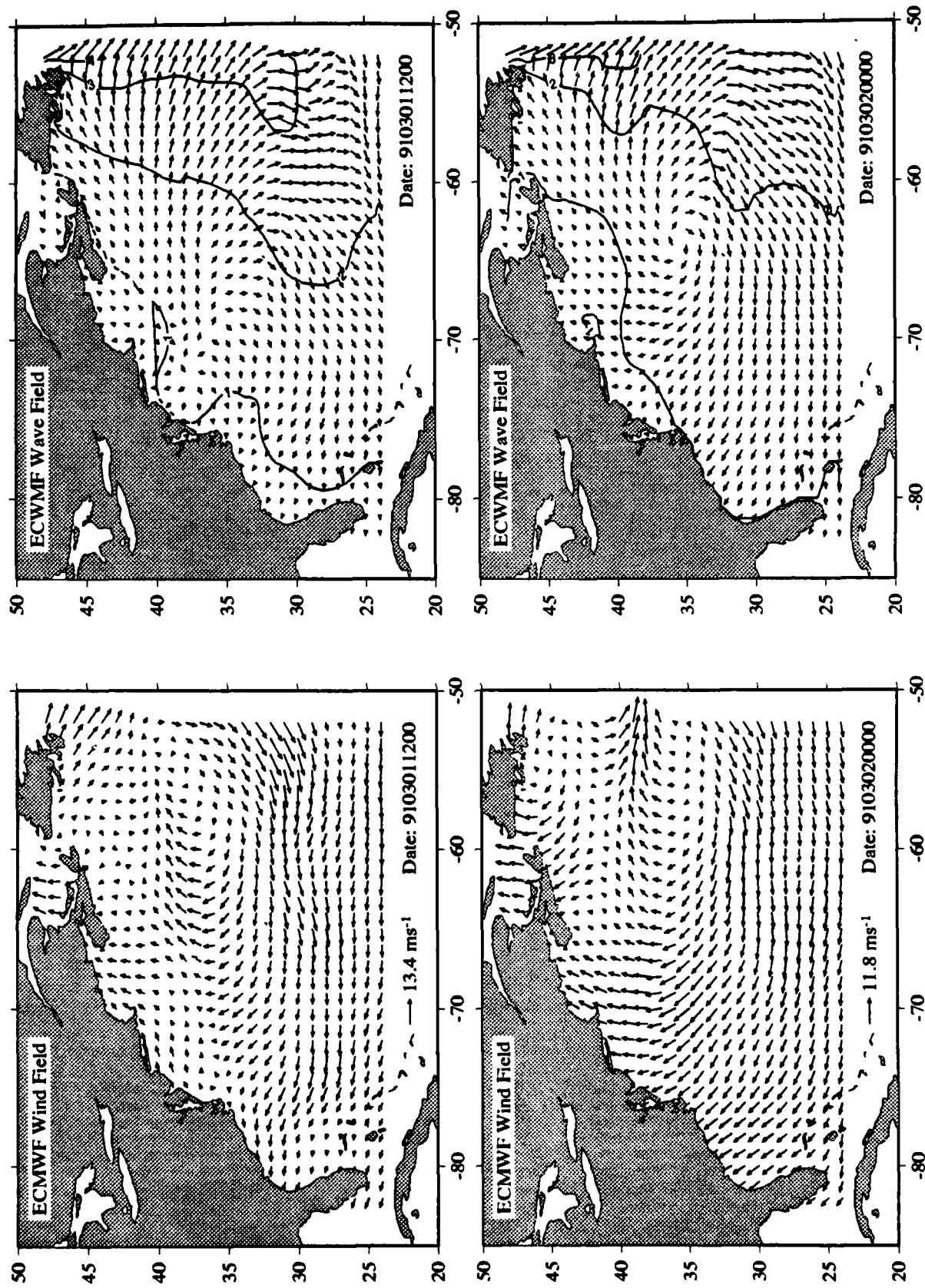




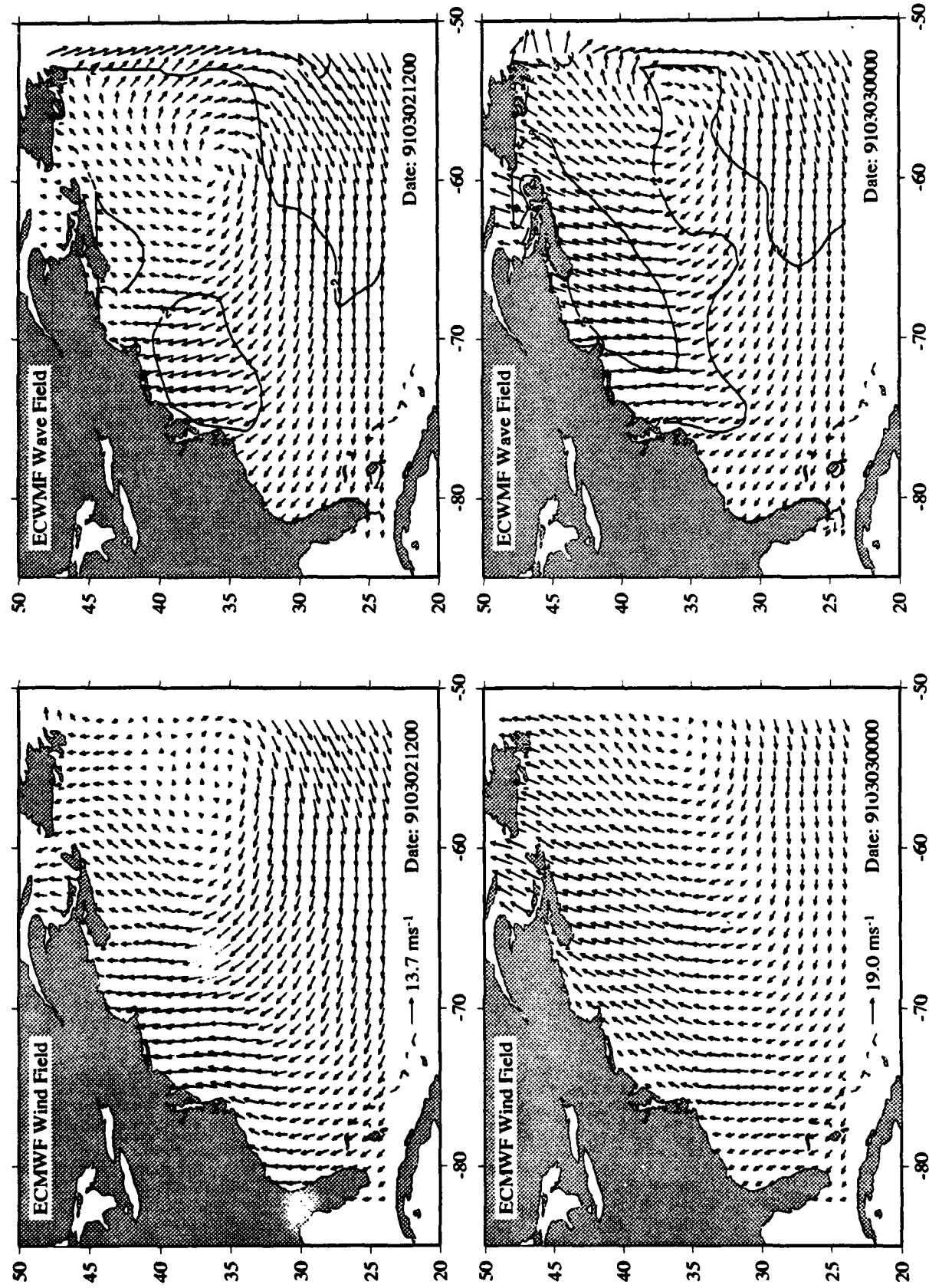


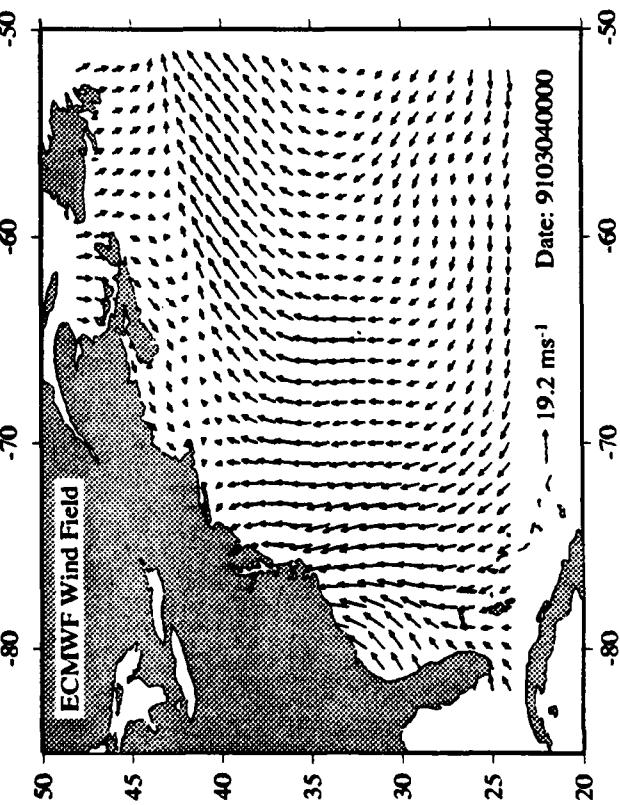
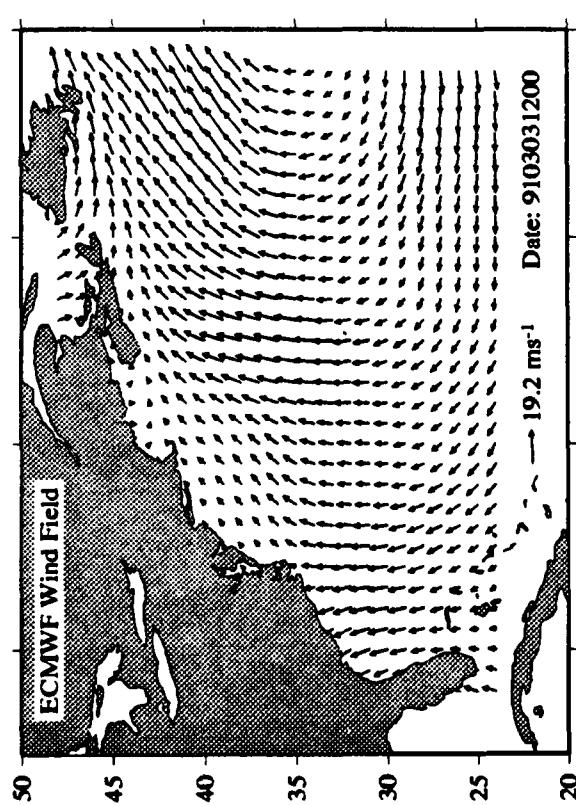
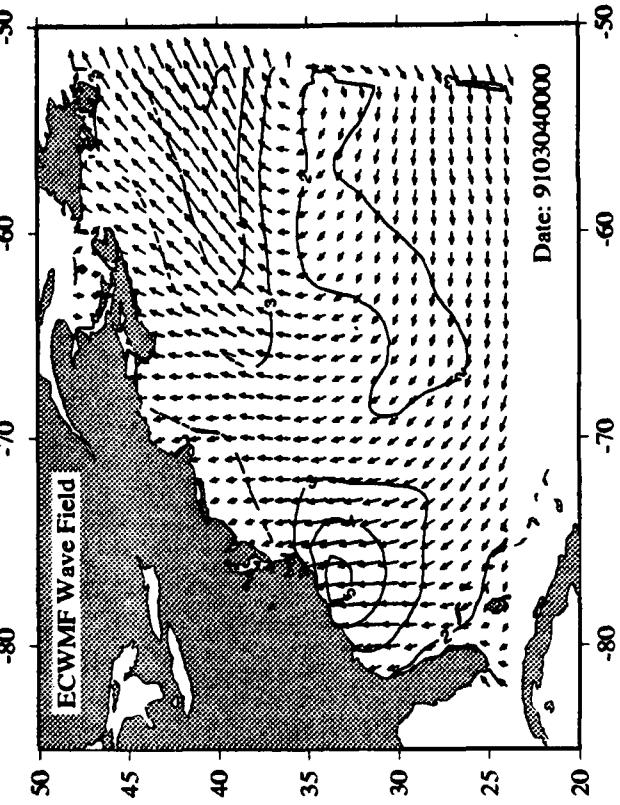
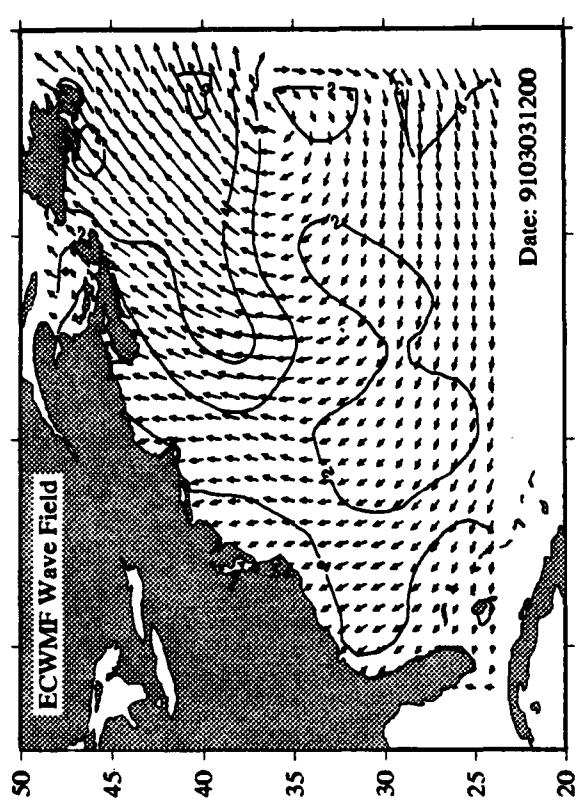


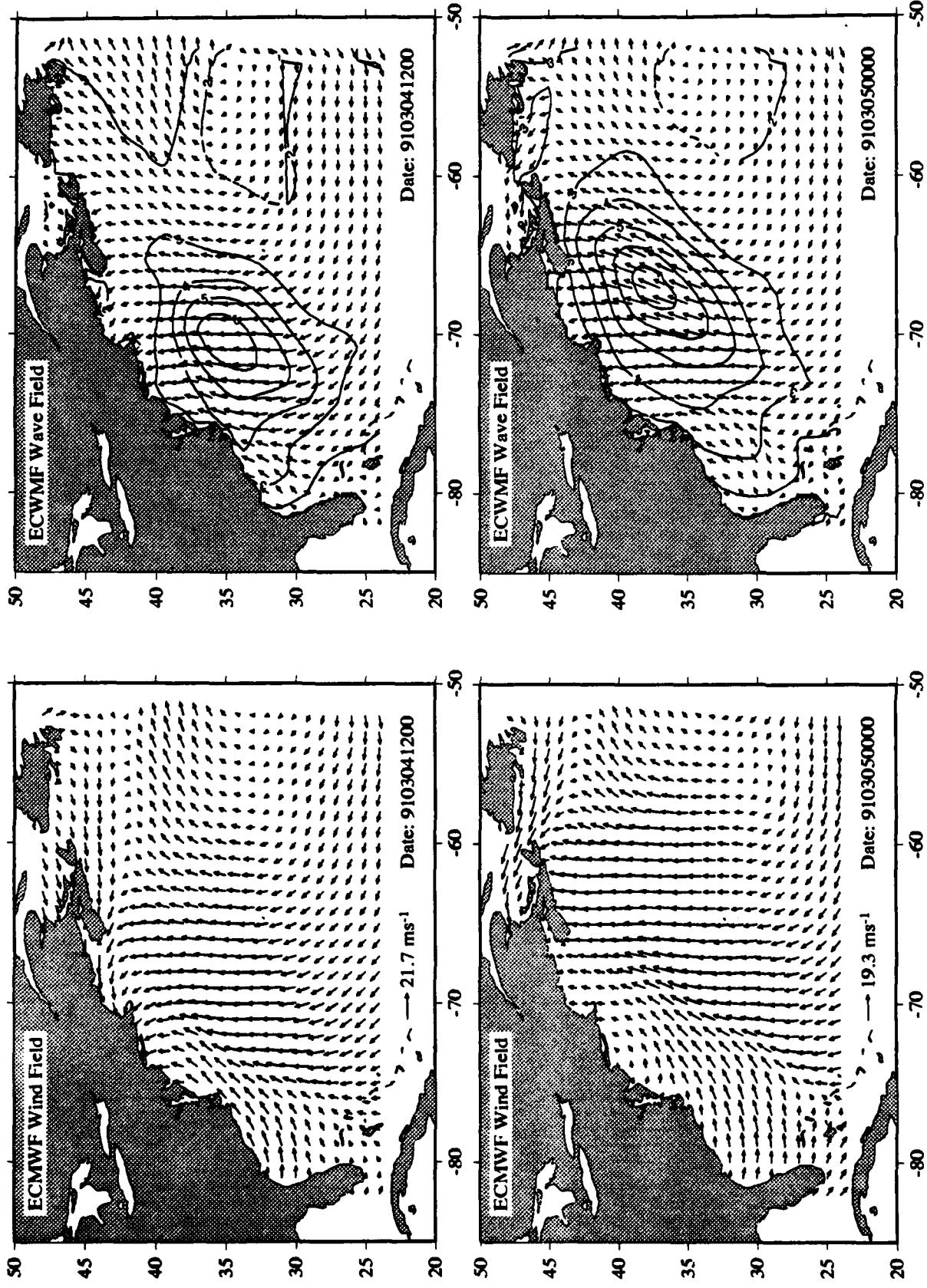


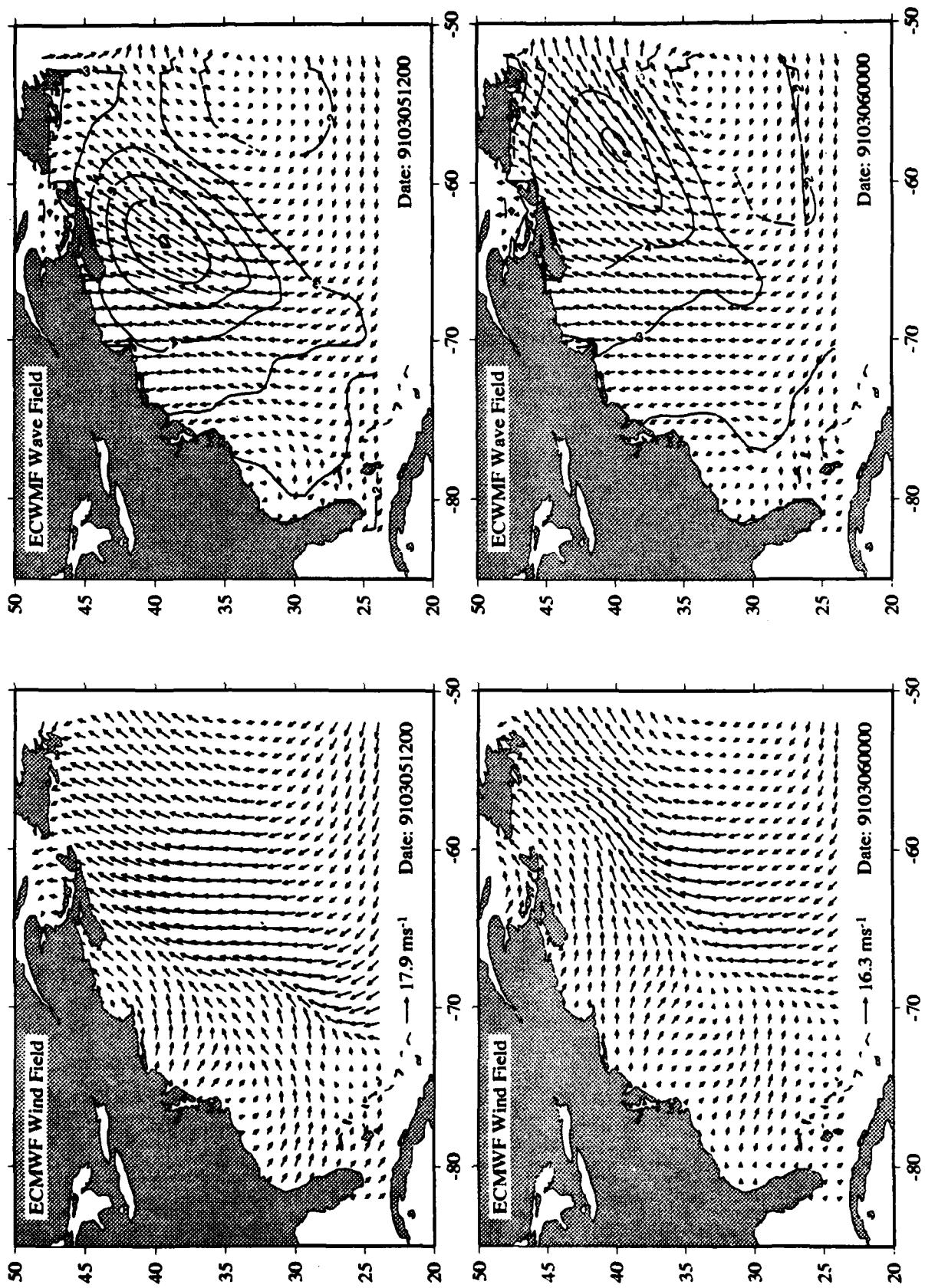


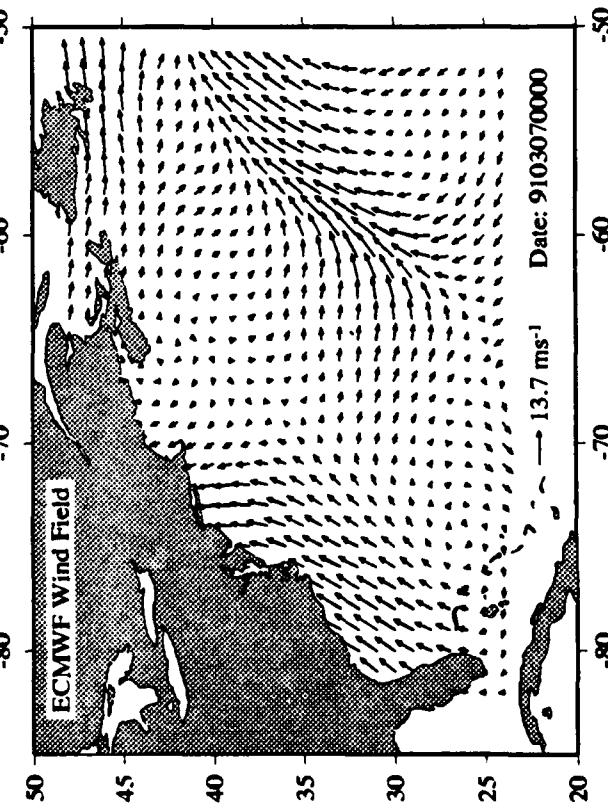
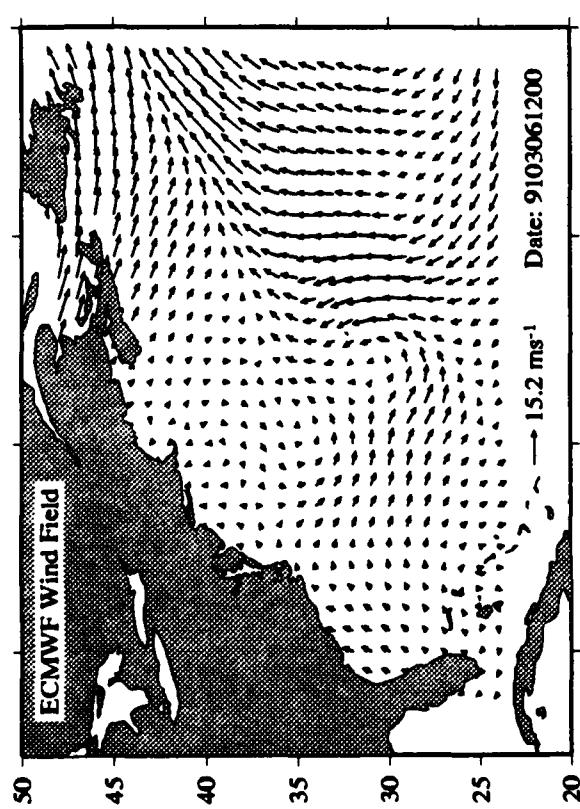
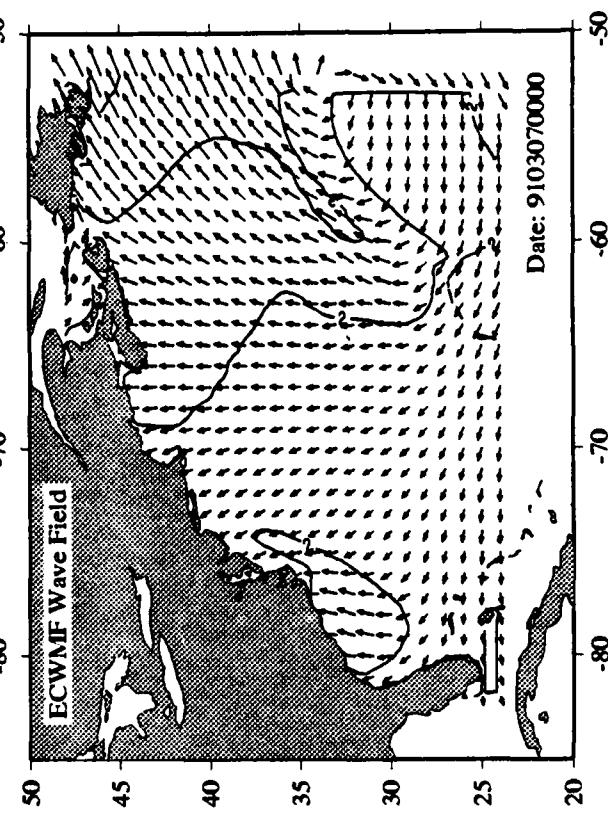
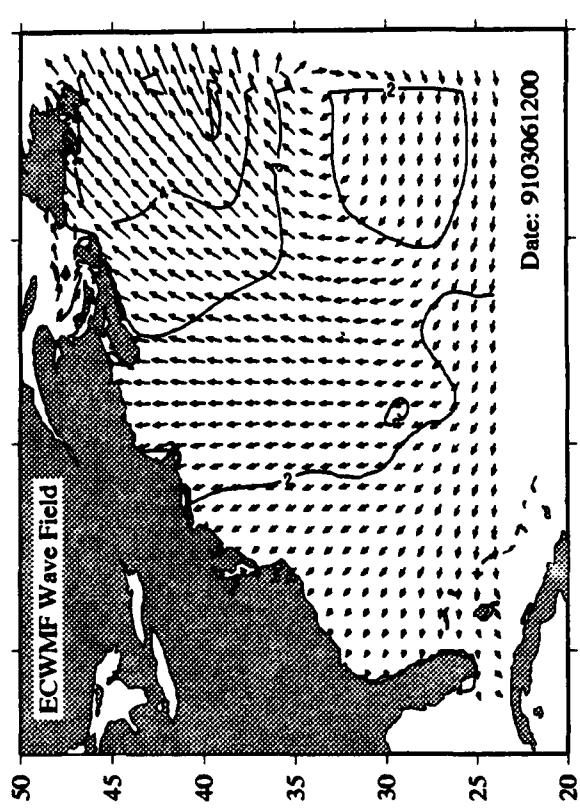
Appendix D Custer Diagrams of Wind fields and Wave Hindcasts

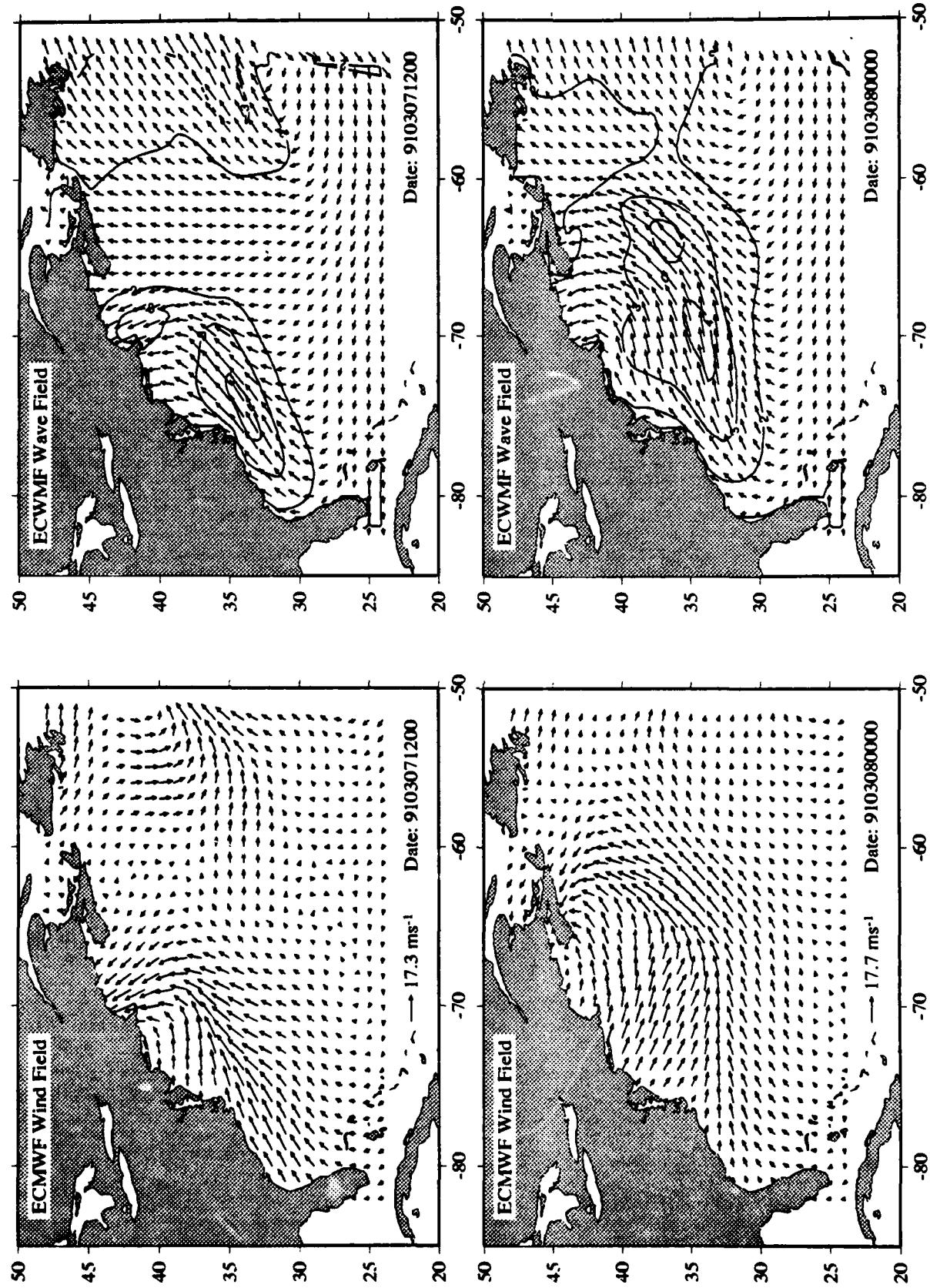




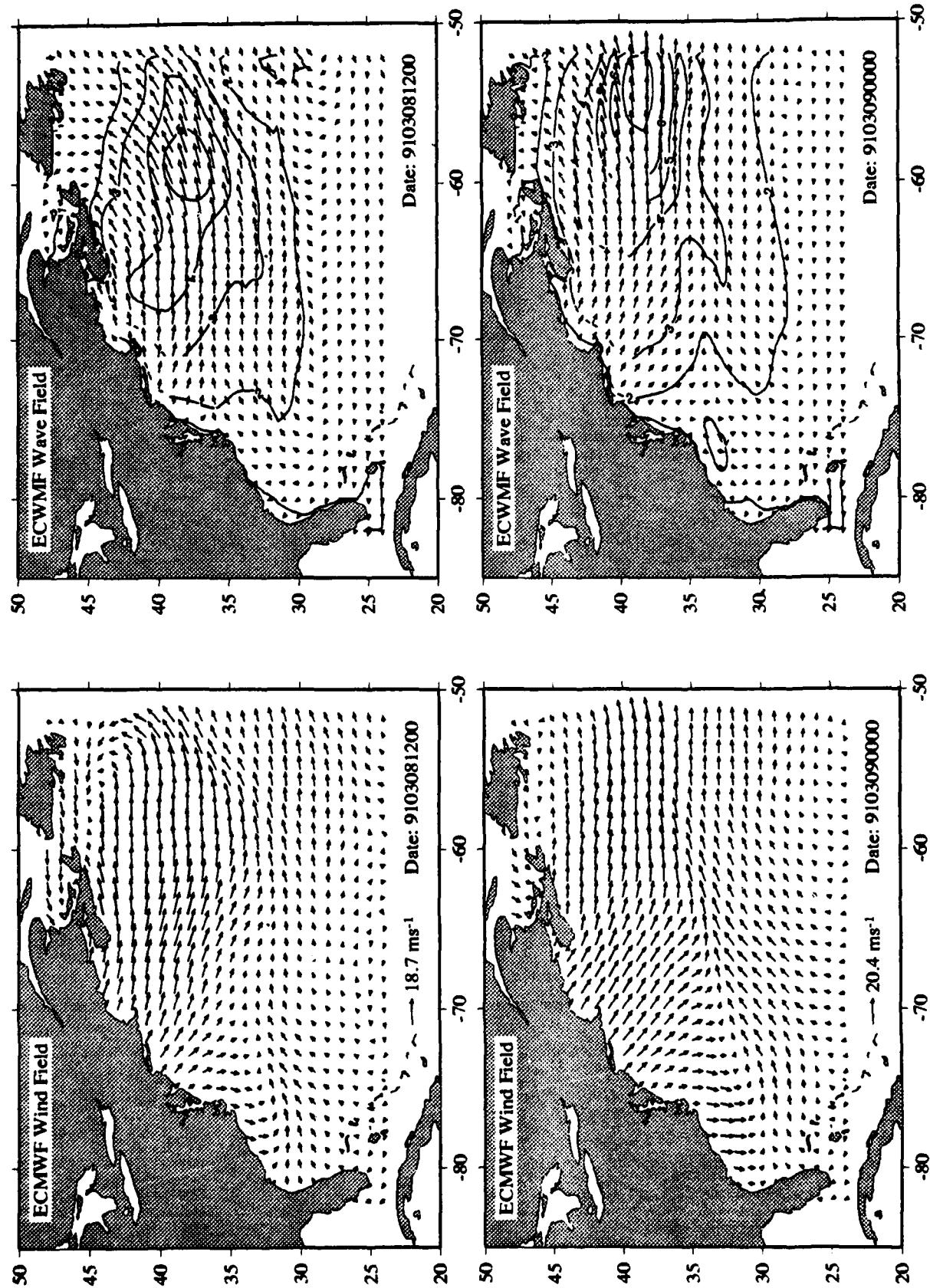






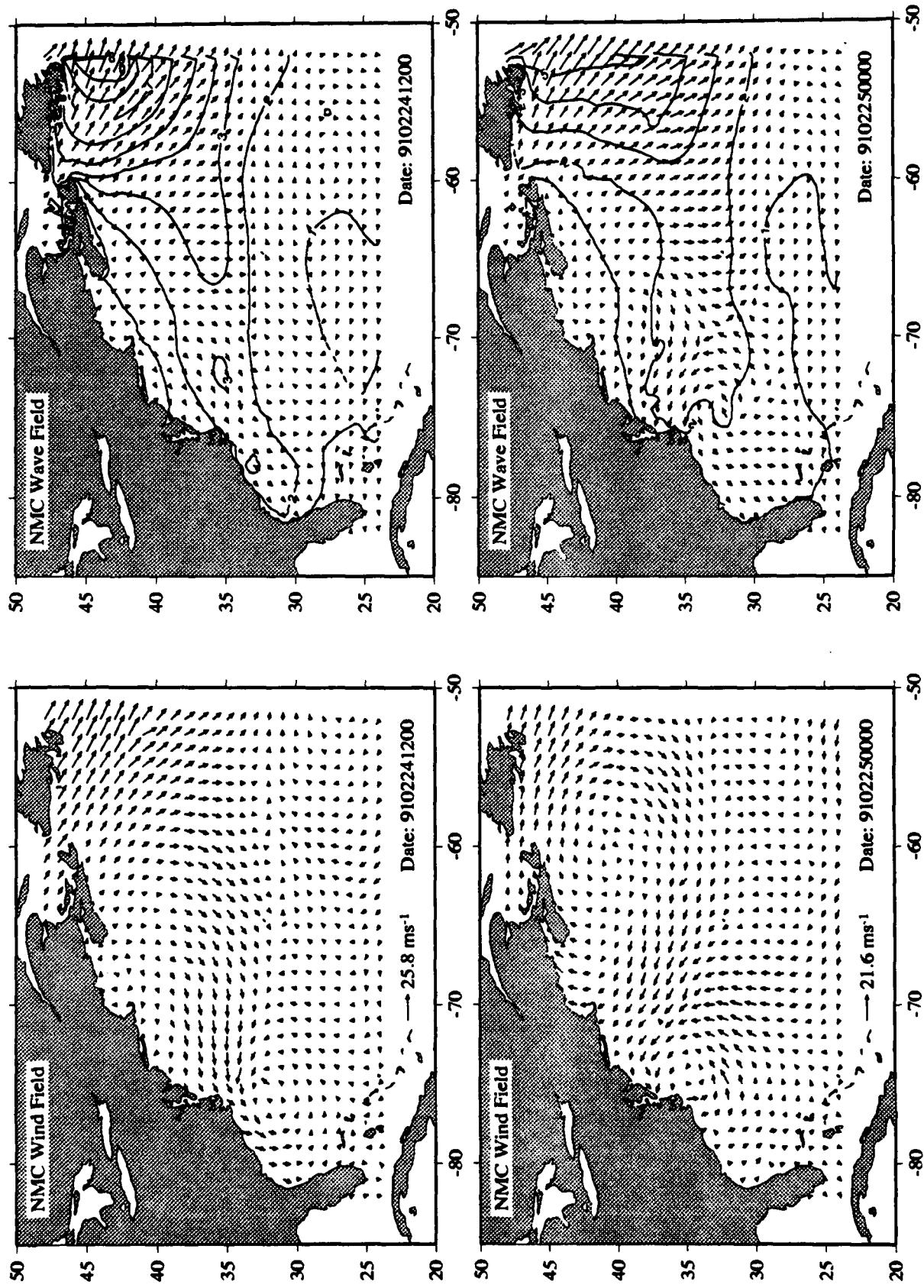


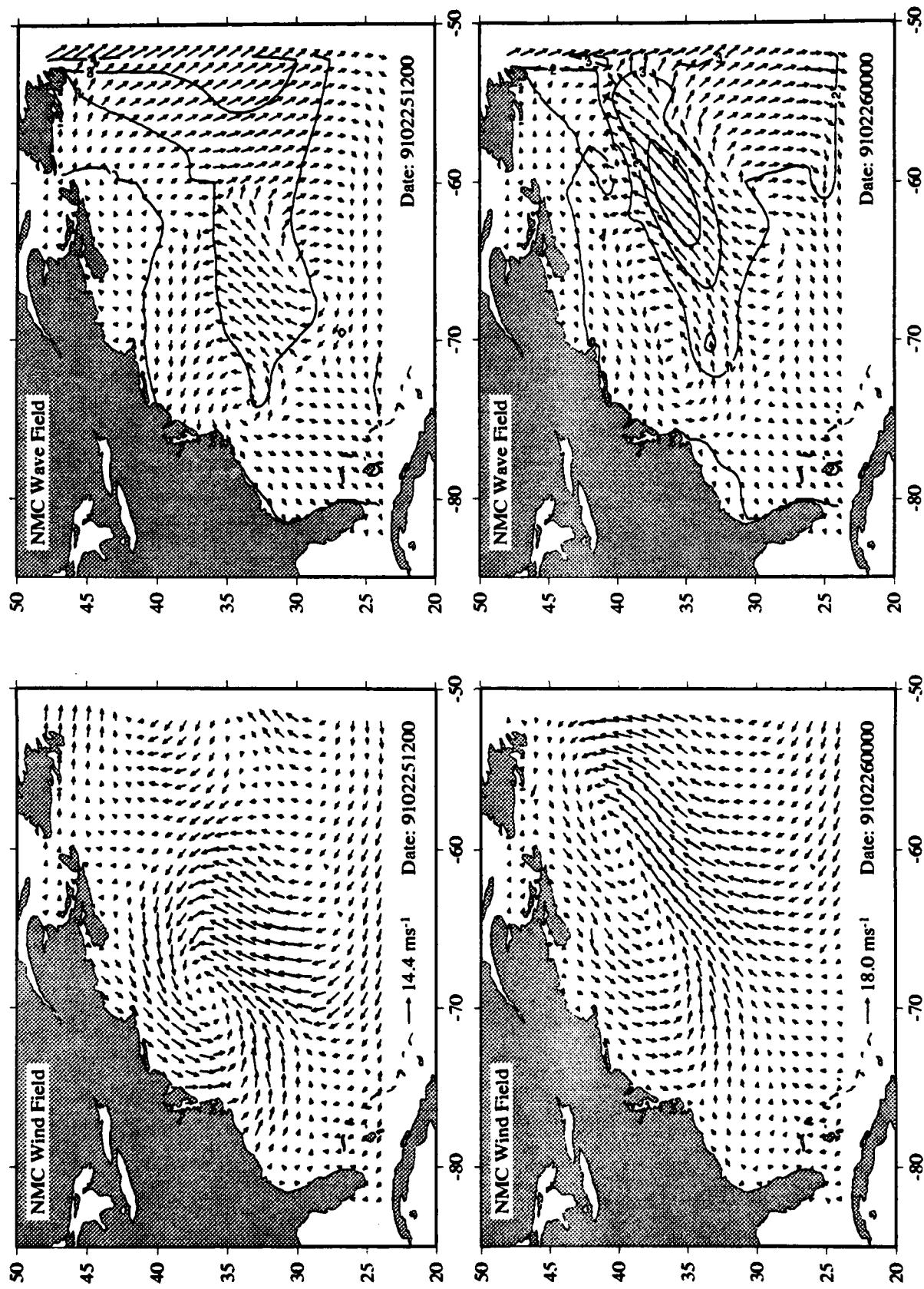
Appendix D Cluster Diagrams of Wind fields and Wave Hindcasts

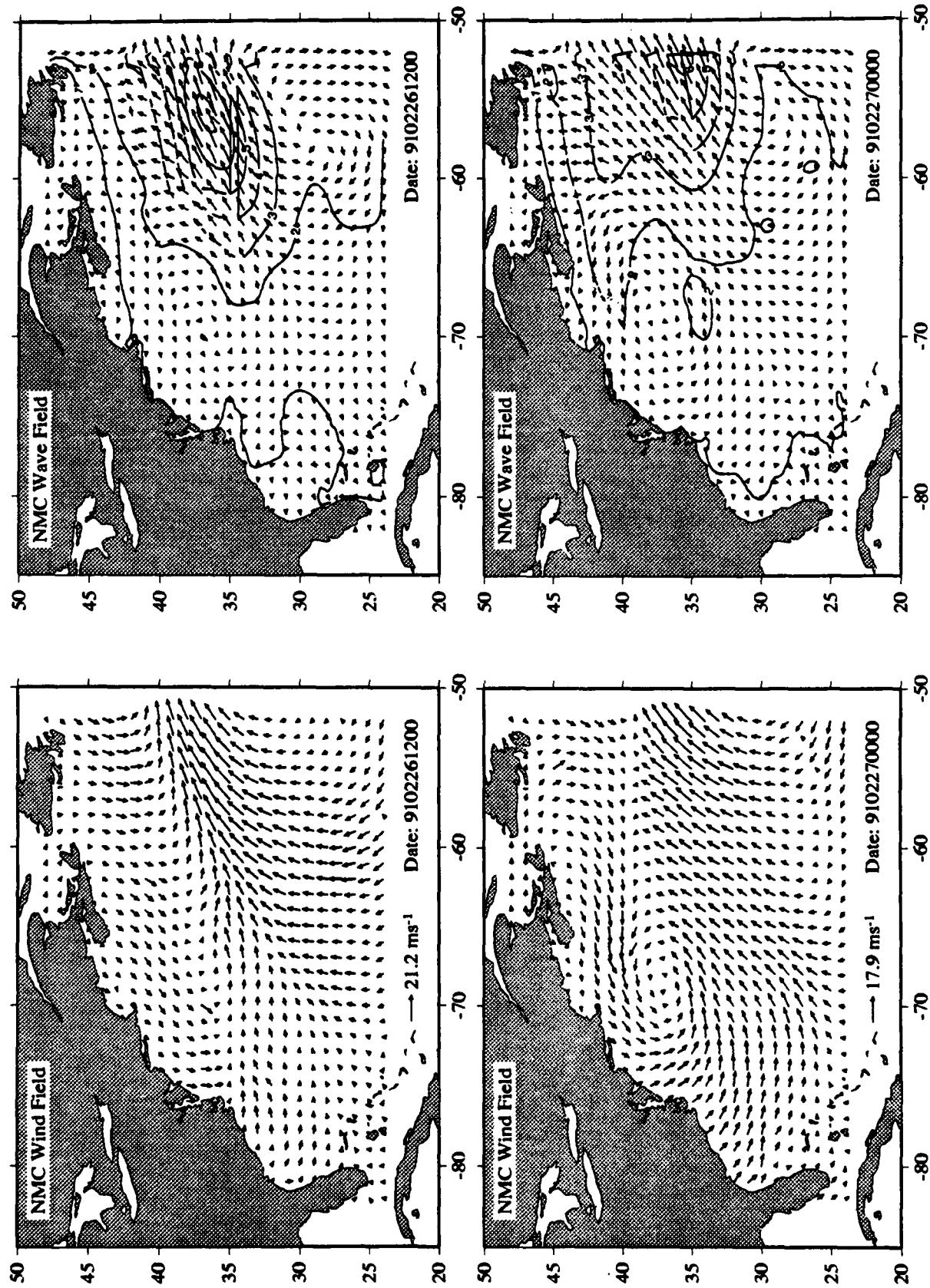


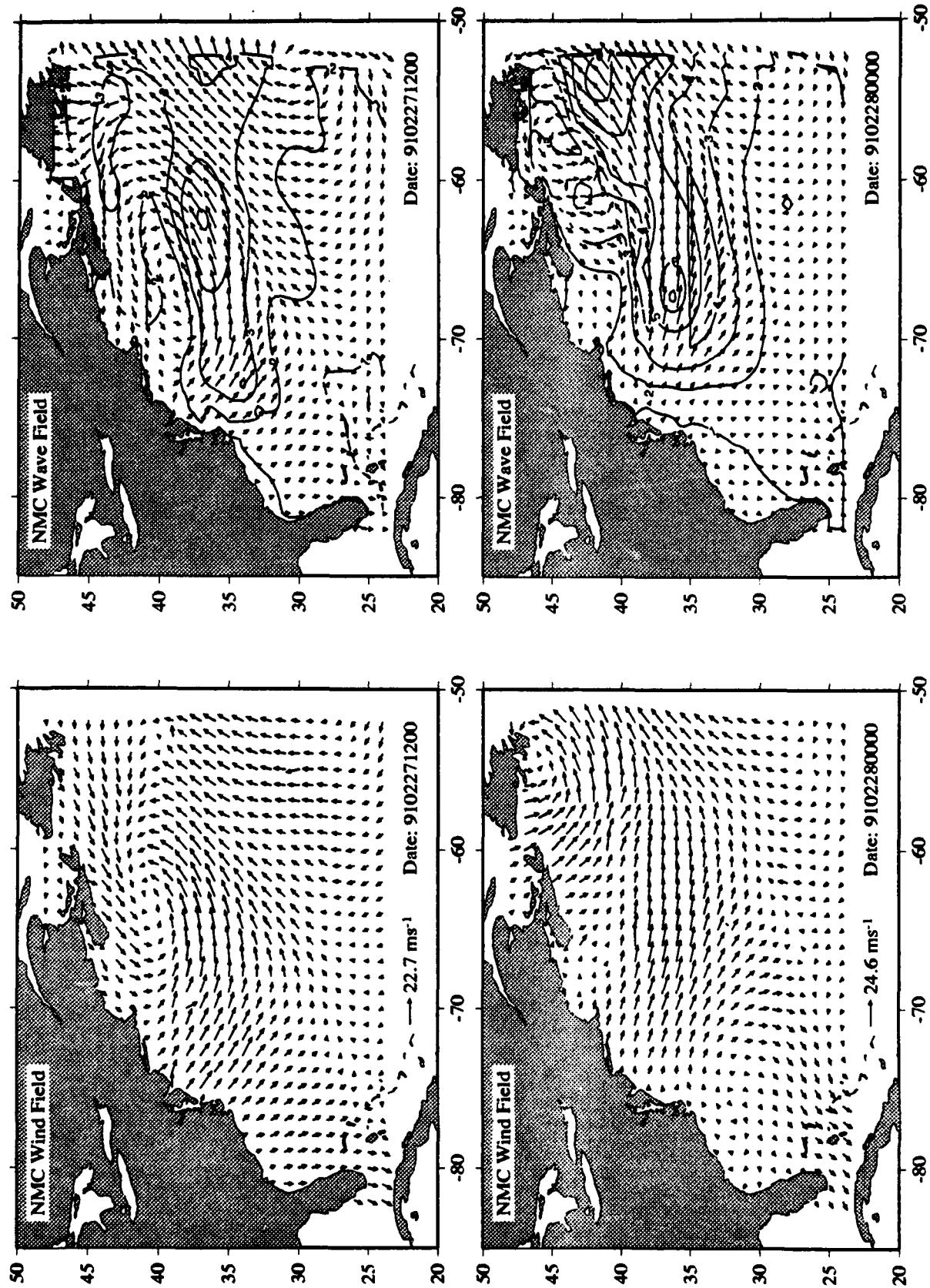
D.4: National Meteorological Center (NMC)

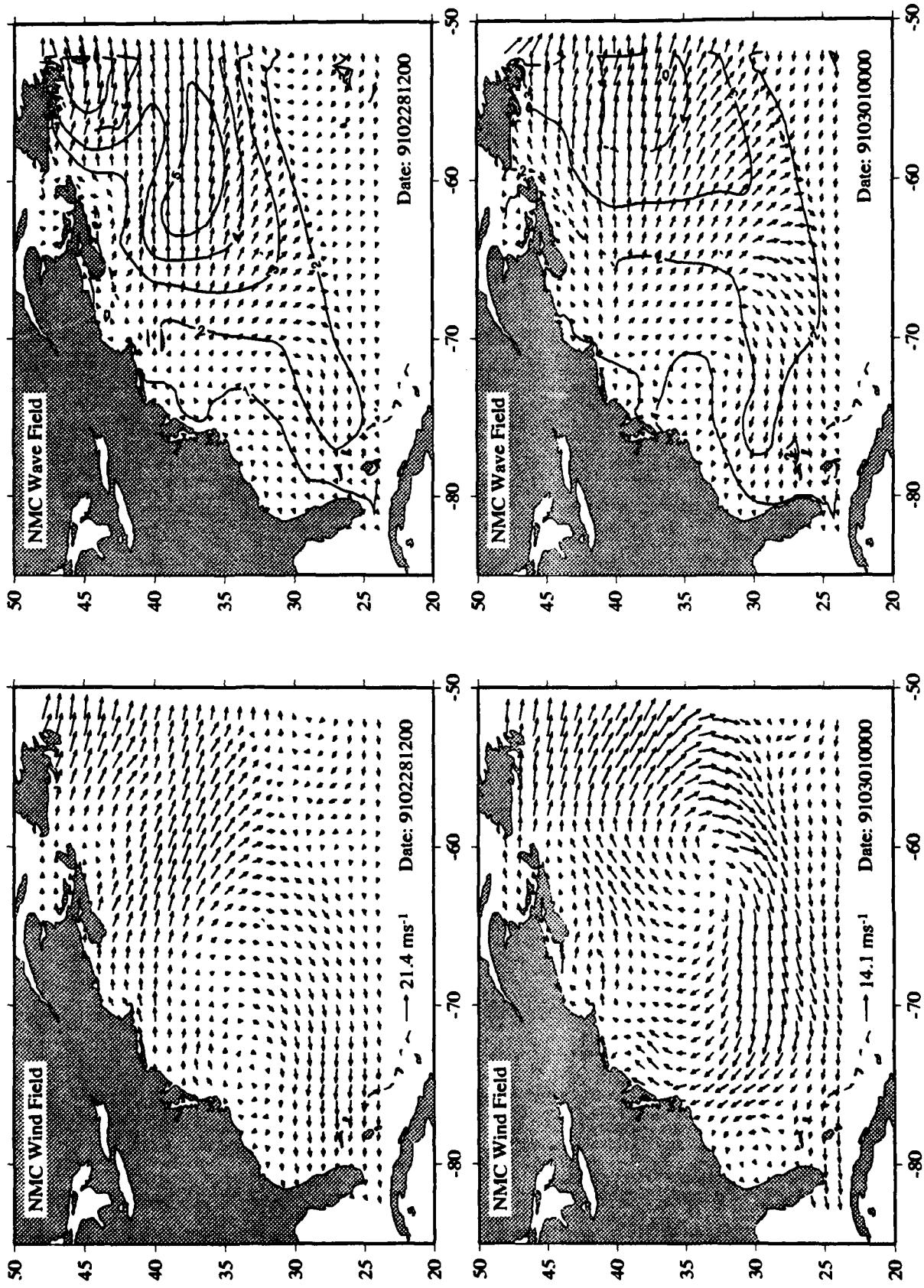
Custer diagrams are presented for the time period from 24 February 1991, 12:00 GMT to 7 March 1991, 12:00 GMT of the wind field and corresponding wave hindcasts. Note that all wind fields for 8 March 1991 were not available and the shown fields were computed from linear interpolation.

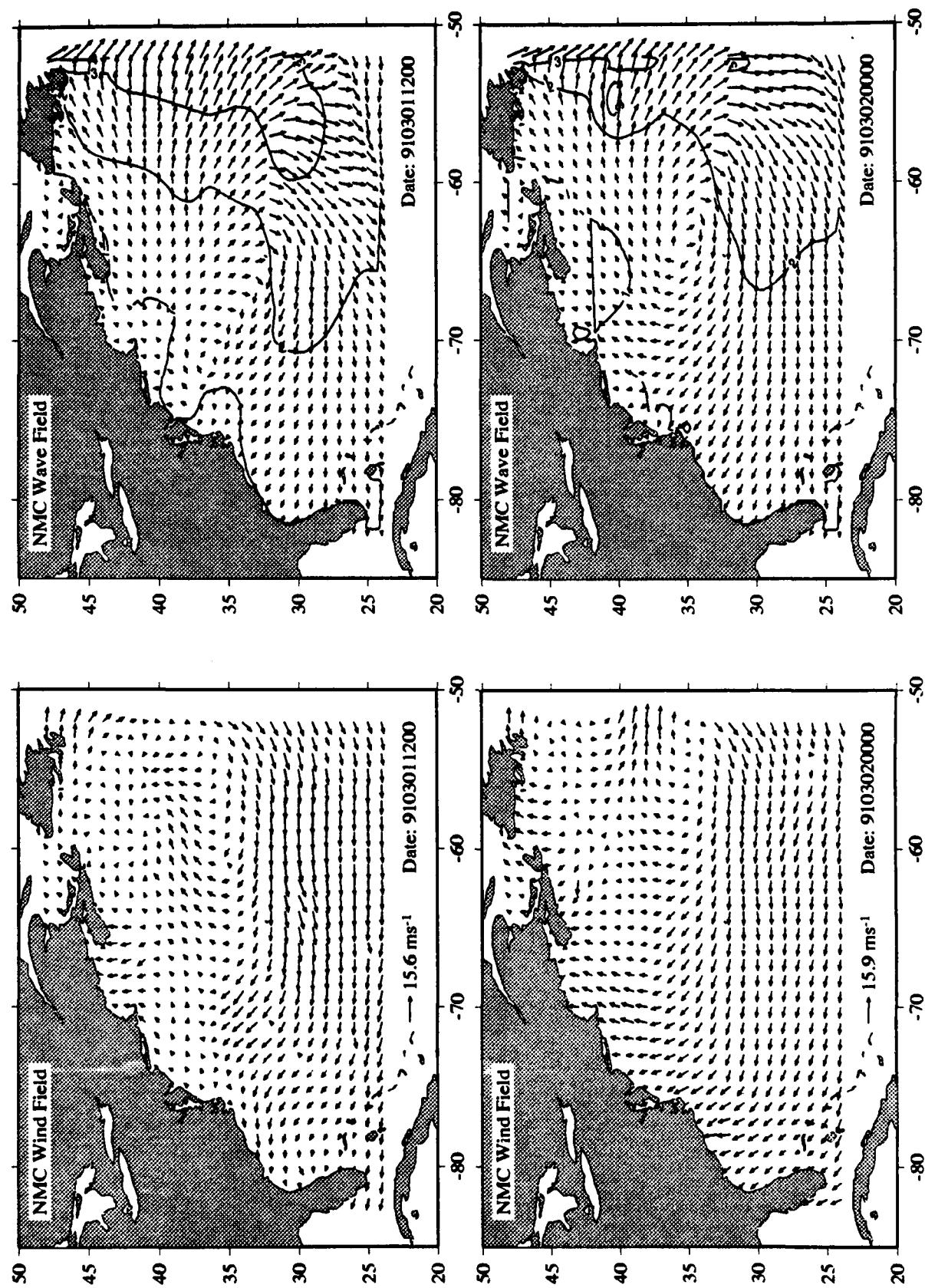




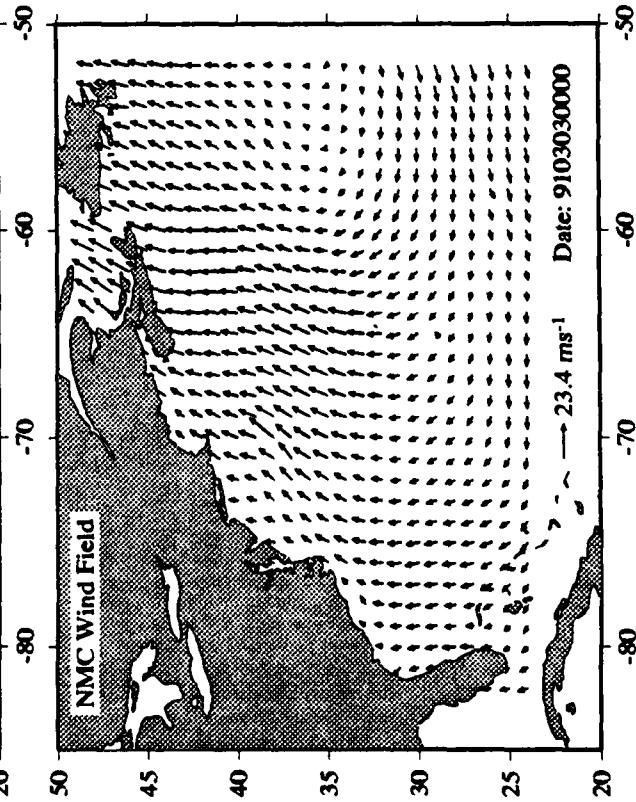
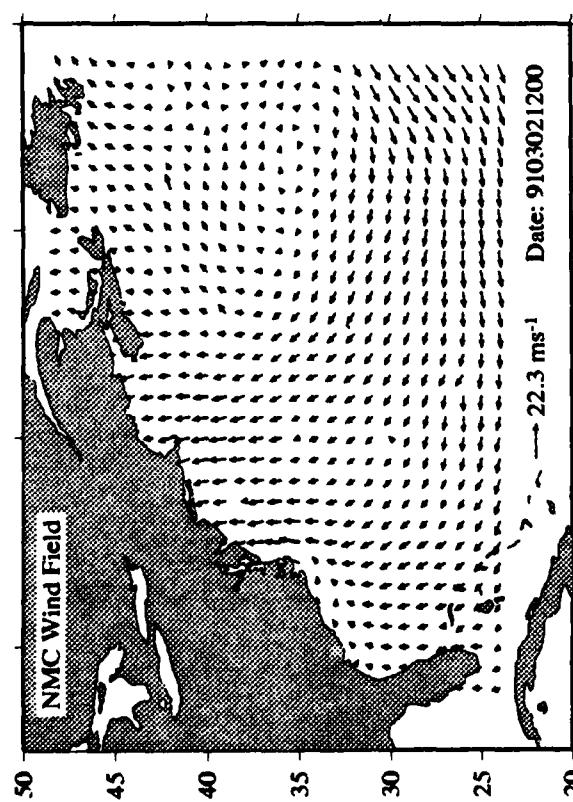
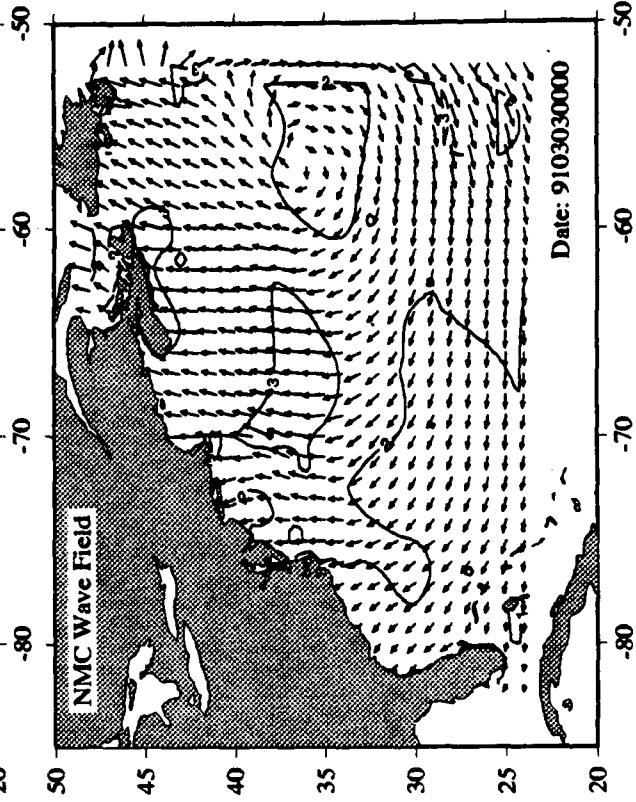
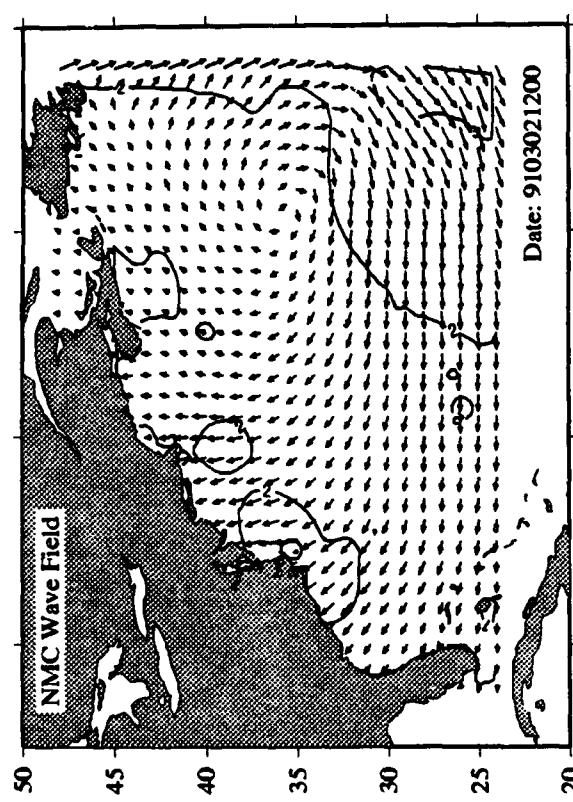


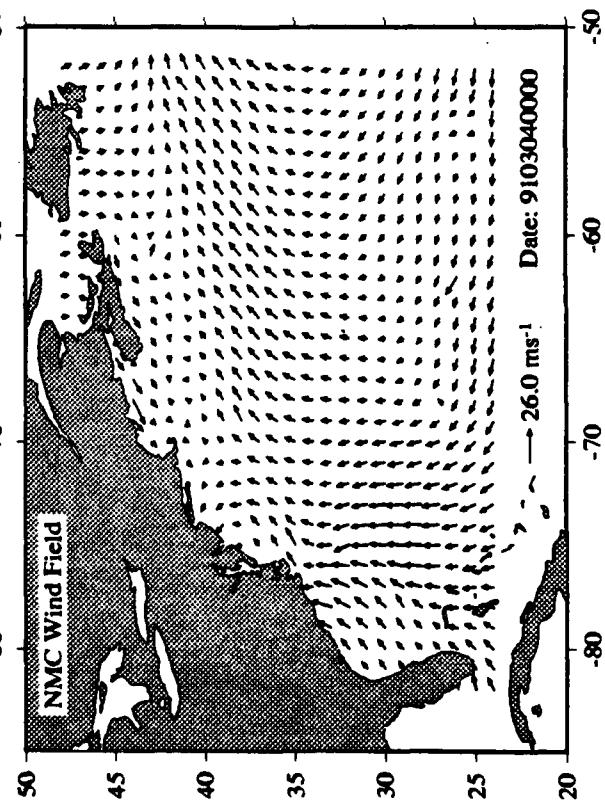
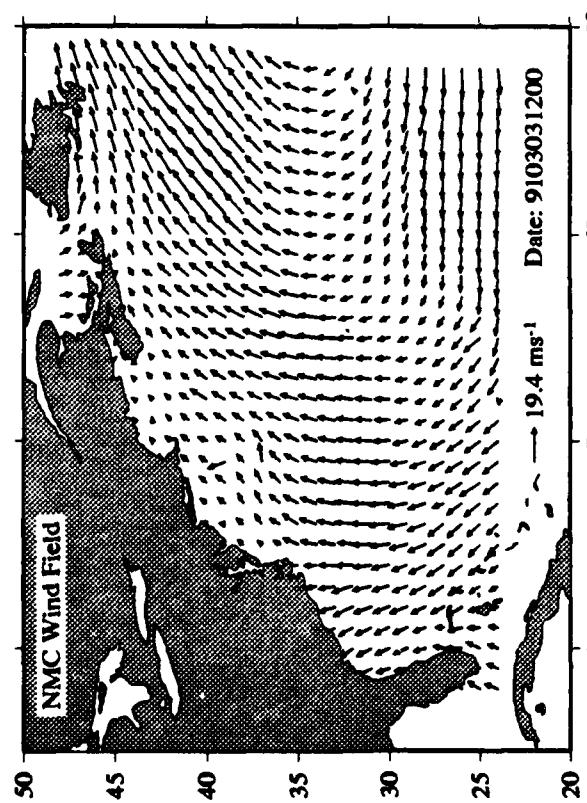
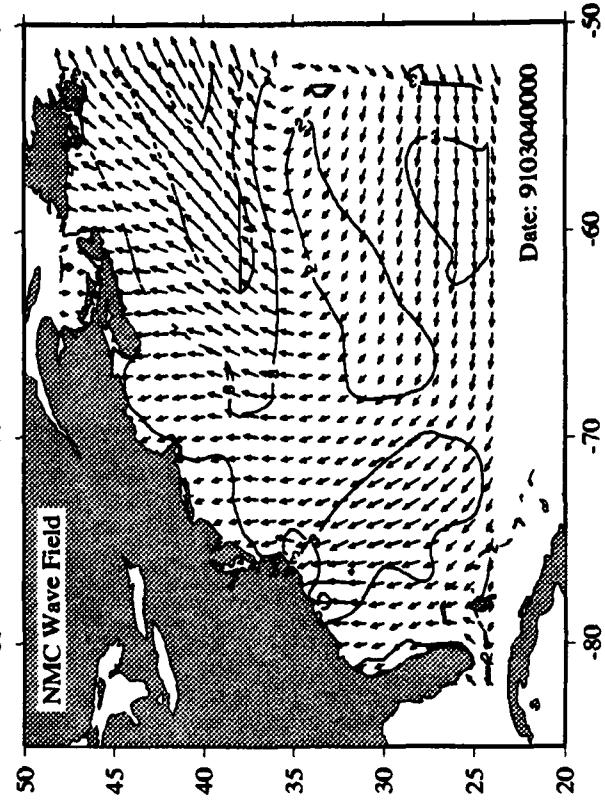
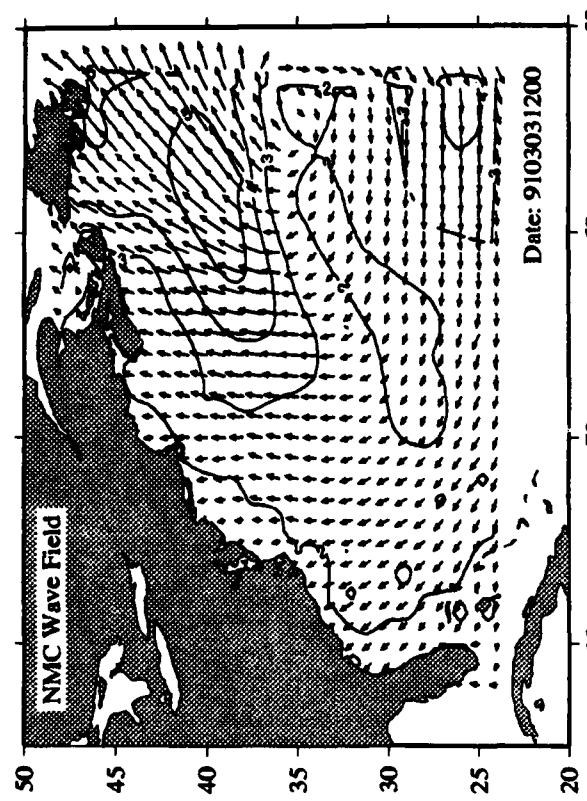


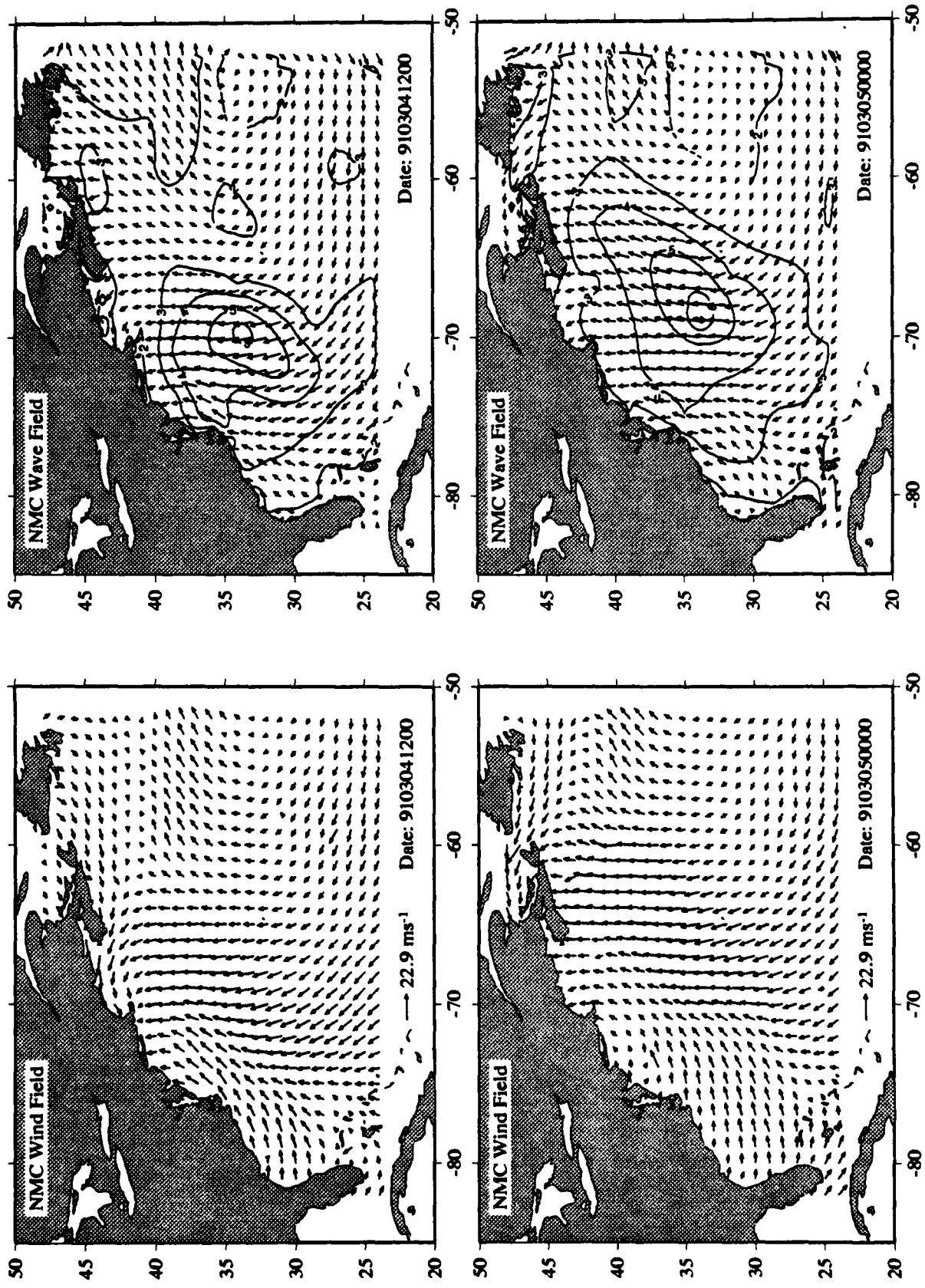


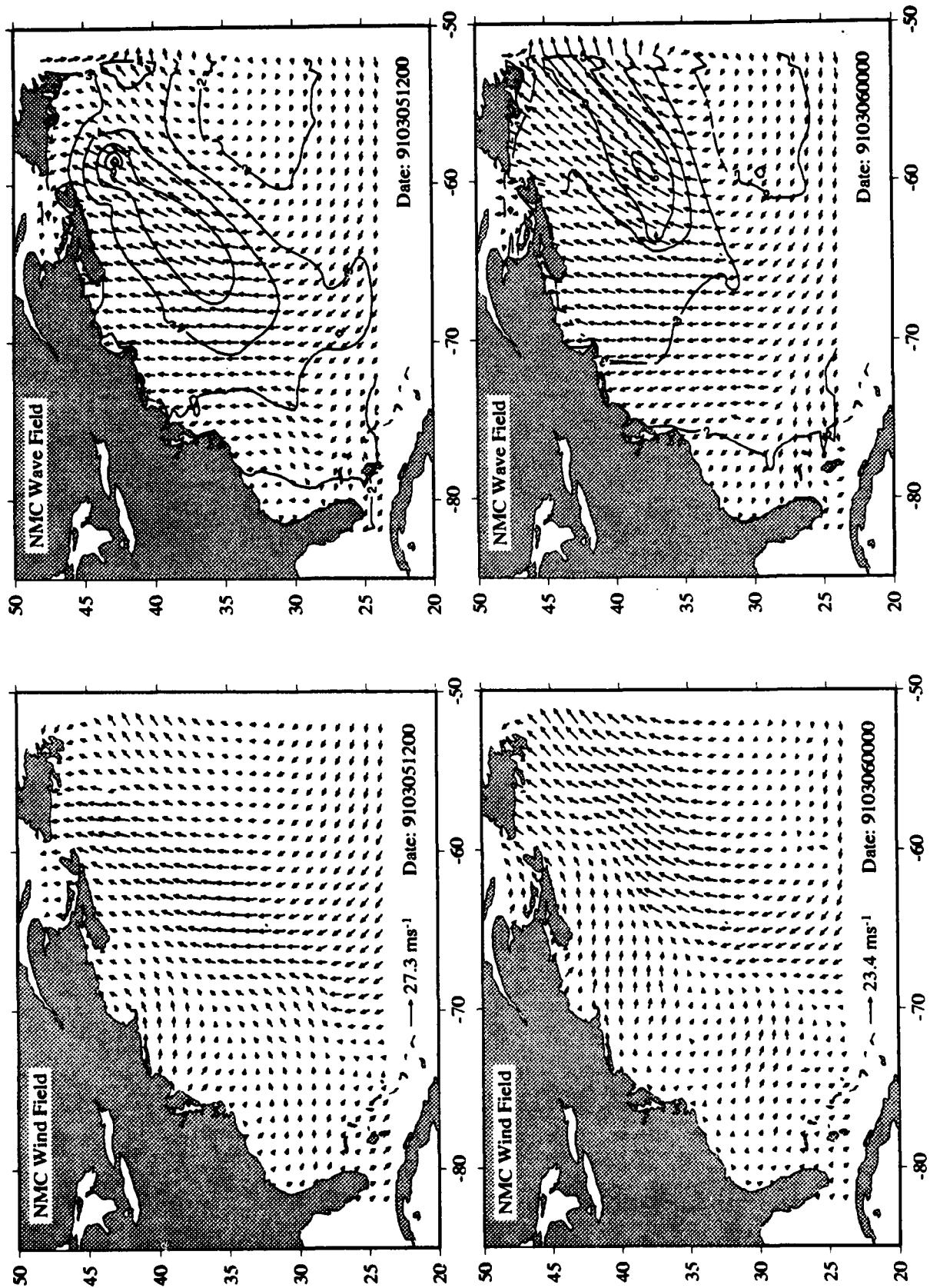


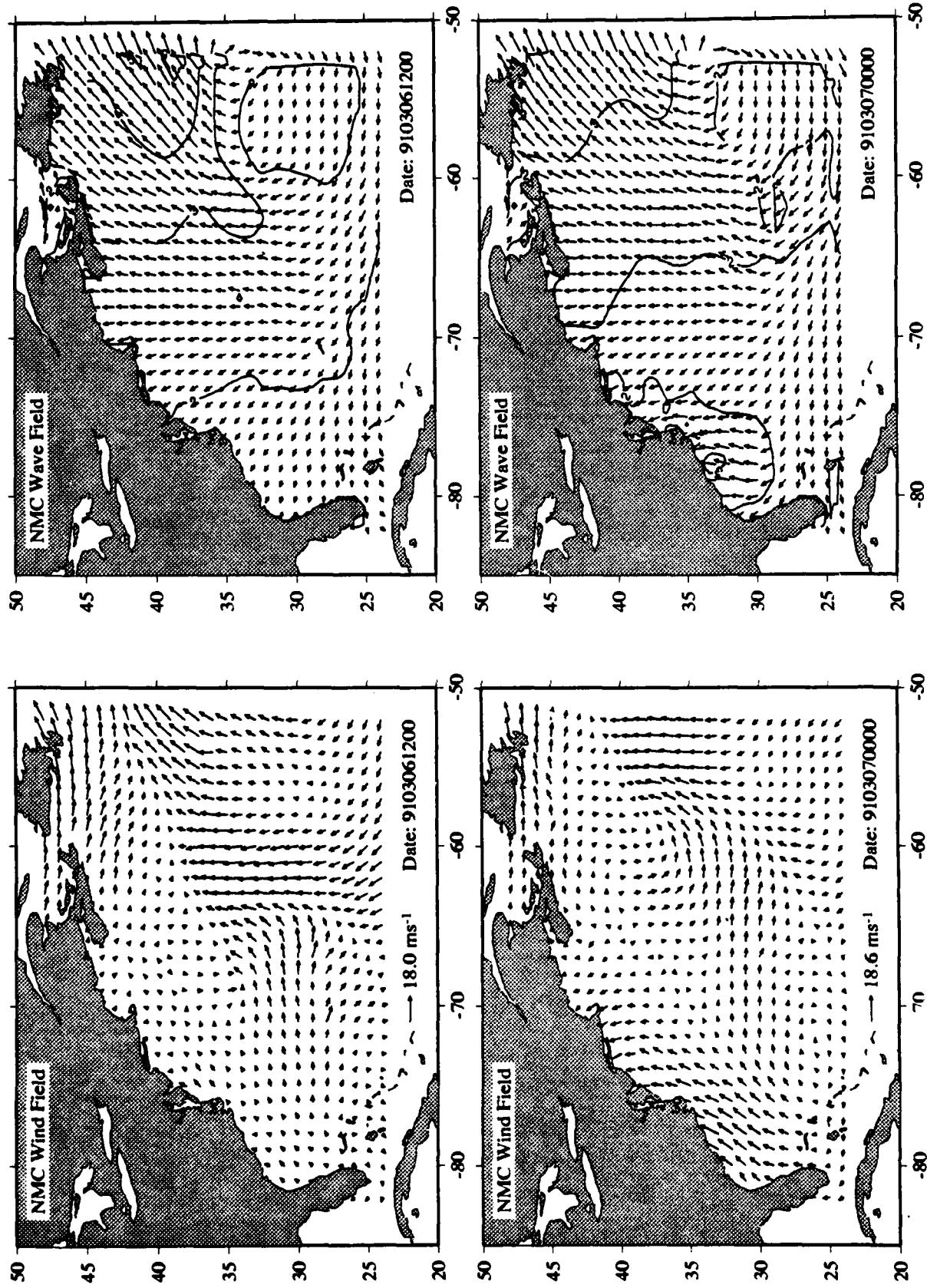
Appendix D Cluster Diagrams of Wind fields and Wave Hindcasts

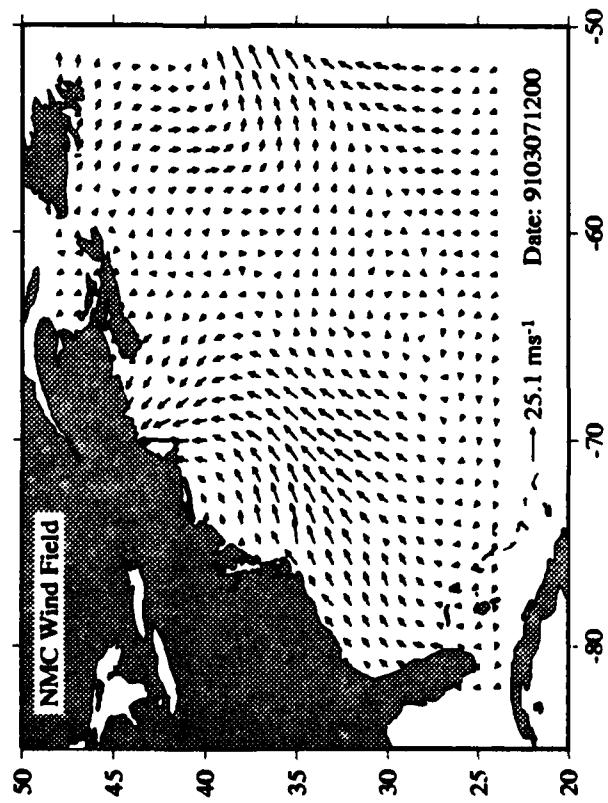
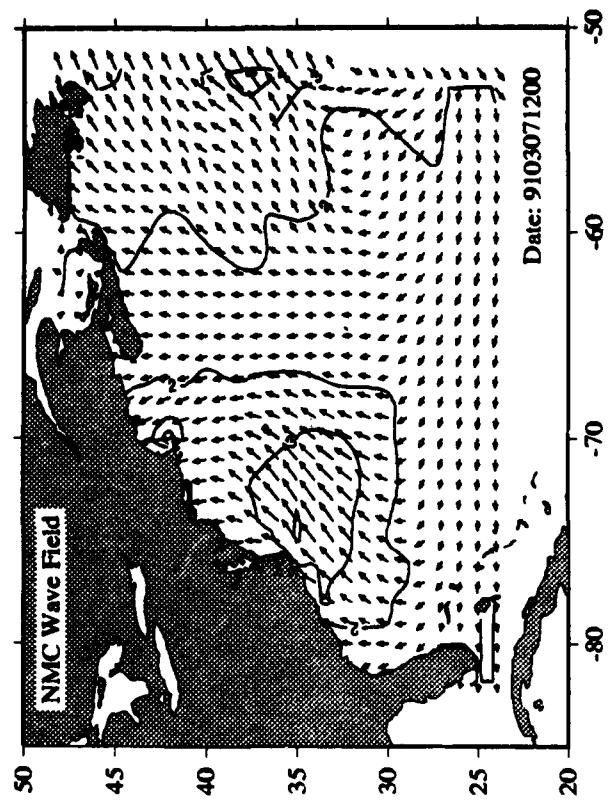






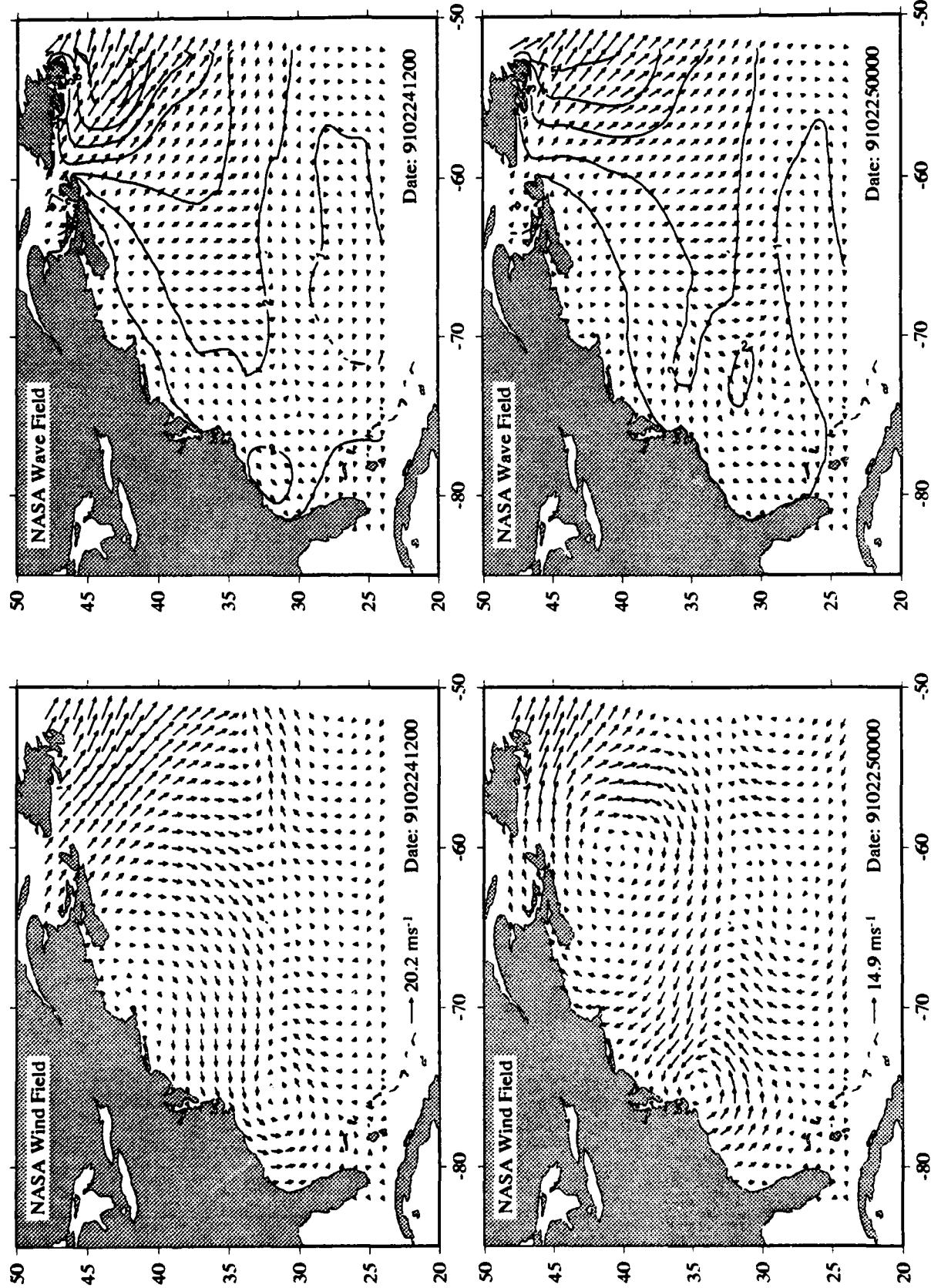


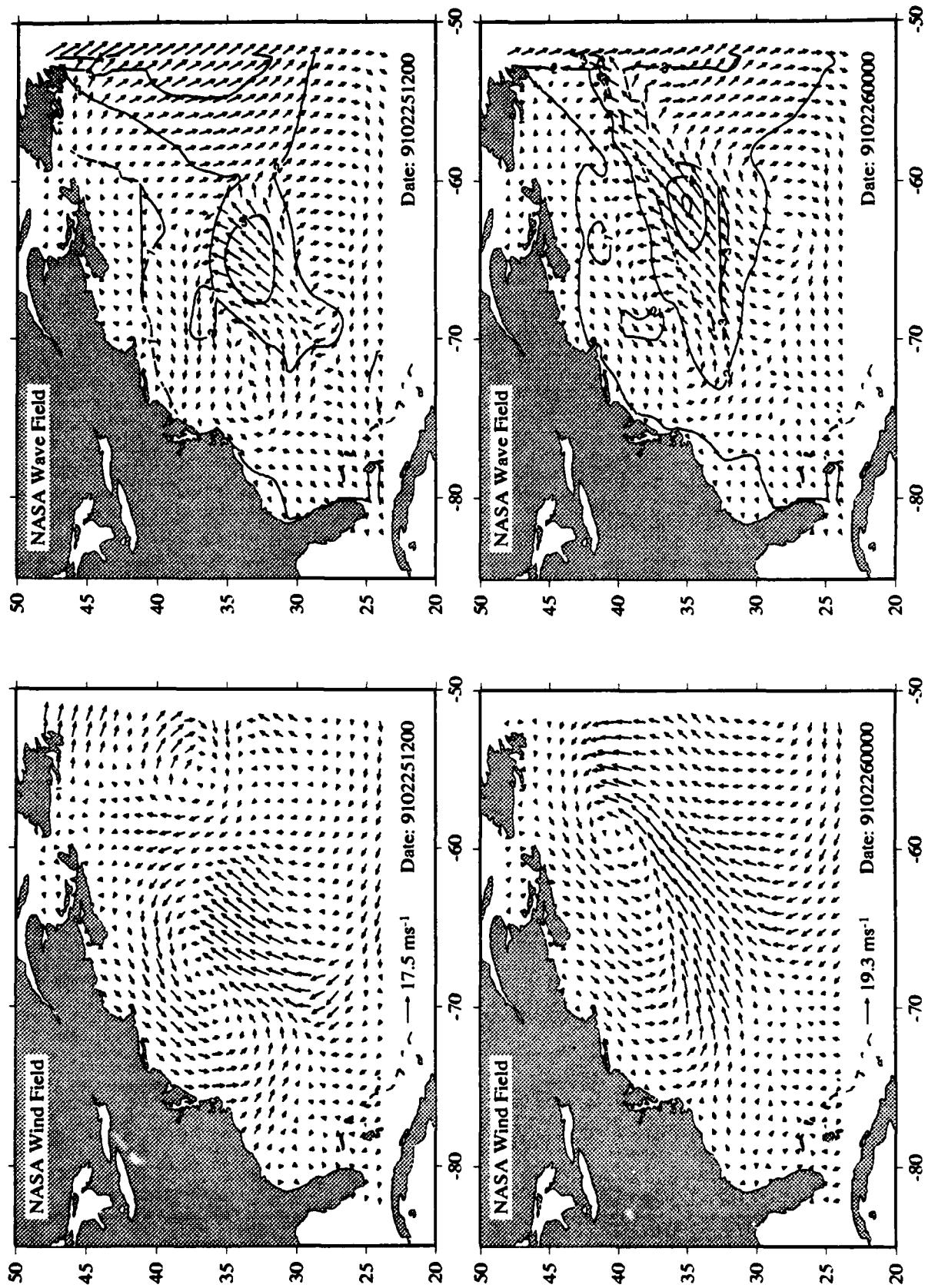




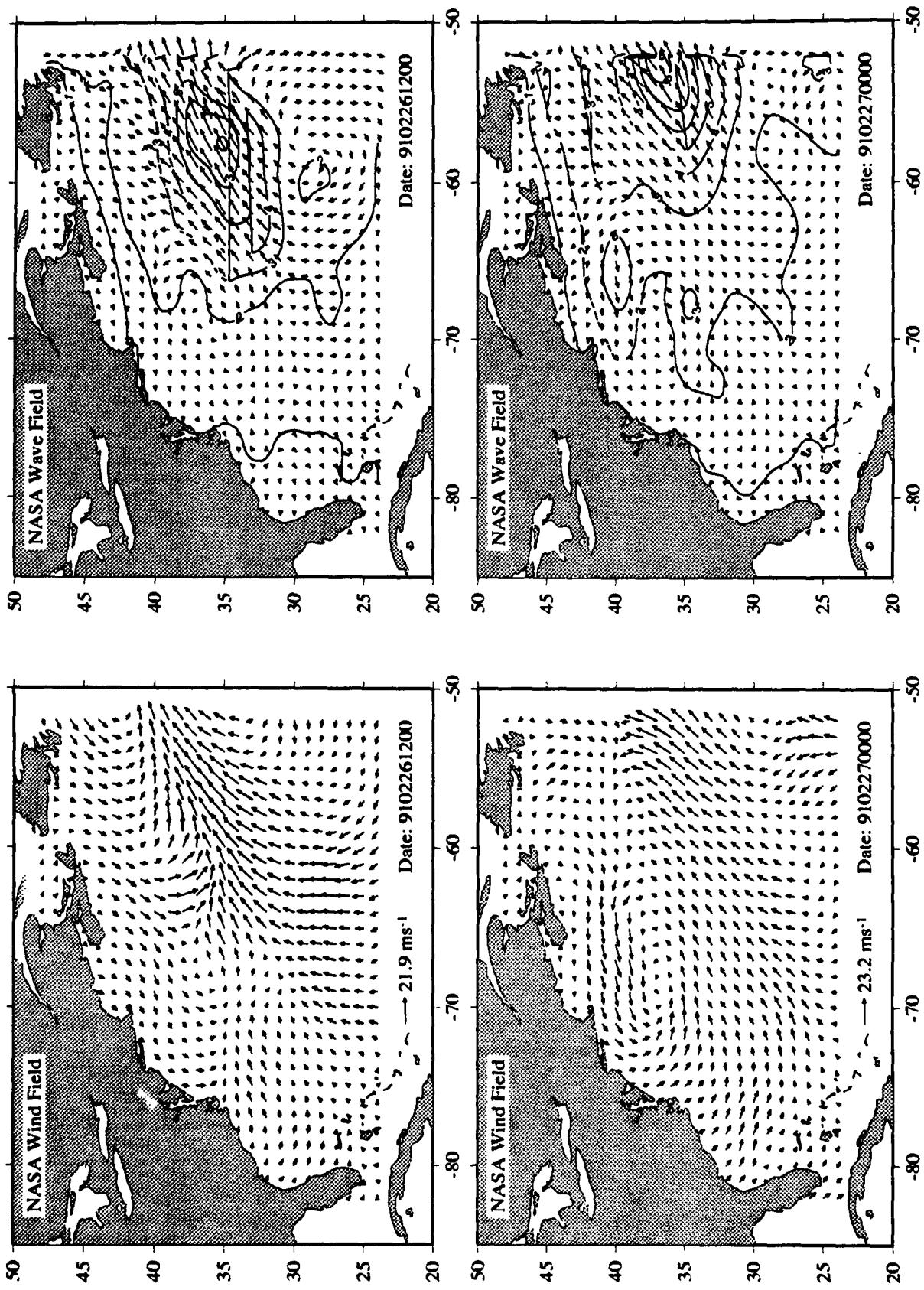
D.5: NASA Goddard Space Flight Facility (GSFC)

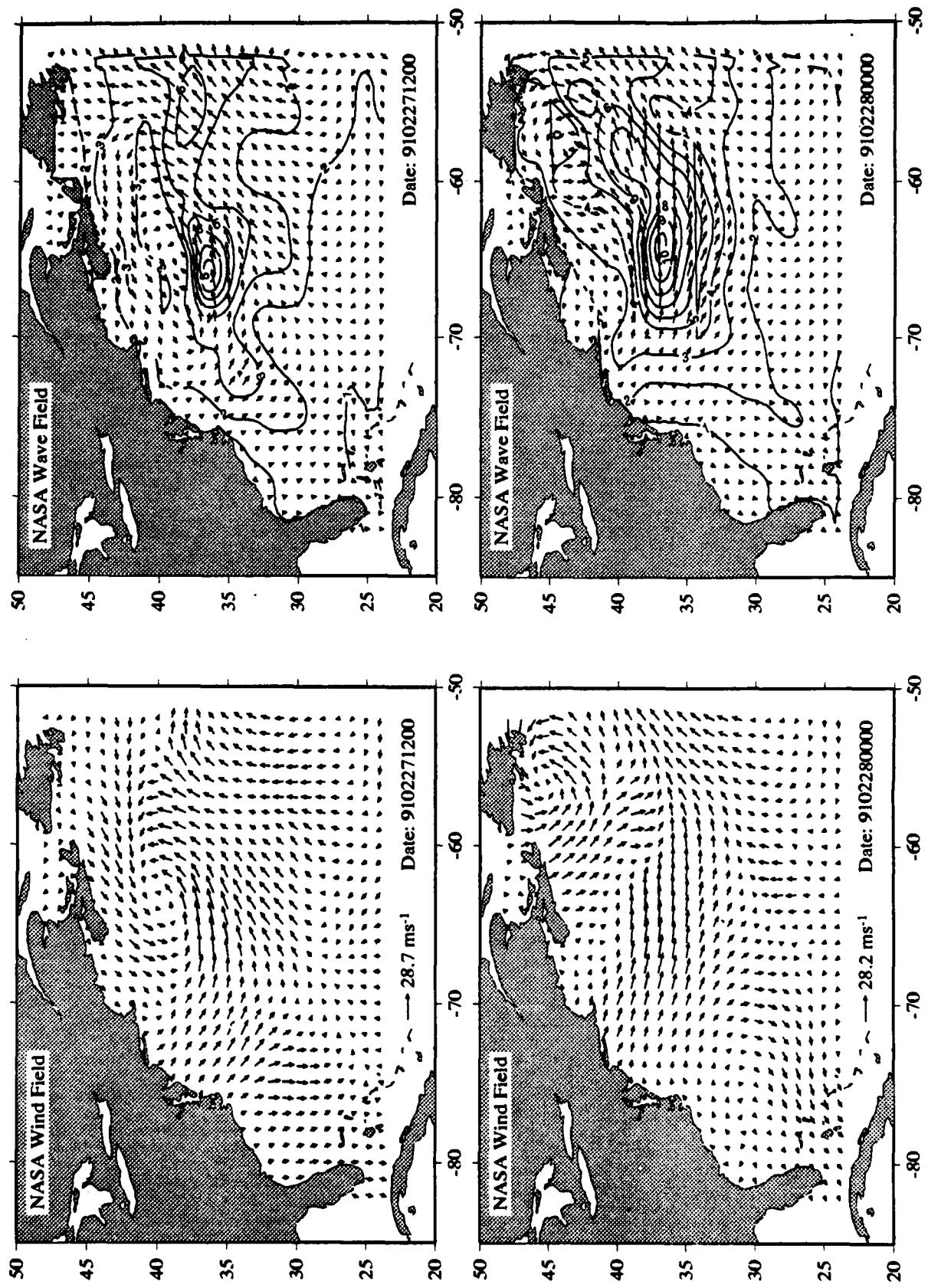
Custer diagrams are presented for the time period from 24 February 1991, 12:00 GMT to 8 March 1991, 12:00 GMT of the wind field and corresponding wave hindcasts. Note that the wind field for 8 March 1991, 12:00 GMT was not available and the shown field was computed from linear interpolation.



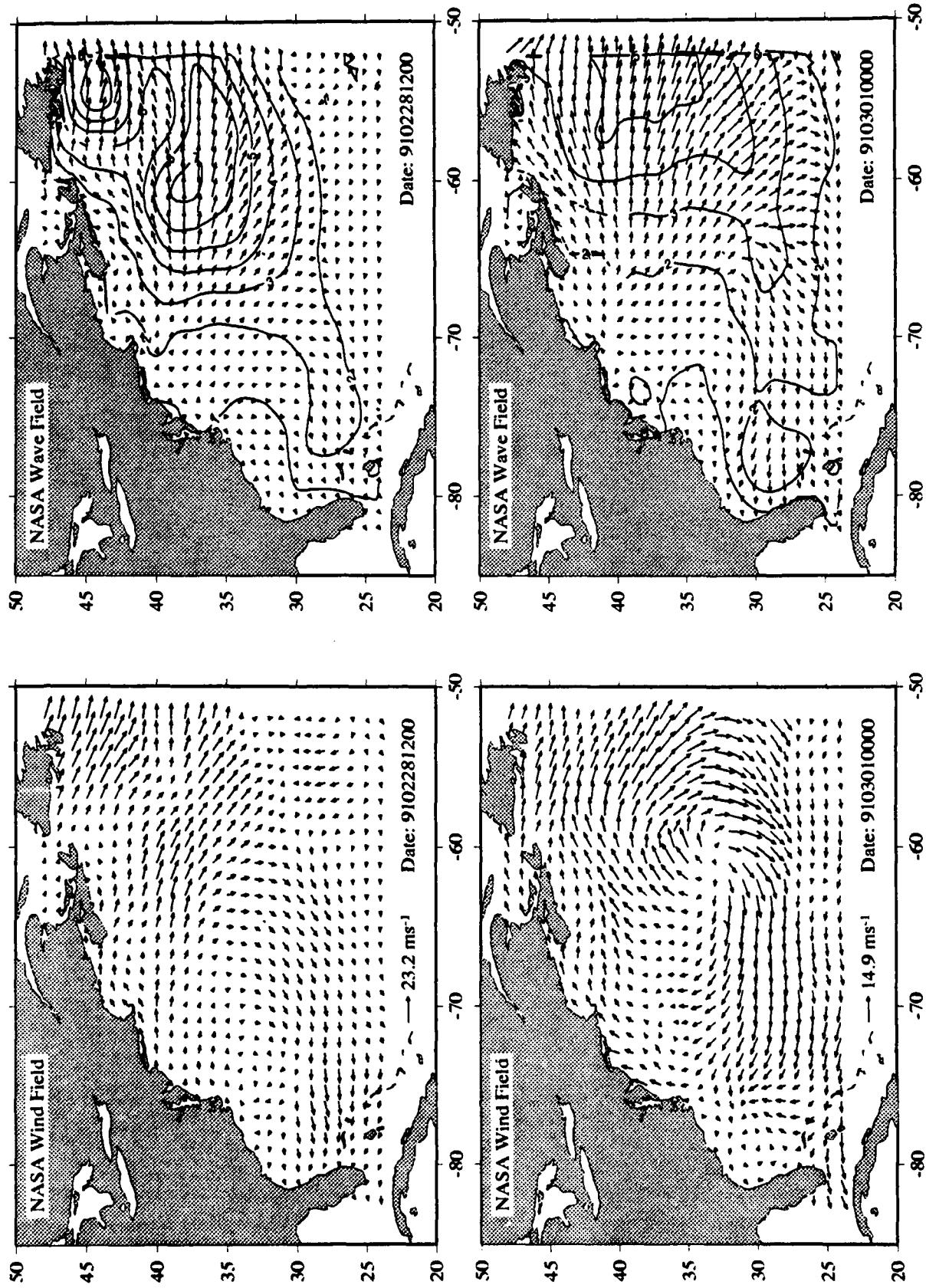


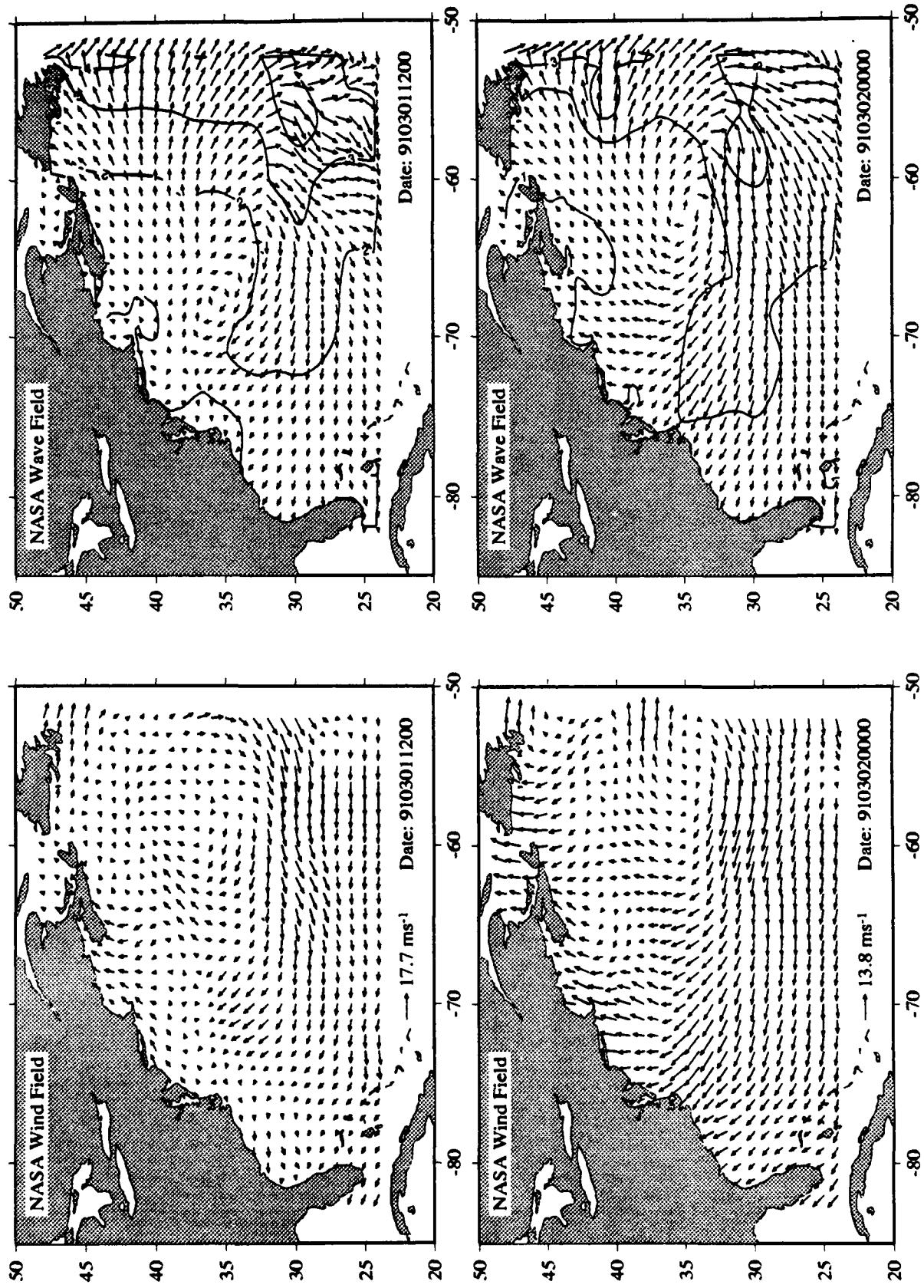
Appendix D Cluster Diagrams of Wind fields and Wave Hindcasts



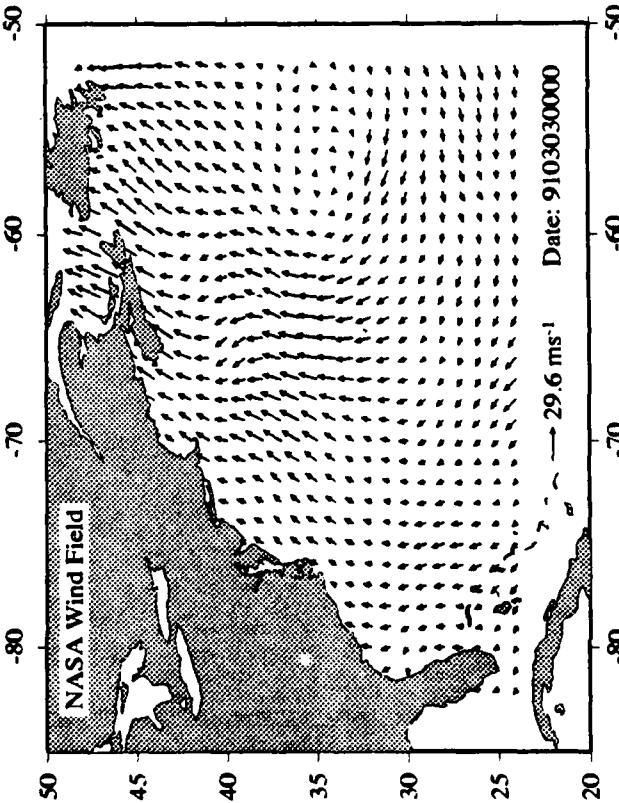
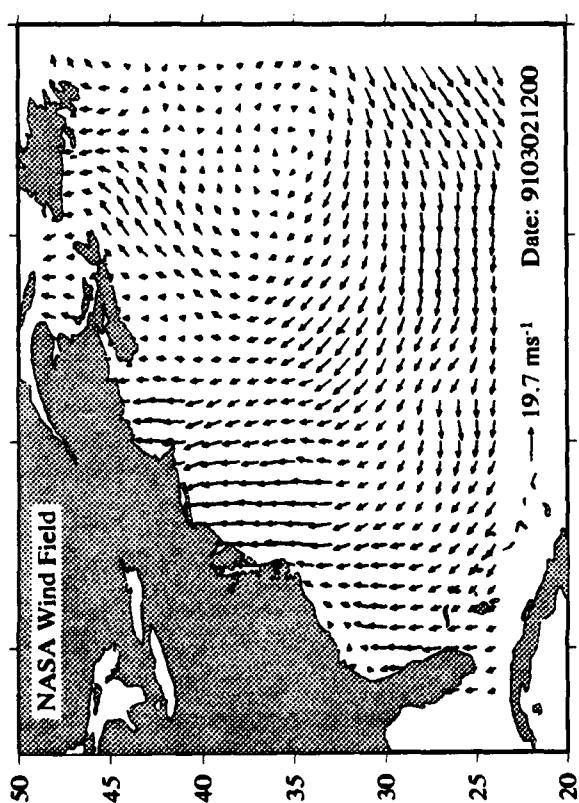
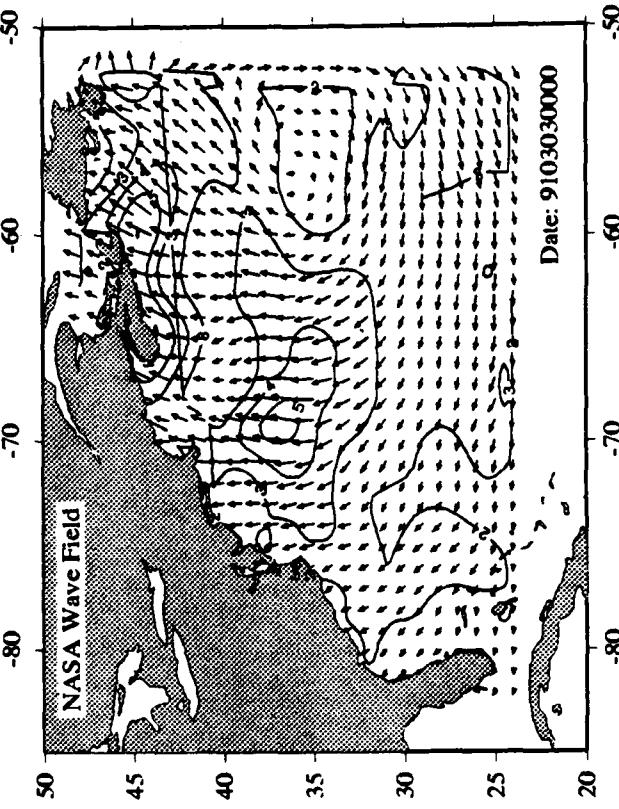
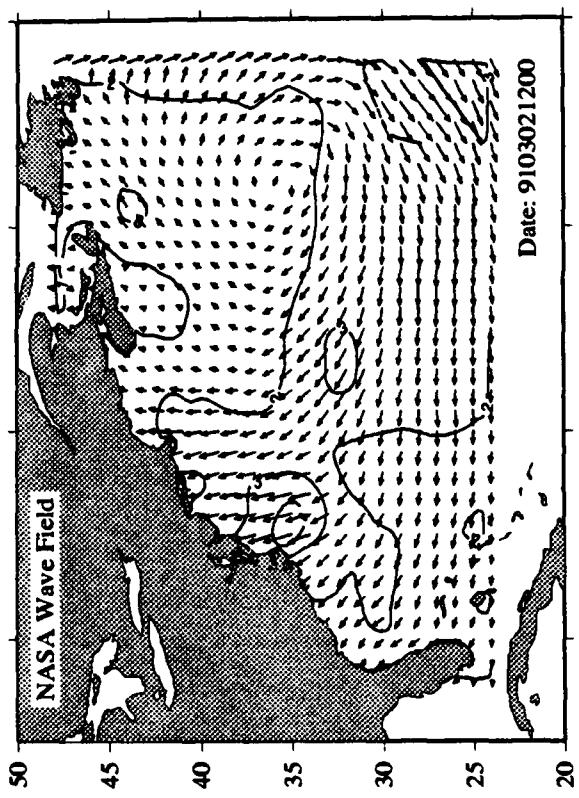


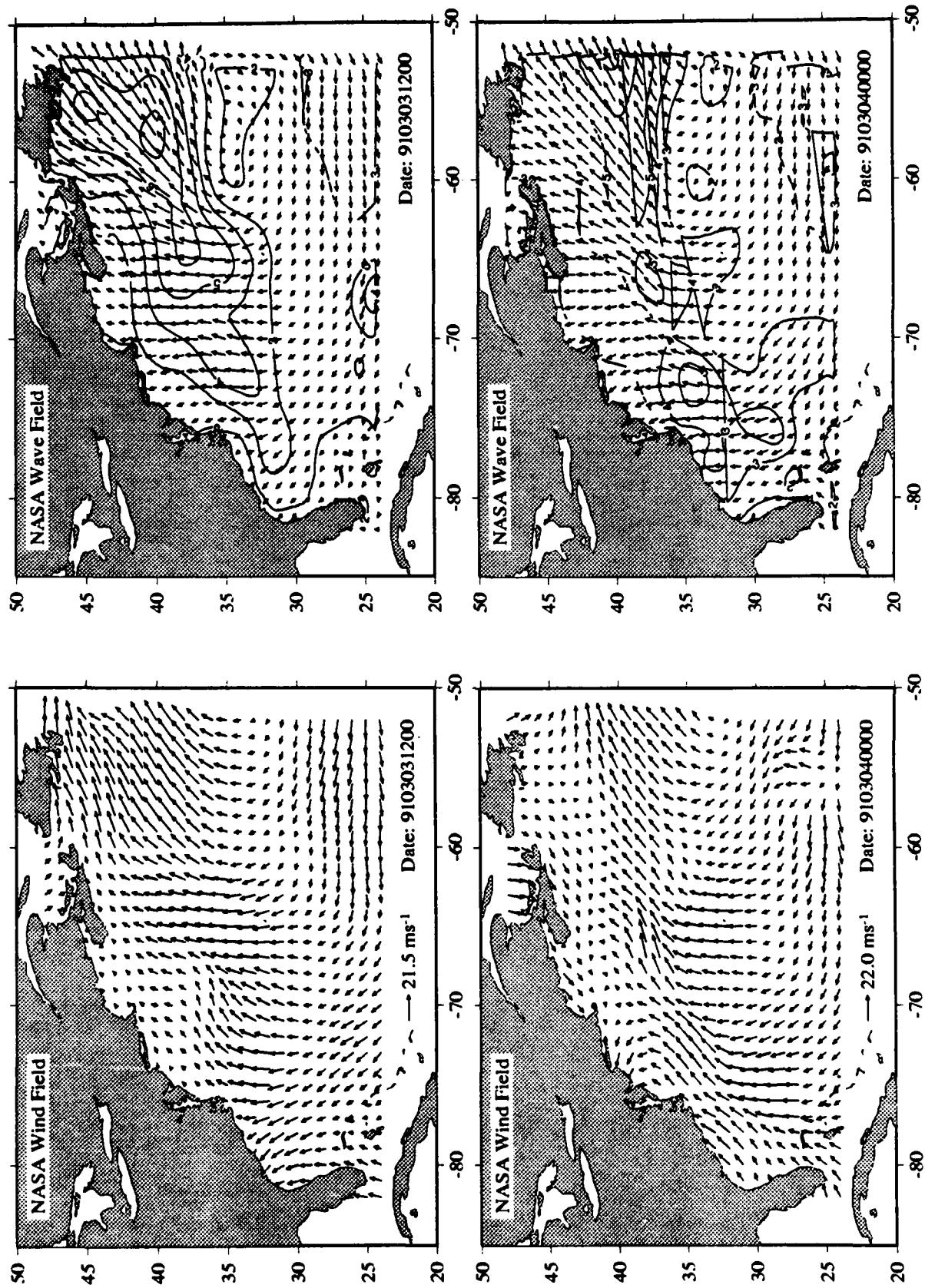
Appendix D Cluster Diagrams of Wind fields and Wave Hindcasts



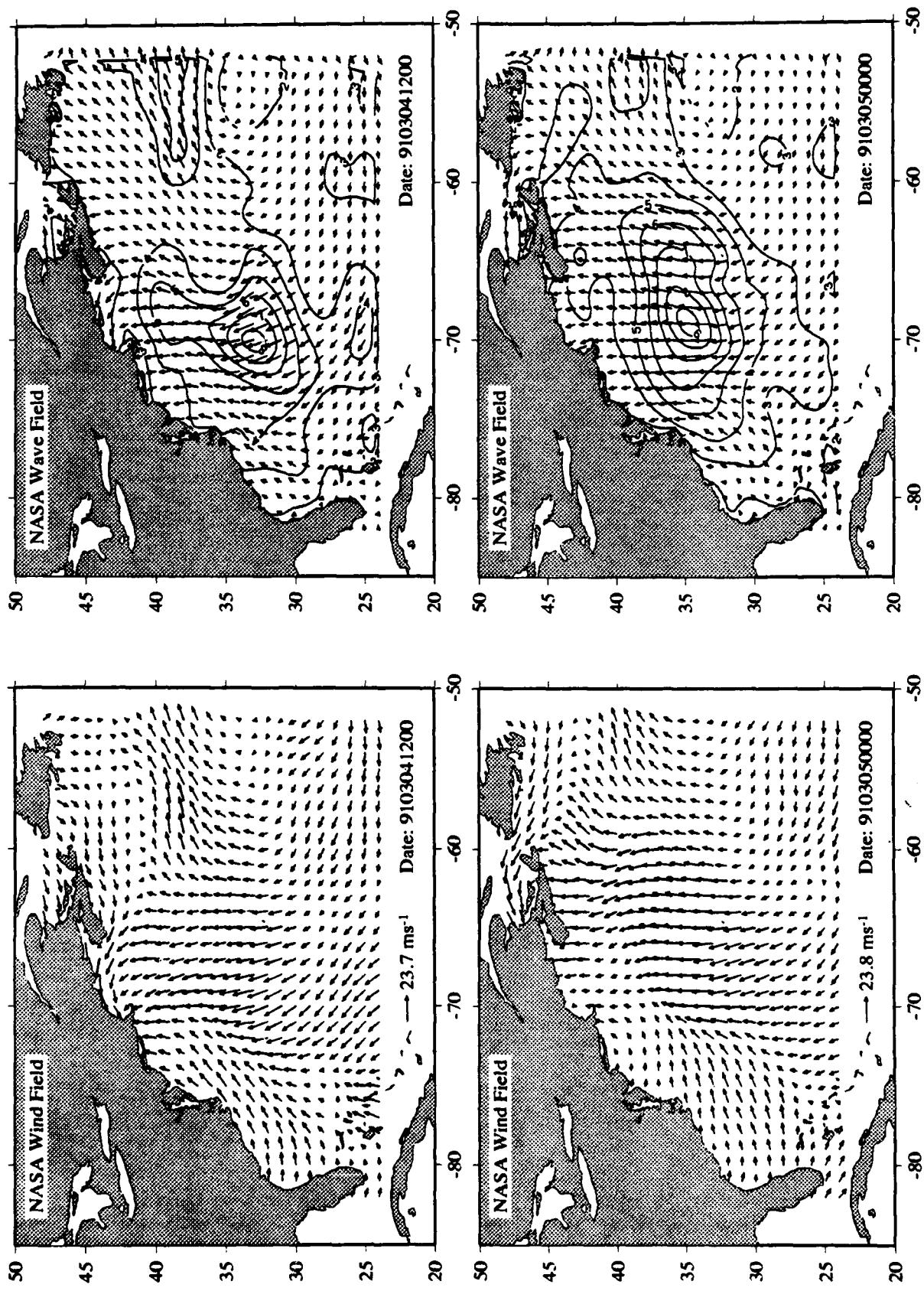


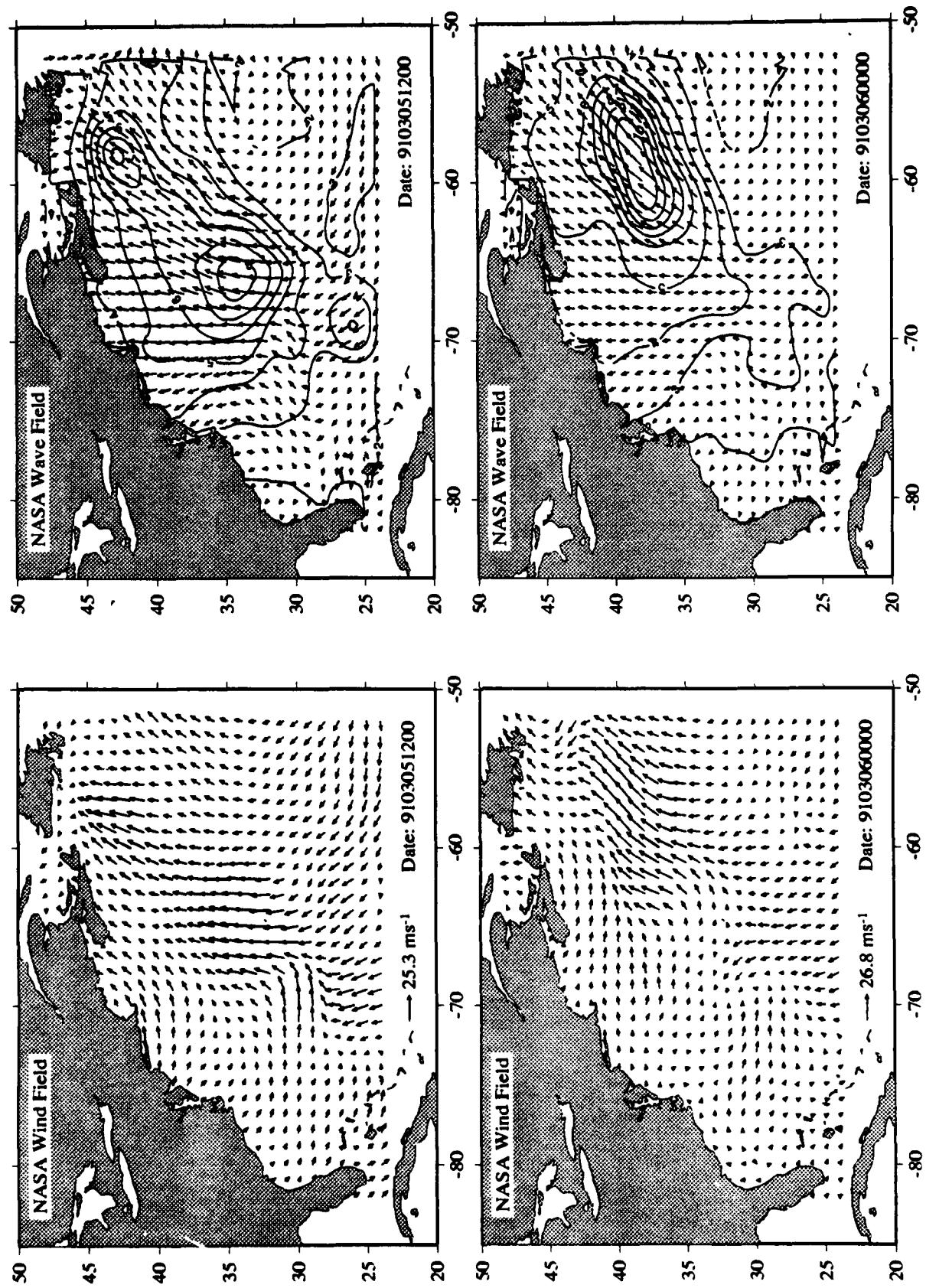
Appendix D Cluster Diagrams of Wind fields and Wave Hindcasts

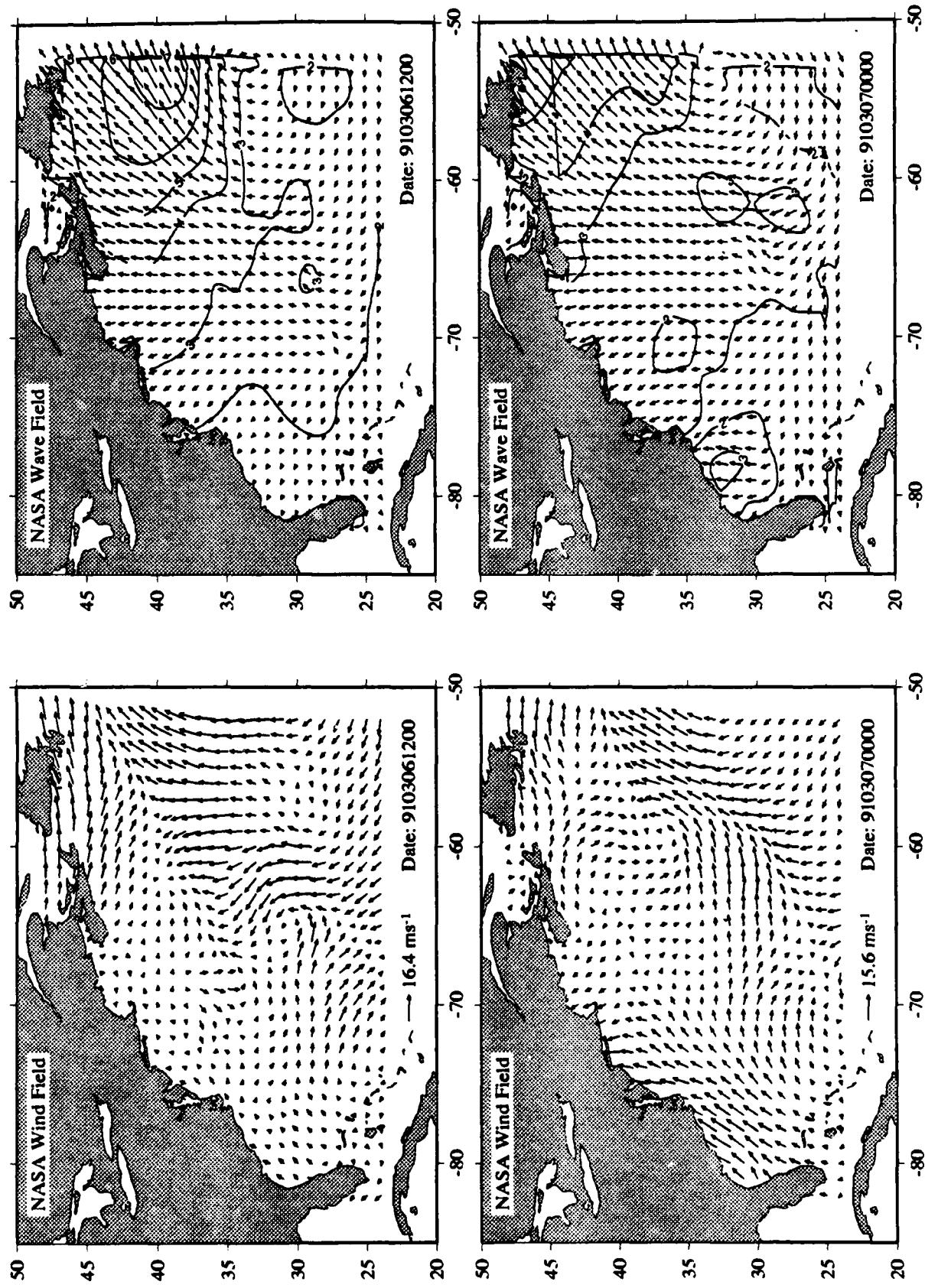


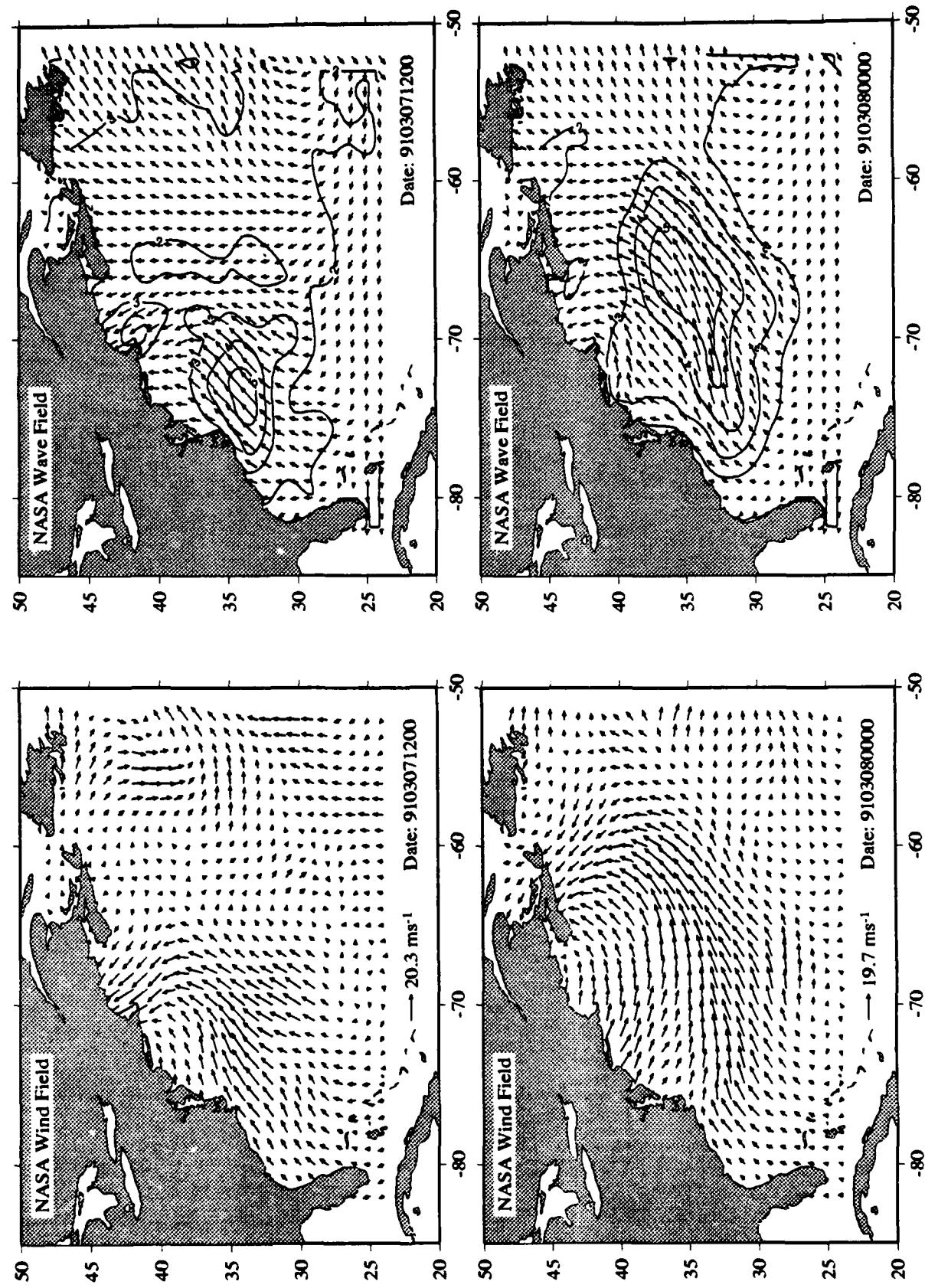


Appendix D Cluster Diagrams of Wind fields and Wave Hindcasts

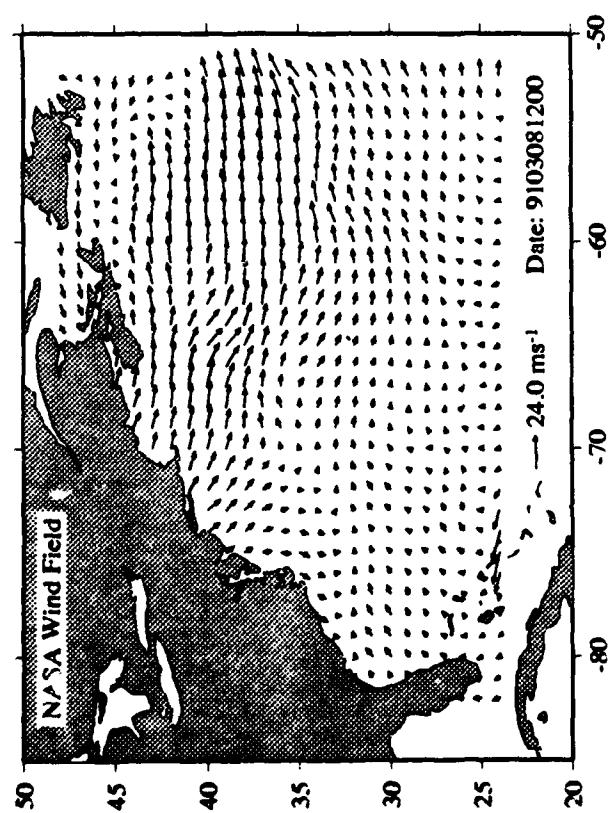
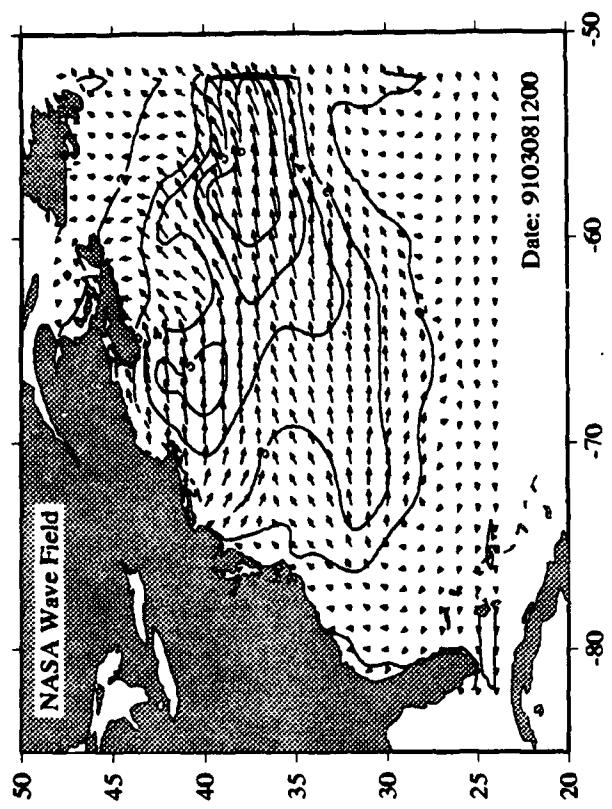






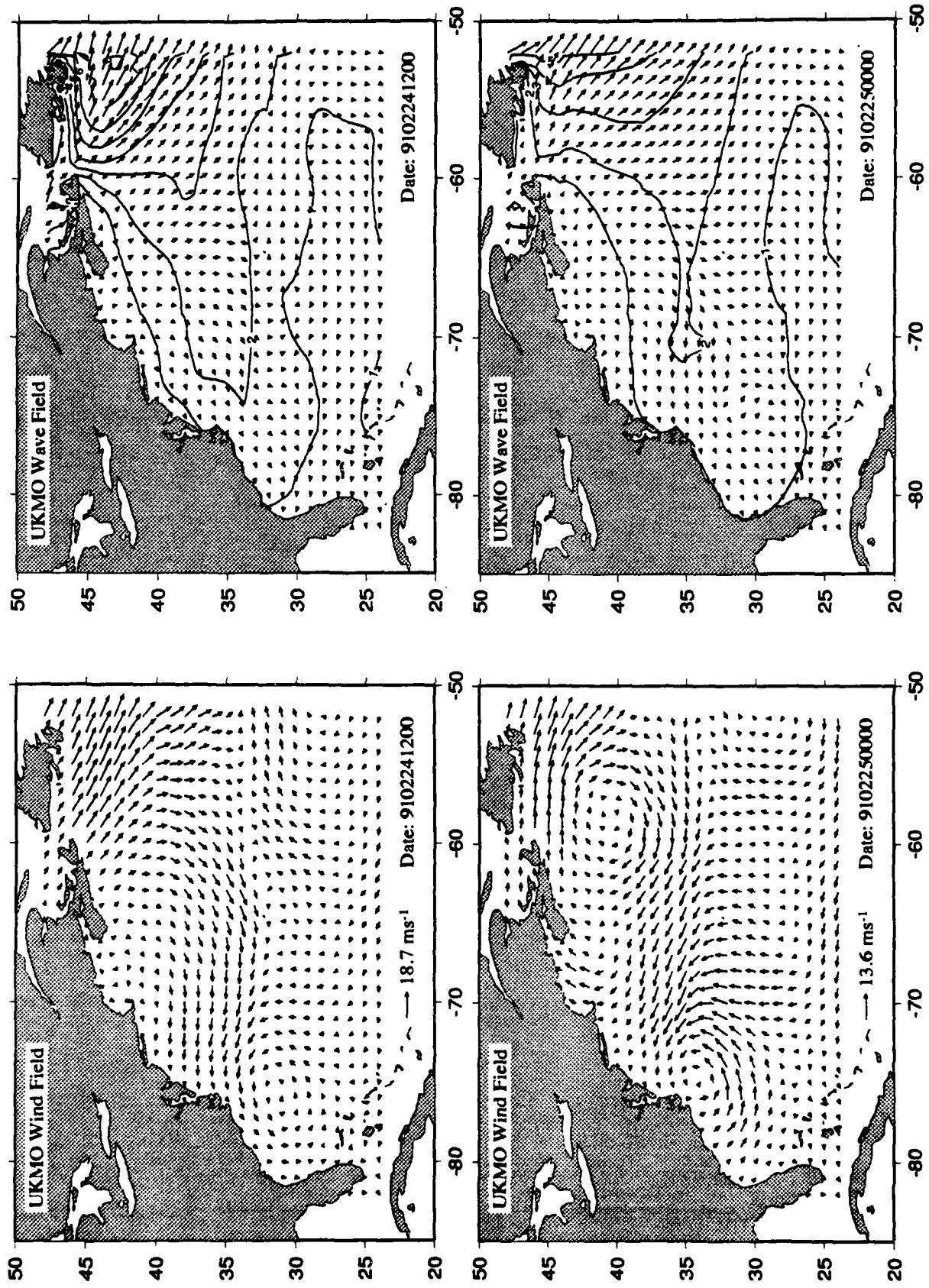


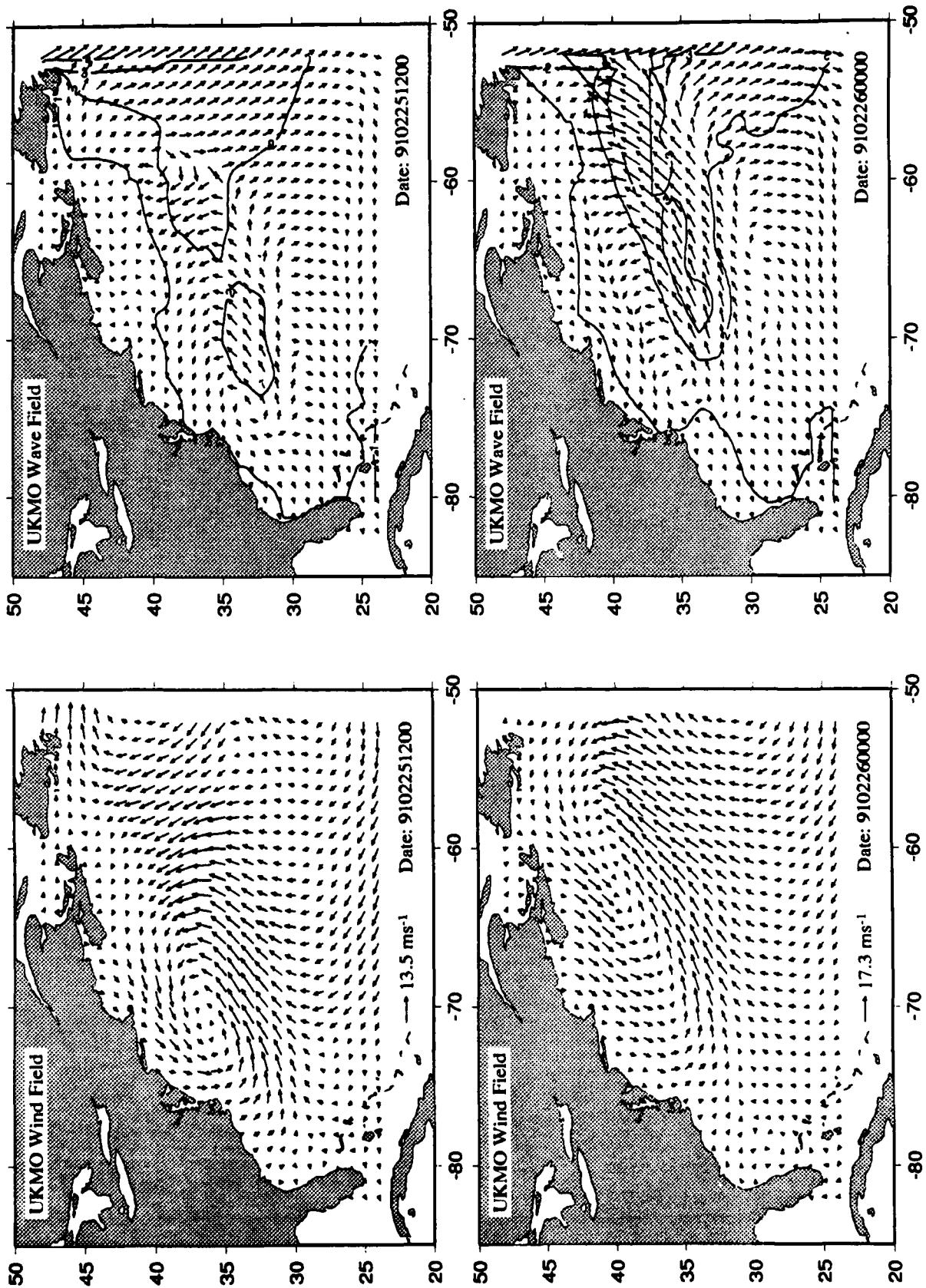
Appendix D Cluster Diagrams of Wind fields and Wave Hindcasts



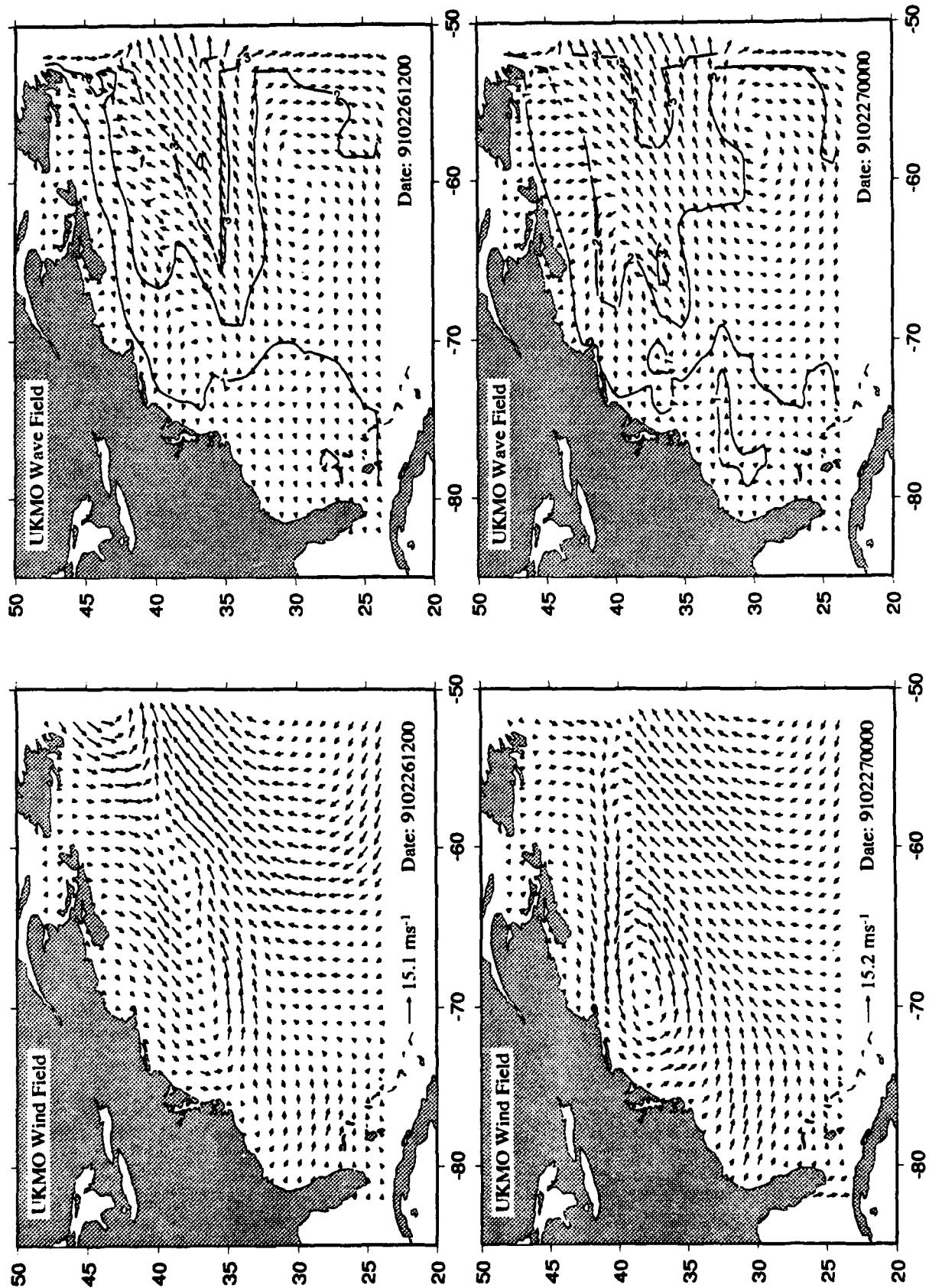
D.6: United Kingdom Meteorological Office (UKMO)

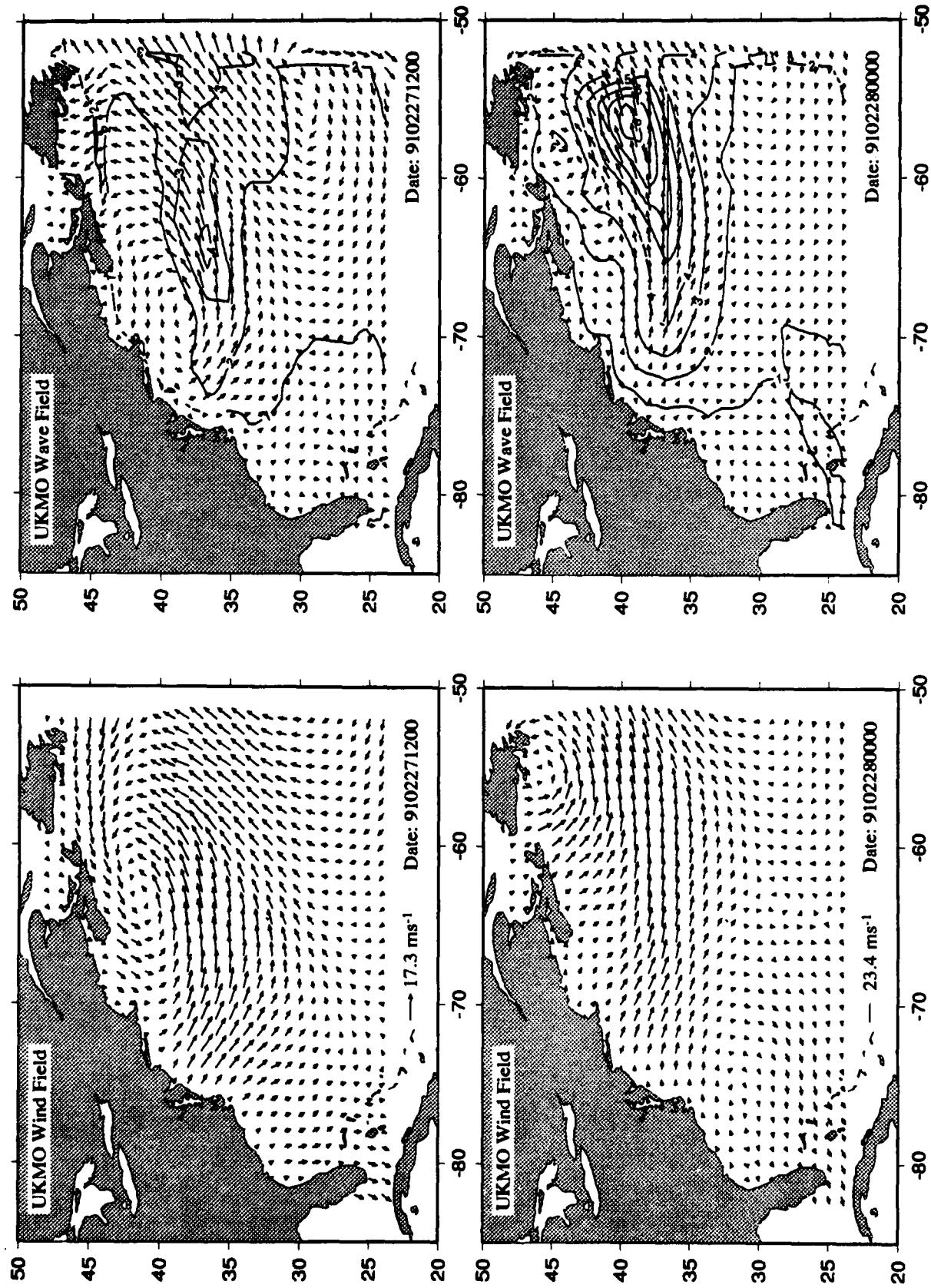
Custer diagrams are presented for the time period from 24 February 1991, 12:00 GMT to 9 March 1991, 00:00 GMT of the wind field and corresponding wave hindcasts. Note that the wind fields for 27 February 1991, 00:00 - 12:00 GMT were not available and the shown fields were computed from linear interpolation.

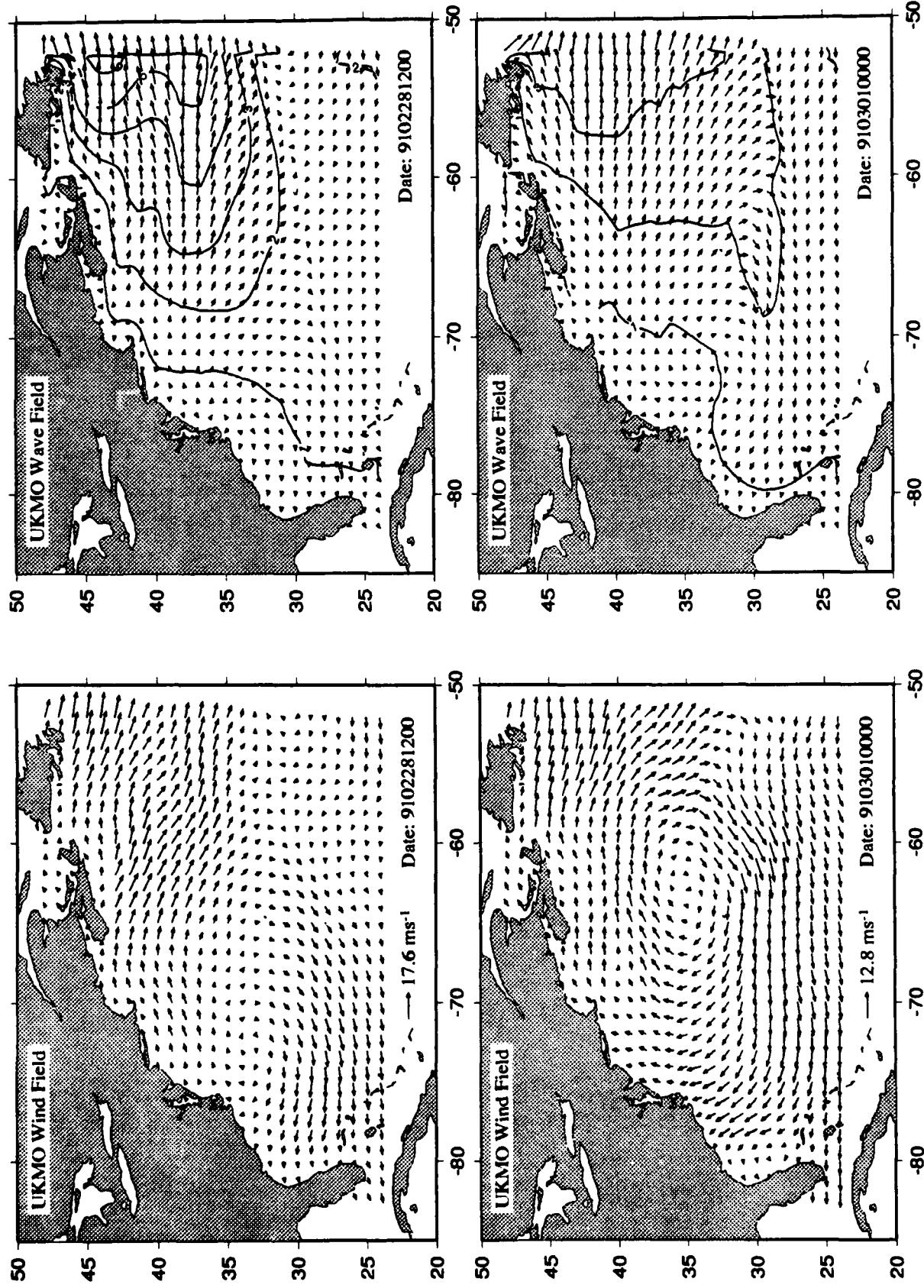


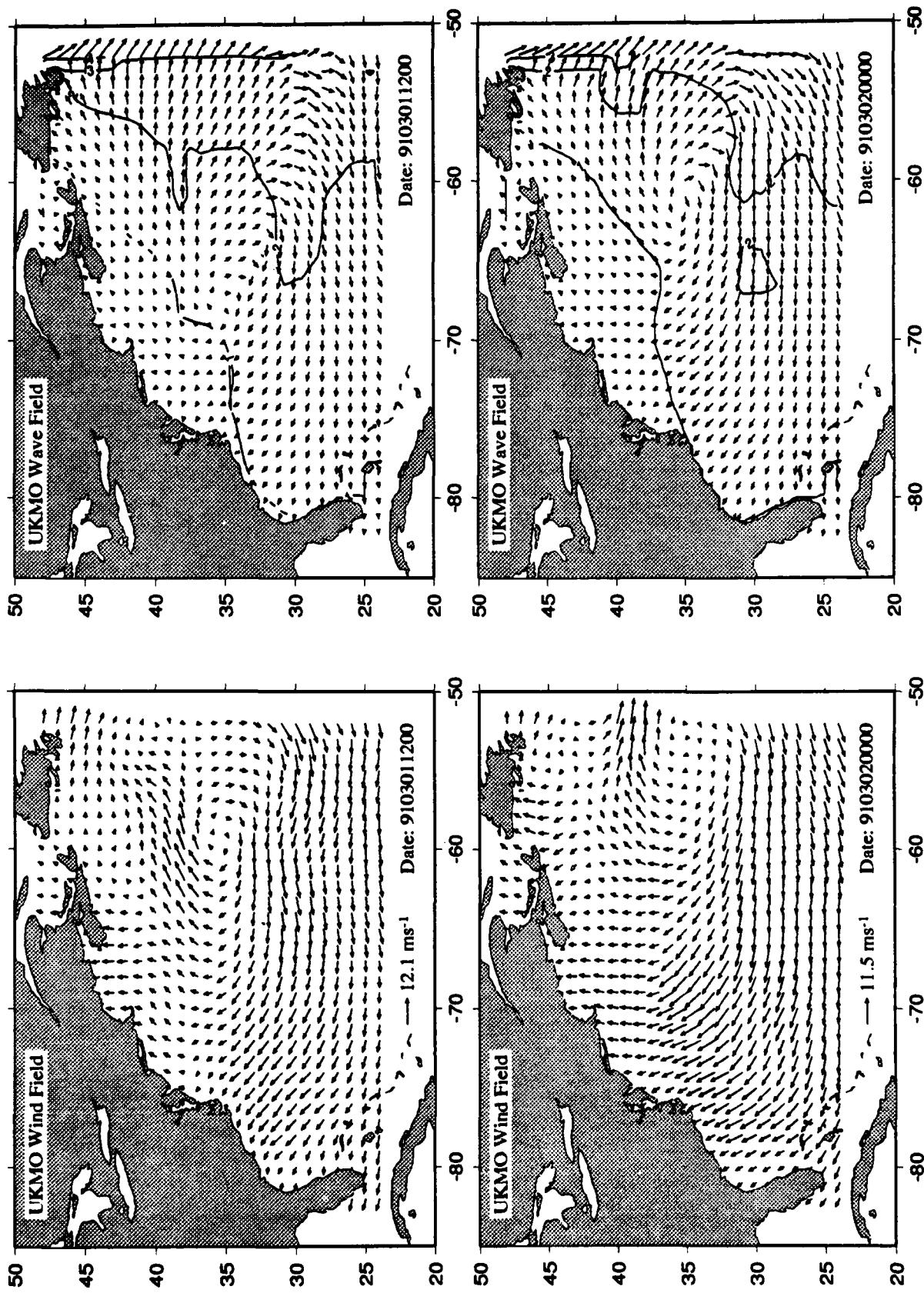


Appendix D Custer Diagrams of Wind fields and Wave Hindcasts

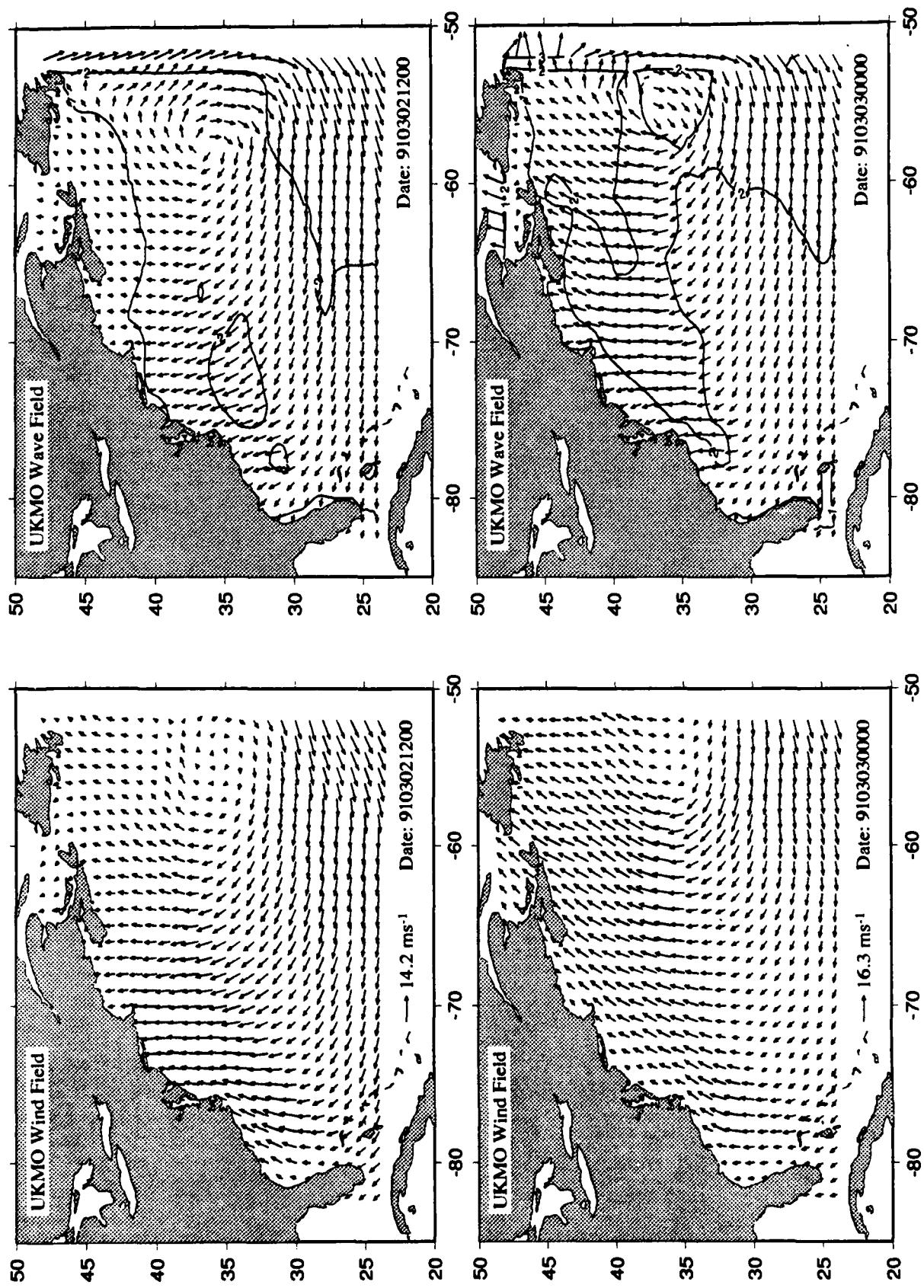


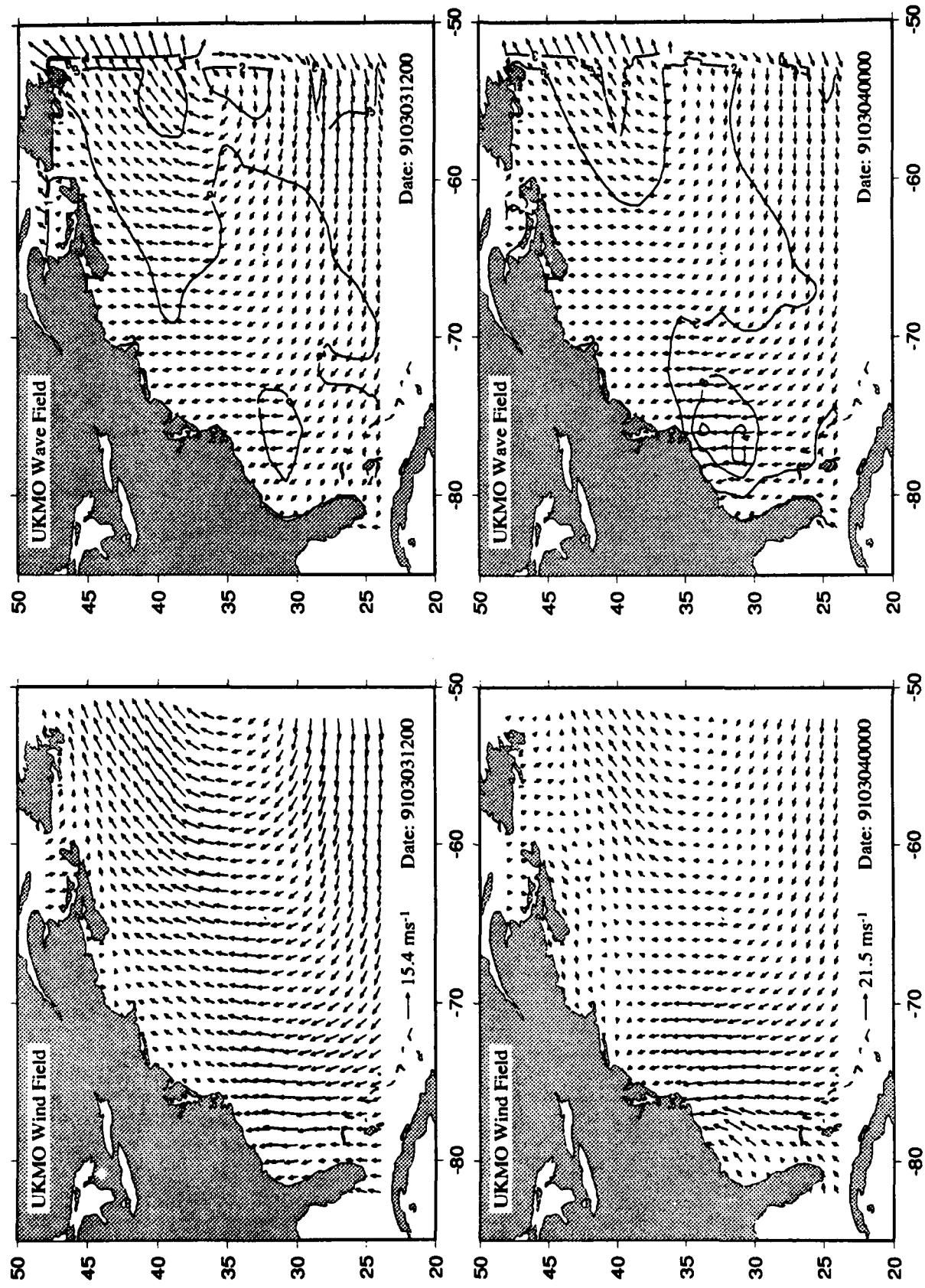


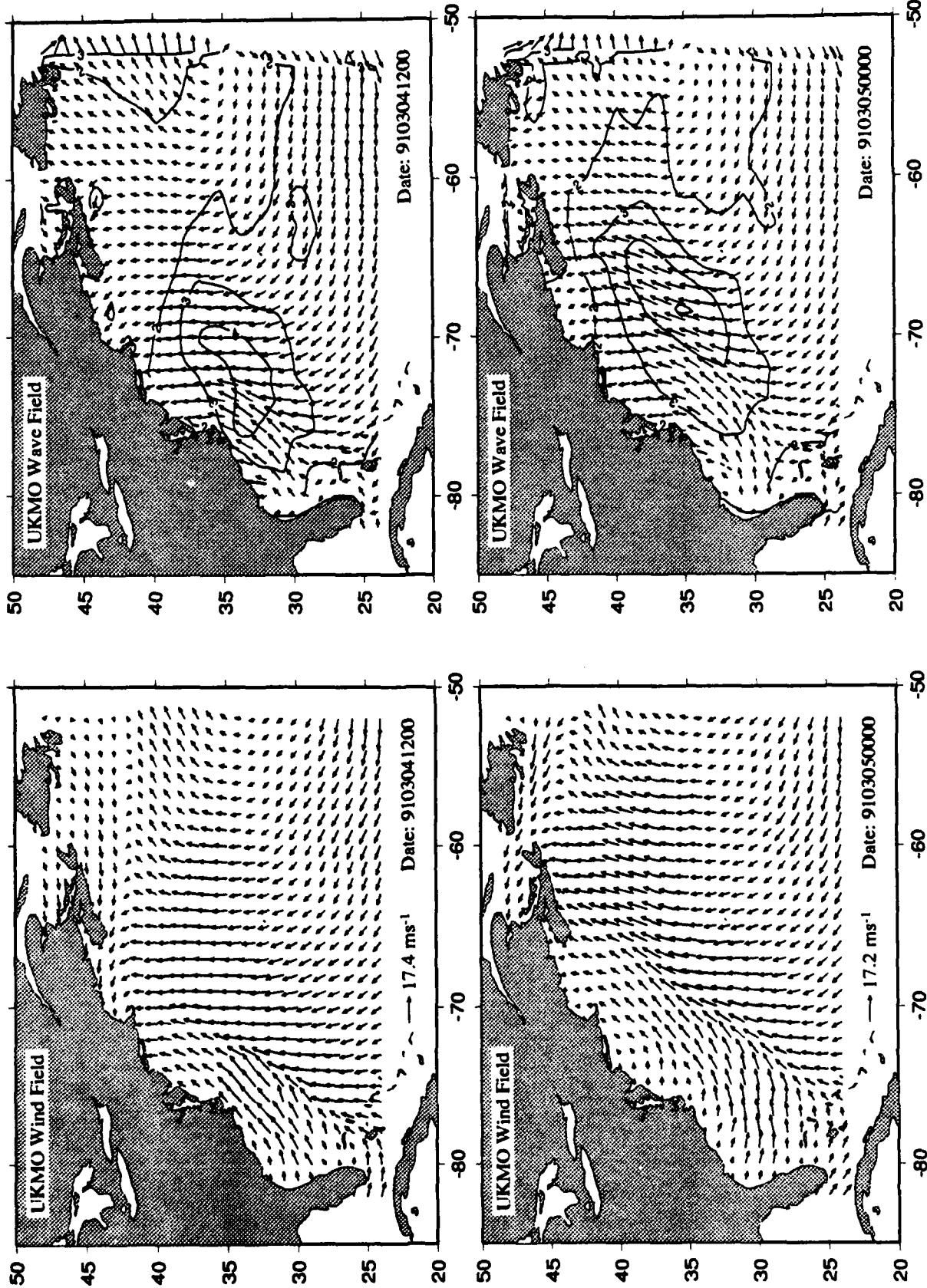


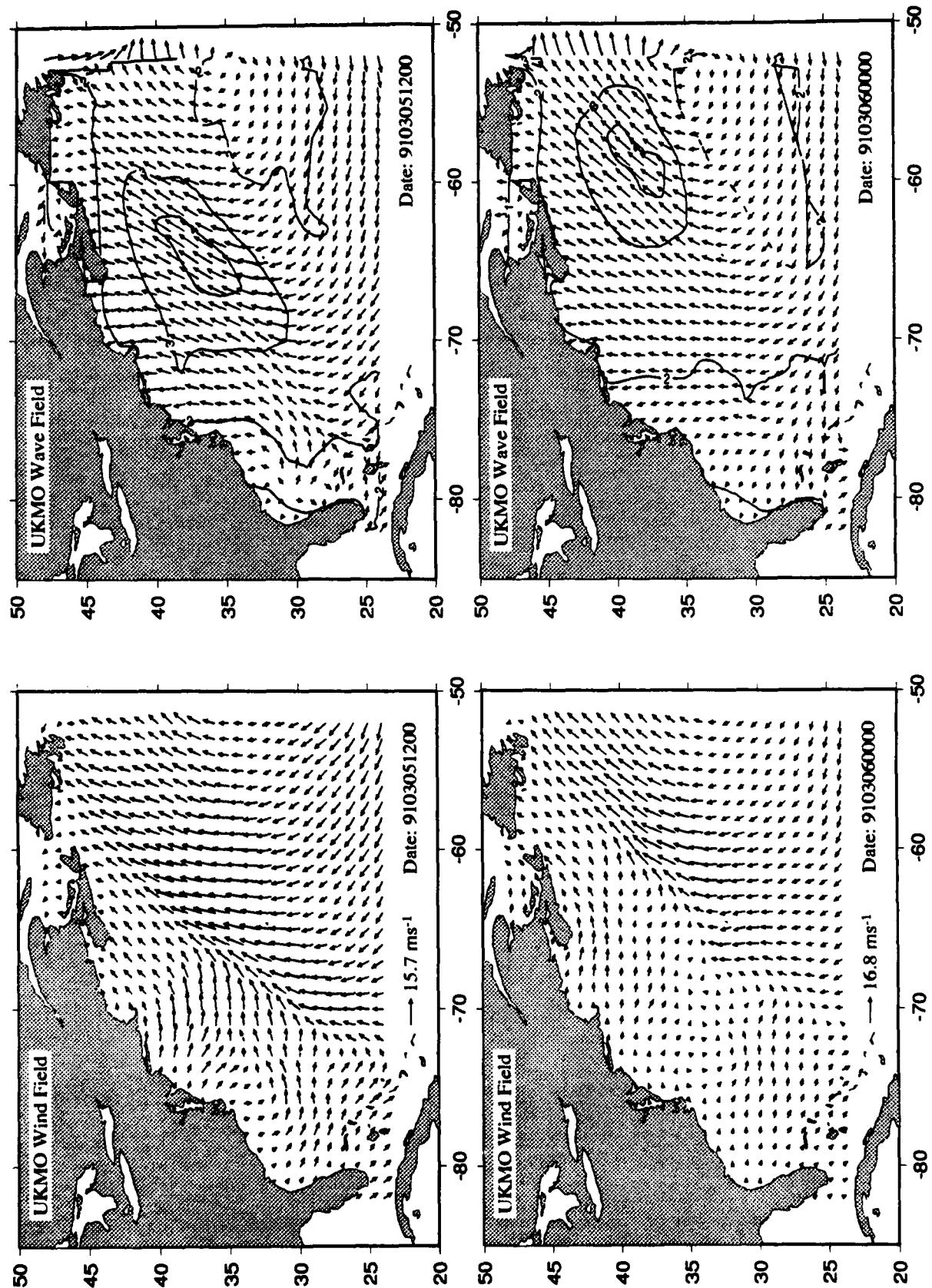


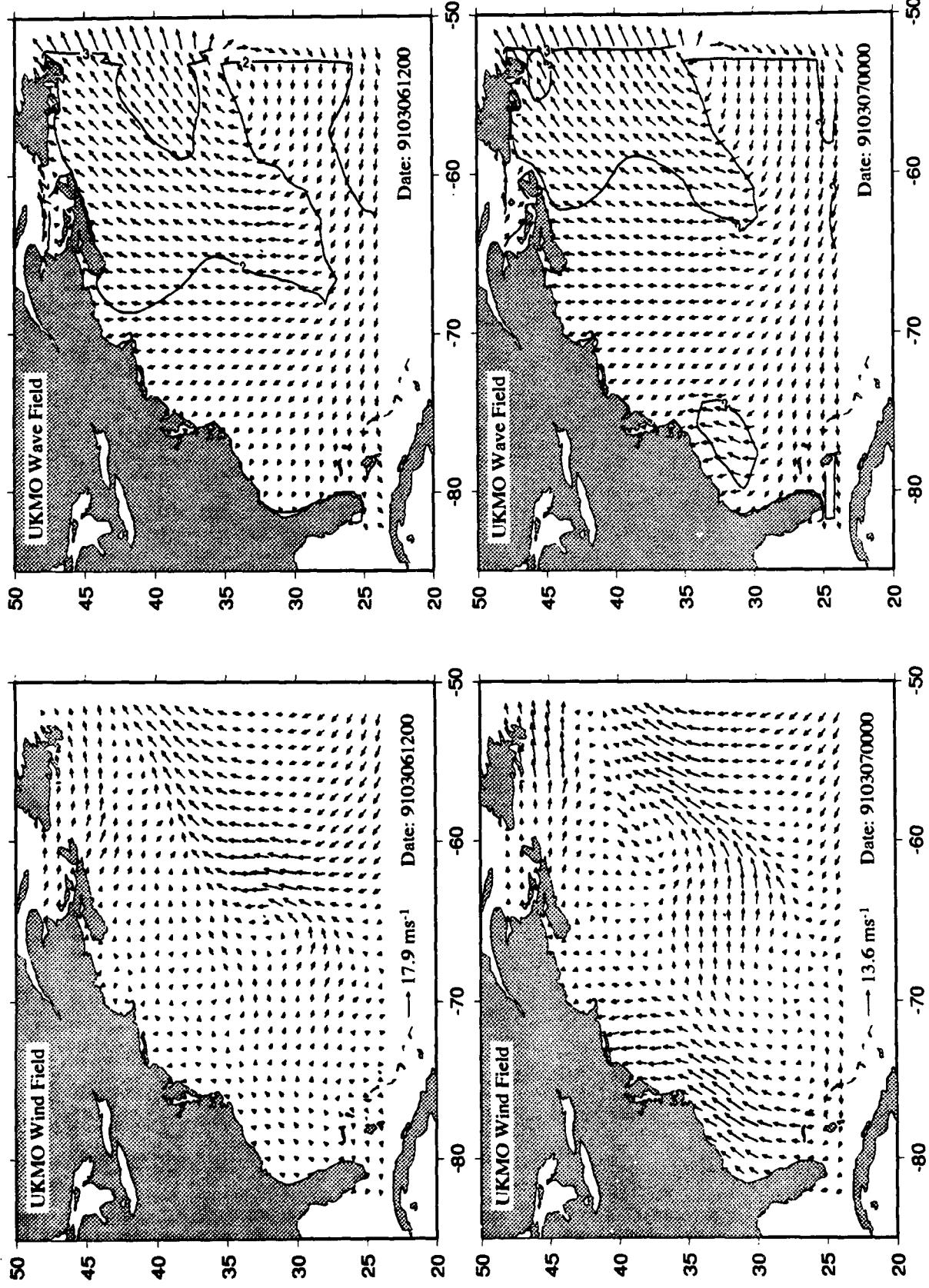
Appendix D Custer Diagrams of Wind fields and Wave Hindcasts

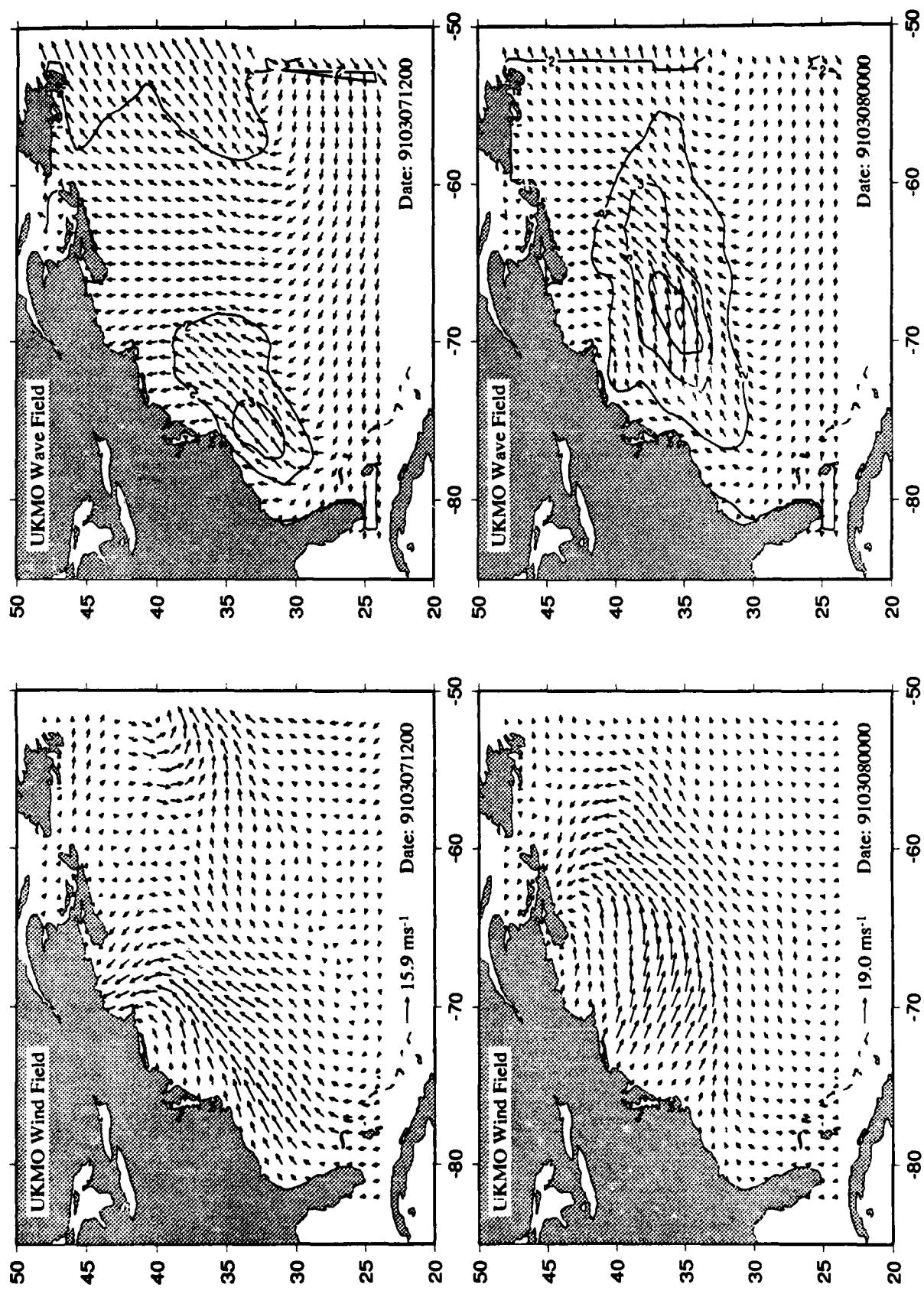




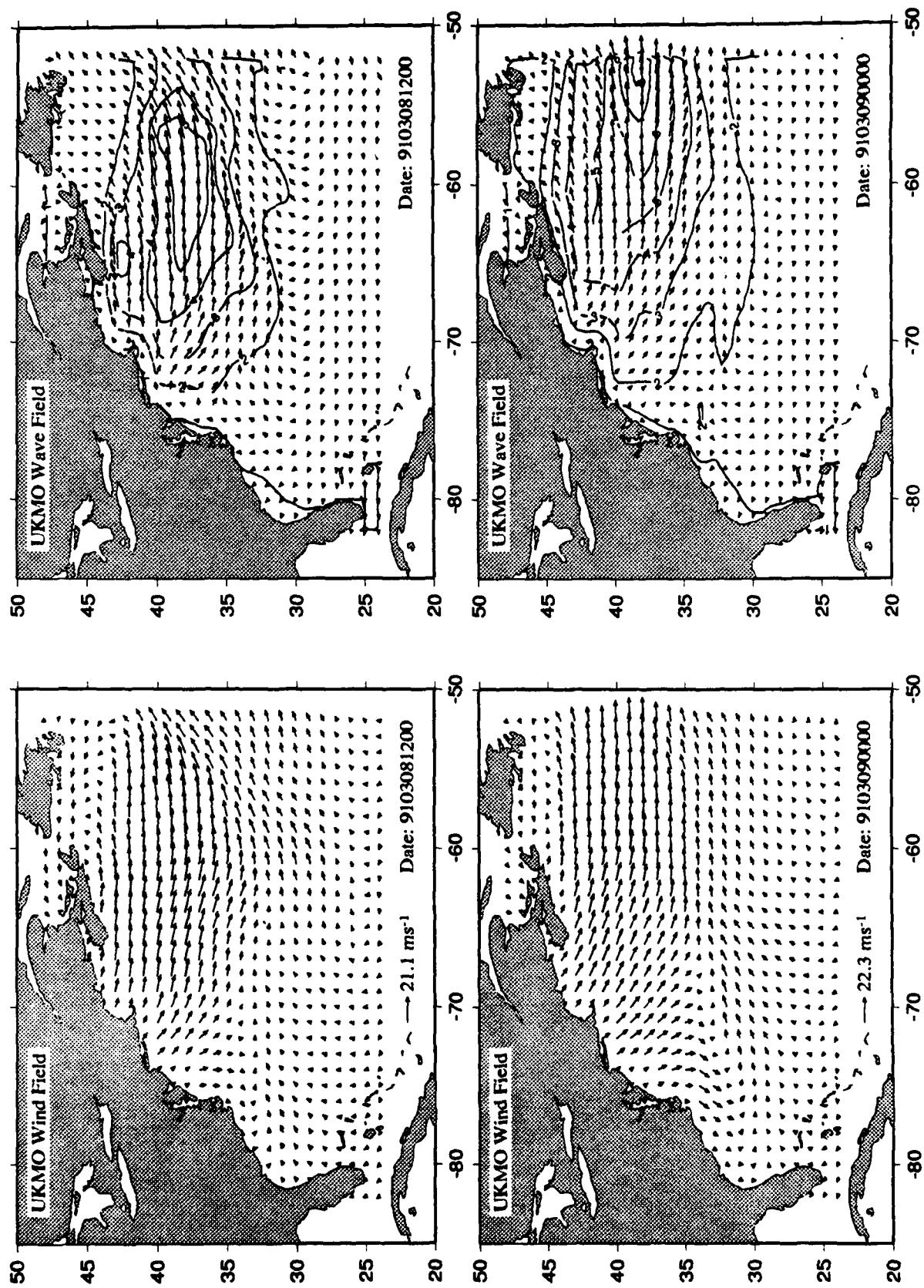








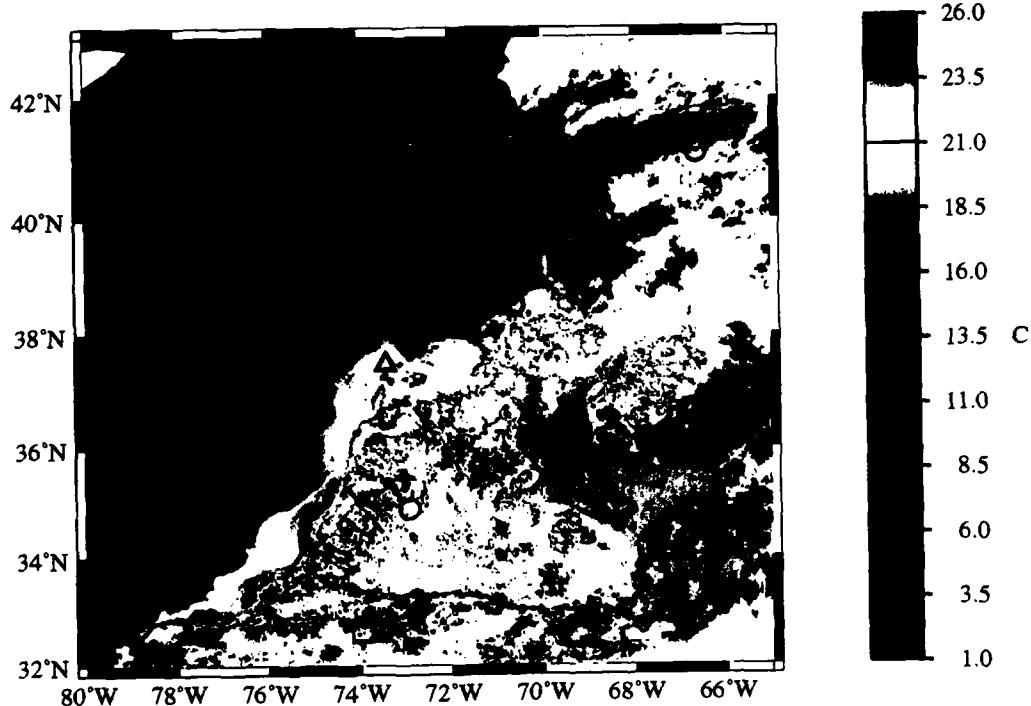
Appendix D Custer Diagrams of Wind fields and Wave Hindcasts



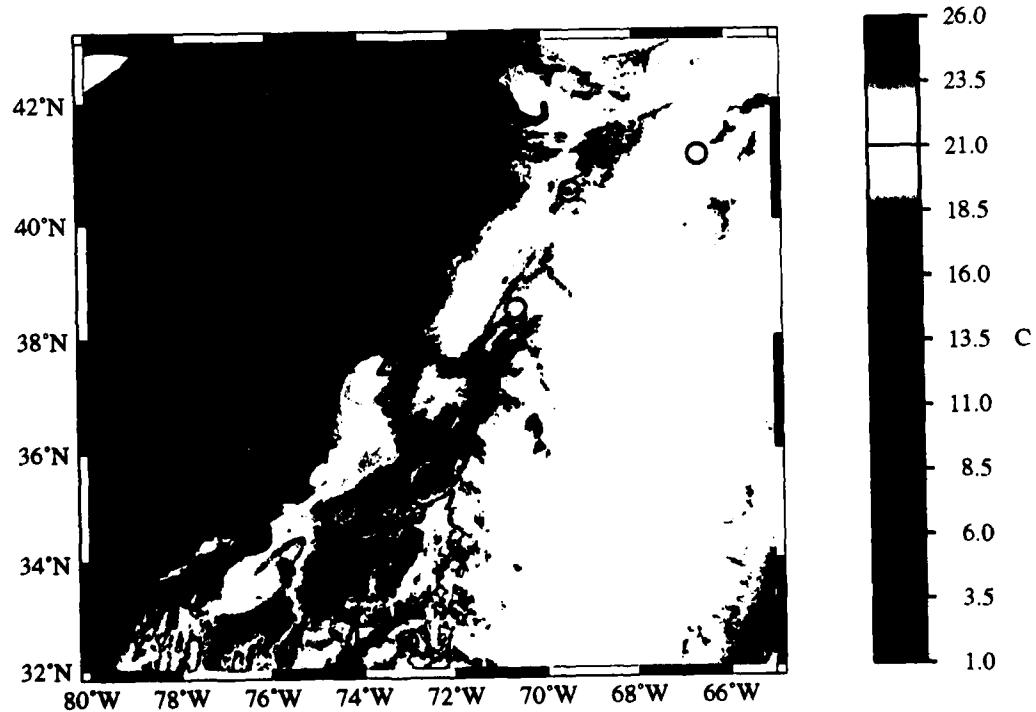
Appendix E: Infrared Imagery of Sea Surface Temperature

Color images of sea surface temperature from NOAA-10 are presented in this appendix for selected, mostly cloud-free days over the SWADE domain. Spatial resolution is approximately 1 km and the accuracy of the temperature field is about 0.125 °C from pixel to pixel.

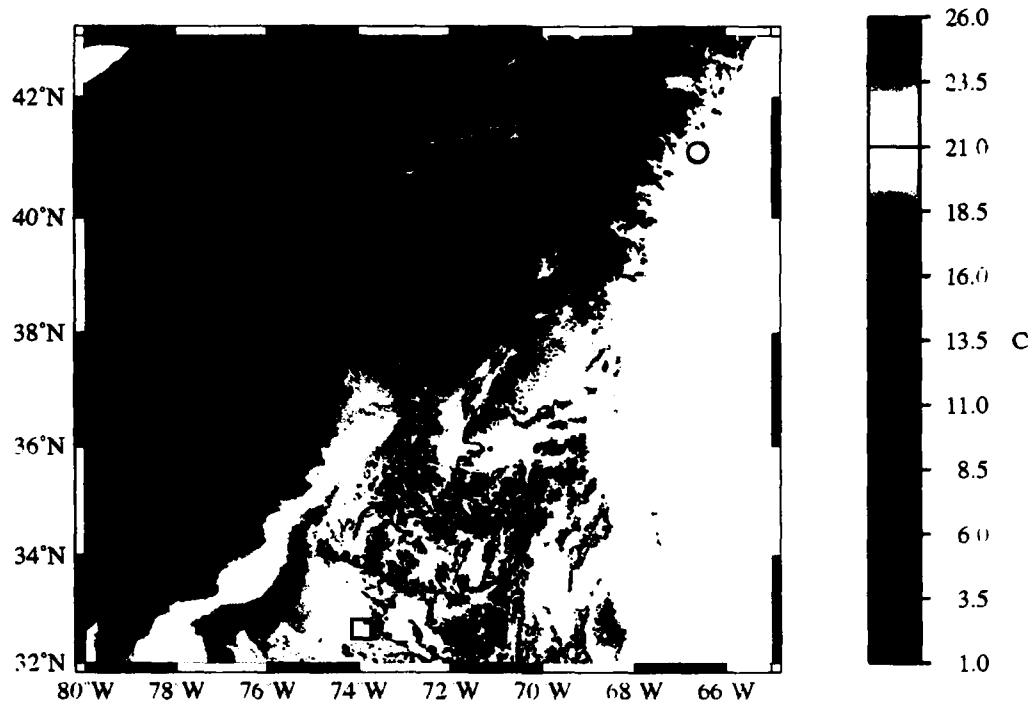
March 1, 1991



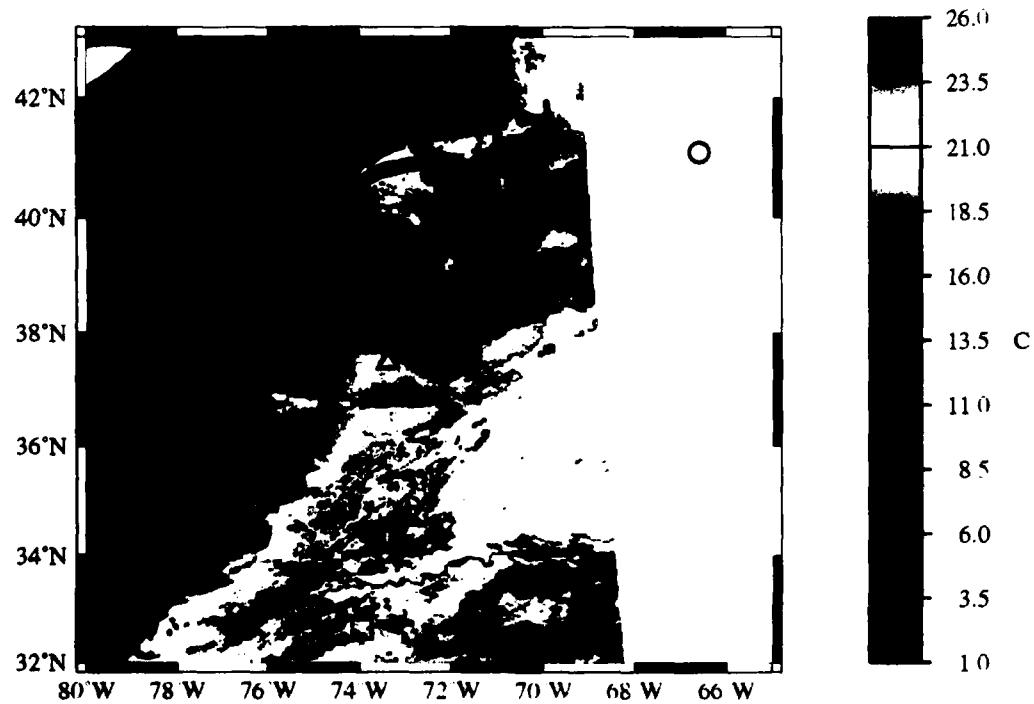
March 5, 1991



March 6, 1991



March 7, 1991



REPORT DOCUMENTATION PAGE

Form Approved
OMB No. 0704-0188

Public reporting burden for this collection of information is estimated to average 1 hour per response, including the time for reviewing instructions, searching existing data sources, gathering and maintaining the data needed, and completing and reviewing the collection of information. Send comments regarding this burden estimate or any other aspect of this collection of information, including suggestions for reducing this burden, to Washington Headquarters Services, Directorate for Information Operations and Reports, 1215 Jefferson Davis Highway, Suite 1204, Arlington, VA 22202-4302, and to the Office of Management and Budget, Paperwork Reduction Project (0704-0188), Washington, DC 20503.

| | | | | |
|---|--|---|---|--|
| 1. AGENCY USE ONLY (Leave blank) | | | 2. REPORT DATE March 1994 | 3. REPORT TYPE AND DATES COVERED Report 2 of a series |
| 4. TITLE AND SUBTITLE Observations and Modelling of Winds and Waves During the Surface Wave Dynamics Experiment; Report 2, Intensive Observation Period IOP-3, 25 February-9 March 1991 | | | 5. FUNDING NUMBERS ORN Contracts N00014-90-J-1464 N00014-92-J-1546 N00014-88-J-1028 WU 32523 | |
| 6. AUTHOR(S) Michael J. Caruso, Hans C. Graber, Robert E. Jensen, Mark A. Donelan | | | | |
| 7. PERFORMING ORGANIZATION NAME(S) AND ADDRESS(ES) See reverse. | | | 8. PERFORMING ORGANIZATION REPORT NUMBER | |
| 9. SPONSORING/MONITORING AGENCY NAME(S) AND ADDRESS(ES) U.S. Army Corps of Engineers, Washington, DC 20314-1000; Office of Naval Research, 800 N. Quincy Street, Arlington, VA 22217 | | | 10. SPONSORING/MONITORING AGENCY REPORT NUMBER Technical Report CERC-93-6 | |
| 11. SUPPLEMENTARY NOTES Available from National Technical Information Service, 5285 Port Royal Road, Springfield, VA 22161. | | | | |
| 12a. DISTRIBUTION / AVAILABILITY STATEMENT Approved for public release; distribution is unlimited. | | | 12b. DISTRIBUTION CODE | |
| 13. ABSTRACT (Maximum 200 words) <p>This report describes the compilation of observed and modelled wind, wave and current parameters during the third intensive observation period (IOP-3) from February 25 to March 9, 1991, of the Surface Wave Dynamics Experiment. The measurements include wind speed and direction, wave heights and periods, air and sea temperatures, and atmospheric pressures from four directional wave buoys, two meteorological buoys, and several routinely operated buoys from the National Data Buoy Center (NDBC). Examples of directional wave spectra obtained from two airborne radars and from a Swath ship are presented along with surface currents from airborne expendable current profilers (AXCP) and acoustic doppler current profilers (ADCP). In addition, a summary of directional wave spectra is presented for this period. The model data include examples of wind fields from six numerical weather prediction models and the corresponding wave height maps as derived from the 3G-WAM ocean wave model. Estimated surface current velocities and directions from the Fleet Numerical Oceanographic Center (FNOC) model and selected satellite images of sea surface temperature fields are also presented for this time period.</p> | | | | |
| 14. SUBJECT TERMS See reverse. | | | 15. NUMBER OF PAGES 294 | |
| | | | 16. PRICE CODE | |
| 17. SECURITY CLASSIFICATION OF REPORT UNCLASSIFIED | 18. SECURITY CLASSIFICATION OF THIS PAGE UNCLASSIFIED | 19. SECURITY CLASSIFICATION OF ABSTRACT | 20. LIMITATION OF ABSTRACT | |

7. (Concluded).

Department of Physical Oceanography, Woods Hole Oceanographic Institution, Woods Hole, MA 02543;
Rosenstiel School of Marine and Atmospheric Science, University of Miami, Miami, FL 33149-1098;

U.S. Army Engineer Waterways Experiment Station, Coastal Engineering Research Center,
3909 Halls Ferry Road, Vicksburg, MS 39180-6199;

National Water Research Institute, Canada Centre for Inland Waters, Burlington, Ontario L7R 4A6, Canada